International Journal of
Rheumatic Diseases

WILEY

International Journal of Rheumatic Diseases

For submission instructions, subscription and all other information visit http://onlinelibrary.wiley.com/journal/10.1111/(ISSN)1756-185X

View this journal online at wileyonlinelibrary.com/journal/apl

WILEY

CLINICAL IMAGE

Red Hot Ears: An Entity Not to be Missed

Bodhibrata Banerjee[1] | Godasi S. R. S. N. K. Naidu[1] | Rajender Kumar[2] | Aman Sharma[1]

[1]Department of Internal Medicine, Post Graduate Institute of Medical Education and Research, Chandigarh, India | [2]Department of Nuclear Medicine, PGIMER, Chandigarh, India

Correspondence: Aman Sharma (amansharma74@yahoo.com)

1 | Case Summary

A 52-year-old diabetic and hypertensive male presented with swelling and redness of the left pinna followed by the right pinna along with pain over the nasal bridge for 5 months. There was easy fatigability and weight loss of 4 kg in 4 months. The swelling used to subside with NSAIDs, but there were multiple recurrences. On examination, both pinnae were warm, red, and tender, with thickening of the ear cartilage and sparing of the ear lobules (Figure 1A). There was tenderness of the nasal cartilage also. Investigations revealed hemoglobin level of 13 g% and C-reactive protein of 25 mg/L. X-ray showed calcification of the pinna (Figure 1B yellow arrow). PET scan showed FDG avidity in auricular and nasal cartilages and no involvement of the trachea-bronchial tree (Figure 1C). A diagnosis of Relapsing Polychondritis (RP) was made. He was started on prednisolone 10 mg along with oral Methotrexate 15 mg/week. He had resolution of chondritis (Figure 1D) with normalization of CRP (1.6 mg/L) without any recurrence until the last follow-up visit at 3 months. Prednisolone was gradually tapered and stopped after 4 weeks.

RP should be suspected in any adult presenting with recurrent inflammation of auricular cartilage sparing the ear lobules or nasal cartilage [1]. The involvement of the cartilaginous part of the trachea and great vessels like the aorta and its branches can be life threatening. Hence, screening for their involvement should be done in all patients. RP can be seen in association with other systemic autoimmune rheumatic diseases [2]. VEXAS should be suspected in elderly males aged more than 50 years who develop cytopenia with MCV > 100 fl [3].
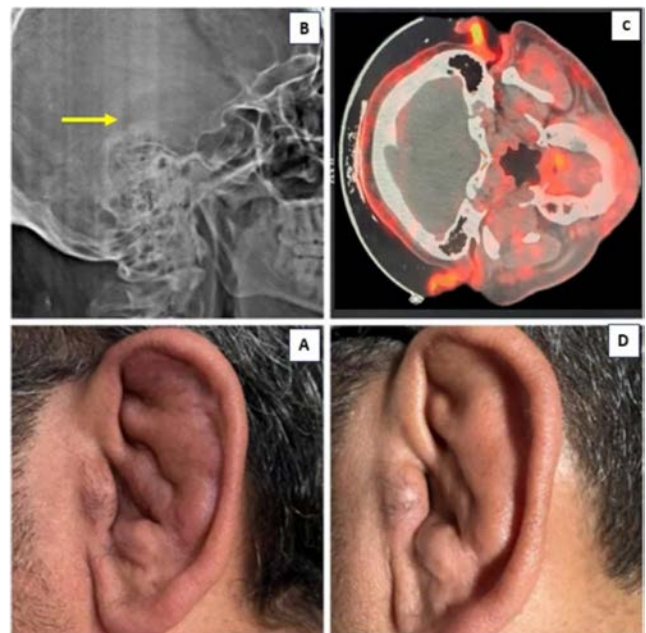
FIGURE 1 | (A) Inflamed auricular cartilage before start of treatment. (B) X ray showing calcification of pinna (yellow arrow). (C) Positron emission tomography showing hypermetabolic FDG uptake over bilateral auricular and nasal cartilages. (D) Resolution of auricular chondritis with treatment after 3 months.

Author Contributions

B.B., G.S.R.S.N.K.N. and A.S. were involved in clinical evaluation and treatment of the patient. Dr Rajender Kumar did the PET CT scan of this patient.

Conflicts of Interest

The authors declare no conflicts of interest.

Data Availability Statement

The data that support the findings of this study are available on request from the corresponding author. The data are not publicly available due to privacy or ethical restrictions.

References

1. F. Borgia, R. Giuffrida, F. Guarneri, and S. P. Cannavò, "Relapsing Polychondritis: An Updated Review," *Biomedicine* 6, no. 3 (2018): 84.

2. E. Zampeli and H. M. Moutsopoulos, "Relapsing Polychondritis: A Diagnosis Not to Be Missed," *Rheumatology* 57, no. 10 (2018): 1768.

3. A. Sharma, A. D. Law, P. Bambery, et al., "Relapsing Polychondritis: Clinical Presentations, Disease Activity and Outcomes," *Orphanet Journal of Rare Diseases* 9 (2014): 198.

ORIGINAL ARTICLE

Decoding PANoptosis in Gout: Signature Gene Identification and Immune Infiltration Profiling

Junjie Cao[1] | Aifang Li[2] | Gaiying Luo[1] | Zhen Wu[3] | Yuan Liu[1]

[1]Department of Laboratory Medicine, Xi'an Fifth Hospital, Xi'an, Shaanxi Province, China | [2]Department of Laboratory Medicine, Xi'an Chest Hospital, Xi'an, Shaanxi Province, China | [3]Department of Rheumatology (Unit 6), Xi'an Fifth Hospital, Xi'an, Shaanxi Province, China

Correspondence: Yuan Liu (ly526621452@163.com)

ABSTRACT

Background: Gout is an inflammatory disorder triggered by the deposition of monosodium urate (MSU) crystals in joints and periarticular tissues. PANoptosis, a recently identified form of inflammatory cell death, remains uncharacterized in gout pathogenesis. This study aims to identify PANoptosis-related genes that may drive gout progression.

Methods: Gout-related datasets, including the human cohort (GSE160170) and murine model (GSE190138), were retrieved from the Gene Expression Omnibus (GEO) database. Differentially expressed genes (DEGs) were screened using thresholds of $|\log_2$ fold change (FC)$| \geq 1$ and adjusted P-value < 0.05. PANoptosis-related biomarkers were identified through the combined use of MCODE and cytoHubba algorithms in Cytoscape. Least Absolute Shrinkage and Selection Operator (LASSO) regression was applied to select hub genes. Subsequently, we performed single—sample gene set enrichment analysis (ssGSEA) for the hub genes, analyzed the infiltration levels of immune cells, constructed a miRNA–mRNA–transcription factor (TF) regulatory network, and identified potential therapeutic drugs via the DSigDB database and the Coremine Medical database. Finally, the expression of the diagnostic gene was validated by real-time quantitative reverse transcription polymerase chain reaction (RT-qPCR).

Results: The PANoptosis-associated gene *SOCS3* was identified via integrative bioinformatics screening. Enrichment analysis and immune infiltration assessment revealed its involvement in gout pathogenesis through pathways linked to inflammation and cell death, with significant correlations observed with specific immune cell subsets. Clinical validation via RT-qPCR confirmed a strong consistency between SOCS3 expression levels in gout patients and computational predictions.

Conclusion: We identified the hub gene *SOCS3* in gout and elucidated its mechanistic roles by integrated bioinformatics analysis, machine learning approach, and clinical validation, providing critical insights for advancing diagnostic biomarkers and therapeutic strategies in gout management.

1 | Introduction

Gout is a metabolic-inflammatory disorder caused by the deposition of monosodium urate (MSU) crystals in joints or periarticular tissues, clinically manifesting as gouty arthritis (GA), urate nephrolithiasis, or chronic gouty kidney disease [1]. The global prevalence of gout exhibits significant geographical variation, ranging from 3% to 5% in developed countries,

---

while China reports a lower prevalence of 1.6%, though both regions show a persistent upward trend [2]. Currently, the gold standard for diagnosing gout is the presence of MSU crystals in synovial fluid or tophi using polarized light microscopy, but the detection of MSU crystals is subject to limitations in medical conditions, examination conditions, and the technician's skill, resulting in suboptimal sensitivity for early-stage diagnosis [3].

Cell death plays a pivotal role in both physiological and pathological processes. Emerging evidence indicates that distinct cell death modalities are associated with the clinical progression of gout, where immune cells release cytokines and chemokines through necroptosis, pyroptosis, or other forms of cell death. This process amplifies immune cell recruitment to joints and exacerbates inflammatory cascades [4]. Key inflammatory mediators such as tumor necrosis factor (TNF)-α and interleukin (IL)-1β, which are critical regulators of apoptosis, necroptosis, and pyroptosis, are predominantly secreted by monocytes. These molecules promote inflammatory cell infiltration in gout patients [5, 6].

PANoptosis, a novel form of programmed cell death, integrates features of pyroptosis, apoptosis, and necroptosis, regulating disease progression through the formation of a multimolecular complex called the PANoptosome. Its core mechanism involves synergistic interactions of key molecules (e.g., ZBP1, NLRP3, Caspase family proteins) that ultimately drive inflammatory factor release and cell death [7]. The pathological hallmark of GA lies in the inflammatory response triggered by MSU crystal deposition. MSU crystals activate the NLRP3 inflammasome, triggering Caspase-1-dependent pyroptosis and subsequent release of pro-inflammatory cytokines like IL-1β [8, 9]. PANoptosis may exacerbate inflammatory signaling cascades and promote joint damage by integrating pyroptosis with other cell death modalities (e.g., apoptosis-related Caspase-8 or necroptosis-associated MLKL) [10]. Therefore, investigating PANoptosis mechanisms in gout could facilitate the discovery of biomarkers for early diagnosis and targeted therapeutic interventions.

This study aims to investigate the relationship between PANoptosis and gout. By analyzing the gout data retrieved from the Gene Expression Omnibus (GEO) database, bioinformatics analysis was used to screen differentially expressed genes (DEGs) related to PANoptosis in gout. A protein–protein interaction (PPI) network was constructed to identify topologically central hub genes, ultimately screening for critical genes. The least absolute shrinkage and selection operator (LASSO) regression model was utilized in machine learning to identify hub genes. Gene set enrichment analysis (GSEA) was performed to identify potential signaling pathways. Correlation analysis was performed between PANoptosis-related biomarkers and immune cell infiltration. Subsequently, relevant miRNAs and transcription factors (TFs) were predicted through online databases, and a miRNA–mRNA–TF network was constructed using Cytoscape software. The DSigDB database and the Coremine Medical database were adopted to screen for drugs targeting biomarkers. This provides potential biomarkers and regulatory pathways for the diagnosis and treatment of gout.

2 | Materials and Methods

2.1 | Study Design

The "GEOquery" package in R was employed to download gene expression datasets GSE160170 and GSE190138 from the GEO database. The GSE160170 dataset comprised peripheral blood mononuclear cell (PBMC) samples from 6 healthy controls and 6 gout patients, while GSE190138 included samples from 9 control mice and 9 gout model mice. Probe IDs were converted to gene symbols using the "idmap3" package based on platform annotation files. Differential expression analysis was performed with the "limma" package, applying thresholds of adjusted P-value < 0.05 and $|\log_2$ fold change (FC)$| \geq 1$ to identify significant DEGs. Volcano plots visualizing DEGs were generated using the "ggplot2" package. A total of 711 PANoptosis-related genes were curated from literature sources, including 681 apoptosis-associated genes, 6 necroptosis-related genes, and 24 pyroptosis-linked genes [11]. Gene Ontology (GO) and Kyoto Encyclopedia of Genes and Genomes (KEGG) enrichment analysis and PPI network analysis were performed on the common DEGs using online databases. Hub genes were prioritized using the MCODE and cytoHubba algorithms. The relative abundance of 28 distinct immune cell subsets was quantified using single-sample Gene Set Enrichment Analysis (ssGSEA) to characterize immune infiltration patterns within the tissue microenvironment. miRNAs and TFs related to the hub genes were predicted through online databases, and a miRNA–mRNA–TF regulatory network was constructed using Cytoscape software. Hub gene-associated drugs were predicted using the DSigDB database and the Coremine Medical database. PBMCs from gout patients and healthy individuals were collected, and the expression level of hub genes was verified by RT-qPCR. The flowchart is shown in Figure S1.

2.2 | Screening of Differentially Expressed Genes

Firstly, the "affy" package in the R software program was used for background correction, normalization, and $\log_2$ transformation of the gout datasets. The Limma package was used to identify DEGs in gout, with the criteria set as: $|\log_2$ Fold change (FC)$| \geq 1$, and P-value < 0.05. A total of 711 PANoptosis-related genes were curated from literature sources, including 681 apoptosis-associated genes, 6 necroptosis-related genes, and 24 pyroptosis-linked genes [11].

2.3 | Functional Enrichment Analysis

The Database for Annotation, Visualization and Integrated Discovery (DAVID, https://david.ncifcrf.gov/) was used for GO analysis. To elucidate the functional implications of DEGs, GO enrichment analysis was performed using the DAVID tool (version 6.8), which interrogates the GO database to annotate biological processes, cellular components, and molecular functions. After downloading the GO analysis data, the "ggplot2" package was used to generate bubble charts. The KEGG Orthology Based Annotation System (KOBAS version 3.0, http://kobas.cbi.pku.edu.cn) was used for pathway analysis. The DAVID tool was used to explore the pathways enriched

by DEGs and the biological significance behind them. After downloading the pathway analysis data, the "ggplot2" package was used to generate bubble charts. Subsequently, GSEA was performed to reveal the specific functions of each gene. The significance threshold was set at an adjusted P-value < 0.05. In this study, based on the intersection of DEGs from gout and genes related to PANoptosis, a common set of genes was subjected to GO and KEGG analysis.

2.4 | Construction of Protein–Protein Interaction (PPI) Network

The PPI network was constructed using the String database (version 11.5; www.string-db.org) with an interaction score set to 0.400. The Cytoscape software was utilized to build this PPI network.

2.5 | Hub Gene Screening

The PPI network was imported into the Cytoscape software to identify key functional modules and hub genes that play significant roles. The Molecular Complex Detection (MCODE) plugin was employed to recognize key functional modules; the identification criteria were: node degree ≥ 2, node score ≥ 0.2, K-core ≥ 2, and maximum depth $= 100$. The top 10 hub genes were identified in the PPI network using the Maximal Clique Centrality (MCC) algorithm of the Cytohubba plugin. Ultimately, the intersection of genes from the MCODE key modules and the cytoHubba key genes was determined as the hub genes.

2.6 | LASSO Regression Model

The R package "glmnet" was utilized to further screen candidate genes for gout diagnosis through LASSO-Cox regression analysis. For the GSE160170 dataset, the optimal λ (lambda) value was 0.07, while for the GSE190138 dataset, λ was set to 0.06. The intersection of genes selected from both datasets was identified as key genes.

2.7 | Immune Infiltration Analysis

The infiltration of 28 immune cell types was analyzed using ssGSEA with the R package "GSVA". The correlations among immune cells were visualized using heatmaps generated by the R package "corrplot" $*p < 0.05$, $**p < 0.01$, $***p < 0.001$.

2.8 | miRNA–mRNA–TF Regulatory Network in Gout

Three online miRNA databases, miRWalk, miRNANet, and miRTarBase, were used to predict miRNAs. The TRRUST database was used to predict associated TFs for the target mRNAs. Using the "merge" function in Cytoscape, a regulatory network of miRNA–mRNA–TF interactions was constructed.

2.9 | Real-Time Quantitative Reverse Transcription Polymerase Chain Reaction (RT-qPCR)

A total of 10 gout patients and 10 healthy controls were recruited from the Xi'an Fifth Hospital. The gout patients met the 2015 EULAR/ACR classification criteria for gout. The PBMCs from gout patients and healthy individuals were collected. Total RNA was isolated from cells using the TRIzol reagent (Invitrogen) according to the manufacturer's instructions. RT-qPCR was performed using SYBR Green PCR Master Mix (Bio-Rad Laboratories) on a MyiQ Single-Color Real-time PCR Detection System (Bio-Rad Laboratories). Sequence-specific primers for the indicated genes were synthesized by Sangon Biotech and are listed in Table S1. The study was approved by the Research Ethics Committee of the Xi'an Fifth Hospital (2023–74).

2.10 | Predicting Drugs for Key Genes

To identify potential therapeutics targeting the key genes, we performed drug enrichment analysis using the DSigDB database. The gene signature was uploaded to the Enrichr platform (https://maayanlab.cloud/Enrichr/) to evaluate associations with drug-induced gene expression profiles. Significantly small-molecule drug candidates were filtered by an adjusted p-value < 0.05. The top 10 drugs ranked by the Combined Score were further analyzed based on their known mechanisms of action and clinical relevance to the disease context. Additionally, the Coremine Medical database (https://www.pubgene.com/coremine-medical/) was utilized to query traditional Chinese medicines (TCMs) statistically associated with the key genes (p-value < 0.05).

2.11 | Statistical Analysis

All statistical analyses were conducted using R software (version 4.3.3) and GraphPad Prism 9 (GraphPad Software Inc., San Diego, CA, USA). Normality of continuous variables was assessed via the Shapiro–Wilk test. For intergroup comparisons: Normally distributed data were analyzed using independent two-tailed Student's t-tests, and non-normally distributed data were evaluated with the Mann–Whitney U test. Spearman's rank correlation analysis was employed to assess variable associations. Statistical significance was defined as $p < 0.05$.

3 | Results

3.1 | Identification and Functional Enrichment Analysis of DEGs in Gout

In the GSE190138 dataset, 1469 DEGs were yielded, with 722 upregulated and 747 downregulated genes (Figure 1A). In the GSE160170 dataset, 790 DEGs were identified, comprising 303 upregulated and 487 downregulated genes (Figure 1B). Intersection analysis with 711 PANoptosis-related genes revealed 17 overlapping genes (Figure 1C).
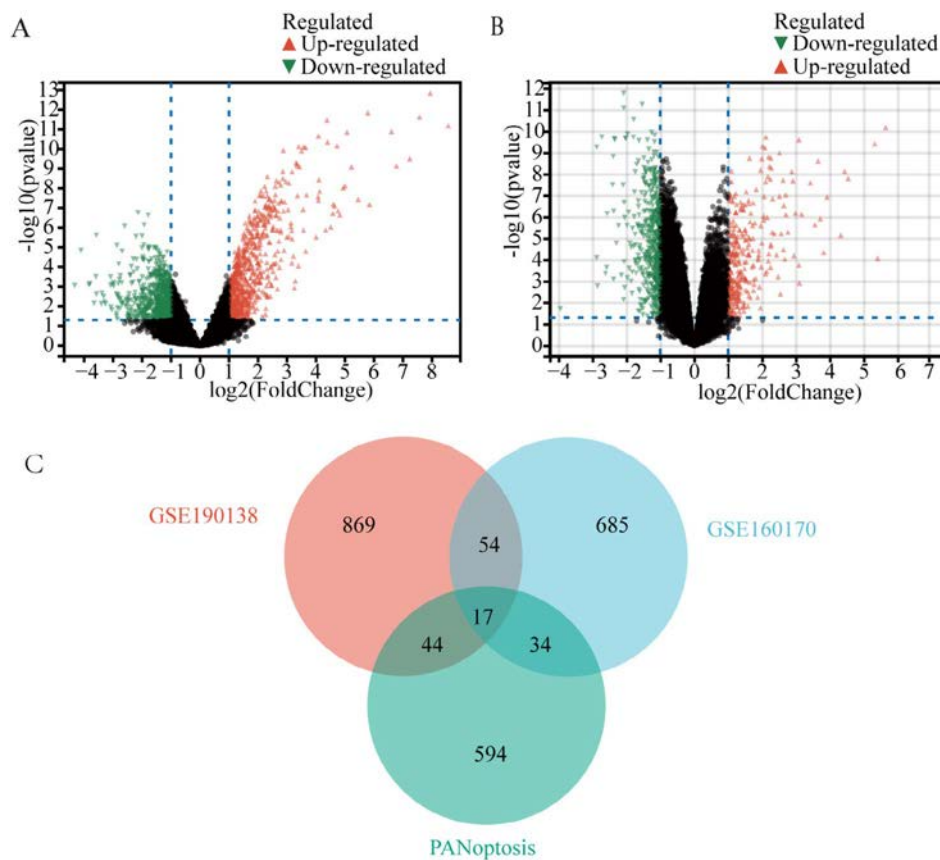
FIGURE 1 | Identification of DEGs in Gout and common genes with PANoptosis. (A) The volcano map of gout dataset GSE190138. (B) The volcano map of Gout dataset GSE160170. Upregulated genes were marked in red; downregulated genes were marked in green. (C) The overlap genes of DEGs in GSE190138, GSE160170, and genes with PANoptosis via a Venn diagram.

To further understand and study the biological functions of the DEGs related to PANoptosis, GO and KEGG enrichment analyses were performed on the above 17 genes. The results were shown in Figure S2. In the KEGG enrichment analysis, most genes were involved in the TNF signaling pathway, the NF-kappa B signaling pathway, the IL-17 signaling pathway, apoptosis, and necroptosis (Figure S2A). Biological Process (BP) was mainly enriched in pathways related to cell death (Figure S2B); Cellular Component (CC) was primarily enriched in the extracellular region, plasma membrane part, lysosomes, etc. (Figure S2C); Molecular Function (MF) were mainly enriched in the molecular function regulators, cytokine activity, cytokine receptor binding, etc. (Figure S2D).

3.2 | Hub Gene Screening

Based on the STRING database, interactions were found among 15 of the 17 DEGs. A visual PPI network diagram was established using the Cytoscape software (Figure 2A). To better understand the potential relationships between DEGs related to PANoptosis, the PPI network was further imported into the Cytoscape software to screen for key functional modules and hub genes that play important roles. One key module (containing 11 genes) was identified using the MCODE plugin (Figure 2B), which may represent important regulatory pathways for genes related to PANoptosis in gout. Second, the top 10 hub genes were

identified using the MCC algorithm in the cytoHubba plugin (Figure 2C). Finally, the intersection of the MCODE key module genes and the cytoHubba key genes resulted in 9 hub genes (*PTGS2*, *SOCS3*, *TNFAIP3*, *IER3*, *DUSP1*, *FOS*, *EGR1*, *IL6*, and *IL1B*) (Figure 2D).

3.3 | Machine Learning Screening for Gout Candidate Genes

The LASSO machine learning algorithm was employed to analyze the previously identified 9 genes in both the GSE160170 and GSE190138 datasets to screen candidate diagnostic genes for gout. In the GSE160170 dataset, the selected genes were *TNFAIP3, SOCS3*, and *DUSP1*, while the GSE190138 dataset yielded *IL6, PTGS2, SOCS3*, and *GZMB* (Figure 3A,B). The shared gene between both datasets was *SOCS3* (Figure 3C).

3.4 | Expression of Key Genes and Gene Set Enrichment Analysis (GSEA)

The expression of *SOCS3* was validated in the GSE160170 and GSE190138 datasets, respectively. Compared to the normal control group, *SOCS3* was significantly upregulated in the gout group (Figure 4A,C), and the area under the ROC curve (AUC) for both datasets reached 100% (Figure 4B,D). GSEA analysis
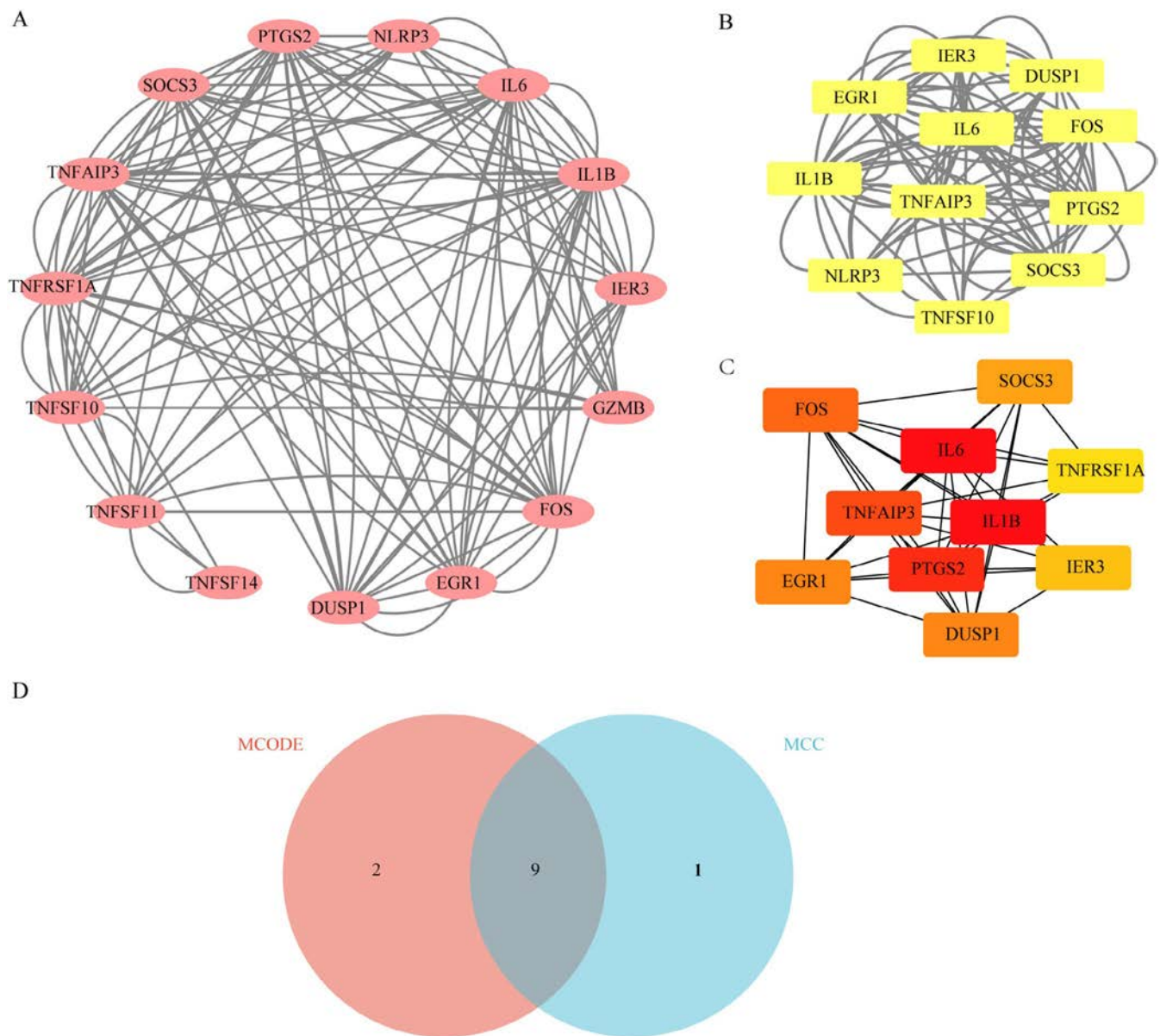
FIGURE 2 | Protein–protein interaction (PPI) network and hub genes screening. (A) PPI network of common genes in Gout and PANoptosis. (B) 11 genes clustered in one module were exhibited by MCODE. (C) The top 10 hub genes identified using the MCC algorithm in the cytoHubba plugin. (D) Intersection of the MCODE key module genes and the MCC algorithm hub genes via a Venn diagram.

revealed that *SOCS3* was mainly concentrated in the purine metabolism, pyrimidine metabolism, and RNA degradation pathways (Figure 4E).

3.5 | Immune Infiltration Analysis

Using ssGSEA, we characterized the infiltration patterns of 28 immune cell subpopulations in gout patients versus healthy controls. Significant differences in immune cell proportions were observed between the two groups. Specifically, 12 out of 28 immune cell subsets exhibited distinct variations, with activated CD4$^+$T cells, CD56^{dim} natural killer cells, eosinophils, and T follicular helper cells, showing marked upregulation in gout patients (Figure 5A). Next, we conducted a comprehensive correlation analysis among these 28 immune cell subtypes, revealing that many subtypes exhibited significant intercorrelations.

(Figure 5B). Subsequently, we conducted an association analysis between the 28 immune cell subtypes and the *SOCS3*. The results indicated that *SOCS3* was negatively correlated with type 2 T helper cells, natural killer T cells, effector memory CD8$^+$T cells, central memory CD4$^+$T cells and activated CD8$^+$T cells, while it was positively correlated with T follicular helper cells, plasmacytoid dendritic cells, natural killer cells, mast cells, immature dendritic cells, gamma delta T cells, eosinophils, CD56^{dim} natural killer cells, and activated CD4$^+$T cells (Figure 5C). These findings suggest that these specific cell types may play a crucial role in the development of gout.

3.6 | Construction of miRNA–mRNA–TF Network

Three online miRNA databases (miRWalk, miRNANet, and miRTarBase) were applied to predict miRNAs, identifying
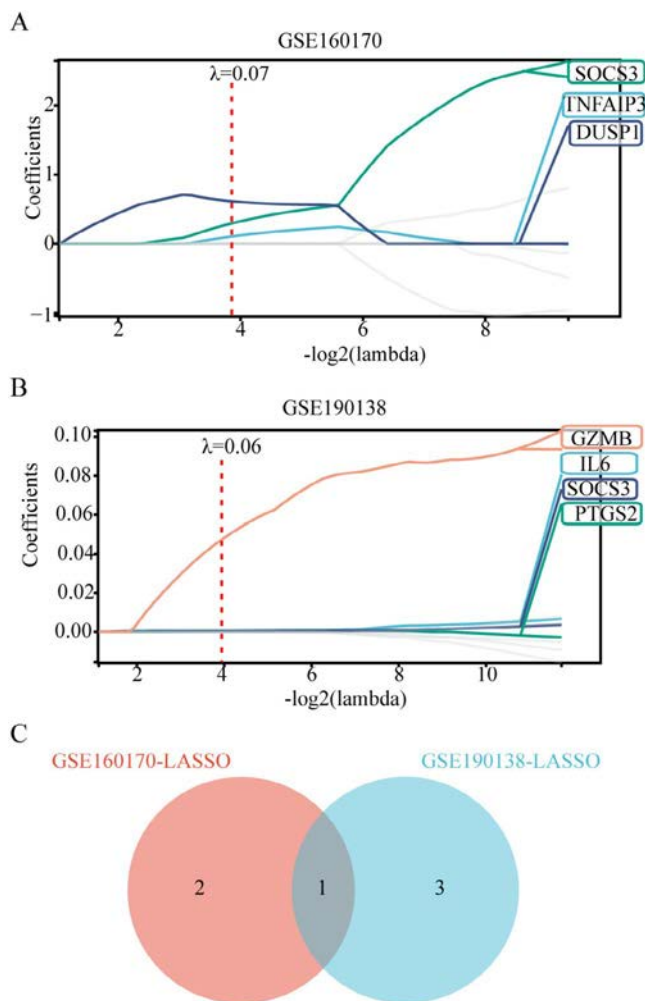
FIGURE 3 | Machine learning screening for gout candidate genes. (A) Identification of biomarkers using the Lasso regression model in the GSE160170 dataset. (B) Identification of biomarkers using the Lasso regression model in the GSE190138 dataset. (C) Intersection of the LASSO candidate genes between GSE160170 and GSE190138 via Venn diagram.

five differentially expressed target miRNAs: *hsa-let-7f-5p, hsa-miR-221-3p, hsa-miR-324-5p, hsa-miR-484*, and *hsa-miR-423-5p* (Figure 6A).

In the TRRUST database, TFs related to the predicted *SOCS3* were identified. A total of 7 important TFs were finally screened out (*CEBPA*, *NFKB1*, *RELA*, *SP3*, *STAT1*, *STAT3*, *STAT4*). A miRNA–mRNA–TF network was constructed using the merge function in Cytoscape (Figure 6B).

3.7 | Expression of Hub Genes in Clinical Samples

Compared with health control, the expression of *SOCS3* was up-regulated in the gout group (Figure S3).

3.8 | Screening for Potential Therapeutic Drugs

Using the DSigDB drug database for *SOCS3*-targeted small-molecule enrichment analysis, the top 10 candidates based on Combined Score (adjusted p-value <0.05) were identified (Table S2). Comprehensive analysis suggested that Isoeugenol and Rofecoxib may exert therapeutic effects on gout via *SOCS3* modulation. Additionally, 5 *SOCS3*-related traditional Chinese herbs were screened from the Coremine Medical database (Table S3).

4 | Discussion

Gout, a chronic metabolic-inflammatory disorder, arises from dysregulated uric acid homeostasis driven by excessive purine catabolism, urate overproduction, and/or impaired renal urate excretion, culminating in persistent hyperuricemia (serum urate >6.8 mg/dL) [12]. Monosodium urate (MSU) crystals form in synovial tissues when serum urate levels exceed saturation, triggering inflammation and pain [12]. The diagnostic gold standard remains the identification of MSU crystals in synovial fluid via joint aspiration; however, this invasive procedure demands specialized expertise and is not universally feasible in clinical practice [13]. Imaging tools like dual-energy computed tomography (DECT) or ultrasound improve accuracy but face accessibility barriers [14]. Serum urate levels may normalize during acute flares due to inflammatory shifts, requiring post-flare retesting for confirmation [15]. These limitations highlight the urgent need for non-invasive biomarkers and diagnostic innovations to optimize gout management.

PANoptosis is a recently identified form of programmed inflammatory cell death characterized by its unique integration of molecular mechanisms from three classical cell death pathways: pyroptosis, apoptosis, and necroptosis. Its regulation relies on a multilayered macromolecular complex termed the PANoptosome, which triggers signaling cascades upon recognition of pathogen-associated molecular patterns (PAMPs) or damage-associated molecular patterns (DAMPs), ultimately leading to irreversible cell death. Unlike singular cell death pathways, the biological effects of PANoptosis cannot be fully explained by any individual mechanism alone. Instead, it operates through shared molecular components (e.g., caspase family proteins) and crosstalk between pathways [7, 16]. Current research suggests that PANoptosis may play a critical role in the pathogenesis and progression of gout by modulating inflammatory signaling pathways, immune cell functionality, and cell death mechanisms [8, 17, 18]. Therefore, elucidating the specific molecular mechanisms of PANoptosis in gout and identifying novel diagnostic biomarkers targeting the PANoptosis pathway could provide precision medicine strategies for gout patients.

Our study identified *SOCS3* as a central hub gene orchestrating gout-associated inflammatory networks through integrated bioinformatics and machine learning approaches. *SOCS3* (Suppressor of Cytokine Signaling 3) is a critical member of the SOCS protein family and primarily functions to negatively regulate cytokine-mediated signaling pathways, particularly the JAK–STAT pathway [19, 20]. Notably, recent mechanistic studies have demonstrated that *SOCS3* indirectly regulates PANoptosis-associated genes (e.g., *CASP8*, *MLKL*) through suppression of STAT3 phosphorylation, thereby establishing a direct link to PANoptosis pathogenesis [21, 22]. Studies demonstrate that *SOCS3* inhibits PANoptosis through dual mechanisms: directly
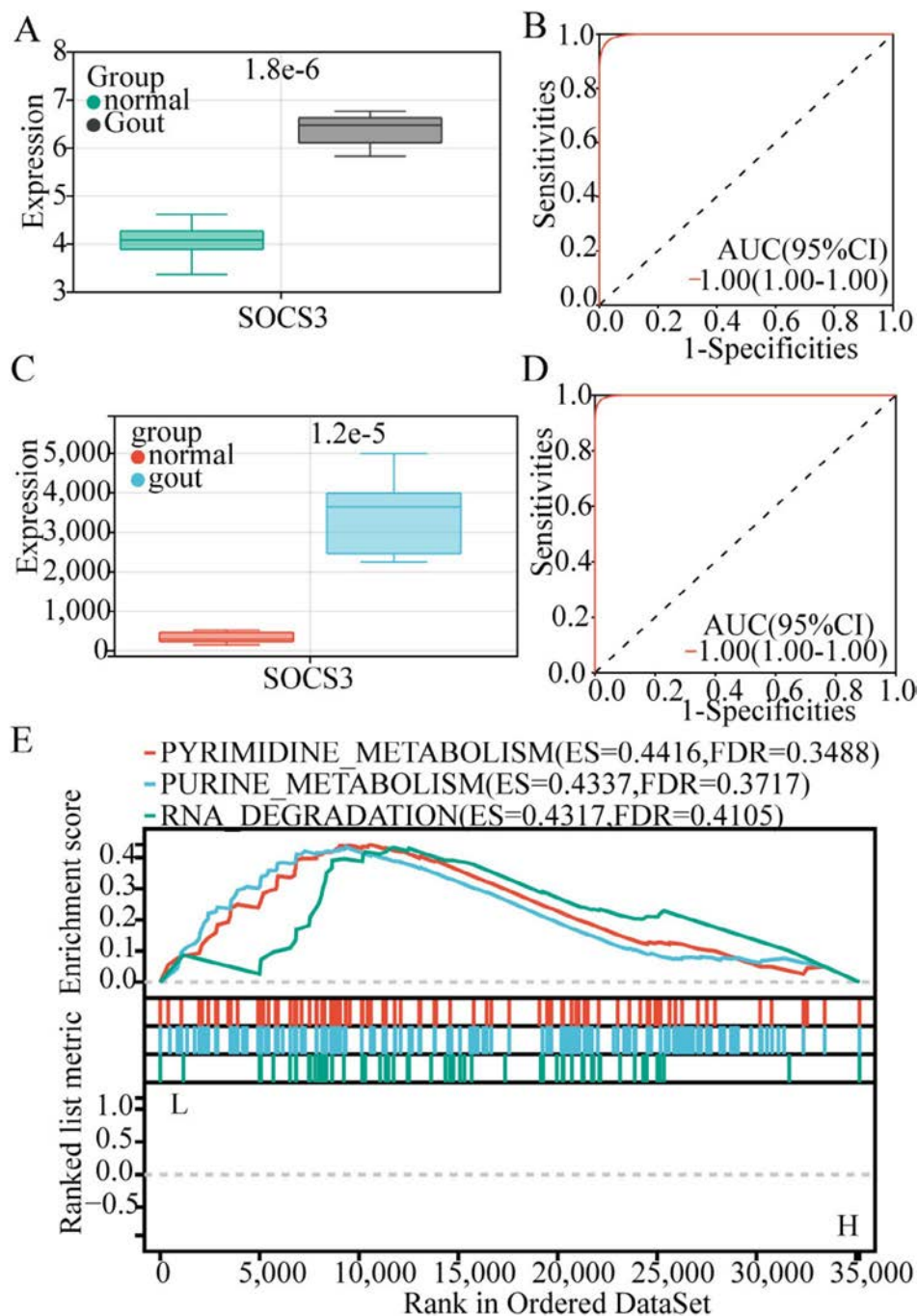
FIGURE 4 | Expression of Key Genes and GSEA Analysis. (A, B) The expression of *SOCS3* and ROC curve validated in the GSE160170. (C, D) The expression of *SOCS3* and ROC curve was validated in the GSE190138. (E) GSEA analysis of *SOCS3*.

attenuating NF-κB pathway activation (via reducing p65 phosphorylation and nuclear translocation) and indirectly modulating signaling mediators such as TLR4 and JAK2/STAT3, thereby downregulating inflammatory cytokines (IL-6, TNF-α) and cell death-associated factors (Caspase-8, RIPK3) [23]. These regulatory roles establish *SOCS3* as a multifunctional hub coordinating inflammatory responses and PANoptosis through crosstalk with core pathways, including JAK–STAT and NF-κB. Recent studies have demonstrated that *SOCS3* exhibits significantly elevated expression in monocytes and inflammatory tissues during the acute phase of gout, showing marked differences compared to individuals with normal serum uric acid (SUA) levels or those with asymptomatic hyperuricemia (AH). Mechanistically,

SOCS3 may regulate the intensity of inflammatory responses by suppressing STAT3 phosphorylation, thereby limiting the signaling transduction of pro-inflammatory cytokines such as IL-6. This molecular regulatory mechanism modulates the amplification of inflammatory cascades and contributes to the pathological progression of gout [19, 24]. Collectively, these findings underscore SOCS3 as a pivotal biomarker influencing PANoptosis-driven inflammatory severity during acute gout episodes.

Based on enrichment analysis findings, our study revealed a significant association between PANoptosis-related genes and immune regulatory networks during the pathogenesis of gout. By

FIGURE 5 | Immune cell infiltration analysis between gout and control. (A) Comparison of the proportions of 28 immune cell types between the gout group and the control group. (B) Association analysis of the 28 immune cell subtypes. Both horizontal and vertical axes demonstrate immune cell subtypes. (C) Correlation analysis between 28 immune cell types and *SOCS3*. *$p < 0.05$, **$p < 0.01$, ***$p < 0.001$.

systematically applying the ssGSEA method to conduct a panoramic characterization of the immune microenvironment in gout patients versus healthy controls, results demonstrated that 12 out of 28 evaluated immune cell subpopulations exhibited significant functional dysregulation. Further correlation analysis identified that the expression level of *SOCS3* showed significant negative correlations with five immune cell subsets, while displaying marked positive correlations with nine immune cell subsets. Notably, this differential association pattern suggests

that *SOCS3* may act as a pivotal regulatory hub in gout-related inflammatory pathology by modulating the functional states of specific immune cell populations. Studies have demonstrated that *SOCS3* enhances allergic responses by promoting the differentiation and activation of T helper 2 cells [25]. Its expression level is positively correlated with the pro-inflammatory activity of mast cells and contributes to the pathogenesis of allergic diseases by regulating mast cell survival/degranulation and eosinophil activation/migration [25]. Current studies demonstrated
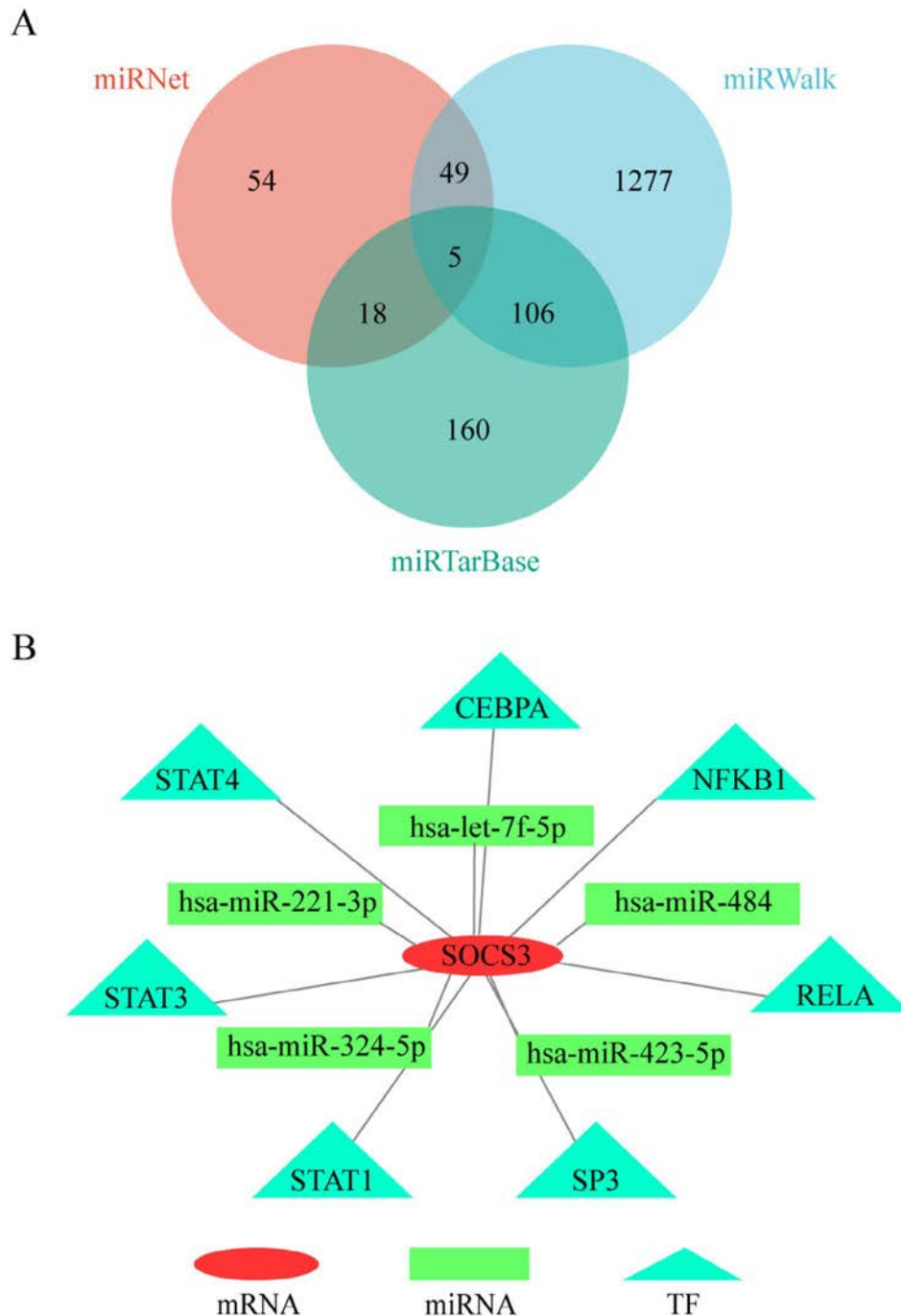
FIGURE 6 | Construction of miRNA-mRNA-TF Network. (A) The overlapping miRNAs of miRWalk, miRNANet, and miRTarbase via Venn diagram. (B) The miRNA–mRNA–TF Network interactions by Cytoscape.

that in inflammatory bowel disease (IBD), *SOCS3* acts on multiple cell types—including epithelial cells, macrophages, dendritic cells, neutrophils, and T cells—to repair mucosal damage and balance immune responses [26]. Studies have revealed that PANoptosis is primarily driven by molecular mechanisms in innate immune cells (e.g., macrophages, neutrophils, and dendritic cells). PANoptosis contributes to autoimmune diseases through chronic inflammation and aberrant immune activation. In conditions like systemic lupus erythematosus (SLE) and rheumatoid arthritis (RA), PANoptosis in innate immune cells (e.g., dendritic cells) may promote the release of self-antigens, disrupt immune tolerance, and exacerbate inflammation via signaling

pathways such as IL-6/JAK-STAT3 [16, 27]. These findings collectively highlight the pleiotropic immunomodulatory functions of *SOCS3* across diverse pathological contexts.

Our study constructed a miRNA–mRNA–TF regulatory network involving seven TFs (*CEBPA, NFKB1, RELA, SP3, STAT1, STAT3, STAT4*), five miRNAs (*hsa-let-7f-5p*, *hsa-miR-221-3p*, *hsa-miR-324-5p*, *hsa-miR-484*, *hsa-miR-423-5p*), and one mRNA (*SOCS3*). The NF-κB signaling pathway plays a central role in gout-associated inflammation. NFKB1 and RELA, key NF-κB family members, directly regulate pro-inflammatory cytokines IL-1β and TNF-α. Monocytes from gout patients exhibit

heightened NF-κB activity, closely linked to urate crystal-triggered inflammatory cascades [28]. The STAT family (STAT1/STAT3/STAT4) mediates cytokine signaling in gout pathogenesis. IL-6 activates STAT3 to promote neutrophil infiltration and joint inflammation, while *SOCS3*, a negative regulator of STAT3, is upregulated during gout flares, potentially mitigating inflammation by suppressing STAT3 signaling [22, 29]. STAT1 and STAT4 may also contribute to immune cell activation in gout pathology [30]. *Hsa-let-7f-5p* is closely associated with inflammatory states in diseases. In macrophages, *hsa-let-7f-5p* alleviates excessive inflammation by specifically downregulating the expression of interferon-induced proteins Gbp2 and Gbp7 [31]. *Hsa-miR-221-3p* exacerbates inflammatory responses by targeting and suppressing SOCS3, a negative regulator of the STAT3 signaling pathway, thereby relieving its inhibitory effect on STAT3 activation. This drives macrophage polarization toward the pro-inflammatory M1 phenotype [32]. *Hsa-miR-423-5p* is implicated in the inflammatory activation mechanisms of salt-sensitive hypertension (SS). It participates in the KCNQ1OT1 long non-coding RNA (lncRNA)-mediated competitive endogenous RNA (ceRNA) network, where KCNQ1OT1 sequesters *hsa-miR-423-5p* to attenuate its repression of downstream target genes. This process ultimately leads to vascular endothelial dysfunction and systemic inflammatory responses [33].

Based on the screening analysis of the DSigDB drug database, Isoeugenol and Rofecoxib were identified as potential small-molecule drugs targeting *SOCS3* for gout treatment. Isoeugenol derivatives, such as ISO-PC, significantly reduced serum uric acid levels by inhibiting xanthine oxidase (XOD) activity to suppress urate production and modulating renal urate transporters (e.g., ABCG2) to enhance uric acid excretion. Animal studies demonstrated that ISO-PC exhibited protective effects against hyperuricemia-induced hepatic and renal injuries [34]. Rofecoxib, a selective COX-2 inhibitor, alleviated acute gout inflammation by blocking prostaglandin E2 (PGE2) synthesis. Notably, COX-2 (PTGS2) and SOCS3 were co-upregulated in gout patients and murine models, suggesting their potential as dual biomarkers for gout [2, 35]. The Coremine Medical database identified five *SOCS3* and Gout-associated traditional Chinese herbs: *Su Tou* (root of *Perilla frutescens*, Lamiaceae), *Bai Su Geng* (stem of *Perilla* species), *Sang Ye* (dried leaf of *Morus alba*, Moraceae), *Sang Zhi* (twig of *Morus alba*), and *Bai Su Zi* (fruit of *Perilla* species). The extract of *Su Tou* inhibits XOD activity to reduce uric acid production, while components from *Perilla* leaves demonstrate hypouricemic effects in hyperuricemic animal models [36]. *Bai Su Geng* contains phenolics, coumarins, terpenoids, and alkaloids that mitigate gout-associated inflammation and oxidative stress by suppressing IL-1β/TNF-α and scavenging free radicals [37, 38]. *Bai Su Zi* is rich in α-linolenic acid (ALA, > 65% in *Perilla* seeds), an ω-3 polyunsaturated fatty acid that alleviates gouty arthritis by modulating lipid metabolism, inhibiting IL-6/TNF-α, and promoting anti-inflammatory mediators like lipoxins [39, 40]. *Perilla* extracts synergize with conventional anti-gout drugs (e.g., allopurinol) to enhance efficacy and reduce adverse effects via multi-target mechanisms [41, 42]. *Sang Ye* aqueous extract lowers uric acid by inhibiting hepatic XOD and upregulating renal ABCG2 expression, while suppressing prostaglandin E2 synthesis to attenuate joint inflammation [43, 44]. *Sang Zhi* bioactive components alleviate gouty arthritis by inhibiting NF-κB signaling to reduce IL-6/

TNF-α release, thereby ameliorating local inflammation and pain [37, 45].

In summary, our integrated bioinformatics analysis, machine learning approach, and clinical validation have identified *SOCS3* as a pivotal diagnostic biomarker for gout, with its regulatory role intricately linked to PANoptosis - related mechanisms. This work not only provides a novel translational framework for developing diagnostic biomarkers and targeted therapeutics in gout but also advances our understanding of shared pathological mechanisms across inflammatory diseases, offering conceptual inspiration for research on common inflammatory pathways. While this study confirmed the biomarker's relevance through clinical samples, limitations include a limited sample size and the lack of stratification by disease stages. Subsequent studies should employ in vitro and in vivo models to elucidate the mechanistic underpinnings of *SOCS3* in gout pathogenesis. Future research may further explore the roles of these molecular pathways in gout progression, offering novel insights and therapeutic targets for the precise diagnosis and treatment of the disease.

Conflicts of Interest

The authors declare no conflicts of interest.

Data Availability Statement

The data that support the findings of this study are available from the corresponding author upon reasonable request.

References

1. N. Dalbeth, A. L. Gosling, A. Gaffo, and A. Abhishek, "Gout," *Lancet* 397, no. 10287 (2021): 1843–1855, https://doi.org/10.1016/S0140-6736(21)00569-9.

2. J. Song, C. Jin, Z. Shan, W. Teng, and J. Li, "Prevalence and Risk Factors of Hyperuricemia and Gout: A Cross-Sectional Survey From 31 Provinces in Mainland China," *Journal of Translational Internal Medicine* 10, no. 2 (2022): 134–145, https://doi.org/10.2478/jtim-2022-0031.

3. H. Tao, Y. Mo, W. Liu, et al., "A Review on Gout: Looking Back and Looking Ahead," *International Immunopharmacology* 117 (2023): 109977, https://doi.org/10.1016/j.intimp.2023.109977.

4. J. Chen, M. Wu, J. Yang, et al., "The Immunological Basis in the Pathogenesis of Gout," *Iranian Journal of Immunology* 14, no. 2 (2017): 90–98.

5. F. A. Amaral, L. F. Bastos, T. H. Oliveira, et al., "Transmembrane TNF-Alpha Is Sufficient for Articular Inflammation and Hypernociception in a Mouse Model of Gout," *European Journal of Immunology* 46, no. 1 (2016): 204–211, https://doi.org/10.1002/eji.201545798.

6. V. Kluck, R. Liu, and L. A. B. Joosten, "The Role of Interleukin-1 Family Members in Hyperuricemia and Gout," *Joint, Bone, Spine* 88, no. 2 (2021): 105092, https://doi.org/10.1016/j.jbspin.2020.105092.

7. X. Sun, Y. Yang, X. Meng, J. Li, X. Liu, and H. Liu, "PANoptosis: Mechanisms, Biology, and Role in Disease," *Immunological Reviews* 321, no. 1 (2024): 246–262, https://doi.org/10.1111/imr.13279.

8. J. Zhao, K. Wei, P. Jiang, et al., "Inflammatory Response to Regulated Cell Death in Gout and Its Functional Implications," *Frontiers in Immunology* 13 (2022): 888306, https://doi.org/10.3389/fimmu.2022.888306.

9. J. Chu, J. Tian, P. Li, et al., "The Impact of AIM2 Inflammasome-Induced Pyroptosis on Acute Gouty Arthritis and Asymptomatic Hyperuricemia Patients," *Frontiers in Immunology* 15 (2024): 1386939, https://doi.org/10.3389/fimmu.2024.1386939.

10. A. Pandeya and T. D. Kanneganti, "Therapeutic Potential of PANoptosis: Innate Sensors, Inflammasomes, and RIPKs in PANoptosomes," *Trends in Molecular Medicine* 30, no. 1 (2024): 74–88, https://doi.org/10.1016/j.molmed.2023.10.001.

11. Z. Lan, Y. Yang, R. Sun, et al., "Characterization of PANoptosis-Related Genes With Immunoregulatory Features in Osteoarthritis," *International Immunopharmacology* 140 (2024): 112889, https://doi.org/10.1016/j.intimp.2024.112889.

12. M. P. Leask, T. O. Crisan, J. I. A, et al., "The Pathogenesis of Gout: Molecular Insights From Genetic, Epigenomic and Transcriptomic Studies," *Nature Reviews Rheumatology* 20, no. 8 (2024): 510–523, https://doi.org/10.1038/s41584-024-01137-1.

13. H. Jum'ah, M. Shribak, A. Keikhosravi, et al., "Detection of Crystals in Joint Fluid Aspirates With Polychromatic Polarisation Microscopy," *Annals of the Rheumatic Diseases* 82, no. 11 (2023): 1501–1502, https://doi.org/10.1136/ard-2023-224331.

14. M. Yan, M. Du, T. Yu, et al., "Concordance of Ultrasound and Dual-Energy CT in Diagnosing Gouty Arthritis in the Knee Joint: A Retrospective Observational Study," *Academic Radiology* 32, no. 1 (2025): 316–325, https://doi.org/10.1016/j.acra.2024.08.041.

15. N. Mbuyi and C. Hood, "An Update on Gout Diagnosis and Management for the Primary Care Provider," *Nurse Practitioner* 45, no. 10 (2020): 16–25, https://doi.org/10.1097/01.NPR.0000696896.83494.fe.

16. K. Liu, M. Wang, D. Li, et al., "PANoptosis in Autoimmune Diseases Interplay Between Apoptosis, Necrosis, and Pyroptosis," *Frontiers in Immunology* 15 (2024): 1502855, https://doi.org/10.3389/fimmu.2024.1502855.

17. N. Xiao, Z. Xie, Z. He, et al., "Pathogenesis of Gout: Exploring More Therapeutic Target," *International Journal of Rheumatic Diseases* 27, no. 4 (2024): e15147, https://doi.org/10.1111/1756-185X.15147.

18. H. Gu, H. Yu, L. Qin, et al., "MSU Crystal Deposition Contributes to Inflammation and Immune Responses in Gout Remission," *Cell Reports* 42, no. 10 (2023): 113139, https://doi.org/10.1016/j.celrep.2023.113139.

19. M. Badii, V. Kluck, O. Gaal, et al., "Regulation of SOCS3-STAT3 in Urate-Induced Cytokine Production in Human Myeloid Cells," *Joint, Bone, Spine* 91, no. 3 (2024): 105698, https://doi.org/10.1016/j.jbspin.2024.105698.

20. M. Morelli, S. Madonna, and C. Albanesi, "SOCS1 and SOCS3 as Key Checkpoint Molecules in the Immune Responses Associated to Skin Inflammation and Malignant Transformation," *Frontiers in Immunology* 15 (2024): 1393799, https://doi.org/10.3389/fimmu.2024.1393799.

21. Y. Liu, Y. Chang, X. Jiang, et al., "Analysis of the Role of PANoptosis in Seizures via Integrated Bioinformatics Analysis and Experimental Validation," *Heliyon* 10, no. 4 (2024): e26219, https://doi.org/10.1016/j.heliyon.2024.e26219.

22. L. Zhuang, Q. Sun, S. Huang, et al., "A Comprehensive Analysis of PANoptosome to Prognosis and Immunotherapy Response in Pan-Cancer [J]," *Scientific Reports* 13, no. 1 (2023): 3877, https://doi.org/10.1038/s41598-023-30934-z.

23. D. Zhao, L. Wu, X. Fang, et al., "Copper Exposure Induces Inflammation and PANoptosis Through the TLR4/NF-κB Signaling Pathway, Leading to Testicular Damage and Impaired Spermatogenesis in Wilson Disease," *Chemico-Biological Interactions* 396 (2024): 111060, https://doi.org/10.1016/j.cbi.2024.111060.

24. J. Peng, Y. Gu, J. Liu, et al., "Identification of SOCS3 and PTGS2 as New Biomarkers for the Diagnosis of Gout by Cross-Species Comprehensive Analysis," *Heliyon* 10, no. 9 (2024): e30020, https://doi.org/10.1016/j.heliyon.2024.e30020.

25. A. Jafarzadeh, P. Chauhan, M. Nemati, S. Jafarzadeh, and A. Yoshimura, "Aberrant Expression of Suppressor of Cytokine Signaling (SOCS) Molecules Contributes to the Development of Allergic Diseases," *Clinical and Experimental Allergy* 53, no. 11 (2023): 1147–1161, https://doi.org/10.1111/cea.14385.

26. P. Zhang, B. Pei, C. Yi, F. A. Akanyibah, and F. Mao, "The Role of Suppressor of Cytokine Signaling 3 in Inflammatory Bowel Disease and Its Associated Colorectal Cancer," *Biochimica et Biophysica Acta, Molecular Basis of Disease* 1871, no. 2 (2025): 167578, https://doi.org/10.1016/j.bbadis.2024.167578.

27. B. R. Sharma, S. M. Choudhury, H. M. Abdelaal, et al., "Innate Immune Sensor NLRP3 Drives PANoptosome Formation and PANoptosis," *Journal of Immunology*, Published online April 18 2025 : 1236–1246, https://doi.org/10.1093/jimmun/vkaf042.

28. F. Li, J. H. Yao, L. Li, Q. Nie, J. J. Cao, and X. R. Ning, "MiRNA-23a-5p Is the Biomarkers for Gouty Arthritis and Promotes Inflammation in Rats of Gouty Arthritis via MyD88/NF-κB Pathway by Induction TLR2," *Archives of Rheumatology* 37, no. 4 (2022): 536–546, https://doi.org/10.46497/ArchRheumatol.2022.9236.

29. Z. Zhang, P. Wang, T. Lei, et al., "The Role and Impact of the IL-6 Mediated JAK2-STAT1/3 Signaling Pathway in the Pathogenesis of Gout," *Frontiers in Pharmacology* 16 (2025): 1480844, https://doi.org/10.3389/fphar.2025.1480844.

30. J. Ji, S. Wu, X. Bao, et al., "Mediating Oxidative Stress Through the Palbociclib/miR-141-3p/STAT4 Axis in Osteoporosis: A Bioinformatics and Experimental Validation Study," *Scientific Reports* 13, no. 1 (2023): 19560, https://doi.org/10.1038/s41598-023-46813-6.

31. Y. J. Liu, H. B. Miao, S. Lin, et al., "Exosomes Derived Let-7f-5p Is a Potential Biomarker of SLE With Anti-Inflammatory Function," *Noncoding RNA Research* 12 (2025): 116–131, https://doi.org/10.1016/j.ncrna.2025.02.004.

32. H. Jia, W. He, B. Wu, et al., "Cigarette Smoke-Induced Exosomal miR-221-3p Facilitates M1 Macrophage Polarization via the STAT3 Pathway in Chronic Obstructive Pulmonary Disease," *Aging (Albany NY)* 16, no. 17 (2024): 12379–12391, https://doi.org/10.18632/aging.206095.

33. W. Peng, Y. Xie, J. Xia, et al., "Integrated Analysis of the lncRNA-Associated Competing Endogenous RNA Network in Salt Sensitivity of Blood Pressure," *Heliyon* 9, no. 12 (2023): e22466, https://doi.org/10.1016/j.heliyon.2023.e22466.

34. F. Zou, H. Zhao, A. Ma, D. Song, X. Zhang, and X. Zhao, "Preparation of an Isorhamnetin Phospholipid Complex for Improving Solubility and Anti-Hyperuricemia Activity," *Pharmaceutical Development and Technology* 27, no. 7 (2022): 842–852, https://doi.org/10.1080/10837450.2022.2123510.

35. A. Bech-Drewes, K. Bonnesen, E. M. Hauge, and M. Schmidt, "Cardiovascular Safety of Using Non-Steroidal Anti-Inflammatory Drugs for Gout: A Danish Nationwide Case-Crossover Study," *Rheumatology International* 44, no. 6 (2024): 1061–1069, https://doi.org/10.1007/s00296-024-05584-7.

36. C. Wu, A. R. Wong, Q. Chen, et al., "Identification of Inhibitors From a Functional Food-Based Plant Perillae Folium Against Hyperuricemia via Metabolomics Profiling, Network Pharmacology and All-Atom Molecular Dynamics Simulations," *Frontiers in*

Endocrinology 15 (2024): 1320092, https://doi.org/10.3389/fendo.2024.1320092.

37. M. H. Frazaei, R. Nouri, R. Arefnezhad, P. M. Pour, M. Naseri, and S. Assar, "A Review of Medicinal Plants and Phytochemicals for the Management of Gout," *Current Rheumatology Reviews* 20, no. 3 (2024): 223–240, https://doi.org/10.2174/0115733971268503723092072503.

38. W. Cao, T. Wu, F. Liang, et al., "Protective Effects of Di-Caffeoylquinic Acids From *Artemisia Selengensis* Turcz Leaves Against Monosodium Urate-Induced Inflammation via the Modulation of NLRP3 Inflammasome and Nrf2 Signaling Pathway in THP-1 Macrophages," *Journal of Food Biochemistry* 46, no. 9 (2022): e14252, https://doi.org/10.1111/jfbc.14252.

39. X. Zou, K. Zhang, D. Wu, et al., "Integrated Analysis of miRNA, Transcriptome, and Degradome Sequencing Provides New Insights Into Lipid Metabolism in Perilla Seed," *Gene* 895 (2024): 147953, https://doi.org/10.1016/j.gene.2023.147953.

40. D. Wu, K. Zhang, C. Y. Li, et al., "Genome-Wide Comprehensive Characterization and Transcriptomic Analysis of AP2/ERF Gene Family Revealed Its Role in Seed Oil and ALA Formation in Perilla (*Perilla Frutescens*)," *Gene* 889 (2023): 147808, https://doi.org/10.1016/j.gene.2023.147808.

41. M. F. Mahomoodally, K. Coodian, M. Hosenally, et al., "Herbal Remedies in the Management of Hyperuricemia and Gout: A Review of In Vitro, In Vivo and Clinical Evidences," *Phytotherapy Research* 38, no. 7 (2024): 3370–3400, https://doi.org/10.1002/ptr.8211.

42. T. Bencsik, O. Balazs, R. G. Vida, et al., "Effects of Catechins, Resveratrol, Silymarin Components and Some of Their Conjugates on Xanthine Oxidase-Catalyzed Xanthine and 6-Mercaptopurine Oxidation," *Journal of the Science of Food and Agriculture* 105, no. 5 (2025): 2765–2776, https://doi.org/10.1002/jsfa.14045.

43. B. Fang, L. Lu, M. Zhao, et al., "Mulberry (Fructus Mori) Extract Alleviates Hyperuricemia by Regulating Urate Transporters and Modulating the Gut Microbiota," *Food & Function* 15, no. 24 (2024): 12169–12179, https://doi.org/10.1039/d4fo03481c.

44. Y. Du, Y. L. Chen, Y. Zhang, et al., "Bio-Affinity Ultrafiltration Combined With UPLC Q-Exactive Plus Orbitrap HRMS to Screen Potential COX-2 and 5-LOX Inhibitors in Mulberry (*Morus Alba* L.) Leaf," *Journal of Ethnopharmacology* 341 (2025): 119325, https://doi.org/10.1016/j.jep.2025.119325.

45. H. J. Kwak, J. Kim, S. Y. Kim, et al., "Moracin E and M Isolated From *Morus alba* Linne Induced the Skeletal Muscle Cell Proliferation via PI3K-Akt-mTOR Signaling Pathway," *Scientific Reports* 13, no. 1 (2023): 20570, https://doi.org/10.1038/s41598-023-47411-2.

Supporting Information

Additional supporting information can be found online in the Supporting Information section.

ORIGINAL ARTICLE

Exploring the Factors Associated With the Discontinuation of Tofacitinib in Patients With Rheumatoid Arthritis: A Retrospective Cohort Study

Li-Huei Chiang[1] [iD] | Chia-Ling Yu[1] | Tzu-Cheng Tsai[1,2] | Yao-Fan Fang[3] [iD]

[1]Department of Pharmacy, Chang Gung Memorial Hospital, Linkou, Taoyuan, Taiwan | [2]Department of Long Term Care, Hsin Sheng Junior College of Medical Care and Management, Taoyuan, Taiwan | [3]Division of Rheumatology, Allergy and Immunology, Department of Internal Medicine, Chang Gung Memorial Hospital, Linkou, Taoyuan, Taiwan

Correspondence: Yao-Fan Fang (fang8802012@gmail.com)

ABSTRACT

Objectives: Tofacitinib is the first oral targeted synthetic disease-modify anti-rheumatic drug for patients with moderate to severe rheumatoid arthritis. This study aimed to identify the factors associated with the discontinuation of tofacitinib in patients with RA in clinical practice.

Methods: RA patients who received tofacitinib between 2015 and 2020 were included in this observational cohort study. The patients were followed for at least 1 year, ending on December 31, 2022. A tofacitinib non-responder was defined as a patient who required discontinuation or switch to another bDMARD. Conversely, tofacitinib responders were defined as those who could continue to receive tofacitinib without experiencing a loss of efficacy or severe adverse events. Univariate and multivariate Cox regression analyses and Kaplan–Meier survival curve analysis were used to investigate the factors associated with the discontinuation of tofacitinib.

Results: A total of 266 patients were enrolled. The average age of the patients was 57.07 ± 12.07 years, and 99 (37.2%) were tofacitinib non-responders. Univariate analysis revealed that the non-responders had a lower rate of concomitant hydroxychloroquine treatment and higher rates of leflunomide, biological disease-modifying antirheumatic drug (bDMARD), and tumor necrosis factor inhibitor (TNFi) treatment compared to the responders. Cox regression adjusted analysis indicated that prior bDMARD treatment (hazard ratio (HR) = 1.423, 95% confidence interval (CI) = 1.024, 1.976, $p = 0.036$), prior TNFi treatment (HR = 1.605, 95% CI = 1.165, 2.212, $p = 0.004$), and prior non-TNFi treatment (HR = 1.326, 95% CI = 1.012, 2.075, $p = 0.048$) were associated with a higher non-response rate. Moreover, Kaplan–Meier survival curve analysis revealed that the patients with prior bDMARD treatment had a higher non-response rate.

Conclusions: The RA patients who received tofacitinib in this study had a good response rate, and the average non-response rate was around 37% after 2 years of treatment. The main factor associated with an inadequate response to tofacitinib was prior bDMARD treatment. Prior TNFi treatment was the strongest factor associated with a non-response to tofacitinib. Patients with a non-response to tofacitinib may consider bDMARDs with other mechanisms if previous treatment with TNFis was unsuccessful.

Summary

- Tofacitinib effectively treats RA, yet about 25% of patients remain unresponsive after 2 years.
- Prior bDMARD use—especially TNFi exposure—is linked to poor tofacitinib response.
- RA patients failing tofacitinib with a TNFi history might benefit from switching to a bDMARD with a new mechanism.

1 | Introduction

RA is a chronic autoimmune disease characterized by inflammation and joint damage which may negatively affect health, reduce the quality of life, and diminish joint function [1, 2]. According to the American College of Rheumatology (ACR) and European Alliance of Associations for Rheumatology (EULAR), the "treat-to-target" strategy represents a fundamental paradigm in RA management, aiming to optimize outcomes through regular disease activity assessment and treatment adjustment [3, 4]. Factors associated with remission include comorbidities and other patient factors, the type of medication, course of treatment, and adherence to treat to target strategies [5–7].

Tofacitinib is the first oral Janus kinase (JAK) inhibitor [8], and it is prescribed for patients with rheumatoid arthritis (RA), psoriatic arthritis, ulcerative colitis, and polyarticular course juvenile idiopathic arthritis [9]. JAK inhibitors are small-molecule drugs that interfere with the activation of JAKs, a family of enzymes related to leukocyte cell signaling. JAK signaling has been confirmed to play a key role in immune cell activation, proliferation, and function [10–13]. Compared to JAK1 and JAK3, JAK2 is less significantly inhibited by tofacitinib [14].

The cornerstone of RA treatment has long been methotrexate (MTX) and other conventional synthetic disease-modifying antirheumatic drugs (csDMARDs) [3, 4, 15]. Over the past few decades, biological disease-modifying antirheumatic drugs (bDMARDs) have greatly improved the clinical outcomes of RA patients. However, even though biologics have revolutionized RA treatment, individuals may still experience adverse effects, or the treatment may lose efficacy over time [16–18]. A 12-year observational study found that nearly one-fifth of RA patients had unmet treatment demands with csDMARDs or bDMARDs, highlighting the need for alternative therapy [19].

A prior systematic review and meta-analysis study found that patients with RA treated with etanercept had better drug survival than those treated with two other tumor necrosis factor inhibitors (TNFis). In addition, the study found that the duration of disease prior to biologic treatment, concurrent DMARD use, and female sex were predictors of the time to cessation [20]. Another study comparing tofacitinib to bDMARD in the treatment of RA found that tofacitinib was associated with a longer persistence in switchers and shorter persistence in new users [21]. This study aimed to identify factors associated with the discontinuation of tofacitinib in RA patients based on real-world data.

2 | Methods

2.1 | Study Design and Setting

In this retrospective study, we reviewed the medical records of patients in our hospital's information system, and enrolled those over 18 years of age who used tofacitinib from January 1, 2015 to December 31, 2020 and were followed up for at least 1 year to December 31, 2021. The regimens used at our hospital were tofacitinib tablets 5 mg bid or tofacitinib extended-release tablets 11 mg qd. Patients with indications other than RA, incomplete data, loss of follow-up for unknown reasons, side effects, death, and those who changed drug treatment due to pregnancy were excluded. The decision to discontinue tofacitinib and all other related treatments was at the discretion of the treating rheumatologists. This study was also approved by the Institutional Review Board of Chang Gung Medical Foundation (IRB No. 202201902B0).

2.2 | Assessments

The patient's basic information, including age, sex, comorbidities (hypertension, diabetes, hyperlipidemia, and osteoporosis), RA disease course during initial tofacitinib treatment, and the duration of tofacitinib use until December 31, 2021, were recorded. The Disease Activity Score (DAS) and its popular variant, the DAS28, were used to evaluate disease activity. The modified DAS28 examines 28 joints and includes the ESR level, making it a more focused and frequently used clinical marker of disease activity. The primary objective of RA treatment is to attain and sustain remission, which is defined as a DAS28 score of < 2.6. If the primary objective is not feasible, then the aim is to achieve low disease activity, defined as a DAS28 score between 2.6 and 3.2. We also recorded the use of bDMARDs before tofacitinib, and the concomitant use of csDMARDs and corticosteroids. Laboratory data, including C-reactive protein, erythrocyte sedimentation rate, rheumatoid factor immunoglobulin M or immunoglobulin G, and anti-cyclic citrullinated peptide antibody, were also recorded. The baseline disease severity and medication adherence in patients with rheumatoid arthritis (RA) were well-managed. This is because patients were required to undergo at least 6 months of treatment with conventional synthetic disease-modifying antirheumatic drugs (csDMARDs) before becoming eligible for biological DMARDs (bDMARDs). Additionally, prior to prescribing bDMARDs to RA patients, approval from the national health insurance institute was mandatory.

A tofacitinib non-responder was defined as a patient who required discontinuation or switch to another bDMARD by a rheumatologist. Non-response was attributed to loss of efficacy, defined as an increase in DAS28 score of more than 1.2 from baseline, or due to severe complications, infections, or medication intolerance during the treatment period. The definition of non-response (DAS28 increase ≥ 1.2 from baseline) aligns with the National Institute for Health and Care Excellence (NICE) guidelines in the United Kingdom, which are adopted as part of Taiwan's reimbursement criteria for biologic DMARDs [22]. Specifically, NICE recommends this threshold to identify inadequate treatment response in RA patients, ensuring consistency with our real-world clinical practice [23]. Conversely, tofacitinib

responders were defined as those who could continue to receive tofacitinib without experiencing a loss of efficacy or severe adverse events.

The pre-defined primary endpoint was discontinuation of tofacitinib due to ineffectiveness. We further classified the prior use of bDMARDs into treatment with tumor necrosis factor inhibitors (TNFis) and non-TNF inhibitors (non-TNFis).

2.3 | Statistical Analysis

Statistical analysis was performed with SAS Enterprise Guide 7.1 (SAS Inc., Cary, NC), Stata 12 (StataCorp, College Station, TX), and Microsoft Excel 2013 (Microsoft Corp., Redmond, WA). Continuous variables are expressed as mean and standard deviation. In univariate analysis, the Student's t-test was used for continuous variables, and the chi-squared test for categorical variables to compare differences between the two groups. A two-tailed p value < 0.05 was considered statistically significant.

Prior to performing Cox regression analyses, we rigorously evaluated the underlying statistical assumptions to ensure the validity of our findings. The proportional hazards assumption, a critical requirement for Cox models, was tested using Schoenfeld residuals and log–log plots. Global tests of residuals across all covariates yielded non-significant p values ($p > 0.05$), confirming that hazard ratios remained constant over time and no time-dependent biases were present. For continuous variables, linearity with respect to the log hazard was assessed graphically using Martingale residual plots, which revealed no systematic deviations from linear trends. To address potential multicollinearity among predictor variables, we calculated variance inflation factors (VIFs) for all covariates included in the multivariate model. All VIF values were below 2.0, well under the conventional threshold of 5–10, indicating negligible correlation between explanatory variables and supporting the stability of regression estimates. For Kaplan–Meier survival analyses, we verified the non-informative censoring assumption by reviewing clinical records to confirm that discontinuation events (e.g., loss to follow-up) were unrelated to study outcomes. Additionally, the log-rank test, used to compare survival curves between groups, assumes independent observations—a condition met by our study design, which excluded patients with overlapping treatments or competing risks. Sensitivity analyses, including stratified Cox models by prior bDMARD exposure, further reinforced the robustness of our results. These comprehensive checks ensure the reliability of our hazard ratio estimates and survival analyses. Subgroups for Kaplan–Meier analysis (TNFi-exposed, non-TNFi-exposed, and bDMARD-naïve patients) were pre-specified based on prior evidence linking biologic exposure to differential JAK inhibitor responses. Log-rank tests compared survival curves between these subgroups.

3 | Results

A total of 266 patients participated in the study, with an average age of 57.07 ± 12.07 years. We included patients who had recently begun using Tofacitinib between 2015/1/1 and 2020/12/31. The start time of use was used as the baseline, and patients were monitored until 2021/12/31. The median follow-up period for tofacitinib is 4.77 years, and the median survival time is 2.64 years. Among these patients, 99 (37.2%) were identified as non-responders to tofacitinib treatment. The missing data were addressed (1) Patients received tofacitinib for indications other than rheumatoid arthritis ($n = 95$), such as dermatitis ($n = 31$), severe cutaneous adverse response ($n = 7$), ulcerative colitis ($n = 1$), alopecia ($n = 29$), or psoriasis ($n = 27$). (2) The medical records contain test results that are either missing or unclear. (3) Patients did not come to our facility for treatment for unknown reasons. (4) Doctors stopped administering tofacitinib because of side effects or patient intolerance. (5) The doctor suggested certolizumab pegol rather than tofacitinib for the patients who planned to get pregnant (Figure 1). The results of univariate analysis revealed that a higher percentage of the non-responders had received prior treatment with leflunomide or bDMARDs (especially TNFis) (Table 1).

To further investigate the factors associated with a non-response to tofacitinib, we conducted multivariate analysis using Cox regression, adjusting for potential confounders. The potential confounders included sex, age, and RA disease duration. Moreover, previously used leflunomide was also considered a confounder due to the difference in Table 1. The patients who had previously received bDMARDs had a hazard ratio (HR) of 1.423, with a 95% confidence interval (CI) ranging from 1.024 to 1.976 ($p < 0.05$) (Table 2).

In addition to the use of bDMARDs, prior TNFis treatment was also found to significantly increase the risk of a non-response to tofacitinib. The HR for non-response in the patients with a history of TNFis treatment was 1.605 (95% CI 1.165–2.212, $p < 0.05$). Furthermore, the analysis indicated that the patients with a history of prior non-TNFi biologic treatment were also at an increased risk of being a non-responder, with an HR of 1.326 (95% CI 1.012–2.075, $p < 0.05$) (Table 2).

Kaplan–Meier survival curve analysis, which is typically used to assess the time to an event such as treatment response, supported the results of the Cox regression analysis. As pre-specified, Kaplan–Meier analysis stratified patients by prior bDMARD exposure (TNFi, non-TNFi, or naïve) to assess non-response risk. The log-rank test comparing survival curves between bDMARD-naïve and bDMARD-experienced groups revealed that patients with prior bDMARD treatment had significantly higher non-response rates compared to those without prior biologic therapy ($p = 0.006$; Figure 2A). Further subgroup analysis comparing TNFi-exposed patients to bDMARD-naïve patients showed significantly higher non-response rates in the TNFi-exposed group ($p = 0.0001$; Figure 2B). In contrast, comparison between non-TNFi-exposed and bDMARD-naïve groups revealed no significant difference in non-response rates ($p = 0.867$; Figure 2B). These results suggest that prior TNFi exposure, but not necessarily non-TNFi bDMARD exposure, may significantly influence the likelihood of treatment response to tofacitinib (Figure 2).

4 | Discussion

This study investigated the factors associated with a non-response to tofacitinib, a JAK inhibitor used in the treatment
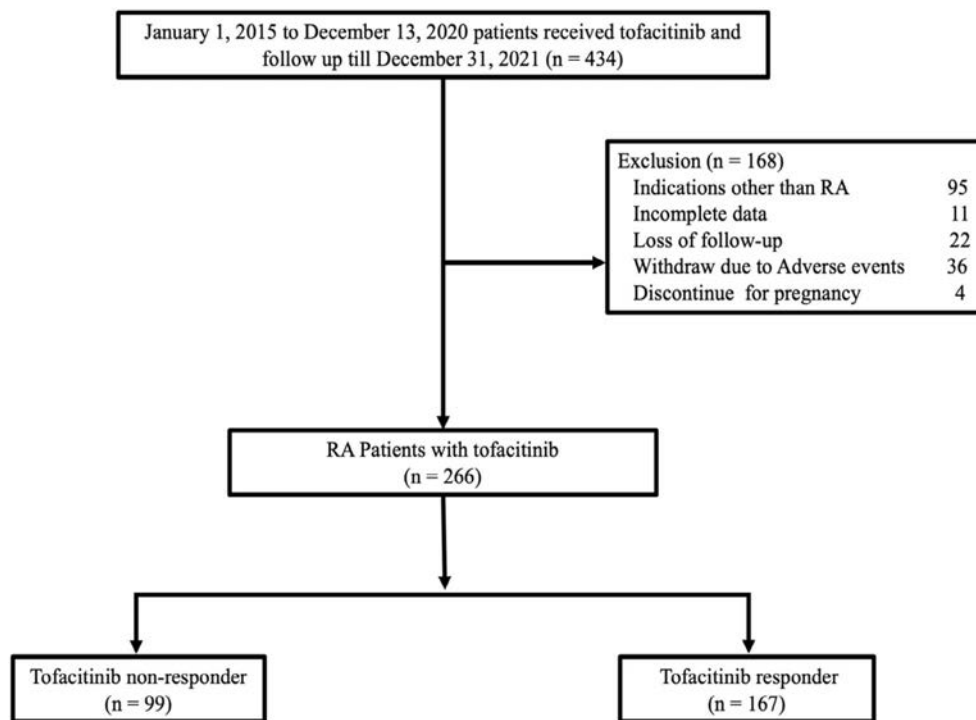
FIGURE 1 | Flowchart for identifying rheumatoid arthritis patients with Tofacitinib in Chang Gung memorial hospital. RA, rheumatoid arthritis.

of various autoimmune conditions including RA. Compared to other bDMARD therapies, tofacitinib has only recently become available. A number of factors have been reported to influence bDMARD drug retention rates, some of which seem to be specific to a particular drug or class of drug [24, 25]. A Canadian study reported that older age (≥ 56 vs. ≤ 45 years), bDMARD naivety (compared with prior bDMARD exposure), and longer time from the diagnosis (15–19 vs. < 5 years) were significantly associated with increased retention to tofacitinib [26]. Our findings revealed a significant association between prior bDMARD exposure, particularly TNFis, and reduced tofacitinib effectiveness. These results have important implications for clinical practice, suggesting that prior biologic therapy should be carefully considered when initiating tofacitinib treatment.

In this study, 37.2% of the patients were non-responders to tofacitinib. Univariate analysis highlighted differences between the responders and non-responders, and notably a lower rate of concomitant hydroxychloroquine treatment in the non-responders. While the role of hydroxychloroquine in conjunction with tofacitinib warrants further investigation, this observation could suggest a potential synergistic effect or reflect differences in disease severity or treatment strategies between the groups. Patients on tofacitinib or bDMARDs may also be taking another csDMARD. Nevertheless, most of these combinations would involve medications such as hydroxychloroquine, which by itself does not usually increase the risk of infection [27]. However, the most striking finding of the univariate analysis was the higher prevalence of prior leflunomide and bDMARD (especially TNFis) treatment among the non-responders. This preliminary observation strongly suggests that prior exposure to immunosuppressive therapies, particularly biologics, could influence the efficacy of tofacitinib.

To rigorously assess the impact of prior therapies on the response to tofacitinib, we performed multivariate analysis using Cox regression, adjusting for potential confounding factors. The results confirmed a strong association between prior bDMARD use and an increased risk of tofacitinib non-response, and showed that the patients with prior bDMARD exposure were nearly twice as likely to be non-responders. This finding is important, as it provides strong evidence that prior biologic therapy can significantly diminish the effectiveness of tofacitinib.

In further analysis of the impact of specific bDMARD classes, our results revealed that prior TNFi treatment also significantly increased the risk of tofacitinib non-response.

Importantly, our analysis also demonstrated that prior exposure to non-TNFi biologics was associated with an increased risk of tofacitinib non-response. Although the confidence interval was wider for this association, likely due to the smaller number of patients receiving non-TNFi biologics, this finding strengthens the overall conclusion that prior biologic exposure, regardless of the specific class, can negatively influence the efficacy of tofacitinib. This suggests a broader phenomenon of reduced responsiveness to subsequent targeted therapies after prior biologic failure.

The Kaplan–Meier survival curve analysis further corroborated these findings, and the curves clearly demonstrated a significantly higher non-responder rate among the patients with prior bDMARD exposure compared to those without. This reinforces the conclusions of the Cox regression analysis, and highlights the substantial impact of prior biologic therapy on the response to tofacitinib.

Several potential mechanisms could explain the observed association between prior biologic exposure and reduced tofacitinib

TABLE 1 | Baseline characteristics of comparing RA patients with Tofacitinib non-responder and responder.

	All	Non-responder	Responder	
	$N = 266$	$N = 99$	$N = 167$	p
Age (years), mean (SD)	57.07 (12.07)	57.28 (12.57)	56.94 (11.80)	0.8234
Female, n (%)	221 (83.08)	86 (86.87)	135 (80.84)	0.205
Disease duration (years), mean (SD)	7.46 (5.36)	7.94 (5.28)	7.17 (5.41)	0.258
Treatment duration (years), mean (SD)	2.81 (1.66)	1.67 (1.21)	3.48 (1.52)	
Comorbidities, n (%)				
Hypertension	83 (31.20)	33 (33.33)	50 (29.94)	0.564
Diabetes mellitus	24 (9.02)	10 (10.10)	14 (8.38)	0.636
Hyperlipidemia	51 (19.17)	19 (19.19)	32 (19.16)	0.995
Osteoporosis	31 (11.65)	8 (8.08)	23 (13.77)	0.162
Concomitant cDMARDs, n (%)	266 (100)	99 (100)	167 (100.0)	
Methotrexate	247 (92.86)	91 (91.92)	156 (93.41)	0.647
Hydroxychroloquine	201 (75.56)	67 (67.68)	134 (80.24)	0.021*
Sulfasalazine	181 (68.05)	71 (71.72)	110 (65.87)	0.323
Leflunomide	89 (33.46)	43 (43.43)	46 (27.54)	0.008*
Others[a]	40 (15.04)	18 (18.18)	22 (13.17)	0.707
Concomitant corticosteroids	209 (78.57)	79 (79.80)	130 (77.84)	0.3503
Prior bDMARDs, n (%)	155 (58.27)	72 (72.73)	83 (49.70)	0.0001*
TNFis	95 (35.71)	46 (46.46)	49 (29.34)	0.005*
Non-TNFis	49 (18.42)	22 (22.22)	27 (16.17)	0.218
DAS28 (ESR), mean (SD)	5.63 (1.08)	5.63 (1.18)	5.63 (1.01)	0.977
ESR (mm/h), mean (SD)	33.72 (26.49)	37.17 (29.60)	31.69 (24.34)	0.104
RF positivity, n (%)	206 (77.44)	72 (72.73)	134 (80.24)	0.156
Anti-CCP positivity, n (%)	120 (45.11)	41 (41.41)	79 (47.31)	0.351

Abbreviations: anti-CCP, anti-cyclic citrullinated peptide antibodies; bDMARDs, biological DMARDs; cDMARDs, conventional DMARDs; DAS28, 28 joint count disease activity score; DMARDs, disease modifying drugs; n, number of subjects; RA, rheumatoid arthritis; RF, rheumatoid factor; SD, standard deviation; TNFis, tumor necrosis factor inhibitors.

[a]Azathioprin, cyclosporine and penicillamine.

*$p < 0.05$.

effectiveness. One possibility is the development of altered immune responses or resistance mechanisms following exposure to previous bDMARDs. Prior treatment with TNFis, for example, may lead to changes in downstream signaling pathways or the upregulation of alternative inflammatory pathways, rendering subsequent JAK inhibition less effective [28–30]. Another potential explanation is a more refractory disease phenotype in patients who have failed prior bDMARD therapies. Such patients may have a more aggressive or complex disease course that is inherently less responsive to subsequent treatments, including JAK inhibitors. It is also possible that the duration of prior bDMARD therapy, the number of prior bDMARDs used, or the reason for discontinuation of the prior bDMARD (e.g., primary or secondary failure) could influence the response to tofacitinib [31–34].

These findings have important clinical implications. The study suggests that a history of biologic therapy, particularly TNFis

and other bDMARDs, may negatively impact the effectiveness of tofacitinib. Patients who have been treated with these therapies prior to starting tofacitinib may be at a higher risk of not responding to treatment. While randomized trials with meta-analysis established tofacitinib's efficacy in TNFi-inadequate responders, our real-world cohort complements this by evaluating durability and predictors of non-response in clinical practice [35]. The consistency between our results and clinical trials with meta-analysis reinforces tofacitinib's role in this population, while our data on prior bDMARD exposure offers pragmatic guidance for sequencing therapies. Clinicians may need to consider these factors when determining whether to initiate tofacitinib therapy in patients with a history of biologic treatments. Additionally, these findings highlight the need for closer monitoring of patients with prior bDMARD therapy to assess their response to tofacitinib and consider alternative treatment strategies if necessary.

TABLE 2 | Multivariate Cox regression analysis: Adjusted hazard ratio of the factors for Tofacitinib in RA patients.

Variable	Multivariate 1[a], HR (95% CI)	Multivariate 2[b], HR (95% CI)	Multivariate 3[c], HR (95% CI)
Male vs. Female	0.774 (0.492–1.219)	0.774 (0.492–1.219)	0.776 (0.492–1.224)
Age	0.998 (0.986–1.011)	0.999 (0.987–1.012)	0.998 (0.986–1.011)
RA disease duration	1.008 (0.968–1.049)	1.011 (0.981–1.043)	1.019 (0.990–1.050)
Previously use of hydroxychloroquine	0.798 (0.564–1.129)	0.794 (0.561–1.121)	0.763 (0.541–1.076)
Previously use of leflunomide	1.329 (0.956–1.848)	1.330 (0.958–1.846)	1.392 (1.005–1.928)
bDMARDs-experienced vs. bDMARDs-näive	1.423* (1.024–1.976)	—	—
Prior TNFis vs. bDMARDs-näive	—	1.605* (1.165–2.212)	—
Prior non-TNFis vs. bDMARDs-näive	—	—	1.326* (1.012–2.075)

Abbreviations: bDMARDs, biological DMARDs; CI, confidence interval; HR, hazard ratio; RA, rheumatoid arthritis; TNFis, tumor necrosis factor inhibitors.
[a]266 subjects with 155 bDMARDs-experienced, adjusting for gender, age, RA disease duration, previously use of Hydroxychloroquine, previously use of Leflunomide.
[b]217 subjects with 95 prior TNFis, adjusting for gender, age, RA disease duration, previously use of Hydroxychloroquine, previously use of Leflunomide.
[c]171 subjects with 49 non-TNFis, adjusting for gender, age, RA disease duration, previously use of Hydroxychloroquine, previously use of Leflunomide.
*$p < 0.05$.
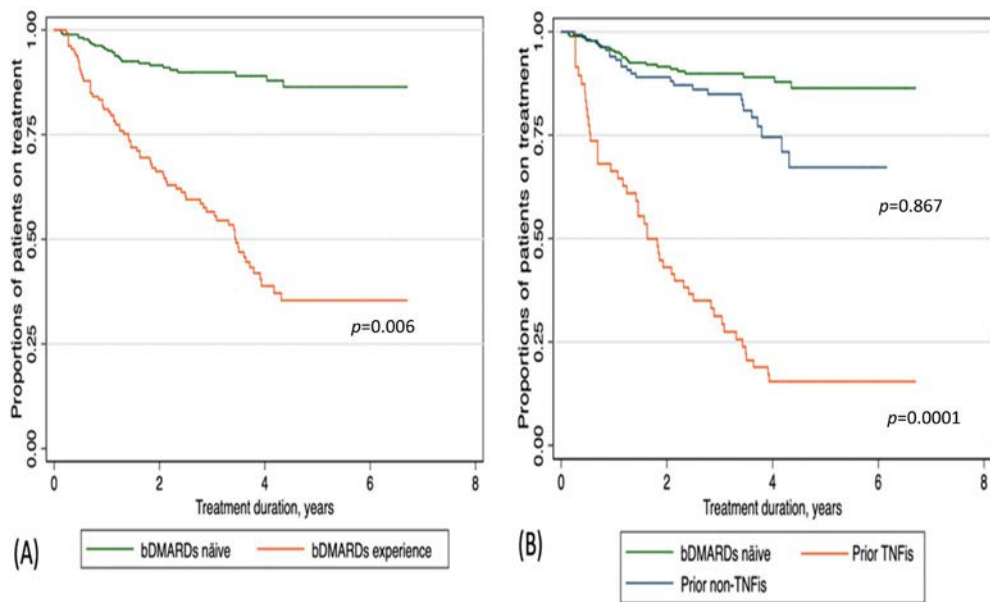
FIGURE 2 | (A) Drug survival curve for comparing RA patients with bDMARDs-näive and bDMARDs-experienced (B) Drug survival curve of comparing RA with Prior TNFis, Prior non-TNFis and bDMARDs näive. RA, rheumatoid arthritis; bDMARDs, biological disease modifying anti-rheumatic drugs; TNFis, tumor necrosis factor inhibitors.

This study has several limitations that should be considered. Because it is retrospective, there is a risk of selection bias and unmeasured confounding, even though we adjusted for some factors in our analysis. The way we defined tofacitinib non-response as a combination of different outcomes-such as loss of efficacy, adverse events, and other clinical decisions-reflects real-world practice but also mixes different reasons for stopping treatment, which can make it harder to interpret the underlying mechanisms. Our study population, which included only patients who had received tofacitinib in clinical trials or at certain institutions, may not fully represent all patients treated with this medication, so our findings may not apply to every setting. Additionally, we did not collect detailed information on why patients stopped previous biologic treatments or how long they were on those therapies, which could have provided more context for our results. We also had to exclude some patients due to missing or incomplete data, such as unclear diagnoses, loss to follow-up, or treatment discontinuation for reasons like adverse effects or pregnancy planning. While these exclusions were necessary to keep the study population consistent, we did not perform sensitivity analyses or data imputation, which could introduce bias and limit how widely our results can be applied. Despite these limitations, we made every effort to carefully review patients' medical histories to ensure accurate inclusion. Future prospective studies with larger and more diverse patient groups, as well as more detailed data collection, will be important to confirm our findings and better understand the mechanisms involved.

Despite these limitations, our study provides compelling evidence that prior biologic therapy, particularly TNFis and other bDMARDs, is a significant predictor of reduced tofacitinib effectiveness. These findings have important clinical implications. Clinicians should carefully consider a patient's history of biologic therapy when deciding whether to initiate tofacitinib treatment. In patients with prior biologic exposure, particularly those who have failed multiple biologics, alternative treatment strategies or closer monitoring of treatment response may be warranted. Furthermore, our findings highlight the need for further research to elucidate the underlying mechanisms and develop strategies to overcome resistance to targeted therapies in patients with autoimmune diseases. This could lead to more personalized treatment approaches and improve outcomes for patients with these challenging conditions.

5 | Conclusion

This study provides important insights into the factors influencing a non-response to tofacitinib in patients with RA. The findings suggest that prior exposure to bDMARD therapies, particularly TNFis, is a significant predictor of a non-response. These results underscore the need for careful patient selection when considering tofacitinib therapy and highlight the importance of treatment history in determining the most appropriate therapeutic approach for RA patients. We recognize that treatment non-response may reflect either drug-specific factors or underlying disease refractoriness. This link probably reflects both medication history and disease severity, even though our adjusted analyses indicate that prior bDMARD exposure independently predicts the discontinuation of tofacitinib. Clinicians could interpret these findings in the context of individual patient characteristics and treatment trajectories. Further research is needed to explore the mechanisms underlying a non-response to tofacitinib and to identify strategies for improving outcomes in this challenging patient population.

References

1. K. Heinimann, J. von Kempis, R. Sauter, et al., "Long-Term Increase of Radiographic Damage and Disability in Patients With RA in Relation to Disease Duration in the Era of Biologics. Results From the SCQM Cohort," *Journal of Clinical Medicine* 7, no. 3 (2018): 57, https://doi.org/10.3390/jcm7030057.

2. K. W. Drossaers-Bakker, A. H. Zwinderman, T. P. Vliet Vlieland, et al., "Long-Term Outcome in Rheumatoid Arthritis: A Simple Algorithm of Baseline Parameters Can Predict Radiographic Damage, Disability, and Disease Course at 12-Year Followup," *Arthritis and Rheumatism* 47, no. 4 (2002): 383–390, https://doi.org/10.1002/art.10513.

3. L. Fraenkel, J. M. Bathon, B. R. England, et al., "2021 American College of Rheumatology Guideline for the Treatment of Rheumatoid Arthritis," *Arthritis and Rheumatology* 73, no. 7 (2021): 1108–1123, https://doi.org/10.1002/art.41752.

4. J. S. Smolen, R. B. M. Landewé, S. A. Bergstra, et al., "EULAR Recommendations for the Management of Rheumatoid Arthritis With Synthetic and Biological Disease-Modifying Antirheumatic Drugs: 2022 Update," *Annals of the Rheumatic Diseases* 82, no. 1 (2023): 3–18, https://doi.org/10.1136/ard-2022-223356.

5. J. S. Smolen, F. C. Breedveld, G. R. Burmester, et al., "Treating Rheumatoid Arthritis to Target: 2014 Update of the Recommendations of an International Task Force," *Annals of the Rheumatic Diseases* 75, no. 1 (2016): 3–15, https://doi.org/10.1136/annrheumdis-2015-207524.

6. P. C. Taylor, B. Fautrel, Y. Piette, et al., "Treat-to-Target in Rheumatoid Arthritis: A Real-World Study of the Application and Impact of Treat-to-Target Within the Wider Context of Patient Management, Patient Centricity and Advanced Therapy Use in Europe," *RMD Open* 8, no. 2 (2022): e002658, https://doi.org/10.1136/rmdopen-2022-002658.

7. C. Webers, I. Essers, M. Been, and A. van Tubergen, "Barriers and Facilitators to Application of Treat-to-Target Management in Psoriatic Arthritis and Axial Spondyloarthritis in Practice: A Systematic Literature Review," *Seminars in Arthritis and Rheumatism* 69 (2024): 152546, https://doi.org/10.1016/j.semarthrit.2024.152546.

8. D. Vyas, K. M. O'Dell, J. L. Bandy, and E. G. Boyce, "Tofacitinib: The First Janus Kinase (JAK) Inhibitor for the Treatment of Rheumatoid Arthritis," *Annals of Pharmacotherapy* 47, no. 11 (2013): 1524–1531, https://doi.org/10.1177/1060028013512790.

9. I. S. Padda, R. Bhatt, and M. Parmar, "Tofacitinib," in *StatPearls* (StatPearls Publishing, 2025).

10. D. M. Meyer, M. I. Jesson, X. Li, et al., "Anti-Inflammatory Activity and Neutrophil Reductions Mediated by the JAK1/JAK3 Inhibitor, CP-690550, in Rat Adjuvant-Induced Arthritis," *Journal of Inflammation* 7, no. 1 (2010): 41, https://doi.org/10.1186/1476-9255-7-41.

11. K. Ghoreschi, A. Laurence, and J. J. O'Shea, "Janus Kinases in Immune Cell Signaling," *Immunological Reviews* 228, no. 1 (2009): 273–287, https://doi.org/10.1111/j.1600-065X.2008.00754.x.

12. R. A. Ortmann, T. Cheng, R. Visconti, D. M. Frucht, and J. J. O'Shea, "Janus Kinases and Signal Transducers and Activators of Transcription: Their Roles in Cytokine Signaling, Development and Immunoregulation," *Arthritis Research* 2, no. 1 (2000): 16–32, https://doi.org/10.1186/ar66.

13. Y. Tanaka, Y. Luo, J. J. O'Shea, and S. Nakayamada, "*Janus* Kinase-Targeting Therapies in Rheumatology: A Mechanisms-Based Approach," *Nature Reviews Rheumatology* 18, no. 3 (2022): 133–145, https://doi.org/10.1038/s41584-021-00726-8.

14. P. C. Taylor, "Clinical Efficacy of Launched JAK Inhibitors in Rheumatoid Arthritis," *Rheumatology (Oxford, England)* 58, no. Suppl 1 (2019): i17–i26, https://doi.org/10.1093/rheumatology/key225.

15. C. Cubberley and A. Maharaj, "Global RA Treatment Recommendations: An Update From the Various International Societies," *Best Practice & Research. Clinical Rheumatology* 39 (2024): 102019, https://doi.org/10.1016/j.berh.2024.102019.

16. A. Finckh, J. F. Simard, J. Duryea, et al., "The Effectiveness of Anti-Tumor Necrosis Factor Therapy in Preventing Progressive Radiographic

Joint Damage in Rheumatoid Arthritis: A Population-Based Study," *Arthritis and Rheumatism* 54, no. 1 (2006): 54–59, https://doi.org/10.1002/art.21491.

17. Y. H. Lee and S. C. Bae, "Comparative Efficacy and Safety of Tocilizumab, Rituximab, Abatacept and Tofacitinib in Patients With Active Rheumatoid Arthritis That Inadequately Responds to Tumor Necrosis Factor Inhibitors: A Bayesian Network Meta-Analysis of Randomized Controlled Trials," *International Journal of Rheumatic Diseases* 19, no. 11 (2016): 1103–1111, https://doi.org/10.1111/1756-185x.12822.

18. J. A. Singh, A. Hossain, E. Tanjong Ghogomu, et al., "Biologics or Tofacitinib for Rheumatoid Arthritis in Incomplete Responders to Methotrexate or Other Traditional Disease-Modifying Anti-Rheumatic Drugs: A Systematic Review and Network Meta-Analysis," *Cochrane Database of Systematic Reviews* 2016, no. 5 (2016): Cd012183, https://doi.org/10.1002/14651858.Cd012183.

19. E. Kaltsonoudis, E. Pelechas, P. V. Voulgari, and A. A. Drosos, "Unmet Needs in the Treatment of Rheumatoid Arthritis. An Observational Study and a Real-Life Experience From a Single University Center," *Seminars in Arthritis and Rheumatism* 48, no. 4 (2019): 597–602, https://doi.org/10.1016/j.semarthrit.2018.06.003.

20. A. Souto, J. R. Maneiro, and J. J. Gómez-Reino, "Rate of Discontinuation and Drug Survival of Biologic Therapies in Rheumatoid Arthritis: A Systematic Review and Meta-Analysis of Drug Registries and Health Care Databases," *Rheumatology* 55, no. 3 (2016): 523–534, https://doi.org/10.1093/rheumatology/kev374.

21. A. Fisher, M. Hudson, R. W. Platt, and C. R. Dormuth, "Tofacitinib Persistence in Patients With Rheumatoid Arthritis: A Retrospective Cohort Study," *Journal of Rheumatology* 48, no. 1 (2021): 16–24, https://doi.org/10.3899/jrheum.191252.

22. S. Jerram, S. Butt, K. Gadsby, and C. Deighton, "Discrepancies Between the EULAR Response Criteria and the NICE Guidelines for Continuation of Anti-TNF Therapy in RA: A Cause for Concern?," *Rheumatology* 47, no. 2 (2008): 180–182, https://doi.org/10.1093/rheumatology/kem331.

23. N. Smith, T. Ding, S. Butt, K. Gadsby, and C. Deighton, "The Importance of the Baseline Disease Activity Score 28 in Determining Responders and Non-Responders to Anti-TNF in UK Clinical Practice," *Rheumatology* 47, no. 9 (2008): 1389–1391, https://doi.org/10.1093/rheumatology/ken233.

24. K. Ebina, M. Hashimoto, W. Yamamoto, et al., "Drug Retention and Discontinuation Reasons Between Seven Biologics in Patients With Rheumatoid Arthritis—The ANSWER Cohort Study," *PLoS One* 13, no. 3 (2018): e0194130, https://doi.org/10.1371/journal.pone.0194130.

25. M. L. Hetland, I. J. Christensen, U. Tarp, et al., "Direct Comparison of Treatment Responses, Remission Rates, and Drug Adherence in Patients With Rheumatoid Arthritis Treated With Adalimumab, Etanercept, or Infliximab: Results From Eight Years of Surveillance of Clinical Practice in the Nationwide Danish DANBIO Registry," *Arthritis and Rheumatism* 62, no. 1 (2010): 22–32, https://doi.org/10.1002/art.27227.

26. J. Pope, L. Bessette, N. Jones, et al., "Experience With Tofacitinib in Canada: Patient Characteristics and Treatment Patterns in Rheumatoid Arthritis Over 3 Years," *Rheumatology* 59, no. 3 (2020): 568–574, https://doi.org/10.1093/rheumatology/kez324.

27. M. Machado, C. S. Moura, S. F. Guerra, J. R. Curtis, M. Abrahamowicz, and S. Bernatsky, "Effectiveness and Safety of Tofacitinib in Rheumatoid Arthritis: A Cohort Study," *Arthritis Research & Therapy* 20, no. 1 (2018): 60, https://doi.org/10.1186/s13075-018-1539-6.

28. S. E. Henrickson, M. A. Ruffner, and M. Kwan, "Unintended Immunological Consequences of Biologic Therapy," *Current Allergy and Asthma Reports* 16, no. 6 (2016): 46, https://doi.org/10.1007/s11882-016-0624-7.

29. J. G. Sathish, S. Sethu, M. C. Bielsky, et al., "Challenges and Approaches for the Development of Safer Immunomodulatory Biologics,"

Nature Reviews Drug Discovery 12, no. 4 (2013): 306–324, https://doi.org/10.1038/nrd3974.

30. D. M. Schwartz, Y. Kanno, A. Villarino, M. Ward, M. Gadina, and J. J. O'Shea, "JAK Inhibition as a Therapeutic Strategy for Immune and Inflammatory Diseases," *Nature Reviews. Drug Discovery* 16, no. 12 (2017): 843–862, https://doi.org/10.1038/nrd.2017.201.

31. S. Singh, M. H. Murad, M. Fumery, et al., "Comparative Efficacy and Safety of Biologic Therapies for Moderate-to-Severe Crohn's Disease: A Systematic Review and Network Meta-Analysis," *Lancet Gastroenterology & Hepatology* 6, no. 12 (2021): 1002–1014, https://doi.org/10.1016/s2468-1253(21)00312-5.

32. M. Movahedi, D. Choquette, L. Coupal, et al., "Discontinuation of Tofacitinib and TNF Inhibitors in Patients With Rheumatoid Arthritis: Analysis of Pooled Data From Two Registries in Canada," *BMJ Open* 13, no. 3 (2023): e063198, https://doi.org/10.1136/bmjopen-2022-063198.

33. K. J. Li, C. L. Chang, C. Y. Hsin, and C. H. Tang, "Switching and Discontinuation Pattern of Biologic Disease-Modifying Antirheumatic Drugs and Tofacitinib for Patients With Rheumatoid Arthritis in Taiwan," *Frontiers in Pharmacology* 12 (2021): 628548, https://doi.org/10.3389/fphar.2021.628548.

34. H. Shimizu, Y. Aonuma, S. Hibiya, et al., "Long-Term Efficacy and Safety of Tofacitinib in Patients With Ulcerative Colitis: 3-Year Results From a Real-World Study," *Intestinal Research* 22, no. 3 (2024): 369–377, https://doi.org/10.5217/ir.2023.00194.

35. M. C. Vieira, S. H. Zwillich, J. P. Jansen, B. Smiechowski, D. Spurden, and G. V. Wallenstein, "Tofacitinib Versus Biologic Treatments in Patients With Active Rheumatoid Arthritis Who Have Had an Inadequate Response to Tumor Necrosis Factor Inhibitors: Results From a Network Meta-Analysis," *Clinical Therapeutics* 38, no. 12 (2016): 2628–2641.e5, https://doi.org/10.1016/j.clinthera.2016.11.004.

WILEY

EDITORIAL

Epidemiology of Juvenile Dermatomyositis—What We Know and What More Is Needed?

Dev Desai[1] | Latika Gupta[2,3] | Pandiarajan Vignesh[1]

[1]Division of Pediatric Rheumatology and Immunology, Allergy Immunology Unit, Department of Pediatrics, Advanced Pediatrics Centre, Postgraduate Institute of Medical Education and Research (PGIMER), Chandigarh, India | [2]Department of Rheumatology, Royal Wolverhampton Hospitals NHS Trust, Wolverhampton, UK | [3]Division of Musculoskeletal and Dermatological Sciences, Centre for Musculoskeletal Research, School of Biological Sciences, the University of Manchester, Manchester, UK

Correspondence: Pandiarajan Vignesh (vigimmc@gmail.com)

Juvenile idiopathic inflammatory myopathies (JIIMs) are a heterogeneous group of immune-mediated disorders—including Juvenile Dermatomyositis (JDM), Juvenile Polymyositis (JPM), immune-mediated necrotizing myositis, myositis associated with other connective tissue diseases, and rare disorders classified under the unified spectrum of idiopathic inflammatory myopathies (IIMs).

The estimated incidence of IIM varies from 1.6 to 19/million/year, and estimated prevalence varyies from 2.4 to 33.8/100000/year [1]. For JDM, the form of JIIM for which most estimates are available, the incidence varies from 1.9 to 3.2/million children/year [2–4]. The exact etiological basis of JIIMs is not yet known, but studies have found associations with several environmental triggers such as ultraviolet (UV) light exposure, air pollution, and a variety of infectious triggers. Genetic associations with HLA haplotypes have also been identified [5, 6]. Historically, JIIMs had a grim prognosis with a chronic and severe course, and as many as a third of all patients succumbing to the disease [7]. With advances in treatment, the prognosis for JIIMs has significantly improved, but mortality rates in JIIM patients remain higher than that in the general population [6], and most patients are seen to have some extent of disease damage [8]. Even among rheumatological disorders, JIIMs are rare, chronic disorders with patients requiring long-term management and rehabilitation at specialist centers. A better understanding of the epidemiology of the JIIMs can help in estimating the burden of disease, which can influence public health policy toward provision of healthcare facilities for these patients. Moreover, studying epidemiological trends over time can contribute toward

recognition of risk factors, some of which may be modifiable. Epidemiological studies can also help guide future research and public health interventions [9].

Nossent et al. conducted a 30-year population-based retrospective study of 40 JIIM patients under 18 years in Western Australia, finding an annual incidence of 2.52/million children, with JDM at 2.02/million, female predominance, and a 94.9% 10-year survival rate. Compared with JIA controls, JIIM patients had significantly higher rates of serious infections, with nonsignificant increases in thromboembolic disease, ILD, osteoporosis, and pregnancy complications. Nossent et al.'s study makes a significant contribution by providing Australian population-based JIIM incidence data and enabling outcome comparisons with JIA as a control group. The extended median follow-up of over 10 years offers valuable insights into the long-term complications and functional impacts of JIIM.

As the understanding of JIIMs has evolved over time, it has been seen that different autoantibodies confer different clinical phenotypes and also have a significant bearing on outcomes in patients with JIIMs [6, 8]. Determining the accurate incidence of JIIMs is met with several challenges. Contemporary research reveals significant heterogeneity in classification criteria usage, with many studies using multiple systems or none at all, highlighting the urgent need for a unified, comprehensive classification framework that can accurately capture all IIM subtypes [10]. Limited access to specialized diagnostic tools, particularly myositis-specific antibody testing in many regions, further complicates accurate case identification. The scarcity of pediatric rheumatologists

and specialists experienced in recognizing early disease features often results in delayed diagnosis or missed cases, especially in resource-limited settings. Limited research funding, given the rarity of the condition, constrains the scope and scale of epidemiological studies, particularly in developing regions. Additionally, cases managed exclusively in outpatient settings or those who never reach tertiary care centers may go unrecorded, leading to potential underestimation of true disease incidence.

The above study while valuable, the absence of autoantibody profile data limits our understanding of the immunological characteristics of the cohort. Additionally, the baseline disease severity metrics were not reported, making it challenging to evaluate the relationship between initial patient status and outcomes. The study also does not specify the exact causes of mortality. The composition of JIA subtypes in the comparison cohort would have provided useful context for interpretation. The study's reliance on hospitalization records for JIIM case identification, though methodologically sound, may not capture the full spectrum of cases, particularly those managed in outpatient settings or those without access to healthcare facilities. These observations may inform the design of future studies in this area. The study nonetheless represents a significant contribution to the field, offering valuable longitudinal data on JIIM incidence, prevalence and associated morbidities. Its particular strengths lie in its comprehensive temporal scope and the inclusion of multiple healthcare facilities across Western Australia, providing a robust regional perspective.

Future epidemiological studies would benefit from prospective multicentric data collection, including autoantibody profiles and outpatient cases. Collaborative networks such as Myositis International Health and Research Collaborative Alliance (MIHRA) play a crucial role in addressing current research gaps, particularly in developing regions where data remains limited [11]. Such international partnerships, guided by principles of inclusivity and equitable representation, are essential for establishing a comprehensive global understanding of JIIM epidemiology.

Conflicts of Interest

The authors declare no conflicts of interest.

Data Availability Statement

Data sharing not applicable to this article as no datasets were generated or analysed during the current study.

References

1. A. Meyer, N. Meyer, M. Schaeffer, J. E. Gottenberg, B. Geny, and J. Sibilia, "Incidence and Prevalence of Inflammatory Myopathies: A Systematic Review," *Rheumatology (Oxford, England)* 54, no. 1 (2015): 50–63.

2. E. P. Mendez, R. Lipton, R. Ramsey-Goldman, et al., "US Incidence of Juvenile Dermatomyositis, 1995-1998: Results From the National Institute of Arthritis and Musculoskeletal and Skin Diseases Registry," *Arthritis & Rheumatism* 49, no. 3 (2003): 300–305.

3. S. Dp, S. Ja, and D. Sm, "The Incidence of Juvenile Dermatomyositis: Results From a Nation-Wide Study," *British Journal of Rheumatology* 34, no. 8 (1995), https://pubmed.ncbi.nlm.nih.gov/7551657/.

4. B. M. Feldman, L. G. Rider, A. M. Reed, and L. M. Pachman, "Juvenile Dermatomyositis and Other Idiopathic Inflammatory Myopathies of Childhood," *Lancet* 371, no. 9631 (2008): 2201–2212.

5. C. Papadopoulou, C. Chew, M. G. L. Wilkinson, L. McCann, and L. R. Wedderburn, "Juvenile Idiopathic Inflammatory Myositis: An Update on Pathophysiology and Clinical Care," *Nature Reviews Rheumatology* 19, no. 6 (2023): 343–362.

6. L. G. Rider and K. Nistala, "The Juvenile Idiopathic Inflammatory Myopathies: Pathogenesis, Clinical and Autoantibody Phenotypes, and Outcomes," *Journal of Internal Medicine* 280, no. 1 (2016): 24–38.

7. H. Am, "Juvenile Idiopathic Inflammatory Myopathies," *Pediatric Clinics of North America* 65, no. 4 (2018), https://pubmed.ncbi.nlm.nih.gov/30031496/.

8. V. Tsaltskan, A. Aldous, S. Serafi, et al., "Long-Term Outcomes in Juvenile Myositis Patients," *Seminars in Arthritis and Rheumatism* 50, no. 1 (2020): 149–155.

9. T. Khoo, J. B. Lilleker, B. Y. H. Thong, V. Leclair, J. A. Lamb, and H. Chinoy, "Epidemiology of the Idiopathic Inflammatory Myopathies," *Nature Reviews Rheumatology* 19, no. 11 (2023): 695–712.

10. I. E. Lundberg, A. Tjärnlund, M. Bottai, et al., "2017 EULAR/ACR Classification Criteria for Adult and Juvenile Idiopathic Inflammatory Myopathies and their Major Subgroups," *Annals Rheumatic Diseases* 76, no. 12 (2017): 1955–1964.

11. L. A. Saketkoo, J. J. Paik, H. Alexanderson, et al., "Collaborative Research in Myositis-Related Disorders: MIHRA, a Global Shared Community Model," *Clinical and Experimental Rheumatology* 42, no. 2 (2024): 207–212.

ORIGINAL ARTICLE

Differential Impact of Concomitant Methotrexate and Glucocorticoids Dosages on Biologics and JAK Inhibitors: The ANSWER Cohort Study

Kosuke Ebina[1,2] | Yuki Etani[2] | Yasutaka Okita[3] | Kohei Tsujimoto[3] | Yuichi Maeda[3] | Takaaki Noguchi[1] | Makoto Hirao[4] | Koichi Murata[5] | Takayuki Fujii[5] | Motomu Hashimoto[6] | Tadashi Okano[7] | Takuya Kotani[8] | Koji Nagai[8] | Takaichi Okano[9] | Iku Shirasugi[9] | Ryota Hara[10] | Yonsu Son[11] | Hideki Amuro[11] | Masaki Katayama[12] | Shotaro Tachibana[13] | Shinya Hayashi[13] | Wataru Yamamoto[14] | Atsushi Kumanogoh[3] | Ken Nakata[15] | Seiji Okada[1] | Akira Onishi[5]

[1]Department of Orthopaedic Surgery, The University of Osaka Graduate School of Medicine Faculty of Medicine, Suita, Japan | [2]Department of Sports Medical Biomechanics, The University of Osaka Graduate School of Medicine Faculty of Medicine, Suita, Japan | [3]Department of Respiratory Medicine and Clinical Immunology, The University of Osaka Graduate School of Medicine Faculty of Medicine, Suita, Japan | [4]Department of Orthopaedic Surgery, Osaka Minami Medical Center, Kawachi-Nagano, Japan | [5]Department of Advanced Medicine for Rheumatic Diseases, Kyoto University Graduate School of Medicine, Kyoto, Japan | [6]Department of Clinical Immunology, School of Medicine, Osaka Metropolitan University Graduate School of Medicine, Osaka, Japan | [7]Center for Senile Degenerative Disorders (CSDD), Osaka Metropolitan University Graduate School of Medicine, Osaka, Japan | [8]Department of Internal Medicine (IV), Osaka Medical and Pharmaceutical University, Takatsuki, Japan | [9]Department of Rheumatology and Clinical Immunology, School of Medicine, Kobe University Graduate School of Medicine, Kobe, Japan | [10]Department of Orthopaedic Surgery, Nara Medical University, Kashihara, Japan | [11]First Department of Internal Medicine, Kansai Medical University, Hirakata, Japan | [12]Department of Rheumatology, Osaka Red Cross Hospital, Osaka, Japan | [13]Department of Orthopaedic Surgery, Kobe University Graduate School of Medicine, Kobe, Japan | [14]Department of Health Information Management, Kurashiki Sweet Hospital, Kurashiki, Japan | [15]Department of Health and Sport Sciences, The University of Osaka Graduate School of Medicine Faculty of Medicine, Suita, Japan

Correspondence: Kosuke Ebina (k-ebina@ort.med.osaka-u.ac.jp)

ABSTRACT

Aim: This multicenter retrospective study evaluated the differential impact of concomitant methotrexate (MTX) and glucocorticoids (GCs) administration by dosage on the effectiveness and safety of biological disease-modifying antirheumatic drugs (bDMARDs) and Janus kinase inhibitors (JAKi) in a real-world cohort of patients with rheumatoid arthritis, adjusting for clinical backgrounds variables.

Methods: The study included 3751 treatment courses (bDMARD- or JAKi-naïve cases, 48.9%; tumor necrosis factor inhibitors: 1668; tocilizumab [TCZ]: 865; abatacept [ABT]: 825; JAKi: 393). Hazard ratios for treatment retention were calculated using multivariate Cox proportional hazards models, adjusted for potential confounders. Improvement in the clinical disease activity index (ΔCDAI) with each formulation was analyzed using mixed-effects models for repeated measures, stratified by concomitant MTX and GCs dosages.

Results: Compared to MTX(−), a lower dose of MTX (< 10 mg/week) was associated with significant improvement in ΔCDAI with golimumab (GLM), TCZ, and JAKi and reduced discontinuation due to ineffectiveness of etanercept (ETN). A higher MTX dose (≥ 10 mg/week) demonstrated a similar trend. Compared to GCs(−), a lower dose of GCs (≤ 5 mg/day; prednisolone equivalent) was associated with a diminished ΔCDAI with GLM and an increased discontinuation due to ineffectiveness of ADA and GLM. A higher dose of GCs (> 5 mg/day) was associated with increased discontinuation due to safety with ETN, CZP, and JAKi.

Conclusions: The effects of concomitant MTX and GCs dosages on the effectiveness and safety of biologics and JAKi vary among agents. MTX did not mitigate safety issues, and GCs did not enhance effectiveness of any agents, regardless of dosage.

Summary

- Methotrexate and glucocorticoids dosages distinctly affect biologics and JAK inhibitors effectiveness and safety among agents.

- Lower-dose methotrexate improves ΔCDAI with golimumab, tocilizumab, and JAK inhibitors and reduces etanercept discontinuation.

- Lower-dose glucocorticoids reduce golimumab effectiveness; higher-dose GCs increase etanercept, certolizumab pegol, and JAK inhibitor discontinuation.

1 | Introduction

The 2022 recommendations from the European Alliance of Associations for Rheumatology (EULAR) advocate for the combination of biological disease-modifying anti-rheumatic drugs (bDMARDs) or targeted synthetic (ts) DMARDs with methotrexate (MTX) in patients with rheumatoid arthritis (RA) [1] due to better clinical outcomes and reduced radiographic progression compared to monotherapy [2]. Previous studies suggest that even lower-dose MTX (as low as 10 mg/week) in combination with tumor necrosis factor inhibitors (TNFi) can provide additional benefit over TNFi monotherapy [3, 4], though the evidence concerning combined MTX dosage for non-TNFi or tsDMARDs is still lacking. Moreover, in real-world clinical settings, unlike randomized controlled trials (RCTs), the use of higher-dose MTX is often constrained by comorbidities such as renal dysfunction or pulmonary diseases, underscoring the need to evaluate the optimal MTX dose necessary to ensure efficacy and safety by specific formulations.

The 2022 EULAR recommendations also address the use of oral glucocorticoids (GCs) in combination with bDMARDs or tsDMARDs, recommending their discontinuation as early as possible due to the increased risk of infection associated with prolonged use [1]. The recommendations further advise against the use of GCs during transitions between bDMARDs or tsDMARDs. However, the recommendations include a research agenda that questions whether the concomitant use of very low doses of GCs (1–3 mg/day prednisone equivalent) could enhance therapeutic outcomes without incurring unacceptable side effects [1].

Recent studies evaluating the efficacy and safety of combining GCs with DMARDs have primarily focused on conventional synthetic DMARDs (csDMARDs), with fewer investigations exploring their use with bDMARDs and tsDMARDs [5, 6]. To our knowledge, the impact of combining lower-dose or standard-dose GCs with bDMARDs or tsDMARDs on efficacy and safety in real-world clinical cohorts remains poorly characterized in contemporary literature.

RCTs have been criticized for occasionally enrolling participants who do not represent typical real-world populations often due to younger ages and fewer comorbidities [7]. Consequently, observational cohort studies are increasingly favored for evaluating the effectiveness of bDMARDs [8] and drug retention [9], despite potential biases in treatment selection and discontinuation influenced by physician practices and patient characteristics [10]. Nevertheless, multicenter studies and the comprehensive national health insurance system in our country may help mitigate these biases.

Our ongoing publications from the multicenter, observational registry of rheumatic disease patients in Japan's Kansai region (the ANSWER cohort) [11–16] have demonstrated that the concomitant administration of MTX and GCs influences the continuation rates of bDMARDs and tsDMARDs differently, depending on the drug category [11]. This finding suggests that the impact of concomitant MTX or GCs administration on the efficacy and safety of bDMARDs or tsDMARDs varies not only by drug class but also among individual drugs, underscoring the complexity of these interactions.

The primary objective of this study was to clarify the differential impact of concomitant MTX and GCs by dosage at the initiation of bDMARDs or tsDMARDs on drug retention due to effectiveness and safety for each agent. The secondary objective was to examine the impact of these combined doses on the improvement in the clinical disease activity index (ΔCDAI) following the introduction of each agent with adjustment for clinical backgrounds, with the aim of informing more precise treatment selection and strategies.

2 | Materials and Methods

2.1 | Patients

The Kansai Consortium for Well-being of Rheumatic Disease Patients (ANSWER) cohort is a multicenter, observational registry of patients with rheumatic disease in Japan's Kansai region [11–16]. The data was retrospectively obtained from patients treated at eight prominent university-affiliated hospitals, including The University of Osaka, Kyoto University, Osaka Metropolitan University, Osaka Medical and Pharmaceutical University, Kansai Medical University, Kobe University, Nara Medical University, and Osaka Red Cross Hospital. RA diagnoses were made following either the American College

of Rheumatology (ACR) 1987 RA classification criteria [17] or the 2010 ACR/EULAR RA classification criteria [18]. The administration of bDMARDs and Janus kinase inhibitor (JAKi) was at the discretion of the attending rheumatologists, consistent with the Japan College of Rheumatology (JCR) guidelines [19, 20]. According to the JCR guidelines (2014), failure to achieve low disease activity during phase I treatment with csDMARDs is an indication for augmenting therapy with additional csDMARDs or bDMARDs during phase II. For patients experiencing treatment failure during phase II, transitioning to alternative bDMARDs or tofacitinib (TOF) is considered. The JCR guidelines of 2020 recommend introducing bDMARDs or JAKi during phase II for patients who fail to achieve low disease activity with csDMARDs in phase I. However, from a long-term safety and cost-effectiveness standpoint, bDMARDs are generally preferred. Non-TNFi, specifically aIL-6R, is recommended when a bDMARD is used without MTX. If an inadequate response to a TNFi occurs, a switch to a non-TNFi agent should be prioritized. The dosing of each agent was determined according to the manufacturer's recommendations.

Patients treated with either bDMARDs, including adalimumab (ADA), golimumab (GLM), etanercept (ETN), certolizumab pegol (CZP), abatacept (ABT), and tocilizumab (TCZ) (both intravenous and subcutaneous forms and biosimilar agents), or JAKi (including tofacitinib [TOF] and baricitinib [BAR]) between January 2011 and March 2024 and for whom complete data on initiation and discontinuation dates and the reasons for discontinuation were available were eligible for inclusion in this study. Patients with missing data regarding age, sex, prior use, and the number of switched bDMARDs or JAKi, initiation and discontinuation dates, and the reasons for discontinuation of bDMARDs or JAKi were excluded [11].

Additional data, including baseline demographic information such as disease duration, the disease activity score in 28 joints using the erythrocyte sedimentation rate (DAS28-ESR), the clinical disease activity index (CDAI) score, concomitant dosages (represented as blank if not combined) and use of MTX and GCs [prednisolone (PSL) equivalent], concomitant use of other csDMARDs (including salazosulfapyridine, bucillamine, iguratimod, tacrolimus, and leflunomide), positivity for rheumatoid factor (RF) and anticyclic citrullinated peptide antibody (ACPA), and health assessment questionnaire disability index score were also collected [21]. The CDAI data every 1–3 months after bDMARDs or JAKi initiation were also collected.

Cut-off values for the combined MTX and GCs dosages were set following previous reports of efficacy and safety in combination with bDMARDs and JAKi [3, 4, 21–23]. Briefly, MTX of < 10 mg/week and GCs of ≤ 5 mg/day were set as lower doses, and MTX of ≥ 10 mg/week and GCs of > 5 mg/day were set as others.

Drug retention was retrospectively assessed based on the time until definitive treatment cessation. The reasons for termination were categorized into four main categories, and physicians were required to cite a single rationale for termination as follows: (1) ineffectiveness (comprising both primary and secondary); (2) toxic adverse events (infection, skin reaction, systemic reaction, and other toxic events, such as haematologic, pulmonary, renal, cardiovascular complications, and malignancies); (3) non-toxic reasons (patient preference, hospital transfer, desire for pregnancy, etc.); and (4) remission [24, 25].

2.2 | Statistical Analysis

Multivariate Cox proportional hazards modeling was used to calculate the hazard ratios (HRs) and Cox *p*-values for each reason for treatment discontinuation in the adjusted model [26], using previously reported potential confounders such as baseline age, sex, disease duration, RF/ACPA positivity, CDAI, concomitant dose of GCs and MTX, use of other csDMARDs, prior used number, categories, and starting date of bDMARDs or JAKi [27–29]. Regarding disease activity, the outcome analysis relied on a difference with a 95% confidence interval (CI) derived from mixed-effects models for repeated measures (MMRM) with an unstructured covariance structure and robust variance. The MMRM analyses included categorical time, treatment-by-time interactions, and confounders as fixed factors for adjustment. Improvement in CDAI from baseline (ΔCDAI) was measured at four post-intervention time points (1, 3, 6, and 12 months). Missing data on post-intervention visits were handled by MMRM, assuming missing at random. Multiple imputations by chained equations were performed to handle missing values at baseline [30]. Consequently, 20 imputed datasets were generated, encompassing all covariates and outcomes [31]. Subsequently, the imputation estimates and standard errors were amalgamated according to Rubin's rule [32].

All statistical analyses were performed using R version 4.4.1 (R Development Core Team, Vienna, Austria). Two-sided *p*-values of < 0.05 were considered indicative of statistical significance.

3 | Results

3.1 | Baseline Characteristics

The study population was selected among patients with RA in the ANSWER cohort. A total of 11 039 patients were recruited from the cohort, and 3751 bDMARD or JAKi treatment courses of 3490 patients qualified the inclusion criteria (Figure S1). Table 1 summarizes the baseline demographic and clinical characteristics of the enrolled patients (the average age was 60.9 years, 81.8% were female, mean disease duration was 7.0 years, 77.3% were positive for RF, the CDAI was 13.3, the combined MTX dose was 8.0 mg/week [proportion 55.1%], the GC dose (PSL equivalent) was 5.0 mg/day [proportion 36.6%], and 48.9% were bio/JAKi-naïve). The details on missing data at each observation point are shown in Table S1.

3.2 | Treatment Retention

Table 2 shows the adjusted HRs for treatment discontinuation due to ineffectiveness or toxic adverse events across different agents, stratified by combined MTX and GCs dosages.

TABLE 1 | Clinical characteristics of patients at the initiation of treatment with each agent.

Variables	ADA	GLM	ETN	CZP	ABT	TCZ	JAKi
Number of treatment courses	374	567	508	219	825	865	393 (TOF = 176, BAR = 217)
Number of patients	356	546	444	214	783	805	342
MTX (−) (%)	122 (32.6)	195 (34.4)	203 (40.0)	81 (37.0)	475 (57.6)	435 (50.3)	175 (44.5)
MTX (<10 mg/week) (%)	98 (26.2)	247 (43.6)	190 (37.4)	88 (40.2)	243 (29.5)	279 (32.3)	126 (32.1)
MTX (≥10 mg/week) (%)	154 (41.2)	125 (22.0)	115 (22.6)	50 (22.8)	107 (13.0)	151 (17.5)	92 (23.4)
GC (−) (%)	283 (75.7)	371 (65.4)	334 (65.7)	140 (63.9)	505 (61.2)	527 (60.9)	220 (56.0)
GC (≤5 mg/day) (%)	57 (15.2)	135 (23.8)	131 (25.8)	55 (25.1)	212 (25.7)	215 (24.9)	126 (32.1)
GC (>5 mg/day) (%)	34 (9.1)	61 (10.8)	43 (8.5)	24 (11.0)	108 (13.1)	123 (14.2)	47 (12.0)
Age (years)	53.8 (13.7)	64.5 (13.6)	56.7 (16.8)	53.3 (16.8)	66.6 (12.4)	59.9 (15.0)	62.2 (13.1)
Female sex (%)	275 (73.5)	474 (83.6)	445 (87.6)	185 (84.5)	671 (81.3)	697 (80.6)	323 (82.2)
Disease duration (years)	3.0 [1.0, 8.0]	8.0 [2.0, 17.0]	8.0 [3.0, 17.0]	4.0 [1.0, 10.0]	7.0 [2.0, 16.0]	7.0 [2.0, 14.0]	9.0 [4.0, 17.0]
RF positivity (%)	188 (70.7)	335 (72.2)	349 (81.0)	151 (80.3)	502 (78.9)	555 (78.2)	266 (78.2)
ACPA positivity (%)	184 (77.6)	316 (76.7)	294 (81.7)	128 (76.6)	460 (83.3)	472 (79.9)	224 (78.0)
DAS28-ESR	4.1 (1.4)	4.2 (1.4)	4.0 (1.4)	4.6 (1.6)	4.4 (1.5)	4.3 (1.4)	4.3 (1.3)
CDAI	12.4 [8.2, 19.5]	13.0 [7.8, 19.0]	11.6 [6.4, 17.2]	15.1 [9.8, 24.7]	14.7 [8.6, 22.2]	13.3 [8.4, 20.4]	13.5 [9.5, 22.5]
HAQ-DI	0.9 (0.8)	1.0 (0.8)	0.8 (0.7)	1.0 (0.8)	1.0 (0.8)	0.9 (0.8)	1.0 (0.8)
eGFR (mL/min/1.73 m^2)	82.7 (20.5)	76.0 (24.7)	78.4 (23.3)	85.0 (25.1)	72.0 (23.4)	79.3 (26.8)	71.3 (19.0)
Oral GCs use (%)	91 (24.3)	196 (34.6)	174 (34.3)	79 (36.1)	320 (38.8)	338 (39.1)	173 (44.0)
GCs dose (mg/day; PSL equivalent)	5.0 [4.0, 8.0]	5.0 [3.0, 6.0]	5.0 [3.0, 5.0]	5.0 [3.2, 7.0]	5.0 [3.0, 7.5]	5.0 [4.0, 8.0]	5.0 [2.5, 6.0]
MTX use (%)	252 (67.4)	372 (65.6)	305 (60.0)	138 (63.0)	350 (42.4)	430 (49.7)	218 (55.5)
MTX dose (mg/week)	10.0 [8.0, 12.0]	8.0 [6.0, 10.0]	8.0 [6.0, 10.0]	8.0 [6.0, 10.0]	8.0 [6.0, 10.0]	8.0 [6.0, 10.0]	8.0 [6.0, 10.0]
Other csDMARDs use (%)	67 (17.9)	156 (27.5)	143 (28.1)	46 (21.0)	274 (33.2)	259 (29.9)	144 (36.6)
Number of bDMARD or JAKi							
bDMARD- or JAKi-naive (%)	253 (67.6)	264 (46.6)	240 (47.2)	110 (50.2)	499 (60.5)	375 (43.4)	94 (23.9)
Second bDMARD or JAKi (%)	77 (20.6)	186 (32.8)	155 (30.5)	52 (23.7)	169 (20.5)	251 (29.0)	93 (23.7)
≥3rd bDMARD or JAKi (%)	44 (11.8)	117 (20.6)	113 (22.2)	57 (26.0)	157 (19.0)	239 (27.6)	206 (52.4)

(Continues)

TABLE 1 | (Continued)

Variables	ADA	GLM	ETN	CZP	ABT	TCZ	JAKi
Prior TNFi use (%)	96 (25.7)	193 (34.0)	218 (42.9)	90 (41.1)	235 (28.5)	391 (45.2)	226 (57.5)
Prior anti-IL-6R use (%)	35 (9.4)	92 (16.2)	65 (12.8)	40 (18.3)	149 (18.1)	118 (13.6)	144 (36.6)
Prior CTLA4-Ig use (%)	25 (6.7)	115 (20.3)	53 (10.4)	30 (13.7)	53 (6.4)	134 (15.5)	120 (30.5)
Prior JAKi use (%)	12 (3.2)	18 (3.2)	13 (2.6)	8 (3.7)	21 (2.5)	20 (2.3)	60 (15.3)

Note: Data are presented as mean (standard deviation), median [interquartile ranges], or percentages.

Abbreviations: ABT, abatacept; ACPA, anticyclic citrullinated peptide antibody; ADA, adalimumab; aIL-6R, anti-interleukin-6 receptor antibodies; BAR, baricitinib; bDMARDs, biological disease-modifying antirheumatic drugs; CDAI, Clinical Disease Activity Index; csDMARDs, conventional synthetic disease-modifying antirheumatic drugs; CTLA4-Ig, cytotoxic T lymphocyte-associated antigen-4-Ig; CZP, certolizumab pegol; DAS28-ESR, Disease Activity Score in 28 joints using erythrocyte sedimentation rate; eGFR, estimated glomerular filtration rate; ETN, etanercept; GCs, glucocorticoids; GLM, golimumab; HAQ-DI, Health Assessment Questionnaire Disability Index; JAKi, Janus kinase inhibitors; MTX, methotrexate; PSL, prednisolone; RF, rheumatoid factor; TCZ, tocilizumab; TNFi, tumor necrosis factor inhibitors; TOF, tofacitinib.

The discontinuation rate of ETN due to ineffectiveness was significantly lower when administered with MTX, either < 10 mg/week or ≥ 10 mg/week, compared to ETN without MTX. MTX < 10 mg/week showed a trend toward a lower rate of discontinuation due to inefficacy for golimumab (GLM) ($p = 0.081$); however, further validation is warranted.

GCs ≤ 5 mg/day were associated with higher rates of discontinuation due to ineffectiveness for ADA and GLM compared to their respective treatments without GCs. For GCs > 5 mg/day administered with GLM or ETN, the ineffectiveness-related discontinuation rate was significantly higher than their respective treatments without GCs.

The discontinuation rate due to adverse events was not significantly affected by the MTX dose in any drug combination, although MTX < 10 mg/week showed a trend toward a higher rate of discontinuation due to adverse events for JAKi ($p = 0.072$).

GCs ≤ 5 mg/day showed a trend toward a higher rate of discontinuation due to adverse events for CZP ($p = 0.060$). GCs > 5 mg/day showed a trend for ABT ($p = 0.071$) and were significantly associated with higher rates of discontinuation due to adverse events for ETN, CZP, or JAK inhibitors compared to without GCs.

The improvement in clinical disease activity (ΔCDAI) was analyzed by drug formulation with adjustment for clinical backgrounds, stratified by MTX (Figure 1) and GCs (Figure 2) dosages. Significant enhancement in ΔCDAI was observed at 12 months post-initiation for GLM, TCZ, and JAKi when combined with MTX < 10 mg/week, compared to without MTX. With MTX ≥ 10 mg/week, significant enhancement in ΔCDAI was observed for GLM, TCZ, and JAKi at any point between 3 and 12 months and for ETN at 3 and 6 months post-initiation, compared to without MTX. A similar trend was noted for CZP at 12 months ($p = 0.075$), although it did not reach statistical significance. ADA, CZP, and ABT effectiveness was not significantly influenced by MTX combination or dosage, suggesting a distinct pharmacologic profile.

For GCs, > 5 mg/day was associated with a tendency toward mitigated ΔCDAI compared to without GCs for ADA at 12 months ($p = 0.081$) and significantly lower ΔCDAI for GLM from 6 to 12 months post-initiation. Conversely, significant enhancement in ΔCDAI was observed at > 5 mg/day for TCZ at only 1 month post-initiation, which disappeared thereafter. No significant differences were observed in other agents based on GC combination.

Summary:

ADA: GCs at ≤ 5 mg/day were associated with a significantly higher discontinuation rate due to ineffectiveness.

GLM: ΔCDAI was greater with the concomitant administration of both MTX < 10 and ≥ 10 mg/week, compared to without MTX at 12 months. However, GCs at ≤ 5 mg/day were associated with diminished ΔCDAI from 6 to 12 months. Both > 5 and ≤ 5 mg/day of GCs were associated with higher discontinuation due to ineffectiveness compared to without GCs.

TABLE 2 | Adjusted hazard ratios for treatment discontinuation by specific reason for each agent, in comparison to without concomitant MTX or GCs (PSL equivalent).

Variables	References	Group	ADA	GLM	ETN	CZP	ABT	TCZ	JAKi
Ineffectiveness	MTX (−)	MTX (<10 mg/week)	0.76 (0.39–1.49)	0.72 (0.50–1.04)	0.58 (0.37–0.92)*	0.69 (0.39–1.22)	1.39 (1.00–1.93)	0.80 (0.52–1.22)	1.04 (0.61–1.76)
		MTX (≥10 mg/week)	0.87 (0.47–1.59)	0.93 (0.61–1.41)	0.45 (0.26–0.78)**	1.34 (0.70–2.59)	1.20 (0.76–1.89)	1.17 (0.73–1.86)	1.23 (0.70–2.15)
	GCs (−)	GCs (≤5 mg/day)	2.04 (1.03–4.07)*	1.48 (1.03–2.13)*	1.47 (0.92–2.34)	0.64 (0.35–1.18)	1.03 (0.72–1.49)	1.26 (0.84–1.88)	1.00 (0.62–1.63)
		GCs (>5 mg/day)	1.86 (0.87–3.98)	2.48 (1.62–3.82)***	2.24 (1.21–4.13)*	0.95 (0.44–2.05)	1.12 (0.71–1.79)	1.35 (0.81–2.24)	0.87 (0.42–1.81)
Toxic adverse events	MTX (−)	MTX (<10 mg/week)	1.08 (0.43–2.73)	0.87 (0.46–1.65)	1.19 (0.59–2.37)	2.66 (0.55–12.73)	0.99 (0.61–1.62)	0.98 (0.64–1.50)	2.08 (0.94–4.63)
		MTX (≥10 mg/week)	1.48 (0.64–3.42)	0.53 (0.23–1.23)	0.85 (0.37–1.94)	1.05 (0.16–6.84)	0.99 (0.52–1.89)	0.74 (0.40–1.34)	1.12 (0.42–2.99)
	GCs (−)	GCs (≤5 mg/day)	0.80 (0.31–2.08)	1.70 (0.89–3.24)	1.04 (0.48–2.23)	3.76 (0.95–14.94)	1.37 (0.82–2.30)	0.80 (0.50–1.28)	1.87 (0.84–4.16)
		GCs (>5 mg/day)	0.76 (0.21–2.74)	1.94 (0.80–4.71)	2.87 (1.15–7.18)*	6.23 (1.18–32.87)*	1.72 (0.96–3.09)	1.23 (0.73–2.07)	4.57 (1.77–11.79)**

Note: Hazard ratios between patients with or without combination of MTX or GCs were assessed using the Cox p value. Adjusted confounders were age at baseline; sex; body mass index; disease duration; RF/ACPA positivity; CDAI; concomitant dose of GCs; MTX; use of other csDMARDs; priory used number, categories, and starting date of bDMARDs or JAKi.

Abbreviations: 95% CI, 95% confidence interval; ABT, abatacept; ADA, adalimumab; BAR, baricitinib; bDMARDs, biological disease-modifying antirheumatic drugs; BS, biosimilar; CDAI, Clinical Disease Activity Index; csDMARDs, conventional synthetic disease-modifying antirheumatic drugs; CZP, certolizumab pegol; ETN, etanercept; GCs, glucocorticoids; GLM, golimumab; HR, hazard ratio; JAKi, Janus kinase inhibitors; MTX, methotrexate; PSL, prednisolone; RF, rheumatoid factor; TCZ, tocilizumab; TOF, tofacitinib.

$*p < 0.05$; $**p < 0.01$; $***p < 0.001$.

ETN: The concomitant use of both MTX <10 and ≥10 mg/week with ETN reduced the discontinuation rate due to ineffectiveness compared to ETN without MTX, with ≥10 mg/week demonstrating significantly greater ΔCDAI. GCs at >5 mg/day were associated with a higher discontinuation rate due to ineffectiveness or adverse events.

CZP: Concomitant administration of GCs at >5 mg/day was associated with a higher discontinuation rate due to adverse events.

ABT: Concomitant administration of MTX or GCs did not significantly impact effectiveness or adverse events compared to ABT without MTX or GCs.

TCZ: Concomitant administration of MTX <10 and ≥10 mg/week significantly enhanced ΔCDAI compared to TCZ without MTX. GCs did not significantly impact CDAI or adverse events compared to TCZ without GCs after 3 months.

JAKi: Concomitant administration of both MTX <10 and ≥10 mg/week significantly enhanced ΔCDAI, while GCs at >5 mg/day increased the discontinuation rate due to adverse events.

4 | Discussion

In a previous RCT, concomitant administration of ADA with lower-dose MTX (6.2 mg/week) effectively suppressed radiographic progression and improved clinical outcomes compared to without MTX [33]. On the other hand, ADA monotherapy also showed significant, rapid, and sustained improvement in disease activity [34]. In the present study, patients who initiated ADA treatment had relatively low disease activity (CDAI = 12.4) and a short disease duration (3.0 years) at baseline. Furthermore, differences in the study design—specifically, the addition of ADA to ongoing MTX therapy, unlike the protocol in RCTs—may have influenced the results. Conversely, background GCs in ADA did not provide additional benefits in clinical, functional, or radiographic outcomes over a 2-year period [35]. Notably, a novel finding of the present study is that even a lower dose of GCs (≤5 mg/day) was associated with higher discontinuation due to ineffectiveness, warranting further investigation into the underlying mechanisms.

Regarding GLM, monotherapy (50 and 100 mg) was effective in reducing active RA symptoms in Japanese patients [36]. However, GLM 100 mg with MTX tended to show better radiographic outcomes compared to GLM 100 mg without MTX [37]. These findings align with the present study, although a novel observation was that GCs combination was associated with higher discontinuation due to ineffectiveness in a dose-dependent manner.

The combination of ETN with MTX reduced disease activity and radiographic progression more effectively than ETN without MTX [38]. Additionally, ETN combined with low-dose MTX was associated with a higher remission rate than ETN monotherapy in Japanese patients with RA [39]. These results align with the present study. However, a novel finding was that a higher dose of MTX (≥10 mg/week) was more effective than a lower dose
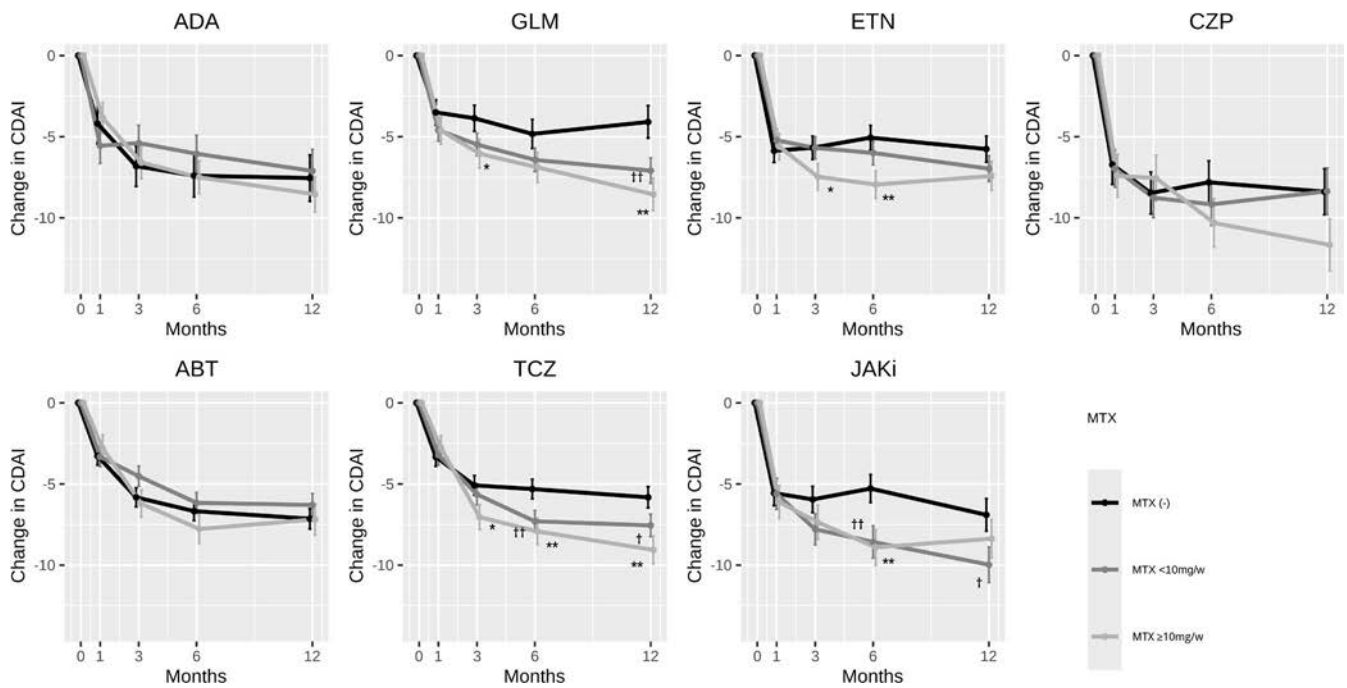
FIGURE 1 | Adjusted change in clinical disease activity index (CDAI) achieved by concomitant administration of different doses of MTX with various bDMARDs and JAKi formulations. ABT, abatacept; ADA, adalimumab; CZP, certolizumab pegol; ETN, etanercept; GLM, golimumab; JAKi, Janus kinase inhibitors; MTX, methotrexate; TCZ, tocilizumab. 【MTX (−) vs. MTX ≥ 10 mg/week】 *$p < 0.05$, **$p < 0.01$. 【MTX (−) vs. MTX < 10 mg/week】 †$p < 0.05$, ††$p < 0.01$.
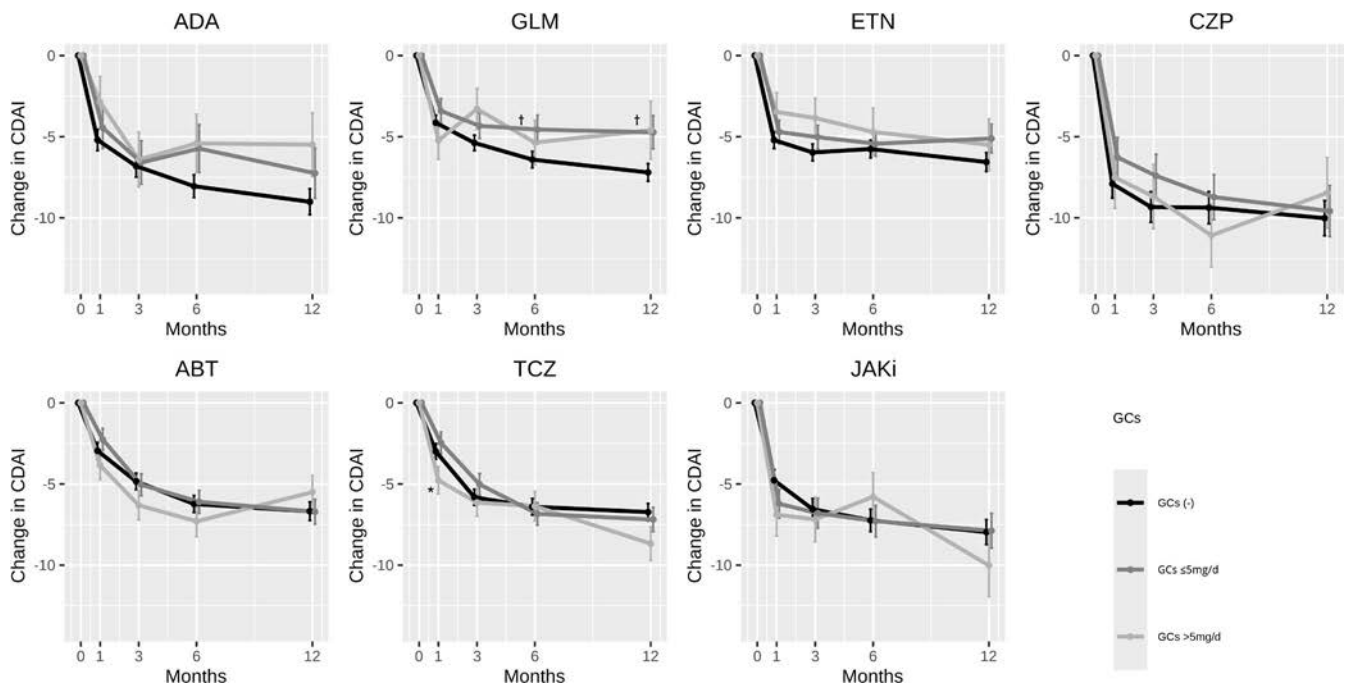
FIGURE 2 | Adjusted change in clinical disease activity index (CDAI) achieved by concomitant administration of different doses of GCs with various bDMARDs and JAKi formulations. ABT, abatacept; ADA, adalimumab; CZP, certolizumab pegol; ETN, etanercept; GCs, glucocorticoids; GLM, golimumab; JAKi, Janus kinase inhibitors; TCZ, tocilizumab. 【GCs (−) vs. GCs > 5 mg/day】 *$p < 0.05$. 【GCs (−) vs. GCs ≤ 5 mg/day】 †$p < 0.05$.

(< 10 mg/week) in improving CDAI and drug retention due to ineffectiveness, and combination with > 5 mg/day of GCs may result in a higher rate of both ineffectiveness and adverse events.

CZP, when administered in combination with or without MTX, was generally well tolerated and significantly improved disease

activity; although CZP with MTX significantly inhibited the radiographic progression more than without MTX [40]. Thus, CZP monotherapy may be clinically acceptable, although the CZP + MTX combination may be more effective in preventing joint destruction. Indeed, CZP tended to show better CDAI improvement when combined with MTX (≥ 10 mg/week) at

12 months ($p = 0.075$) in the present study. However, our findings highlight that a higher dose of GCs (> 5 mg/day) may increase the risk of adverse events without improving disease activity.

ABT was equally effective and safe in ACPA-positive RA patients, regardless of baseline MTX dose [41]. Additionally, baseline GCs therapy did not significantly impact the efficacy of ABT in patients with active RA [35]. These reports are consistent with the present study, which further demonstrated that combined MTX or GCs did not significantly impact effectiveness or safety, irrespective of their doses.

In a previous study, adding MTX (mean 15.4 mg/week) to TCZ (8 mg/kg) tended to achieve a higher rate of low disease activity and remission and lower joint destruction compared to TCZ without MTX [42]. In TCZ treatment without MTX, combined GCs did not significantly impact the efficacy or safety outcomes [43]. These results are aligned with the present study, while also highlighting that both lower (< 10 mg/week) and higher (≥ 10 mg/week) doses of MTX were associated with better CDAI improvement compared to TCZ without MTX.

In previous studies, TOF without MTX failed to demonstrate non-inferiority to TOF with MTX in achieving ACR50 response [44], and TOF with MTX showed greater improvement in patient-reported outcomes compared to TOF without MTX [45]. However, background MTX dose did not affect the efficacy of TOF in Japanese RA patients [46]. Collectively, these findings suggest that the clinical efficacy of TOF may be enhanced even by a small dose of MTX combination, which is consistent with the present study. Conversely, concomitant use of GCs with TOF did not affect clinical or radiographic efficacy [47]. Moreover, the usage of PSL ≥ 5 mg/day with TOF or BAR significantly increased the risk of treatment discontinuation due to adverse events [21], which also aligns with the present study.

The effectiveness of lower-dose MTX may be particularly relevant in Asian populations. The intra-erythrocyte concentration of MTX-polyglutamate, a key biomarker of MTX efficacy, was found to be 65 nmol/L with a MTX 13.4 mg/week in patients from the United States, whereas it was 94 nmol/L with a 10.3 mg/week in Japanese patients [48]. This suggests that lower-dose MTX may be more effective in Asian patients due to the higher levels of MTX-polyglutamate at lower doses compared to western populations.

Several limitations of this study should be considered while interpreting the results. First, treatment discontinuation was based on individual physician decisions without standardized criteria, and improvement in disease activity may not fully match the continuation rate due to effectiveness, and drug discontinuation rates due to adverse events may not fully reflect the actual incidence of adverse events despite monitoring by experienced senior rheumatologists in university-affiliated hospitals. Second, the progression of joint destruction was difficult to evaluate. Third, the initial dosages of each agent were determined based on the manufacturer's recommendations, though minor dosage adjustments over the study course are difficult to monitor. In Japan, GLM is available in 50 and 100 mg formulations, which may influence both efficacy and continuation rates. However, due to the lack of dosage data in this study, further investigation is required in future study. In addition, patients treated with sarilumab, filgotinib, peficitinib, and upadacitinib were excluded due to their small sample size, which made meaningful comparisons with other drugs difficult while avoiding selection bias. Fourth, this study could not distinguish between intravenous and subcutaneous administration or between original and biosimilar bDMARDs. Fifth, as shown in Table S1, the percentage of missing data during this period was approximately 30%–40%, which should be taken into consideration when interpreting the results although compensated by multiple imputation. Finally, the difference in the number of treatment courses between the agents may have influenced the results.

Nevertheless, the strength of this study lies in it being the first to determine the impact of combined dosages of MTX and GCs on the efficacy and safety of bDMARDs and JAKi in real-world clinical practice, by adjusting background factors.

5 | Conclusions

This study reveals that the impact of concomitant administration of varying dosages of MTX and GCs on the effectiveness and safety of bDMARDs and JAKi differs among formulations. These findings may aid in the selection of appropriate therapeutic agents in daily clinical practice.

Author Contributions

K.E. was responsible for conceptualization, formal analysis, investigation, methodology, project administration, and validation. K.E., Y.E., Y.O., K.T., Y.M., T.N., M.Hirao, K.M., T.F., M.Hashimoto, Tadashi Okano, T.K., Koji Nagai, Takaichi Okano, I.S., R.H., Y.S., H.A., M.K., S.T., S.H., and A.O. contributed to data curation and validation. K.E., W.Y., and A.O. contributed to the design and conduction of statistical analysis. K.E. and A.O. prepared the manuscript and visualization. A.K., S.O., and Ken Nakata supervised the manuscript. All the authors read and approved the final manuscript.

Ethics Statement

The representative facility for this registry was Kyoto University. This observational study was conducted in accordance with the Declaration of Helsinki and approved by the ethics committees of the following seven institutes: Kyoto University (granted on 2016-03-24/approval No. R053), The University of Osaka (granted on 2015-11-04/approval No. 15300), Osaka Metropolitan University (granted on 2021-6-09/approval No. 2021-074), Osaka Medical and Pharmaceutical University (granted on 2014-07-14/approval No. 1529), Kansai Medical University (granted on 2017-11-21/approval No. 2014625), Kobe University (granted on 2015-03-20/approval No. 1738), Nara Medial University (granted on 2018-01-23/approval No. 1692), and Osaka Red Cross Hospital (granted on 2015-09-01/approval No. 644). Written informed consent to participate in the ANSWER cohort was obtained from the patients. The ethics committee at The University of Osaka Hospital waived the requirement for patient informed consent by posting the opt-out information in the hospital's homepage.

Consent

Written informed consent to publish the study results was obtained from the patients. The ethics committee at The University of Osaka Hospital waived the requirement for patient informed consent by posting the opt-out information on the hospital's homepage.

Data Availability Statement

The datasets used and/or analyzed in the current study are available from the corresponding author on reasonable request.

References

1. J. S. Smolen, R. B. M. Landewe, S. A. Bergstra, et al., "EULAR Recommendations for the Management of Rheumatoid Arthritis With Synthetic and Biological Disease-Modifying Antirheumatic Drugs: 2022 Update," *Annals of the Rheumatic Diseases* 82, no. 1 (2023): 3–18, https://doi.org/10.1136/ard-2022-223356.

2. J. L. Nam, K. Takase-Minegishi, S. Ramiro, et al., "Efficacy of Biological Disease-Modifying Antirheumatic Drugs: A Systematic Literature Review Informing the 2016 Update of the EULAR Recommendations for the Management of Rheumatoid Arthritis," *Annals of the Rheumatic Diseases* 76, no. 6 (2017): 1113–1136, https://doi.org/10.1136/annrheumdis-2016-210713.

3. G. R. Burmester, A. J. Kivitz, H. Kupper, et al., "Efficacy and Safety of Ascending Methotrexate Dose in Combination With Adalimumab: The Randomised CONCERTO Trial," *Annals of the Rheumatic Diseases* 74, no. 6 (2015): 1037–1044, https://doi.org/10.1136/annrheumdis-2013-204769.

4. R. N. Maini, F. C. Breedveld, J. R. Kalden, et al., "Therapeutic Efficacy of Multiple Intravenous Infusions of Anti-Tumor Necrosis Factor Alpha Monoclonal Antibody Combined With Low-Dose Weekly Methotrexate in Rheumatoid Arthritis," *Arthritis and Rheumatism* 41, no. 9 (1998): 1552–1563, https://doi.org/10.1002/1529-0131(199809)41:9<1552::AID-ART5>3.0.CO;2-W.

5. M. Boers, L. Hartman, D. Opris-Belinski, et al., "Low Dose, Add-On Prednisolone in Patients With Rheumatoid Arthritis Aged 65+: The Pragmatic Randomised, Double-Blind Placebo-Controlled GLORIA Trial," *Annals of the Rheumatic Diseases* 81, no. 7 (2022): 925–936, https://doi.org/10.1136/annrheumdis-2021-221957.

6. C. Hua, F. Buttgereit, and B. Combe, "Glucocorticoids in Rheumatoid Arthritis: Current Status and Future Studies," *RMD Open* 6, no. 1 (2020): e000536, https://doi.org/10.1136/rmdopen-2017-000536.

7. F. Wolfe, K. Michaud, and E. M. Dewitt, "Why Results of Clinical Trials and Observational Studies of Antitumour Necrosis Factor (Anti-TNF) Therapy Differ: Methodological and Interpretive Issues," *Annals of the Rheumatic Diseases* 63, no. Suppl 2 (2004): ii13–ii17.

8. K. Lauper, M. Iudici, D. Mongin, et al., "Effectiveness of TNF-Inhibitors, Abatacept, IL6-Inhibitors and JAK-Inhibitors in 31 846 Patients With Rheumatoid Arthritis in 19 Registers From the 'JAK-Pot' Collaboration," *Annals of the Rheumatic Diseases* 81, no. 10 (2022): 1358–1366, https://doi.org/10.1136/annrheumdis-2022-222586.

9. M. Neovius, E. V. Arkema, H. Olsson, et al., "Drug Survival on TNF Inhibitors in Patients With Rheumatoid Arthritis Comparison of Adalimumab, Etanercept and Infliximab," *Annals of the Rheumatic Diseases* 74, no. 2 (2015): 354–360, https://doi.org/10.1136/annrheumdis-2013-204128.

10. K. L. Hyrich, K. D. Watson, M. Lunt, and D. P. Symmons, "Changes in Disease Characteristics and Response Rates Among Patients in the United Kingdom Starting Anti-Tumour Necrosis Factor Therapy for Rheumatoid Arthritis Between 2001 and 2008," *Rheumatology (Oxford, England)* 50, no. 1 (2011): 117–123, https://doi.org/10.1093/rheumatology/keq209.

11. K. Ebina, Y. Etani, Y. Maeda, et al., "Drug Retention of Biologics and Janus Kinase Inhibitors in Patients With Rheumatoid Arthritis: The ANSWER Cohort Study," *RMD Open* 9, no. 3 (2023): e003160, https://doi.org/10.1136/rmdopen-2023-003160.

12. K. Ebina, M. Hashimoto, W. Yamamoto, et al., "Drug Tolerability and Reasons for Discontinuation of Seven Biologics in 4466 Treatment Courses of Rheumatoid Arthritis – The ANSWER Cohort Study," *Arthritis Research and Therapy* 21, no. 1 (2019): 91, https://doi.org/10.1186/s13075-019-1880-4.

13. S. Hayashi, S. Tachibana, T. Maeda, et al., "Real-World Comparative Study of the Efficacy of Janus Kinase Inhibitors in Patients With Rheumatoid Arthritis: The ANSWER Cohort Study," *Rheumatology (Oxford, England)* 63 (2024): 3033–3041, https://doi.org/10.1093/rheumatology/kead543.

14. S. Jinno, A. Onishi, S. Hattori, et al., "Comparison of Retention of Biologics in Japanese Patients With Elderly-Onset Rheumatoid

Arthritis-The ANSWER Cohort Study," *Rheumatology (Oxford, England)* 64, no. 2 (2024): 509–516.

15. Y. Nakayama, R. Watanabe, W. Yamamoto, et al., "IL-6 Inhibitors and JAK Inhibitors as Favourable Treatment Options for Patients With Anaemia and Rheumatoid Arthritis: ANSWER Cohort Study," *Rheumatology (Oxford, England)* 63, no. 2 (2024): 349–357, https://doi.org/10.1093/rheumatology/kead299.

16. H. Yamada, S. Jinno, T. Maeda, et al., "Trends of Disease Activity in Japanese Patients Over 75 Years With Rheumatoid Arthritis From 2014 to 2021 – The ANSWER Cohort Study," *Rheumatology (Oxford, England)* 63 (2023): 2147–2151, https://doi.org/10.1093/rheumatology/kead539.

17. F. C. Arnett, S. M. Edworthy, D. A. Bloch, et al., "The American Rheumatism Association 1987 Revised Criteria for the Classification of Rheumatoid Arthritis," *Arthritis and Rheumatism* 31, no. 3 (1988): 315–324.

18. D. Aletaha, T. Neogi, A. J. Silman, et al., "Rheumatoid Arthritis Classification Criteria: An American College of Rheumatology/European League Against Rheumatism Collaborative Initiative," *Annals of the Rheumatic Diseases* 69, no. 9 (2010): 1580–1588, https://doi.org/10.1136/ard.2010.138461.

19. Y. Kawahito, "Guidelines for the Management of Rheumatoid Arthritis," *Nihon Rinsho* 74, no. 6 (2016): 939–943.

20. R. Koike, M. Harigai, T. Atsumi, et al., "Japan College of Rheumatology 2009 Guidelines for the Use of Tocilizumab, a Humanized Anti-Interleukin-6 Receptor Monoclonal Antibody, in Rheumatoid Arthritis," *Modern Rheumatology* 19, no. 4 (2009): 351–357, https://doi.org/10.1007/s10165-009-0197-6.

21. K. Ebina, T. Hirano, Y. Maeda, et al., "Factors Affecting Drug Retention of Janus Kinase Inhibitors in Patients With Rheumatoid Arthritis: The ANSWER Cohort Study," *Scientific Reports* 12, no. 1 (2022): 134, https://doi.org/10.1038/s41598-021-04075-0.

22. M. Harigai, N. Ishiguro, S. Inokuma, et al., "Postmarketing Surveillance of the Safety and Effectiveness of Abatacept in Japanese Patients With Rheumatoid Arthritis," *Modern Rheumatology* 26, no. 4 (2016): 491–498, https://doi.org/10.3109/14397595.2015.1123211.

23. T. Koike, M. Harigai, S. Inokuma, et al., "Effectiveness and Safety of Tocilizumab: Postmarketing Surveillance of 7901 Patients With Rheumatoid Arthritis in Japan," *Journal of Rheumatology* 41, no. 1 (2014): 15–23, https://doi.org/10.3899/jrheum.130466.

24. K. Ebina, M. Hashimoto, W. Yamamoto, et al., "Drug Tolerability and Reasons for Discontinuation of Seven Biologics in Elderly Patients With Rheumatoid Arthritis – The ANSWER Cohort Study," *PLoS One* 14, no. 5 (2019): e0216624, https://doi.org/10.1371/journal.pone.0216624.

25. K. Ebina, M. Hashimoto, W. Yamamoto, et al., "Drug Retention and Discontinuation Reasons Between Seven Biologics in Patients With Rheumatoid Arthritis – The ANSWER Cohort Study," *PLoS One* 13, no. 3 (2018): e0194130, https://doi.org/10.1371/journal.pone.0194130.

26. S. M. Du Pan, S. Dehler, A. Ciurea, H. R. Ziswiler, C. Gabay, and A. Finckh, "Comparison of Drug Retention Rates and Causes of Drug Discontinuation Between Anti-Tumor Necrosis Factor Agents in Rheumatoid Arthritis," *Arthritis and Rheumatism* 61, no. 5 (2009): 560–568, https://doi.org/10.1002/art.24463.

27. E. G. Favalli, M. Biggioggero, A. Marchesoni, and P. L. Meroni, "Survival on Treatment With Second-Line Biologic Therapy: A Cohort Study Comparing Cycling and Swap Strategies," *Rheumatology (Oxford, England)* 53, no. 9 (2014): 1664–1668, https://doi.org/10.1093/rheumatology/keu158.

28. C. Gabay, M. Riek, A. Scherer, and A. Finckh, "Effectiveness of Biologic DMARDs in Monotherapy Versus in Combination With Synthetic DMARDs in Rheumatoid Arthritis: Data From the Swiss Clinical Quality Management Registry," *Rheumatology (Oxford, England)* 54, no. 9 (2015): 1664–1672, https://doi.org/10.1093/rheumatology/kev019.

29. T. S. Jorgensen, L. E. Kristensen, R. Christensen, et al., "Effectiveness and Drug Adherence of Biologic Monotherapy in Routine Care of Patients With Rheumatoid Arthritis: A Cohort Study of Patients Registered in the Danish Biologics Registry," *Rheumatology (Oxford, England)* 54, no. 12 (2015): 2156–2165, https://doi.org/10.1093/rheumatology/kev216.

30. R. Watanabe, K. Ebina, T. Gon, et al., "Predictive Factors and Treatment Outcomes Associated With Difficult-To-Treat Rheumatoid Arthritis Conditions: The ANSWER Cohort Study," *Rheumatology (Oxford, England)* 63, no. 9 (2024): 2418–2426, https://doi.org/10.1093/rheumatology/keae265.

31. M. Kobayashi, D. Kudo, H. Ohbe, and S. Kushimoto, "Antiplatelet Pretreatment and Mortality in Patients With Severe Sepsis: A Secondary Analysis From a Multicenter, Prospective Survey of Severe Sepsis in Japan," *Journal of Critical Care* 69 (2022): 154015, https://doi.org/10.1016/j.jcrc.2022.154015.

32. D. B. Rubin and N. Schenker, "Multiple Imputation in Health-Care Databases: An Overview and Some Applications," *Statistics in Medicine* 10, no. 4 (1991): 585–598, https://doi.org/10.1002/sim.4780100410.

33. T. Takeuchi, H. Yamanaka, N. Ishiguro, et al., "Adalimumab, a Human Anti-TNF Monoclonal Antibody, Outcome Study for the Prevention of Joint Damage in Japanese Patients With Early Rheumatoid Arthritis: The HOPEFUL 1 Study," *Annals of the Rheumatic Diseases* 73, no. 3 (2014): 536–543, https://doi.org/10.1136/annrheumdis-2012-202433.

34. L. B. van de Putte, C. Atkins, M. Malaise, et al., "Efficacy and Safety of Adalimumab as Monotherapy in Patients With Rheumatoid Arthritis for Whom Previous Disease Modifying Antirheumatic Drug Treatment has Failed," *Annals of the Rheumatic Diseases* 63, no. 5 (2004): 508–516, https://doi.org/10.1136/ard.2003.013052.

35. Y. Degboe, M. Schiff, M. Weinblatt, R. Fleischmann, H. A. Ahmad, and A. Constantin, "Background Glucocorticoid Therapy has No Impact on Efficacy and Safety of Abatacept or Adalimumab in Patients with Rheumatoid Arthritis," *Journal of Clinical Medicine* 9, no. 6 (2020): 2017, https://doi.org/10.3390/jcm9062017.

36. T. Takeuchi, M. Harigai, Y. Tanaka, et al., "Golimumab Monotherapy in Japanese Patients With Active Rheumatoid Arthritis Despite Prior Treatment With Disease-Modifying Antirheumatic Drugs: Results of the Phase 2/3, Multicentre, Randomised, Double-Blind, Placebo-Controlled GO-MONO Study Through 24 Weeks," *Annals of the Rheumatic Diseases* 72, no. 9 (2013): 1488–1495, https://doi.org/10.1136/annrheumdis-2012-201796.

37. P. Emery, R. Fleischmann, D. van der Heijde, et al., "The Effects of Golimumab on Radiographic Progression in Rheumatoid Arthritis: Results of Randomized Controlled Studies of Golimumab Before Methotrexate Therapy and Golimumab After Methotrexate Therapy," *Arthritis and Rheumatism* 63, no. 5 (2011): 1200–1210, https://doi.org/10.1002/art.30263.

38. D. van der Heijde, L. Klareskog, V. Rodriguez-Valverde, et al., "Comparison of Etanercept and Methotrexate, Alone and Combined, in the Treatment of Rheumatoid Arthritis: Two-Year Clinical and Radiographic Results From the TEMPO Study, a Double-Blind, Randomized Trial," *Arthritis and Rheumatism* 54, no. 4 (2006): 1063–1074, https://doi.org/10.1002/art.21655.

39. T. Koike, M. Harigai, S. Inokuma, et al., "Safety and Effectiveness of 6 Months' Etanercept Monotherapy and Combination Therapy in Japanese Patients With Rheumatoid Arthritis: Effect of Concomitant Disease-Modifying Antirheumatic Drugs," *Journal of Rheumatology* 40, no. 10 (2013): 1658–1668, https://doi.org/10.3899/jrheum.120490.

40. P. J. Mease, "Certolizumab Pegol in the Treatment of Rheumatoid Arthritis: A Comprehensive Review of Its Clinical Efficacy and Safety,"

Rheumatology (Oxford, England) 50, no. 2 (2011): 261–270, https://doi.org/10.1093/rheumatology/keq285.

41. Y. Tanaka, T. Matsubara, K. Hashizume, N. Amano, and T. Takeuchi, "Efficacy and Safety of Abatacept in Biologic-Naive Patients With Active Rheumatoid Arthritis by Background Methotrexate Dose: Post Hoc Analysis of a Randomized, Placebo-Controlled, Phase 4 Study," *Modern Rheumatology* 32, no. 3 (2022): 500–507, https://doi.org/10.1093/mr/roab029.

42. G. R. Burmester, E. Choy, A. Kivitz, et al., "Low Immunogenicity of Tocilizumab in Patients With Rheumatoid Arthritis," *Annals of the Rheumatic Diseases* 76, no. 6 (2017): 1078–1085, https://doi.org/10.1136/annrheumdis-2016-210297.

43. M. Safy-Khan, J. W. G. Jacobs, M. J. H. de Hair, et al., "Effect on Efficacy and Safety Trial Outcomes of Also Enrolling Patients on Ongoing Glucocorticoid Therapy in Rheumatoid Arthritis Clinical Trials of Tocilizumab or Adalimumab or Methotrexate Monotherapy," *Annals of the Rheumatic Diseases* 79, no. 4 (2020): 460–463, https://doi.org/10.1136/annrheumdis-2019-216537.

44. R. Fleischmann, E. Mysler, S. Hall, et al., "Efficacy and Safety of Tofacitinib Monotherapy, Tofacitinib With Methotrexate, and Adalimumab With Methotrexate in Patients With Rheumatoid Arthritis (ORAL Strategy): A Phase 3b/4, Double-Blind, Head-To-Head, Randomised Controlled Trial," *Lancet* 390, no. 10093 (2017): 457–468, https://doi.org/10.1016/S0140-6736(17)31618-5.

45. V. Strand, E. Mysler, R. J. Moots, et al., "Patient-Reported Outcomes for Tofacitinib With and Without Methotrexate, or Adalimumab With Methotrexate, in Rheumatoid Arthritis: A Phase IIIB/IV Trial," *RMD Open* 5, no. 2 (2019): e001040, https://doi.org/10.1136/rmdopen-2019-001040.

46. T. Takeuchi, H. Yamanaka, K. Yamaoka, et al., "Efficacy and Safety of Tofacitinib in Japanese Patients With Rheumatoid Arthritis by Background Methotrexate Dose: A Post Hoc Analysis of Clinical Trial Data," *Modern Rheumatology* 29, no. 5 (2019): 756–766, https://doi.org/10.1080/14397595.2018.1553489.

47. C. Charles-Schoeman, D. van der Heijde, G. R. Burmester, et al., "Effect of Glucocorticoids on the Clinical and Radiographic Efficacy of Tofacitinib in Patients With Rheumatoid Arthritis: A Posthoc Analysis of Data From 6 Phase III Studies," *Journal of Rheumatology* 45, no. 2 (2018): 177–187, https://doi.org/10.3899/jrheum.170486.

48. C. Takahashi, Y. Kaneko, Y. Okano, et al., "Association of Erythrocyte Methotrexate-Polyglutamate Levels With the Efficacy and Hepatotoxicity of Methotrexate in Patients With Rheumatoid Arthritis: A 76-Week Prospective Study," *RMD Open* 3, no. 1 (2017): e000363, https://doi.org/10.1136/rmdopen-2016-000363.

Supporting Information

Additional supporting information can be found online in the Supporting Information section.

LETTER TO THE EDITOR

Clinical Characteristics and Risk Factors for Lupus Nephritis in Tunisian Patients With Systemic Lupus Erythematosus

Mourad Elghali[1] 🟢 | Imene Chaabane[2] | Marwa Cherichi[2] | Mahbouba Jguirim[3] | Nabil Sakly[1,4] | Sonia Hammami[2,5]

[1]Laboratory of Immunology FB Monastir, University of Monastir, Monastir, Tunisia | [2]Department of Internal Medicine FB Monastir, University of Monastir, Monastir, Tunisia | [3]Department of Rheumatology FB Monastir, University of Monastir, Monastir, Tunisia | [4]Laboratory of Medical and Molecular Parasitology-Mycology (Code LR12ES08), Department of Clinical Biology B, Faculty of Pharmacy, University of Monastir, Monastir, Tunisia | [5]Research Laboratory LR12ES05, Lab-NAFS 'Nutrition – Functional Food & Health', Faculty of Medicine Monastir, University of Monastir, Monastir, Tunisia

Correspondence: Mourad Elghali (mouradghali3@gmail.com)

Dear Editor,

Systemic lupus erythematosus (SLE) is a common connective tissue disease characterized by pleomorphic clinical expression and production of antinuclear antibodies (ANA) [1]. Statistics on SLE epidemiology in Africa remain rare and unavailable. Rees et al. estimated in their systematic review that the incidence of SLE in Africa is 0.3/100 000 person-years [2]. Lupus nephritis (LN) is one of the most serious manifestations of SLE and refers to the development of renal tissue inflammation responsible for glomerular, vascular, and/or tubulointerstitial lesions [1]. Most Tunisian and African studies on LN have focused on the clinical aspects, management, or prognostic factors of the disease, but very few have sought to identify the risk factors associated with the development of LN in patients with SLE [3, 4]. Therefore, we conducted a retrospective study to investigate the clinical, biological, and histological presentations of patients with LN at the time of diagnosis of the disease and to determine the risk factors for developing this complication in Tunisian patients with SLE.

In this retrospective study, we reviewed the medical records of 138 SLE patients recruited from the internal medicine and rheumatology departments of Fattouma Bourguiba University Hospital in Monastir between January 2000 and December 2022. The features were collected at the time of the diagnosis. The inclusion criteria were any patient who fulfilled at least four of the 1997 American College of Rheumatology (ACR) criteria or the 2012 Systemic Lupus Erythematosus International Collaborating Clinics (SLICC) criteria for SLE classification. We excluded all patients who had been diagnosed with incomplete SLE without going on to develop the disease, patients without follow-up, or patients in whom anti-double-stranded DNA (dsDNA) were positive only with an enzyme-linked immunosorbent assay (ELISA) without confirmation with an indirect immunofluorescence (IIF) assay using *Crithidia luciliae* slides (CLIF). Neuropsychiatric SLE (NPSLE) manifestations were classified according to the ACR 1999 nomenclature. Disease activity was measured using the SLE Disease Score Index 2000 (SLEDAI 2k).

The diagnosis of LN was exclusively histological through renal puncture biopsy (RPB). RPB indications were as follows: an acute increase in serum creatinine level (26.4 µmol/L or more within 48 h), proteinuria > 500 mg/24 h, presence of figured blood in the urinary sediment (> 5 red blood cells per field), nephrotic (presence of edema, proteinuria ≥ 3 g/day, and a serum

albumin level < 3.5 g/dL), or nephritic syndrome (presence of hematuria, elevated creatinine serum levels, and edema and/or elevated blood pressure).

Absolute contraindications to RPB included a major bleeding risk, an uncontrollable severe high blood pressure, an active renal or perirenal infection, the presence of a solitary kidney, and the patient's refusal to undergo a kidney biopsy.

RPB was performed after ultrasound identification under local anesthesia. All samples obtained were subjected to a conventional histological study using light microscopy and immunofluorescence by the same pathologist. After diagnosis, we periodically checked all relevant kidney parameters for all our patients.

We divided LN patients into three groups according to the results of RPB: Group 1 (G1, $n = 6$), including patients with class I and II LN; Group 2 (G2, $n = 23$), including patients with class III and IV LN; and Group 3 (G3 = 7), including patients with class V LN. This classification stems from large clinical studies [5] and histopathological reviews [6], highlighting the importance of separating patients with proliferative lesions (class III/IV LN) from those with non-proliferative lesions (mesangial class I + II, membranous class V). All statistical analyses were performed using SPSS for Windows (version 21; SPSS, Chicago, IL, USA). A p value (asymptotic significance [two-sided]) < 0.05 was defined as statistically significant.

The mean age at the time of SLE diagnosis was 38.9 ± 15 years. Women constituted 88.4% ($n = 122$) of all the patients, with a sex ratio of man/women = 0.1. In our study, RPB was performed in 37 patients; 36 patients (26.1%) had LN, of whom 36.2% had class IV LN. Only one patient was diagnosed with LN during the follow-up of patients with SLE. The comparison between SLE patients according to the presence of LN (Table 1) showed that cases with LN were younger than cases without LN (33.6 ± 14.3 years vs. 40.7 ± 14.9 years, $p = 0.014$), and they presented principally with a higher frequency of high titers of ANA (17/25 [68%] vs. 31/87 [35.6%], $p = 0.004$), anti-dsDNA (25/33 [75.8%] vs. 38/95 [40%], $p \leq 0.001$), anti-Sm (14/33 [42.4%] vs. 15/96 [15.6%], $p \leq 0.001$), anti-SSA (18/33 [54.5%] vs. 33/96 [34.4%], $p = 0.041$), and need for immunosuppressive drugs (22/36 [61.1%] vs. 31/101 [30.7%], $p \leq 0.001$). These patients also presented with higher levels of SLEDAI (14 vs. 6, $p \leq 0.001$).

The comparison between Group 1 (patients with class I and II LN), Group 2 (patients with class III and IV LN), and Group 3 (patients with class V LN) resumed in Table 1 showed that G1 had the highest positivity of anti-dsDNA (5/6 [83.3%] vs. 18/23 [78.3%] vs. 2/7 [28.6%], $p = 0.027$) and anti-nucleosome antibodies (5/6 [83.3%] vs. 11/23 [47.8%] vs. 0/7, $p = 0.013$). However, G2 showed the highest levels of creatininemia (63.5 vs. 97 vs. 56 μmol/L, $p = 0.036$) and G3 showed the highest levels of daily proteinuria (1 vs. 1.9 vs. 3 g/day, $p = 0.036$). After binary logistic regression analysis (Table 2), we found that high titers of ANA ($p = 0.009$, OR = 4.708, 95% CI = 1.470–15.075), anti-dsDNA positivity ($p = 0.029$, OR = 3.809, 95% CI = 1.144–12.682), and a high

SLEDAI score ($p \leq 0.001$, OR = 1.185, 95% CI = 1.082–1.298) were associated with LN development.

Our study is among the few Tunisian case–control studies (SLE with or without LN) to explore factors associated with LN in patients with SLE [7, 8]. We found that the prevalence of LN in our patients was 26.1%. A recent review showed that LN prevalence at the time of SLE diagnosis ranged from 7% to 31%, with the lower range derived from studies that relied on biopsy confirmation alone [9].

In our study, LN was associated with immunological abnormalities, particularly anti-dsDNA, anti-Sm, and anti-SSA. Although anti-dsDNA has been reported to be associated with LN [10], the association between LN and anti-Sm or anti-SSA (Ro) remains controversial. While Alba et al. reported that anti-Sm but not anti-SSA (Ro) was associated with LN [11], Li et al. found that anti-SSA (Ro) but not anti-Sm was associated with LN [12].

Regarding the comparison between LN classes, Mavragani et al. reported that patients with classes III and IV LN had more positive anti-dsDNA antibodies and increased levels of creatinine and that patients with class V LN had the highest levels of severe proteinuria (> 3 g/L) [5]. It is known that anti-dsDNA and anti-nucleosomes come early during the disease course and might disappear later [13], which supports our results regarding the association of these antibodies with early classes of LN. Moreover, the literature reports that, although classes I and II are characterized by minimal urinary abnormalities, LN patients with classes III and IV have more renal insufficiency and patients with class V have more nephrotic proteinuria [14].

In our study, we reported that anti-dsDNA antibodies, high titers of ANA, and a high disease activity score were risk factors for developing LN in patients with SLE. To the best of our knowledge, our results are the first on the African and Arab scales to approach the literature data. In fact, the interconnection between the titers of ANA and anti-dsDNA antibodies and the disease activity score is logical. Usually, the quantification of anti-dsDNA is performed by ELISA, and it has been recently reported that high levels of this antibody can predict LN, disease activity, and flare [15]. In contrast, the only African study (from Tunisia) that investigated risk factors for developing LN found that young age (≤ 34 years) was the only predictor of LN [8]. These differences may be due to the time of diagnosis of LN (follow-up) and the variation of tools used to identify LN (urinary abnormalities) or assess immunological biomarkers (not defined).

In conclusion, despite some technical limitations such as interpretation of the RPB by a single pathologist, and statistical and histopathological limitations such as the small number of analyzed LN biopsies and the absence of histological data of activity (NIH activity and chronicity index), our study showed that anti-dsDNA antibodies, high titers of ANA, and a high disease activity score were risk factors for developing LN in patients with SLE. Conducting genetic investigation might be of great interest to elucidate other risk factors for developing LN in our population.

TABLE 1 | Clinical, biological, therapeutic, and follow-up comparisons between patients according to the presence of lupus nephritis.

Features	Patients with LN (n=36)[a]				Patients without LN (n=102)[a]	p	p*
	G1*[b] (n=6)	G2*[b] (n=23)	G3*[b] (n=7)	All LN			
Age (years)	34.8±11.5	31.3±15.2	40.4±12.3	33.6±14.3	40.7±14.9	**0.014**	0.337
Old SLE (>50 years)	0	5 (21.7)	2 (28.6)	7 (19.4)	30 (29.4)	0.246	0.387
Sex, n (%)	4 (66.7)	20 (87)	7 (100)	31 (86.1)	91 (89.2)	0.219	0.219
Diabetes, n (%)	0	2 (8.7)	2 (28.6)	4 (11.1)	4 (3.9)	0.206	0.218
Hypertension, n (%)	0	3 (13)	2 (28.6)	5 (13.9)	8 (7.8)	0.286	0.326
Cutaneous features, n (%)	3 (50)	16 (69.6)	3 (42.9)	22 (61.1)	58 (56.9)	0.657	0.371
Malar rash	2 (33.3)	9 (39.1)	3 (42.9)	14 (38.9)	31 (30.4)	0.350	0.939
Discoid lupus	1 (16.7)	1 (4.3)	0	2 (5.6)	4 (3.9)	0.679	0.389
Ulcerations	0	4 (17.4)	0	4 (11.1)	10 (9.8)	0.522	0.28
Photosensitivity	3 (50)	11 (47.8)	2 (28.6)	16 (44.4)	32 (31.4)	0.157	0.639
Alopecia	1 (16.7)	4 (17.4)	0	5 (13.9)	21 (20.6)	0.377	0.496
Serositis, n (%)	1 (16.7)	9 (39.1)	0	10 (27.8)	11 (10.8)	**0.015**	0.103
Pleural effusion	1 (16.7)	8 (34.8)	0	9 (25)	8 (7.8)	**0.007**	0.155
Pericarditis	1 (16.7)	8 (34.8)	0	9 (25)	6 (5.9)	**0.002**	0.155
Thrombosis, n (%)	3 (18.8)	3 (13)	0	3 (18.8)	3 (2.9)	0.076	0.637
Nephrotic syndrome, n (%)	0	5 (21.7)	4 (57.1)	9 (25)	0 (0)	**≤0.001**	0.05
Nephritic syndrome, n (%)	0	7 (38.9)	1 (16.7)	8 (22.2)	1 (0.9)	**≤0.001**	0.228
Arthritis, n (%)	3 (50)	7 (38.9)	4 (57.1)	14 (38.9)	48 (47.1)	0.397	0.371
NPSLE, n (%)	2 (33.3)	5 (21.7)	3 (42.9)	10 (27.8)	27 (26.5)	0.879	0.521
Inflammation laboratory disorders							
Erythrocyte sedimentation rate (mm/1st hour)	77.8±51.2	101.3±43.3	76.4±52.8	92.5±46.3	63.9±37.1	**≤0.001**	0.4
C-reactive protein (mg/L)	50.1 [5–82]	16 [3.9–69.3]	6 [2.4–12]	13 [4–63.7]	13 [2.5–39.4]	0.424	0.272
Kidney laboratory disorders							
Creatininemia (μmol/L)	63.5 [58.5–76.7]	97 [77–129.2]	56 [51.5–99]	92.5 [58.5–111.7]	64 [52.7–74]	**≤0.001**	**0.036**
Creatinine clearance (mL/min/1.72 m²)	102.3 [82.1–125.6]	65 [43–104.8]	115.1 [58.1–119.1]	78.4 [51.6–113.8]	98.5 [83.8–124.4]	**0.003**	0.127
Daily proteinuria (g/24h)	1 [0.7–1.7]	1.9 [1.3–2.7]	3 [1.5–3.4]	1.8 [1.2–2.9]	0.15 [0.07–0.24]	**≤0.001**	**0.036**
Hematological disorders, n (%)							
Anemia	5 (83.3)	21 (91.3)	5 (71.4)	31 (86.1)	66 (64.7)	**0.016**	0.403

(Continues)

TABLE 1 | (Continued)

Features	Patients with LN (n = 36)[a]				Patients without LN (n = 102)[a]	p	p*
	G1*[b] (n = 6)	G2*[b] (n = 23)	G3*[b] (n = 7)	All LN			
Leukopenia	2 (33.3)	12 (52.2)	4 (57.1)	18 (50)	29 (28.4)	**0.019**	0.653
Lymphopenia	4 (66.7)	8 (34.8)	4 (57.1)	16 (44.4)	34 (33.3)	0.233	0.283
Thrombopenia	0	8 (34.8)	2 (28.6)	10 (27.8)	12 (11.8)	**0.024**	0.238
ANA, n (%)	5 (83.3)	100 (100)	100 (100)	35 (97.2)	101 (99)	0.455	0.076
High titers (≥ 1600)	3 (60)	11 (68.8)	4 (80)	17 (47.2)	31 (35.6)	**0.005**	0.789
Anti ds-DNA	5 (83.3)	18 (85.7)	2 (33.3)	25 (75.8)	38 (40)	**≤0.001**	**0.027**
Anti-Sm	2 (33.3)	9 (42.9)	3 (50)	14 (42.2)	15 (15.6)	**≤0.001**	0.841
Anti-Sm/RNP	4 (66.7)	11 (52.4)	2 (33.3)	17 (51.5)	25 (26)	**0.007**	0.509
Anti-SSA/Ro	4 (66.7)	12 (57.1)	2 (33.3)	18 (54.4)	33 (34.4)	**0.041**	0.472
Anti-SSB/La	1 (16.7)	6 (28.6)	2 (33.3)	9 (27.3)	17 (17.7)	0.237	0.791
Anti-nucleosomes	5 (83.3)	11 (52.4)	0	16 (48.5)	47 (49)	0.963	**0.013**
C3 (g/L)	1.1 ± 0.3	0.7 ± 0.3	0.9	0.8 ± 0.3	1.2 ± 0.3	**≤0.001**	0.37
C4 (g/L)	0.2 ± 0.1	0.14 ± 0.1	0.13	0.16 ± 0.1	0.22 ± 0.1	0.096	0.571
SLEDAI	10 [7–20]	16 [11–21]	12 [9–18]	14 [9.2–20.7]	6 [4–11.2]	**≤0.001**	0.202
Corticotherapy, n (%)	6 (100)	23 (100)	7 (100)	36 (100)	72 (71.3)	**≤0.001**	
High dose (1 mg/Kg)	1 (16.7)	8 (34.8)	5 (71.4)	14 (38.9)	14 (13.9)	**0.004**	0.104
Bolus	6 (100)	22 (95.7)	7 (100)	35 (97.2)	19 (18.8)	**≤0.001**	0.748
Immunosuppressive drugs, n (%)	1 (16.7)	16 (69.6)	5 (71.4)	22 (61.1)	31 (30.7)	**≤0.001**	0.05
Cyclophosphamide	0	12 (52.2)	4 (57.1)	16 (44.4)	9 (9)	**≤0.001**	0.055
Azathioprine	0	4 (17.4)	3 (42.9)	7 (19.4)	5 (5)	**0.016**	0.138
Mycophenolate mofetil	0	8 (34.8)	2 (28.6)	10 (27.8)	0 (0)	**≤0.001**	0.238
Follow-up complications, n (%)							
Infections	3 (50)	5 (21.7)	1 (14.3)	9 (25)	12 (11.8)	0.057	0.278
Proteinuria persistence	1 (16.7)	2 (2.7)	2 (28.6)	5 (13.9)	1 (1)	**0.005**	0.403

Note: Serositis: pleural effusion and/or pericarditis; nephrotic syndrome: presence of edema, proteinuria ≥ 3 g/day, and a serum albumin level l < 3.5 g/dL; nephritic syndrome: presence of hematuria and elevated creatinine serum levels and edema or elevated blood pressure; C3 (normal range: 0.81–1.57 g/L) and C4 (normal range: 0.13–0.39 g/L) fractions. *p*: Comparison between SLE patients with and without LN. *p**: Comparison between I + II versus III + IV versus V classes. Bold values refer to significant associations (*p*-value < 0.05).

Abbreviations: ANA, anti-nuclear antibodies; CRP, C-reactive protein; ds, double stranded; LN, lupus nephritis; NPSLE, neuropsychiatric SLE; SLE, systemic lupus erythematosus; SLEDAI, SLE disease activity index.

[a] Comparisons between SLE patients with and without LN were performed using the chi-square test or the Fisher exact test when appropriate for qualitative variables and the Student's *t*-test (when data followed a normal distribution) or Mann–Whitney *U* test (when the distribution was non-normal) for quantitative variables, according to the normality test results (Kolmogorov–Smirnov test).

[b] Comparisons between G1, G2, and G3 were performed using the Chi square test or the Fisher exact test when appropriate for qualitative variables and one-way ANOVA (when data followed a normal distribution) or Kruskal–Wallis test (when the distribution was non-normal) for quantitative variables, according to the normality tests results (Kolmogorov–Smirnov test).

TABLE 2 | Risk factors associated with lupus nephritis.

Features	Univariate *p*	Multivariate *p*	Multivariate OR (95% CI)
Age	0.454		
Old SLE (> 50 years)	0.136		
Diabetes	0.057		
Photosensitivity	0.455		
Pleural effusion	0.129		
Pericarditis	0.225		
Serositis	0.14		
Thrombosis	0.802		
Erythrocytes sedimentation rate	0.408		
High titers of ANA (> 1600)	**0.012**	**0.009**	4.708 (1.470–15.075)
Anti-dsDNA	**0.032**	**0.029**	3.809 (1.144–12.682)
Anti-Sm	0.396		
Anti-Sm/RNP	0.054		
Anti-SSA/Ro	0.606		
C3	**0.018**	0.082	
Anemia	0.825		
Leucopenia	**0.021**	0.109	
Lymphopenia	0.081		
Thrombopenia	0.089		
SLEDAI	**0.017**	**≤ 0.001**	1.185 (1.082–1.298)

Note: Serositis: pleural effusion and/or pericarditis. *p*: Risk factors for LN development were determined using univariate and multivariate binary logistic regression analyses. Variables with $p \leq 0.25$ were introduced for the univariate analysis. Variables with $p < 0.05$ in the univariate analysis were included in the multivariate analyses. Bold values refer to significant associations (p-value < 0.05).
Abbreviations: ANA, anti-nuclear antibodies; ds, double stranded; SLE, systemic lupus erythematosus; SLEDAI: SLE disease activity index.

Author Contributions

All the authors participated in the data collection. M.E. and N.S. were responsible for the conception, design, analysis, and interpretation of the data. M.E. and N.S. wrote the manuscript, and the other authors revised it critically for intellectual content. All authors approved the final version.

Ethics Statement

This study was conducted in accordance with the guidelines of the Declaration of Helsinki. The ethics committee of the Hospital of Fattouma Bourguiba Monastir confirmed that no ethical approval was required.

Consent

Written informed consent was obtained from all patients for publication of details of their medical cases.

Conflicts of Interest

The authors declare no conflicts of interest.

Data Availability Statement

The datasets generated during and/or analyzed during the current study are available from the corresponding author on reasonable request.

Mourad Elghali
Imene Chaabane
Marwa Cherichi
Mahbouba Jguirim
Nabil Sakly
Sonia Hammami

References

1. N. Alforaih, L. Whittall-Garcia, and Z. Touma, "A Review of Lupus Nephritis," *Journal of Applied Laboratory Medicine* 7, no. 6 (2022): 1450–1467.

2. F. Rees, M. Doherty, M. J. Grainge, P. Lanyon, and W. Zhang, "The Worldwide Incidence and Prevalence of Systemic Lupus Erythematosus: A Systematic Review of Epidemiological Studies," *Rheumatology (Oxford, England)* 56, no. 11 (2017): 1945–1961.

3. A. Boussetta, D. Louati, M. Jellouli, et al., "Lupus Nephritis in Tunisian Children: Predictive Factors of Poor Outcomes," *Saudi Journal of Kidney Diseases and Transplantation* 33, no. 3 (2022): 440–448.

4. O. I. Ameh, A. P. Kengne, D. Jayne, et al., "Standard of Treatment and Outcomes of Adults With Lupus Nephritis in Africa: A Systematic Review," *Lupus* 25, no. 11 (2016): 1269–1277.

5. C. P. Mavragani, G. E. Fragoulis, G. Somarakis, A. Drosos, A. G. Tzioufas, and H. M. Moutsopoulos, "Clinical and Laboratory Predictors of Distinct Histopathogical Features of Lupus Nephritis," *Medicine (Baltimore)* 94, no. 21 (2015): e829.

6. S. Rodriguez-Ramirez, N. Wiegley, and J. M. Mejia-Vilet, "Kidney Biopsy in Management of Lupus Nephritis: A Case-Based Narrative Review," *Kidney Medicine* 6, no. 2 (2023): 100772.

7. M. H. Houman, M. Smiti-Khanfir, I. Ben Ghorbell, and M. Miled, "Systemic Lupus Erythematosus in Tunisia: Demographic and Clinical Analysis of 100 Patients," *Lupus* 13, no. 3 (2004): 204–211.

8. M. Somai, F. Daoud, I. Rachdi, et al., "Predictive Factors of the Lupus Nephritis in a Tunisian Cohort," *La Tunisie Médicale* 97, no. 12 (2019): 1399–1406.

9. A. Mahajan, J. Amelio, K. Gairy, et al., "Systemic Lupus Erythematosus, Lupus Nephritis and End-Stage Renal Disease: A Pragmatic Review Mapping Disease Severity and Progression," *Lupus* 29, no. 9 (2020): 1011–1020.

10. J. M. Shin, D. Kim, Y. C. Kwon, et al., "Clinical and Genetic Risk Factors Associated With the Presence of Lupus Nephritis," *Journal of Rheumatic Diseases* 28, no. 3 (2021): 150–158.

11. P. Alba, L. Bento, M. J. Cuadrado, et al., "Anti-dsDNA, Anti-Sm Antibodies, and the Lupus Anticoagulant: Significant Factors Associated With Lupus Nephritis," *Annals of the Rheumatic Diseases* 62, no. 6 (2003): 556–560.

12. J. Li, X. Leng, Z. Li, et al., "Chinese SLE Treatment and Research Group Registry: III. Association of Autoantibodies With Clinical Manifestations in Chinese Patients With Systemic Lupus Erythematosus," *Journal of Immunology Research* 2014 (2014): 809389.

13. O. P. Rekvig, J. van der Vlag, and N. Seredkina, "Review: Antinucleosome Antibodies: A Critical Reflection on Their Specificities and Diagnostic Impact," *Arthritis & Rhematology* 66, no. 5 (2014): 1061–1069.

14. C. W. Devadass, V. V. Mysorekar, M. Eshwarappa, L. Mekala, M. G. Siddaiah, and K. G. Channabasappa, "Clinical Features and Histological Patterns of Lupus Nephritis in a Single Center of South India," *Saudi Journal of Kidney Diseases and Transplantation* 27, no. 6 (2016): 1224–1230.

15. Y. Renaudineau, W. Brooks, and J. Belliere, "Lupus Nephritis Risk Factors and Biomarkers: An Update," *International Journal of Molecular Sciences* 24, no. 19 (2023): 14526.

WILEY

LETTER TO THE EDITOR

Case Report: Atypical Form of Jaccoud's Arthropathy With Distal Interphalangeal Joints Dislocation

Maria de Lourdes Castro de Oliveira Figueiroa[1] | Izabela Prado Viana[2] | Anna Paula Mota Duque Sousa[2] | Ana Luisa Souza Pedreira[1] | Mittermayer Barreto Santiago[1,2]

[1]Escola Bahiana de Medicina e Saúde Pública, Salvador, BA, Brazil | [2]Hospital Universitário Professor Edgard Santos, UFBA, Salvador, BA, Brazil

Correspondence: Mittermayer Barreto Santiago (mbsantiago2014@gmail.com)

Received: 1 December 2024 | **Revised:** 19 May 2025 | **Accepted:** 17 June 2025

Dear Editor,

Jaccoud's arthropathy (JA) is marked by reducible joint deformities, such as swan neck, thumb subluxation, ulnar deviation, and boutonniere deformities, similar to those seen in rheumatoid arthritis (RA), but without bone erosions on radiographs. Initially described in rheumatic fever patients, JA is now more commonly observed in systemic lupus erythematosus (SLE) patients. Besides SLE, other diffuse connective tissue diseases may present with similar joint deformities. Sjögren's syndrome, systemic sclerosis, dermatomyositis, and mixed connective tissue disease have all been associated with JA-like deformities [1].

While JA deformities are typically mild to moderate and often under-recognized, some cases can progress to a "severe" or "*mutilans*" form, despite standard treatment [2].

Here, we report a case of atypical JA, presenting with subluxation of the distal interphalangeal (DIP) joints in the context of secondary hyperparathyroidism.

A 41-year-old female was diagnosed with SLE in 2005, presenting with alopecia, photosensitivity, oral ulcers, nephritis, anti-dsDNA, antinuclear antibodies positivity, and low complement levels. Despite treatment with corticosteroids, hydroxychloroquine, cyclophosphamide, and azathioprine, she developed end-stage renal failure and began dialysis in 2016. Examination revealed reversible swan neck deformities and subluxation of the second DIP joints (Figure 1A), with no other notable findings.

Laboratory tests showed renal dysfunction (creatinine 5.8 mg/dL—reference < 1.2 mg/dL, urea 80 mg/dL—reference < 40 mg/dL) and normocytic normochromic anemia (hemoglobin 10.2 g/dL—reference > 12 g/dL). White blood cell and platelet count were normal. Elevated parathyroid hormone (PTH) levels (282 pg/mL—reference 12–88 pg/mL) were noted, although calcium, magnesium, and phosphorus levels were normal at the time of the clinical evaluation. Radiographs showed reduced joint space and subluxation of the second DIP joints bilaterally, without bone erosion (Figure 1B). The power Doppler ultrasound of the hands showed no erosions or synovitis. During 3 years of follow-up of the patient, the deformities remained stable.

The pathophysiology of JA is not fully understood but may involve ligament and joint capsule laxity, joint tissue fibrosis, and hypermobility. Hyperparathyroidism has been proposed as another contributing factor. Babini et al. suggested that increased PTH levels, as seen in renal failure patients like ours, might lead to collagenase activity, resulting in ligament and tendon laxity and subsequent joint deformities [3].

Musculoskeletal manifestations of hyperparathyroidism typically include bone pain, arthralgias, chondrocalcinosis, Milwaukee shoulder, pseudoclubbing, fibrocystic osteitis, and brown tumor. JA is a rare manifestation, seen in 1% of patients, according to Pappu et al. [4]. This report presents the first description of atypical JA with DIP joint involvement secondary to hyperparathyroidism. The DIP joint involvement may represent either an underrecognized manifestation within the JA spectrum or a clinical overlap with other deforming arthropathies, potentially triggered by metabolic abnormalities like chronic PTH elevation.

There have been reports of multiple DIP joint dislocations associated with Sjogren's syndrome, interstitial lung disease, and anti-SSA/Jo1 antibodies, described as a "new syndrome" [5]. Additionally, DIP joint subluxations without bone erosions have

FIGURE 1 | (A) Swan-neck deformity and subluxation of the second right distal interphalangeal joints, more prominent on the right hand. (B) Plain radiograph showing subluxation of the second distal interphalangeal joints but not bone erosion.

been noted in inflammatory myopathy patients with anti-Jo1 antibodies [6]. However, our patient had no muscle weakness, xerostomia, or xerophthalmia, and anti-SSA/Ro antibodies were negative.

In conclusion, secondary hyperparathyroidism due to chronic renal failure should be considered as a contributing factor, acting synergistically with autoimmunity, to promote atypical patterns of joint deformity in SLE patients. Whether DIP joint subluxations are part of a "new syndrome" in diffuse connective tissue diseases remains to be determined.

Conflicts of Interest

The authors declare no conflicts of interest.

Data Availability Statement

Data sharing is not applicable to this article as no new data were created or analyzed in this study.

Maria de Lourdes Castro de Oliveira Figueiroa
Izabela Prado Viana
Anna Paula Mota Duque Sousa
Ana Luisa Souza Pedreira
Mittermayer Barreto Santiago

References

1. M. B. Santiago, "Jaccoud-Type Lupus Arthropathy," *Lupus* 31, no. 4 (2022): 398–406, https://doi.org/10.1177/09612033221082908.

2. M. B. Santiago, V. Machicado, and D. S. Ribeiro, ""Mutilans-Type" Jaccoud Arthropathy," *Journal of Rheumatology* 42, no. 4 (2015): 725–726.

3. S. M. Babini, J. A. Cocco, M. de la Sota, et al., "Tendinous Laxity and Jaccoud's Syndrome in Patients With Systemic Lupus Erythematosus: Possible Role of Secondary Hyperparathyroidism," *Journal of Rheumatology* 16, no. 4 (1989): 494–498.

4. R. Pappu, S. A. Jabbour, A. M. Reginato, and A. J. Reginato, "Musculoskeletal Manifestations of Primary Hyperparathyroidism," *Clinical Rheumatology* 35, no. 12 (2016): 3081–3087. Erratum in: Clin Rheumatol. 2017;36(3):735.

5. Y. Nanke, S. Kotake, H. Akama, and N. Kamatani, "A New Syndrome: Multiple Dislocations of Distal Interphalangeal Joints Associated With Interstitial Pneumonia, Sjögren's Syndrome, and Positive Autoantibodies," *Modern Rheumatology* 13, no. 2 (2003): 103–106.

6. C. V. Oddis, T. A. Medsger, Jr., and L. A. Cooperstein, "A Subluxing Arthropathy Associated With the Anti-Jo-1 Antibody in Polymyositis/Dermatomyositis," *Arthritis and Rheumatism* 33, no. 11 (1990): 1640–1645.

International Journal of
Rheumatic Diseases

ORIGINAL ARTICLE

Evaluation of Vertebrae in Patients With Ankylosing Spondylitis Using Hounsfield Unit Values

Junya Hasegawa[1] | Mochihito Suzuki[1] | Kenji Kishimoto[2] | Ryo Sato[1] | Yusuke Ohno[1] | Takaya Sugiura[1] | Hiroto Yamamoto[1] | Kenya Terabe[1] | Shuji Asai[1] | Shiro Imagama[1]

[1]Department of Orthopedic Surgery and Rheumatology, Nagoya University Graduate School of Medicine, Aichi, Japan | [2]Department of Orthopedic Surgery, Kishimoto Clinic, Aichi, Japan

Correspondence: Mochihito Suzuki (suzuki.mochihito.z9@f.mail.nagoya-u.ac.jp)

ABSTRACT

Objective: To evaluate vertebral Hounsfield Unit (HU) values on computed tomography (CT) in patients with ankylosing spondylitis (AS) compared to patients without AS and to examine differences in HU values between ankylosed and nonankylosed vertebrae in patients with AS.

Methods: This cross-sectional study included 34 patients with AS and 73 patients without AS who underwent spinal CT between 2004 and 2022. HU values were measured from C3 to L5 in patients with AS and from L1 to L5 in patients without AS. Propensity score (PS) matching based on age and sex was performed to compare HU values between groups. Additionally, HU values were compared between ankylosed and nonankylosed vertebrae within the AS group.

Results: After PS matching, vertebral HU values were significantly lower in patients with AS than in patients without AS (136.4 vs. 197.1, $p = 0.009$). Among patients with AS, HU values were highest in the cervical spine, followed by the thoracic and lumbar regions. Ankylosed vertebrae showed significantly lower HU values than nonankylosed vertebrae across all spinal levels ($p < 0.001$).

Conclusion: Vertebral HU values were lower in patients with AS compared to age- and sex-matched patients without AS. HU values were highest in the cervical spine, and ankylosed vertebrae consistently exhibited lower HU values than nonankylosed vertebrae across all spinal regions.

1 | Introduction

Ankylosing spondylitis (AS) is a chronic inflammatory disease that primarily affects the axial skeleton, especially the spine and sacroiliac joints, leading to ankylosis or the fusion of vertebrae [1, 2]. This condition belongs to the broader category of spondyloarthritis, characterized by inflammation of the entheses—regions where tendons and ligaments insert into the bone. In AS, persistent inflammation can cause new bone formation, ultimately resulting in fusion of the spine. This fusion, or ankylosis,

leads to stiffness and reduced mobility in affected individuals, significantly impacting their quality of life [3, 4].

As the disease progresses, vertebrae lose their flexibility and the lever arm increases, which renders patients with AS more susceptible to vertebral fractures, even from relatively minor external forces [5]. This increased fragility is particularly dangerous because vertebral fractures in patients with AS are often unstable, leading to a higher risk of complications such as spinal cord injury [5, 6]. Vertebral fractures reportedly occur predominantly

Summary

- After age- and sex-matching, patients with AS had lower HU values than patients without AS.
- Cervical spine had the highest HU value among spinal regions in patients with AS.
- Ankylosed vertebrae showed significantly lower HU values than nonankylosed vertebrae.

in the cervical spine (78%), followed by the thoracic spine (12%) and lumbar spine (9%) [5].

Osteoporosis, another well-known complication of AS that affects 11%–30% of patients [7, 8], further increases the risk of fractures. According to one study, patients with AS are more likely to suffer vertebral fractures compared to healthy individuals [9]. Osteoporosis is typically diagnosed using dual-energy X-ray absorptiometry (DEXA), which measures bone mineral density (BMD). However, DEXA can overestimate BMD in patients with AS due to the presence of new bone formation around the vertebrae. These ossifications, which occur in response to inflammation, can lead to artificially higher BMD readings on DEXA, making it difficult to accurately assess osteoporosis in these patients [10].

Given the limitations of DEXA in patients with AS, other imaging modalities, such as computed tomography (CT), are increasingly being explored for evaluating bone density in this population [11]. CT imaging allows for a more detailed assessment of the spine and sacroiliac joints, which are often affected in AS. One of the key metrics used in CT imaging is the Hounsfield Unit (HU), which quantifies the density of tissues based on their radiographic attenuation properties [12]. Previous studies have demonstrated a strong correlation between HU values and BMD as measured by DEXA [10]. However, to date, no study has compared HU values between patients with and without AS, and between ankylosed and nonankylosed vertebrae in patients with AS.

The present study aimed to assess CT-derived HU values of vertebrae in patients with AS. Specifically, we aimed to investigate whether HU values of patients with AS differed from those of patients without AS as well as whether vertebral ankylosis is related to HU values in patients with AS. The goal was to explore whether CT-derived HU values could serve as a reliable surrogate for assessing bone density in patients with AS, particularly in cases where DEXA may provide inaccurate readings due to ossification.

2 | Methods

2.1 | Patients

This was a cross-sectional imaging analysis study of patients with AS who were treated at the Department of Orthopedic Surgery in our hospital between January 2004 and December 2022. A total of 82 patients were diagnosed with AS based on the revised New York criteria [13]. Patients who were unable to undergo whole-spine CT scans or whose CT scans did not include the full vertebral range from C3 to L5 were excluded, resulting in a final study population of 34 patients.

To establish the comparison group, we included patients without AS who visited the Department of Orthopedic Surgery and underwent both lumbar CT and DEXA within a 3-month period. A total of 73 patients met these criteria. Their primary diagnoses included lumbar degenerative disease ($n = 47$), lumbar disc herniation ($n = 1$), idiopathic scoliosis ($n = 8$), ossification of the posterior longitudinal ligament ($n = 3$), compression fractures ($n = 4$), spinal tumors ($n = 8$), and bone metastasis ($n = 2$).

This study was approved by the Ethics Committee of the Nagoya University Graduate School of Medicine (2023-0263) and was conducted in accordance with the principles of the Declaration of Helsinki. Patient anonymity was maintained throughout the data collection process, and informed consent was obtained via an opt-out procedure. All personal information was stored securely and managed in strict compliance with ethical guidelines.

2.2 | Evaluation of Images

CT imaging was performed using a Canon Aquilion Prime SP scanner. The scanning protocol included a slice thickness of 1.0 mm, a voltage of 120 kVp, and an adjustable current of approximately 200 mAs, depending on the patient's body size. This protocol ensured that the images captured high-resolution, detailed views of the vertebral bodies while minimizing radiation exposure. On average, the estimated equivalent absorbed radiation dose for each patient was 5 mSv, a dose typically considered safe in clinical practice. Images from CT scans were acquired for all vertebrae from C3 to L5, providing a comprehensive view of the entire spine for analysis. Ankylosed vertebrae were defined as those with partial or complete bony continuity with adjacent vertebrae, while nonankylosed vertebrae were those without any such continuity [14].

The HU scale was calibrated such that water has a value of 0, whereas air has a value of −1000. Bone typically exhibits HU values ranging from 300 to 1000, depending on its density. Vertebral HU values were measured by selecting regions of interest (ROIs) in the cancellous bone of each vertebra [12, 15, 16]. First, sagittal CT images were used to identify specific vertebral levels. Next, axial images were selected at the central level of each vertebral body's height (Figure S1). The ROI was placed within the cancellous bone, avoiding the cortical bone to ensure that the measurement reflected the density of the trabecular bone, which is more prone to changes in bone quality and density [10, 15]. HU values were recorded for each vertebra from C3 to L5 in patients with AS and from L1 to L5 in patients without AS. HU values of patients with AS were then compared with those of patients without AS to determine whether there were significant differences between the two groups. In addition, within the AS group, vertebrae were classified as either ankylosed or nonankylosed, and their HU values were compared to examine the impact of vertebral ankylosis on bone density.

2.3 | Data Collection

We collected the following information on patients: age and disease duration at time of CT, sex, body mass index (BMI), human leukocyte antigen B-27 (HLA-B27) positivity, C-reactive protein (CRP) levels at diagnosis, Ankylosing Spondylitis Disease Activity (ASDAS), and previous b/tsDMARDs use.

2.4 | Statistical Analysis

Continuous variables are presented as mean ± SD, and categorical variables as number and percentage. To compare vertebral HU values between patients with and without AS as well as between ankylosed and nonankylosed vertebrae in patients with AS, we used the unpaired t-test. For multiple comparisons across three vertebral regions (cervical, thoracic, and lumbar), we used one-way analysis of variance. Post hoc pairwise comparisons between groups were conducted with Bonferroni correction. Statistical significance was set at $p < 0.05$.

Age and sex were identified as potential confounders in the comparison between patients with and without AS. To adjust for these confounders, we applied propensity score (PS) matching based on age and sex. This approach facilitated a comparison between patients with and without AS with similar demographic characteristics, allowing for a more accurate assessment of AS on vertebral HU values.

Statistical analyses were conducted using EZR, a graphical user interface for R statistical software that is widely used in medical research [17].

3 | Results

3.1 | Demographics and Clinical Characteristics of Patients With AS

Table 1 shows demographics and clinical characteristics of the 34 patients who participated in this study. The mean age and mean disease duration were 43.8 ± 16.8 years and 13.2 ± 13.2 years, respectively, at the time of CT imaging. Of these 34 patients, 24 (70.6%) were male, 16 (47.1%) tested positive for HLA-B27, and the mean CRP level at diagnosis was 2.0 ± 3.3. b/tsDMARDs were used in 15 patients (44%), including 13 treated with tumor necrosis factor (TNF) inhibitors and two treated with IL-17 inhibitors.

3.2 | Comparison of HU Values Between Patients With and Without AS

A comparison of HU values from L1 to L5 between 34 patients with AS and 73 patients without AS was performed. Patients without AS were significantly older than patients with AS, with a mean age of 64 years vs. 45 years ($p < 0.001$). In addition, the proportion of male patients was higher in patients with AS (71%) than in those without AS (29%). The mean HU value for patients with AS was 159.1 ± 60.3, while that for patients without AS was 136.9 ± 65.5 ($p = 0.096$).

TABLE 1 | Patient demographics and clinical characteristics.

Characteristics	Total ($n = 34$)
Age at time of CT, years	43.8 ± 16.8
Male, n (%)	24 (71)
Disease duration at time of CT, years	13.2 ± 13.2
BMI, kg/m^2[a]	21.8 ± 3.3
HLA-B27 positive, n (%)[b]	16 (47)
CRP at diagnosis, mg/dl[c]	2.0 ± 3.3
ASDAS[d]	1.9 ± 0.7
Previous use of b/tsDMARDs, n (%)	15 (44)

Note: Data are presented as mean ± SD or number (percentage).
Abbreviations: ASDAS, Ankylosing Spondylitis Disease Activity Score; b/tsDMARDs, biological/targeted-synthetic disease modifying antirheumatic drugs; BMI, body mass index; CRP, C-reactive protein; CT, computed tomography; HLA, human leukocyte antigen.
[a]Data were available for 30 patients.
[b]Data were available for 29 patients.
[c]Data were available for 32 patients.
[d]Data were available for 21 patients.

As age and sex differences may affect vertebral HU values, PS matching was performed to control for these variables, resulting in a re-analysis of 19 matched pairs of patients with and without AS. Following PS matching, the mean age was 51 years in patients with AS and 47 years in patients without AS ($p = 0.464$), while the proportion of male patients was 63% and 47%, respectively ($p = 0.515$). The mean HU value for patients with AS was 136.4 ± 57.2, compared to 197.2 ± 77.6 for patients without AS ($p = 0.009$) (Figure 1).

3.3 | Whole Spine HU Values in Patients With AS

Mean HU values of each vertebra for all 34 patients with AS are shown in Figure 2. Mean HU values in patients with AS were as follows: cervical spine 300.6 ± 85.0, thoracic spine 188.9 ± 62.8, and lumbar spine 158.2 ± 60.3. HU values in the cervical spine were significantly higher than those in the thoracic spine ($p < 0.001$) and lumbar spine ($p < 0.001$), but there was no significant difference in HU values between the thoracic spine and lumbar spine ($p = 0.190$).

3.4 | Comparison of HU Values Between Ankylosed Vertebrae and Nonankylosed Vertebrae in Patients With AS

Among the 748 vertebrae analyzed in the 34 patients with AS, 333 were classified as ankylosed and 415 as nonankylosed. Mean HU values for all vertebrae from C3 to L5 were 178.7 ± 88.6 for ankylosed vertebrae and 231.7 ± 89.3 for nonankylosed vertebrae, with a significantly lower HU value in ankylosed vertebrae ($p < 0.001$).

When examining specific spinal regions, mean HU values for ankylosed and nonankylosed vertebrae were cervical spine 259.1 ± 86.0 vs. 354.1 ± 80.9 ($p < 0.001$), thoracic spine 166.7 ± 72.7 vs. 214.1 ± 51.6 ($p < 0.001$), and lumbar spine
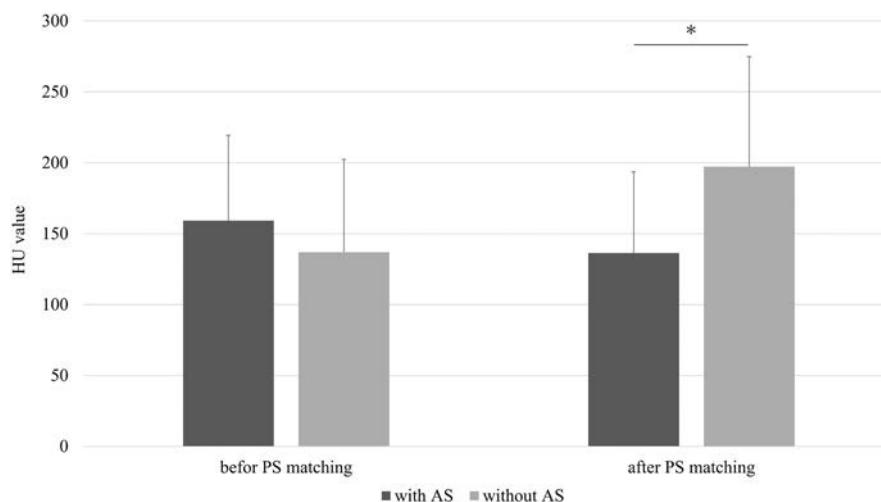
FIGURE 1 | Comparison of HU values from L1 to L5 between patients with and without AS before and after propensity score matching based on age and sex. Bars represent mean values, and error bars indicate SD. Dark gray bars represent patients with AS, and light gray bars represent patients without AS. AS, Ankylosing spondylitis; HU, Hounsfield Unit. *$p < 0.05$.
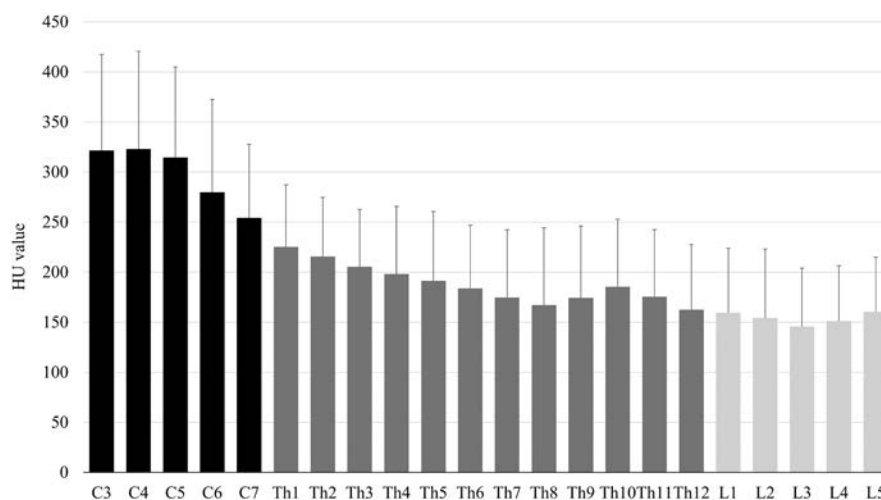
FIGURE 2 | HU values of all vertebrae (C3–L5) in patients with AS. Mean HU values of all vertebrae (C3–L5) in patients with AS are shown. C, cervical; HU, Hounsfield Unit; L, lumbar; Th, thoracic.

105.1 ± 64.3 vs. 167.8 ± 44.5 ($p < 0.001$). In each spinal region, HU values of ankylosed vertebrae were significantly lower than those of nonankylosed vertebrae (Figure 3).

4 | Discussion

The present study revealed significant differences in HU values across different spinal regions and between ankylosed and nonankylosed vertebrae in patients with AS. HU values for patients with AS were lower than those for patients without AS after PS matching based on age and sex. Among patients with AS, HU values of ankylosed vertebrae were consistently lower than those of nonankylosed vertebrae across all spinal regions.

To evaluate vertebral bone density, we utilized CT-derived HU values. While DEXA, which is widely used for bone density evaluation, can provide accurate assessments in patients with AS

without ankylosis [18], it may overestimate bone density in cases with ankylosis due to new bone formation [10]. In contrast, HU values have been reported to correlate with bone density and are not affected by new bone formation, enabling a more accurate evaluation.

HU values were lower in patients with AS compared to patients without AS. In terms of the biological mechanisms underlying the reduced HU values in patients with AS, previous research by Taams et al. [19] suggests that inflammatory cytokines such as TNF and interleukin-17A (IL-17A) play a key role. These cytokines promote the differentiation of mesenchymal stem cells into osteoblasts, leading to increased bone formation. However, they also increase the expression of receptor activator of nuclear factor kappa-B ligand, which stimulates osteoclast differentiation and enhances bone resorption. The balance between these processes likely resulted in the net loss of bone density observed in patients with AS, as reflected by the lower HU values in both ankylosed and nonankylosed vertebrae.
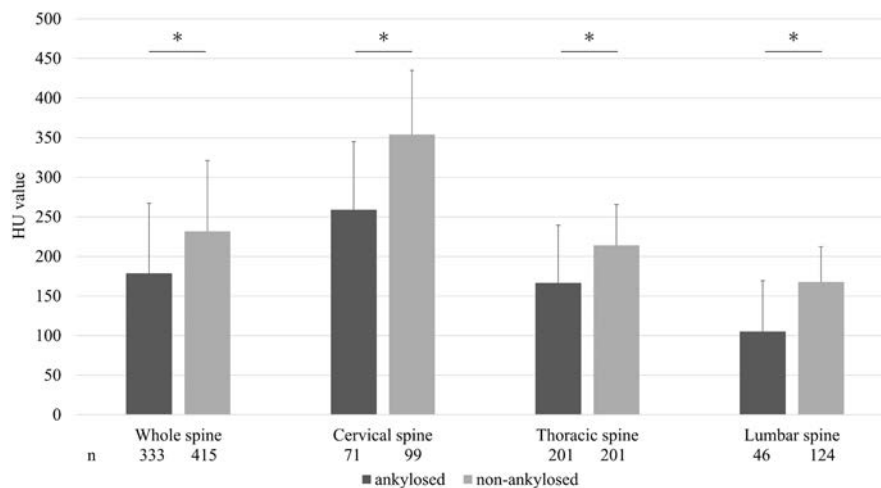
FIGURE 3 | Comparison of HU values between ankylosed and nonankylosed vertebrae in the whole spine, and cervical, thoracic, and lumbar regions. Bars represent mean values, and error bars indicate SD. Dark gray bars represent ankylosed vertebrae, whereas light gray bars represent nonankylosed vertebrae. Numbers below each bar indicate the number of vertebral levels analyzed in each group. AS, ankylosing spondylitis; HU, Hounsfield Unit. $*p < 0.05$.

HU values in patients with AS were highest in the cervical spine, followed by the thoracic spine and lumbar spine. Marques et al. conducted a study on axial spondyloarthritis patients, measuring vertebral HU values and evaluating interobserver reliability [15]. They found that cervical HU values were higher than those in the thoracic and lumbar regions, likely due to the smaller volume and greater mobility of the cervical vertebrae, subjecting them to greater mechanical loads. Our findings are consistent with these results, as we also found that cervical HU values were higher than those in the thoracic and lumbar regions. This pattern may reflect the greater mechanical demands placed on the cervical spine compared to the lower regions of the spine.

HU values of ankylosed vertebrae in patients with AS were significantly lower compared to non-ankylosed vertebrae. Hamano et al. reported that in a mouse model of diffuse idiopathic skeletal hyperostosis, the ossified continuity of vertebrae due to ankylosis led to stress shielding, resulting in bone fragility [20]. Normally, the stress transmitted to vertebral bodies through intervertebral discs is thought to decrease in ankylosed regions because the stress is instead transmitted through the bridged parts. Additionally, reduced mobility caused by ankylosis further decreases the load, potentially leading to additional vertebral fragility. In patients with AS of the present study, a similar mechanism may have weakened the vertebrae, resulting in a decrease in HU values. These findings align with previous research showing that patients with AS are at increased risk of osteoporosis and fractures. Lower HU values in patients with AS may reflect the complex interplay between inflammation, bone formation, and bone resorption that occurs in this disease.

This study has several limitations. First, the sample size was relatively small, which may affect the generalizability of the findings. This limitation reflects an inherent challenge in studying patients with AS in Japan, where the prevalence of AS is significantly lower compared to Western countries [20]. Future studies with larger cohorts are warranted to provide more comprehensive insights and enhance the external validity of the results.

Second, the cross-sectional design of the study precluded an evaluation of the longitudinal effects of disease duration on bone quality in patients with AS. Although we attempted to mitigate this limitation by comparing ankylosed and non-ankylosed vertebrae within the same patients, a prospective study design would offer more robust evidence of the progression of bone density changes over time. Third, we did not assess the impact of disease activity or therapeutic interventions on HU values. Future research should explore whether treatments aimed at reducing inflammation, such as TNF inhibitors and IL-17 inhibitors, could improve vertebral bone density as reflected by HU values. Fourth, BMD measurements were not available for patients with AS, which precluded a direct comparison between HU and BMD in this population. We are currently developing a predictive model that estimates BMD based on HU values and patient characteristics. This model is expected to contribute to the assessment of BMD in situations where direct BMD measurements are not available. Fifth, full-spine CT imaging was not consistently available in patients without AS, as it involves radiation exposure and is not routinely performed in healthy individuals or those with uncomplicated osteoporosis. Therefore, they had CT scans available only when the scans were taken for other clinical purposes. As a result, vertebrae from C3 to Th12 could not be evaluated in a uniform manner. Finally, there was radiation exposure associated with CT imaging. However, these concerns were minimized since all CT scans were obtained for clinical purposes, with no additional imaging performed solely for research.

In conclusion, vertebral HU values were significantly lower in patients with AS compared to patients without AS, which may reflect reduced bone density in AS. Furthermore, ankylosed vertebrae in patients with AS had significantly lower HU values compared to non-ankylosed vertebrae, suggesting that the process of ankylosis may lead to bone weakening. CT-derived HU values provide a valuable tool for evaluating bone density in patients with AS and may offer a more accurate assessment than DEXA in cases where ossification complicates BMD measurements. Future research should investigate the potential

effectiveness of osteoporosis treatments in patients with AS and identify effective strategies for preventing fractures.

References

1. J. Braun and J. Sieper, "Ankylosing Spondylitis," *Lancet* 369, no. 9570 (2007): 1379–1390, https://doi.org/10.1016/S0140-6736(07)60635-7.

2. J. Sieper and D. Poddubnyy, "Axial Spondyloarthritis," *Lancet* 390, no. 10089 (2017): 73–84, https://doi.org/10.1016/S0140-6736(16)31591-4.

3. P. Agrawal, S. Tote, and B. Sapkale, "Diagnosis and Treatment of Ankylosing Spondylitis," *Cureus* 16, no. 1 (2024): e52559, https://doi.org/10.7759/cureus.52559.

4. O. Ozdemir, "Quality of Life in Patients With Ankylosing Spondylitis: Relationships With Spinal Mobility, Disease Activity and Functional Status," *Rheumatology International* 31, no. 5 (2011): 605–610, https://doi.org/10.1007/s00296-009-1328-2.

5. B. C. Werner, D. Samartzis, and F. H. Shen, "Spinal Fractures in Patients With Ankylosing Spondylitis: Etiology, Diagnosis, and Management," *Journal of the American Academy of Orthopaedic Surgeons* 24, no. 4 (2016): 241–249, https://doi.org/10.5435/JAAOS-D-14-00149.

6. W. B. Jacobs and M. G. Fehlings, "Ankylosing Spondylitis and Spinal Cord Injury: Origin, Incidence, Management, and Avoidance," *Neurosurgical Focus* 24, no. 1 (2008): E12, https://doi.org/10.3171/FOC/2008/24/1/E12.

7. K. Briot and C. Roux, "Inflammation, Bone Loss and Fracture Risk in Spondyloarthritis," *RMD Open* 1, no. 1 (2015): e000052, https://doi.org/10.1136/rmdopen-2015-000052.

8. I. Ghozlani, M. Ghazi, A. Nouijai, et al., "Prevalence and Risk Factors of Osteoporosis and Vertebral Fractures in Patients With Ankylosing Spondylitis," *Bone* 44, no. 5 (2009): 772–776, https://doi.org/10.1016/j.bone.2008.12.028.

9. F. Yan, L. Wu, J. Lang, and Z. Huang, "Bone Density and Fracture Risk Factors in Ankylosing Spondylitis: A Meta-Analysis," *Osteoporosis International* 35, no. 1 (2024): 25–40, https://doi.org/10.1007/s00198-023-06925-1.

10. M. K. Choi, S. M. Kim, and J. K. Lim, "Diagnostic Efficacy of Hounsfield Units in Spine CT for the Assessment of Real Bone Mineral Density of Degenerative Spine: Correlation Study Between T-Scores Determined by DEXA Scan and Hounsfield Units From CT," *Acta Neurochirurgica* 158, no. 7 (2016): 1421–1427, https://doi.org/10.1007/s00701-016-2821-5.

11. S. Tan and M. M. Ward, "Computed Tomography in Axial Spondyloarthritis," *Current Opinion in Rheumatology* 30, no. 4 (2018): 334–339, https://doi.org/10.1097/BOR.0000000000000507.

12. J. J. Schreiber, P. A. Anderson, and W. K. Hsu, "Use of Computed Tomography for Assessing Bone Mineral Density," *Neurosurgical Focus* 37, no. 1 (2014): E4, https://doi.org/10.3171/2014.5.FOCUS1483.

13. S. van der Linden, H. A. Valkenburg, and A. Cats, "Evaluation of Diagnostic Criteria for Ankylosing Spondylitis. A Proposal for Modification of the New York Criteria," *Arthritis and Rheumatism* 27, no. 4 (1984): 361–368, https://doi.org/10.1002/art.1780270401.

14. K. Kishimoto, "Intervertebral Fusion Sites in Patients With Ankylosing Spondylitis: A Computed Tomography Study," *Modern Rheumatology* 34, no. 3 (2024): 599–606, https://doi.org/10.1093/mr/road088.

15. M. L. Marques, N. Pereira da Silva, D. van der Heijde, et al., "Low-Dose CT Hounsfield Units: A Reliable Methodology for Assessing Vertebral Bone Density in Radiographic Axial Spondyloarthritis," *RMD Open* 8, no. 2 (2022): e002149, https://doi.org/10.1136/rmdopen-2021-002149.

16. T. Akabane, T. Suzuki, Y. Konno, et al., "Bone Density as a Risk of Early Loss of Correction After Percutaneous Posterior Spinal Fixation for Traumatic Thoracolumbar Fracture: A Study on the Usefulness of Hounsfield Unit Values on Computed Tomography Scan," *European Spine Journal* 34, no. 2 (2025): 498–505, https://doi.org/10.1007/s00586-024-08508-y.

17. Y. Kanda, "Investigation of the Freely Available Easy-To-Use Software 'EZR' for Medical Statistics," *Bone Marrow Transplantation* 48, no. 3 (2013): 452–458, https://doi.org/10.1038/bmt.2012.244.

18. M. N. Magrey, S. Lewis, and K. M. Asim, "Utility of DXA Scanning and Risk Factors for Osteoporosis in Ankylosing Spondylitis-A Prospective Study," *Seminars in Arthritis and Rheumatism* 46, no. 1 (2016): 88–94, https://doi.org/10.1016/j.semarthrit.2016.03.003.

19. L. S. Taams, K. J. A. Steel, U. Srenathan, L. A. Burns, and B. W. Kirkham, "IL-17 in the Immunopathogenesis of Spondyloarthritis," *Nature Reviews Rheumatology* 14, no. 8 (2018): 453–466, https://doi.org/10.1038/s41584-018-0044-2.

20. H. Hamano, M. Takahata, M. Ota, et al., "Teriparatide Improves Trabecular Osteoporosis but Simultaneously Promotes Ankylosis of the Spine in the Twy Mouse Model for Diffuse Idiopathic Skeletal Hyperostosis," *Calcified Tissue International* 98, no. 2 (2016): 140–148, https://doi.org/10.1007/s00223-015-0068-4.

Supporting Information

Additional supporting information can be found online in the Supporting Information section.

WILEY

| **REVIEW**

The Effects of Calcitonin Gene-Related Peptide on Cartilage in Osteoarthritis

Yucan Ju[1] | Leyao Shen[2] | Qiang Huang[1] | Zeyu Huang[1] (iD)

[1]Department of Orthopaedic Surgery, Orthopaedic Research Institute, West China Hospital, West China Medical School, Sichuan University, Chengdu, Sichuan Province, People's Republic of China | [2]School of Dentistry, University of Michigan, Ann Arbor, Michigan, USA

Correspondence: Qiang Huang (huangqiang4325@126.com) | Zeyu Huang (zey.huang@gmail.com)

ABSTRACT

Osteoarthritis (OA) is the most common age-related joint disease, which affects articular cartilage and joint structures, causing severe pain and disability. Owing to limited understanding of the underlying disease pathogenesis, there are currently no disease-modifying drugs for OA. Recent studies have demonstrated that calcitonin gene-related peptide (CGRP) plays an important role in OA synovial inflammation. Here, we first provide a fundamental basis for the physiological and pathological effects of CGRP in cartilage. Then we summarize current evidence of CGRP's roles in OA-affected tissues. We then focus on the potential innovative strategies for targeting CGRP to enhance cartilage regeneration. Further research into CGRP's role in OA may have broader implications in the understanding of OA pathogenesis, the standardization of biomarker detection, and the development of novel therapeutic routes for the prevention and management of OA.

1 | Introduction

Osteoarthritis (OA) is a prevalent degenerative joint disease characterized by degenerative articular cartilage lesions, subchondral bone sclerosis, bone formation abnormalities, and cartilage angiogenesis [1]. These pathologic changes are closely linked to pain in OA [2]. Epidemiologic data show that the incidence of OA rises progressively with age, with a particularly notable rise in prevalence among individuals over 50 years old [3]. OA primarily affects weight-bearing joints, such as the knee, and hip joints. Symptoms are primarily manifested as joint pain,

which is the primary cause for seeking medical intervention [4]. Pain is often persistent during joint movement and is typically accompanied by stiffness and reduced range of motion [5].

Previous research has demonstrated a strong correlation between calcitonin gene-related peptide (CGRP) levels and joint pain in individuals with OA [6]. Additionally, CGRP levels are significantly elevated in synovial tissue during OA-related pain [7]. CGRP is a neuropeptide that is widely distributed in both the peripheral and central nervous systems [8]. It is primarily secreted by sensory nerve endings in the peripheral region. A study has also found

---

an increase in the presence of CGRP-positive sensory nerves within the cartilage and subchondral regions as OA progresses [9]. Therefore, investigating the role of CGRP in OA is crucial for developing targeted interventions aimed at reducing pain and improving the overall quality of life for OA patients.

CGRP is a neuroendocrine peptide that is highly involved in bone metabolism. CGRP is a member of the calcitonin family with two isoforms, α-CGRP and β-CGRP. α-CGRP is encoded by the *Calca* gene in humans and mice, and β-CGRP by the *Calcb* gene [10, 11]. Sensory neurons preferentially express α-CGRP [12], and the human and rodent α-CGRP genes have been studied much more extensively than β-CGRP. Therefore, unless otherwise specified, "CGRP" in this article refers to α-CGRP.

Previous studies have extensively acknowledged the crucial role of CGRP in promoting bone formation, facilitating blood vessel growth, inhibiting osteoclasts, and modulating the immune microenvironment [13, 14]. Specifically, CGRP plays a significant pathological role in subchondral angiogenesis, subchondral bone sclerosis, and the metabolism of chondrocytes and the extracellular matrix. The delicate balance between cartilage tissue and the subchondral bone microenvironment critically impacts the extent of cartilage damage. Additionally, subchondral angiogenesis plays a key role in cartilage destruction [15, 16]. Furthermore, CGRP regulates the expression of inflammatory factors and vascular endothelial growth factor (VEGF), thereby influencing the synthesis and metabolism of cartilage [17–19]. Therefore, exploring the role of CGRP in osteoarthritis provides important insights for understanding and treating OA. This paper aims to review recent studies that elucidate the pathological effects of CGRP and the peripheral nervous system (PNS) on articular cartilage in OA, examines its impact on the peripheral environment of articular cartilage, and explores the neuropharmacological potential of CGRP in OA treatment.

1.1 | Fundamental Basis for the Physiological and Pathological Effects of CGRP in Cartilage

1.1.1 | Distribution of sensory and sympathetic nerve fibers is highly correlated with cartilage in OA

Healthy cartilage is avascular and lacks innervation by nerve fibers. However, a few studies have shown that sensory nerve fibers are in contact with subpopulations of chondrocytes in the outer layer of growth plate cartilage and the outer layer of articular cartilage, as well as with chondrocytes in the deeper layers of articular cartilage. This may affect the trophic metabolism of healthy chondrocytes and chondrocyte differentiation [20–22]. Additionally, the sensory and sympathetic nervous system affects the tissue cells surrounding the nerve fibers, and the tissue cells surrounding the nerve fibers in turn synthesize growth factors, cytokines, proteases, and other factors that further affect the function of the surrounding chondrocytes [23].

Although nerves are rarely distributed in healthy cartilage [24], a marked increase in the distribution of sensory nerve fibers (SP and CGRP positive) and sympathetic nerve fibers (NPY positive) has been observed in OA articular cartilage [25]. These fibers are primarily located in the area where articular cartilage contacts the subchondral bone, with nerve fibers predominantly surrounding blood vessels (Figure 1), closely associated with cartilage vascularization [9, 26]. The density of CGRP-positive nerve fibers is significantly correlated with the rate of ossification of the cartilage [27]. Therefore, in diseased joints, the increased distribution of both these nerve fibers here may exacerbate joint inflammation and lead to cartilage damage [9, 28]. Furthermore, inflammatory factors (such as interleukin-6) produced during OA can also contribute to CGRP release from sensory neurons [29]. These studies suggest that sensory and sympathetic nerves play an important role in OA pathology and are involved in CGRP secretion in OA.
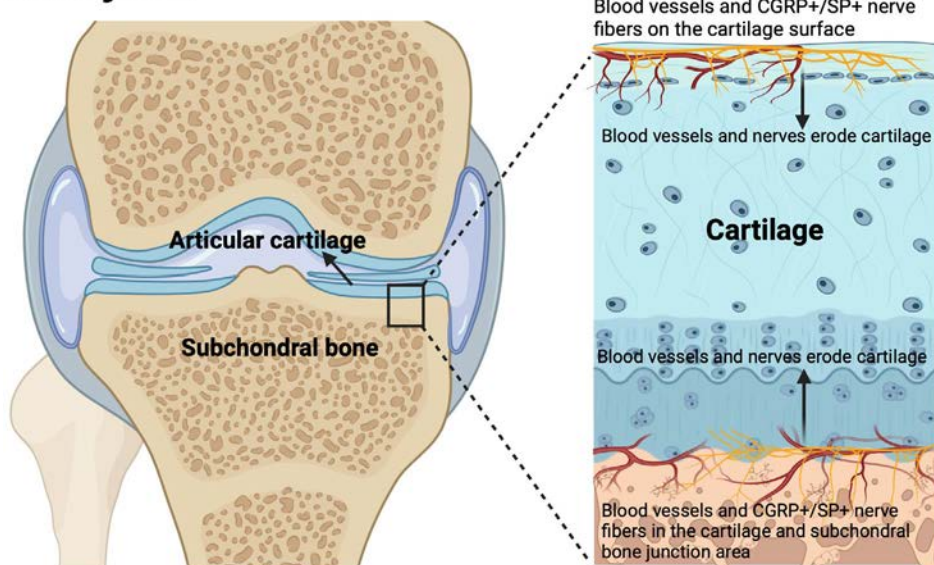
FIGURE 1 | Distribution of CGRP+/SP+ nerve fibers on the cartilage surface and in the cartilage-bone junction area in knee osteoarthritis, and the vascular alignment is consistent with the distribution of nerve fibers.

1.1.2 | Receptors and Signaling Pathways of CGRP

The CGRP receptor has two subunits, calcitonin receptor-like receptor (CLR) and receptor activity modifying protein 1 (RAMP1) (Figure 2) [30–32]. In the classical pathway, the CGRP receptor acts as a G Protein Coupled Receptor (GPCR), regulating the downstream target via the Gαs—cAMP-protein kinase A (PKA) axis. Additionally, CGRP can also regulate through Gαq/11-mediated phospholipase C (PLC) action, mitogen-activated protein kinase (MAPK) action, and nitric oxide (NO) production, generating a series of transcriptional events [33–35]. Downstream of CGRP receptor activation, PKA regulates downstream signaling components, including K+ channels [36], L-type Ca2+ channels [37], and cAMP response element-binding protein (CREB) (Figure 2) [38]. In OA chondrocytes, CGRP induces pro-inflammatory and chondro-destructive effects via MAPK signaling pathway activation and NO production. However, it can also produce anti-inflammatory and anabolic effects via the cAMP signaling pathway [22, 39, 40]. Studies show that increasing cAMP levels can protect cartilage by inhibiting matrix mineralization, delaying chondrocyte hypertrophy, attenuating inflammation, and slowing cartilage degeneration [20, 41].

Upon binding with GPCR kinase-2 (GRK2), activated GPCR leads to phosphorylation of serine and threonine residues on the receptor, which triggers receptor desensitization and internalization (Figure 2) [42]. Upregulation of GRK2 expression leads to reduced cAMP production, which inhibits the protective effects of GPCR-cAMP signaling in OA chondrocytes; thus, downregulation of GRK2 prevents the progression of OA and promotes cartilage regeneration [43]. In addition to GRK-mediated desensitization, GPCR is phosphorylated by PKA and PKC, resulting in inhibition of GPCR-cAMP signaling [10].

Overall, the CGRP receptor consists of two subunits, CLR and RAMP1, and functions as a GPCR. It activates downstream signaling through the Gαs-cAMP-PKA axis and also via Gαq/11-mediated pathways like PLC, MAPK, and NO production. In OA chondrocytes, CGRP can either induce pro-inflammatory effects through MAPK and NO or produce anti-inflammatory effects via the cAMP pathway. Elevated cAMP levels protect cartilage by reducing mineralization and inflammation. GPCR activation leads to receptor desensitization and internalization via GRK2, which decreases cAMP production and diminishes its protective effects, while downregulating GRK2 may slow OA progression and promote cartilage regeneration.

2 | Pathologic Effects of CGRP in OA

2.1 | Effects of CGRP on Inflammation

While OA has traditionally been viewed as primarily a mechanical wearing and tearing process, recent research has highlighted the crucial role of inflammation in its development. The inflammation in OA is complex, involving the
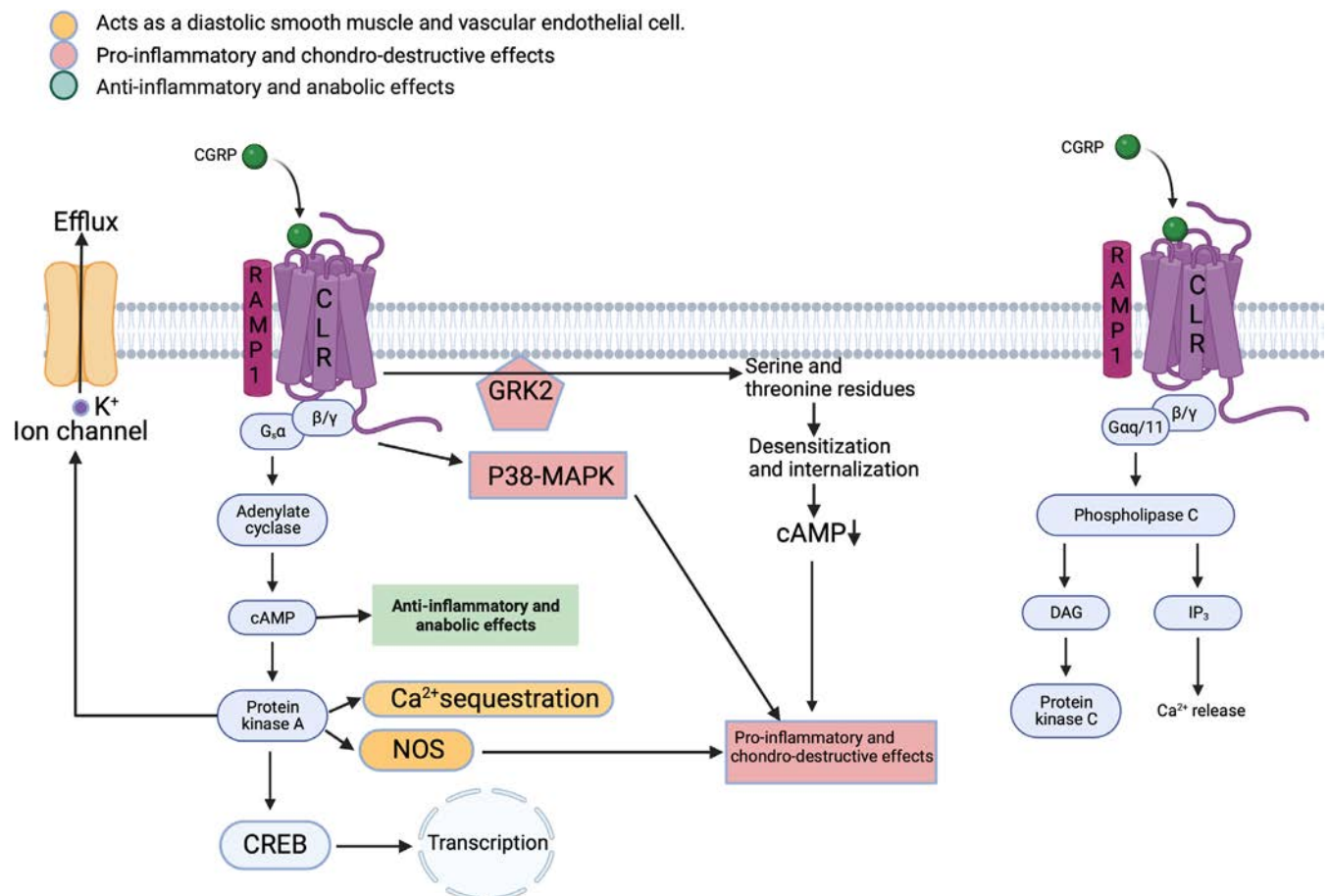
FIGURE 2 | Intracellular signaling and downstream effectors of CGRP receptors.

interaction of multiple cell types and molecular signaling pathways (Figure 3a) [44, 45]. Studies have demonstrated that activated chondrocytes in OA produce various proteins involved in inflammatory responses, including interleukin-1β (IL-1β), interleukin-6 (IL-6), and tumor necrosis factor-α (TNF-α), as well as matrix-degrading enzymes, such as metalloproteinases (MMPs) and a disintegrin and metalloproteinase with thrombospondin-like motifs (ADAMTS), MMP1, 3, and 13, and ADAMTS 4 and 5 [46, 47] included. Pro-inflammatory cytokines like IL-1β and TNF-α are significantly upregulated in OA. These cytokines stimulate the production of matrix metalloproteinases (MMPs) [48]. MMPs break down various components of cartilage tissue, including type II collagen, proteoglycans, type IV and IX collagen, osteoconjugates, and perlecan proteins [49–51]. This degradation ultimately leads to the destruction of articular cartilage. Furthermore, the catabolized cartilage extracellular matrix can also trigger inflammatory and immune responses through the complement pathway and the classical pathway [47, 52].

In vitro experiments have demonstrated that CGRP induces the expression and release of TNF-α and IL-1β, both of which contribute to the inflammatory response associated with macrophages [53]. IL-6 has been found to increase the number of sensory neurons and CGRP release, further exacerbating inflammation [29]. Released by sensory nerve fibers, CGRP can recruit both innate and adaptive immune cells to participate in the inflammatory process in OA [54]. Additionally, CGRP promotes the polarization of M2 macrophages via PKA and PKC [55] and facilitates the recruitment of human T lymphocytes [56, 57]. M2 macrophages release growth factors and angiogenic factors, including TGF-β, VEGF, and epidermal growth factor (EGF), and also regulate T-cell function, contributing to damage and remodeling of OA cartilage [57, 58]. Increased numbers of Th1, Th9, and Th17 cells in OA synovial fluid, along with Th1, Th17, and cytotoxic T-cells in synovial tissues, produce cytokines, such as IL-2, IFN-γ, and TNF-α, enhancing cartilage catabolism [59]. However, a study also demonstrated that T-helper cells drive macrophages toward a regenerative phenotype [60], potentially aiding in the control of inflammation and tissue repair. Thus, further investigation to elucidate the role that T-cells play in the progression of OA is warranted. Macrophage activation in OA joints enhances the innate immune system, particularly including several complement components [61]. The complement system not only directly induces cell death but also promotes chemotaxis of neurotrophoblasts and monocytes (role of C5a) [62], which are directly involved in OA cartilage damage and repair. Thus, the role of CGRP in OA inflammation encompasses both innate and adaptive immunity, activating the macrophage and complement systems related to cartilage damage and repair.

2.2 | Effects of CGRP on Subchondral Bone Microenvironment

Maintaining an appropriate balance between cartilage tissue and the microenvironment of the subchondral bone is crucial in OA. This sclerosis alters the mechanical support for cartilage, which in turn impacts chondrocyte metabolism (Figure 3b), as well as the synthesis and breakdown of the cartilage matrix [63, 64]. Ultimately, this imbalance exacerbates cartilage destruction [15, 16]. Subchondral bone sclerosis is closely related to the dysregulation of osteoblasts and osteoclasts. A study has demonstrated increased expression of CGRP in the subchondral bone of OA, especially during the acute arthritic phase, which promotes joint inflammation and contributes to disease progression [41]. Notably, CGRP promotes osteogenesis while inhibiting osteoclast differentiation [14, 65], thereby altering the microenvironment of the subchondral bone. Additionally, this study presents evidence showing that the use of CGRP receptor antagonists can counteract the effects of CGRP [66]. The CGRP receptor antagonists, olcegepant, shift the balance toward osteoclast predominance by inhibiting CGRP function. And in the study [66], olcegepan significantly reduced alkaline phosphatase (ALP) activity, decreased the proportion of MMP-13-positive cells, increased the proportion of TRAP-positive multinucleated cells, and reduced the volume of subchondral bone tissue.
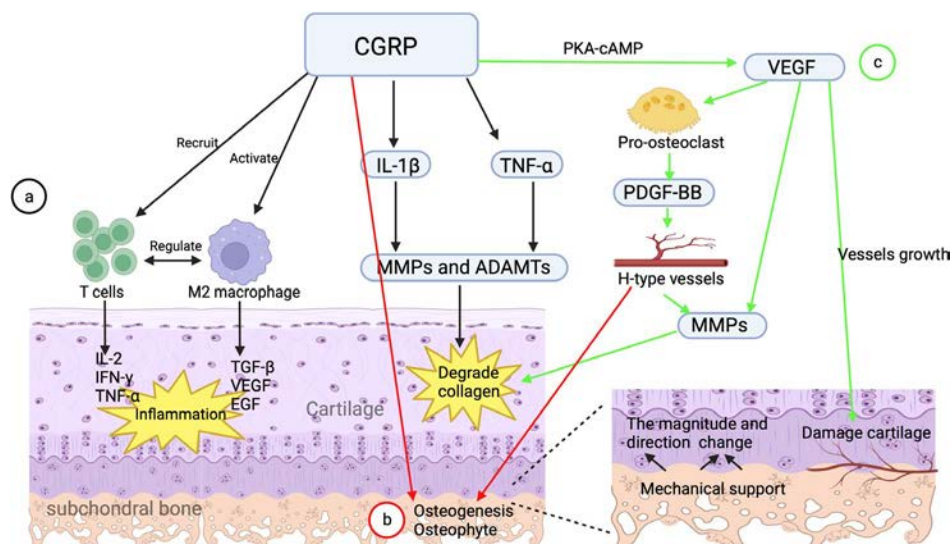
FIGURE 3 | Pathological roles played by CGRP in OA cartilage. (a) (Black) CGRP plays a role in OA inflammation. (b) (Red) CGRP promotes subchondral osteosclerosis leading to altered cartilage support. (c) (Green) CGRP stimulates subchondral neoangiogenesis thereby destroying cartilage.

2.3 | Effects of CGRP on Vascular Growth

Subchondral angiogenesis plays a pivotal role in cartilage degradation. The proliferating endothelial cells in the region between cartilage and subchondral bone erode the cartilage matrix and promote ossification, leading to ossification within the cartilage [16, 19]. The invasion of the articular cartilage and meniscus by neovascularization further intensifies the progression of OA [47, 67]. Neovascularization also induces alterations in the structure of subchondral bone trabeculae, which affects stress distribution at the osteochondral interface, resulting in cartilage degeneration. Moreover, vascular growth facilitates the distribution of subchondral nerves. The combined invasion of avascular cartilage and calcified cartilage by neovascularization and nerves ultimately leads to an increase in OA pain [68].

VEGF plays a crucial role in the growth of subchondral blood vessels, with its expression significantly elevated in various tissues and fluids of patients with OA, including articular cartilage, synovium, synovial fluid, subchondral bone, and serum [17, 18]. Notably, VEGF influences the formation of H-type blood vessels [69, 70]. Multiple experimental models have demonstrated a strong association between H-vessels in subchondral bone and the development of OA [71, 72]. H-vessels are predominantly found around the growth plate in young animals and contribute to cartilage resorption and endochondral ossification during long bone development. The endothelium of H-vessels also releases proteases, such as matrix metalloproteinase-9 (MMP-9), which facilitate cartilage matrix resorption [73]. Additionally, VEGF plays an important role in the remodeling of cartilage extracellular matrix, angiogenesis, and bone formation [17]. It can stimulate OA chondrocytes to produce MMP-1 and MMP-3, both of which degrade the cartilage extracellular matrix.

In vitro experiments have demonstrated that CGRP upregulates the expression of VEGF through the cAMP-PKA pathway, thereby promoting endothelial cell proliferation and angiogenesis [74, 75]. CGRP promotes vascularization of OA cartilage and subchondral bone, particularly driving abnormal angiogenesis in the subchondral bone, which leads to vascular invasion of the osteochondral junction and further destruction of cartilage tissue (Figure 3c) [76]. Additionally, CGRP elevates the proportion of pro-osteoclasts [65], which secrete platelet-derived growth factor BB (PDGF-BB) in OA, further promoting the formation of H-type blood vessels [77, 78]. PDGF-BB also directly induces endothelial cell proliferation, migration, and vascularization and stimulates the secretion of vascular endothelial growth factor, which induces *de novo* formation of blood vessels in the subchondral bone of OA [79].

Significantly, in the subchondral bone microenvironment of OA, angiogenesis and osteogenesis are coupled [80, 81]. First, vascular endothelial growth factor involves vascularization [69]. H-vessels also promote the proliferation and differentiation of osteoblasts in the bone marrow, actively contributing to bone formation in subchondral osteosclerosis in OA [81–83]. Furthermore, the vasodilatory effects and increased angiogenesis impact blood flow, further promoting osteogenesis [84, 85]. Increased subchondral bone porosity, bone remodeling, and decreased bone density in the early stage of OA are associated with vascular invasion [86]. High concentrations of VEGF may also increase osteoclast recruitment and promote bone resorption, leading to bone loss [87, 88]. This suggests that VEGF can exacerbate the imbalance of the subchondral bone microenvironment in OA, where incoordination between the biomechanical and biochemical interactions between subchondral bone and cartilage accelerates OA progression. Therefore, the mechanism of CGRP on the subchondral bone microenvironment and subchondral neovascularization in OA deserves further investigation.

2.4 | Effects of CGRP on Chondrocytes and Cartilage Matrix

Cartilage homeostasis is regulated by the balance between anabolism and catabolism within chondrocytes, CGRP enhances chondrocyte metabolism and offers a protective effect on healthy chondrocytes [89]. In a study using a-CGRP gene-deficient model of rheumatoid arthritis (RA), knockout of a-CGRP attenuates clinical arthritis, intra-articular inflammation, and cartilage degeneration whereas reduces the expression of pro-inflammatory cytokines (TNF-a, IL-1b, cluster of differentiation 80, MMP-13) and expression of cartilage markers (COL1A1, COL2A1, Sox9) [41]. Additionally, CGRP deficiency accelerates the onset of cartilage matrix degradation after OA, though this is likely to be the result of an imbalance in neuropeptide expression rather than a CGRP-independent effect [90]. In conclusion, the metabolic effects of CGRP on the cartilage matrix can be influenced by the physiological state of chondrocytes, the surrounding environment, and the specific disease model. Additionally, the combined effects of CGRP and other neuropeptides influences the metabolism and signaling pathways of the cartilage matrix. However, there is a dearth of studies in this area. Although the synthetic and catabolic effects of neuropeptides like CGRP on the chondrocytes require further explored, the fact that CGRP damages the cartilage matrix by promoting subchondral osteosclerosis and subchondral angiogenesis is well established [15, 16, 76].

3 | Innovative Strategies for CGRP to Enhance Cartilage Regeneration

CGRP plays a crucial role in the pathogenesis of OA. However, the effects of CGRP on cartilage and plasma concentration in the disease are influenced by the physiological state of the body, the degree of disease progression, and the interaction of various cytokines. Moreover, there is a dearth of research investigating the direct effects of CGRP on chondrocytes and its potential for ameliorating cartilage degeneration. Based on the results of the above studies, CGRP is one of the main factors involved in cartilage damage in OA. It is reasonable to assume that the degeneration of cartilage in OA can be effectively controlled through the reduction of CGRP's effects on articular cartilage, the subchondral bone microenvironment, subchondral neoangiogenesis, and inflammatory cytokines.

3.1 | CGRP Receptor Antagonists

A basic study on the rat monosodium iodoacetate (MIA) model showed that behavioral tests and neurophysiological tests in rats

suggest [91] the effectiveness of CGRP inhibitors in relieving OA pain. A basic study on the rat MIA model showed that the potential use of CGRP inhibitors to alleviate the degeneration of articular cartilage in OA [92]. Additionally, another study on the histologic results of a mouse model of destabilization of the medial meniscus (DMM) showed that the administration of CGRP receptor antagonists (olcegepant) prevents the hardening of the subchondral bone during the early stage of OA, consequently inhibiting the degeneration of the cartilage [66]. A mouse DMM model and senescence-accelerated mice (SAM)-prone 8 (SAMP8) model study showed that the use of CGRP inhibitors (rimegepant) was effective in reducing synovial inflammation [93].

3.2 | Bone Marrow Mesenchymal Stem Cells (BMSCs) Exosomes

A study on the mouse lumbar facet joint (LFJ) osteoarthritis (OA) model showed that BMSC-exosomes reduce CGRP-positive fibers and H-vessels, and inhibit abnormal neuroinvasion and angiogenesis in subchondral bone [94]. Additionally, BMSC-exosomes attenuated the inhibitory effects of IL-1β on chondrocyte proliferation and migration, and maintained the expression of cartilage extracellular matrix components through the upregulation of anabolic markers (C 0 L2-A1, ACAN) and the down-regulation of catabolic markers (MMP-13, ADAMTS-5). Moreover, BMSC-exosomes can inhibit IL-1β-induced chondrocyte apoptosis through the p38 MAPK, ERK, and Akt pathways [95]. Thus, exosomes not only directly promote cartilage growth but also inhibit the growth of nerve fibers into cartilage. However, there is a lack of research evidence in knee osteoarthritis models to support these effects. A study showed a significant reduction in serum CGRP after intra-articular injection of BMSC-exosomes in a rat MIA model [96]. The addition of different actives to exosomes has superior cartilage protection. For example, exosome miR-125a-5p attenuates the degradation of cartilage extracellular matrix in an OA rat model [97, 98]. A study validated the protective effect of hypoxia-treated adipose mesenchymal stem cell-derived exosomes in the LFJ OA mouse model, effectively reducing pain and cartilage degradation [99].

3.3 | Other Therapeutic Targets

Doxycycline, a potent inhibitor of matrix metalloproteinases, improves joint space narrowing but is suboptimal in improving pain and function. Further studies should be done to reveal its side effects, off-target effects, and the general benefits [47]. The bisphosphonates can inhibit the proliferation, adhesion, and migration of vascular smooth muscle cells and vascular endothelial cells, with some antiangiogenic effects [71]. Moreover, Strontium Ranelate can promote the synthesis of cartilage extracellular matrix in vitro, but its effect on the microenvironment of OA articular cartilage and subchondral bone needs further study [100]. Metformin protects articular cartilage and reverses the abnormal expression of iron-defeat-related proteins in chondrocytes of the mouse DMM model [101]. This further attenuates subchondral osteosclerosis and reduces heterogeneous angiogenesis in OA mice. Surprisingly, in this study, we found that Pazopanib also reduced the distribution of sensory nerve

fibers in the synovium of the knee. And based on the abovementioned finding, Pazopanib holds promise as a potential treatment to reduce the distribution of sensory nerves beneath the cartilage in OA [102]. A gene therapy study demonstrated that TissueGene-C, which overexpresses transforming growth factor-β1 (TGF-β1), significantly inhibited the expression of nerve growth factor (NGF) and CGRP in OA inflammation [103].

4 | Challenges

CGRP′s effects on cartilage in OA primarily lead to cartilage degradation, and potential treatments may involve CGRP receptor antagonists or the reduction of CGRP secretion. However, in menopausal and postmenopausal women with a high risk of developing OA, the implementation of these methods may lead to further bone loss or interfere with fracture healing [104, 105]. Clinical studies are needed to address this issue further. Combinations with other approaches may reduce adverse effects, such as the addition of oral magnesium supplements or the use of bisphosphonates in the treatment of osteoporosis, as well as magnesium-containing implants for fractures and bone defects [106]. However, their specific clinical efficacy and side effects need to be further explored.

5 | Perspectives

Many advances have been made on the role of CGRP in OA, which provides us with new ideas for the treatment of OA. In OA, CGRP promotes the production of inflammatory factors and the growth of H-vessels, contributing to the imbalance of cartilage's microenvironment, which leads to cartilage degeneration. However, in the cartilage microenvironment, it is crucial not to solely concentrate on the function of individual cytokines. Instead, a comprehensive approach should consider the potential synergistic effects of various cytokines. The delicate balance among multiple cytokines is crucial for preserving the synthesis and degradation of the cartilage matrix [107]. CGRP has different effects on cytokines, neoangiogenesis, subchondral osteosclerosis, and the synthesis and degradation of cartilage extracellular matrix. Notably, the significant increase in CGRP-positive sensory nerves around the cartilage in OA highlights the need to address both cartilage matrix repair and the combined effects of cytokines, angiogenesis, and nerve distribution in OA treatment.

6 | Conclusions

In the progression of OA, the distribution of sensory nerves at the osteochondral junction increases, leading to an increase in CGRP release. In addition to its well-established role in OA pain, CGRP is also involved in the process of cartilage degeneration in OA. It regulates pro-inflammatory factors and immune cells in OA, promoting the up-regulation of inflammatory factors, such as IL-1 and TNF-α, and the expression of matrix-degrading enzymes, like MMPs, thereby aggravating cartilage damage. Additionally, CGRP-induced recruitment and activation of immune cells significantly impact the inflammatory environment around OA chondrocytes. CGRP can activate macrophages of

different phenotypes, with M2 macrophages promoting repair of damaged articular cartilage. Moreover, CGRP promotes the coupling of subchondral bone to angiogenesis, thereby altering the subchondral bone microenvironment and aggravating cartilage degeneration. However, studies on CGRP's involvement in chondrocyte proliferation, differentiation, and apoptosis are limited and should be further investigated. We list some drugs that can block the signaling pathway of CGRP and some drugs that can ameliorate the pathological changes induced by CGRP, which are expected to guide future research and clinical treatment. Future work should focus on understanding the functional role of CGRP involved in OA cartilage degradation, as well as the specific regulatory pathways associated with CGRP, to discover more targets that can be intervened.

Author Contributions

Acknowledgments

Ethics Statement

The authors have nothing to report.

Consent

All authors approved the final manuscript.

Conflicts of Interest

The authors declare no conflicts of interest.

Data Availability Statement

The authors have nothing to report.

References

1. M. G. Cisternas, L. Murphy, J. J. Sacks, D. H. Solomon, D. J. Pasta, and C. G. Helmick, "Alternative Methods for Defining Osteoarthritis and the Impact on Estimating Prevalence in a US Population-Based Survey," *Arthritis Care & Research (Hoboken)* 68, no. 5 (2016): 574–580.

2. T. W. O'Neill and D. T. Felson, "Mechanisms of Osteoarthritis (OA) Pain," *Current Osteoporosis Reports* 16, no. 5 (2018): 611–616.

3. H. Long, Q. Liu, H. Yin, et al., "Prevalence Trends of Site-Specific Osteoarthritis From 1990 to 2019: Findings From the Global Burden of Disease Study 2019," *Arthritis & Rhematology* 74, no. 7 (2022): 1172–1183.

4. H. Yu, T. Huang, W. W. Lu, L. Tong, and D. Chen, "Osteoarthritis Pain," *International Journal of Molecular Sciences* 23, no. 9 (2022): 4642.

5. B. Abramoff and F. E. Caldera, "Osteoarthritis: Pathology, Diagnosis, and Treatment Options," *Medical Clinics of North America* 104, no. 2 (2020): 293–311.

6. S. Orita, T. Ishikawa, M. Miyagi, et al., "Pain-Related Sensory Innervation in Monoiodoacetate-Induced Osteoarthritis in Rat Knees That Gradually Develops Neuronal Injury in Addition to Inflammatory Pain," *BMC Musculoskeletal Disorders* 12 (2011): 134.

7. W. S. Schou, S. Ashina, F. M. Amin, P. J. Goadsby, and M. Ashina, "Calcitonin Gene-Related Peptide and Pain: A Systematic Review," *Journal of Headache and Pain* 18, no. 1 (2017): 34.

8. X. Wang, J. Xu, and Q. Kang, "Neuromodulation of Bone: Role of Different Peptides and Their Interactions (Review)," *Molecular Medicine Reports* 23, no. 1 (2021): 32.

9. G. Saxler, F. Loer, M. Skumavc, J. Pfortner, and U. Hanesch, "Localization of SP- and CGRP-Immunopositive Nerve Fibers in the Hip Joint of Patients With Painful Osteoarthritis and of Patients With Painless Failed Total Hip Arthroplasties," *European Journal of Pain* 11, no. 1 (2007): 67–74.

10. A. F. Russo and D. L. Hay, "CGRP Physiology, Pharmacology, and Therapeutic Targets: Migraine and Beyond," *Physiological Reviews* 103, no. 2 (2023): 1565–1644.

11. A. K. Huebner, J. Keller, P. Catala-Lehnen, et al., "The Role of Calcitonin and Alpha-Calcitonin Gene-Related Peptide in Bone Formation," *Archives of Biochemistry and Biophysics* 473, no. 2 (2008): 210–217.

12. P. K. Mulderry, M. A. Ghatei, R. A. Spokes, et al., "Differential Expression of Alpha-CGRP and Beta-CGRP by Primary Sensory Neurons and Enteric Autonomic Neurons of the Rat," *Neuroscience* 25, no. 1 (1988): 195–205.

13. J. Xu, J. Wang, X. Chen, Y. Li, J. Mi, and L. Qin, "The Effects of Calcitonin Gene-Related Peptide on Bone Homeostasis and Regeneration," *Current Osteoporosis Reports* 18, no. 6 (2020): 621–632.

14. H. He, J. Chai, S. Zhang, et al., "CGRP May Regulate Bone Metabolism Through Stimulating Osteoblast Differentiation and Inhibiting Osteoclast Formation," *Molecular Medicine Reports* 13, no. 5 (2016): 3977–3984.

15. D. Bobinac, J. Spanjol, S. Zoricic, and I. Maric, "Changes in Articular Cartilage and Subchondral Bone Histomorphometry in Osteoarthritic Knee Joints in Humans," *Bone* 32, no. 3 (2003): 284–290.

16. Y. Hu, X. Chen, S. Wang, Y. Jing, and J. Su, "Subchondral Bone Microenvironment in Osteoarthritis and Pain," *Bone Research* 9, no. 1 (2021): 20.

17. H. Enomoto, I. Inoki, K. Komiya, et al., "Vascular Endothelial Growth Factor Isoforms and Their Receptors Are Expressed in Human Osteoarthritic Cartilage," *American Journal of Pathology* 162, no. 1 (2003): 171–181.

18. M. Nagao, J. L. Hamilton, R. Kc, et al., "Vascular Endothelial Growth Factor in Cartilage Development and Osteoarthritis," *Scientific Reports* 7, no. 1 (2017): 13027.

19. T. Hayami, M. Pickarski, Y. Zhuo, G. A. Wesolowski, G. A. Rodan, and L. T. Duong, "Characterization of Articular Cartilage and Subchondral Bone Changes in the Rat Anterior Cruciate Ligament Transection and Meniscectomized Models of Osteoarthritis," *Bone* 38, no. 2 (2006): 234–243.

20. S. G. Grassel, "The Role of Peripheral Nerve Fibers and Their Neurotransmitters in Cartilage and Bone Physiology and Pathophysiology," *Arthritis Research & Therapy* 16, no. 6 (2014): 485.

21. S. Grassel and D. Muschter, "Peripheral Nerve Fibers and Their Neurotransmitters in Osteoarthritis Pathology," *International Journal of Molecular Sciences* 18, no. 5 (2017): 931.

22. W. Schwab, A. Bilgiçyildirim, and R. H. W. Funk, "Microtopography of the Autonomic Nerves in the Rat Knee: A Fluorescence Microscopic Study," *Anatomical Record* 247, no. 1 (1997): 109–118.

23. S. Grässel, R. H. Straub, and Z. Jenei-Lanzl, "The Sensory and Sympathetic Nervous System in Cartilage Physiology and Pathophysiology," in *Cartilage Physiology and Pathophysiology*, ed. S. Grässel and A. Aszódi (Springer, 2017), 191–227.

24. S. Imai, Y. Tokunaga, T. Maeda, M. Kikkawa, and S. Hukuda, "Calcitonin Gene-Related Peptide, Substance P, and Tyrosine Hydroxylase-Immunoreactive Innervation of Rat Bone Marrows: An Immunohistochemical and Ultrastructural Investigation on Possible Efferent and Afferent Mechanisms," *Journal of Orthopaedic Research* 15, no. 1 (1997): 133–140.

25. K. Aso, S. M. Shahtaheri, R. Hill, et al., "Contribution of Nerves Within Osteochondral Channels to Osteoarthritis Knee Pain in Humans and Rats," *Osteoarthritis and Cartilage* 28, no. 9 (2020): 1245–1254.

26. S. Suri, S. E. Gill, S. Massena de Camin, D. Wilson, D. F. McWilliams, and D. A. Walsh, "Neurovascular Invasion at the Osteochondral Junction and in Osteophytes in Osteoarthritis," *Annals of the Rheumatic Diseases* 66, no. 11 (2007): 1423–1428.

27. K. Murakami, H. Nakagawa, K. Nishimura, and S. Matsuo, "Changes in Peptidergic Fiber Density in the Synovium of Mice With Collagenase-Induced Acute Arthritis," *Canadian Journal of Physiology and Pharmacology* 93, no. 6 (2015): 435–441.

28. B. Lehner, F. X. Koeck, S. Capellino, T. E. Schubert, R. Hofbauer, and R. H. Straub, "Preponderance of Sensory Versus Sympathetic Nerve Fibers and Increased Cellularity in the Infrapatellar Fat Pad in Anterior Knee Pain Patients After Primary Arthroplasty," *Journal of Orthopaedic Research* 26, no. 3 (2008): 342–350.

29. M. Ebbinghaus, G. Segond von Banchet, J. Massier, et al., "Interleukin-6-Dependent Influence of Nociceptive Sensory Neurons on Antigen-Induced Arthritis," *Arthritis Research & Therapy* 17 (2015): 334.

30. L. M. McLatchie, N. J. Fraser, M. J. Main, et al., "RAMPs Regulate the Transport and Ligand Specificity of the Calcitonin-Receptor-Like Receptor," *Nature* 393, no. 6683 (1998): 333–339.

31. C. S. Walker, A. C. Conner, D. R. Poyner, and D. L. Hay, "Regulation of Signal Transduction by Calcitonin Gene-Related Peptide Receptors," *Trends in Pharmacological Sciences* 31, no. 10 (2010): 476–483.

32. D. R. Poyner, P. M. Sexton, I. Marshall, et al., "XXXII. The Mammalian Calcitonin Gene-Related Peptides, Adrenomedullin, Amylin, and Calcitonin Receptors," *Pharmacological Reviews* 54, no. 2 (2002): 233–246.

33. H. Drissi, F. Lasmoles, V. Le Mellay, P. J. Marie, and M. Lieberherr, "Activation of Phospholipase C-beta1 via Galphaq/11 During Calcium Mobilization by Calcitonin Gene-Related Peptide," *Journal of Biological Chemistry* 273, no. 32 (1998): 20168–20174.

34. H. Drissi, M. Lieberherr, M. Hott, P. J. Marie, and F. Lasmoles, "Calcitonin Gene-Related Peptide (CGRP) Increases Intracellular Free Ca2+ Concentrations but Not Cyclic AMP Formation in CGRP Receptor-Positive Osteosarcoma Cells (OHS-4)," *Cytokine* 11, no. 3 (1999): 200–207.

35. S. D. Brain and A. D. Grant, "Vascular Actions of Calcitonin Gene-Related Peptide and Adrenomedullin," *Physiological Reviews* 84, no. 3 (2004): 903–934.

36. G. C. Wellman, J. M. Quayle, and N. B. Standen, "ATP-Sensitive K+ Channel Activation by Calcitonin Gene-Related Peptide and Protein Kinase A in Pig Coronary Arterial Smooth Muscle," *Journal of Physiology* 507, no. Pt 1 (1998): 117–129.

37. S. Hosokawa, T. Endoh, Y. Shibukawa, et al., "Calcitonin Gene-Related Peptide- and Adrenomedullin-Induced Facilitation of Calcium Current by Different Signal Pathways in Nucleus Tractus Solitarius," *Brain Research* 1327 (2010): 47–55.

38. T. Kawase, K. Okuda, and D. M. Burns, "Immature Osteoblastic MG63 Cells Possess Two Calcitonin Gene-Related Peptide Receptor Subtypes That Respond Differently to [Cys(Acm)(2,7)] Calcitonin Gene-Related Peptide and CGRP(8-37)," *American Journal of Physiology. Cell Physiology* 289, no. 4 (2005): C811–C818.

39. M. Bastepe, L. S. Weinstein, N. Ogata, et al., "Stimulatory G Protein Directly Regulates Hypertrophic Differentiation of Growth Plate Cartilage in Vivo," *Proceedings of the National Academy of Sciences of the United States of America* 101, no. 41 (2004): 14794–14799.

40. A. Eitner, S. Muller, C. Konig, et al., "Inhibition of Inducible Nitric Oxide Synthase Prevents IL-1beta-Induced Mitochondrial Dysfunction in Human Chondrocytes," *International Journal of Molecular Sciences* 22, no. 5 (2021): 2477, https://doi.org/10.3390/ijms22052477.

41. T. Maleitzke, A. Hildebrandt, J. Weber, et al., "Proinflammatory and Bone Protective Role of Calcitonin Gene-Related Peptide Alpha in Collagen Antibody-Induced Arthritis," *Rheumatology (Oxford)* 60, no. 4 (2021): 1996–2009.

42. K. Watari, M. Nakaya, and H. Kurose, "Multiple Functions of G Protein-Coupled Receptor Kinases," *Journal of Molecular Signaling* 9, no. 1 (2014): 1.

43. E. L. Carlson, V. Karuppagounder, W. J. Pinamont, et al., "Paroxetine-Mediated GRK2 Inhibition is a Disease-Modifying Treatment for Osteoarthritis," *Science Translational Medicine* 13, no. 580 (2021): eaau8491.

44. U. Nedunchezhiyan, I. Varughese, A. R. Sun, X. Wu, R. Crawford, and I. Prasadam, "Obesity, Inflammation, and Immune System in Osteoarthritis," *Frontiers in Immunology* 13 (2022): 907750.

45. M. B. Goldring and S. R. Goldring, "Articular Cartilage and Subchondral Bone in the Pathogenesis of Osteoarthritis," *Annals of the New York Academy of Sciences* 1192 (2010): 230–237.

46. A. Burleigh, A. Chanalaris, M. D. Gardiner, et al., "Joint Immobilization Prevents Murine Osteoarthritis and Reveals the Highly Mechanosensitive Nature of Protease Expression in Vivo," *Arthritis and Rheumatism* 64, no. 7 (2012): 2278–2288.

47. S. Glyn-Jones, A. J. Palmer, R. Agricola, et al., "Osteoarthritis," *Lancet* 386, no. 9991 (2015): 376–387.

48. M. P. Vincenti and C. E. Brinckerhoff, "Transcriptional Regulation of Collagenase (MMP-1, MMP-13) Genes in Arthritis: Integration of Complex Signaling Pathways for the Recruitment of Gene-Specific Transcription Factors," *Arthritis Research* 4, no. 3 (2002): 157–164.

49. P. S. Burrage, K. S. Mix, and C. E. Brinckerhoff, "Matrix Metalloproteinases: Role in Arthritis," *Frontiers in Bioscience* 11 (2006): 529–543.

50. Y. J. Ha, Y. S. Choi, E. H. Kang, et al., "SOCS1 Suppresses IL-1beta-Induced C/EBPbeta Expression via Transcriptional Regulation in Human Chondrocytes," *Experimental & Molecular Medicine* 48, no. 6 (2016): e241.

51. B. Ji, Y. Ma, H. Wang, X. Fang, and P. Shi, "Activation of the P38/CREB/MMP13 Axis Is Associated With Osteoarthritis," *Drug Design, Development and Therapy* 13 (2019): 2195–2204.

52. K. E. Happonen, T. Saxne, A. Aspberg, M. Morgelin, D. Heinegard, and A. M. Blom, "Regulation of Complement by Cartilage Oligomeric Matrix Protein Allows for a Novel Molecular Diagnostic Principle in Rheumatoid Arthritis," *Arthritis and Rheumatism* 62, no. 12 (2010): 3574–3583.

53. R. Yaraee, M. Ebtekar, A. Ahmadiani, and F. Sabahi, "Neuropeptides (SP and CGRP) Augment Pro-Inflammatory Cytokine Production in HSV-Infected Macrophages," *International Immunopharmacology* 3, no. 13–14 (2003): 1883–1887.

54. G. Pongratz and R. H. Straub, "Role of Peripheral Nerve Fibres in Acute and Chronic Inflammation in Arthritis," *Nature Reviews Rheumatology* 9, no. 2 (2013): 117–126.

55. S. Matsui, M. Tanaka, A. Kamiyoshi, et al., "Endogenous Calcitonin Gene-Related Peptide Deficiency Exacerbates Postoperative Lymphedema by Suppressing Lymphatic Capillary Formation and M2 Macrophage Accumulation," *American Journal of Pathology* 189, no. 12 (2019): 2487–2502.

56. T. Talme, Z. Liu, and K. G. Sundqvist, "The Neuropeptide Calcitonin Gene-Related Peptide (CGRP) Stimulates T Cell Migration Into Collagen Matrices," *Journal of Neuroimmunology* 196, no. 1–2 (2008): 60–66.

57. J. Tao, X. Wang, and J. Xu, "Expression of CGRP in the Trigeminal Ganglion and Its Effect on the Polarization of Macrophages in Rats With Temporomandibular Arthritis," *Cellular and Molecular Neurobiology* 44, no. 1 (2024): 22.

58. D. L. Laskin, V. R. Sunil, C. R. Gardner, and J. D. Laskin, "Macrophages and Tissue Injury: Agents of Defense or Destruction?," *Annual Review of Pharmacology and Toxicology* 51 (2011): 267–288.

59. Y. S. Li, W. Luo, S. A. Zhu, and G. H. Lei, "T Cells in Osteoarthritis: Alterations and Beyond," *Frontiers in Immunology* 8 (2017): 356.

60. K. Sadtler, K. Estrellas, B. W. Allen, et al., "Developing a Pro-Regenerative Biomaterial Scaffold Microenvironment Requires T Helper 2 Cells," *Science* 352, no. 6283 (2016): 366–370.

61. R. Gobezie, A. Kho, B. Krastins, et al., "High Abundance Synovial Fluid Proteome: Distinct Profiles in Health and Osteoarthritis," *Arthritis Research & Therapy* 9, no. 2 (2007): R36.

62. J. E. Woodell-May and S. D. Sommerfeld, "Role of Inflammation and the Immune System in the Progression of Osteoarthritis," *Journal of Orthopaedic Research* 38, no. 2 (2020): 253–257.

63. C. Sanchez, M. A. Deberg, N. Piccardi, P. Msika, J. Y. Reginster, and Y. E. Henrotin, "Subchondral Bone Osteoblasts Induce Phenotypic Changes in Human Osteoarthritic Chondrocytes," *Osteoarthritis and Cartilage* 13, no. 11 (2005): 988–997.

64. T. Schinke, S. Liese, M. Priemel, et al., "Decreased Bone Formation and Osteopenia in Mice Lacking Alpha-Calcitonin Gene-Related Peptide," *Journal of Bone and Mineral Research* 19, no. 12 (2004): 2049–2056.

65. L. Wang, X. Shi, R. Zhao, et al., "Calcitonin-Gene-Related Peptide Stimulates Stromal Cell Osteogenic Differentiation and Inhibits RANKL Induced NF-kappaB Activation, Osteoclastogenesis and Bone Resorption," *Bone* 46, no. 5 (2010): 1369–1379.

66. T. Nakasa, M. Ishikawa, T. Takada, S. Miyaki, and M. Ochi, "Attenuation of Cartilage Degeneration by Calcitonin Gene-Related Paptide Receptor Antagonist via Inhibition of Subchondral Bone Sclerosis in Osteoarthritis Mice," *Journal of Orthopaedic Research* 34, no. 7 (2016): 1177–1184.

67. Y. Chen, T. Wang, M. Guan, et al., "Bone Turnover and Articular Cartilage Differences Localized to Subchondral Cysts in Knees With Advanced Osteoarthritis," *Osteoarthritis and Cartilage* 23, no. 12 (2015): 2174–2183.

68. D. Syx, P. B. Tran, R. E. Miller, and A. M. Malfait, "Peripheral Mechanisms Contributing to Osteoarthritis Pain," *Current Rheumatology Reports* 20, no. 2 (2018): 9.

69. G. Ji, R. Xu, Y. Niu, et al., "Vascular Endothelial Growth Factor Pathway Promotes Osseointegration and CD31(Hi)EMCN(Hi) Endothelium Expansion in a Mouse Tibial Implant Model: An Animal Study," *Bone & Joint Journal* 101-B, no. 7_Supple_C (2019): 108–114.

70. J. Zhang, J. Pan, and W. Jing, "Motivating Role of Type H Vessels in Bone Regeneration," *Cell Proliferation* 53, no. 9 (2020): e12874.

71. Y. Liu, H. Q. Xie, and B. Shen, "Type H Vessels-a Bridge Connecting Subchondral Bone Remodelling and Articular Cartilage Degeneration in Osteoarthritis Development," *Rheumatology (Oxford)* 62, no. 4 (2023): 1436–1444.

72. Y. Peng, S. Wu, Y. Li, and J. L. Crane, "Type H Blood Vessels in Bone Modeling and Remodeling," *Theranostics* 10, no. 1 (2020): 426–436.

73. S. G. Romeo, K. M. Alawi, J. Rodrigues, A. Singh, A. P. Kusumbe, and S. K. Ramasamy, "Endothelial Proteolytic Activity and Interaction With Non-Resorbing Osteoclasts Mediate Bone Elongation," *Nature Cell Biology* 21, no. 4 (2019): 430–441.

74. P. I. Mapp, D. F. McWilliams, M. J. Turley, E. Hargin, and D. A. Walsh, "A Role for the Sensory Neuropeptide Calcitonin Gene-Related Peptide in Endothelial Cell Proliferation in Vivo," *British Journal of Pharmacology* 166, no. 4 (2012): 1261–1271.

75. S. Zheng, W. Li, M. Xu, et al., "Calcitonin Gene-Related Peptide Promotes Angiogenesis via AMP-Activated Protein Kinase," *American Journal of Physiology-Cell Physiology* 299, no. 6 (2010): C1485–C1492.

76. D. A. Walsh, C. S. Bonnet, E. L. Turner, D. Wilson, M. Situ, and D. F. McWilliams, "Angiogenesis in the Synovium and at the Osteochondral Junction in Osteoarthritis," *Osteoarthritis and Cartilage* 15, no. 7 (2007): 743–751.

77. H. Xie, Z. Cui, L. Wang, et al., "PDGF-BB Secreted by Preosteoclasts Induces Angiogenesis During Coupling With Osteogenesis," *Nature Medicine* 20, no. 11 (2014): 1270–1278.

78. W. Su, G. Liu, X. Liu, et al., "Angiogenesis Stimulated by Elevated PDGF-BB in Subchondral Bone Contributes to Osteoarthritis Development," *JCI Insight* 5, no. 8 (2020): e135446, https://doi.org/10.1172/jci.insight.135446.

79. G. Sufen, Y. Xianghong, C. Yongxia, and P. Qian, "bFGF and PDGF-BB Have a Synergistic Effect on the Proliferation, Migration and VEGF Release of Endothelial Progenitor Cells," *Cell Biology International* 35, no. 5 (2011): 545–551.

80. W. C. Liu, S. Chen, L. Zheng, and L. Qin, "Angiogenesis Assays for the Evaluation of Angiogenic Properties of Orthopaedic Biomaterials - A General Review," *Advanced Healthcare Materials* 6, no. 5 (2017): 1600434.

81. A. P. Kusumbe, S. K. Ramasamy, and R. H. Adams, "Coupling of Angiogenesis and Osteogenesis by a Specific Vessel Subtype in Bone," *Nature* 507, no. 7492 (2014): 323–328.

82. R. Xu, A. Yallowitz, A. Qin, et al., "Targeting Skeletal Endothelium to Ameliorate Bone Loss," *Nature Medicine* 24, no. 6 (2018): 823–833.

83. S. K. Ramasamy, A. P. Kusumbe, L. Wang, and R. H. Adams, "Endothelial Notch Activity Promotes Angiogenesis and Osteogenesis in Bone," *Nature* 507, no. 7492 (2014): 376–380.

84. R. E. Tomlinson and M. J. Silva, "Skeletal Blood Flow in Bone Repair and Maintenance," *Bone Research* 1, no. 4 (2013): 311–322.

85. S. K. Ramasamy, A. P. Kusumbe, M. Schiller, et al., "Blood Flow Controls Bone Vascular Function and Osteogenesis," *Nature Communications* 7 (2016): 13601.

86. Q. Yao, X. Wu, C. Tao, et al., "Osteoarthritis: Pathogenic Signaling Pathways and Therapeutic Targets," *Signal Transduction and Targeted Therapy* 8, no. 1 (2023): 56.

87. Y. Matsumoto, K. Tanaka, G. Hirata, et al., "Possible Involvement of the Vascular Endothelial Growth Factor-Flt-1-Focal Adhesion Kinase Pathway in Chemotaxis and the Cell Proliferation of Osteoclast Precursor Cells in Arthritic Joints," *Journal of Immunology* 168, no. 11 (2002): 5824–5831.

88. M. Nakagawa, T. Kaneda, T. Arakawa, et al., "Vascular Endothelial Growth Factor (VEGF) Directly Enhances Osteoclastic Bone Resorption and Survival of Mature Osteoclasts," *FEBS Letters* 473, no. 2 (2000): 161–164.

89. S. Stockl, A. Eitner, R. J. Bauer, M. Konig, B. Johnstone, and S. Grassel, "Substance P and Alpha-Calcitonin Gene-Related Peptide Differentially Affect Human Osteoarthritic and Healthy Chondrocytes," *Frontiers in Immunology* 12 (2021): 722884.

90. D. Muschter, L. Fleischhauer, S. Taheri, A. F. Schilling, H. Clausen-Schaumann, and S. Grassel, "Sensory Neuropeptides Are Required for Bone and Cartilage Homeostasis in a Murine Destabilization-Induced Osteoarthritis Model," *Bone* 133 (2020): 115181.

91. S. Hirsch, L. Corradini, S. Just, K. Arndt, and H. Doods, "The CGRP Receptor Antagonist BIBN4096BS Peripherally Alleviates Inflammatory Pain in Rats," *Pain* 154, no. 5 (2013): 700–707.

92. R. J. Benschop, E. C. Collins, R. J. Darling, et al., "Development of a Novel Antibody to Calcitonin Gene-Related Peptide for the Treatment of Osteoarthritis-Related Pain," *Osteoarthritis and Cartilage* 22, no. 4 (2014): 578–585.

93. A. Nekomoto, T. Nakasa, Y. Ikuta, C. Ding, S. Miyaki, and N. Adachi, "Feasibility of Administration of Calcitonin Gene-Related Peptide Receptor Antagonist on Attenuation of Pain and Progression in Osteoarthritis," *Scientific Reports* 13, no. 1 (2023): 15354.

94. J. Li, Z. Ding, Y. Li, et al., "BMSCs-Derived Exosomes Ameliorate Pain via Abrogation of Aberrant Nerve Invasion in Subchondral Bone in Lumbar Facet Joint Osteoarthritis," *Journal of Orthopaedic Research* 38, no. 3 (2020): 670–679.

95. H. Qi, D. P. Liu, D. W. Xiao, D. C. Tian, Y. W. Su, and S. F. Jin, "Exosomes Derived From Mesenchymal Stem Cells Inhibit Mitochondrial Dysfunction-Induced Apoptosis of Chondrocytes via p38, ERK, and Akt Pathways," *In Vitro Cellular & Developmental Biology. Animal* 55, no. 3 (2019): 203–210.

96. A. Noorwali, F. Aljoud, A. Alghamdi, et al., "Evaluation of Serum Biomarkers After Intra-Articular Injection of Rat Bone Marrow-Derived Mesenchymal Stem Cells in a Rat Model of Knee Osteoarthritis," *Heliyon* 10, no. 21 (2024): e39940.

97. S. C. Tao, T. Yuan, Y. L. Zhang, W. J. Yin, S. C. Guo, and C. Q. Zhang, "Exosomes Derived From miR-140-5p-Overexpressing Human Synovial Mesenchymal Stem Cells Enhance Cartilage Tissue Regeneration and Prevent Osteoarthritis of the Knee in a Rat Model," *Theranostics* 7, no. 1 (2017): 180–195.

98. Q. Xia, Q. Wang, F. Lin, and J. Wang, "miR-125a-5p-Abundant Exosomes Derived From Mesenchymal Stem Cells Suppress Chondrocyte Degeneration via Targeting E2F2 in Traumatic Osteoarthritis," *Bioengineered* 12, no. 2 (2021): 11225–11238.

99. J. Zhao, Y. Sun, X. Sheng, et al., "Hypoxia-Treated Adipose Mesenchymal Stem Cell-Derived Exosomes Attenuate Lumbar Facet Joint Osteoarthritis," *Molecular Medicine* 29, no. 1 (2023): 120.

100. Y. Henrotin, A. Labasse, S. X. Zheng, et al., "Strontium Ranelate Increases Cartilage Matrix Formation," *Journal of Bone and Mineral Research* 16, no. 2 (2001): 299–308.

101. J. Yan, G. Feng, L. Ma, Z. Chen, and Q. Jin, "Metformin Alleviates Osteoarthritis in Mice by Inhibiting Chondrocyte Ferroptosis and Improving Subchondral Osteosclerosis and Angiogenesis," *Journal of Orthopaedic Surgery and Research* 17, no. 1 (2022): 333.

102. K. Ma, G. Singh, J. Wang, et al., "Targeting Vascular Endothelial Growth Factor Receptors as a Therapeutic Strategy for Osteoarthritis and Associated Pain," *International Journal of Biological Sciences* 19, no. 2 (2023): 675–690.

103. E. H. Park, J. Seo, Y. Lee, et al., "TissueGene-C Induces Long-Term Analgesic Effects Through Regulation of Pain Mediators and Neuronal Sensitization in a Rat Monoiodoacetate-Induced Model of Osteoarthritis Pain," *Osteoarthritis and Cartilage* 31, no. 12 (2023): 1567–1580.

104. X. Liu, H. Liu, Y. Xiong, et al., "Postmenopausal Osteoporosis Is Associated With the Regulation of SP, CGRP, VIP, and NPY," *Biomedicine & Pharmacotherapy* 104 (2018): 742–750.

105. Z. Huan, Y. Wang, M. Zhang, et al., "Follicle-Stimulating Hormone Worsens Osteoarthritis by Causing Inflammation and Chondrocyte Dedifferentiation," *FEBS Open Bio* 11, no. 8 (2021): 2292–2303.

106. L. Z. Zheng, J. L. Wang, J. K. Xu, et al., "Magnesium and Vitamin C Supplementation Attenuates Steroid-Associated Osteonecrosis in a Rat Model," *Biomaterials* 238 (2020): 119828.

107. S. Liu, Z. Deng, K. Chen, et al., "Cartilage Tissue Engineering: From Proinflammatory and Anti-Inflammatory Cytokines to Osteoarthritis Treatments (Review)," *Molecular Medicine Reports* 25 (2022): 99.

WILEY

LETTER TO THE EDITOR

Letter to the Editor: "Cerebral Perfusion Features in Takayasu Arteritis: Insights From pCASL MRI"

Bhaskar Kambhampati[1] | Leelakrishna Ayanambakam[2] | Ranjana Sah[3,4]

[1]Rangaraya Medical College, Kakinada, Andhra Pradesh, India | [2]Sri Venkateswara Medical College, Tirupati, Andhra Pradesh, India | [3]Department of Paediatrics, Dr. D. Y. Patil Medical College Hospital and Research Centre, Dr. D. Y. Patil Vidyapeeth (Deemed-To-Be-University), Pune, Maharashtra, India | [4]Department of Public Health Dentistry, Dr. D. Y. Patil Dental College Hospital and Research Centre, Dr. D. Y. Patil Vidyapeeth (Deemed-To-Be-University), Pune, Maharashtra, India

Correspondence: Bhaskar Kambhampati (bhaskar.k.research@gmail.com)

Dear Editor,

We read with great interest the study by Zhao et al. [1], which utilized pseudo-continuous arterial spin labeling (pCASL) MRI to characterize cerebral perfusion in Takayasu arteritis (TA) patients with supra-aortic and/or intracranial artery lesions. While the study contributes important observational data, several key limitations undermine its translational validity and mechanistic insight.

First, the methodological design suffers from insufficient statistical power across key subgroup analyses. Despite using linear mixed models to adjust for age, post hoc power remained well below the 0.80 threshold for non-significant comparisons, particularly between patients with and without prior cerebral infarction. Such underpowered comparisons limit interpretability and may have masked clinically relevant perfusion disparities, especially in regions supplied by affected vertebrobasilar vessels.

Second, the homogeneity of the study cohort, restricted to female patients, limits external validity. Although the rationale relates to the gender distribution in TA, excluding male patients precludes generalization of perfusion metrics to the entire TA population [2]. Furthermore, the absence of structured control for medication classes, specifically corticosteroids, biologics, and cytotoxics, raises the possibility that treatment-related vascular modulation could have confounded cerebral blood flow (CBF) and arterial transit time (ATT) measurements [3].

Third, the pathophysiological interpretation presented by the authors underemphasizes microvascular contributions to perfusion deficits. While macrovascular stenoses were graded and correlated with perfusion, the possibility of concomitant small vessel vasculopathy, well-documented in TA through histopathological studies, was not addressed [4]. Additionally, the discussion did not account for neurovascular autoregulatory responses that could alter ATT in the setting of chronic hypoperfusion, nor did it evaluate the role of cortical versus subcortical hypoperfusion patterns, which may offer higher discriminatory value for cognitive and functional correlates [5].

From a translational standpoint, the clinical utility of pCASL-MRI remains speculative without longitudinal validation or correlation with cognitive decline, stroke recurrence, or treatment response. The claim that pCASL offers dynamic evaluation is weakened by its single time-point design and the absence of follow-up scans post-immunosuppression. Moreover, the observation that vertebral artery lesions of grade 3 or higher are associated with global perfusion deficits is noteworthy, although it may be considered somewhat tautological, given the well-established hemodynamic significance of the posterior circulation.

In conclusion, while this study advances the application of pCASL in vasculitis imaging, its limitations in sample power, generalizability, and mechanistic interpretation constrain its

clinical relevance. Future studies must incorporate multicenter cohorts, include both sexes, stratify by medication class, and embed longitudinal pCASL data aligned with cerebrovascular outcomes and cognitive assessments. Only through such integrative efforts can pCASL transition from a research modality to a clinical decision-making tool in Takayasu arteritis.

Author Contributions

Bhaskar Kambhampati: conceptualisation, methodology, writing – original draft, writing – review and editing. **Leelakrishna Ayanambakam:** writing – original draft, writing – review and editing. **Ranjana Sah:** validation, supervision, project administration, writing – original draft, writing – review and editing.

Conflicts of Interest

The authors declare no conflicts of interest.

Data Availability Statement

Data sharing is not applicable to this article, as no new data were created or analyzed in this study.

<div align="right">

Bhaskar Kambhampati
Leelakrishna Ayanambakam
Ranjana Sah

</div>

References

1. Y. Zhao, H. Zhang, F. Kong, et al., "Cerebral Perfusion Features in Takayasu Arteritis: Insights From pCASL MRI," *International Journal of Rheumatic Diseases* 28 (2025): e70326, https://doi.org/10.1111/1756-185X.70326.

2. A. Y. Lim, G. Y. Lee, S. Y. Jang, et al., "Gender Differences in Clinical and Angiographic Findings of Patients With Takayasu Arteritis," *Clinical and Experimental Rheumatology* 33, no. 2 Suppl 89 (2015): S132–S137.

3. M. Samaan, A. Abramyan, S. Sundararajan, et al., "Cerebrovascular Implications of Takayasu Arteritis: A Review," *Neuroradiology* 67 (2024): 125–136, https://doi.org/10.1007/s00234-024-03472-2.

4. C. Svensson, N. Bjarnegård, P. Eriksson, et al., "Affected Microcirculation and Vascular Hemodynamics in Takayasu Arteritis," *Frontiers in Physiology* 13 (2022): 926940, https://doi.org/10.3389/fphys.2022.926940.

5. Y. Sun, W. Cao, W. Ding, et al., "Cerebral Blood Flow Alterations as Assessed by 3D ASL in Cognitive Impairment in Patients With Subcortical Vascular Cognitive Impairment: A Marker for Disease Severity," *Frontiers in Aging Neuroscience* 8 (2016): 211, https://doi.org/10.3389/fnagi.2016.00211.

WILEY

International Journal of
Rheumatic Diseases

LETTER TO THE EDITOR

Successful Treatment for Recurrent Histiocytic Necrotizing Lymphadenitis With Low-Dose Hydroxychloroquine

Shuya Kaneko ⬤ | Hitoshi Irabu | Masaki Shimizu ⬤

Department of Paediatrics and Developmental Biology, Graduate School of Medical and Dental Sciences, Institute of Science Tokyo, Tokyo, Japan

Correspondence: Masaki Shimizu (mshimizu.ped@tmd.ac.jp)

Dear Editor,

Histiocytic necrotizing lymphadenitis (HNL), also known as Kikuchi-Fujimoto disease, is an inflammatory disease characterized by painful lymph node (LN) swelling and sustained high fever for several weeks [1, 2], with some patients experiencing relapses despite treatment or even developing autoimmune diseases, including systemic lupus erythematosus (SLE) [2, 3]. Typically, HNL is treated with antipyretic agents, such as nonsteroidal anti-inflammatory drugs and glucocorticoids (GC); however, some patients may develop recurrences or disease flares as the GC dosage is reduced, requiring adjunctive treatment to counter the side effects of GC.

Hydroxychloroquine (HCQ) is an effective treatment for SLE and other rheumatic diseases, which suppresses the excessive production of interferon-alfa (IFN-α) by inhibiting toll-like receptors 7 and 9 [4]. Recent studies have revealed that overproduction of IFNα is related to the pathogenesis of HNL, making it a potential therapeutic target [5, 6]. There are a few reports on the clinical efficacy of HCQ in patients with HNL; however, the optimal dosage and duration are yet to be established [7, 8]. Herein, we describe the management of two pediatric HNL cases who relapsed after GC reduction or discontinuation; remission was maintained with low-dose HCQ initiation, which led to decreased serum IFNα levels.

Patient 1 is a Japanese 15-year-old boy who presented with fever and painful cervical LN swelling at 13 years of age. He was diagnosed with HNL following an LN biopsy. Although general blood tests revealed no significant abnormalities at the time of diagnosis, his serum IFNα levels were at 32 pg/mL (normal range: < 1 pg/mL; Table S1). Although his symptoms improved upon prednisolone (PSL) initiation (0.8 mg/kg/day), fever and painful LN swelling recurred 24 months following onset (Figure 1). Accordingly, he was diagnosed with an HNL relapse. PSL was initiated again and his symptoms improved rapidly; however, the painful LN swelling flared up 1 month after tapering and discontinuation of PSL. PSL was restarted; however, a reduction in the PSL dosage worsened the fever and lymphadenopathy, thereby making the discontinuation difficult. During the course of PSL administration, we noted that his serum IFNα levels increased with every relapse. Alternating doses of HCQ (400 and 200 mg/day) (7.3 and 3.6 mg/kg/day, respectively; averaging 5.5 mg/kg/day) were initiated, which ameliorated the fever and lymphadenopathy; PSL was eventually discontinued. HCQ was also discontinued 7 months later, and there have been no relapses for 13 months since HCQ discontinuation.

Patient 2 is a Japanese 15-year-old boy who was referred to our department with complaints of high fever, painful cervical LN swelling, and intermittent erythema for more than 2 weeks, with mildly elevated C-reactive protein and ferritin levels (Table S1). He was also diagnosed with HNL based on LN biopsy results, and PSL (1.0 mg/kg/day) was initiated. At the time of diagnosis, his serum IFNα levels increased to 52 pg/mL. Subsequently, the dose of PSL was reduced and discontinued over 3 months; however, he relapsed 5 months after PSL discontinuation (Figure 2). PSL was reinitiated, and the serum sample collected 3 days after recommencing showed increased serum IFNα levels. An alternative HCQ dose (400 and 200 mg/day [6.7 and 3.3 mg/kg/day, respectively] averaging 5.0 mg/kg/day) was administered, following which the fever and cervical LN swelling ameliorated. PSL could be promptly discontinued, and the patient has had no relapses for 6 months since HCQ initiation.
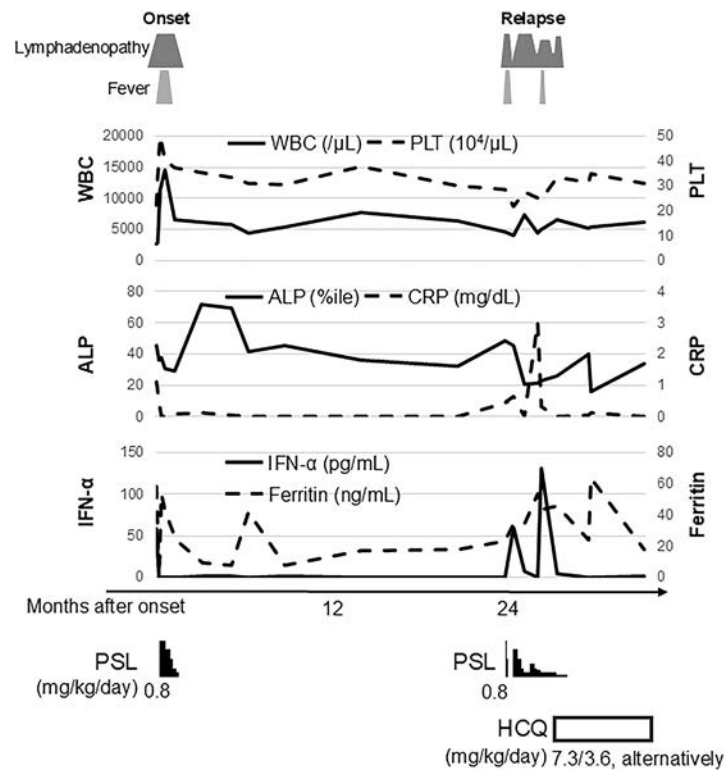
FIGURE 1 | Clinical course of patients 1.
Serum IFNα levels were measured using enzymelinked immunosorbent assay kits as per manufacturer's instructions (PBL Assay Science, Piscataway, NJ, USA). Serum alkaline phosphatase (ALP) has recently been reported as a useful biomarker for HNL [9, 10]. AD, Alternative-day Dosing; ALP, alkaline phosphatase; HCQ, hydroxychloroquine; PLT, platelet counts; PSL, prednisolone.
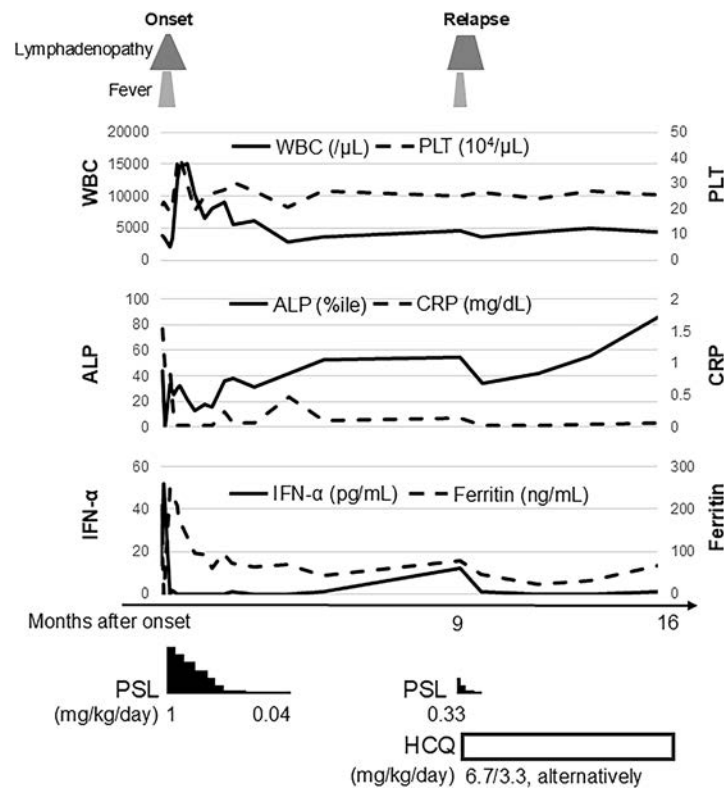
FIGURE 2 | Clinical course of patients 2.
Serum IFNα levels were measured using enzymelinked immunosorbent assay kits as per manufacturer's instructions (PBL Assay Science, Piscataway, NJ, USA). Serum alkaline phosphatase (ALP) has recently been reported as a useful biomarker for HNL [9, 10]. AD, Alternative-day Dosing; ALP, alkaline phosphatase; HCQ, hydroxychloroquine; PLT, platelet counts; PSL, prednisolone.

To date, there is no standardized treatment for HNL. Over the years, HCQ is emerging as a potential therapy with some case reports exhibiting the efficacy of HCQ for HNL. We previously reported the usefulness of serum IFNα for diagnosing and assessing the disease activity of HNL [6]. In the present study, serum IFN-α levels decreased and eventually normalized after starting HCQ in both patients, highlighting the importance of IFN-α in the pathogenesis of HNL and the therapeutic role of HCQ in suppressing IFN-α.

So far, only six pediatric cases of HNL treated with HCQ have been reported (Table S2) [7, 8]. All previously reported patients were approximately 10 years of age and did not exhibit relapse after discontinuing an HCQ treatment of 3–9 months, although the details of the clinical courses are unknown. Notably, the HCQ dosage used in these studies (6.5 to 16.5 kg/mg/day) was higher than those of our two cases. We tried to maintain the dose as low as possible to avoid toxicity, including retinopathy and gastroenteropathy. Accordingly, we can recommend that HCQ treatment of 5 mg/kg/day for 6 months may be adequate in HNL patients. Nevertheless, prospective studies with large sample sizes are warranted.

In conclusion, low-dose HCQ can be used to manage recurrent HNL in pediatric patients.

Author Contributions

S.K. wrote the manuscript; S.K. and H.I. collected data; H.I. and M.S. critically reviewed the manuscript. M.S. supervised the whole study process. All authors read and approved the final manuscript.

Consent

Informed consent was obtained from both patients and their parents for using and publishing their data in this manuscript.

Conflicts of Interest

The authors declare no conflicts of interest.

Data Availability Statement

The data that support the findings of this study are available from the corresponding author upon reasonable request.

Shuya Kaneko
Hitoshi Irabu
Masaki Shimizu

References

1. X. Bosch, A. Guilabert, R. Miquel, and E. Campo, "Enigmatic Kikuchi–Fujimoto Disease: A Comprehensive Review," *American Journal of Clinical Pathology* 122 (2004): 141–152.

2. A. M. Perry and S. M. Choi, "Kikuchi–Fujimoto Disease: A Review," *Archives of Pathology & Laboratory Medicine* 142 (2018): 1341–1346.

3. D. Biasi, P. Caramaschi, A. Carletto, et al., "Three Clinical Reports of Kikuchi's Lymphadenitis Combined With Systemic Lupus Erythematosus," *Clinical Rheumatology* 15 (1996): 81–83.

4. G. RuizIrastorza and G. Bertsias, "Treating Systemic Lupus Erythematosus in the 21st Century: New Drugs and New Perspectives on Old Drugs," *Rheumatology* 59 (2020): v69–v81.

5. E. Y. Li, J. Xu, N. D. Nelson, et al., "Kikuchi–Fujimoto Disease Is Mediated by an Aberrant Type I Interferon Response," *Modern Pathology* 35 (2022): 462–469.

6. S. Kaneko, A. Shimbo, H. Irabu, et al., "Pathogenic Role and Diagnostic Utility of Interferonα in Histiocytic Necrotizing Lymphadenitis," *Clinical Immunology* 266 (2024): 110324.

7. P. H. Chen, Y. F. Huang, C. W. Tang, S. R. Wann, and H. T. Chang, "Kikuchi–Fujimoto Disease: An Amazing Response to Hydroxychloroquine," *European Journal of Pediatrics* 169 (2010): 1557–1559.

8. Y. C. Lin, H. H. Huang, B. R. Nong, et al., "Pediatric Kikuchi–Fujimoto Disease: A Clinicopathologic Study and the Therapeutic Effects of Hydroxychloroquine," *Journal of Microbiology, Immunology, and Infection* 52 (2019): 395–401.

9. Y. Inamo, "Low Serum Alkaline Phosphatase Activity in Kikuchi-Fujimoto Disease," *Medicine (Baltimore)* 96, no. 9 (2017): e6228.

10. S. Fujiwara, Y. Higuchi, and J. Shimizu, "Serum Alkaline Phosphatase Levels in Pediatric Kikuchi-Fujimoto Disease: A Retrospective Observational Analysis," *Immunity, Inflammation and Disease* 13, no. 1 (2025): e70129.

Supporting Information

Additional supporting information can be found online in the Supporting Information section.

Case Report: Two Cases of Autoimmune/Inflammatory Syndrome Induced by Adjuvants

Karlygash Karina[1,2] 🔟 | Lina Zaripova[3] 🔟 | Bayan Ainabekova[1] | Argul Issilbayeva[1] | Nurzhan Asanov[4] | Dinara Sadykova[1] 🔟 | Diana Makimova[5] 🔟

[1]Department of Internal Medicine with Gastroenterology, Endocrinology and Pulmonology Courses, Astana Medical University, Astana, Kazakhstan | [2]The General Clinical Department, National Scientific Center of Traumatology and Orthopedics Named after N.D. Batpenov, Astana, Kazakhstan | [3]Department of Scientific and Innovation Management, National Scientific Medical Center, Astana, Kazakhstan | [4]Department of Arthroscopy and Sports Medicine, National Scientific Center of Traumatology and Orthopedics Named after N.D. Batpenov, Astana, Kazakhstan | [5]Department of Internal Medicine no. 4, Astana Medical University, Astana, Kazakhstan

Correspondence: Lina Zaripova (zaripova_lina@list.ru)

Received: 24 December 2024 | **Revised:** 10 March 2025 | **Accepted:** 22 June 2025

Dear Editor,

Autoimmune/inflammatory syndrome induced by adjuvants (ASIA syndrome) encompasses a spectrum of immune-mediated disorders triggered by exposure to environmental factors. In 2011, Shoenfeld and Agmon-Levin introduced the concept of ASIA syndrome to describe immune-mediated disorders linked to adjuvants [1]. Since then, more than 4000 cases of this disease have been documented, with differing histories and varying degrees of severity [2]. While the syndrome remains controversial due to its broad diagnostic criteria and overlap with other conditions, its recognition is essential for understanding certain unexplained autoimmune phenomena.

Over the past few decades, new adjuvants have been added to the list of potential causes of the syndrome including vaccine adjuvants, aluminum hydroxide, silica, silicone implants, polypropylene meshes [3–6], and other environmental substances such as infectious agents [7, 8]. Adjuvants do not directly trigger an immune response themselves, but they assist in creating a strong reaction against the antigens they are introduced to. They influence both the adaptive and innate immune responses through various mechanisms, leading to the initiation and maintenance of an immune response through the activation of pattern recognition receptors such as toll-like receptors, NOD-like receptors, and C-type lectin receptors [9]. The activation of these molecules gives rise to a cascade of events, culminating in the recruitment and subsequent activation of proteins, which in turn contribute to the production of cytokines. Moreover, adjuvants facilitate specific aspects of dendritic cell chemotaxis and the activation of antigen-presenting cells, promoting cytokine release, further enhancing the transfer of antigens to a B- and T-cell-rich environment, thereby stimulate the adaptive immune response against antigens [10]. Commonly used biomaterials for implants are designed to be non-immunogenic and non-cytotoxic, yet they can still elicit an immune response with the granulomatous inflammation in people with genetic predisposition according to HLA-DRB1, HLA-DQ8 [11, 12].

Following the implantation of biomaterials, a protein layer of the host forms on its surface, attracting phagocytes, primarily pro-inflammatory macrophages. In addition, if a biofilm forms after implantation, the microorganisms in the biofilm can act as adjuvants, activating. Exposure to these adjuvants mimic patterns associated with damage and pathogens by activating Toll-like receptors and inflammasomes, resulting in the release of inflammatory cytokines, activation of dendritic cells, and macrophages, leading to apoptosis of macrophages, release of particles containing the adjuvant, further stimulating inflammation. IL-17 production is also stimulated, as well as the influx of neutrophils, leading to formation of reactive oxygen species and release of myeloperoxidase that potentiate inflammation. This, in turn, leads to increased local and systemic responses to antigens present in regional lymph nodes, dysregulation of T and B lymphocytes, inability to recognize autoantigens, inflammation, tissue damage, and autoimmunity [13]. The breakdown of own tissues is facilitated by an imbalance between effector T cells and regulatory T cells, which further increases the production of autoantibodies [14].

The ASIA syndrome can be identified if a patient meets two major or one major and two minor following criteria [7]. Main criteria for this diagnose of ASIA syndrome include exposure to adjuvants previous clinical manifestations; typical arthralgia and/or arthritis, cognitive impairment and memory loss, fever, dryness of mouth and/or eyes, neurological symptoms especially those associated with demyelination; the improvement after removal of the inciting factor; a typical changes on the biopsy of affected organs [1, 7, 15]. Minor criteria include the presence of autoantibodies or antibodies directed against the putative adjuvant; additional clinical symptoms such as irritable bowel syndrome or Raynaud's phenomenon; explicit HLA associations DRB1, DQB1; the development of any autoimmune diseases (systemic lupus erythematosus, multiple sclerosis, arthritis, Sjögren's disease) [7].

The alleviation of post-operative symptoms following the removal of implants is a key indicator in the assessment of ASIA [7, 16, 17], which were observed in a range of 50%–98% of patients [18].

Patient I., aged 38, underwent dental surgery on May 5th, 2022, during which four teeth were extracted and five dental implants were installed. Ten days later, on May 15th, the patient presented with pain, stiffness, and restricted movement in their right elbow and left ankle. Additionally, the patient experienced pain in the sacral area, muscle weakness, fatigue, disturbed sleep, and weight loss. Both the right ankle and the left elbow were swollen, right achilles tendinitis and left talalgia were present. Radiographs did not reveal any pathological changes. Despite this, the patient continued to suffer from generalized weakness, pain and fever up to 39°C. The patient underwent a comprehensive examination for suspected infections, which yielded negative results, and consulted with a surgeon, a traumatologist, and a rheumatologist. Given the presence of symptoms such as asymmetric polyarthritis, left-sided sacroiliitis, right-sided achilles tendinitis, and talalgia, a diagnosis of reactive arthritis was considered. Nonsteroidal anti-inflammatory medications, antibiotics, and sulfasalazine were prescribed at appropriate doses. During the initial three months of therapy, joint inflammation and systemic manifestations persisted, accompanied by laboratory findings indicating anemia, leukocytosis, thrombocytosis, an erythrocyte sedimentation rate of 55 mm/h, and C-reactive protein level of 104.8 units/mL. Negative rheumatoid factor (RF), positive antibodies to human leukocyte antigen (HLA)-B27 and antibodies against β2-glycoprotein-1 were observed. No evidence of any pathological alterations was detected in the radiographs of the sacroiliac joints, elbows, and ankles.

Considering oligoarthritis, unilateral achilles tendonitis, and clinical sacroiliitis on the right side (Figure 1), after excluding all suspected infectious and inflammatory bowel disorders, the
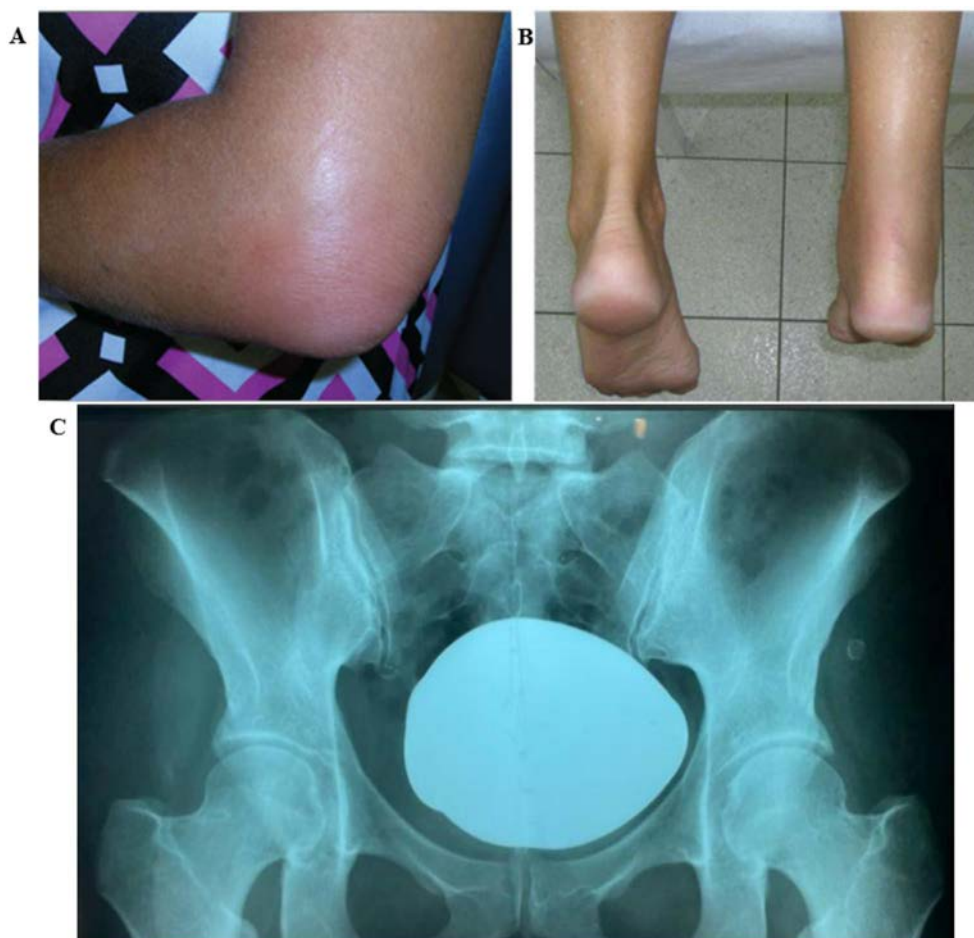
FIGURE 1 | ASIA syndrome development in Patients I. (A) elbow arthritis with synovitis; (B) unilateral Achilles tendinitis; (C) unilateral sacroiliitis.

following diagnosis was made: seronegative polyarthritis with sacroiliitis and achilles tenosynovitis, talalgia. A change in the primary treatment was made with sulfasalazine replaced by methotrexate at a dose of 10 mg per week with folic acid supplementation. Systemic corticosteroids were added for six days (90–60–30 mg). Oral methylprednisolone was then prescribed at a daily dose of 16 mg.

During treatment with methotrexate and corticosteroids, the patient demonstrated sustained clinical and laboratory improvements. However, after a month, methotrexate was discontinued due to adverse reactions in the form of skin dermatitis, and leflunomide at a dose of 20 mg per day was initiated. After five months of therapy with 20 mg leflunomide daily, the patient's condition has been fully stabilized. There were no indications of joint pain or intoxication, and the blood test results remained within the normal range, with no radiological signs of sacroiliitis or arthritis. After nine months from the onset of the illness, the patient discontinued all medication, due to improvement in general condition and the absence of joint pain and intoxicating symptoms. Over the subsequent thirteen months without medication, there was no change in the patient's clinical or laboratory findings or any deterioration in well-being.

Patient G., aged 22, was admitted to the Arthroscopy Department on March 14, 2024. The patient presented with complaints of pain in knee joints at rest and upon movement, mild stiffness, fevers 37°C–38°C, hemorrhagic rashes on the skin, intermittent redness of the eyes, dryness of the ocular mucosa, hair loss, lethargy, excessive sweating, sleep disturbances, constipation, and weight loss of three kilograms over a period of four months.

In the course of the medical history, the patient had recurrent episodes of chronic tonsillitis occurring two to three times annually. Between the years 2017 and 2018, she underwent multiple tattooing procedures using Dynamic black ink (USA). Additionally, in 2021, she received her first hyaluronic acid lip augmentation. On November 7, 2023, she underwent a subsequent hyaluronic lip implant after the previous implant was removed using hyaluronidase. Within a period of 3 weeks following the readmission, the patient began to experience complaints. It is noteworthy that there had been no history of exacerbation of tonsillitis at that time or prior to it. During the examination, multiple tattoos were observed on the patient's skin, as well as solitary hemorrhagic rashes visible on various parts of the body, which did not fade upon pressure. Both eyes exhibited injection (Figure 2A), while the lips appeared enlarged without local inflammatory changes. Hair loss was diffuse, and the hair itself was sparse. The tonsils were hypertrophied in the pharyngeal area with no evidence of hyperemia. The thyroid was enlarged, but not tender. The knee joints displayed swelling, with the presence of painful Baker's
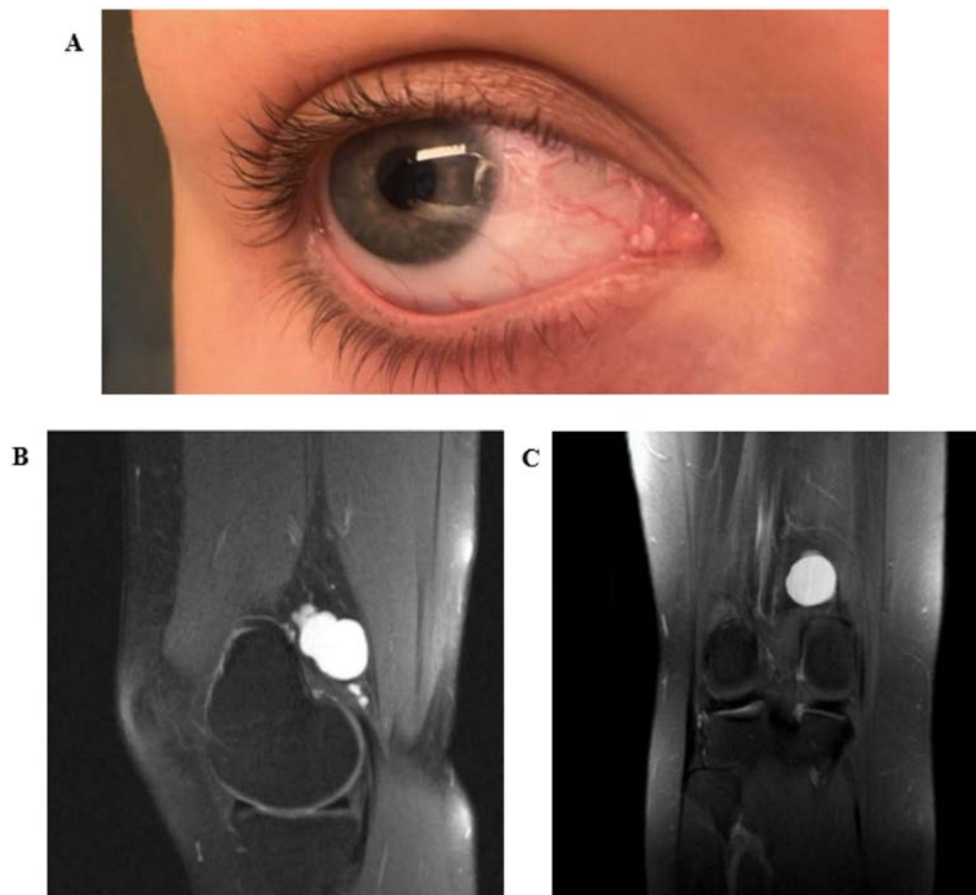
FIGURE 2 | Clinical and instrumental examination of the Patient G. (A) xerophthalmia, eye injection; (B), (C) Baker's cysts on MRI of both knee joints.

cysts palpable in the popliteal fossa. The other joints were unremarkable, and there was no evidence of any abnormalities in the respiratory or cardiovascular systems.

Laboratory and instrumental investigations showed no signs of inflammation, with a negative rheumatoid factor and a C-reactive protein level of 0.1 mg/dL. However, high levels of antibodies to thyroid peroxidase were detected (401.89 IU/mL), along with elevated levels of thyroid-stimulating hormone (9.40 μIU/mL). Additionally, the anticardiolipin, anti-Scl-100, and antinuclear antibody (ANA) tests were mildly positive, with titers of 1:80. The tests for antibodies to double-stranded DNA and cancer markers (CA125 and CA-15-3) came back negative. Magnetic resonance imaging (MRI) of the knee joints on both sides revealed the presence of cysts (Figure 2B,C).

The patient was consulted with an endocrinologist who diagnosed acute thyroiditis and prescribed appropriate treatment, and traumatologist who identified Baker's cyst. Punctures of the popliteal cysts on both sides were performed, and microscopic examination of the cystic contents revealed minor signs of inflammation.

Based on the administration of hyaluronidase, repeated implants, articular syndrome after the placement of lips implant, dry eye syndrome, alopecia, chronic fatigue, severe sweating, subfertility, and weight loss, positivity for anticardiolipin antibodies and high levels of antibodies to thyroid peroxidase, anti-PM-Scl-100, and antinuclear antibodies, the following diagnosis was established: undifferentiated systemic mixed connective tissue disease, associated with the use of adjuvants, acute thyroiditis, xerophthalmia, alopecia.

The patient continued to receive thyroid hormone therapy (levothyroxine at a dosage of 75 mg/day), non-steroidal anti-inflammatory medications (NSAIDs), platelet aggregation inhibitors (dipyridamole 75 mg/day), and basic medications (hydroxychloroquine 200 mg/day). During treatment, including evacuation of the Baker's cyst, the patient's temperature became normal and inflammatory articular syndrome reduced.

ASIA syndrome is identified as a pre-nosological state, which is equivalent to permanent hyperstimulation of the immune system that may develop into a precarious state of connective tissue disease in the future. The relationship between implants and the risk of developing rheumatic diseases remains uncertain, necessitating further research and monitoring. Herein we described two clinical cases of ASIA syndrome: (1) a 38-year-old with seronegative polyarthritis induced by dental implants, and (2) a 22-year-old with mixed connective tissue disease triggered by lip implants. In both cases, systemic symptoms developed shortly after exposure to implants, suggesting immune system overstimulation. Although treatments alleviated symptoms, immune tolerance breakdown persisted. Further research is needed to elucidate the mechanisms and optimize management strategies for ASIA syndrome.

Karlygash Karina
Lina Zaripova
Bayan Ainabekova
Argul Issilbayeva
Nurzhan Asanov
Dinara Sadykova
Diana Makimova

References

1. Y. Shoenfeld and N. Agmon-Levin, "'ASIA' - Autoimmune/Inflammatory Syndrome Induced by Adjuvants," *Journal of Autoimmunity* 36, no. 1 (2011): 4–8, https://doi.org/10.1016/j.jaut.2010.07.003.

2. A. Watad, K. Sharif, and Y. Shoenfeld, "The ASIA Syndrome: Basic Concepts," *Mediterranean Journal of Rheumatology* 28, no. 2 (2017): 64–69, https://doi.org/10.31138/mjr.28.2.64.

3. J. W. C. Tervaert, "Autoinflammatory/Autoimmunity Syndrome Induced by Adjuvants (ASIA; Shoenfeld's Syndrome): A New Flame," *Autoimmunity Reviews* 17, no. 12 (2018): 1259–1264.

4. M. Singh, G. Singh, A. S. Chauhan, et al., "Impact of FDA Updates on Public Interest in Breast Implant-Associated Anaplastic Large Cell Lymphoma," *Plastic and Reconstructive Surgery* 8, no. 11 (2020): e3240.

5. J. W. Cohen Tervaert, "Autoinflammatory/Autoimmunity Syndrome Induced by Adjuvants (Shoenfeld's Syndrome) in Patients After a Polypropylene Mesh Implantation," *Best Practice & Research Clinical Rheumatology* 32, no. 4 (2018): 511–520, https://doi.org/10.1016/j.berh.2019.01.003.

6. J. W. Cohen Tervaert and R. M. Kappel, "Silicone Implant Incompatibility Syndrome (SIIS): A Frequent Cause of ASIA (Shoenfeld's Syndrome)," *Immunologic Research* 56, no. 2–3 (2013): 293–298, https://doi.org/10.1007/s12026-013-8401-3.

7. J. W. Cohen Tervaert, M. Martinez-Lavin, L. J. Jara, et al., "Autoimmune/Inflammatory Syndrome Induced by Adjuvants (ASIA) in 2023," *Autoimmunity Reviews* 2023/05/01/ 22, no. 5 (2023): 103287, https://doi.org/10.1016/j.autrev.2023.103287.

8. J. T. Ruiz, L. Luján, M. Blank, and Y. Shoenfeld, "Adjuvants- and Vaccines-Induced Autoimmunity: Animal Models," *Immunologic Research* 65, no. 1 (2017): 55–65, https://doi.org/10.1007/s12026-016-8819-5.

9. R. L. Coffman, A. Sher, and R. A. Seder, "Vaccine Adjuvants: Putting Innate Immunity to Work," *Immunity* 33, no. 4 (2010): 492–503, https://doi.org/10.1016/j.immuni.2010.10.002.

10. E. Israeli, N. Agmon-Levin, M. Blank, and Y. Shoenfeld, "Adjuvants and Autoimmunity," *Lupus* 18, no. 13 (2009): 1217–1225, https://doi.org/10.1177/0961203309345724.

11. D. Butnaru and Y. Shoenfeld, "Adjuvants and Lymphoma Risk as Part of the ASIA Spectrum," *Immunologic Research* 61 (2015): 79–89.

12. M. R. Major, V. W. Wong, E. R. Nelson, M. T. Longaker, and G. C. Gurtner, "The Foreign Body Response: At the Interface of Surgery and Bioengineering," *Plastic and Reconstructive Surgery* 135, no. 5 (2015): 1489–1498.

13. I. Cavazzana, T. Vojinovic, P. Airo, et al., "Systemic Sclerosis-Specific Antibodies: Novel and Classical Biomarkers," *Clinical Reviews in Allergy & Immunology* 64, no. 3 (2023): 412–430, https://doi.org/10.1007/s12016-022-08946-w.

14. A. Owczarczyk-Saczonek and K. De Boulle, "Hyaluronic Acid Fillers and ASIA Syndrome: Case Studies," *Clinical, Cosmetic and Investigational Dermatology* 16 (2023): 2763–2771.

15. J. W. Cohen Tervaert, "Autoinflammatory/Autoimmunity Syndrome Induced by Adjuvants (ASIA; Shoenfeld's Syndrome): A New Flame," *Autoimmunity Reviews* 17, no. 12 (2018): 1259–1264, https://doi.org/10.1016/j.autrev.2018.07.003.

16. J. M. Anderson, A. Rodriguez, and D. T. Chang, *Foreign Body Reaction to Biomaterials* (Elsevier, 2008), 86–100.

17. M. De Boer, M. Colaris, R. Van Der Hulst, and J. Cohen Tervaert, "Is Explantation of Silicone Breast Implants Useful in Patients With Complaints?," *Immunologic Research* 65 (2017): 25–36.

18. J. Cohen Tervaert, N. Mohazab, D. Redmond, C. van Eeden, and M. Osman, "Breast Implant Illness: Scientific Evidence of Its Existence," *Expert Review of Clinical Immunology* 18, no. 1 (2022): 15–29.

WILEY

LETTER TO THE EDITOR

Case Report: Chalk-Like Synovial Fluid and Calcified Synovium in Systemic Sclerosis Overlapping With Rheumatoid Arthritis Stabilized by Rituximab

Amphay Khounthep[1] | Punthip Thummaroj[2] | Ajanee Mahakkanukrauh[1] | Siraphop Suwannaroj[1] |
Chingching Foocharoen[1]

[1]Department of Medicine, Faculty of Medicine, Khon Kaen University, Khon Kaen, Thailand | [2]Department of Radiology, Faculty of Medicine, Khon Kaen University, Khon Kaen, Thailand

Correspondence: Chingching Foocharoen (fching@kku.ac.th)

Dear Editor,

Systemic sclerosis (SSc) overlapping with rheumatoid arthritis (SSc-RA overlap) is rare [1]. The treatment of SSc-RA overlap mainly depends on the extent of organ involvement and the severity of arthritis symptoms.

Calcinosis cutis, the deposition of calcium in the skin and subcutaneous tissues, is a debilitating manifestation of both the diffuse cutaneous SSc (dcSSc) and limited cutaneous SSc (lcSSc) subsets [2] and is often refractory to conventional therapies [3]. We report a patient with SSc-RA overlap complicated by periarticular calcinosis cutis, calcified synovium in both wrists, and chalk-like synovial fluid, who was unresponsive to multiple immunosuppressants. However, the calcified synovium and skin stabilized after treatment with rituximab, a B-cell depleting agent. The objective of this report is to illustrate the clinical, laboratory, and radiographic features of this rare presentation and to evaluate the therapeutic response to rituximab in a patient with complicated SSc-RA overlap. This description contributes to the understanding of atypical manifestations in SSc-RA overlap and provides insight into potential treatment options.

A 55-year-old female with a known diagnosis of dcSSc-RA overlap since 2015 was referred to us in March 2021 due to uncontrolled arthritis. She had type 2 diabetes mellitus and was on multiple medications, including metformin, low-dose aspirin, nifedipine, prednisolone, sulfasalazine, cyclosporine A, and folic acid. Initially, she presented with sclerodactyly, polyarthritis, and dyspnea on exertion. Serological findings revealed positive anti-topoisomerase I antibody, anti-cyclic citrullinated peptide antibody (anti-CCP; 143 U/mL), and rheumatoid factor (RF; 86.8 U/mL). High-resolution computed tomography demonstrated chronic fibrosis with honeycombing, traction bronchiectasis, interlobular septal thickening, subpleural reticulation—predominantly in the lower lobes—and esophageal dilatation. Spirometry revealed severe restrictive lung disease with a forced vital capacity (FVC) of 36% (0.90 L) and a forced expiratory volume in 1 s (FEV1) of 41%. Echocardiography in March 2021 revealed a severely elevated right ventricular systolic pressure of 90.3 mmHg with a preserved ejection fraction of 81.3%. Pulmonary arterial hypertension was suspected. Right heart catheterization confirmed precapillary pulmonary hypertension (mPAP 53 mmHg, PCWP 9 mmHg, PVR 5.2 WU), and sildenafil was prescribed to control pulmonary arterial pressure.

Hand radiography revealed erosive changes in the left wrist and calcinosis cutis in the fingers. She was started on cyclophosphamide and 10 mg/day prednisolone.

She developed worsening arthritis in both wrists 2 years later. Radiographic imaging revealed progressive bone erosions, extensive calcifications in the left wrist, and calcinosis cutis in the fingers (Figure 1A). Arthrocentesis was performed and revealed chalk-like synovial fluid, as shown in Figure 1B. Synovial fluid

FIGURE 1 | (A) Radiographic findings of the hands demonstrated concentric joint space narrowing at both wrists, more severe on the right side. Bony erosions are seen at the right distal radius and right distal ulna. Severe calcinosis cutis is indicated by the Simple Scoring System, based on evidence of multiple sites of high or mix density calcium deposits in both hands, mostly notably at the left wrist (arrowhead) and the left second and third distal interphalangeal joints (thick arrows). Acro-osteolysis is observed in the right second finger (thin arrow), with normal bone mineralization. (B) Chalk-like synovial fluid from left wrist.

analysis showed white blood cell count of 43 580 cells/mm^3, with 87% neutrophils and 13% lymphocytes, glucose 90 mg/dL, calcium 345.4 mg/dL, phosphorus 230.3 mg/dL, magnesium 4.0 mg/dL, no crystals detected by fresh smear, and no organisms detected by gram stain or culture. Polymerase chain reaction for *Mycobacterium* spp. was negative. Her blood calcium, phosphorus, and magnesium levels were within the normal range (9.1, 2.9, and 2.2 mg/dL, respectively). Synovial biopsy confirmed calcified synovial tissue and revealed several foci of calcification, along with mild synovitis without granulomatous inflammation. C-reactive protein (CRP) was 29.04 mg/L with normal complete blood count, renal, and liver function.

Cyclophosphamide was discontinued, and rituximab was initiated to control her arthritis symptoms. One year after starting rituximab, her arthritis symptoms were controlled, with a reduction in pain—from 8 to 3 on the visual analog scale—and a decrease in CRP levels to 2.19 mg/L.

Two years after starting rituximab treatment, improvements in joint symptoms and skin thickness, as well as stabilization of calcinosis cutis, were observed (Figure 2). Inflammatory markers returned to normal, and the modified Rodnan skin score (mRSS) decreased from 14 to 4. Spirometry showed unchanged restrictive lung disease, with an FVC of 38% predicted (0.91 L).

This case illustrates a rare but clinically significant overlap syndrome involving dcSSc and RA, complicated by calcified synovium, calcinosis cutis, and ILD. The presence of anti-CCP antibody and RF positivity supported a true overlap syndrome, rather than SSc-associated arthritis alone, which is typically nonerosive and noninflammatory arthritis [4]. However,

FIGURE 2 | Hand radiography 2 years after rituximab treatment showed stable calcinosis cutis in the left hand (arrowhead) and a noticeable decrease in the size and density of calcinosis cutis at the left third distal interphalangeal joint (thick arrow). Acro-osteolysis at the right second finger (thin arrow) also remained stable.

SSc-specific autoantibodies other than anti-topoisomerase I antibody were not evaluated as part of our routine practice, due to their low prevalence among Thais and the lack of confirmed clinical correlation [5]. Therefore, we could not provide details of other serological profiles for SSc.

The patient's refractory polyarthritis and cutaneous calcifications posed considerable therapeutic challenges, particularly after an inadequate response to conventional immunosuppressive

therapy with cyclophosphamide, sulfasalazine, cyclosporin A, and low-dose steroids. The introduction of rituximab, a monoclonal anti-CD20 antibody, resulted in notable clinical improvement in joint symptoms and stabilization of calcinosis, underscoring its potential utility in complex autoimmune overlap syndromes.

Calcinosis cutis is a manifestation frequently observed in patients with lcSSc subset who are positive for anti-centromere antibody [6]. However, it can also be present in the dcSSc subset [2]. Currently, there are no established reports of calcified synovium and chalk-like synovial fluid in SSc. Our patient had anti-topoisomerase I positive dcSSc and developed calcinosis cutis, along with extensive calcified synovium and calcium-rich synovial fluid, which are extremely rare findings. In addition, she also had coexisting RA, which made the disease more complicated. Calcinosis cutis is notoriously difficult to treat and often refractory to standard immunosuppressants [7].

Rituximab is a biologic treatment used to control arthritis in RA, particularly in seropositive and treatment-resistant cases [8]. It has also shown a positive effect on skin thickness by improving skin fibrosis [9], stabilization of lung function in patients with ILD [9, 10], and treating calcinosis cutis in SSc [3]. In this context, rituximab was chosen for treatment in our patient due to its potential multiple effects on the disease, including controlling arthritis, improvement of skin thickness, stabilization of ILD, and reduction of calcinosis cutis. By its mechanism of action, rituximab has immunomodulatory effects through B-cell depletion and downregulation of pro-inflammatory cytokines, such as interleukin-6 and tumor necrosis factor-α, which have been reported to be present at sites of calcium deposition [6]. Therefore, it may help stabilize or reduce calcinosis cutis and calcified synovium, as observed in our case. In overlap syndromes, rituximab may offer a dual benefit by addressing both RA-related synovitis and SSc-related fibrotic or inflammatory manifestations.

This case highlights a rare presentation of calcified synovium and calcium-rich synovial fluid, in a patient with SSc-RA overlap and emphasize the promising role of RTX in effectively managing refractory arthritis and stabilizing calcinosis cutis in complex SSc-RA overlap. Management requires a multidisciplinary approach. Ultimately, this case contributes valuable clinical insight into the potential benefits of RTX in this challenging patient population.

Author Contributions

Amphay Khounthep and **Chingching Foocharoen:** conceptualization. **Amphay Khounthep, Siraphop Suwannaroj, Ajanee Mahakkanukrauh** and **Chingching Foocharoen:** data curation. **Amphay Khounthep** and **Chingching Foocharoen:** methodology. **Siraphop Suwannaroj** and **Ajanee Mahakkanukrauh:** supervision. **Amphay Khounthep:** writing – original draft. **Chingching Foocharoen:** writing – review and editing. All authors have read and approved the final manuscript.

Conflicts of Interest

The authors declare no conflicts of interest.

Data Availability Statement

The data that support the findings of this study are available on request from the corresponding author. The data are not publicly available due to privacy or ethical restrictions.

Amphay Khounthep
Punthip Thummaroj
Ajanee Mahakkanukrauh
Siraphop Suwannaroj
Chingching Foocharoen

References

1. C. Foocharoen, S. Netwijitpan, A. Mahakkanukrauh, S. Suwannaroj, and R. Nanagara, "Clinical Characteristics of Scleroderma Overlap Syndromes: Comparisons With Pure Scleroderma," *International Journal of Rheumatic Diseases* 19, no. 9 (2016): 913–923.

2. C. Muktabhant, P. Thammaroj, P. Chowchuen, and C. Foocharoen, "Prevalence and Clinical Association With Calcinosis Cutis in Early Systemic Sclerosis," *Modern Rheumatology* 31, no. 6 (2021): 1113–1119.

3. H. Elahmar, B. M. Feldman, and S. R. Johnson, "Management of Calcinosis Cutis in Rheumatic Diseases," *Journal of Rheumatology* 49, no. 9 (2022): 980–989.

4. S. B. Randone, S. Guiducci, and M. M. Cerinic, "Musculoskeletal Involvement in Systemic Sclerosis," *Best Practice & Research: Clinical Rheumatology* 22, no. 2 (2008): 339–350.

5. C. Foocharoen, P. Watcharenwong, S. Netwijitpan, A. Mahakkanukrauh, S. Suwannaroj, and R. Nanagara, "Relevance of Clinical and Autoantibody Profiles in Systemic Sclerosis Among Thais," *International Journal of Rheum Atic Diseases* 20, no. 10 (2017): 1572–1581.

6. N. Boulman, G. Slobodin, M. Rozenbaum, and I. Rosner, "Calcinosis in Rheumatic Diseases," *Seminars in Arthritis and Rheumatism* 34, no. 6 (2005): 805–812.

7. S. Davuluri, C. Lood, and L. Chung, "Calcinosis in Systemic Sclerosis," *Current Opinion in Rheumatology* 34, no. 6 (2022): 319–327.

8. J. S. Smolen, R. B. M. Landewé, S. A. Bergstra, et al., "EULAR Recommendations for the Management of Rheumatoid Arthritis With Synthetic and Biological Disease-Modifying Antirheumatic Drugs: 2022 Update," *Annals of the Rheumatic Diseases* 82, no. 1 (2023): 3–18.

9. M. M. V. de Figueiredo, K. P. M. de Azevedo, V. H. de Oliveira, et al., "Is Rituximab Effective for Systemic Sclerosis? A Systematic Review and Meta-Analysis," *Advances in Rheumatology* 61, no. 1 (2021): 15.

10. R. P. Goswami, A. Ray, M. Chatterjee, A. Mukherjee, G. Sircar, and P. Ghosh, "Rituximab in the Treatment of Systemic Sclerosis-Related Interstitial Lung Disease: A Systematic Review and Meta-Analysis," *Rheumatology (Oxford, England)* 60, no. 2 (2021): 557–567.

International Journal of
Rheumatic Diseases

ORIGINAL ARTICLE

The Effects of Tocilizumab on Inflammatory and Differentiation Pathways in Primary Human Chondrocytes: A Bioinformatic and In Vitro Approaches

Bugrahan Regaip Kilinc[1] | Feyza Kostak[2] | Omer Faruk Yilmaz[3] | Suray Pehlivanoglu[2] | Duygu Yasar Sirin[1] 📷

[1]Department of Biology, Institute of Natural and Applied Sciences, Namık Kemal University, Tekirdag, Turkey | [2]Department of Molecular Biology and Genetics, Necmettin Erbakan University, Konya, Turkey | [3]Corlu State Hospital, Tekirdag, Turkey

Correspondence: Duygu Yasar Sirin (dysirin@nku.edu.tr)

ABSTRACT

Introduction: This study investigates the effects of Tocilizumab, an interleukin-6 (IL-6) receptor inhibitor, on human primary chondrocyte cells, focusing on bone morphogenetic protein 2 (BMP-2), hypoxia-inducible factor 1-alpha (HIF-1α), interleukin-1 beta (IL-1β), SRY-box transcription factor 9 (SOX-9), and IL-6 genes.

Methods: Combining bioinformatic and experimental approaches, we assessed Tocilizumab's impact on inflammatory signaling pathways, cellular differentiation, and viability. Reactome and Gene Ontology (GO) enrichment analyses revealed the involvement of interleukin signaling, BMP, and mitogen-activated protein kinase (MAPK) pathways.

Results: Protein–protein interaction (PPI) network analysis indicated strong interactions among the studied genes, with BMP-2 and SOX-9 identified as central nodes. Western blot analysis demonstrated a 71% reduction in SOX-9, a 55% reduction in HIF-1α, and an 81% reduction in BMP-2 expression levels by day 15. Conversely, IL-1β levels decreased by 67% after prolonged treatment. MTT assays showed a 27.7% reduction in cell viability at day 15 compared to controls. Despite these changes, staining analyses confirmed preserved cell membrane integrity and nuclear morphology, indicating minimal cytotoxic effects.

Conclusion: These findings highlight Tocilizumab's role in modulating inflammation and differentiation pathways in human primary chondrocytes. Further studies should explore the long-term effects of IL-6 blockade on cartilage remodeling and regenerative capacity in chronic inflammatory settings.

1 | Introduction

Cartilage tissue damage and inflammation are central features in the progression of various musculoskeletal disorders, including osteoarthritis (OA) and rheumatoid arthritis (RA) [1].

Chondrocytes, the primary cellular component (CC) of cartilage, play a crucial role in maintaining the structural and functional integrity of the cartilage matrix [2]; however, inflammatory cytokines can disrupt this balance, leading to cartilage degradation and loss of function [3]. Among these cytokines, interleukin-6

(IL-6) is recognized as a key mediator of inflammation and joint degeneration, promoting catabolic activities that accelerate cartilage breakdown [4]. Consequently, targeting the IL-6 signaling pathway has emerged as a promising therapeutic strategy for modulating inflammation and preserving cartilage health [5, 6].

Tocilizumab, a humanized monoclonal antibody targeting the IL-6 receptor, has shown clinical efficacy in reducing inflammation and inhibiting IL-6-mediated pathways [7, 8]. While its effects on systemic inflammatory diseases such as RA are well-documented, the specific molecular mechanisms by which Tocilizumab influences chondrocyte functionality remain less explored. Understanding these mechanisms is essential for optimizing therapeutic strategies for cartilage preservation in inflammatory diseases. Although Tocilizumab has proven systemic anti-inflammatory effects, little is known about its direct impact on cartilage-resident chondrocytes at the molecular and cellular levels. Understanding these mechanisms is essential for optimizing therapeutic strategies for cartilage preservation in inflammatory diseases.

This study focuses on four key genes: bone morphogenetic protein 2 (BMP-2), hypoxia-inducible factor 1-alpha (HIF-1α), IL-1β, SRY-box transcription factor 9 (SOX-9), and IL-6 due to their critical roles in chondrocyte function, inflammation, and cellular stress response. BMP-2 is integral to cartilage development and repair [9], while HIF-1α regulates cellular adaptation to hypoxic conditions commonly observed in damaged cartilage [10]. SOX-9 is a master regulator of chondrocyte differentiation and cartilage matrix synthesis [11, 12]. BMP-2 promotes SOX-9 expression, and HIF-1α can further regulate SOX-9 under hypoxic conditions, suggesting cross-regulatory interactions among these factors critical for cartilage homeostasis [6]. Interleukin-1 beta (IL-1β) is a potent pro-inflammatory cytokine that plays a key role in cartilage degradation by promoting catabolic processes and inhibiting extracellular matrix synthesis [13]. In addition, IL-6 is not only a major inflammatory cytokine but also directly impacts chondrocyte metabolism and cartilage degradation [14, 15].

To elucidate the regulatory effects of Tocilizumab on these key pathways, we employed a combination of bioinformatic and experimental approaches. Reactome and Gene Ontology (GO) enrichment analyses were utilized to identify pathways significantly impacted by Tocilizumab treatment, while protein–protein interaction (PPI) network analysis provided insight into the interconnected roles of these genes. Complementary in vitro analyses, including MTT assays and staining analyses for cell viability and Western blot for protein expression, further explored Tocilizumab's effects on chondrocyte functionality. This study aims to provide a comprehensive understanding of Tocilizumab's role in modulating inflammation and chondrocyte survival, contributing to the development of targeted therapies for cartilage-related inflammatory diseases.

2 | Materials and Methods

2.1 | Data Collection and Gene Selection

In this study, we examined the regulatory effects of Tocilizumab on human primary chondrocytes by focusing on four key genes: BMP-2, HIF-1α, IL-1β, SOX-9, and IL-6. These genes were selected due to their critical roles in inflammation, cartilage degradation, and stress response, which are integral to chondrocyte functionality and the progression of cartilage-related diseases. To facilitate pathway enrichment analysis, gene symbols were converted into Entrez IDs using the bitr() function from the R package clusterProfiler, with the human genome annotation database org.Hs.eg.db serving as the reference [16].

2.2 | Functional Enrichment Analysis

To investigate the regulatory pathways influenced by Tocilizumab in human primary chondrocytes, Reactome pathway enrichment analysis and GO enrichment analysis were performed. Reactome pathway analysis was conducted using the enrichPathway() function from the ReactomePA package in R, with a statistical significance threshold of $p < 0.05$. The analysis utilized the org.Hs.eg.db database for gene annotation, and significant pathways were visualized using ggplot2. For functional classification, GO enrichment analysis was performed using the enrichGO() function from the clusterProfiler package. The selected genes were categorized into three principal domains: biological process (BP), molecular function (MF), and CC. GO terms with p-values < 0.05 were considered statistically significant, and the results were visualized in a combined dot plot. All analyses were conducted in R (version 4.3.3.), and gene annotation was referenced against the org.Hs.eg.db database. Data preprocessing and normalization steps were performed prior to enrichment analysis to ensure the accuracy and reliability of pathway associations [16, 17].

2.3 | Protein–Protein Interaction (PPI) Analyses

PPI networks were constructed to explore the broader interaction landscape of the identified genes, including BMP-2, HIF-1α, IL-1β, SOX-9, and IL-6, in the context of Tocilizumab treatment. The Search Tool for the Retrieval of Interacting (STRING) database was utilized for the prediction and visualization of interaction networks, applying a confidence score threshold of > 0.4 to ensure the robustness of the analysis. The threshold of 0.4 (medium confidence) was selected to balance sensitivity and specificity, minimizing false-positive interactions while capturing relevant biological associations. Key hub gene identification was directly performed using the Maximal Clique Centrality (MCC) algorithm in Cytoscape's CytoHubba plugin to determine the most critical proteins within the network. This approach provided insights into the molecular mechanisms potentially regulated by Tocilizumab treatment [18, 19].

2.4 | Preparation of Human Primary Chondrocyte Cultures

Human primary chondrocyte cultures were established using cartilage tissue obtained from patients classified as Kellgren–Lawrence radiographic grade IV undergoing total knee arthroplasty (four males, four females; mean age: 44.12 ± 4.87 years). Tissues from patients with neutropenia, leukopenia, thrombocytopenia, active tuberculosis, or active hepatitis B or C were excluded from the preparation of primary cell cultures.

Individuals with a history of liver or kidney dysfunction, pregnant women, and those with known allergies or hypersensitivity to Tocilizumab were not included in the study. Additionally, tissues from patients who received nonsteroidal anti-inflammatory drugs, disease-modifying antirheumatic drugs, or biological agents within the last month were also excluded from the present study. Tissues were transported aseptically in sterile Falcon tubes containing Dulbecco's Modified Eagle Medium (DMEM; cat no: 11965092, Thermo Fisher Scientific) supplemented with 5% penicillin–streptomycin (cat no: 15140122, Thermo Fisher Scientific). Following arrival, tissues were washed with phosphate-buffered saline (PBS), mechanically dissociated, and digested overnight in Hank's balanced salt solution (HBSS; cat no: 14170070, Thermo Fisher Scientific) using a combination of *Clostridium histolyticum* collagenase type I (cat no: J13820.03, Thermo Fisher Scientific) ($475 \mu g/mL$) and type II (cat no: 17101015, Thermo Fisher Scientific) ($125 \mu g/mL$) at 37.4°C and 5% CO_2. The resulting cells were centrifuged at 1300 rpm for 10 min, resuspended in DMEM with 10% fetal bovine serum (FBS; cat no: A5670801, Thermo Fisher Scientific), and incubated at 37°C with 5% CO_2. Cells were cultured for 21 days before being used in experiments [20].

2.5 | Application of Tocilizumab

The study involved untreated (control) and Tocilizumab-treated groups. Tocilizumab was prepared at a concentration of $10 \mu g/mL$ by diluting a 100 mL stock solution of Actemra with isotonic saline and DMEM. The drug was applied to the primary chondrocyte cultures, and analyses were performed at 1, 7, and 15 days post-treatment. Half maximal inhibitory concentrations (IC50) were tested by MTT (Vybrant MTT Cell Proliferation Assay Kit (V-13154), Invitrogen) assay to detect cellular sensitivity to Tocilizumab.

2.6 | MTT Assay for Cell Viability and Proliferation

Cell viability was assessed using the MTT assay. Cells were seeded in 96-well plates at a density of 1.6×10^4 cells per well. After treatment, $100 \mu L$ of MTT solution (12 mM) was added to each well and incubated for 2 h at 37°C. The resulting formazan crystals were dissolved using dimethyl sulfoxide (DMSO), and absorbance was measured at 540 nm to determine cell viability. The viability of control cells was set to 100%, and the percentage viability of treated groups was calculated accordingly [21].

2.7 | AO/PI and Hoechst Staining

To evaluate membrane integrity and nuclear morphology, cells were stained with acridine orange (AO)/propidium iodide (PI) and Hoechst 33342. For AO/PI staining, cells were incubated with $5 \mu g/mL$ AO and $5 \mu g/mL$ PI in PBS for 5 min at room temperature. Live cells exhibited green fluorescence (AO-positive), while apoptotic or necrotic cells displayed red fluorescence (PI-positive) under a fluorescence microscope. For Hoechst staining, cells were fixed with 4% paraformaldehyde for 10 min,

washed with PBS, and stained with Hoechst 33342 ($1 \mu g/mL$) for 10 min. Microscopic observations were performed using a phase contrast microscope (Leica DM2500) and an inverted microscope (Olympus CKX41) at 500× magnification. Stained cells were visualized to assess nuclear integrity and chromatin condensation, providing additional insights into potential apoptotic changes [22].

2.8 | Western Blotting for BMP-2, HIF-1α, IL-1β, SOX-9, and IL-6 Expression

Proteins were extracted from control and treated cells using RIPA buffer and quantified by the Bradford assay. Equal protein amounts were separated by 10% SDS-PAGE and transferred to polyvinylidene difluoride (PVDF) membranes. Membranes were blocked with 5% nonfat milk and incubated overnight with primary antibodies against BMP-2 (Cat no: PA5-85956, Thermo Fisher Scientific), HIF-1α (Cat no: MA1-516, Thermo Fisher Scientific), IL-1β (Cat no: MA5-23691, Thermo Fisher Scientific), SOX-9 (Cat no: MA5-17177, Thermo Fisher Scientific), and β-actin (Cat no: MA1-140, Thermo Fisher Scientific). After washing, membranes were incubated with HRP-conjugated secondary antibodies, and protein bands were visualized using the WesternBreeze Chemiluminescent Kit (Cat no: WB7104, Thermo Fisher Scientific). Band intensities were analyzed with ImageJ software, with β-actin serving as the loading control [23].

2.9 | Statistical Analysis

All experiments were conducted in triplicate, with data expressed as mean ± standard deviation (SD). Statistical significance was determined using one-way analysis of variance (ANOVA) followed by Tukey's post hoc test. Statistical analyses were performed using R software (v4.3.3), and *p*-values less than 0.05 were considered statistically significant.

3 | Results

In this study, we investigated the regulatory effects of Tocilizumab on key molecular pathways in human primary chondrocytes, focusing on the roles of BMP-2, HIF-1α, IL-1β, SOX-9, and IL-6. Utilizing a combination of bioinformatic and in vitro analyses, we explored the involvement of these genes in inflammatory signaling, differentiation processes, and cellular viability. Reactome and GO enrichment analyses revealed significant pathways and GO terms associated with inflammation and chondrocyte functionality. Additionally, PPI network analysis highlighted the interconnected roles of these genes within cellular signaling networks. Complementary experiments, including Western blot and MTT assays and staining analyses, provided further insight into the dynamic expression of these proteins over time and the cytostatic effects of Tocilizumab on chondrocytes. Together, these findings underscore the multifaceted impact of Tocilizumab on chondrocyte biology, with implications for cartilage health and inflammation modulation.

The Reactome pathway enrichment analysis revealed several significant pathways associated with the BMP-2, HIF-1α, IL-6, and SOX-9 genes in human primary chondrocytes treated with Tocilizumab (Figure 1). Among the most significantly enriched pathways were interleukin-4 and interleukin-13 signaling, Transcriptional regulation by Runt-related transcription factor 2 (RUNX2), and signaling by interleukins. These pathways are highly relevant to immune regulation and inflammation [24–26], suggesting that Tocilizumab may influence chondrocyte function through the modulation of cytokine signaling and transcriptional regulation.

Interleukin-4 and interleukin-13 signaling were the most significantly enriched pathways, highlighting the potential role of these cytokines in the inflammatory responses of chondrocytes [25]. RUNX2, a key transcription factor involved in bone and cartilage development [27], also appeared prominently in the analysis, indicating that Tocilizumab may influence cartilage differentiation and repair processes. Additionally, pathways such as MAPK3 (ERK1) activation and (IL-6) signaling were also enriched, reflecting the involvement of these signaling cascades in cellular responses to inflammation and tissue stress [28, 29]. Overall, the results suggest that Tocilizumab may exert its therapeutic effects
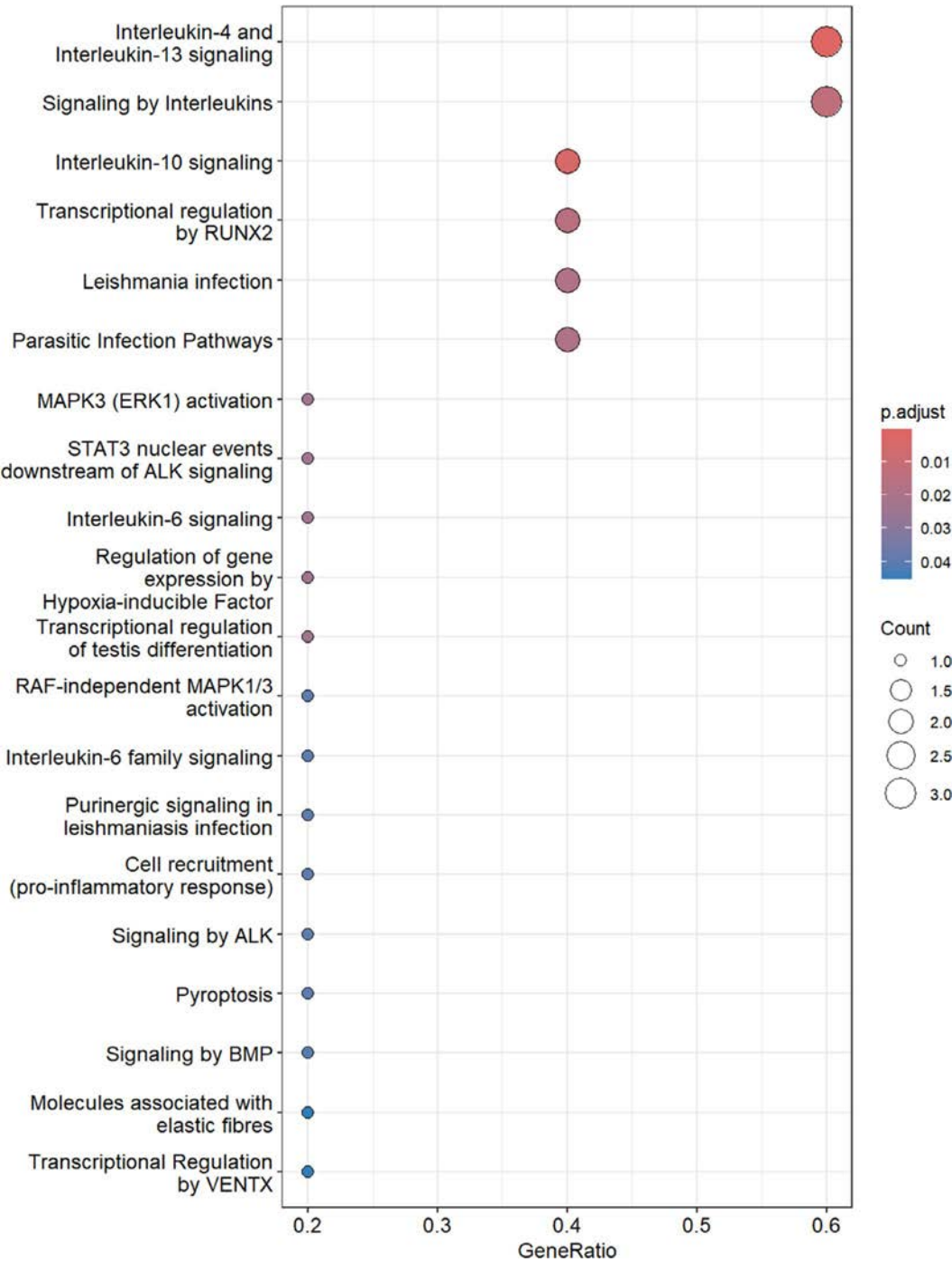
FIGURE 1 | Reactome pathway enrichment analysis of BMP-2, HIF-1α, IL-1β, SOX-9, and IL-6.

on human chondrocytes by modulating both inflammatory and transcriptional regulation pathways, with potential impacts on cartilage maintenance and repair [23, 30].

The GO enrichment analysis revealed significant BPs, MFs, and CCs associated with the BMP-2, HIF-1α, IL-6, and SOX-9 genes in human primary chondrocytes treated with Tocilizumab (Figure 2). In the BP category, key enriched terms included epithelial to mesenchymal transition, mesenchymal cell differentiation, and regulation of extracellular matrix organization, all of which are crucial in tissue remodeling and repair mechanisms. The high enrichment of epithelial to mesenchymal transition [31] and mesenchymal cell differentiation suggests that these processes may play a significant role in the chondrocyte response to Tocilizumab treatment. In the MF category, important enriched terms such as growth factor activity, cytokine activity, and BMP receptor binding were identified. These MFs are closely related to the regulation of cellular communication, inflammation, and growth responses, which are critical for maintaining chondrocyte function and cartilage integrity. For the CC category, the most significantly enriched term was the plasma membrane signaling receptor complex. These results highlight the potential of Tocilizumab to modulate both inflammatory responses and cellular differentiation processes in human primary chondrocytes, suggesting that the drug may exert its effects through pathways related to tissue repair, inflammation, and extracellular matrix organization [8, 32].
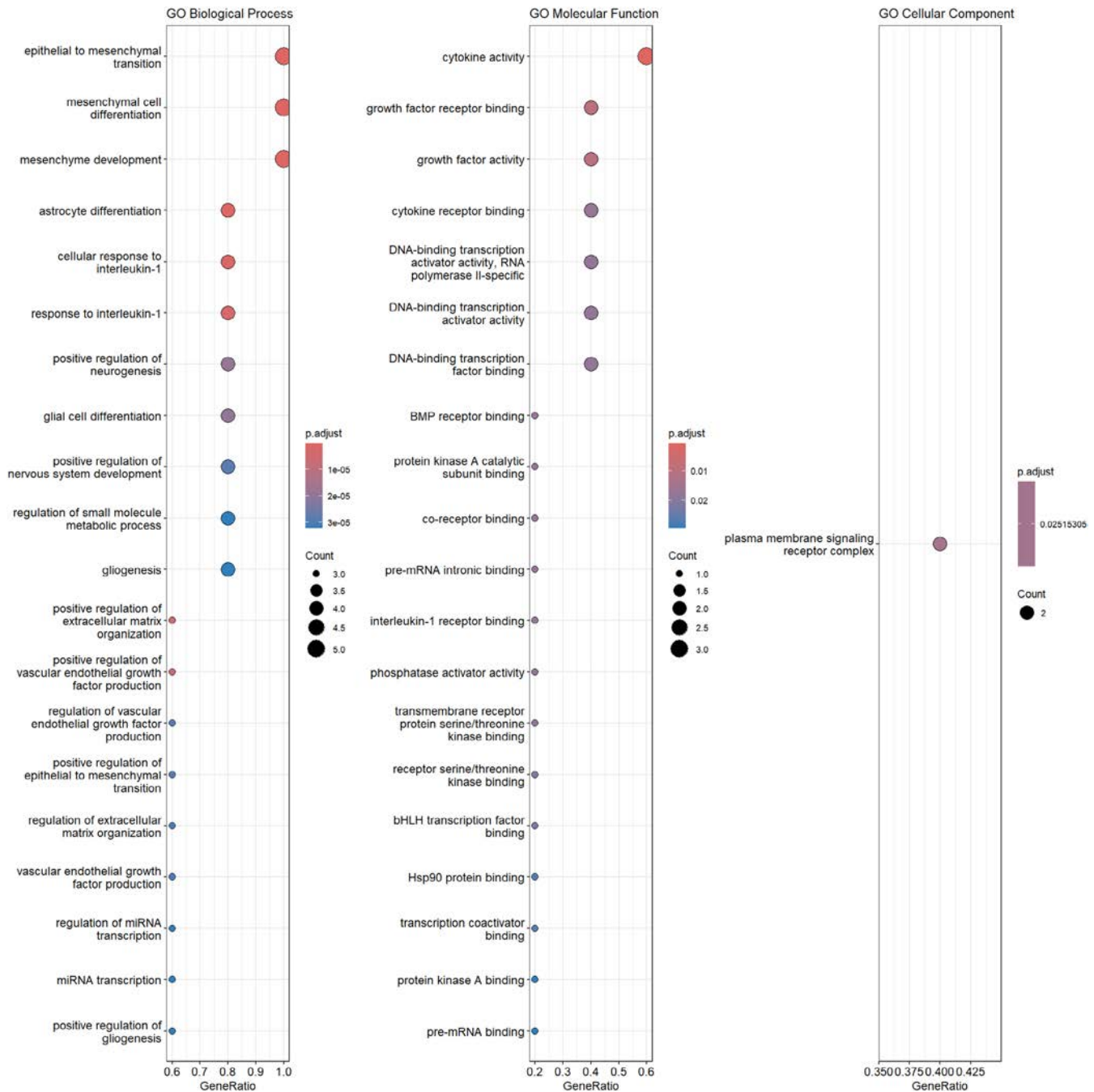
FIGURE 2 | GO enrichment analysis of BMP-2, HIF-1α, IL-1β, SOX-9, and IL-6 genes. The analysis includes three categories: biological process, molecular function, and cellular component.

The PPI network analysis identified a dense interaction network involving the BMP-2, HIF-1α, IL-1β, SOX-9, and IL-6 genes, along with several key interacting proteins in human primary chondrocytes treated with Tocilizumab (Figure 3). Notably, the network includes numerous high-confidence interactions, with a focus on pathways related to cartilage development, inflammation, and matrix organization. Key proteins such as RUNX2, MMP13, COL2A1, ACAN, and BMP-2 were identified as central nodes, indicating their crucial roles in maintaining cartilage integrity and regulating inflammatory responses [24]. Additionally, HIF-1α, a major regulator of hypoxic responses, and IL-6, a key inflammatory mediator, were identified as significant hubs in the network, reflecting their central roles in both cellular stress responses and inflammation modulation [10]. The analysis also highlighted several proteins involved in matrix remodeling, including A Disintegrin and Metalloproteinase

with Thrombospondin motifs (ADAMTS) and MMP13, which are known to be involved in extracellular matrix breakdown and cartilage degradation [33–35], suggesting that Tocilizumab may influence matrix homeostasis in chondrocytes. Overall, the STRING PPI network suggests that Tocilizumab may exert its effects on chondrocytes by modulating key proteins involved in cartilage development, extracellular matrix organization, and inflammatory signaling pathways, which are essential for maintaining cartilage health and reducing degeneration.

Microscopic staining results are shown in Figure 4, presenting the viability and nuclear morphology of chondrocytes treated with Tocilizumab (Figure 4). AO/PI staining reveals predominantly green fluorescence, indicating a high proportion of viable chondrocytes across both control and Tocilizumab-treated groups. The lack of red fluorescence (propidium iodide) suggests minimal cell
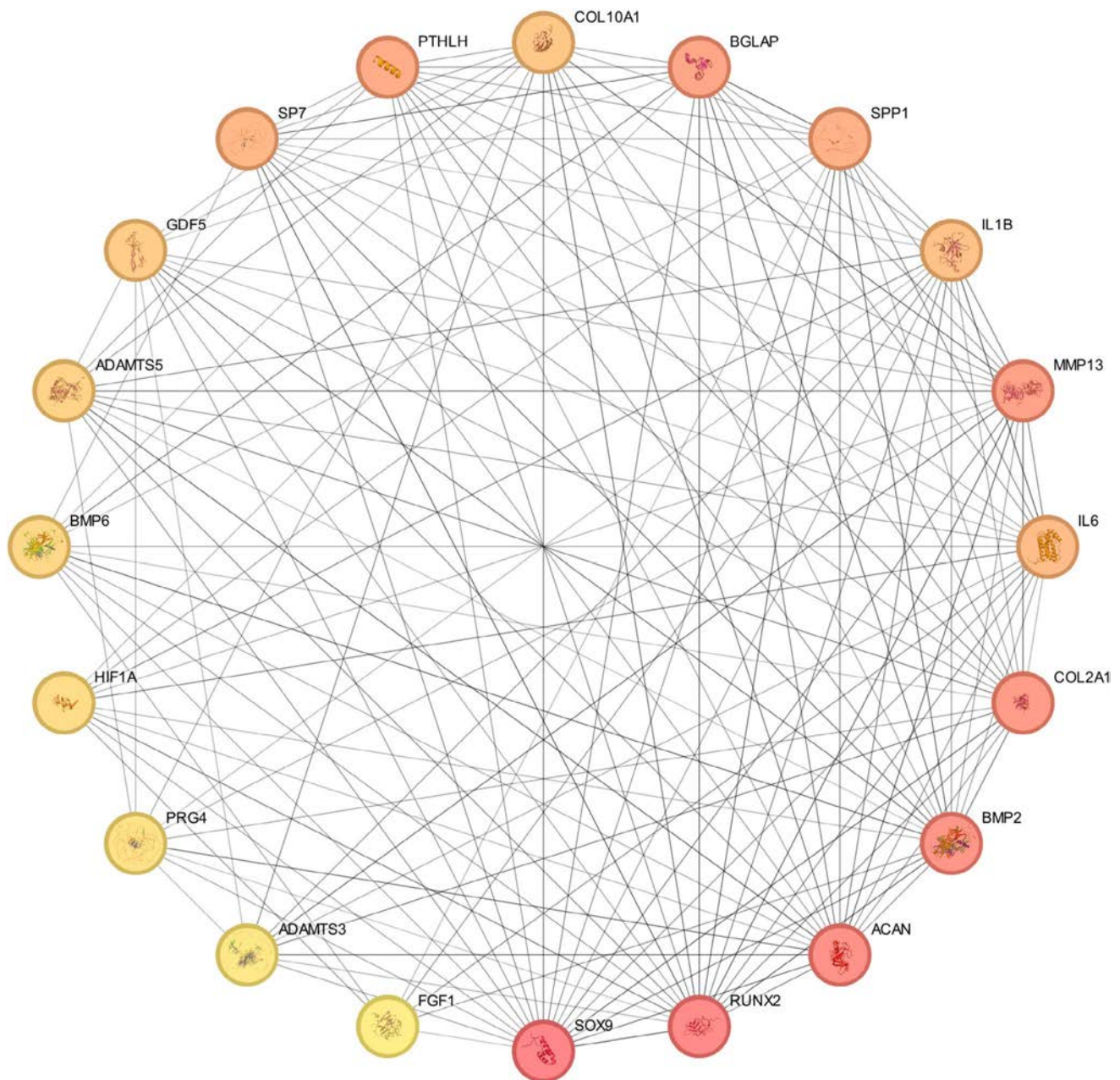
FIGURE 3 | PPI network analysis of BMP-2, HIF-1α, IL-1β, SOX-9, and IL-6. The network displays high-confidence interactions between proteins involved in key biological processes such as cartilage development, extracellular matrix organization, and inflammation.

death or membrane compromise, even with extended exposure to Tocilizumab. Similarly, Hoechst staining results highlight intact nuclear morphology in both control and treated groups. The nuclei appear uniformly stained and well defined, with no evidence of chromatin condensation or nuclear fragmentation typically associated with apoptosis. These results suggest that Tocilizumab does not induce significant cytotoxic effects or nuclear alterations in primary human chondrocytes under the conditions tested [23].

The effects of Tocilizumab on cell viability in human primary chondrocytes were evaluated using MTT analysis at different time points. The control group exhibited the highest cell viability, whereas the 15-day treatment group showed the lowest viability levels. Statistical evaluation of the MTT assay results revealed a significant, time-dependent reduction in chondrocyte viability after Tocilizumab treatment ($p < 0.005$) (Figure 5). These findings suggest that changes in cell viability may reflect the potential impact of the drug on chondrocyte physiology [23].

Western blot analysis examined the expression of HIF-1α, SOX-9, BMP-2, and IL-1β proteins in chondrocytes exposed to Tocilizumab treatment. A notable downward trend was observed in SOX-9 and BMP-2 protein levels by day 15, while HIF-1α and IL-1β showed a more moderate decrease over the treatment period (Figure 6). Compared to the control (0 day), a statistically significant time-dependent decrease in protein expression was observed at 1, 7, and 15 days following Tocilizumab treatment ($p < 0.005$) [23].
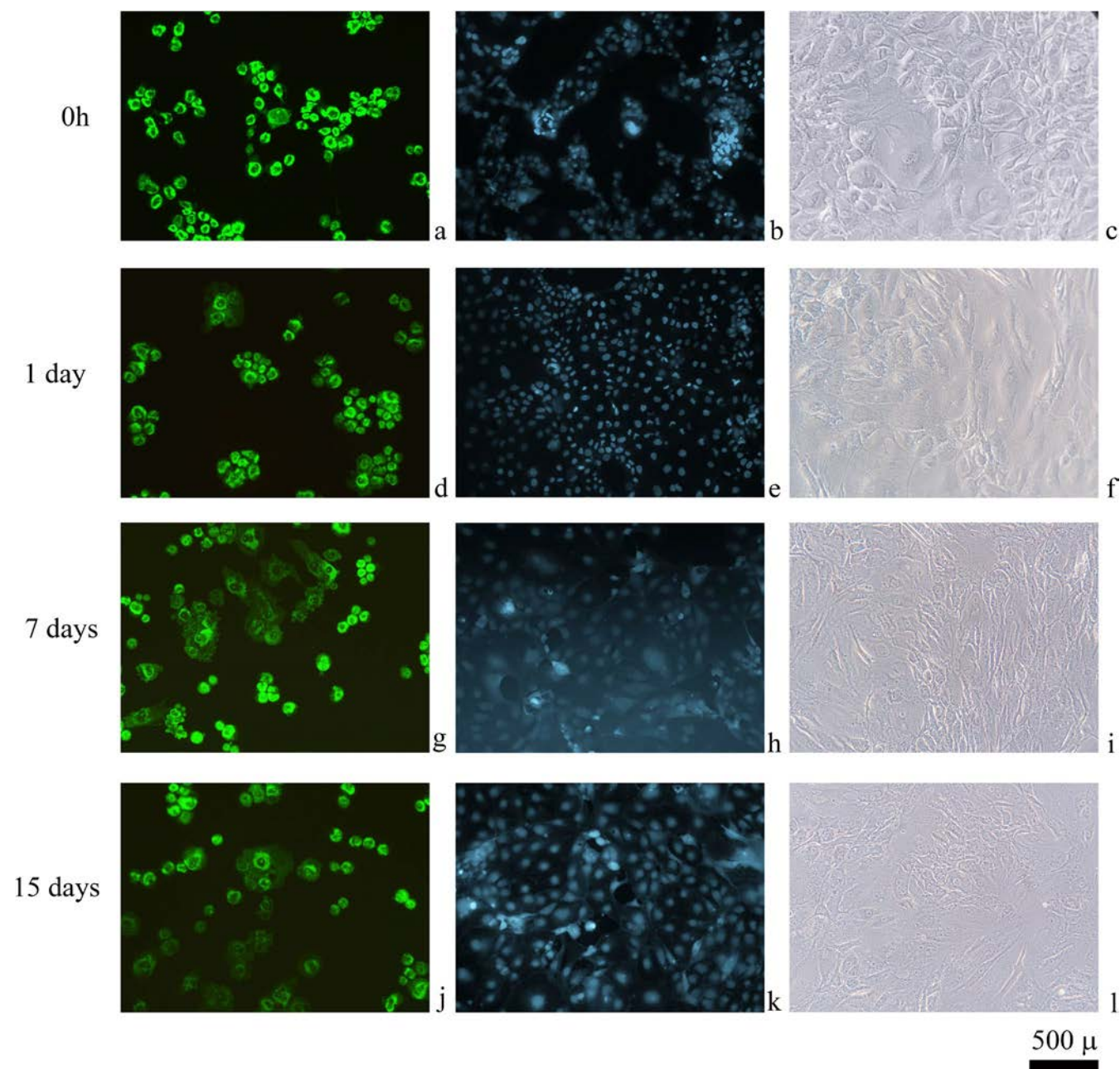
FIGURE 4 | Microscopic staining of chondrocytes with AO/PI and Hoechst stains, first lane (a–c) control group samples, (d–f) micrographs of Tocilizumab-applied cultures for 1 day, (g–i) 7 days, and (j–l) 15 days. First column: acridine orange/propidium iodide-stained cultures (20× magnification), second column: Hoechst-stained cultures (20× magnification). Third column: inverted microscopy images.
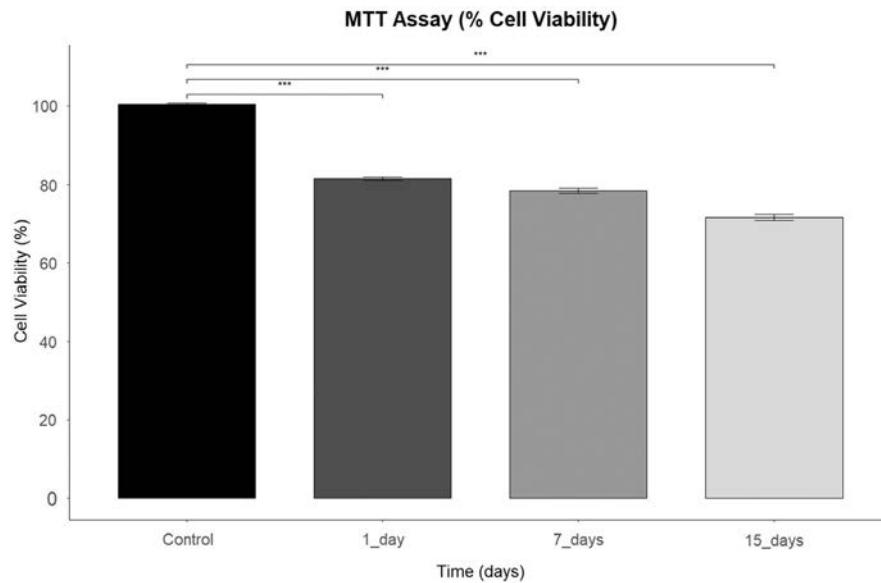
FIGURE 5 | MTT assay showing the percentage cell viability of human primary chondrocytes treated with Tocilizumab at different time points (Control, 1, 7, 15 days). Error bars represent standard deviation across replicates. ***Data represent mean ± SD of at least three independent experiments. Statistical significance was determined using one-way ANOVA followed by post hoc analysis ($p < 0.05$ considered significant).
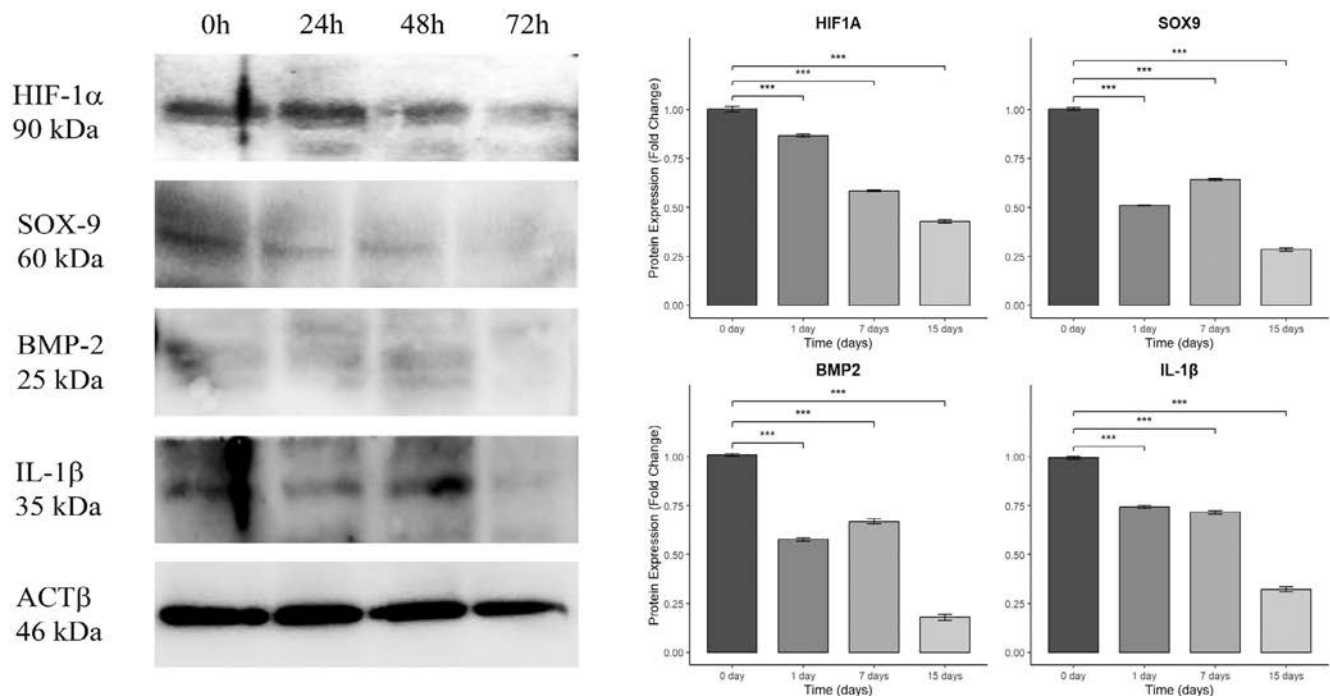
FIGURE 6 | Western blot analysis of HIF-1α, SOX-9, BMP-2, and IL-1β protein expression levels in human primary chondrocytes treated with Tocilizumab across different time points. Representative Western blot images showing the expression levels of HIF-1α, SOX-9, BMP-2, and IL-1β in human primary chondrocytes following Tocilizumab treatment at 0, 1, 7, and 15 days. Protein bands were quantified by densitometric analysis and normalized to β-actin. Data are representative of at least three independent experiments. ***Data are expressed as mean ± SD from replicate experiments.

4 | Discussion

In this study, the effects of Tocilizumab on human primary chondrocyte cells were evaluated through BMP-2, HIF-1α, IL-1β, SOX-9, and IL-6 genes. The Reactome and GO enrichment analyses indicated significant involvement of pathways such as interleukin signaling, BMP signaling, and mitogen-activated protein kinase (MAPK) pathways in chondrocyte regulation. Specifically, Reactome pathways like "Interleukin-6 signaling" and "MAPK3 (ERK1) activation" are central to inflammation and cellular response regulation. Given Tocilizumab's inhibitory effects on IL-6 signaling, it may influence metabolic processes and differentiation pathways critical to chondrocyte health and function.

The STRING PPI network further highlighted the interaction between BMP-2, HIF-1α, IL-1β, SOX-9, and IL-6, alongside additional proteins associated with inflammation and developmental processes, such as RUNX2 and tenomodulin (TNMD). This dense interaction network underscores the interconnected roles of these genes, with potential downstream effects on chondrocyte differentiation and function. In particular, BMP-2 and SOX-9 play crucial roles in chondrogenesis and differentiation, while HIF-1α is vital for cellular adaptation under low oxygen conditions. HIF-1α has also been shown to transcriptionally regulate SOX-9 expression during hypoxic stress, thereby linking hypoxia response to chondrocyte differentiation processes [36]. The observed reduction in SOX-9 and HIF-1α expression over time suggests that Tocilizumab may impact the differentiation and oxygen sensitivity of chondrocytes, especially under prolonged inflammatory conditions [36].

In the Western blot analysis, an early increase in BMP-2 and IL-1β protein expression was observed, which may be related to the initial activation of inflammatory pathways. The subsequent reduction in BMP-2 expression could be interpreted as a compensatory feedback mechanism to limit excessive matrix remodeling, as sustained BMP-2 activation can potentially promote chondrocyte hypertrophy [9]. However, the subsequent decrease in HIF-1α and SOX-9 protein levels over time indicates that Tocilizumab could suppress regulatory mechanisms essential to chondrocyte differentiation and cellular adaptation in the long term. This reduction suggests a potential decrease in the cells' ability to adapt within an anti-inflammatory environment, impacting their functionality and differentiation capabilities [36].

The MTT cell viability assay results demonstrated a time-dependent decline in cell viability, potentially reflecting the cytostatic effects of Tocilizumab on chondrocytes. IL-6 has been reported to inhibit chondrocyte proliferation [15]; however, in our study, the blockade of IL-6 signaling by Tocilizumab was associated with a time-dependent reduction in chondrocyte viability, indicating that additional regulatory mechanisms may be involved in the cytostatic effects observed. This reduction in viability may arise from the drug's inhibitory effects on inflammatory signaling pathways, which could subsequently decrease chondrocyte growth and proliferation capacity. The response of chondrocytes to prolonged Tocilizumab exposure highlights essential findings regarding cartilage integrity and viability, particularly in treating chronic inflammatory conditions.

In the AO/PI and Hoechst staining analyses, chondrocytes treated with Tocilizumab exhibited consistent green fluorescence and intact nuclear morphology, with no observable increase in red-stained (nonviable) cells or signs of nuclear deformation. This outcome suggests that while Tocilizumab may have a cytostatic effect, as indicated by reduced proliferation in MTT assays, it does not compromise membrane integrity or induce apoptosis within the timeframe assessed. These findings emphasize Tocilizumab's favorable safety profile concerning cellular integrity in chondrocytes, even though prolonged treatment could affect cell viability and proliferation. These findings emphasize that Tocilizumab preserves cellular and nuclear integrity under the tested conditions, although prolonged treatment may impact overall cell viability and proliferation capacity.

Overall, the findings of this study demonstrate that Tocilizumab significantly modulates pathways influencing inflammatory and differentiation processes in human primary chondrocytes. The inhibition of IL-6 signaling may indirectly impact cartilage synthesis and repair mechanisms and could lead to a gradual reduction in cellular viability over time. These results provide a valuable foundation for future studies to elucidate the long-term effects of Tocilizumab on cartilage tissue in chronic inflammatory diseases and to assess its therapeutic potential in cartilage preservation and regeneration.

Ethics Statement

This study was conducted in accordance with the ethical standards of the (TNKÜ Girişimsel Olmayan Klinik Araştırmalar Etik Kurulu) and was approved under Ethics Approval Number: 2024.302.11.09.

Consent

Written informed consent was obtained from all donors prior to cartilage tissue collection.

Conflicts of Interest

The authors declare no conflicts of interest.

Data Availability Statement

The data that support the findings of this study are available from the corresponding author upon reasonable request.

References

1. T. Pap and A. Korb-Pap, "Cartilage Damage in Osteoarthritis and Rheumatoid Arthritis—Two Unequal Siblings," *Nature Reviews Rheumatology* 11, no. 10 (2015): 606–615, https://doi.org/10.1038/NRRHEUM.2015.95.

2. H. Muir, "The Chondrocyte, Architect of Cartilage. Biomechanics, Structure, Function and Molecular Biology of Cartilage Matrix Macromolecules," *BioEssays* 17, no. 12 (1995): 1039–1048, https://doi.org/10.1002/BIES.950171208.

3. S. R. Goldring and M. B. Goldring, "The Role of Cytokines in Cartilage Matrix Degeneration in Osteoarthritis," *Clinical Orthopaedics and*

Related Research 427 (2004): S27–S36, https://doi.org/10.1097/01.BLO.0000144854.66565.8F.

4. A. J. Schuerwegh, E. J. Dombrecht, W. J. Stevens, J. F. Van Offel, C. H. Bridts, and L. S. De Clerck, "Influence of Pro-Inflammatory (IL-1α, IL-6, TNF-α, IFN-γ) and Anti-Inflammatory (IL-4) Cytokines on Chondrocyte Function," *Osteoarthritis and Cartilage* 11, no. 9 (2003): 681–687, https://doi.org/10.1016/S1063-4584(03)00156-0.

5. R. Wiegertjes, F. A. J. Van De Loo, and E. N. Blaney Davidson, "A Roadmap to Target Interleukin-6 in Osteoarthritis," *Rheumatology (Oxford)* 59, no. 10 (2020): 2681–2694, https://doi.org/10.1093/RHEUMATOLOGY/KEAA248.

6. Q. Yao, X. Wu, C. Tao, et al., "Osteoarthritis: Pathogenic Signaling Pathways and Therapeutic Targets," *Signal Transduction and Targeted Therapy* 8, no. 1 (2023): 1–31, https://doi.org/10.1038/s41392-023-01330-w.

7. M. Mihara, Y. Ohsugi, and T. Kishimoto, "Tocilizumab, a Humanized Anti-Interleukin-6 Receptor Antibody, for Treatment of Rheumatoid Arthritis," *Open Access Rheumatology: Research and Reviews* 3 (2011): 19–29, https://doi.org/10.2147/OARRR.S17118.

8. M. Hashizume, S. L. Tan, J. Takano, et al., "Tocilizumab, a Humanized Anti-IL-6R Antibody, as an Emerging Therapeutic Option for Rheumatoid Arthritis: Molecular and Cellular Mechanistic Insights," *International Reviews of Immunology* 34, no. 3 (2015): 265–279, https://doi.org/10.3109/08830185.2014.938325.

9. Z. H. Deng, Y. S. Li, X. Gao, G. H. Lei, and J. Huard, "Bone Morphogenetic Proteins for Articular Cartilage Regeneration," *Osteoarthritis and Cartilage* 26, no. 9 (2018): 1153–1161, https://doi.org/10.1016/J.JOCA.2018.03.007.

10. C. Y. Zeng, X. F. Wang, and F. Z. Hua, "HIF-1α in Osteoarthritis: From Pathogenesis to Therapeutic Implications," *Frontiers in Pharmacology* 13 (2022): 927126, https://doi.org/10.3389/FPHAR.2022.927126.

11. H. Song and K. H. Park, "Regulation and Function of SOX9 During Cartilage Development and Regeneration," *Seminars in Cancer Biology* 67 (2020): 12–23, https://doi.org/10.1016/J.SEMCANCER.2020.04.008.

12. K. Hino, A. Saito, M. Kido, et al., "Master Regulator for Chondrogenesis, Sox9, Regulates Transcriptional Activation of the Endoplasmic Reticulum Stress Transducer BBF2H7/CREB3L2 in Chondrocytes," *Journal of Biological Chemistry* 289, no. 20 (2014): 13810–13820, https://doi.org/10.1074/JBC.M113.543322.

13. P. Kongdang, C. Chokchaitaweesuk, S. Tangyuenyong, and S. Ongchai, "Proinflammatory Effects of IL-1β Combined With IL-17A Promoted Cartilage Degradation and Suppressed Genes Associated With Cartilage Matrix Synthesis In Vitro," *Molecules* 24, no. 20 (2019): 3682, https://doi.org/10.3390/MOLECULES24203682.

14. C. R. Flannery, C. B. Little, C. E. Hughes, C. L. Curtis, B. Caterson, and S. A. Jones, "IL-6 and Its Soluble Receptor Augment Aggrecanase-Mediated Proteoglycan Catabolism in Articular Cartilage," *Matrix Biology* 19, no. 6 (2000): 549–553, https://doi.org/10.1016/S0945-053X(00)00111-6.

15. A. Jikko, T. Wakisaka, M. Iwamoto, et al., "Effects of INTERLEUKIN-6 on Proliferation and Proteoglycan Metabolism in Articular Chondrocyte Cultures," *Cell Biology International* 22, no. 9–10 (1998): 615–621, https://doi.org/10.1006/CBIR.1998.0304.

16. G. Yu, L. G. Wang, Y. Han, and Q. Y. He, "ClusterProfiler: An R Package for Comparing Biological Themes Among Gene Clusters," *OMICS: A Journal of Integrative Biology* 16, no. 5 (2012): 284–287, https://doi.org/10.1089/OMI.2011.0118.

17. G. Yu and Q. Y. He, "ReactomePA: An R/Bioconductor Package for Reactome Pathway Analysis and Visualization," *Molecular BioSystems* 12, no. 2 (2016): 477–479, https://doi.org/10.1039/C5MB00663E.

18. C. von Mering, M. Huynen, D. Jaeggi, S. Schmidt, P. Bork, and B. Snel, "STRING: A Database of Predicted Functional Associations Between Proteins," *Nucleic Acids Research* 31, no. 1 (2003): 258–261, https://doi.org/10.1093/NAR/GKG034.

19. C. H. Chin, S. H. Chen, H. H. Wu, C. W. Ho, M. T. Ko, and C. Y. Lin, "cytoHubba: Identifying Hub Objects and Sub-Networks From Complex Interactome," *BMC Systems Biology* 8, no. Suppl 4 (2014): S11, https://doi.org/10.1186/1752-0509-8-S4-S11.

20. M. Isyar, I. Yilmaz, D. Yasar Sirin, S. Yalcin, O. Guler, and M. Mahirogullari, "A Practical Way to Prepare Primer Human Chondrocyte Culture," *Journal of Orthopaedics* 13, no. 3 (2016): 162–167, https://doi.org/10.1016/J.JOR.2016.03.008.

21. P. Kumar, A. Nagarajan, and P. D. Uchil, "Analysis of Cell Viability by the MTT Assay," *Cold Spring Harbor Protocols* 2018, no. 6 (2018): 469–471, https://doi.org/10.1101/PDB.PROT095505.

22. C. Lema, A. Varela-Ramirez, and R. J. Aguilera, "Differential Nuclear Staining Assay for High-Throughput Screening to Identify Cytotoxic Compounds," *Current Cell Biology* 1, no. 1 (2011): 1, https://pmc.ncbi.nlm.nih.gov/articles/PMC4816492/.

23. I. Yilmaz, H. Akalan, D. Y. Sirin, et al., "Effects of Tocilizumab on Intervertebral Disc Degeneration, Cell Senescence and Inflammation via BMP-2, Hif-1α, IL-1β and SOX9," *International Journal of Pharmacology* 19, no. 6 (2023): 825–833, https://doi.org/10.3923/IJP.2023.825.833.

24. M. Lv, Y. Zhou, S. W. Polson, et al., "Identification of Chondrocyte Genes and Signaling Pathways in Response to Acute Joint Inflammation," *Scientific Reports* 9, no. 1 (2019): 93, https://doi.org/10.1038/s41598-018-36500-2.

25. M. Iwaszko, S. Biały, and K. Bogunia-Kubik, "Significance of Interleukin (IL)-4 and IL-13 in Inflammatory Arthritis," *Cells* 10 (2021): 3000, https://doi.org/10.3390/CELLS10113000.

26. S. Wahlen, F. Matthijssens, W. van Loocke, et al., "The Transcription Factor RUNX2 Drives the Generation of Human NK Cells and Promotes Tissue Residency," *eLife* 11 (2022): e80320, https://doi.org/10.7554/ELIFE.80320.

27. D. Chen, D. J. Kim, J. Shen, Z. Zou, and R. J. O'Keefe, "Runx2 Plays a Central Role in Osteoarthritis Development," *Journal of Orthopaedic Translation* 23 (2020): 132–139, https://doi.org/10.1016/J.JOT.2019.11.008.

28. T. Tanaka, M. Narazaki, and T. Kishimoto, "IL-6 in Inflammation, Immunity, and Disease," *Cold Spring Harbor Perspectives in Biology* 6, no. 10 (2014): a016295, https://doi.org/10.1101/CSHPERSPECT.A016295.

29. J. M. Kyriakis and J. Avruch, "Mammalian MAPK Signal Transduction Pathways Activated by Stress and Inflammation: A 10-Year Update," *Physiological Reviews* 92, no. 2 (2012): 689–737, https://doi.org/10.1152/PHYSREV.00028.2011.

30. A. Rubbert-Roth, D. E. Furst, J. M. Nebesky, A. Jin, and E. Berber, "A Review of Recent Advances Using Tocilizumab in the Treatment of Rheumatic Diseases," *Rheumatology and Therapy* 5, no. 1 (2018): 21–42, https://doi.org/10.1007/S40744-018-0102-X.

31. J. P. Thiery, H. Acloque, R. Y. J. Huang, and M. A. Nieto, "Epithelial-Mesenchymal Transitions in Development and Disease," *Cell* 139, no. 5 (2009): 871–890, https://doi.org/10.1016/J.CELL.2009.11.007.

32. M. Shimasaki, S. Ueda, M. Sakurai, N. Kawahara, Y. Ueda, and T. Ichiseki, "Celecoxib Combined With Tocilizumab has Anti-Inflammatory Effects and Promotes the Recovery of Damaged Cartilage via the Nrf2/HO-1 Pathway In Vitro," *Biomolecules* 14, no. 12 (2024): 1636, https://doi.org/10.3390/BIOM14121636.

33. T. Li, J. Peng, Q. Li, Y. Shu, P. Zhu, and L. Hao, "The Mechanism and Role of ADAMTS Protein Family in Osteoarthritis," *Biomolecules* 12 (2022): 959, https://doi.org/10.3390/BIOM12070959.

34. R. H. Song, M. D. Tortorella, A. M. Malfait, et al., "Aggrecan Degradation in Human Articular Cartilage Explants Is Mediated by Both

ADAMTS-4 and ADAMTS-5," *Arthritis and Rheumatism* 56, no. 2 (2007): 575–585, https://doi.org/10.1002/ART.22334.

35. Q. Hu and M. Ecker, "Overview of MMP-13 as a Promising Target for the Treatment of Osteoarthritis," *International Journal of Molecular Sciences* 22, no. 4 (2021): 1742, https://doi.org/10.3390/IJMS22041742.

36. R. Amarilio, S. V. Viukov, A. Sharir, I. Eshkar-Oren, R. S. Johnson, and E. Zelzer, "HIF1alpha Regulation of Sox9 Is Necessary to Maintain Differentiation of Hypoxic Prechondrogenic Cells During Early Skeletogenesis," *Development (Cambridge, England)* 134, no. 21 (2007): 3917–3928, https://doi.org/10.1242/DEV.008441.

The Role of TYK2 Inhibitors in the Evolving Landscape of Rheumatologic and Dermatologic Treatment

I-Chang Lai[1] | Yung-Heng Lee[2,3,4,5] | Po-Cheng Shih[6,7] | Meng-Che Wu[8,9,10]

[1]Department of Education, China Medical University Hospital, China Medical University, Taichung, Taiwan | [2]Department of Orthopedics, Feng Yuan Hospital, Ministry of Health and Welfare, Taichung, Taiwan | [3]Institute of Medical Science and Technology, National Sun Yat-Sen University, Kaohsiung, Taiwan | [4]Department of Senior Services Industry Management, Minghsin University of Science and Technology, Hsinchu, Taiwan | [5]Department of Recreation and Sport Management, Shu-Te University, Kaohsiung, Taiwan | [6]Division of Allergy, Immunology and Rheumatology, Department of Internal Medicine, Changhua Christian Hospital, Changhua, Taiwan | [7]Institute of Medicine, Chung Shan Medical University, Taichung, Taiwan | [8]School of Medicine, Chung Shan Medical University, Taichung, Taiwan | [9]Division of Pediatric Gastroenterology, Children's Medical Center, Taichung Veterans General Hospital, Taichung, Taiwan | [10]Department of Post-Baccalaureate Medicine, College of Medicine, National Chung Hsing University, Taichung, Taiwan

Correspondence: Po-Cheng Shih (robertpcshih@gmail.com) | Meng-Che Wu (wumengche@gmail.com)

Tyrosine kinase 2 (TYK2) is a non-receptor tyrosine kinase and a key member of the Janus kinase (JAK) family, playing an essential role in the intracellular signaling of several cytokine pathways. Specifically, TYK2 mediates the signal transduction of interleukin-12 (IL-12), interleukin-23 (IL-23), and type I interferons (IFN-α/β), which are crucial regulators of innate and adaptive immune responses. These pathways are central to the pathogenesis of multiple autoimmune and inflammatory diseases, including psoriasis, psoriatic arthritis (PsA), systemic lupus erythematosus (SLE), and inflammatory bowel disease (IBD) [1, 2]. Unlike conventional JAK inhibitors, which target the active catalytic domain (JH1 domain) and broadly suppress multiple cytokine pathways, TYK2 inhibitors function through selective allosteric inhibition of the regulatory JH2 (pseudokinase) domain. This unique mechanism allows for precise modulation of TYK2 activity without directly affecting the ATP-binding site, thereby reducing off-target inhibition of JAK1, JAK2, and JAK3 [2]. By preserving partial physiological cytokine signaling, TYK2 inhibitors demonstrate a potentially improved safety profile compared to broader JAK inhibitors, particularly in terms of infection risk, malignancy concerns, and cardiovascular adverse events [1, 3].

From a clinical perspective, TYK2 inhibitors have emerged as promising therapeutic agents with an improved safety profile compared to conventional JAK inhibitors. Deucravacitinib, the first FDA-approved allosteric TYK2 inhibitor, has demonstrated efficacy in the treatment of moderate-to-severe plaque psoriasis, with ongoing trials exploring its potential in PsA and SLE [4–10]. Other TYK2 inhibitors, such as Brepocitinib and Ropsacitinib, are in earlier phases of clinical development and are being investigated for a range of autoimmune conditions [11–20]. This editorial aims to review the evidence-based medicine (EBM) level of TYK2 inhibitors across different autoimmune and dermatologic indications, compare their clinical positioning relative to biologic agents such as IL-17 and IL-23 inhibitors, and discuss the existing unmet needs and future research directions for TYK2-targeted therapies.

TYK2 inhibitors have been extensively studied across various immune-mediated diseases, with different levels of evidence supporting their use (Table 1). Among the available agents, Deucravacitinib has the most robust clinical data, particularly in psoriasis, where multiple Phase III trials confirm its efficacy, earning it Level 1A evidence [4–8]. Meanwhile, other TYK2

Dr. Meng-Che Wu and Dr. Po-Cheng Shih contributed equally as corresponding authors to this work.

TABLE 1 | Summary of TYK2 inhibitor clinical trials and evidence-based medicine (EBM) levels across autoimmune diseases.

TYK2 inhibitor	Indication	Trial stage	Main outcome measure	Treatment protocol	Efficacy results (compared to placebo)	EBM level	Ref.
Deucravacitinib	PsO	Phase III	PASI 75 at week 16	6 mg/day	58.4% versus 12.7%; $p < 0.0001$	Level 1A	[5]
	PsO	Phase III	PASI 75 at week 16	6 mg/day	53.0% versus 9.4%; $p < 0.0001$	Level 1A	[4]
	PsO	Phase III	PASI 75 at week 16	6 mg/day	76.2% (achievement rate)	Level 2B	[6]
	PsO	Real-world data	PASI 75 at week 16	6 mg/day	78.3% (achievement rate)	Level 3	[7]
	PsO	Real-world data	PASI 75 at week 52	6 mg/day	86.36% (achievement rate)	Level 3	[8]
	PsA	Phase II	ACR20 at week 16	6 mg/day	52.9% versus 31.8%; $p = 0.0134$	Level 2A	[9]
				12 mg/day	62.7% versus 31.8%; $p = 0.0004$		
	SLE	Phase II	SRI-4 at week 32	3 mg twice/day	58% versus 34%; $p < 0.001$	Level 2A	[10]
				6 mg twice/day	49.5% versus 34.4%; $p = 0.02$		
				12 mg/day	44.9% versus 34.4%; $p = 0.08$		
Brepocitinib	PsO	Phase II	Mean change in PASI at week 12	30 mg/day	−17.3% versus 7%; $p < 0.0001$	Level 2B	[11]
	PsO	Phase IIb	PASI-50, PASI-75, PASI-90 and PASI-100 at week 12	Topical 0.1% once daily to 3% twice daily	Did not reach statistical significance	Level 1B	[12]
	PsA	Phase II	ACR20 at week 16	10 mg/day	64.5% versus 44.3% (did not reach statistical significance)	Level 2A	[20]
				30 mg/day	66.7% versus 44.3%; $p = 0.0197$		
				60 mg/day	74.6% versus 44.3%; $p = 0.0006$		
	UC	Phase II	Total Mayo Score at week 8	10 mg/day	6.1 versus 7.9; $p = 0.009$	Level 2B	[13]
				30 mg/day	5.6 versus 7.9; $p = 0.001$		
				60 mg/day	4.7 versus 7.9; $p < 0.001$		
	AD	Phase IIb	Mean percentage change in EASI total score at week 6	Topical 1% once daily	−70.1% versus −44.4%; $p < 0.05$	Level 1B	[14]
				Topical 1% twice daily	−75.0% versus −47.6%; $p < 0.05$		
				Topical 0.1%, 0.3%, 3% once daily and 0.3% twice daily	Did not reach statistical significance		
	AA	Phase IIa	Mean change in SALT score at week 24	30 mg/day	−38.8 versus −7.6 (p value not provided)	Level 1B	[15]
	AA	Phase IIa	Mean change in SALT score at week 24	60 mg/day for 4 weeks then 30 mg/day for 20 weeks	−49.2 versus −1.4; $p < 0.001$	Level 1B	[16]
	CA	Phase IIa	CCL5 expression at week 24 (log2-fold change)	45 mg/day	−1.47 ($p = 0.004$) versus −0.43 ($p = 0.01$)	Level 1B	[18]
	HS	Phase IIa	Participants achieving HiSCR at week 16	45 mg/day	51.9% versus 33.3%; $p = 0.03$	Level 1B	[17]
Ropsacitinib	PsO	Phase II	PASI 90 at week 16	400 mg/day	Risk difference 46.5%; $p < 0.0001$	Level 2B	[19]
	HS	Phase IIa	Participants achieving HiSCR at week 16	400 mg/day	37.0% versus 33.3%; $p = 0.36$	Level 1B	[17]

Abbreviations: AA, alopecia areata; AD, atopic dermatitis; CA, cicatricial alopecia; CCL5, C-C motif chemokine ligand 5; EASI, eczema area and severity index; HiSCR, hidradenitis suppurativa clinical response; HS, hidradenitis suppurativa; PASI, psoriasis area and severity index; PsA, psoriatic arthritis; PsO, psoriasis; SALT, severity of alopecia tool; SLE, systemic lupus erythematosus; SRI-4, SLE responder index 4; UC, ulcerative colitis.

inhibitors such as Brepocitinib and Ropsacitinib remain in earlier phases of development, with supporting data primarily from Phase II trials, resulting in Level 2A or lower evidence across different indications [11–20].

In psoriasis, Deucravacitinib's FDA approval is backed by strong Phase III trial results, demonstrating PASI 75 response rates comparable to biologic agents. The real-world studies further support its durability, with long-term PASI 75 achievement rates exceeding 85% in observational settings [4–8]. These findings suggest that Deucravacitinib may represent a valuable oral systemic option for patients with moderate-to-severe psoriasis, especially those who prefer non-injectable treatments or encounter logistical or economic barriers to accessing biologics. Compared to apremilast, Deucravacitinib has demonstrated superior efficacy with a comparable safety profile, potentially expanding the role of oral therapies in this setting. Its selective allosteric inhibition of the TYK2 pseudokinase domain allows for targeted cytokine modulation—primarily IL-12, IL-23, and type I interferons—while avoiding broader JAK1–3 suppression. This selectivity may translate into a more favorable safety profile, with a lower risk of adverse effects such as cytopenias, thromboembolic events, or dyslipidemia. In contrast, Brepocitinib and Ropsacitinib remain in earlier clinical trials, with Phase II data suggesting promising efficacy, but without Phase III validation, they remain investigational for this indication [11, 19]. Within the current therapeutic landscape, which includes an array of biologics with proven efficacy, TYK2 inhibition offers a potential intermediary step in treatment sequencing—positioned after failure of conventional systemics but before escalation to biologics in appropriately selected patients.

For psoriatic arthritis (PsA), Deucravacitinib has reached Phase II trials, demonstrating clinically meaningful efficacy, leading to a Level 2A evidence rating [9]. However, no Phase III trials have been completed, limiting its immediate clinical application. Brepocitinib has also shown positive results in Phase II trials for PsA, though larger studies are necessary to confirm its efficacy and safety in this population [20]. Compared to IL-17 and IL-23 inhibitors, which are supported by robust Phase III data and widespread real-world use, TYK2 inhibitors remain in earlier stages of clinical development for PsA. However, their mechanism—targeting IL-23 and type I interferon pathways—offers a distinct approach. Given their oral formulation and emerging safety data, TYK2 inhibitors such as Deucravacitinib may be considered in patients with mild-to-moderate or early PsA, particularly those with limited joint involvement and concurrent skin disease. In such cases, oral TYK2 inhibition may provide a practical alternative prior to initiating biologics, especially when patient preference, tolerability, or access are important considerations.

In systemic lupus erythematosus (SLE), Deucravacitinib has been evaluated in Phase II trials, showing potential benefits, but its evidence level remains at Level 2A due to the lack of Phase III confirmation [10]. Given the complexity of SLE, where multiple immune pathways are involved, additional studies are needed to establish TYK2 inhibitors as a viable treatment alternative.

For ulcerative colitis (UC), results have been mixed. While TYK2 inhibition is a biologically plausible target given its role in IL-23 signaling, clinical trials have produced inconsistent findings, with some failing to meet their primary endpoints [13].

Consequently, the evidence level remains at Level 2B or lower, and further optimization of dosing strategies or combination therapies may be required to improve outcomes.

Despite their therapeutic potential, TYK2 inhibitors face several critical challenges, particularly regarding long-term safety, real-world effectiveness, and broader clinical applications. A key concern is malignancy risk, as prolonged JAK inhibition has been linked to increased cancer incidence. While Deucravacitinib's selective allosteric inhibition suggests a lower oncogenic risk, long-term surveillance data are still lacking. Similarly, cardiovascular safety remains uncertain, given the association between JAK inhibitors and increased MACE risk [1, 3]. Although TYK2 inhibitors theoretically have a more favorable safety profile, definitive conclusions require extended follow-up and real-world studies.

Another major gap is the lack of large-scale real-world evidence, which is crucial for assessing drug persistence, effectiveness across diverse patient populations, and rare adverse events. While RCTs indicate that Deucravacitinib is superior to placebo and Apremilast in psoriasis, direct comparisons with biologics are limited, making it difficult to determine its true positioning in treatment guidelines [3–5].

Beyond psoriasis, expanding indications remains a challenge. Phase II trials in PsA and SLE have shown promising efficacy, but Phase III validation is still pending [9, 10, 20]. Similarly, Brepocitinib and Ropsacitinib, though showing potential in psoriasis and inflammatory conditions, remain in early-stage clinical development, requiring multi-center trials to establish efficacy and safety [11–20].

To fully integrate TYK2 inhibitors into clinical practice, long-term safety monitoring, real-world studies, and head-to-head trials against biologics and JAK inhibitors are essential to clarify their benefits and risks. Addressing these gaps will be crucial for defining their role in autoimmune disease management.

In conclusion, TYK2 inhibitors have emerged as a promising therapeutic option for immune-mediated diseases, offering a selective mechanism that distinguishes them from both traditional JAK inhibitors and biologic therapies. Their efficacy in psoriasis is well established, with Deucravacitinib achieving Phase III approval, while other indications, including PsA, SLE, and UC, remain under investigation. Despite their potential advantages in safety and convenience, long-term real-world data and direct comparative studies with biologics are essential to determine their optimal role in clinical practice. Future research should focus on head-to-head trials with IL-17 and IL-23 inhibitors, as well as expanding Phase III studies in autoimmune diseases beyond psoriasis to strengthen their evidence base. Additionally, real-world registries and long-term pharmacovigilance programs will be critical in confirming their long-term safety, particularly regarding malignancy and cardiovascular risks. With further validation, TYK2 inhibitors have the potential to bridge the gap between conventional systemic therapies and biologics, providing a well-tolerated, effective, and convenient oral option for patients with chronic inflammatory diseases. Their continued development could significantly reshape treatment paradigms, offering an alternative for patients who require long-term disease control with a favorable safety profile.

References

1. E. Morand, J. F. Merola, Y. Tanaka, D. Gladman, and R. Fleischmann, "TYK2: An Emerging Therapeutic Target in Rheumatic Disease," *Nature Reviews Rheumatology* 20, no. 4 (2024): 232–240, https://doi.org/10.1038/s41584-024-01093-w.

2. D. P. McLornan, J. E. Pope, J. Gotlib, and C. N. Harrison, "Current and Future Status of JAK Inhibitors," *Lancet* 398, no. 10302 (2021): 803–816, https://doi.org/10.1016/s0140-6736(21)00438-4.

3. M. G. Haggett, S. Lee, and F. Y. X. Lai, "A Systematic Review of the Efficacy of TYK2 Inhibitors in Patients With Dermatological Disease," *Australasian Journal of Dermatology* 66 (2024): 1, https://doi.org/10.1111/ajd.14391.

4. B. Strober, D. Thaçi, H. Sofen, et al., "Deucravacitinib Versus Placebo and Apremilast in Moderate to Severe Plaque Psoriasis: Efficacy and Safety Results From the 52-Week, Randomized, Double-Blinded, Phase 3 Program fOr Evaluation of TYK2 Inhibitor Psoriasis Second Trial," *Journal of the American Academy of Dermatology* 88, no. 1 (2023): 40–51, https://doi.org/10.1016/j.jaad.2022.08.061.

5. A. W. Armstrong, M. Gooderham, R. B. Warren, et al., "Deucravacitinib Versus Placebo and Apremilast in Moderate to Severe Plaque Psoriasis: Efficacy and Safety Results From the 52-Week, Randomized, Double-Blinded, Placebo-Controlled Phase 3 POETYK PSO-1 Trial," *Journal of the American Academy of Dermatology* 88, no. 1 (2023): 29–39, https://doi.org/10.1016/j.jaad.2022.07.002.

6. S. Imafuku, Y. Okubo, Y. Tada, et al., "Deucravacitinib, an Oral, Selective, Allosteric Tyrosine Kinase 2 Inhibitor, in Japanese Patients With Moderate to Severe Plaque, Erythrodermic, or Generalized Pustular Psoriasis: Efficacy and Safety Results From an Open-Label, Phase 3 Trial," *Journal of Dermatology* 51, no. 3 (2024): 365–379, https://doi.org/10.1111/1346-8138.17074.

7. T. Hagino, H. Saeki, E. Fujimoto, and N. Kanda, "Effectiveness and Safety of Deucravacitinib Treatment for Moderate-To-Severe Psoriasis in Real-World Clinical Practice in Japan," *Journal of Dermatological Treatment* 35, no. 1 (2024): 2307489, https://doi.org/10.1080/09546634.2024.2307489.

8. T. Hagino, M. Onda, H. Saeki, E. Fujimoto, and N. Kanda, "Real-World 52-Week Effectiveness of Deucravacitinib in Psoriasis: A Stratified Analysis by Age and Body Mass Index," *Journal of Dermatology* 52 (2025): 663–671, https://doi.org/10.1111/1346-8138.17617.

9. P. J. Mease, A. A. Deodhar, D. van der Heijde, et al., "Efficacy and Safety of Selective TYK2 Inhibitor, Deucravacitinib, in a Phase II Trial in Psoriatic Arthritis," *Annals of the Rheumatic Diseases* 81, no. 6 (2022): 815–822, https://doi.org/10.1136/annrheumdis-2021-221664.

10. E. Morand, M. Pike, J. T. Merrill, et al., "Deucravacitinib, a Tyrosine Kinase 2 Inhibitor, in Systemic Lupus Erythematosus: A Phase II, Randomized, Double-Blind, Placebo-Controlled Trial," *Arthritis and Rheumatology* 75, no. 2 (2023): 242–252, https://doi.org/10.1002/art.42391.

11. S. B. Forman, D. M. Pariser, Y. Poulin, et al., "TYK2/JAK1 Inhibitor PF-06700841 in Patients With Plaque Psoriasis: Phase IIa, Randomized, Double-Blind, Placebo-Controlled Trial," *Journal of Investigative Dermatology* 140, no. 12 (2020): 2359–2370.e5, https://doi.org/10.1016/j.jid.2020.03.962.

12. M. N. Landis, S. R. Smith, G. Berstein, et al., "Efficacy and Safety of Topical Brepocitinib Cream for Mild-To-Moderate Chronic Plaque Psoriasis: A Phase IIb Randomized Double-Blind Vehicle-Controlled Parallel-Group Study," *British Journal of Dermatology* 189, no. 1 (2023): 33–41, https://doi.org/10.1093/bjd/ljad098.

13. W. J. Sandborn, S. Danese, J. Leszczyszyn, et al., "Oral Ritlecitinib and Brepocitinib for Moderate-To-Severe Ulcerative Colitis: Results From a Randomized, Phase 2b Study," *Clinical Gastroenterology and Hepatology* 21, no. 10 (2023): 2616–2628.e7, https://doi.org/10.1016/j.cgh.2022.12.029.

14. M. N. Landis, M. Arya, S. Smith, et al., "Efficacy and Safety of Topical Brepocitinib for the Treatment of Mild-To-Moderate Atopic Dermatitis: A Phase IIb, Randomized, Double-Blind, Vehicle-Controlled, Dose-Ranging and Parallel-Group Study," *British Journal of Dermatology* 187, no. 6 (2022): 878–887, https://doi.org/10.1111/bjd.21826.

15. E. Guttman-Yassky, A. B. Pavel, A. Diaz, et al., "Ritlecitinib and Brepocitinib Demonstrate Significant Improvement in Scalp Alopecia Areata Biomarkers," *Journal of Allergy and Clinical Immunology* 149, no. 4 (2022): 1318–1328, https://doi.org/10.1016/j.jaci.2021.10.036.

16. B. King, E. Guttman-Yassky, E. Peeva, et al., "A Phase 2a Randomized, Placebo-Controlled Study to Evaluate the Efficacy and Safety of the Oral Janus Kinase Inhibitors Ritlecitinib and Brepocitinib in Alopecia Areata: 24-Week Results," *Journal of the American Academy of Dermatology* 85, no. 2 (2021): 379–387, https://doi.org/10.1016/j.jaad.2021.03.050.

17. A. B. Kimball, E. Peeva, S. Forman, et al., "Brepocitinib, Zimlovisertib, and Ropsacitinib in Hidradenitis Suppurativa," *NEJM Evidence* 3, no. 3 (2024): EVIDoa2300155, https://doi.org/10.1056/EVIDoa2300155.

18. E. David, N. Shokrian, E. del Duca, et al., "A Phase 2a Trial of Brepocitinib for Cicatricial Alopecia," *Journal of the American Academy of Dermatology* 92 (2024): 427–434, https://doi.org/10.1016/j.jaad.2024.09.073.

19. C. Tehlirian, R. S. P. Singh, V. Pradhan, et al., "Oral Tyrosine Kinase 2 Inhibitor PF-06826647 Demonstrates Efficacy and an Acceptable Safety Profile in Participants With Moderate-To-Severe Plaque Psoriasis in a Phase 2b, Randomized, Double-Blind, Placebo-Controlled Study," *Journal of the American Academy of Dermatology* 87, no. 2 (2022): 333–342, https://doi.org/10.1016/j.jaad.2022.03.059.

20. P. Mease, P. Helliwell, P. Silwinska-Stanczyk, et al., "Efficacy and Safety of the TYK2/JAK1 Inhibitor Brepocitinib for Active Psoriatic Arthritis: A Phase IIb Randomized Controlled Trial," *Arthritis & Rheumatology* 75, no. 8 (2023): 1370–1380, https://doi.org/10.1002/art.42519.

ORIGINAL ARTICLE

Gamified Telerehabilitation in Oligoarticular Juvenile Idiopathic Arthritis: A Randomized Controlled, Single-Blind Trial

Gokce Leblebici[1] | Eylul Pinar Kısa[2] | Ela Tarakci[3] | Iremnur Gunhan[4] | Emine Nur Yenici[5] | Ozgur Kasapcopur[6]

[1]Division of Physiotherapy and Rehabilitation, Faculty of Health Science, Istanbul Medeniyet University, Istanbul, Turkey | [2]Department of Occupational Therapy, Istanbul Medipol University, Istanbul, Turkey | [3]Division of Physiotherapy and Rehabilitation, Faculty of Health Science, Istanbul University-Cerrahpasa, Istanbul, Turkey | [4]Department of Physiotherapy and Rehabilitation, Istanbul University-Cerrahpasa, Institute of Graduate Studies, Istanbul, Turkey | [5]Private Clinic, Istanbul, Turkey | [6]Cerrahpaşa Faculty of Medicine- Department of Pediatric Rheumatology, Istanbul University-Cerrahpasa, Istanbul, Turkey

Correspondence: Gokce Leblebici (leblebicigokce@gmail.com)

ABSTRACT

Introduction: This study aimed to investigate the effect of the 6-week gamified exercise program, delivered via telerehabilitation, on pain, kinesiophobia, quality of life, and mobility in children with oligoarticular juvenile arthritis (JIA).

Methods: Forty children with oligoarticular JIA (mean age: 11.86 ± 3.79 years) were randomly divided into two groups: Group I received game-based exercises via a telerehabilitation protocol, while Group II followed a home exercise program. The Wong Baker Pain Scale, Tampa Kinesiophobia Scale (TKS) and Pediatric Quality of Life Inventory (PedsQL) 3.0 Arthritis Module were completed by the patients. Patients' joint range of motion (ROM) and walking speed were measured by a blinded physiotherapist. The gamified exercises in the telerehabilitation program were supervised by another physiotherapist via WhatsApp video calls three times a week. Additionally, the exercise program was scheduled in the patients' calendars using Google Fit to provide reminders.

Results: There was a significant improvement in the ROM, walking speed, pain, kinesiophobia, and quality of life in the telerehabilitation group ($p < 0.05$). After the intervention, the telerehabilitation group showed greater improvements compared to the control group in hip and ankle ROM values, walking speed, and quality of life scores for ages 13–18 ($p < 0.05$).

Conclusion: The 6-week gamified telerehabilitation program reduced pain symptoms and kinesiophobia behaviors while improving the participants' quality of life and mobility.

Trial Registration: ClinicalTrials.gov NCT05837247

1 | Introduction

Juvenile idiopathic arthritis (JIA) is the most common rheumatic disease in childhood [1, 2]. Children with JIA often encounter issues such as pain, restricted mobility, morning stiffness, growth impairment, frequent hospital visits, decreased participation in activities, and school attendance problems [3]. Pain constitutes a significant component of the symptoms that contribute to disability

Summary

- A 6-week gamified telerehabilitation program may improve pain, ROM, walking speed, kinesiophobia, and quality of life in children with oligoarticular JIA.
- Gamified telerehabilitation has greater benefits compared to home exercises in improving joint ROM, walking speed, and quality of life.

and persistent outcomes in JIA [4]. Chronic pain in individuals with various etiologies may lead to the development of an avoidance behavior, known as kinesiophobia [5].

Mobility is critically important for people to preserve their functional independence, and research indicates higher morbidity and mortality rates in children with decreased mobility [6]. Regular physical activity and therapeutic exercises can help prevent and treat kinesiophobia [7].

Children with rheumatic diseases may have doubts about participating in standard physiotherapy programs that include stretching exercises, strength training, and joint range of motion exercises [8]. To address this, delivering a game-based exercise program that actively engages and interests the child can be beneficial [9].

Recently, telerehabilitation has gained popularity due to its ability to improve adherence, monitor development, apply treatment options through electronic communication, reduce post-discharge healthcare expenses, decrease home visits by physiotherapists, save time and costs related to travel, and reduce hospital stays [10].

The use of game-based telerehabilitation applications for therapeutic purposes has increased in chronically painful children. Game-based telerehabilitation applications, which involve repetitive and enjoyable performance of goal-oriented functional movements, are becoming increasingly popular, especially in the treatment of patients with chronic and long-term follow-up conditions [11]. Therefore, using game-based applications is a viable option to overcome kinesiophobia, alleviate pain, boost motivation, encourage movement, and provide an enjoyable rehabilitation program for children with chronic painful rheumatic conditions. However, while studies using play-based therapy and telerehabilitation within traditional physiotherapy in different pediatric diseases are common, these studies are relatively limited in children with JIA [12]. Therefore, this study aimed to investigate the effect of the 6-week gamified exercise program, delivered via telerehabilitation, on pain, kinesiophobia, quality of life, and mobility in children with oligoarticular JIA.

2 | Materials and Methods

2.1 | Patients

A total of 40 patients (11.86 ± 3.79 years) diagnosed with JIA from the Pediatric Rheumatology unit of Istanbul University-Cerrahpasa, Faculty of Medicine between March 2023 and December 2023 were included in this study. The participants were divided into two groups randomly using a sealed envelope;

the telerehabilitation group received game-based exercises via the telerehabilitation protocol, whereas the control group was followed with a home exercises program.

Inclusion criteria were as follows: having been diagnosed with oligoarticular JIA for at least 6 months ago according to ILAR criteria [13], suffering from pain in any lower extremity joint (hip, knee, ankle), being on stable doses of their routine pharmacological treatment, being between the ages of 6 and 16, and being able to understand games mentally. Since this age group of participants is more suitable for the gamified telerehabilitation method without disrupting their education programs and the commitment of older students preparing for national university exams, the upper limit was determined as 16 years. Participants with the following conditions were not included in the study: being diagnosed with any other orthopedic/neurological pathology; having another chronic disease; experiencing any exacerbation during the study. All patients and their parents were informed about the study, and written informed consent forms were obtained from patients and families.

The study was approved by the Ethics Committee of Istanbul University-Cerrahpasa (Number 2023/16) and was conducted in accordance with the Declaration of Helsinki.

2.2 | Sampling

Due to the unavailability of sufficient data and minimum clinically important change values for the outcomes of interest in pediatric rheumatologic patients, the sample size was determined considering the mean, standard deviation, and effect size of the quality-of-life parameter by using G Power. The PedsQL score was estimated using the data from the study of JIA patients by Varni et al. [14]. The minimal clinically important improvement was a reduction in score of 0.58. The sample size was determined as $n = 17$ for a 90% confidence interval. To account for possible dropouts, we planned to include at least 20 participants per group.

2.3 | Study Design

This study was designed as a single-center, single-blind randomized controlled study. A demographic information survey, Wong Baker Pain Scale, Tampa Kinesiophobia Scale, and Pediatric Quality of Life Inventory (PedsQL) Arthritis Module 3.0 were completed by the patients. Patients' joint range of motion was measured with an electronic goniometer, and mean walking speed was obtained during walking. All evaluations were conducted by a physiotherapist (IG) who was blinded to the interventions in a clinical setting before and after treatment. Another physiotherapist (ENY) supervised the exercise program. The patients continued their routine pharmacological treatments throughout the study.

Telerehabilitation program was followed via synchronous WhatsApp video calls. The exercise program was scheduled in the telerehabilitation group participants' calendars using Google Fit to provide reminders. The control group was followed with a home exercises program only.

The flowchart of the study was given in Figure 1.
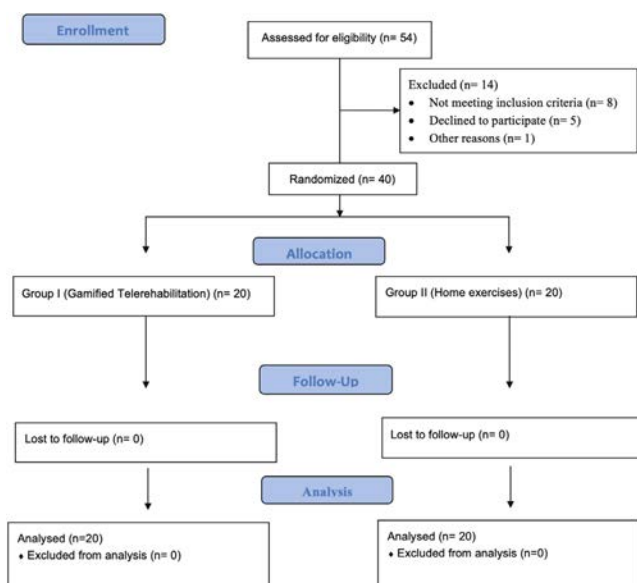
FIGURE 1 | The flow diagram of the study.

2.4 | Outcome Measures

2.4.1 | Range of Motion

Hip flexion/extension, hip internal/external rotation, hip abduction/adduction, knee flexion and extension, ankle dorsiflexion, and plantar flexion passive ranges of motion (pROM) were measured by goniometer [15].

2.4.2 | Mobility

Participants were asked to walk on the 25-m walkway at a speed that matched their own pace. Before testing, the participants walked for a minute on the walkway for familiarization. To record the walking speed data, Google Fit was used [16].

2.4.3 | Wong Baker Pain Scale

The Wong-Baker FACES Pain Rating Scale (WBS), used in children aged 3–18 years to rate pain severity, has been validated, mostly for chronic pain [17, 18]. There are 6 faces on the Wong-Baker Pain Scale. All the faces have a meaning. "Face 0 doesn't hurt at all." Face 2 hurts just a little. Face 4 hurts a little more. Face 6 hurts even more. Face 8 hurts a whole lot. Face 10 hurts as much as you can imagine, although you do not have to be crying to have this worst pain.

2.4.4 | Pediatric Quality-of-Life Inventory (PedsQL 3.0 Arthritis Module)

The PedsQL Measurement Model is a modular approach to measuring health-related quality of life (HRQOL) in healthy children and adolescents and those with acute and chronic health conditions. The PedsQL has demonstrated reliability, validity, sensitivity, and responsiveness for child self-report

for ages 5–18 years and parent proxy report for ages 2–18 years [19]. Each item is rated on a 5-point Likert scale, and the total score ranges from 0 to 100. Higher scores on the PedsQL Arthritis Module indicate a better quality of life and less disease impact on the child.

2.4.5 | Tampa Kinesiophobia Scale (TKS)

TKS is a 17-question scale that aims to hide the fear of movement and re-injury and is valid for various pediatric populations [20, 21]. A 4-point Likert scoring system is used in the scale, which contains parameters (1 = strongly disagree, 4 = completely agree) [22].

2.5 | Intervention

Exercises were gamified to motivate participants to exercise. A protocol was prepared based on various games in line with the needs of the participants [23]. A detailed description of the gamified exercises and the instructions given to the child are summarized in (Appendix 1). Among 15 different gamified exercises created for the general needs of children with lower extremity involvement, a structured game-based exercise program was created for each child with the minimum level of play that best suits the child's needs because of the initial evaluation for the telerehabilitation group.

Exercises were selected and taught to the child and his family in a clinical setting for telerehabilitation group. Additionally, ENY recorded videos of these exercises to create an archive (Figures 2 and 3). These videos were shared with the family to ensure they correctly remembered and performed the exercises at home.

The participants' sessions were monitored three times a week through telerehabilitation. The exercises were followed via synchronous Whatsapp video calls by ENY. Sessions were applied three times a week for 6 weeks, each session lasting 25–30 min.

For the control group, a structured home exercise program was planned for each participant with the minimum level of play that best suits the child's needs because of the initial evaluation. The home exercise program consisted of stretching, strengthening, weight-bearing, and proprioceptive exercises designed to reduce joint limitations and pain, increase functionality, and reduce limitation in daily life activities. A detailed description of the home exercises is summarized in (Appendix 2). The control group was asked to keep an exercise diary, and their records were checked by ENY at their evaluation 6 weeks later.

2.6 | Statistics

"Statistical Package for Social Sciences" (SPSS) Version 20.0 (SPSS inc., Chicago, IL, USA) statistical program was used and significance was determined in data analysis. The level was accepted as $p < 0.05$. The variables were described with
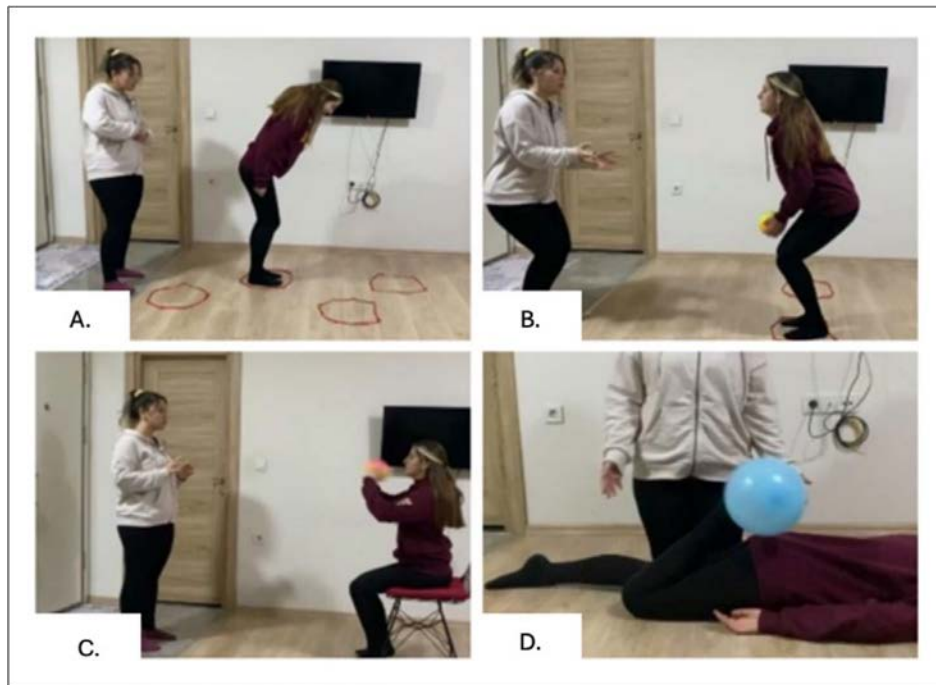
FIGURE 2 | Samples from Game-based exercises. (A) Grasshopper in circles; (B) Carrying watermelon; (C) Sit up and catch, sit down and catch; D, Squeezing the balloon.
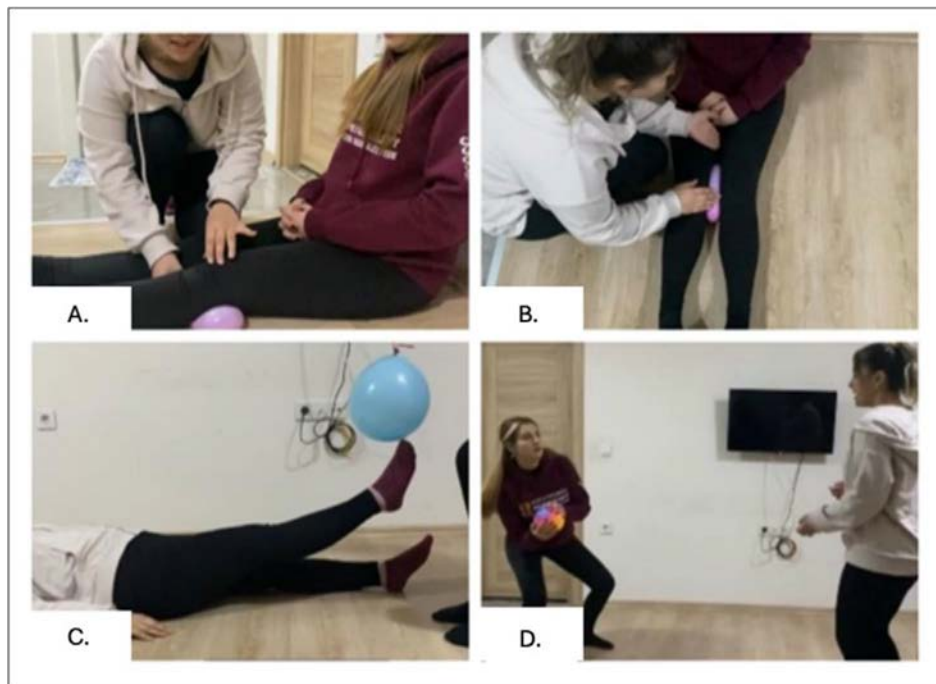
FIGURE 3 | Samples from Game-based exercises. (A) Squeezing the balloon under knee; (B) Squeezing the balloon between the legs; (C) Touch the balloon!; (D) Catch and swing.

mean (mean), standard deviation (SD), and percentage values. To compare the demographic and clinical characteristics of the study groups, Dependent Groups t test or Wilcoxon Signed-Rank test were employed. In comparisons between two independent groups, the Student's t test or Mann–Whitney U test was used according to the distribution of data. Cohen's d was used for effect size, interpreted as small (0.2), medium (0.5), and large (0.8) [24].

3 | Results

Forty children with oligoarticular JIA were included. The demographics and clinical features of the participants were given in Table 1.

After the intervention, there was a significant improvement in all the ROM values of the lower extremity compared to the

TABLE 1 | Demographics and the clinical characteristics of the participants.

	Telerehabilitation Group ($n = 20$) Mean $\pm$ SD (min–max)/n (%)	Control Group ($n = 20$) Mean $\pm$ SD (min–max)/n (%)	p
Age (years)	10.85 ± 3.89 (6–16)	12.87 ± 3.69 (6–16)	0.578
BMI (kg/m^2)	21.9 ± 2.18 (14.40–25.21)	21.8 ± 1.92 (16.51–25.17)	0.832
Disease duration (months)	78 ± 42.72 (12–144)	69 ± 40.77 (12–144)	0.656
Sex (n)			
Female	11 (55%)	13 (65%)	
Male	9 (45%)	7 (35%)	
Involved joints (n)			
Hip	2 (10%)	3 (15%)	
Knee	14 (70%)	14 (70%)	
Ankle	9 (45%)	7 (35%)	

Abbreviations: BMI, body mass index; kg, kilogram; m, meter; max, maximum; min, minimum; SD, standard deviation.

baseline evaluation in the telerehabilitation group ($p < 0.05$) (Table 2). In the control group, only knee flexion-extension and ankle dorsi-plantar flexion ROM values were increased ($p < 0.05$) (Table 2). After the intervention, hip and ankle ROM values improved more in the telerehabilitation group compared to the control group ($p < 0.05$) (Table 2).

The walking speed was significantly increased in the telerehabilitation group ($p < 0.001$) (Table 2).

Pain and kinesiophobia exhibited a significant decrease ($p = 0.001$; 0.001, respectively) in both groups (Table 2).

In terms of quality of life, PedsQL scores for ages 5–7 and PedsQL scores for ages 13–18 significantly decreased while PedsQL scores for ages 8–12 remained the same compared to the baseline after the intervention in the telerehabilitation group ($p = 0.063$) (Table 2). In the control group, only PedsQL scores for ages 5–7 were significantly decreased after the intervention, compared to the baseline ($p = 0.039$) (Table 2). Only in PedsQL scores for ages 13–18, the telerehabilitation group showed greater improvement compared to the control group ($p = 0.043$) (Table 2).

4 | Discussion

We aimed to investigate the effect of the gamified exercise program delivered via telerehabilitation on pain, kinesiophobia, quality of life, and mobility in children with oligoarticular JIA, and we found that the 6-week gamified telerehabilitation program reduced pain and kinesiophobia while improving the participants' quality of life and mobility.

Similar to our study, a telerehabilitation-based study in children with JIA investigated the effects of a 30-min tele-session exercise program twice a week for 2 weeks under the supervision of a pediatric physiotherapist [12]. They found that the telerehabilitation group performed the home exercise program significantly more often, for longer durations, and with less difficulty. Additionally, it was observed that the quality of life and functionality of the

participants increased, while pain decreased. This study serves as a good example of telerehabilitation implementations, as it demonstrated increased interest and motivation for exercise, as well as an improvement in quality of life, similar to our findings.

Previous telerehabilitation and home-based exercise studies conducted on children with JIA have reported a decrease in joint limitation and kinesiophobia and an increase in quality of life, parallel to our study [12, 23]. However, in these studies, exercises were generally applied in their traditional form, whereas in our study, these traditional exercises were gamified to enhance the child's participation in the program and promote sustainability. Stavrakidou et al. investigated the effects of a 12-week physiotherapy telerehabilitation program and reported significant improvements in pain reduction, functional ability, and quality of life, along with increased compliance with home-based exercises [12], similar to our results. A key distinction of our study is the incorporation of gamification, which not only maintained engagement but also significantly reduced kinesiophobia—an outcome not explicitly addressed in the Stavrakidou et al. study. Given that fear of movement can hinder participation in physical therapy, the use of interactive and game-based rehabilitation strategies may offer an effective approach to overcoming psychological barriers in children with JIA. These findings suggest that gamification can further enhance the benefits of telerehabilitation by promoting adherence and fostering a more enjoyable rehabilitation experience. Additionally, as previously mentioned [10], smartphone applications used for monitoring or motivating individuals to exercise can enhance patients' adherence to their exercise programs. In this study, the use of the Google Fit app likely facilitated the exercise process. Therefore, telerehabilitation programs incorporating gamified home exercises, as opposed to traditional exercises, can be effective and safely preferred for children with JIA.

The strength of this study lies in being the first to demonstrate that exercises applied through telerehabilitation, which have proven effective in children with JIA, are gamified and presented in the home environment. This gamified home exercise program has shown improvements in participants' mobility,

TABLE 2 | Comparison of the relevant parameters between the groups before and after treatment.

	Telerehabilitation group				Control group				Δ Grup I–II	
Outcomes	Baseline (n=20) Mean±SD	After treatment (n=20) Mean±SD	p	Effect size (Cohen's d)	Baseline (n=20) Mean±SD	After treatment (n=20) Mean±SD	p	Effect size (Cohen's d)	Z	p
Range of motion (°)										
Hip flexion	119.70±2.99	123.35±1.98	**<0.001**	1.22	115.61±3.19	117.66±2.75	0.124	0.68	2.371	**<0.001**
Hip extension	8.00±0.97	9.55±0.68	**<0.001**	1.59	8.10±0.92	8.57±1.09	0.120	0.46	1.073	**<0.001**
Hip internal rotation	41.90±1.65	43.90±1.21	**0.001**	1.21	40.93±1.15	41.95±2.04	0.721	0.61	1.162	**<0.001**
Hip external rotation	42.50±2,23	44.10±1.48	**<0.001**	0.71	41.69±1,24	41.44±2,20	0.765	0.13	1.410	**<0.001**
Hip abduction	42.35±1.53	44.40±1.23	**<0.001**	1.33	41.86±1.21	42.15±1.55	0.288	0.20	1.601	**<0.001**
Hip adduction	7.70±0.97	9.35±0.67	**<0.001**	1.70	7.01±0.98	8.02±0.34	0.210	1.37	2.508	**<0.001**
Knee flexion	130.30±9.06	135.50±8.14	**<0.001**	0.57	128.33±8.97	133.92±8.55	**<0.001**	0.63	0.188	0.187
Knee extension	−1.70±0.92	−0.15±0.48	**<0.001**	1.68	−1.71±1.12	−1.01±0.82	**0.041**	2.77	1.284	0.061
Ankle dorsiflexion	16.75±1.20	19.55±0.75	**<0.001**	2.33	17.85±1.10	18.75±0.20	**0.022**	1.13	1.465	**0.043**
Ankle plantarflexion	41.10±2.29	43.90±1.21	**<0.001**	1.22	40.20±2.19	41.90±2.33	**0.030**	0.75	1.077	**0.049**
Walking speed (km/h)	4.70±0.97	5.65±0.99	**<0.001**	0.96	4.79±1.18	4.65±1.02	0.862	0.12	0.994	**0.038**
Pain and Kinesiophobia										
Wong Baker	2.15±0.98	1.05±0.88	**0.001**	2.15	2.19±1.02	1.07±0.85	**0.001**	1.19	0.023	0.188
Tampa Kinesiophobia	40.55±9.01	33.55±9.29	**0.001**	0.77	41.14±8.98	34.15±8.30	**0.001**	0.80	0.068	0.282

(Continues)

TABLE 2 | (Continued)

Outcomes	Telerehabilitation group				Control group				Δ Grup I–II	
	Baseline (n = 20) Mean ± SD	After treatment (n = 20) Mean ± SD	p	Effect size (Cohen's d)	Baseline (n = 20) Mean ± SD	After treatment (n = 20) Mean ± SD	p	Effect size (Cohen's d)	Z	p
Quality of life										
PedsQL (5–7 ages) ($n_1 = 5$, $n_2 = 6$)	56.20 ± 20.17	32.80 ± 7.91	**0.043**	1.16	55.22 ± 21.19	30.75 ± 6.01	**0.039**	1.56	0.291	0.885
PedsQL (8–12 ages) ($n_1 = 7$, $n_2 = 9$)	51.14 ± 30.74	31.00 ± 22.74	0.063	0.65	50.98 ± 31.14	30.98 ± 25.14	0.062	0.70	0.000	0.676
PedsQL (13–18 ages) ($n_1 = 8$, $n_2 = 5$)	68.00 ± 16.52	41.00 ± 14.90	**0.012**	1.63	67.89 ± 15.92	45.60 ± 13.99	0.061	1.48	0.318	**0.043**

Abbreviations: h, hour; km, kilometer; PedsQL, Pediatric Quality of Life Inventory; SD, standard deviation. Bold values indicate statistical significance at $p < 0.05$.

---

kinesiophobia, and quality of life. Furthermore, the successful completion of the telerehabilitation program by all participants included in the study, without any dropouts, underscores the effectiveness of the gamified telerehabilitation program in terms of program adherence. Considering the 2016 Ottawa Panel guideline emphasizing the crucial role of home exercises in enhancing the quality of life and functionality in children with JIA, it is important to underscore the significance of the telerehabilitation program implemented in this study [25]. The gamified telerehabilitation program may increase treatment participation by gamifying home exercises.

5 | Limitations

In this study, a study design was initially proposed to compare pre- and post-treatment evaluations with comparing the home exercise group, aiming to reveal the pure effect of gamified exercises via telerehabilitation on pain, quality of life, kinesiophobia, and mobility. However, future studies should incorporate randomized controlled trials comparing telerehabilitation supported gamified exercises with telerehabilitation supported traditional exercise applications. Another limitation of this study is the inclusion of only a single subtype of JIA and the fact that it was conducted in a single center, which may limit the generalizability of the findings. Since the kinesiophobia scale is only valid for children aged 10–18 years, a valid and reliable kinesiophobia assessment is needed in the younger age group to evaluate the effect of gamified telerehabilitation on kinesiophobia. Additionally, future studies should include a larger number of participants and follow-up periods to better assess the efficacy of these interventions.

6 | Conclusion

The gamified telerehabilitation program effectively improves pain, kinesiophobia, functionality, and quality of life in children with JIA. By leveraging the interest of these children in gamified exercises as a treatment opportunity, it may encourage active participation in exercise programs, thereby reducing exercise-related kinesiophobia and enhancing quality of life. Our study has successfully implemented a gamified telerehabilitation program, demonstrating its effectiveness and offering an alternative treatment option for physiotherapists working in this field, alongside traditional physiotherapy methods.

University-Cerrahpasa (Number 2023/16) and was conducted in accordance with the Declaration of Helsinki.

Consent

All study participants provided informed consent.

Conflicts of Interest

The authors declare no conflicts of interest.

Data Availability Statement

The data that support the findings of this study are available from the corresponding author upon reasonable request.

References

1. R. Cimaz, "Systemic-Onset Juvenile Idiopathic Arthritis," *Autoimmunity Reviews* 15, no. 9 (2016): 931–934, https://doi.org/10.1016/j.autrev.2016.07.004.

2. L. N. Zaripova, A. Midgley, S. E. Christmas, M. W. Beresford, E. M. Baildam, and R. A. Oldershaw, "Juvenile Idiopathic Arthritis: From Aetiopathogenesis to Therapeutic Approaches," *Pediatric Rheumatology Online Journal* 19, no. 1 (2021): 135, https://doi.org/10.1186/s12969-021-00629-8.

3. B. Gudjonsdottir, S. A. Oskarsdottir, A. Kristjansdottir, et al., "Impact of Musculoskeletal Pain on Functioning and Disability in Children With Juvenile Idiopathic Arthritis in Iceland," *Physical & Occupational Therapy in Pediatrics* 44, no. 4 (2024): 554–571, https://doi.org/10.1080/01942638.2023.2299028.

4. J. Roelofs, J. K. Sluiter, M. H. Frings-Dresen, et al., "Fear of Movement and (Re)injury in Chronic Musculoskeletal Pain: Evidence for an Invariant Two-Factor Model of the Tampa Scale for Kinesiophobia Across Pain Diagnoses and Dutch, Swedish, and Canadian Samples," *Pain* 131, no. 1–2 (2007): 181–190, https://doi.org/10.1016/j.pain.2007.01.008.

5. L. U. Woolnough, L. Lentini, S. Sharififar, C. Chen, and H. K. Vincent, "The Relationships of Kinesiophobia and Physical Function and Physical Activity Level in Juvenile Idiopathic Arthritis," *Pediatric Rheumatology Online Journal* 20, no. 1 (2022): 73, https://doi.org/10.1186/s12969-022-00734-2.

6. M. Bordeleau, M. Vincenot, S. Lefevre, et al., "Treatments for Kinesiophobia in People With Chronic Pain: A Scoping Review," *Frontiers in Behavioral Neuroscience* 16 (2022): 933483, https://doi.org/10.3389/fnbeh.2022.933483.

7. B. Gualano, E. Bonfa, R. M. R. Pereira, and C. A. Silva, "Physical Activity for Paediatric Rheumatic Diseases: Standing Up Against Old Paradigms," *Nature Reviews Rheumatology* 13, no. 6 (2017): 368–379, https://doi.org/10.1038/nrrheum.2017.75.

8. E. Tarakci, E. P. Kisa, N. Arman, and A. Albayrak, "Physical Activity and Exercise in Patients With Pediatric Rheumatic Disease: A Systematic Search and Review," *Turkish Archives of Pediatrics* 56, no. 3 (2021): 179–186, https://doi.org/10.5152/TurkArchPediatr.2021.21034.

9. F. SUBAŞI, "Sağlıkta Dijitalleşme ve rehabilitasyon," *Turkiye Klinikleri Physiotherapy and Rehabilitation-Special Topics* 8, no. 3 (2022): 1–4.

10. J. C. Polese, G. S. EF, G. A. Ribeiro-Samora, et al., "Google Fit Smartphone Application or Gt3X Actigraph: Which Is Better for Detecting the Stepping Activity of Individuals With Stroke? A Validity Study," *Journal of Bodywork and Movement Therapies* 23, no. 3 (2019): 461–465, https://doi.org/10.1016/j.jbmt.2019.01.011.

11. M. Iosa, C. M. Verrelli, A. E. Gentile, M. Ruggieri, and A. Polizzi, "Gaming Technology for Pediatric Neurorehabilitation: A Systematic Review," *Frontiers in Pediatrics* 10 (2022): 775356, https://doi.org/10.3389/fped.2022.775356.

12. M. Stavrakidou, M. Trachana, A. Koutsonikoli, K. Spanidou, and A. Hristara-Papadopoulou, "The Impact of a Physiotherapy Tele-Rehabilitation Program on the Quality of Care for Children With Juvenile Idiopathic Arthritis," *Mediterranean Journal of Rheumatology* 34, no. 4 (2023): 443–453, https://doi.org/10.31138/mjr.310823.tio.

13. R. E. Petty, T. R. Southwood, P. Manners, et al., "International League of Associations for Rheumatology Classification of Juvenile Idiopathic Arthritis: Second Revision, Edmonton, 2001," *Journal of Rheumatology* 31, no. 2 (2004): 390–392.

14. J. W. Varni, M. Seid, T. Smith Knight, T. Burwinkle, J. Brown, and I. S. Szer, "The PedsQL in Pediatric Rheumatology: Reliability, Validity, and Responsiveness of the Pediatric Quality of Life Inventory Generic Core Scales and Rheumatology Module," *Arthritis and Rheumatism* 46, no. 3 (2002): 714–725, https://doi.org/10.1002/art.10095.

15. M. A. Watkins, D. L. Riddle, R. L. Lamb, and W. J. Personius, "Reliability of Goniometric Measurements and Visual Estimates of Knee Range of Motion Obtained in a Clinical Setting," *Physical Therapy* 71, no. 2 (1991): 90–96; discussion 96-7, https://doi.org/10.1093/ptj/71.2.90.

16. R. Y. C. Kwan, J. Y. W. Liu, D. Lee, C. Y. A. Tse, and P. H. Lee, "A Validation Study of the Use of Smartphones and Wrist-Worn ActiGraphs to Measure Physical Activity at Different Levels of Intensity and Step Rates in Older People," *Gait & Posture* 82 (2020): 306–312.

17. G. Garra, A. J. Singer, B. R. Taira, et al., "Validation of the Wong-Baker FACES Pain Rating Scale in Pediatric Emergency Department Patients," *Academic Emergency Medicine* 17, no. 1 (2010): 50–54, https://doi.org/10.1111/j.1553-2712.2009.00620.x.

18. A. Twycross, J. Stinson, W. Zempsky, and A. Jordan, *Managing Pain in Children and Young People: A Clinical Guide* (John Wiley & Sons, 2024).

19. J. W. Varni, T. M. Burwinkle, and M. Seid, "The PedsQL as a Pediatric Patient-Reported Outcome: Reliability and Validity of the PedsQL Measurement Model in 25,000 Children," *Expert Review of Pharmacoeconomics & Outcomes Research* 5, no. 6 (2005): 705–719.

20. D. A. White, W. R. Black, E. Cramer, et al., "Validity and Reliability of the Tampa Scale for Kinesiophobia for Adolescents With Heart Disease," *Medicine and Science in Sports and Exercise* 57 (2025): 1246–1256, https://doi.org/10.1249/MSS.0000000000003642.

21. D. L. Ye, I. Plante, M. Roy, J. A. Ouellet, and C. E. Ferland, "The Tampa Scale of Kinesiophobia: Structural Validation Among Adolescents With Idiopathic Scoliosis Undergoing Spinal Fusion Surgery," *Physical & Occupational Therapy in Pediatrics* 40, no. 5 (2020): 546–556, https://doi.org/10.1080/01942638.2020.1720054.

22. J. D. Weermeijer and A. Meulders, "Clinimetrics: Tampa Scale for Kinesiophobia," *Journal of Physiotherapy* 64, no. 2 (2018): 126, https://doi.org/10.1016/j.jphys.2018.01.001.

23. E. Tarakci, I. Yeldan, S. N. Baydogan, S. Olgar, and O. Kasapcopur, "Efficacy of a Land-Based Home Exercise Programme for Patients With Juvenile Idiopathic Arthritis: A Randomized, Controlled, Single-Blind Study," *Journal of Rehabilitation Medicine* 44, no. 11 (2012): 962–967, https://doi.org/10.2340/16501977-1051.

24. J. Cohen, *Statistical Power Analysis for the Behavioral Sciences*, 2nd ed. (Lawrence Erlbaum Associates, 1988).

25. M. White, J. N. Stinson, P. Lingley-Pottie, P. J. McGrath, N. Gill, and A. Vijenthira, "Exploring Therapeutic Alliance With an Internet-Based Self-Management Program With Brief Telephone Support for Youth With Arthritis: A Pilot Study," *Telemedicine and e-Health* 18, no. 4 (2012): 271–276, https://doi.org/10.1089/tmj.2011.0150.

A Detailed Description of the Gamified Exercises and the Instructions Given to the Child

Game-based exercise	Instructions	Targeted muscles	Dose
Grasshopper in circles 	The participant is asked to jump with both feet in the circles on the ground.	Lower extremity muscles, core muscles.	10 repetitions, 3 sets
Grasshopper single leg 	The participant is asked to jump with single leg in the circles on the ground. The exercise is repeated with the other leg.	Lower extremity muscles, core muscles.	10 repetitions, 1 set
Big and little grasshopper 	The participant is asked to jump with both feet in the circles on the ground. When the participant is stable in a circle, it is asked to be a big (stand up) and be a little (sit down).	Lower extremity muscles, core muscles.	10 repetitions, 3 sets

Game-based exercise	Instructions	Targeted muscles	Dose
Grasshopper in all directions 	The circles on the ground are placed in four directions as right, left, front and back. The participant is asked to jump with both feet in the circles on the ground.	Lower extremity muscles, core muscles.	10 repetitions for every direction, 1 set
Carrying watermelon 	The participant is asked to catch the oncoming ball and to squat by bending his knees while catching it, like carrying a watermelon. Afterward, he/she is asked to rise again and throw the ball across.	Core muscles, quadriceps femoris, hamstring muscles.	10 repetitions, 3 set
Carrying watermelon on heel and toe 	The participant is asked to catch the incoming ball while standing on his/her toes. Afterward, he/she is asked to rise again and throw the ball across. He/she is asked to do the same while standing on her heels.	Core muscles, quadriceps femoris, hamstring muscles, dorsi and plantar flexors.	10 repetitions, 3 set

Game-based exercise	Instructions	Targeted muscles	Dose

Game-based exercise	Instructions	Targeted muscles	Dose
Catch like a warrior!	The participant is asked to catch the oncoming ball with one foot in front and the other foot behind, in a warrior stance with knees bent, and to throw it back across.	Core muscles, quadriceps femoris, hamstring muscles, dorsi and plantar flexors.	10 repetitions, 3 set
Catch and swing!	The participant is asked to catch the oncoming ball and throw it back as if swinging by transferring weight to the right leg and to the left leg.	Core muscles, quadriceps femoris, hamstring muscles.	10 repetitions, 3 set
Sit up and catch, sit down and catch	The participant is asked to catch the oncoming ball and throw it back while sitting on the chair and getting up.	Core muscles, quadriceps femoris, hamstring muscles.	10 repetitions, 1 set
Cars under the bridge	The participant is asked to build a bridge by lifting his/her pelvis on the ground and to keep the bridge as vertical as possible while cars pass under the bridge and not to destroy the bridge.	Core muscles and gluteal muscles.	10 repetitions, 1 set

Game-based exercise	Instructions	Targeted muscles	Dose
Squeezing the balloon	The participant is asked to bend his/her knee while lying face down and press the balloon on her pelvis with her foot, but not to pop it.	Hamstring muscles	10 repetitions, 3 sets
Robe jumping	Two rows of ropes are stretched side by side with closed strip tires attached to the chair legs, and the participant is asked to jump left and right without touching these tires.	Lower extremity muscles, core muscles.	10 repetitions, 3 sets
Squeezing the balloon under knee	The participant is asked to compress the balloon under him/her knee by pressing it with him/her knee, but not to burst it. The same game is repeated with the other knee.	Quadriceps muscles.	10 repetitions, 1 set
Squeezing the balloon between the legs	The participant is asked to compress the balloon between him/her legs by pressing it with him/her knee, but not to burst it.	Hip adductor muscles.	10 repetitions, 3 sets

Game-based exercise	Instructions	Targeted muscles	Dose
Touch the balloon!	The participant is asked to touch the balloon held above with the tips of his/her toes while his/her leg is straight and lower his/her leg again. The same game is repeated with the other leg.	Hip flexor muscles.	10 repetitions, 1 set

Appendix 2

A Detailed Description of the Structured Home Exercises and the Instructions Given to the Child

Home exercises	Instructions	Targeted muscles	Dose
Hamstring stretch	Sit with legs extended, reach toward toes without straining.	Hamstring	10 repetitions, 1 set
Quadriceps stretch	Stand and pull one ankle toward the buttocks while holding onto a support.	Quadriceps	10 repetitions, 1 set
Seated leg lifts	Sit in a chair and lift legs one at a time to strengthen the quadriceps.	Quadriceps	10 repetitions, 3 sets
Bridging	Lie on the back, bend knees, and lift hips to strengthen the core and lower back.	Core muscles	10 repetitions, 3 sets
Mini squats	Stand with feet shoulder-width apart, bend knees slightly, and rise back up.	Lower extremity muscles.	10 repetitions, 3 sets
Walking on tiptoes and heels	Walk on your tiptoes for a few minutes, then walk on your heels.	Ankle dorsi and plantar flexors, intrinsic muscles of the foot.	3 sets
Standing on one leg	Stand on one leg and try to keep your balance.	Lower extremity muscles	10 repetitions, 3 sets
Ball toss during lunge	Catching and throwing a soft ball during mini squat.	Lower extremity muscles	10 repetitions, 3 sets
Step-ups	Step up onto a low platform or stair and step down.	Lower extremity muscles	10 repetitions, 3 sets
Jumping	Jump by lifting both feet off the ground and then stand on both feet again, maintaining your balance.	Lower extremity muscles	10 repetitions, 1 sets

ORIGINAL ARTICLE

Palmitoylation Dynamics in Systemic Lupus Erythematosus: Multi-Omics Insights and Potential Therapeutic Implications

Zeyu Liu[1] | Yanggang Hong[1] | Guo Hua[2] | Zixi Li[1] | Chunyan Hua[3] | Sheng Gao[4]

[1]The Second School of Medicine, Wenzhou Medical University, Zhejiang, China | [2]School of Ophthalmology & Optometry, School of Biomedical Engineering, Wenzhou Medical University, Zhejiang, China | [3]School of Basic Medical Sciences, Wenzhou Medical University, Zhejiang, China | [4]Laboratory Animal Center, Wenzhou Medical University, Zhejiang, China

Correspondence: Yanggang Hong (hongyanggang@wmu.edu.cn) | Chunyan Hua (huachunyan@wmu.edu.cn) | Sheng Gao (gaosheng@wmu.edu.cn)

ABSTRACT

Objective: Systemic lupus erythematosus (SLE) is a complex autoimmune disorder characterized by immune dysregulation. The role of palmitoylation in regulating immune responses and its contribution to SLE pathogenesis remains insufficiently understood.

Methods: We conducted a multi-omics analysis using the GSE61635 dataset to identify differentially expressed genes (DEGs) in SLE. Palmitoylation-related genes (PRGs) were identified through differential expression analysis, weighted gene co-expression network analysis (WGCNA), and machine learning models. Single-cell RNA sequencing (scRNA-seq) was used to assess immune cell dynamics, and Mendelian randomization (MR) was employed to explore causal relationships between metabolites and SLE.

Results: We identified 3946 DEGs and 13 key PRGs associated with palmitoylation in SLE. Four hub genes (ACSL1, ZDHHC12, GPX1, and DDHD2) were highlighted as potential biomarkers. Functional enrichment analysis revealed that these genes are involved in fatty acid metabolism and immune signaling. scRNA-seq analysis showed increased palmitoylation activity in neutrophils and cytotoxic T lymphocytes (CTLs) in SLE. MR analysis identified four phospholipids containing palmitic acid as causally linked to SLE.

Conclusion: This study identifies ACSL1 and ZDHHC12 as potential therapeutic targets for modulating palmitoylation and immune responses in SLE. Further research is required to validate these findings and explore their clinical implications for SLE treatment.

1 | Introduction

Systemic lupus erythematosus (SLE) is a chronic autoimmune disorder characterized by a profound disruption of immune tolerance, culminating in sustained inflammation and progressive multi-organ damage. This complex disease presents with a wide spectrum of clinical manifestations ranging from cutaneous lesions to life-threatening nephritis, driving a cascade of inflammatory responses that can amplify tissue damage and organ dysfunction [1]. Although the precise etiology of SLE remains elusive, its pathogenesis is thought to involve a complex interplay of genetic predisposition, environmental triggers, and aberrant immune cell function [2–4]. Despite significant advances in understanding the immunopathology of SLE, its heterogeneity and multifactorial etiology continue to pose challenges for accurate diagnosis and effective treatments.

Consequently, SLE remains one of the most challenging conditions faced by healthcare professionals, highlighting the critical need for early detection and targeted therapeutic strategies [5, 6].

In recent years, post-translational modifications (PTMs) have gained increasing attention for their role in regulating immune cell function. Among these, palmitoylation, the reversible attachment of palmitic acid to cysteine residues on proteins, has emerged as a pivotal mechanism influencing diverse cellular processes, including protein transport, membrane anchoring, and signal transduction. This modification is facilitated by DHHC protein acyltransferases, which can modify proteins in the Golgi apparatus, cytosol, or cell membrane [7, 8]. In the immune system, palmitoylation is essential for modulating critical signaling pathways, including STAT3, MYD88, and NOD1/2 signaling, which are crucial for immune cell activation and function [9]. Dysregulation of palmitoylation, particularly driven by altered activity of palmitoyl acyltransferases (PATs) and depalmitoylases (PPTs), has been implicated in aberrant immune responses, potentially contributing to the initiation and progression of autoimmune diseases like SLE. For instance, palmitoylation has been shown to regulate T cell receptor (TCR) signaling, B cell receptor (BCR) endocytosis, and the secretion of inflammatory cytokines. Notably, previous study suggests that DHHC3-mediated palmitoylation and PPT1-mediated depalmitoylation of TLR9 can influence its trafficking and activation, thereby impacting systemic autoimmunity [10]. Additionally, the STING pathway' dependence on palmitoylation for type I interferon production suggesting its potential role in SLE-related inflammation [10]. However, the precise mechanisms by which palmitoylation contributes to SLE remain poorly understood. Understanding how palmitoylation affects immune cell function in the context of SLE could unveil novel disease mechanisms and more effective therapeutic strategies. Given the potential implications of palmitoylation in SLE, a comprehensive investigation into palmitoylation-related genes (PRGs) and their regulatory mechanisms is warranted.

Our study employs multi-omics integration through machine-learning methods to investigate the role of palmitoylation in SLE and explore its potential for identifying novel therapeutic strategies. We identified differentially expressed PRGs between healthy individuals and SLE patients, analyzed gene expression patterns, and examined their correlations with immune cells. Furthermore, we constructed a transcription network to elucidate the relationships between PRGs and specific immune cell populations. Our findings offer novel insights into the intricate interplay among protein palmitoylation, immune dysregulation, and SLE pathogenesis, paving the way for more precise and effective treatments.

2 | Methods

2.1 | Data Acquisition and Preprocessing

The GSE61635 dataset was selected from the Gene Expression Omnibus database (GEO, http://www.ncbi.nlm.nih.gov/geo/) for its large sample size (30 healthy controls and 99 SLE samples), which provides robust statistical power for identifying disease-associated genes. Recent articles validate the accuracy of this dataset [11, 12]. The original expression matrices were normalized via the "limma" R package for subsequent analyses. Between-array normalization was performed using the normalizeBetweenArrays() function from the limma R package with default parameters (scaling arrays to have the same median absolute deviation) [13]. Box plots of our original and normalized expression matrices are provided in Figures S1A and S1B, respectively. We firstly performed a preliminary analysis of the expression matrix by the IOBR R package and obtained a series of significantly enriched pathways ($p < 0.0001$) (Figure S2A). From these, we focused on pathways related to palmitoylation, specifically fatty acid elongation and coenzyme A biosynthesis. We then obtained the associated genes for these pathways from the Gene Ontology (GO) database. Additionally, we obtained the genes related to palmitoylation through the Molecular Signatures Database (http://www.gsea-msigdb.org/gsea/index.jsp). Given that palmitic acid used for post-translational modification of proteins may be derived from the catabolism of triglycerides, we also included genes related to triglyceride metabolism through the GO database, which together form the set of genes we consider PRGs (Table S1).

2.2 | Differential Gene Expression Analysis

We normalized the data from GSE61635 using the "limma" package and obtained differentially expressed genes (DEGs) between SLE and control samples with thresholds of |log2 fold change (FC)| > 0.5 and adjusted P-value < 0.05. Subsequently, DEGs were visualized using volcano plots generated with the "ggplot2" package. Furthermore, a clustering heatmap illustrating the expression patterns of the top 50 DEGs was constructed using the "pheatmap" package.

2.3 | Weighted Gene Co-Expression Network Analysis (WGCNA)

WGCNA was performed to explore gene co-expression modules associated with SLE using the "WGCNA" package (version 1.73) on the GSE61635 [14, 15]. Initially, we conducted hierarchical clustering on all samples using the hclust function. Upon visual inspection of the sample dendrogram, no samples were deemed to be extreme outliers that would significantly affect the WGCNA analysis. Therefore, a cut-off height of 120 was not applied to exclude any samples, preserving all data points for a more inclusive analysis. Subsequently, a soft-thresholding power was determined to achieve a scale-free network topology. The similarity between genes was assessed to construct a phylogenetic tree, followed by module detection using a dynamic tree-cutting algorithm with a minimum module size of 100 genes. Furthermore, a univariate Cox proportional hazards regression analysis was performed for each module. All modules with an HR greater than 0.6 were considered to be associated with the SLE clinical trait.

2.4 | Acquisition of PR-DEGs and Functional Enrichment Analysis

The intersection genes of DEGs and PRGs were defined as palmitoylation-related differential expression genes (PR-DEGs). The overlap was in the Venn diagram generated with an online application (https://jvenn.toulouse.inra.fr/app/example.html) [16]. The chromosomal locations of these PR-DEGs were

mapped using RCircos (version 1.2.2). To elucidate the biological functions and pathways affected by the differentially expressed PRGs, functional enrichment analysis, including GO and Kyoto Encyclopedia of Genes and Genomes (KEGG) pathway analyses, was performed via the "clusterProfiler" package (version 4.12.6) with a significance threshold of adjusted P-value < 0.05. The "clusterProfiler" R package was utilized to evaluate the impact of PRGs on biological processes (BP), molecular functions (MF) and cellular components (CC). The results of these analyses were visualized using R packages such as "GOplot" and "ggplot2", providing insights into the biological role of PR-DEGs.

2.5 | Machine-Learning and Statistical Regression

To further filter the selected genes thus enhancing the precision of our findings, we employed two machine learning methods: Random Forest and Elastic Net Regression. In random forest analysis, we trained a model using 500 trees. This parameter was optimized through pre-experimental testing, which revealed that this value yielded lower error rates compared to the commonly used 1000 trees. On top of that, five repetitions of ten-fold cross-validation was conducted to ensure accuracy. Genes with importance scores greater than 1.5 were selected as our screening results. For Elastic Net Regression, an alpha of 1 would correspond to pure LASSO (L1) and an alpha of 0 to pure Ridge (L2). In order to optimize the regularization parameter α in elastic net regression, we generated 101 α values by cross-validation in the range of 0 to 1 in 0.01 steps and calculated the minimum cross-validation error corresponding to each α value. The α value with the lowest CV error ($\alpha = 0.23$) was finally selected as the optimal parameter, which balanced the L1 (LASSO) and L2 (Ridge) regularization penalties. Subsequently, after evaluating the Bias-Reduced Generalized Linear Model (BRGLM) and Bayesian Logistic Regression through calibration curves, these two statistical regression models were employed to further rank the machine learning screening results. The genes identified by both machine learning methods were considered critical genes.

2.6 | ROC Curve Analysis

Receiver operating characteristic (ROC) curve analysis evaluated the diagnostic capability of the hub gene-based model. The area under the ROC curve (AUC), which quantifies the model's ability to distinguish between SLE and control samples, was calculated. The model exhibiting the highest mean AUC was identified as the best-performing. The "pROC" R package (version 1.18.5) was used to generate ROC curves and compute AUC values with a 95% confidence interval (CI), using the DeLong method for statistical accuracy. External validation across GSE12374 and GSE50772 datasets confirmed generalizability, with ROC curves and AUC values calculated to assess predictive accuracy through the "pROC" R package.

2.7 | GSEA And Immune Cells Analysis

Single-gene gene set enrichment analysis (GSEA) was conducted to investigate the biological functions of four hub PR-DEGs and their interactions with the immune microenvironment via the

IOBR R package. We used the "c2.cp.v2023.2.Hs.symbols.gmt" gene sets from the Molecular Signatures Database to compute the enrichment scores and simulated enrichment scores. Adjusted P-values less than 0.05 were considered statistically significant. To characterize the immune microenvironment, the CIBERSORT algorithm was employed to estimate the proportions of 22 immune cells infiltrated in the SLE microenvironment [17]. While flow cytometry and scRNA-seq are gold standards for immune cell profiling, our study utilized bulk transcriptomic data (GSE61635) derived from peripheral blood mononuclear cells (PBMCs). CIBERSORT was selected for its ability to infer immune cell proportions from bulk RNA-seq data, enabling retrospective analysis of existing datasets and integration with transcriptome-wide differential expression and machine learning results. This approach allowed us to systematically correlate palmitoylation-related gene expression with immune cell dynamics across all samples in the cohort. Bulk deconvolution links ACSL1/ZDHHC12 to neutrophil infiltration, while scRNA-seq reveals elevated palmitoylation in SLE neutrophils and ACSL1 upregulation in cytotoxic T cells, demonstrating multi-scale immune dysregulation through palmitoylation-mediated mechanisms.

Spearman correlation analysis was subsequently conducted to assess the relationship between hub gene expression and immune cell abundance. Finally, single-sample GSEA (ssGSEA) was performed to analyze the infiltration of 24 immune cell types from the GSE61635 datasets [18]. Scatter plots illustrating the Spearman correlation between the expression of each of four hub PR-DEGs and the abundance of various immune cells were generated using the ggplot2 and ggExtra R packages. For each gene, significant correlations ($p < 0.05$) were visualized in individual scatter plots with marginal density distributions. A lollipop plot was created to summarize the correlation coefficients and their corresponding P-values.

2.8 | Single-Cell RNA-Sequencing Data Analysis

Single-cell RNA-sequencing data (GSE162577) from the GEO database, comprising PBMCs from healthy controls and SLE patients, were analyzed using the "Seurat" R package (version 5.1.0) [19]. The data preprocessing involved quality control, including filtering low-quality cells based on metrics such as nCount_RNA, nFeature_RNA and mitochondrial contamination. To achieve cell clustering, we used uniform manifold approximation and projection (UMAP) after principal component analysis (PCA) [20, 21]. Enrichment scores were calculated using AUCell and statistical significance was assessed via the Wilcoxon test. Differential analyses for immune cell subtypes were also performed using the Wilcoxon test, which evaluates the results of differential analyses for the GSEA palmitoylated gene set and key genes, demonstrating differential results in immune cell subtypes. Cell clusters were visualized using scatter plots, gene expression distributions were visualized using bubble plots and results of differential analysis of key gene is shown in violin plot.

2.9 | Construction of "TF-Gene" Networks

To construct transcription factor (TF)-gene networks, we first identified topologically credible TFs that tend to bind to our

four hub PR-DEGs genes using the JASPAR database [22]. Then, we utilized the online tool TF Target Finder web application (https://jingle.shinyapps.io/TF_Target_Finder/) to predict TF-target gene interactions. After retrieving the target gene lists for each TF, we then constructed the interaction networks. Subsequently, visualizations were generated using the same application.

2.10 | Identification of Causal Association Between Plasma Metabolites and SLE

Mendelian randomization (MR) is a statistical method that leverages genetic variants as instrumental variables (IVs) to infer causal relationships between exposures and outcomes, offering advantages over traditional observational studies by reducing confounding and reverse causation [23]. In this study, we executed MR analysis using the TwoSampleMR R package (version 0.6.6) [24]. Summary statistics of plasma metabolomics were acquired on the GWAS Catalog (https://www.ebi.ac.uk/gwas/) under the study accession numbers GCST90199621-GCST90201020, which included 1091 plasma metabolites and 309 metabolite ratios from 8299 European individuals [25]. SLE statistics (ebi-a-GCST003156) were obtained with the relatively largest number of cases from the IEU OpenGWAS platform (https://gwas.mrcieu.ac.uk/). Detailed information on selecting the criterion of IV was included in Supporting Information. Five MR methods, including inverse variance weighted (IVW), MR-Egger, weighted median, simple mode, and weighted mode, were conducted to assess the exposure-outcome relationship [26]. To validate our findings, sensitivity analyses were conducted for significant causal associations. We conducted MR-Egger intercept tests to evaluate horizontal pleiotropy and calculated Cochran's Q statistic using both the IVW method to assess heterogeneity [27]. Additionally, the leave-one-out method was employed, where each SNP was sequentially excluded to identify any SNPs with a significant influence on the overall results [28].

3 | Results

3.1 | Identification of Differentially Expressed Genes in SLE

The whole research design is provided in Figure 1. The original expression matrix was obtained and subsequently normalized using the "limma" R package based on box plots (Figure S1A,B), resulting in the expression matrix necessary for further analysis. Our analysis of GSE61635 revealed a multitude of significantly enriched pathways, which highlighted fatty acid elongation and coenzyme A biosynthesis as pivotal pathways linked to palmitoylation-related genetic elements (Figure S2A). We identified 3946 DEGs between control samples and SLE samples, comprising 1797 down-regulated genes and 2149 up-regulated genes (Figure S2B). Subsequently, we selected the 25 most significantly up-regulated and 25 most significantly down-regulated genes based on logFC. A heatmap was generated to visualize the results of the differential analysis (Figure S2C).

3.2 | Identification of Key Module Genes Associated With SLE

To identify key modules associated with SLE, WGCNA was applied. Sample clustering results revealed no outliers (Figure S3). In the analysis of scale-free fit index and mean connectivity for various soft-thresholding powers, we determined the optimal soft threshold to be 10, beyond which the scale-free fit index increased and signed R^2 approached the critical value of 0.7 (Figure S4A). Hierarchical clustering generated a gene dendrogram, from which a total of 6 modules were obtained using the Dynamic Tree Cut algorithm and similar merging techniques (Figure S4B). A heatmap revealed that the MEblack, MEgreen, MEpink, MEred, and MEgrey modules ($|cor| > 0.6$, $p < 0.05$) were significantly correlated with SLE status (Figure S4C). From these, a total of 2955 key genes associated with SLE were extracted for subsequent analysis, with their significance in relation to module membership plotted in the scatter plots (Figure S4D).

3.3 | Identification and Functional Enrichment Analysis of Key PR-DEGs

Key PR-DEGs were identified by intersecting the DEGs, key module genes, and PRGs (Figure 2A, Table S2). Intersecting DEGs, WGCNA modules, and PRGs prioritizes genes both differentially expressed and functionally linked to SLE pathogenesis, reducing false positives by excluding non-DEGs and irrelevant genes. This integration captures low-expression synergistic regulators missed by DEGs alone, validated in multi-omics studies [29].

Box plots were generated to illustrate the differences in gene expression between control and SLE groups (Figure 2B). Subsequently, chromosomal distribution of the identified genes revealed that they were spread across chromosomes (Figure 2C). To further investigate the functional roles of the PR-DEGs in SLE, functional enrichment analysis was performed. GO analysis revealed significant enrichment in pathways on BP, MF and CC (Figure 2D–G). Additionally, the KEGG analysis implied that these PR-DEGs were mainly enriched in the "Fatty acid metabolism" (Figure 2H).

3.4 | Evaluation of Four Hub Biomarkers via Machine Learning and Regression Model-Based Approaches

Elastic Net Regression (Figure 3A,B), which was chosen to simultaneously perform feature selection and prevent overfitting, prioritized 12 feature genes, including ZDHHC12, ABHD10, GPX1, DDHD2, LIPA, ACSL1, LPIN1, CPT1A, ELOVL4, GLUL, LYPLAL1, ZDHHC12. For the Random Forest classifier (Figure 3C,D), we filtered out 7 feature genes, including ZDHHC12, ABHD10, GPX1, DDHD2, LIPA, ACSL1, LPIN1. Correspondingly, the cross-referencing results from both algorithms highlighted seven core genes, including ZDHHC12, ABHD10, GPX1, DDHD2, LIPA, ACSL1, LPIN1 (Figure 3E, Table S3). To assess the reliability of our model, we constructed
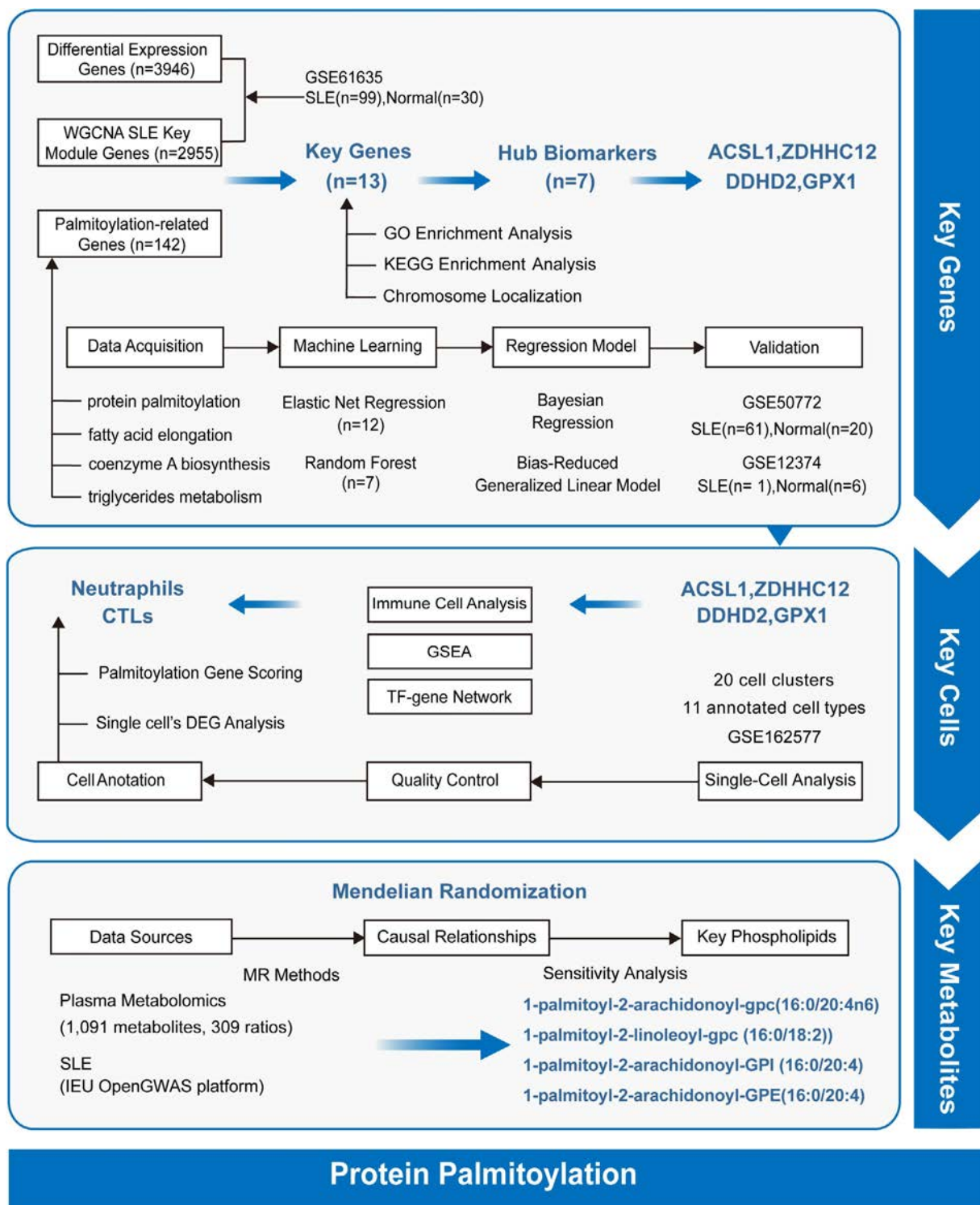
FIGURE 1 | The flow diagram of the research design.

a BayesGLM model and Bias-Reduced Generalized Linear Model (BRGLM) using these hub genes and generated a calibration plot (Figure S5A,B). Furthermore, we generated a key gene importance plot (Figure 3F) to visualize the contribution of each hub gene to the model, resulting in four prominent hub genes: ACSL1, DDHD2, GPX1, ZDHHC12. In external validation GSE61635, GSE50772 and GSE12374, these four genes showed strong diagnostic and predictive values for SLE with AUC values in aggregate greater than

or equal to 2.2, which were established as palmitoylation-related biomarkers for SLE (Figure 3G, Table S4).

3.5 | GSEA Analysis of Four Hub Biomarkers

To explore the roles of ZDHHC12, ACSL, GPX1 and DDHD2 in SLE pathogenesis, GSEA was performed for each biomarker.
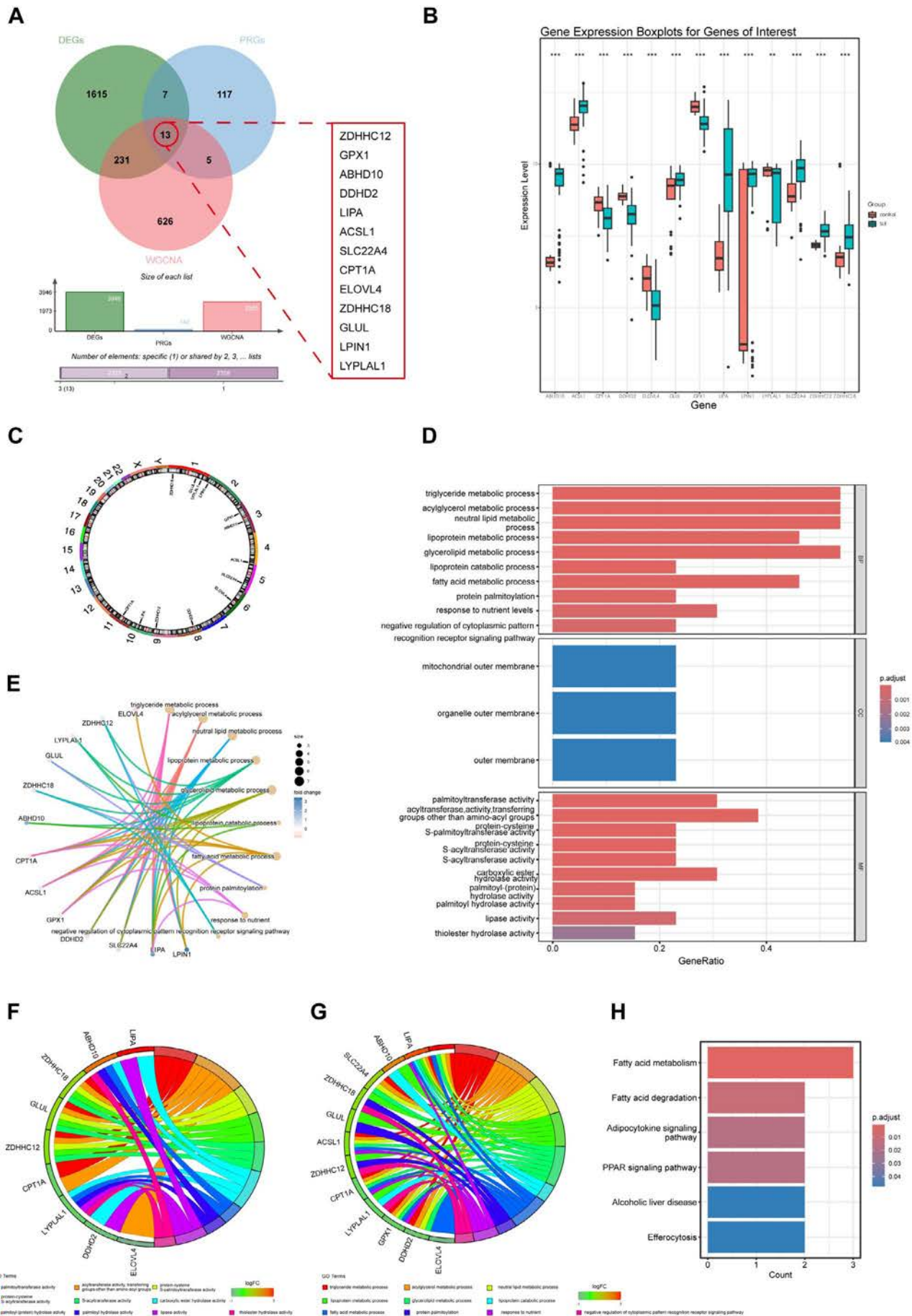
FIGURE 2 | Legend on next page.

FIGURE 2 | Identification and functional enrichment analysis of key palmitoylation-related DEGs. (A) Venn diagram showing 13 Key PR-DEGs in SLE that overlapped DEGs, key module genes, and PRGs. (B) Boxplot showing the 13 Key PR-DEGs. (C) Chromosome localization circles of Key PR-DEGs. (D–G) Barplot, Network plot and chord plots showing the GO enrichment analysis of 13 Key PR-DEGs. TOP10 GO results indicated that these Key PR-DEGs were principally involved in the "palmitoyltransferase activity", "triglyceride metabolic process". (H) Barplot showing the KEGG enrichment analysis of 13 Key PR-DEGs. Fatty acid metabolism was significantly enriched.

KEGG pathway enrichment revealed associations with multiple biological processes, including Toll-like receptor signaling pathway and leishmania infection (Figures S6A–D). Notably, the Toll-like receptor signaling pathway is considered to be a key pathway in the pathogenesis of SLE.

3.6 | The Role of Four Hub Biomarkers in SLE Immune Microenvironment

Given the close relationship between the pathophysiology of SLE and the immune microenvironment, the immune microenvironment in SLE was further explored. The expression abundance of 22 types of immune cells was analyzed (Figure 4A). Notably, 7 immune cell abundances differed significantly in SLE samples, including CD8$^+$ T cells, CD4$^+$ native T cells, resting NK cells, M2 Macrophages, activated Dendritic cells (DCs), resting Mast cells and Neutrophils. Red boxes indicate significantly increased immune cells ($p < 0.05$), while blue boxes indicate significantly decreased immune cells ($p < 0.05$) (Figure 4B). In particular, CD8$^+$ T cells were significantly downregulated, contrasting with the marked upregulation of neutrophils. To further validate and confirm our findings, we performed a dedicated immune infiltration analysis using the IOBR R package (Figure 4C). Subsequently, we analyzed the correlation between these four biomarkers (ZDHHC12, ACSL, GPX1 and DDHD2) and differential immune cells. A positive correlation was observed between neutrophil infiltration and expression levels of ACSL and ZDHHC12, further supporting the increased expression of ACSL1 and ZDHHC12 in SLE (Figure 4D,E). Conversely, a negative correlation was found between CD8$^+$ T cell infiltration and ACSL1, ZDHHC12 expression, while DDHD2 and GPX1 showed a positive correlation with CD8$^+$ T cells infiltration (Figure 4F,G).In addition, other immune cells predominantly consisting of CD8$^+$ T cells also exhibit a strong correlation with the four key biomarkers (Figures S7A–D).

3.7 | Transcription Factor and Molecular Networks Associated With Four Hub Biomarkers

We used the JASPAR database to analyze the transcription factors of four key genes (Figure S8A), in which FOXC1 and GATA2 were linked to three of the key genes filtered. FOXC1, as a transcription factor related to bone development [30], has been associated with the regulation of the autoimmune disorder rheumatoid arthritis [31], suggesting a potential regulatory role in SLE. GATA2, as an important hematopoietic transcription factor, regulates the proliferation and differentiation potential of hematopoietic stem cells and pluripotent progenitor cells [32, 33], which can regulate the differentiation direction of myeloid-derived suppressor cells (MDSCs) [34]. Under pathological conditions, GATA2 may lead to an increase in the number of monocyte myeloid-derived suppressor cells (M-MDSCs)and thus exacerbate SLE progression

[35]. We then mapped the PPI network (Figure S8B,C) for the two significantly upregulated genes (ACSL1 and ZDHHC12), which further showed a close link between these two genes and the enzymes involved in palmitoylation.

3.8 | Palmitoylation-Mediated Neutrophil and T Cells Engagement in SLE

The single-cell transcriptome sequencing analysis was conducted. We performed quality control, batch effect removal, and double cells removal on the single cell data (Figure S9A,B), followed by exclusion of cell cycle effects, dimensionality reduction, clustering, and cell annotation (Figures S9C–F). A total of 20 cell clusters were acquired and annotated into 11 cell types, encompassing Neutrophils, Cytotoxic T Lymphocytes (CTLs), M2 macrophages, Central Memory T cells (TCM), T helper cell 2 (Th2 cells), Naive B cells, NK cells, Eosinophils, Platelets, M1 macrophages, and Plasma cells (Figure 5A,B). Subsequently, we categorized cells according to sample source and scored them using the palmitoylation gene set obtained directly from the GSEA database (Table S1, Figure 5C–E). Notably, cells from SLE samples exhibited higher scores, implying that the probability of palmitoylation occurring in cells from SLE samples was higher than that of control samples, thereby validating the potential for palmitoylation in cells in the context of SLE.

To further explore the cells affected by protein palmitoylation modification, we performed differential analysis on each of the 11 immune cells separately and screened GSEA palmitoylation genes and previously singled out core genes from them (Figure 5F). Some palmitoylation-related genes were significantly down-regulated in neutrophils and plasma cells, whereas ACSL1 showed a significant up-regulation in a variety of immune cells, suggesting the important role of ACSL1 regulation in the pathologic process of SLE. For ACSL1, we show the results of the specific differential analysis of ACSL1 in five immune cells, suggesting a significant role of ACSL1 in T cells (Figure 5G).

3.9 | Causal Effects of Plasma Metabolites With Palmitic Acid on SLE

Based on the IVW method, the results suggested 88 causal relationships between plasma metabolomics and SLE ($p < 0.05$). Among these, four phospholipids containing palmitic acid were identified (Figure 6). The analysis showed that higher levels of 1-palmitoyl-2-arachidonoyl-GPE (16:0/20:4) are associated with an increased risk of SLE (OR = 1.120, 95% CI: 1.002–1.250, $p = 0.045$). Similarly, 1-palmitoyl-2-arachidonoyl-GPI (16:0/20:4) levels were strongly positively associated with SLE (OR = 1.383, 95% CI: 1.181–1.620, $p = 5.83E-05$). On the other hand, 1-palmitoyl-2-linoleoyl-GPC (16:0/18:2) levels showed a negative association (OR = 0.809, 95% CI: 0.710–0.923, $p = 0.0016$),
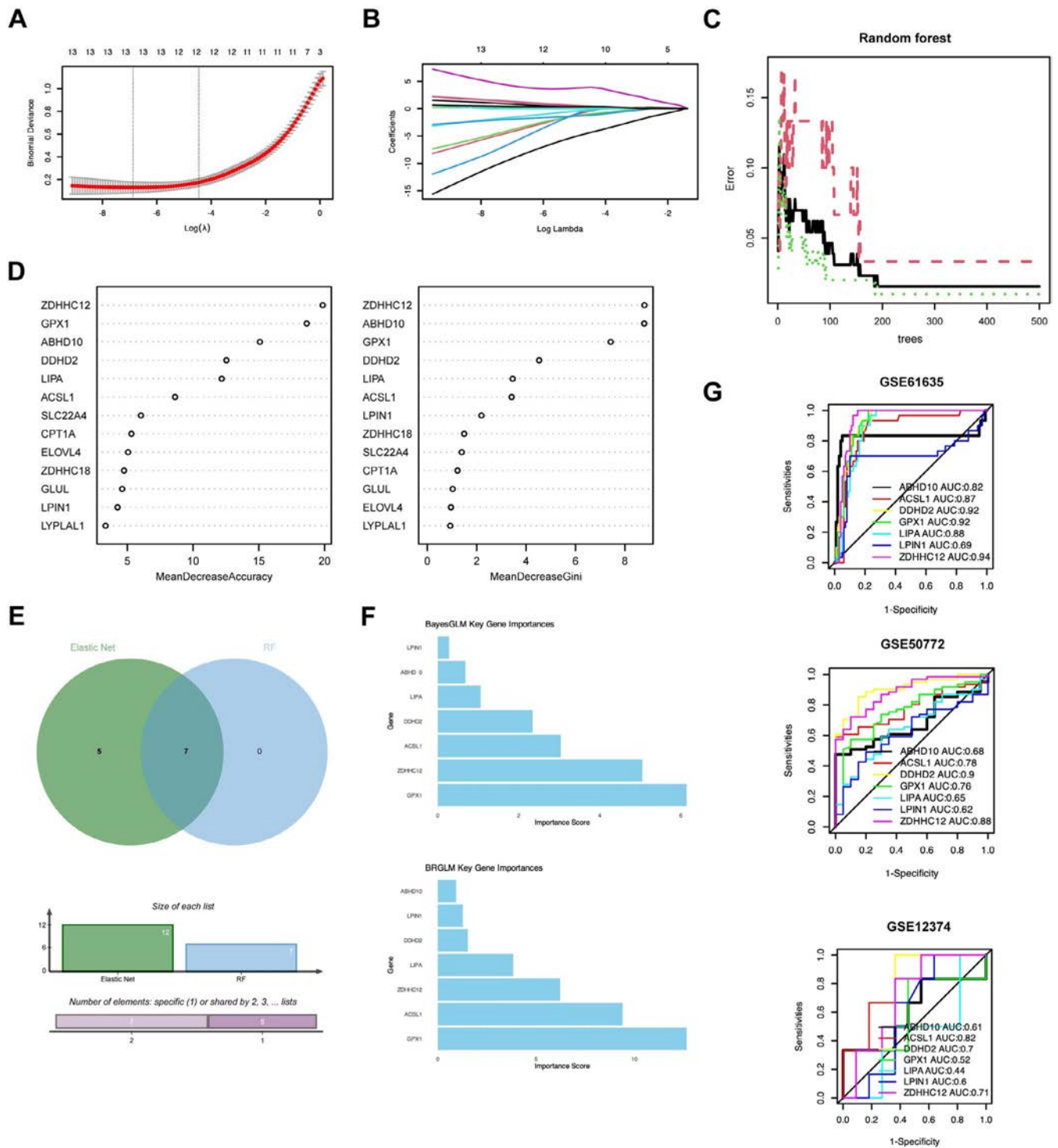
FIGURE 3 | Evaluation of four hub biomarkers via machine learning and regression model-based approaches. (A) Binomial Deviance Plot showing the binomial deviance as a function of the logarithm of lambda (λ). The red line represents the fitted values, and the gray shaded area indicates the confidence interval. (B) Coefficient Plot showing the coefficients of the model as a function of the logarithm of lambda (λ). Each colored line represents a different coefficient. (C) Random Forest performance plot shows the error rate of a random forest model as a function of the number of trees. The black solid line represents the out-of-bag (OOB) error, and the red dashed line represents the test set error. The green dotted lines represent the 95% confidence interval for the OOB error. (D) Mean Decrease Accuracy plot showing the mean decrease in accuracy for each feature when it is permuted. Mean Decrease Gini plot showing the mean decrease in Gini impurity for each feature. (E) Venn diagram identified 7 key PR-DEGs via the intersection of two machine-learning algorithms. (F) Gene importance plot showing the importance scores of key genes using the BayesGLM model and BRGLM model. (G) ROC curves of the 7 key genes in the training set and the external validation set. ACSL1, ZDHHC12, GPX1 and DDHD2 demonstrated strong diagnostic values for SLE in the external validation set.

FIGURE 4 | Legend on next page.

FIGURE 4 | The role of four hub biomarkers in SLE immune microenvironment. (A) Barplot showing the relative percentages of different immune cell subpopulations across multiple samples. (B) Violin Plot showing the proportions of different immune cell subpopulations in normal individuals and patients with SLE. (C) Boxplot showing the application of diverse immune infiltration methods for scoring SLE signatures in neutrophils and T cells. (D–G) Lolipop plots showing the correlation of 4 hub biomarkers with Various Immune Cell Subpopulations and scatter plots showing the correlation of 4 hub biomarkers expression with neutrophil abundance.
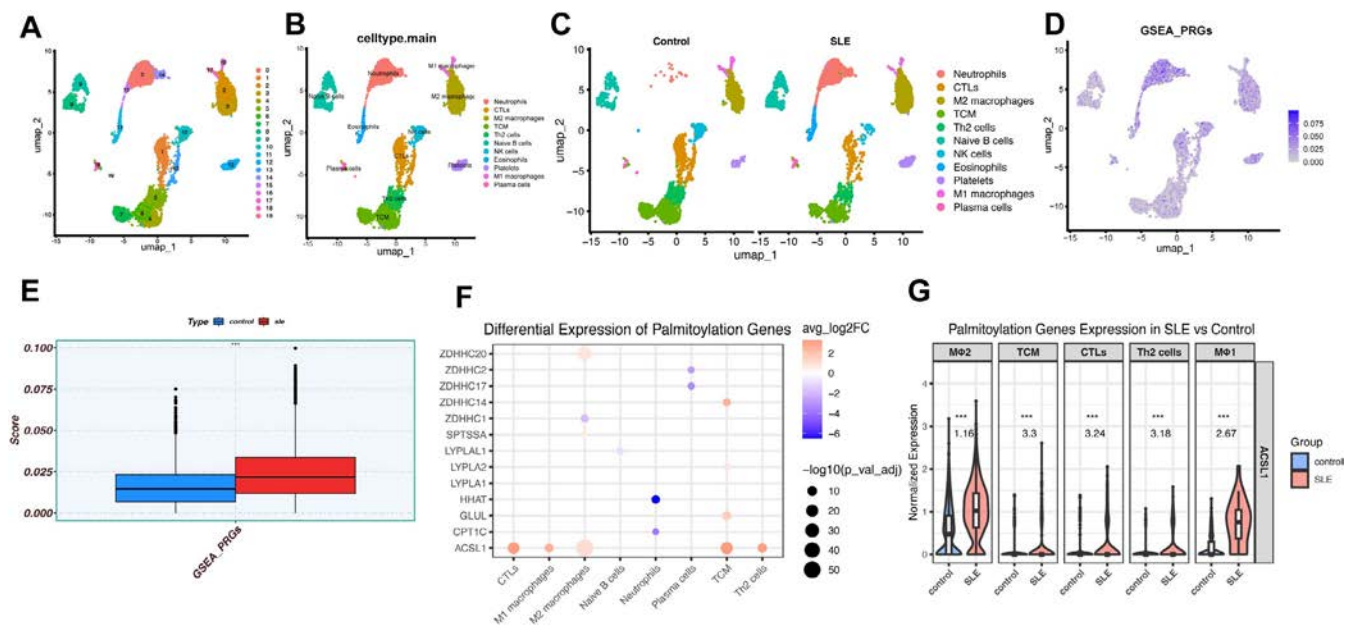
FIGURE 5 | Palmitoylation-mediated neutrophil and CTL engagement in SLE. (A) UMAP plot visualization of all cell clusters. (B) UMAP plot of 11 distinct cell types, the different cell clusters were annotated by the Seurat algorithm. (C) UMAP plot showing categories of cells between SLE groups and control groups. (D) UMAP plot of AUCell score of palmitoylation-related genes derived directly from GSEA database. (E) Boxplot showing the AUCell scores between SLE and normal. (F) Bubble plots showing expression levels of palmitoylated gene sets and key genes in different immune cells. (G) Violin plots show the differential expression of ACSL1 in five key immune cells, *** represents *P*-value less than 0.001, and the numbers below represent Log2 fold change.

FIGURE 6 | Causal effects of four plasma metabolites with palmitic acid on SLE.

4 | Discussion

The persistent clinical challenges in SLE underscore critical gaps in our understanding of its molecular triggers. While dysregulated crosstalk between innate and adaptive immunity forms the disease cornerstone [36], evidenced by aberrant

suggesting a protective effect against SLE. Additionally, 1-palmitoyl-2-arachidonoyl-GPC (16:0/20:4n6) levels were also positively associated with SLE (OR = 1.118, 95% CI: 1.017–1.229, $p = 0.021$). Sensitivity analyses supported these findings, as no evidence of horizontal pleiotropy or heterogeneity was detected, except for weak heterogeneity in 1-palmitoyl-2-arachidonoyl-GPE (16:0/20:4) (Table S5). Consistent trends across four additional MR models and stability in the leave-one-out analysis confirmed the robustness of these findings (Figure S10,11).

interferon signatures and autoantibody-mediated tissue injury [37], the dynamics of immune dysregulation remain mechanistically unclear. Recent studies have highlighted the critical role of PTM in modulating immune cell function [9], with particular attention to palmitoylation's emerging regulatory functions in lymphocyte signaling and antigen presentation. This lipid modification not only influences the subcellular localization of key signaling molecules, but also potentially drives the metabolic reprogramming observed in hyperactive immune cells.

Our multi-omics analysis identifies ACSL1 as the central regulator of palmitoylation dysregulation in SLE. Single-cell RNA sequencing reveals that ACSL1 is significantly upregulated in residual CD8$^+$ T cells, driving compensatory fatty acid oxidation (FAO) to sustain energy homeostasis, while GPX1 deficiency exacerbates oxidative stress, ultimately leading to CD8$^+$ T cell exhaustion and peripheral depletion. Concurrently, ACSL1

overexpression in macrophages and Th2 cells promotes M2 polarization and pro-inflammatory cytokine secretion, synergizing with neutrophil infiltration to amplify tissue damage. Mendelian randomization implicates palmitoylated phospholipids as causal mediators, fueling ACSL1-dependent palmitoyl-CoA synthesis and hyperactivation of STING/TLR pathways. ZDHHC12 acts as a palmitoyltransferase to assist in the process of protein palmitoylation, and down-regulation of DDHD2 leads to impaired phospholipid catabolism and exacerbates palmitic acid accumulation, while GPX1 defects trigger lipid peroxidation and destabilize palmitoylation, which further destabilizes lipid metabolism and forms a vicious "oxidation-inflammation" cycle.

The identified palmitoylation-related biomarkers (ACSL1, ZDHHC12) hold dual diagnostic and therapeutic potential. Elevated ACSL1/ZDHHC12 expression in CD8$^+$ T cells could serve as non-invasive biomarkers for SLE activity monitoring via routine PBMC profiling, particularly in early-stage or seronegative patients. Therapeutically, targeting ACSL1 (using inhibitors like Triacsin C) or ZDHHC12 (via RNAi/ small-molecule modulators) may normalize pathogenic palmitoylation in hyperactive neutrophils and restore CD8$^+$ T cell function, potentially reducing glucocorticoid dependence. Notably, the causal link between palmitoyl-containing phospholipids and SLE risk supports dietary interventions targeting lipid metabolism. Future clinical validation should focus on correlating biomarker levels with organ-specific involvement like lupus nephritis and testing repurposed metabolic agents like etomoxir in stratified patient cohorts.

Author Contributions

Zeyu Liu and Chunyan Hua conceived the study. Zeyu Liu, Yanggang Hong, and Chunyan Hua supervised the statistical analysis. Zeyu Liu and Yanggang Hong performed the data analysis. Zeyu Liu interpreted the results. Zeyu Liu, Yanggang Hong and Guo Hua wrote the first draft of the manuscript. Zeyu Liu and Zixi Li visualized the results. Yanggang Hong, Sheng Gao, and Chunyan Hua reviewed and edited the manuscript. The authors read and approved the final manuscript.

Acknowledgments

Consent

The authors have nothing to report.

Conflicts of Interest

The authors declare no conflicts of interest.

Data Availability Statement

The data that support the findings of this study are available from the corresponding author upon reasonable request.

References

1. C. Mohan, T. Zhang, and C. Putterman, "Pathogenic Cellular and Molecular Mediators in Lupus Nephritis," *Nature Reviews Nephrology* 19, no. 8 (2023): 491–508.

2. S. Almaani, A. Meara, and B. H. Rovin, "Update on Lupus Nephritis," *Clinical Journal of the American Society of Nephrology* 12, no. 5 (2017): 825–835.

3. Y. Hong, D. Wang, Y. Lin, et al., "Environmental Triggers and Future Risk of Developing Autoimmune Diseases: Molecular Mechanism and Network Toxicology Analysis of Bisphenol A," *Ecotoxicology and Environmental Safety* 288 (2024): 117352.

4. Y. Hong, W. Shu, X. Jiang, et al., "Prioritizing Endocrine-Disrupting Chemicals Targeting Systemic Lupus Erythematosus Genes via Mendelian Randomization and Colocalization Analyses," *Ecotoxicology and Environmental Safety* 295 (2025): 118126.

5. T. Dorner and R. Furie, "Novel Paradigms in Systemic Lupus Erythematosus," *Lancet* 393, no. 10188 (2019): 2344–2358.

6. Y. Hong, D. Wang, H. Qian, et al., "Exploring the Molecular Mechanism of Tripterygium Wilfordii Hook F in Treating Systemic Lupus Erythematosus via Network Pharmacology and Molecular Docking," *Clinical Rheumatology* 44, no. 4 (2025): 1549–1569.

7. Y. Zhang, Z. Qin, W. Sun, F. Chu, and F. Zhou, "Function of Protein S-Palmitoylation in Immunity and Immune-Related Diseases," *Frontiers in Immunology* 12 (2021): 661202.

8. T. Lanyon-Hogg, M. Faronato, R. A. Serwa, and E. W. Tate, "Dynamic Protein Acylation: New Substrates, Mechanisms, and Drug Targets," *Trends in Biochemical Sciences* 42, no. 7 (2017): 566–581.

9. J. Cai, J. Cui, and L. Wang, "S-Palmitoylation Regulates Innate Immune Signaling Pathways: Molecular Mechanisms and Targeted Therapies," *European Journal of Immunology* 53, no. 10 (2023): e2350476.

10. A. L. Hansen, G. J. Buchan, M. Ruhl, et al., "Nitro-Fatty Acids Are Formed in Response to Virus Infection and Are Potent Inhibitors of STING Palmitoylation and Signaling," *Proceedings of the National Academy of Sciences of the United States of America* 115, no. 33 (2018): E7768–E7775.

11. J. Yu, J. Yang, Q. He, Z. Zhang, and G. Xu, "Comprehensive Bioinformatics Analysis Reveals the Crosstalk Genes and Immune Relationship Between the Systemic Lupus Erythematosus and Venous Thromboembolism," *Frontiers in Immunology* 14 (2023): 1196064.

12. A. Hejrati, R. Maddah, S. Parvin, et al., "Evaluation of Genes and Molecular Pathways Common Between Diffuse Large B-Cell Lymphoma (DLBCL) and Systemic Lupus Erythematosus (SLE): A Systems Biology Approach," *Medical Journal of the Islamic Republic of Iran* 38 (2024): 129.

13. M. E. Ritchie, B. Phipson, D. Wu, et al., "Limma Powers Differential Expression Analyses for RNA-Sequencing and Microarray Studies," *Nucleic Acids Research* 43, no. 7 (2015): e47.

14. B. Zhang and S. Horvath, "A General Framework for Weighted Gene Co-Expression Network Analysis," *Statistical Applications in Genetics and Molecular Biology* 4 (2005).

15. P. Langfelder and S. Horvath, "WGCNA: An R Package for Weighted Correlation Network Analysis," *BMC Bioinformatics* 9 (2008): 559.

16. P. Bardou, J. Mariette, F. Escudie, C. Djemiel, and C. Klopp, "jvenn: an interactive Venn diagram viewer," *BMC Bioinformatics* 15, no. 1 (2014): 293.

17. A. M. Newman, C. L. Liu, M. R. Green, et al., "Robust Enumeration of Cell Subsets From Tissue Expression Profiles," *Nature Methods* 12, no. 5 (2015): 453–457.

18. A. Subramanian, P. Tamayo, V. K. Mootha, et al., "Gene Set Enrichment Analysis: A Knowledge-Based Approach for Interpreting Genome-Wide Expression Profiles," *Proceedings of the National Academy of Sciences of the United States of America* 102, no. 43 (2005): 15545–15550.

19. Y. Hao, T. Stuart, M. H. Kowalski, et al., "Dictionary Learning for Integrative, Multimodal and Scalable Single-Cell Analysis," *Nature Biotechnology* 42, no. 2 (2024): 293–304.

20. Y. Hong, D. Wang, Z. Liu, Y. Chen, Y. Wang, and J. Li, "Decoding Per- and Polyfluoroalkyl Substances (PFAS) in Hepatocellular Carcinoma: A Multi-Omics and Computational Toxicology Approach," *Journal of Translational Medicine* 23, no. 1 (2025): 504.

21. J. Li, N. Xu, L. Hu, et al., "Chaperonin Containing TCP1 Subunit 5 as a Novel Pan-Cancer Prognostic Biomarker for Tumor Stemness and Immunotherapy Response: Insights From Multi-Omics Data, Integrated Machine Learning, and Experimental Validation," *Cancer Immunology, Immunotherapy* 74, no. 7 (2025): 224.

22. I. Rauluseviciute, R. Riudavets-Puig, R. Blanc-Mathieu, et al., "JASPAR 2024: 20th Anniversary of the Open-Access Database of Transcription Factor Binding Profiles," *Nucleic Acids Research* 52, no. D1 (2024): D174–D182.

23. Y. Hong, Y. Wang, and W. Shu, "Deciphering the Genetic Underpinnings of Neuroticism: A Mendelian Randomization Study of Druggable Gene Targets," *Journal of Affective Disorders* 370 (2025): 147–158.

24. G. Hemani, J. Zheng, B. Elsworth, et al., "The MR-Base Platform Supports Systematic Causal Inference Across the Human Phenome," *eLife* 7 (2018): e34408.

25. Y. Chen, T. Lu, U. Pettersson-Kymmer, et al., "Genomic Atlas of the Plasma Metabolome Prioritizes Metabolites Implicated in Human Diseases," *Nature Genetics* 55, no. 1 (2023): 44–53.

26. Y. Hong and Y. Wang, "Causal Relationship Between Antibody-Mediated Immune Responses of *Chlamydia Trachomatis* Infection and Reproductive Tract Complications: A Bidirectional Mendelian Randomization Study," *American Journal of Reproductive Immunology* 93, no. 1 (2025): e70036.

27. M. F. Greco, C. Minelli, N. A. Sheehan, and J. R. Thompson, "Detecting Pleiotropy in Mendelian Randomisation Studies With Summary Data and a Continuous Outcome," *Statistics in Medicine* 34, no. 21 (2015): 2926–2940.

28. Y. Hong, J. Li, N. Xu, et al., "Integrative Genomic and Single-Cell Framework Identifies Druggable Targets for Colorectal Cancer Precision Therapy," *Frontiers in Immunology* 16 (2025): 1604154.

29. Z. Sun, Z. Gao, M. Xiang, et al., "Comprehensive Analysis of Lactate-Related Gene Profiles and Immune Characteristics in Lupus Nephritis," *Frontiers in Immunology* 15 (2024): 1329009.

30. A. Almubarak, Q. Zhang, C. H. Zhang, et al., "FOXC1 and FOXC2 Regulate Growth Plate Chondrocyte Maturation Towards Hypertrophy in the Embryonic Mouse Limb Skeleton," *Development (Cambridge, England)* 151, no. 16 (2024): dev202798.

31. Y. Wei, X. Huang, Y. Ma, and L. Dai, "FOXC1-Mediated TRIM22 Regulates the Excessive Proliferation and Inflammation of Fibroblast-Like Synoviocytes in Rheumatoid Arthritis via NF-kappaB Signaling Pathway," *Molecular Medicine Reports* 26, no. 4 (2022): 304.

32. E. H. Bresnick, M. M. Jung, and K. R. Katsumura, "Human GATA2 Mutations and Hematologic Disease: How Many Paths to Pathogenesis?," *Blood Advances* 4, no. 18 (2020): 4584–4592.

33. C. Koyunlar, E. Gioacchino, D. Vadgama, et al., "Gata2-Regulated Gfi1b Expression Controls Endothelial Programming During Endothelial-To-Hematopoietic Transition," *Blood Advances* 7, no. 10 (2023): 2082–2093.

34. K. Tomela, B. Pietrzak, L. Galus, et al., "Myeloid-Derived Suppressor Cells (MDSC) in Melanoma Patients Treated With Anti-PD-1 Immunotherapy," *Cells* 12, no. 5 (2023): 789.

35. L. Tan, W. Kong, K. Zhou, et al., "FoxO1 Deficiency in Monocytic Myeloid-Derived Suppressor Cells Exacerbates B Cell Dysfunction in Systemic Lupus Erythematosus," *Arthritis and Rheumatology* 77 (2024): 424–436.

36. S. Lazar and J. M. Kahlenberg, "Systemic Lupus Erythematosus: New Diagnostic and Therapeutic Approaches," *Annual Review of Medicine* 74 (2023): 339–352.

37. R. K. Perez, M. G. Gordon, M. Subramaniam, et al., "Single-Cell RNA-Seq Reveals Cell Type-Specific Molecular and Genetic Associations to Lupus," *Science* 376, no. 6589 (2022): eabf1970.

Supporting Information

Additional supporting information can be found online in the Supporting Information section.

WILEY

LETTER TO THE EDITOR

Endocarditis Presenting as Arthritis With Positive Autoantibodies Mimicking Rheumatoid Arthritis

C. A. Mansoor[1] ⬤ | Ayman H. K. Alserr[2] | Amal Ibrahim Abdel Latif Mohamed[1] | Hashim Ahmed Ba Wazir[3]

[1]Department of General Medicine, Sultan Qaboos Hospital, Salalah, Oman | [2]Department of Vascular Surgery, Sultan Qaboos Hospital, Salalah, Oman | [3]Department of Infectious Diseases, Sultan Qaboos Hospital, Salalah, Oman

Correspondence: C. A. Mansoor (drcamans@gmail.com)

Dear Editor,

Infective endocarditis (IE) can present with musculoskeletal symptoms, including arthritis, which may mimic autoimmune rheumatic diseases and often precede the diagnosis of IE, leading to misdiagnosis as inflammatory arthritis. We present a case of *Streptococcus mitis* IE presenting with arthritis, high rheumatoid factor (RF) and anti-cyclic citrullinated peptide (anti-CCP) antibodies mimicking rheumatoid arthritis (RA).

A 30-year-old male presented to the rheumatology outpatient department with a two-month history of bilateral knee and ankle pain with swelling. His investigations revealed elevated inflammatory markers, normocytic normochromic anemia with a high RF level and anti-CCP antibodies (48 U/ML). He was asked to review it in the outpatient department but did not follow up. Two weeks later, he presented to the emergency department with high-grade fever and left lower limb pain. He had no significant medical history, was not on any medications, and denied weight loss, sick contacts, or substance use. On examination, he was found to have high-grade fever, tachycardia, low blood pressure (90/50 mmHg), and weak pulsations over the left lower limb. The rest of the examination was normal.

Hemoglobin was 9.6 g/dL, total leukocyte count was 23 800/μl with neutrophilic predominance, platelet count was 103 000/L, erythrocyte sedimentation rate was 88 mm/h, and c-reactive protein was 113 mg per deciliter. Peripheral smear showed normocytic normochromic red blood cells with leucocytosis and thrombocytopenia without any abnormal cells. His urea was 20 mmol/L and creatinine was 341 mmol/L. Urine analysis showed 3–4 red blood cells per high-power field and fractional

excretion of sodium 1.5. Electrocardiogram showed sinus tachycardia; chest x-ray and ultrasonography of the abdomen were normal. Arterial Doppler showed reduced flow in the left lower limb arteries and a possible thrombus in the left external iliac artery. The patient was started on ceftriaxone, intravenous fluids, and noradrenaline after adequate fluid resuscitation.

Echocardiogram showed a large vegetation (19 mm X 23 mm) attached to the anterior mitral leaflet with severe mitral regurgitation and mild tricuspid regurgitation (Figure 1A,B). He was intubated and mechanically ventilated on the second day of admission due to pulmonary edema and was started on continuous venovenous hemodialysis for his renal failure. Computed tomography aortogram showed acute thrombotic occlusion of the left common iliac and external iliac arteries (Figure 1C,D). The patient underwent mitral valve replacement (Edwards perimount size 31 bioprosthesis) with removal of the vegetation and left iliac thrombectomy.

His repeated blood cultures and the tissue cultures (vegetation and iliac artery thrombus) were sterile. The 16S rRNA sequencing of the vegetation showed growth of *Streptococcus mitis* sensitive to ceftriaxone. The histopathology of the vegetation showed acute inflammatory exudates with plenty of bacterial colonies. He received ceftriaxone for 6 weeks along with aspirin and anticoagulation.

HIV, venereal disease research laboratory test, hepatitis B, and hepatitis C serology were negative. Autoantibody profiles, including antinuclear antibody, c-antineutrophil cytoplasmic antibody, and p-antineutrophil cytoplasmic antibody, were all

---
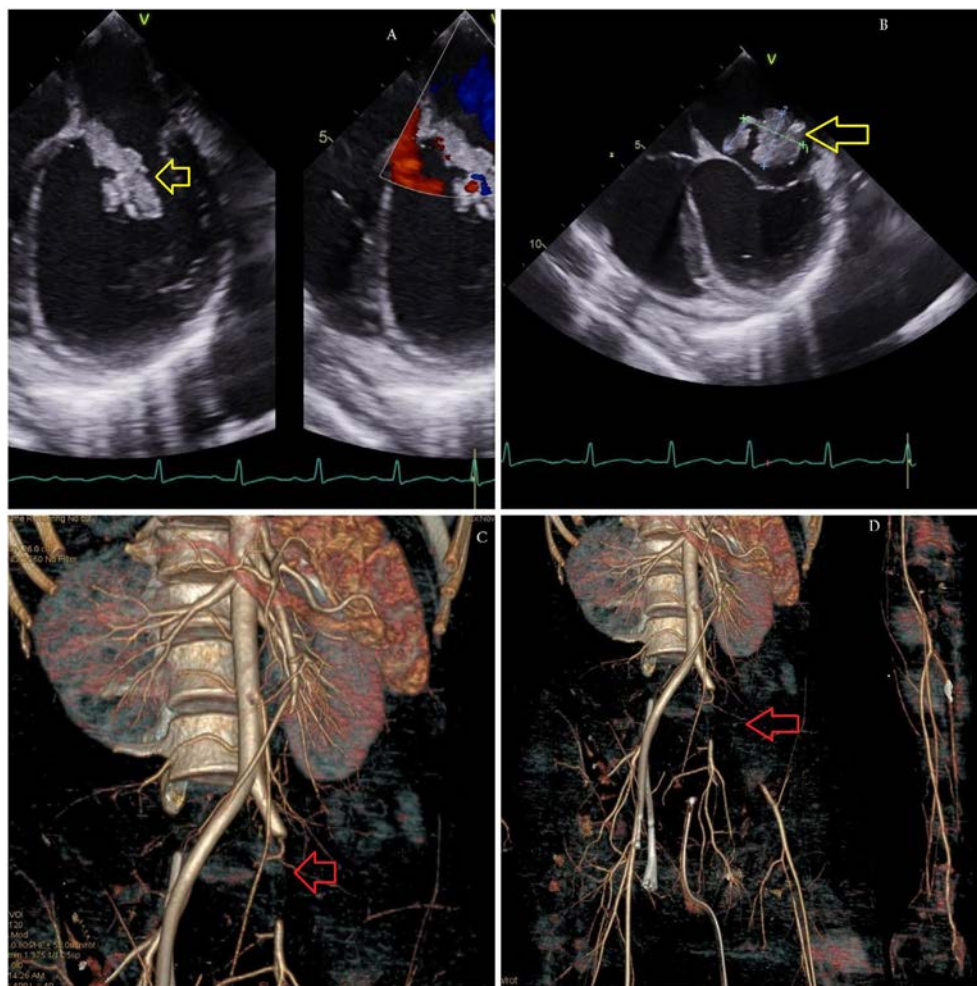
FIGURE 1 | Echocardiogram shows a large vegetation (19 mm × 23 mm) attached to the anterior mitral leaflet (yellow arrow, A, B). Computed tomography aortogram shows acute thrombotic occlusion of the left common iliac and external iliac arteries (red arrow, C, D).

negative. He improved clinically, and laboratory parameters normalized following treatment, and he was discharged after 6 weeks following the admission and followed up in the outpatient departments.

Rheumatic manifestations have been reported in more than 30% of patients with IE, often preceding this diagnosis by several months [1]. A Spanish study over a 12-year period of 100 patients with IE found peripheral arthritis in 13.6%, sacroiliitis in 0.9%, low back pain in 12.7%, and septic discitis in 1.8% of the cases [2].

A study by Gouriet and colleagues observed that RF levels were elevated in 36% of the definite IE cases, suggesting that the immune system's response to persistent infection can lead to the production of autoantibodies [3]. Another study by Bojalil et al. showed that 68% of patients with definite IE had elevated RF levels, 47% tested positive for antinuclear antibodies (ANA), and 58% had anticardiolipin/IgG antibodies [4]. One patient was found to have anti-CCP antibodies positive [4]. IE cases mimicking the clinical presentation of RA were reported previously [5]. RA can indeed present with cardiovascular manifestations that mimic IE, including severe aortic regurgitation and aortic root abscesses [6]. The clinical presentations of RA and IE can overlap, leading to diagnostic challenges.

The presence of anti-CCP antibodies in IE, though rare, may be explained by generalized autoimmune mechanisms commonly triggered by infections. Molecular mimicry and cross-reactivity, where microbial antigens resemble host proteins, are well-established processes that can lead to autoantibody production in various autoimmune diseases and are likely applicable to anti-CCP generation in the context of infection [7]. In both mechanisms, immune responses initially targeting microbial antigens may inadvertently recognize structurally similar self-antigens, leading to a breakdown in self-tolerance and the generation of pathogenic autoantibodies. Additionally, infection-induced citrullination has been demonstrated in studies on *Porphyromonas gingivalis*, where bacterial enzymes generate citrullinated proteins [8]. This mechanism has been studied primarily in RA but can provide a plausible link between infection and anti-CCP positivity. These processes may be further amplified by the pro-inflammatory milieu in IE, which facilitates the breakdown of tolerance and activation of autoreactive lymphocytes [9]. While the exact pathogenesis remains incompletely understood, these mechanisms suggest that infection can occasionally mimic autoimmunity not only clinically but also serologically.

Thromboembolism of the arteries in the extremities is uncommon, with an incidence of 4%–5% in patients with native valve endocarditis [10]. Common pathogens associated with these

embolic events include methicillin-resistant *Staphylococcus aureus* (MRSA), methicillin-susceptible *Staphylococcus aureus* (MSSA), and Candida species [10]. Our patient presented to the outpatient department with musculoskeletal complaints and positive autoantibodies and was later admitted with lower limb ischemia. He had negative blood cultures, and 16S rRNA sequencing of the vegetation identified *Streptococcus mitis*, a known cause of IE. He was successfully managed by both the medical and surgical teams.

Conclusions

The case described above is important for the following reasons:

1. Physicians should be aware of the rheumatological mimics of IE. Prompt diagnosis and appropriate treatment are crucial to prevent complications and improve patient outcomes.

2. Only one case of IE having positive anti-CCP antibodies was previously reported.

3. This case highlights the diagnostic challenge posed by IE presenting with musculoskeletal symptoms and elevated autoantibodies, which can mimic autoimmune rheumatic diseases like RA.

Consent

The authors certify that they have obtained all appropriate patient consent forms. In the form, the patient has given his consent for his images and other clinical information to be reported in the journal. The patient understands that his name and initials will not be published and due efforts will be made to conceal identity, but anonymity cannot be guaranteed.

Conflicts of Interest

The authors declare no conflicts of interest.

Data Availability Statement

Data sharing is not applicable to this article as no new data were created or analyzed in this study.

C. A. Mansoor
Ayman H. K. Alserr
Amal Ibrahim Abdel Latif Mohamed
Hashim Ahmed Ba Wazir

References

1. D. P. Misra, A. C. Chowdhury, S. Edavalath, et al., "Endocarditis: The Great Mimic of Rheumatic Diseases," *Tropical Doctor* 46, no. 4 (2016): 180–186.

2. C. A. González-Juanatey, M. A. González-Gay, J. Llorca, et al., "Rheumatic Manifestations of Infective Endocarditis in Non-Addicts: A 12-Year Study," *Medicine (Baltimore)* 80, no. 1 (2001): 9–19.

3. F. Gouriet, E. Botelho-Nevers, B. Coulibaly, et al., "Evaluation of Sedimentation Rate, Rheumatoid Factor, C-Reactive Protein, and Tumor Necrosis Factor for the Diagnosis of Infective Endocarditis," *Clinical and Vaccine Immunology* 13, no. 2 (2006): 301.

4. R. Bojalil, B. Mazón-González, J. R. Carrillo-Córdova, R. Springall, and L. M. Amezcua-Guerra, "Frequency and Clinical Significance of a Variety of Autoantibodies in Patients With Definite Infective Endocarditis," *Journal of Clinical Rheumatology* 18, no. 2 (2012): 67–70.

5. B. Peechakara, A. Kadam, M. Mewada, and A. Nakrani, "Infective Endocarditis Masquerading as Rheumatoid Arthritis," *Cureus* 11, no. 9 (2019): e5626.

6. F. Kyhl, R. V. Rasmussen, J. Lindhardsen, M. Smerup, and E. L. Fosbøl, "Rheumatoid Arthritis Mimicking Infective Endocarditis With Severe Aortic Regurgitation and Aortic Root Abscess: A Case Report," *European Heart Journal* 5, no. 1 (2021): ytaa561.

7. K. W. Wucherpfennig, "Mechanisms for the Induction of Autoimmunity by Infectious Agents," *Journal of Clinical Investigation* 108, no. 8 (2001): 1097–1104.

8. N. Wegner, K. Lundberg, A. Kinloch, et al., "Peptidylarginine Deiminase From *Porphyromonas Gingivalis* Citrullinates Human Fibrinogen and α-Enolase: Implications for Autoimmunity in Rheumatoid Arthritis," *Arthritis and Rheumatism* 62, no. 9 (2010): 2662–2672.

9. S. Rantapää-Dahlqvist, B. A. de Jong, E. Berglin, et al., "Antibodies Against Cyclic Citrullinated Peptide and IgA Rheumatoid Factor Predict the Development of Rheumatoid Arthritis," *Arthritis & Rheumatism* 48, no. 10 (2003): 2741–2749.

10. E. Sung, E. H. Awtry, D. J. Koh, et al., "Peripheral Vascular Emboli in Patients With Infective Endocarditis Are Common," *Journal of Vascular Surgery* 81, no. 6 (2025): 1450–1455.

International Journal of
Rheumatic Diseases

ORIGINAL ARTICLE

Incidence and Risk of Malignancy in Japanese Patients With Rheumatoid Arthritis in the National Database of Rheumatic Diseases in Japan (NinJa Database)

Toshihiro Matsui[1] | Aosa Kamezaki-Nakagawa[2,3] | Masato Hoshi[3] | Hiroshi Hirano[3] | Naonobu Sugiyama[3] | Toshitaka Hirano[3] | Miwa Enami[3] | Shigeyuki Toyoizumi[4] | Fujio Matsuyama[5] | Tatsunori Murata[5] | Yukitomo Urata[6] | Kimito Kawahata[7] | Shigeto Tohma[8]

[1]Department of Rheumatology Research, Clinical Research Center for Allergy and Rheumatology, National Hospital Organization Sagamihara National Hospital, Kanagawa, Japan | [2]RWE Platform, Chief Medical Affairs Office, Pfizer Inc., New York, New York, USA | [3]Medical Affairs, Pfizer Japan Inc., Tokyo, Japan | [4]Pfizer R&D Japan G.K, Tokyo, Japan | [5]CRECON Medical Assessment Inc., Tokyo, Japan | [6]Department of Rheumatology, Tsugaru General Hospital, United Municipalities of Tsugaru, Aomori, Japan | [7]Department of Rheumatology and Allergology, St. Marianna University School of Medicine, Kawasaki, Japan | [8]Department of Rheumatology, National Hospital Organization Tokyo National Hospital, Tokyo, Japan

Correspondence: Toshihiro Matsui (ninja02matsui@gmail.com)

ABSTRACT

Objective: The study aimed to evaluate the incidence rate and potential risk factors of malignancies in Japanese patients with rheumatoid arthritis (RA).

Methods: This retrospective observational study analyzed data of adult patients with RA from April 2013 to March 2019 using the NinJa database. Patients were categorized into the overall RA cohort and sub-cohorts: biologic disease-modifying antirheumatic drug (bDMARDs) or Janus kinase inhibitors (JAKi-s)-exposed, bDMARDs exposed, and bDMARDs or JAKi-s naïve conventional synthetic DMARDs exposed. The incidence of overall and each type of malignancy was calculated, and the associated risk factors were analyzed using multivariate logistic regression.

Results: Overall, 26 607 patients were included in the overall RA cohort (mean age: 64.16 ± 13.29 years; female: 78.87%) with 1018 malignancies. The incidence of malignancies was similar to that in the general population, with a standardized incidence ratio (SIR) of 0.97 (95% confidence interval [CI]: 0.91–1.03). It was consistent across the sub-cohorts and each year. The most frequent malignancies were lung cancer ($n = 158$), lymphoma ($n = 151$) and colorectal cancer ($n = 145$). The incidence of lymphoma and skin cancer was higher than the general population, with SIRs of 4.00 (3.39–4.68) and 1.70 (1.25–2.30), respectively. Multivariate analysis showed older age, male sex, smoking, Steinbrocker stage score 2 versus 1, 4 versus 1, and higher Disease Activity Score 28 using C-reactive protein as potential risk factors for malignancies.

Conclusion: Japanese patients with RA did not have an elevated risk of overall malignancies, whereas the incidence of lymphoma and skin cancer was higher in patients with RA than in the general population.

Rheumatoid arthritis (RA) is a chronic autoimmune disease primarily affecting joints, with a global prevalence of 0.46% [1]. In Japan, the prevalence of RA is estimated to be 0.6%–1% [2–4]. In patients with RA, malignancy has emerged as a challenging and unforeseen life-threatening complication [5, 6]. Several epidemiological studies have shown an association between RA and

---

Summary

- The incidence of malignancies from 2013 to 2018 was similar between patients with rheumatoid arthritis (RA) and the general population in Japan and that was consistent across the overall RA cohort and sub-cohorts.

- The incidence rates of lymphoma (standardized incidence ratio [SIR]: 4.00) and skin cancer (1.73) were higher in patients with RA versus the general population.

- Older age, male sex, smoking, and higher disease activity were potential risk factors for malignancies in patients with RA.

- Overall, this comprehensive research addresses the potential risk factors for malignancies and the incidence of malignancy types, which may be considered by Japanese physicians in the treatment of RA.

malignancies [7, 8], including site-specific malignancies [8–10]. The results of meta-analyses revealed a higher risk of lymphoma and lung cancer in patients with RA versus the general population, whereas that of colorectal and breast cancer is lower [9, 10]. However, studies from East Asian countries, including China, Taiwan, South Korea, and Japan, reported a similar risk of lung cancer in patients with RA versus the general population [11–13], suggesting regional and/or racial differences in malignancy risk in patients with RA.

RA treatment option, which has transformed significantly with the advent of new antirheumatic drugs over the past two decades, is also a factor that affects malignancy risk [14]. Current treatment options for RA include conventional synthetic disease-modifying antirheumatic drugs (csDMARDs), biologic DMARDs (bDMARDs), and targeted synthetic DMARDs such as Janus kinase inhibitors (JAKi-s) [15]. These treatments modify different immunological pathways involved in the pathogenesis of RA to alleviate symptoms; however, this may increase malignancy risk [9]. A meta-analysis (22 studies; 371 311 patients with RA) assessing the association of DMARDs use with malignancies found that patients on csDMARDs had a 1.15-fold risk of overall cancer, while patients on bDMARDs had a 0.91-fold risk versus the general population. Additionally, patients treated with csDMARDs exhibited a 1.77-fold risk of lung cancer and a 2.15-fold risk of lymphoma versus the general population [16]. Furthermore, evidence showed that treatment with tumor necrosis factor inhibitor (TNFi) increases the risk of skin cancer, including melanoma [17, 18].

Overall, malignancy risk in patients with RA could vary by regional and/or racial features and treatment options. A post-marketing surveillance study of tofacitinib in Japan (July 2013–December 2018) reported malignancy incidences in patients with RA treated with JAKi-s [19], which highlighted an increased need for an update on malignancy risk in Japanese patients with RA in the JAKi-s era. Additionally, there has been limited comprehensive research addressing potential risk factors for malignancies and the incidence of individual cancer types in Japanese patients with RA, which could provide valuable insights for

Japanese physicians treating RA. Therefore, we conducted a study to evaluate the incidences and potential risk factors of malignancies in patients with RA using the NinJa registry from April 2013 to March 2019.

1 | Patients and Methods

1.1 | Study Design

In this retrospective observational study, we analyzed the data of patients with RA (from April 2013 to March 2019) from the NinJa database to assess the incidence and risk factors of malignancies. The NinJa data from April 2012 to March 2018 were utilized to determine the baseline characteristics; data of patients with a cancer diagnosis in 2012 were excluded from the analysis.

1.2 | Data Source

Data were collected from the NinJa registry, a nationwide, multicenter, observational database of patients with RA, which was established in 2002 [20]. The registry is supported by grants from the Ministry of Health, Labour and Welfare of the Japanese Government and the National Hospital Organization. Currently, the NinJa registry includes clinical data from >50 facilities across Japan, including hospitals belonging to the National Hospital Organization, university hospitals, public hospitals, city hospitals, and private clinics.

The NinJa registry collects data on >15000 patients/year, representing approximately 2% of patients with RA in Japan. Of these, about 85%–90% have been followed up continuously for 1 year after registration. All registered patients were diagnosed with RA per standard diagnostic criteria (including American College of Rheumatology [ACR]) by their individual physicians [21, 22]. Data from all patients, accumulated from both existing and newly registered patients, are collected every fiscal year (from April of the current year to March of the following year) as part of an open prospective cohort registry.

The registry includes individual patient-level information on patient background (e.g., date of birth, sex, date of RA onset, attending physician, and last consultation date), RA treatment information (e.g., Disease Activity Score 28 [DAS28], Simplified Disease Activity Index [SDAI], Clinical Disease Activity Index [CDAI], Hospital Anxiety and Depression Scale [HADS], antirheumatic drug use, and surgery details), quality-of-life measures (e.g., Health Assessment Questionnaire Disability Index [HAQ-DI]), and comorbidities or adverse events since 2002, with annual updates. Each patient is tracked using a unique identifier for as long as they continue treatment (inpatient or outpatient) at the same hospital.

1.3 | Study Cohorts

The study included patients with RA aged ≥ 18 years at the index year, with a recorded diagnosis of RA and no definitive diagnosis record of psoriasis in the hospital-based NinJa database. The

RA cohort included patients who received any treatment for RA. Furthermore, patients with RA were categorized into different sub-cohorts based on the types of treatments received: the bDMARDs or JAKi-s-exposed sub-cohort (bio or JAKi-s-exposed) included patients who received ≥ 1 bDMARDs (adalimumab, certolizumab pegol, etanercept, golimumab, infliximab, abatacept, or tocilizumab) or JAKi-s (tofacitinib and baricitinib); the bDMARDs-exposed sub-cohort (bio-exposed) included patients who received ≥ 1 bDMARDs; and the bDMARDs or JAKi-s naïve csDMARDs-exposed sub-cohort (bio or JAKi-s naïve csDMARDs-exposed) included patients who received ≥ 1 csDMARDs (auranofin, bucillamine, iguratimod, leflunomide, MTX, mizoribine, D-penicillamine, salazosulfapyridine, sodium aurothiomalate, or tacrolimus monohydrate) but none of the bDMARDs or JAKi-s. Patients who had malignancies before the index year were excluded from the study.

1.4 | Study Follow-Up

For each RA cohort, the index year was the year in which the relevant treatment data were first recorded in the NinJa database. The earliest and last index years were 2013 and 2018, respectively. A 1-year baseline period before the index date was used to obtain baseline information for covariates. The follow-up for each RA cohort began in the index year. The end of follow-up was the earliest year of the first occurrence of the outcomes of interest, the end of the study period (March 2019), withdrawal from the NinJa database, or loss to follow-up, whichever occurred first.

As the NinJa database provides data at annual intervals, the exact start date for initiation of each treatment of interest cannot be captured. Therefore, follow-up periods were calculated using four patterns: one primary pattern and three other patterns to assess the sensitivity of the follow-up period definitions. The follow-up patterns were based on three criteria: the estimated exposure period in the index year (start of follow-up), occurrence of malignancy within a year (earliest year of event occurrence), and end of the year (final year of the patient's record; Figure S1). Based on discussions with the NinJa registry investigators and advisory board members, the primary pattern was deemed the most appropriate for estimating the follow-up period, considering an annual data entry into the NinJa database, which was conducted retrospectively from medical records. In this pattern, follow-up began at the start of the year (April 1) and ended either at mid-year (September 30) if malignancy was present or at the end of the year (March 31) if malignancy was absent. The other patterns were used for sensitivity analyses.

1.5 | Study Outcomes and Assessments

For each RA cohort, demographics (age and sex) and clinical characteristics were obtained during the baseline period (1 year pre-index). Clinical characteristics included RA severity (mild: DAS28 < 3.2; moderate: DAS28 ≥ 3.2 to ≤ 5.1; and severe: DAS28 > 5.1) during the baseline period; any orthopedic surgeries (excluding cancer-related surgeries); and concomitant drug use (MTX mean dosage, mg/week: ≤ 8 and > 8, NSAIDs use) before inclusion in the NinJa database till the index date.

Data on the study endpoint, the occurrence of malignancy, were collected based on physician declarations, by reference to medical records or referral letters. The study also assessed the risk factors associated with malignancy incidence. As malignant lymphoma affects RA treatment, we further analyzed the risk factors for the occurrence of lymphoma.

1.6 | Statistical Analysis

The longitudinal and cross-sectional incidences of malignancies between 2013 and 2018 were calculated as crude incidence rates (IRs) and age- and sex-adjusted standardized rates (ASRs) for each RA cohort. Person-time was calculated by summing the number of enrolled years between the index date and end of the follow-up period. Longitudinal cumulative IRs of malignancies were calculated by dividing the number of patients with events by total patient-years of observation in each RA cohort. Cross-sectional IRs of malignancies, at each calendar year, were calculated by dividing the number of patients with events by the total number of patients in that year for each RA cohort. These IRs were reported as estimated rates per 100 patient-years of follow-up, with 95% CIs.

The longitudinal cumulative IRs and cross-sectional IRs of malignancies in each RA cohort were compared with those in the Japanese general population; SIRs with 95% CIs were calculated for malignancy incidence. Data for the Japanese general population were obtained from a Japanese population database of malignancy incidence provided by the Center for Cancer Control and Information Services and the National Cancer Center (NCC), Japan [23]. SIRs were calculated for the duration of 2013–2018, adjusted by age and sex as well as ASR, comparing each RA cohort from the NinJa data and using the NCC data as reference. As the NCC data for 2018 were unavailable, data from 2017 were extrapolated.

To adjust the longitudinal cumulative IRs and cross-sectional IRs of malignancies in each RA cohort for the key prognostic factors of age and sex, ASRs per 100 patient-years with 95% CIs were calculated. The reference population was the Japanese general population, as provided by NCC. The incidence of each type of malignancy was calculated as IR, SIR, and ASR for malignancies with > 10 confirmed events reported within the overall RA cohort and sub-cohorts.

Additionally, exploratory analyses were conducted to evaluate risk factors for the development of malignancies using univariate and multivariate logistic regression analyses. The model predictors included age, RA duration, Steinbrocker stage score, global functional status, DAS28 using erythrocyte sedimentation rate (DAS28-ESR) or C-reactive protein (DAS28-CRP), CDAI, SDAI, sex, body mass index, glucocorticoid use, MTX use, JAKi-s use, calcineurin inhibitor use (including tacrolimus and cyclosporine), other immunosuppressant use (including azathioprine, mizoribine, and cyclophosphamide), NSAID use, TNFi use, non-TNFi use (including tocilizumab and abatacept), and smoking status.

The analysis was performed using each patient's data in the year before the onset of malignancies [5]. Drug use and smoking status were analyzed as predictors in patients with cancer (if drug

use/smoking occurred in the year before cancer diagnosis) and without cancer (if drug use/smoking occurred at least once between the index year and end of follow-up). For other factors, data from the year before cancer diagnosis, in patients with cancer, and data from the last year of follow-up, in patients without cancer, were used for analysis.

The multivariate analysis included all predictor variables that were significant at the 5% level in the univariate analysis, using a model with a stepwise selection method (selection criterion: $p < 0.05$). For the multivariate analysis, among the variables indicating disease activity, such as DAS28-ESR, DAS28-CRP, CDAI, and SDAI, we used the DAS28-CRP data due to missing data for DAS28-ESR and to avoid multicollinearity with CDAI and SDAI. Furthermore, bDMARDs were classified into TNFi and non-TNFi categories, and we excluded bDMARDs and abatacept from the predictor variables to further address multicollinearity issues.

2 | Results

2.1 | Demographics and Clinical Characteristics

Overall, data of 26 607 patients with RA were identified and analyzed. Of these, 8400 patients were bio- or JAKi-s-exposed; 8092 were bio-exposed only; and 16 445 were csDMARD-exposed and were bio-/JAKi-s-naïve. Table 1 shows the demographics and clinical characteristics of the overall RA cohort and sub-cohorts. In the overall RA cohort, mean age (± standard deviation [SD]) was 64.16 ± 13.29 years at index, with 78.87% of patients being female and 43.41% having mild RA. MTX use (mean ± SD dose: 8.27 ± 3.02 mg/week) was observed in 62.36% of patients, with most (39.90%) receiving an MTX dose of ≤ 8 mg/week. NSAIDs use was observed in 42.32% of the overall RA cohort, and the levels of NSAIDs use in the sub-cohorts were similar.

TABLE 1 | Demographics and clinical characteristics of the overall RA cohort and sub-cohorts.

Characteristics	Overall RA cohort ($n = 26607$)	Bio- or JAKi-s-exposed sub-cohort ($n = 8400$)	Bio-exposed sub-cohort ($n = 8092$)	Bio- or JAKi-s naïve csDMARDs-exposed sub-cohort ($n = 16445$)
Age (years), mean ± SD	64.16 ± 13.29	61.99 ± 13.87	61.95 ± 13.90	65.11 ± 12.70
Female patients, n (%)	20 984 (78.87)	6944 (82.67)	6696 (82.75)	12 704 (77.25)
RA severity, n (%)				
Mild (DAS28 < 3.2), n (%)	11 549 (43.41)	4117 (49.01)	3962 (48.96)	7383 (44.90)
Moderate (DAS28 ≥ 3.2 to ≤ 5.1), n (%)	7647 (28.74)	2466 (29.36)	2368 (29.26)	4524 (27.51)
Severe (DAS28 > 5.1), n (%)	1706 (6.41)	533 (6.35)	513 (6.34)	774 (4.71)
Not available, n (%)	5705 (21.44)	1284 (15.29)	1249 (15.43)	3764 (22.89)
Any orthopedic surgery, n (%)	3917 (14.72)	1780 (21.19)	1714 (21.18)	2052 (12.48)
History of MTX use				
Patients receiving treatment, n (%)	16 593 (62.36)	5440 (64.76)	5208 (64.36)	11 612 (70.61)
Dose (mg/week), mean ± SD	8.27 ± 3.02	8.49 ± 2.99	8.45 ± 3.00	8.17 ± 2.99
Dose ≤ 8 mg/week, n (%)	10 615 (39.90)	3223 (38.37)	3132 (38.70)	7576 (46.07)
Dose > 8 mg/week, n (%)	5976 (22.46)	2217 (26.39)	2076 (25.65)	4034 (24.53)
History of NSAIDs use				
Patients receiving treatment, n (%)	11 162 (42.32)	3923 (46.74)	3742 (46.28)	7004 (42.60)

Note: The overall RA cohort included patients who received any treatment for RA; bio- or JAKi-s-exposed sub-cohort included patients who received bDMARDs or JAKi-s; bio-exposed sub-cohort included patients who received bDMARDs; bio- or JAKi-s-naïve csDMARDs-exposed sub-cohort included patients who received csDMARDs (excluding actarit) but did not receive bDMARDs/JAKi-s.

Abbreviations: bDMARDs, biologic disease-modifying antirheumatic drugs; csDMARDs, conventional synthetic disease-modifying antirheumatic drug; DAS, disease activity score; JAKi-s, janus kinase inhibitors; MTX, methotrexate; RA, rheumatoid arthritis; SD, standard deviation.

2.2 | Incidence of Malignancies

Cumulative longitudinal incidences and cross-sectional incidences (at each calendar year) of malignancies between 2013 and 2018 in the overall RA cohort and sub-cohorts, per the primary pattern, are shown in Figures 1 and 2, respectively. The SIR of malignancies among all patients with RA was 0.97 (95% CI: 0.91–1.03) between 2013 and 2018. In the cross-sectional analysis, SIR between 2013 and 2018 for all patients with RA remained consistent around 1.0 each year, with all CIs including 1.0; SIR was slightly lower at 0.86 (95% CI: 0.73–1.00) in 2017

and slightly higher at 1.10 (95% CI: 0.95–1.25) in 2018. Crude IR was 1.16 (95% CI: 1.09–1.24) in the overall RA cohort, whereas it was numerically higher in the bio or JAKi-s-naïve csDMARDs-exposed sub-cohort than the others; however, ASRs and SIRs were similar in the overall RA cohort and sub-cohorts.

Cumulative longitudinal crude IRs, ASRs, and SIRs of malignancies in the overall RA cohort and sub-cohorts, based on the follow-up period per other patterns, are shown in Tables S1–S3. Cumulative longitudinal incidences of malignancies in the overall RA cohort and sub-cohorts based on the follow-up

FIGURE 1 | Cumulative analysis of the incidence of malignancies in the overall RA cohort and sub-cohorts (follow-up per primary pattern). The overall RA cohort included patients who received any treatment for RA; bio or JAKi-s-exposed sub-cohort included patients who received bDMARDs or JAKi-s; bio-exposed sub-cohort included patients who received bDMARDs; bio or JAKi-s-naïve csDMARDs-exposed sub-cohort included patients who received csDMARDs but did not receive bDMARDs/JAKi-s. [a]Standardized using data from a Japanese general population database of malignancy incidence (2013–2017), provided by the Center for Cancer Control and Information Services and the National Cancer Center, Japan. SIRs greater than or lower than 1.0 (dashed line) indicate that the malignancy incidence is higher or lower than the general population, respectively. The primary pattern follow-up began at the start of the year (April 1) and ended either at mid-year (September 30) if malignancy was present or at the end of the year (March 31) if malignancy was absent. For the RA sub-cohorts, follow-up began in the year of exposure to their respective drug class. ASR, age- and sex-adjusted standardized rate; bDMARDs, biologic disease-modifying antirheumatic drugs; CI, confidence interval; csDMARDs, conventional synthetic disease-modifying antirheumatic drugs; IR, incidence rate; JAKi-s, janus kinase inhibitors; RA, rheumatoid arthritis; SIR, standardized incidence ratio.
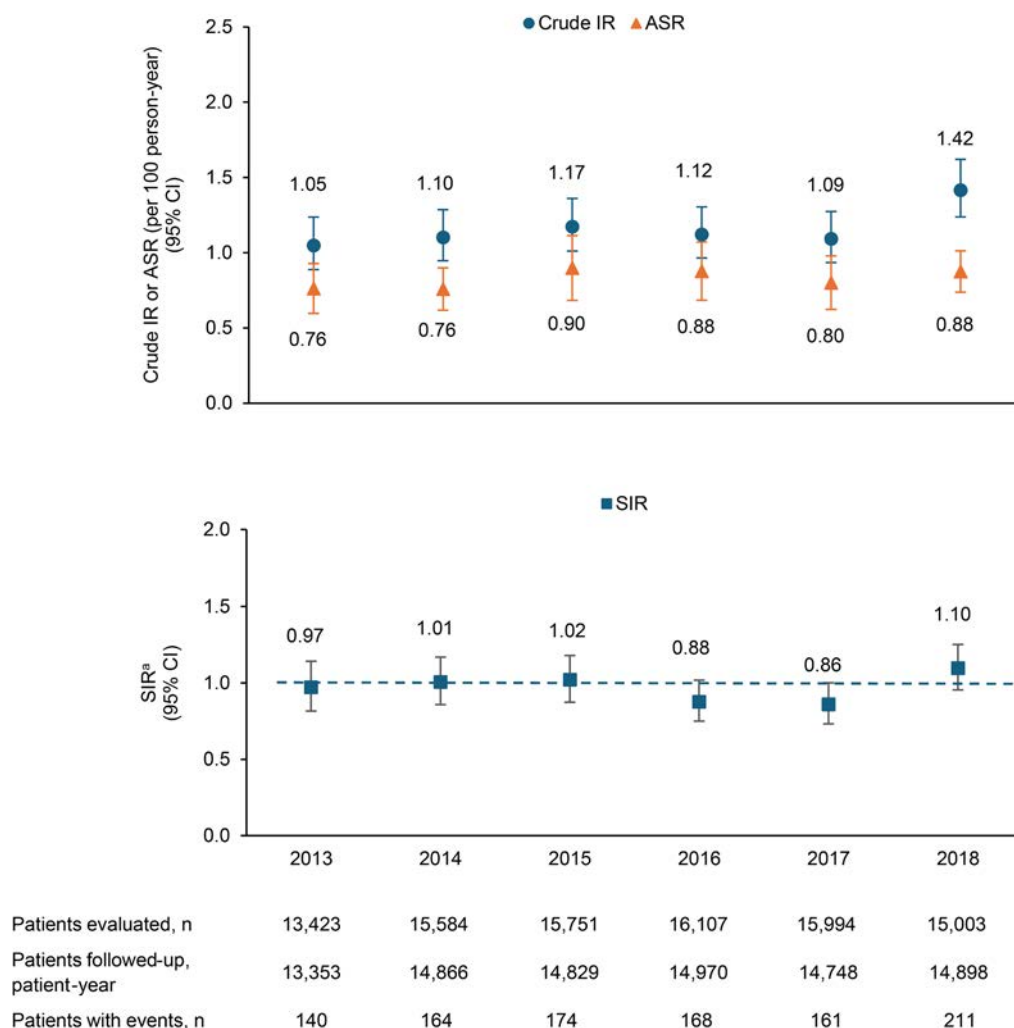
FIGURE 2 | Cross-sectional analysis of the incidence of malignancies in the overall RA cohort (follow-up per primary pattern). The overall RA cohort included patients who received any treatment for RA. [a]Standardized using data from a Japanese general population database of malignancy incidence (2013–2017), provided by the Center for Cancer Control and Information Services and the National Cancer Center, Japan. SIRs greater than or lower than 1.0 (dashed line) indicate that the malignancy incidence is higher or lower than the general population, respectively. The primary pattern follow-up began at the start of the year (April 1) and ended either at mid-year (September 30) if malignancy was present or at the end of the year (March 31) if malignancy was absent. For the RA sub-cohorts, follow-up began in the year of exposure to their respective drug class. ASR, age- and sex-adjusted standardized rate; CI, confidence interval; IR, incidence rate; RA, rheumatoid arthritis; SIR, standardized incidence ratio.

period per pattern 3 were similar to those obtained per the primary pattern.

2.3 | Incidence of Malignancies Per Type

Total 1018 malignancy events were observed in the overall RA cohort. The number of events and SIRs for malignancy types (≥ 10 events) are shown in Figure 3. The most frequent malignancy in the overall RA cohort was lung cancer ($n = 158$), followed by lymphoma ($n = 151$), colorectal cancer ($n = 145$), gastric cancer ($n = 129$), breast cancer (female patients only, $n = 115$), prostate cancer (male patients only, $n = 44$), and skin cancer ($n = 43$), with respective SIRs (95% CIs) of 1.18 (0.999–1.37), 4.00 (3.39–4.68), 0.84 (0.71–0.99), 0.92 (0.77–1.09), 0.79 (0.65–0.94), 0.70 (0.51–0.93), and 1.73 (1.25–2.30). The SIR trend in the RA sub-cohorts was generally similar to that in the overall RA cohort.

2.4 | Potential Risk Factors for the Development of Malignancies

The results of univariate and multivariate analyses are shown in Table 2. Univariate analysis showed that older age (odds ratio [OR]: 1.03; $p < 0.0001$), Steinbrocker stage score of 2 and 4 versus 1 (OR: 1.55; $p < 0.0001$ and 1.49; $p = 0.0002$, respectively), higher DAS28-CRP (OR: 1.21; $p < 0.0001$), higher DAS28-ESR (OR: 1.22; $p < 0.0001$), higher SDAI (OR: 1.02; $p = 0.0001$), higher CDAI (OR: 1.02; $p = 0.0008$), male sex (OR: 1.86; $p < 0.0001$), and a history of smoking (OR: 1.76; $p < 0.0001$) were associated with malignancies. In multivariate analysis, older age (OR: 1.02; $p < 0.0001$), male sex (OR: 1.53; $p = 0.001$), history of smoking (OR: 1.55; $p = 0.0003$), Steinbrocker stage score of 2 and 4 versus 1 (OR: 1.43; $p = 0.0077$ and 1.47; $p = 0.0104$, respectively), and higher DAS28-CRP (OR: 1.15; $p = 0.0023$) were significantly associated with malignancies in patients with RA (Table 2). Furthermore, univariate analysis

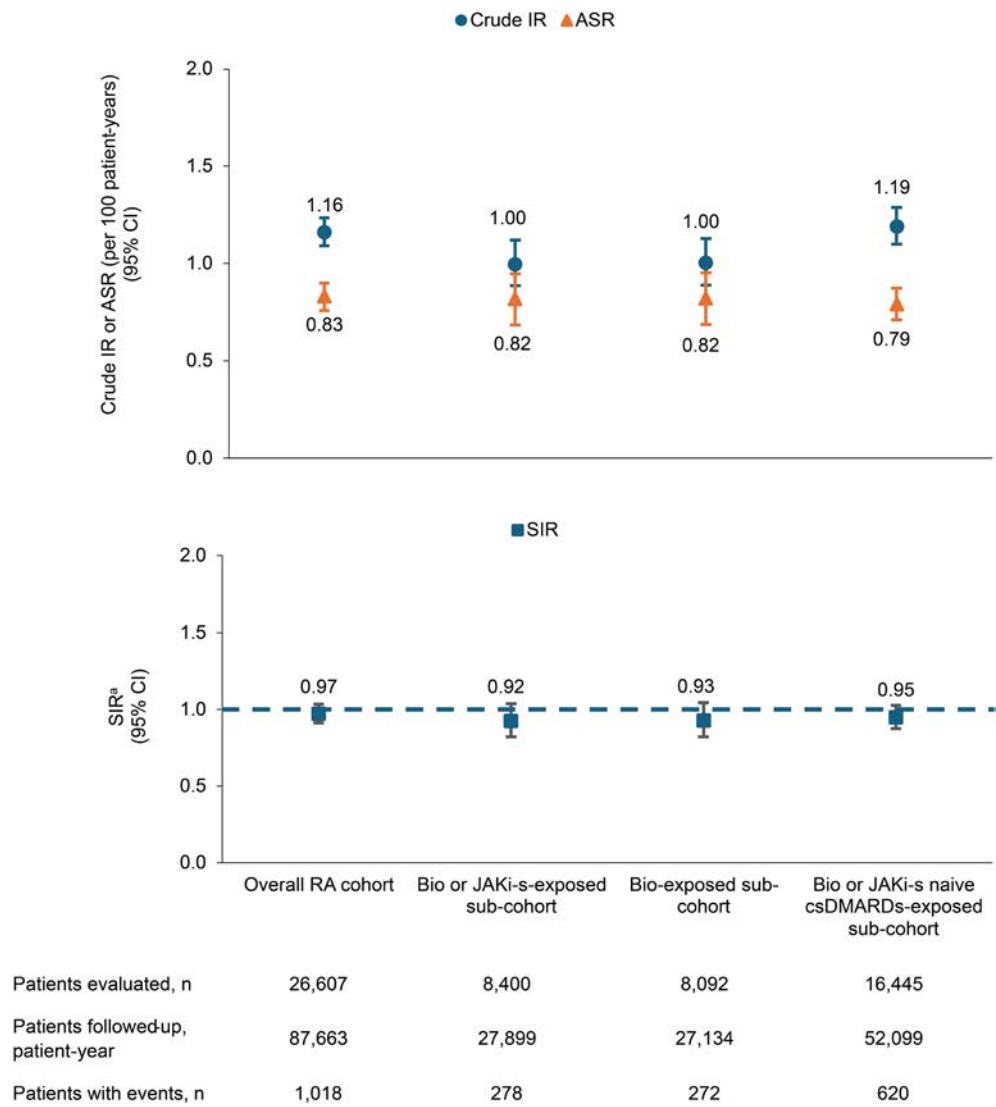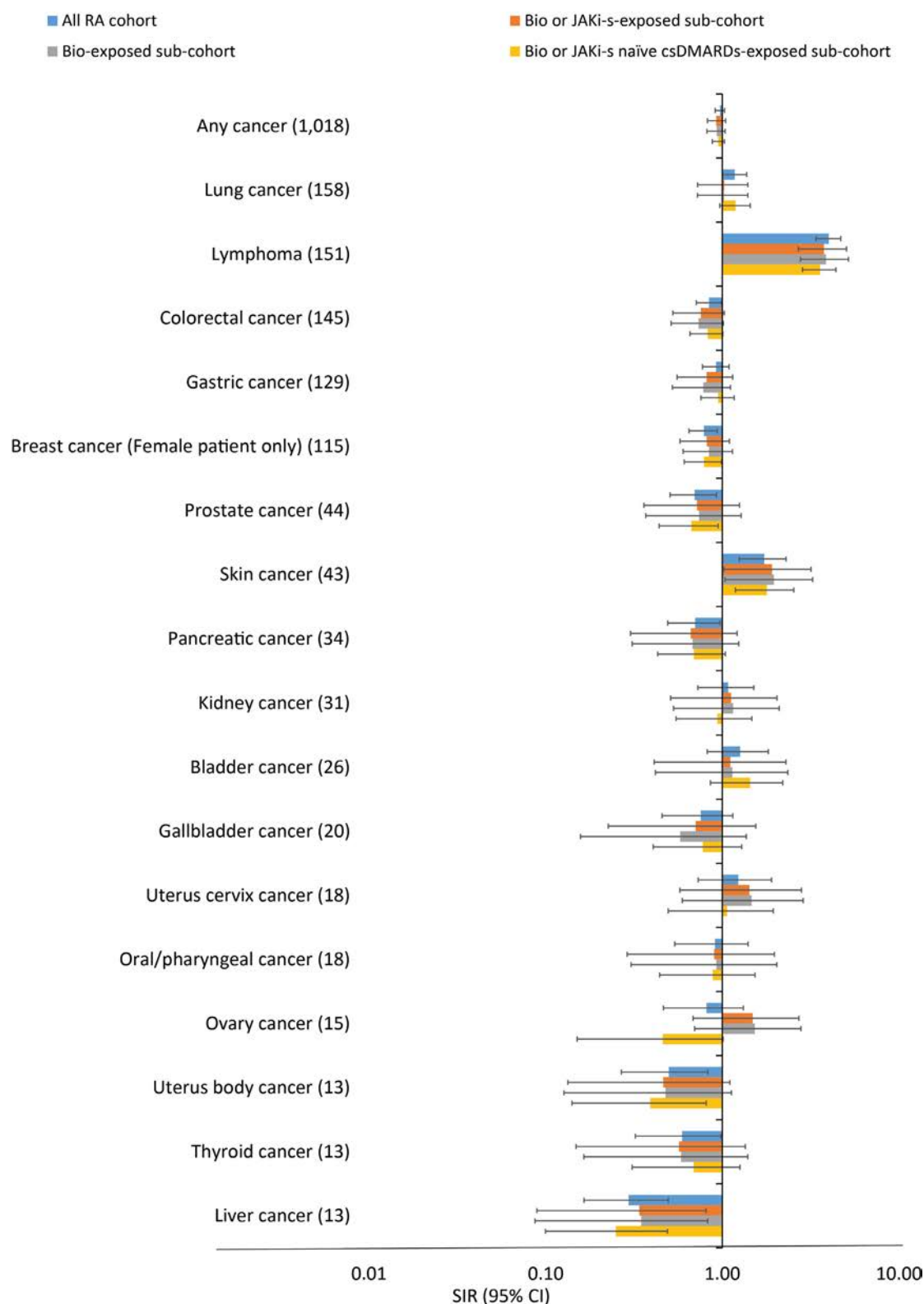**FIGURE 3** | SIRs[a] for each type of malignancy in the overall RA cohort (follow-up per primary pattern). The overall RA cohort included patients who received any treatment for RA; the bio- or JAKi-s-exposed sub-cohort included patients who received bDMARDs or JAKi-s; the bio-exposed sub-cohort included patients who received bDMARDs; the bio- or JAKi-s-naïve csDMARDs-exposed sub-cohort included patients who received csDMARDs but did not receive bDMARDs/JAKi-s. [a]Standardized using data from a Japanese general population database of malignancy incidence (2013–2017), provided by the Center for Cancer Control and Information Services and the National Cancer Center, Japan. SIRs greater than or lower than 1.0 (dashed line) indicate that the malignancy incidence is higher or lower versus the general population, respectively. bDMARDs, biologic disease-modifying antirheumatic drugs; CI, confidence interval; csDMARDs, conventional synthetic disease-modifying antirheumatic drugs; JAKi-s, janus kinase inhibitors; RA, rheumatoid arthritis; SIR, standardized incidence ratio.

showed that the use of MTX, JAKi-s, NSAIDs, bDMARDs, TNFi-s, non-TNFi-s, and abatacept in the preceding year was associated with a significant decrease in malignancy risk. However, multivariate analysis showed no significant association between incidence of malignancies and use of these drugs other than NSAIDs (OR: 0.48; $p < 0.0001$; Table 2). In the multivariate analysis including abatacept, abatacept (but not bDMARDs) was likely associated with a reduced risk of developing malignancies (data not shown).

Additionally, both univariate and multivariate analyses in patients between the index year and year before the onset of malignancy (drug use; ever exposed) indicated that older age, Steinbrocker stage score 2 versus 1, higher DAS28-CRP, male sex, smoking, glucocorticoids, and calcineurin inhibitors were likely associated with a higher risk of developing malignancies (Table S4).

Finally, the risk factors for the development of lymphoma were assessed (Table S5). In univariate analysis, older age, Steinbrocker stage score of 4 versus 1, higher DAS28-CRP, and male sex were associated with the onset of lymphoma. Furthermore, multivariate analysis showed that Steinbrocker stage score of 4 versus 1, higher DAS28-CRP, and male sex were

TABLE 2 | Potential risk factors associated with malignancies in the overall RA cohort in the year before the onset of malignancies.

Risk factors	Univariate analysis		Multivariate analysis	
	OR (95% CI)	*p*	OR (95% CI)	*p*
Age[a]	1.03 (1.02–1.03)	< 0.0001	1.02 (1.01–1.03)	< 0.0001
RA disease duration[a]	1.00 (1.00–1.01)	0.3316	—	—
Steinbrocker stage score of 2 vs. 1	1.55 (1.26–1.90)	< 0.0001	1.43 (1.10–1.87)	0.0077
Steinbrocker stage score of 3 vs. 1	1.16 (0.91–1.47)	0.2255	1.06 (0.77–1.45)	0.7424
Steinbrocker stage score of 4 vs. 1	1.49 (1.21–1.84)	0.0002	1.47 (1.09–1.97)	0.0104
Steinbrocker stage score of 2–4 vs. 1	1.42 (1.19–1.70)	0.0001	—	—
Global functional status of 2 vs. 1	1.05 (0.89–1.24)	0.5672	—	—
Global functional status of 3 vs. 1	1.16 (0.94–1.44)	0.1659	—	—
Global functional status of 4 vs. 1	0.94 (0.61–1.46)	0.7899	—	—
DAS28-ESR	1.22 (1.15–1.30)	< 0.0001	—	—
DAS28-CRP	1.21 (1.13–1.29)	< 0.0001	1.15 (1.05–1.27)	0.0023
SDAI	1.02 (1.01–1.03)	0.0001	—	—
CDAI	1.02 (1.01–1.03)	0.0008	—	—
Male sex	1.86 (1.59–2.18)	< 0.0001	1.53 (1.19–1.97)	0.001
BMI	1.00 (0.98–1.03)	0.6823	—	—
Smoking	1.76 (1.45–2.14)	< 0.0001	1.55 (1.22–1.97)	0.0003
Glucocorticoids	0.98 (0.85–1.14)	0.8268	—	—
MTX	0.64 (0.55–0.74)	< 0.0001	0.83 (0.67–1.03)	0.0849
JAKi-s	0.43 (0.22–0.83)	0.0124	0.67 (0.31–1.43)	0.2992
Calcineurin inhibitors	1.19 (0.98–1.45)	0.0858	—	—
Other immunosuppressants	1.02 (0.62–1.66)	0.9441	—	—
NSAIDs	0.57 (0.49–0.66)	< 0.0001	0.48 (0.40–0.60)	< 0.0001
Biologics	0.76 (0.65–0.90)	0.0015	—	—
TNFi-s	0.71 (0.58–0.87)	0.0009	0.88 (0.67–1.16)	0.3750
Non-TNFi-s	0.75 (0.60–0.94)	0.0141	0.79 (0.59–1.07)	0.1293
Abatacept	0.60 (0.42–0.85)	0.0043	—	—
Tocilizumab	0.84 (0.64–1.10)	0.2095	—	—

Abbreviations: BMI, body mass index; CDAI, clinical disease activity index; CI, confidence interval; CRP, C-reactive protein; DAS, disease activity score; ESR, erythrocyte sedimentation rate; JAKi-s, janus kinase inhibitors; MTX, methotrexate; NSAIDs, nonsteroidal anti-inflammatory drugs; OR, odds ratio; RA, rheumatoid arthritis; SDAI, simplified disease activity index; TNFi-s, tumor necrosis factor inhibitors.
[a]Per an additional year.

significantly associated with the onset of lymphoma. Although both univariate and multivariate analyses showed that the use of non-TNFi-s was associated with a reduced risk of developing lymphoma.

3 | Discussion

Data from 26 607 patients in the overall RA cohort from the NinJa registry showed no difference in overall malignancy incidence (SIR: 0.97 from 2013 to 2018) between patients with RA and the Japanese general population. SIRs of malignancies were similar among the RA sub-cohorts. The most frequently observed malignancies in patients with RA were lung cancer, lymphoma, colorectal cancer, gastric cancer, breast cancer, prostate cancer, and skin cancer. Lymphoma and skin cancer incidences were higher in Japanese patients with RA versus the general population, whereas colorectal and breast cancer incidences were lower.

Studies in Western populations showed an association between malignancy and RA, with SIRs of 0.99–1.23 [17, 24–26]. Studies conducted in East Asian populations reported SIRs (95% CI) for malignancies in patients with RA versus the general population (high SIRs: 1.23 [1.22–1.23] [7], 1.35 [1.02–1.74] [27]; low SIR: 0.93 [0.88–0.97] [11]; similar SIRs: 1.28 [0.88–1.87] for males and 1.21 [0.99–1.46] [28] for females). The inconsistent results among studies may have stemmed from differences in region, race, treatments, study designs, cohort definitions, or follow-up periods. In Japan, a single-institute-based large prospective observational study (the Institute of Rheumatology, Rheumatoid Arthritis [IORRA]; 2001–2005) reported a slightly higher malignancy incidence (SIR: 1.18; 95% CI: 1.02–1.37) among patients with RA versus the general population [8]. However, recent reports (2013–2018 and 14-year follow-up) from the same cohort showed a similar malignancy incidence to the general population, with SIRs 0.90 and 0.92 [13, 29]. Our study, based on the NinJa registry data (2013–2018), reported an SIR 0.97 (95% CI: 0.91–1.03) (Figure 1); this was consistent with previous data from the same registry (2003–2012) showing a similar malignancy incidence (SIR: 0.89; 95% CI: 0.82–0.97) in patients with RA versus the Japanese general population [5]. The SIRs of both registries were similar in individual cancer types. Additionally, ASRs and SIRs of malignancies were consistent among the overall RA cohort and sub-cohorts in our study, suggesting that the population belonging to each cohort/sub-cohort has similar malignancy risk. However, the crude IR in the bio or JAKi-s naïve csDMARDs-exposed sub-cohort was numerically higher than in the other sub-cohorts, which could be attributed to older age and fewer female patients in the sub-cohort.

Lymphoma is the most frequent cancer in patients with RA, with approximately 2-fold increased risk versus the general population, as reported in a meta-analysis [9, 10]. In studies from Japan, the reported SIR of lymphoma in patients with RA varied from 3.43 to 6.07 [5, 8, 13]. Lymphoma risks were also higher in patients with RA in other East Asian countries [7, 11, 28, 30, 31]. In Taiwan, the SIRs for non-Hodgkin's lymphoma were 3.40 and Hodgkin's lymphoma were 5.12 [30]. In China, the SIR for non-Hodgkin's lymphoma was 26.19 [32]. In our study, the relative incidence of lymphoma was high in the overall RA cohort (SIR: 4.0) and sub-cohorts (SIR: 3.57–4.11) (Figure 3), which aligned with previous studies conducted in East Asian countries, including Japan. This suggests the relative risk of lymphoma in patients with RA might be higher in the East Asian population than in other populations, which is possibly due to differences in both genetic and environmental factors [33]. Further studies are needed to conclude Japanese or East Asian features associated with lymphoma risk in patients with RA.

Skin cancer rates are rising globally, especially that of non-melanoma skin cancer (NMSC) in many regions, including East Asia [34]. In Japan, a single-center (Niigata Cancer Center Hospital, Japan) retrospective study showed that skin cancer incidences increased these three decades [35], and similar results were confirmed for squamous cell carcinoma (SCC), NMSC subtype, in studies from other region [36]. However, there is very limited evidence regarding skin cancer risks in Japanese patients with RA. Although previous results from the NinJa registry showed that the incidence of skin cancer in RA patients was similar to that in the general population [5], our study showed that the SIR was 1.73 (95% CI: 1.25–2.30) for skin cancer in the overall RA cohort, suggesting a higher risk of skin cancer versus the general population in Japan (Figure 3). One possible reason for this inconsistency may be the change in the treatment options, that is, advents of the various types of immunosuppressive drugs. Immunosuppression, the key strategy of RA treatment, is a significant risk factor for SCC [37]. There have been several evidences showing the increased risks of NMSC by cs/b/tsD-MARDs including MTX [38], hydroxychloroquine [39], TNFi-s [17, 18, 40, 41], and JAKi-s [42]. Although further studies are needed to characterize the skin cancer risk in Japanese patients with RA, our results suggest a need for attention to the risk of skin cancer in RA patients.

Lung cancer is also a malignancy with an increased risk in patients with RA, with reported SIRs ranged 1.36–2.29 [9, 10]. However, studies from East Asian countries reported either similar [11–13] or higher [7, 8] risk of lung cancer in patients with RA versus the general population. The results of our study showed that the incidence of lung cancer is similar to the general population (Figure 3), consistent with those findings, although the 95% CI for SIR almost exceeded 1. These variations in SIRs of lung cancer in patients with RA among studies may be attributed to differences in study design, cohort characteristics such as regional/racial characteristics, and lifestyle differences. Smoking, in particular, is a major risk factor for both RA and lung cancer; therefore, differences in smoking habits in patients with RA might also affect the results.

In our study, the incidence of liver cancer tended to be lower than that in the general population (Figure 3). A low incidence of liver cancer in RA patients was reported in several studies across countries and races including Japan [5], Taiwan [43], China [44], and French [17], being consistent with our results. One possible reason for this is the cancer-suppressing effects of NSAIDs and aspirin. The use of aspirin and NSAIDs has been reported to contribute to the reduction of liver cancer risk [45–47]. In addition, a previous study using the NinJa registry reported a tendency for NSAIDs use to suppress the occurrence of cancers other than lymphoma [48], which may support the finding of our study. From a different viewpoint, the guidelines

for RA treatment in Japan recommend screening for HBV and HCV, and thorough implementation of these screenings might contribute to the suppression of liver cancer occurrence.

Furthermore, studies have shown reduced or no increased risk of colorectal cancer [13, 49], gastric cancer [12, 13], and breast cancer [13, 50, 51], aligning with our findings (Figure 3).

In the multivariate analysis of our study, the predictors for increased malignancy risk were older age, male sex, high disease severity, and smoking status, whereas NSAID use in the preceding year reduced malignancy risk in patients with RA (Table 2). Previous studies also showed similar predictors such as older age, male sex, and disease activity [5, 8, 24, 29]. The comparison using Steinbrocker stage score showed a tendency for higher malignancy risk with a higher score versus score 1, with a significant difference observed when comparing a score of 2 or 4 in the multivariate analysis; the risk was significantly higher with scores of 2–4 when comparing patients with a score of 2–4 versus 1 (Table 2). The difference observed when comparing patients with a score of 3 versus 1 was not statistically significant, and the exact reason for this is unclear. One possible explanation is that the number of patients with a score of 3 was smaller compared to the other scores, whereas the number of patients with scores of 1, 2, and 4 was similar (score 1: 6384, score 2: 6278, score 3: 4391, score 4: 5845). These findings suggest that patients with Steinbrocker stage score > 1 need to be cautious about developing malignancies, while the significant difference between Steinbrocker stage scores 2 versus 1 may indicate the importance of early intervention in patients with RA. Furthermore, in the univariate analysis, MTX, JAKi-s, TNFi-s, and non-TNFi-s use were associated with lower malignancy incidence; however, the association was not significant ($p = 0.0849$; 0.2992; 0.3750; and 0.1293, respectively) after adjusting for other relevant factors in the multivariate analysis (Table 2). MTX use was identified as a risk factor for lymphoma in patients with RA from the NinJa registry (2002–2011) [5]. This study also showed similar results. Although no significant difference was observed, maybe because of the limited number of patients, the use of MTX tended to increase the risk of lymphoma (Table S5). Therefore, the incidence of malignancies other than lymphoma could have affected the results.

NSAID have a protective effect against colorectal cancer [52–54], although this has not been well-verified in patients with RA. A recent study using the NinJa registry database (2012–2018) identified NSAID use as a strong factor for developing lymphoma in patients with RA, when risk was compared between the development of lymphoma and that of other malignancies (OR for malignant lymphoma versus other malignancies: 2.51; 95% CI: 1.58–3.98; $p < 0.001$) [48]. The multivariate analysis for predictors of malignancy development (not focusing on lymphoma) in our study showed that NSAID use is associated with a significantly decreased malignancy risk (Table 2). It is possible that NSAID prevents malignancies other than lymphoma, such as colorectal cancer, in patients with RA. Given the observational nature of this study, causal inferences cannot be established, and the findings should be interpreted with caution.

Limitations of our study were mostly related to the study design, including the inability to completely control for residual confounding regarding drug therapy choice by the physician (i.e., confounding by indication) and to obtain clinical information for patients with certain events that may increase the risk of selection and under-reporting bias. As the follow-up rate is not 100%, there is a possibility of data loss, which could introduce bias in the results. Unreported malignancies by patients also increase the chances of misclassification bias, although the likelihood of this bias is low. Regarding the selection bias, although the participating facilities are limited to those registered in the NinJa registry, this potential bias is considered to have been mitigated by the inclusion of a diverse range of medical institutions, including university hospitals, large and small hospitals, and clinics. Furthermore, as with other hospital-based observational studies, the possibility of information bias cannot be excluded.

Additionally, as the NinJa registry provides annual data, the actual start date of observation for treatment initiation and the occurrence of cancer cannot be captured. However, the follow-up period was carefully defined, and sensitivity analyses were conducted using multiple follow-up period patterns to assess the potential impact of this limitation. In our study, reference data for the Japanese general population for 2018 were not available at the time of conducting this study and were extrapolated using the 2017 data. Comparing the 2017 and the 2018 data from the NCC, no significant differences were observed (crude IR [per 100 000 population] 2017: 771.4, 2018: 775.7; ASR based on world population 2017: 283.6, 2018: 280.6), and the impact on the results of this study is likely limited.

The multivariate analysis was not conducted for potential risk factors of each malignancy type.

Considering the limitations discussed above, the results of this study should be interpreted with caution.

4 | Conclusion

The malignancy incidence in Japanese patients with RA included in the NinJa registry (2013–2018) was similar to that in the Japanese general population. The incidences of lymphoma and skin cancer were higher, whereas those of colorectal and breast cancers were lower among patients with RA versus the Japanese general population. The results also suggested that malignancy incidence was consistent across all patients with RA and the subcohorts. Furthermore, the study revealed that older age, higher disease activity, male sex, and smoking increased the risk, whereas NSAID use in the preceding year decreased the risk of developing malignancies in Japanese patients with RA. These findings provide valuable insights into the malignancy risks in Japanese patients with RA under recent therapeutic practices, which may be considered by physicians in RA treatment.

Ethics Statement

The study was conducted in accordance with legal and regulatory requirements, emphasizing scientific purpose, value, and rigor. The study adhered to the Guidelines for Good Pharmacoepidemiology Practices issued by the International Society of Pharmacoepidemiology and the Good Practices for Outcomes Research issued by the International Society for Pharmacoeconomics and Outcomes Research. This study was reviewed and approved by the ethics committee of National Hospital Organization Sagamihara National Hospital (Approval number: 2015102213). Informed consent was not required for this study as it involved anonymized structured data, which, per applicable legal requirements, are not subject to privacy laws (Appendix S2).

Data Availability Statement

The data that support the findings of this study are restricted from sharing.

References

1. K. B. Almutairi, J. C. Nossent, D. B. Preen, H. I. Keen, and C. A. Inderjeeth, "The Prevalence of Rheumatoid Arthritis: A Systematic Review of Population-Based Studies," *Journal of Rheumatology* 48, no. 5 (2021): 669–676, https://doi.org/10.3899/jrheum.200367.

2. H. Yamanaka, N. Sugiyama, E. Inoue, A. Taniguchi, and S. Momohara, "Estimates of the Prevalence of and Current Treatment Practices for Rheumatoid Arthritis in Japan Using Reimbursement Data From Health Insurance Societies and the IORRA Cohort (I)," *Modern Rheumatology* 24, no. 1 (2014): 33–40, https://doi.org/10.3109/14397595.2013.854059.

3. K. Kubota, M. Yoshizawa, S. Takahashi, Y. Fujimura, H. Nomura, and H. Kohsaka, "The Validity of the Claims-Based Definition of Rheumatoid Arthritis Evaluated in 64 Hospitals in Japan," *BMC Musculoskeletal Disorders* 22, no. 1 (2021): 373, https://doi.org/10.1186/s12891-021-04259-9.

4. A. Nakajima, R. Sakai, E. Inoue, and M. Harigai, "Prevalence of Patients With Rheumatoid Arthritis and Age-Stratified Trends in Clinical Characteristics and Treatment, Based on the National Database of Health Insurance Claims and Specific Health Checkups of Japan," *International Journal of Rheumatic Diseases* 23, no. 12 (2020): 1676–1684, https://doi.org/10.1111/1756-185X.13974.

5. A. Hashimoto, N. Chiba, H. Tsuno, et al., "Incidence of Malignancy and the Risk of Lymphoma in Japanese Patients With Rheumatoid Arthritis Compared to the General Population," *Journal of Rheumatology* 42, no. 4 (2015): 564–571, https://doi.org/10.3899/jrheum.140533.

6. P. C. Taylor, F. Atzeni, A. Balsa, L. Gossec, U. Müller-Ladner, and J. Pope, "The Key Comorbidities in Patients With Rheumatoid Arthritis: A Narrative Review," *Journal of Clinical Medicine* 10, no. 3 (2021): 509, https://doi.org/10.3390/jcm10030509.

7. Y. J. Chen, Y. T. Chang, C. B. Wang, and C. Y. Wu, "The Risk of Cancer in Patients With Rheumatoid Arthritis: A Nationwide Cohort Study in Taiwan," *Arthritis and Rheumatism* 63, no. 2 (2011): 352–358, https://doi.org/10.1002/art.30134.

8. T. Yamada, A. Nakajima, E. Inoue, et al., "Incidence of Malignancy in Japanese Patients With Rheumatoid Arthritis," *Rheumatology International* 31, no. 11 (2011): 1487–1492, https://doi.org/10.1007/s00296-010-1524-0.

9. A. L. Smitten, T. A. Simon, M. C. Hochberg, and S. Suissa, "A Meta-Analysis of the Incidence of Malignancy in Adult Patients With Rheumatoid Arthritis," *Arthritis Research & Therapy* 10, no. 2 (2008): R45, https://doi.org/10.1186/ar2404.

10. T. A. Simon, A. Thompson, K. K. Gandhi, M. C. Hochberg, and S. Suissa, "Incidence of Malignancy in Adult Patients With Rheumatoid Arthritis: A Meta-Analysis," *Arthritis Research & Therapy* 17, no. 1 (2015): 212, https://doi.org/10.1186/s13075-015-0728-9.

11. W. K. Huang, M. J. Chiou, C. F. Kuo, Y. C. Lin, K. H. Yu, and L. C. See, "No Overall Increased Risk of Cancer in Patients With Rheumatoid Arthritis: A Nationwide Dynamic Cohort Study in Taiwan," *Rheumatology International* 34, no. 10 (2014): 1379–1386, https://doi.org/10.1007/s00296-014-2982-6.

12. K. M. Ko and S. J. Moon, "Prevalence, Incidence, and Risk Factors of Malignancy in Patients With Rheumatoid Arthritis: A Nationwide Cohort Study From Korea," *Korean Journal of Internal Medicine* 38, no. 1 (2023): 113–124, https://doi.org/10.3904/kjim.2021.146.

13. M. Harigai, E. Tanaka, E. Inoue, et al., "Incidence of Malignancies and the Association With Biological Disease-Modifying Antirheumatic Drugs in Japanese Patients With Rheumatoid Arthritis: A Time-Dependent Analysis From the IORRA Patient Registry," *Rheumatology and Therapy* 11, no. 5 (2024): 1181–1195, https://doi.org/10.1007/s40744-024-00689-8.

14. E. Mysler, M. Caubet, and A. Lizarraga, "Current and Emerging DMARDs for the Treatment of Rheumatoid Arthritis," *Open Access Rheumatology: Research and Reviews* 13 (2021): 139–152, https://doi.org/10.2147/OARRR.S282627.

15. G. D. Kalliolias, E. K. Basdra, and A. G. Papavassiliou, "Solid Cancers and Rheumatoid Arthritis," *Cancers* 15, no. 22 (2023): 5441, https://doi.org/10.3390/cancers15225441.

16. Y. Zhang, J. Lin, Z. You, et al., "Cancer Risks in Rheumatoid Arthritis Patients Who Received Immunosuppressive Therapies: Will Immunosuppressants Work?," *Frontiers in Immunology* 13 (2022): 1050876, https://doi.org/10.3389/fimmu.2022.1050876.

17. M. Beydon, S. Pinto, Y. De Rycke, et al., "Risk of Cancer for Patients With Rheumatoid Arthritis Versus General Population: A National Claims Database Cohort Study," *Lancet Regional Health. Europe* 35 (2023): 100768, https://doi.org/10.1016/j.lanepe.2023.100768.

18. X. Mariette, M. Matucci-Cerinic, K. Pavelka, et al., "Malignancies Associated With Tumour Necrosis Factor Inhibitors in Registries and Prospective Observational Studies: A Systematic Review and Meta-Analysis," *Annals of the Rheumatic Diseases* 70, no. 11 (2011): 1895–1904, https://doi.org/10.1136/ard.2010.149419.

19. M. Kuwana, N. Sugiyama, S. Momohara, et al., "Six-Month Safety and Effectiveness of Tofacitinib in Patients With Rheumatoid Arthritis in Japan: Interim Analysis of Post-Marketing Surveillance," *Modern Rheumatology* 34, no. 2 (2024): 272–286, https://doi.org/10.1093/mr/road063.

20. T. Matsui, T. Yoshida, T. Nishino, S. Yoshizawa, T. Sawada, and S. Tohma, "Trends in Treatment for Patients With Late-Onset Rheumatoid Arthritis in Japan: Data From the NinJa Study," *Modern Rheumatology* 34, no. 5 (2024): 881–891, https://doi.org/10.1093/mr/roae006.

21. F. C. Arnett, S. Edworthy, D. Bloch, et al., "The American Rheumatism Association 1987 Revised Criteria for the Classification of Rheumatoid Arthritis," *Arthritis & Rheumatism* 31, no. 3 (1988): 315–324, https://doi.org/10.1002/art.1780310302.

22. D. Aletaha, T. Neogi, A. J. Silman, et al., "2010 Rheumatoid Arthritis Classification Criteria: An American College of Rheumatology/European League Against Rheumatism Collaborative Initiative," *Annals of the Rheumatic Diseases* 69, no. 9 (2010): 1580–1588, https://doi.org/10.1136/ard.2010.138461.

23. A. Matsuda, T. Matsuda, A. Shibata, et al., "Cancer Incidence and Incidence Rates in Japan in 2007: A Study of 21 Population-Based Cancer Registries for the Monitoring of Cancer Incidence in Japan (MCIJ) Project," *Japanese Journal of Clinical Oncology* 43, no. 3 (2013): 328–336, https://doi.org/10.1093/jjco/hys233.

24. L. Abásolo, E. Júdez, M. Á. Descalzo, I. González-Álvaro, J. A. Jover, and L. Carmona, "Cancer in Rheumatoid Arthritis: Occurrence, Mortality, and Associated Factors in a South European Population," *Seminars in Arthritis and Rheumatism* 37, no. 6 (2008): 388–397, https://doi.org/10.1016/j.semarthrit.2007.08.006.

25. R. Seror, A. Lafourcade, Y. De Rycke, et al., "Risk of Malignancy in Rheumatoid Arthritis Patients Initiating Biologics: An Historical Propensity Score Matched Cohort Study Within the French Nationwide Healthcare Database," *RMD Open* 8, no. 2 (2022): e002139, https://doi.org/10.1136/rmdopen-2021-002139.

26. F. Wang, N. Palmer, K. Fox, K. P. Liao, K. H. Yu, and S. C. Kou, "Large-Scale Real-World Data Analyses of Cancer Risks Among Patients With Rheumatoid Arthritis," *International Journal of Cancer* 153, no. 6 (2023): 1139–1150, https://doi.org/10.1002/ijc.34606.

27. Y. J. Kim, J. S. Shim, C. B. Choi, et al., "Mortality and Incidence of Malignancy in Korean Patients With Rheumatoid Arthritis," *Journal of Rheumatology* 39, no. 2 (2012): 226–232, https://doi.org/10.3899/jrheum.110704.

28. X. R. Lim, W. Xiang, J. W. L. Tan, et al., "Incidence and Patterns of Malignancies in a Multi-Ethnic Cohort of Rheumatoid Arthritis Patients," *International Journal of Rheumatic Diseases* 22, no. 9 (2019): 1679–1685, https://doi.org/10.1111/1756-185X.13655.

29. N. Sugimoto, E. Tanaka, E. Inoue, et al., "Trends in Risks of Malignancies in Japanese Patients With Rheumatoid Arthritis: Analyses From a 14-Year Observation of the IORRA Cohort," *Modern Rheumatology* 33, no. 4 (2023): 715–722, https://doi.org/10.1093/mr/roac085.

30. K. H. Yu, C. F. Kuo, L. H. Huang, W. K. Huang, and L. C. See, "Cancer Risk in Patients With Inflammatory Systemic Autoimmune Rheumatic Diseases a Nationwide Population-Based Dynamic Cohort Study in Taiwan," *Medicine (Baltimore)* 95, no. 18 (2016): e3540, https://doi.org/10.1097/MD.0000000000003540.

31. B. Choi, H. J. Park, Y. K. Song, et al., "The Risk of Newly Diagnosed Cancer in Patients With Rheumatoid Arthritis by TNF Inhibitor Use: A Nationwide Cohort Study," *Arthritis Research & Therapy* 24, no. 1 (2022): 238, https://doi.org/10.1186/s13075-022-02929-0.

32. Z. Zhou, H. Liu, Y. Yang, et al., "The Five Major Autoimmune Diseases Increase the Risk of Cancer: Epidemiological Data From a Large-Scale Cohort Study in China," *Cancer Communications* 42, no. 5 (2022): 435–446, https://doi.org/10.1002/cac2.12283.

33. S. Honda, R. Sakai, E. Inoue, et al., "Association of Methotrexate Use and Lymphoproliferative Disorder in Patients With Rheumatoid Arthritis: Results From a Japanese Multi-Institutional Retrospective Study," *Modern Rheumatology* 32, no. 1 (2022): 16–23, https://doi.org/10.1080/14397595.2020.1869370.

34. K. Urban, S. Mehrmal, P. Uppal, R. L. Giesey, and G. R. Delost, "The Global Burden of Skin Cancer: A Longitudinal Analysis From the Global Burden of Disease Study, 1990–2017," *JAAD International* 2 (2021): 98–108, https://doi.org/10.1016/j.jdin.2020.10.013.

35. A. Nakamura, K. Kataoka, S. Takatsuka, and T. Takenouchi, "Aging Trends in Skin Cancer: A Long-Term Observational Study in Japan," *JAAD International* 13 (2023): 32–34, https://doi.org/10.1016/j.jdin.2023.07.003.

36. Y. Umezono, Y. Sato, M. Noto, et al., "Incidence Rate of Cutaneous Squamous Cell Carcinoma Is Rapidly Increasing in Akita Prefecture: Urgent Alert for Super-Aged Society," *Journal of Dermatology* 46, no. 3 (2019): 259–262, https://doi.org/10.1111/1346-8138.14759.

37. P. Nagarajan, M. M. Asgari, A. C. Green, et al., "Keratinocyte Carcinomas: Current Concepts and Future Research Priorities," *Clinical Cancer Research* 25, no. 8 (2019): 2379–2391, https://doi.org/10.1158/1078-0432.CCR-18-1122.

38. D. H. Solomon, R. J. Glynn, E. W. Karlson, et al., "Adverse Effects of Low-Dose Methotrexate: A Randomized Trial," *Annals of Internal Medicine* 172, no. 6 (2020): 369–380, https://doi.org/10.7326/M19-3369.

39. H. Lee, S. K. Chen, N. Gautam, et al., "Risk of Malignant Melanoma and Non-Melanoma Skin Cancer in Rheumatoid Arthritis Patients Initiating Methotrexate Versus Hydroxychloroquine: A Cohort Study," *Clinical and Experimental Rheumatology* 41, no. 1 (2023): 110–117, https://doi.org/10.55563/clinexprheumatol/staplf.

40. E. F. Chakravarty, K. Michaud, and F. Wolfe, "Skin Cancer, Rheumatoid Arthritis, and Tumor Necrosis Factor Inhibitors," *Journal of Rheumatology* 32, no. 11 (2005): 2130–2135.

41. P. Raaschou, J. F. Simard, C. A. Hagelberg, et al., "Rheumatoid Arthritis, Anti-Tumour Necrosis Factor Treatment, and Risk of Squamous Cell and Basal Cell Skin Cancer: Cohort Study Based on Nationwide Prospectively Recorded Data From Sweden," *BMJ (Clinical Research Ed.)* 352 (2016): i262, https://doi.org/10.1136/bmj.i262.

42. V. Huss, H. Bower, K. Hellgren, et al., "Cancer Risks With JAKi and Biological Disease-Modifying Antirheumatic Drugs in Patients With Rheumatoid Arthritis or Psoriatic Arthritis: A National Real-World Cohort Study," *Annals of the Rheumatic Diseases* 82, no. 7 (2023): 911–919, https://doi.org/10.1136/ard-2022-223636.

43. C. S. Hsu, H. C. Lang, K. Y. Huang, et al., "Risks of Hepatocellular Carcinoma and Cirrhosis-Associated Complications in Patients With Rheumatoid Arthritis: A 10-Year Population-Based Cohort Study in Taiwan," *Hepatology International* 12, no. 6 (2018): 531–541, https://doi.org/10.1007/s12072-018-9905-7.

44. Y. Zhang, Y. Zhang, P. He, F. Ge, Z. Huo, and G. Qiao, "The Genetic Liability to Rheumatoid Arthritis May Decrease Hepatocellular Carcinoma Risk in East Asian Population: A Mendelian Randomization Study," *Arthritis Research & Therapy* 25, no. 1 (2023): 49, https://doi.org/10.1186/s13075-023-03029-3.

45. Y. H. Liao, R. J. Hsu, T. H. Wang, et al., "Aspirin Decreases Hepatocellular Carcinoma Risk in Hepatitis C Virus Carriers: A Nationwide Cohort Study," *BMC Gastroenterology* 20, no. 1 (2020): 6, https://doi.org/10.1186/s12876-020-1158-y.

46. S. Wang, Y. Yu, P. M. Ryan, et al., "Association of Aspirin Therapy With Risk of Hepatocellular Carcinoma: A Systematic Review and Dose-Response Analysis of Cohort Studies With 2.5 Million Participants,"

Pharmacological Research 151 (2020): 104585, https://doi.org/10.1016/j.phrs.2019.104585.

47. C. Selmi, M. De Santis, and M. E. Gershwin, "Liver Involvement in Subjects With Rheumatic Disease," *Arthritis Research & Therapy* 13, no. 3 (2011): 226, https://doi.org/10.1186/ar3319.

48. M. Mizushima, T. Sugihara, T. Matsui, Y. Urata, S. Tohma, and K. Kawahata, "Comparison Between Rheumatoid Arthritis With Malignant Lymphoma and Other Malignancies: Analysis of a National Database of Rheumatic Disease in Japan," *Seminars in Arthritis and Rheumatism* 63 (2023): 152301, https://doi.org/10.1016/j.semarthrit.2023.152301.

49. Q. Li, L. Zhou, D. Xia, and J. Wang, "Rheumatoid Arthritis Reduces the Risk of Colorectal Cancer Through Immune Inflammation Mediation," *Journal of Cellular and Molecular Medicine* 28, no. 13 (2024): e18515, https://doi.org/10.1111/jcmm.18515.

50. H. Wadström, A. Pettersson, K. E. Smedby, and J. Askling, "Risk of Breast Cancer Before and After Rheumatoid Arthritis, and the Impact of Hormonal Factors," *Annals of the Rheumatic Diseases* 79, no. 5 (2020): 581–586, https://doi.org/10.1136/annrheumdis-2019-216756.

51. G. Tian, J. N. Liang, Z. Y. Wang, and D. Zhou, "Breast Cancer Risk in Rheumatoid Arthritis: An Update Meta-Analysis," *BioMed Research International* 2014 (2014): 453012, https://doi.org/10.1155/2014/453012.

52. J. Cuzick, F. Otto, J. A. Baron, et al., "Aspirin and Non-Steroidal Anti-Inflammatory Drugs for Cancer Prevention: An International Consensus Statement," *Lancet Oncology* 10, no. 5 (2009): 501–507, https://doi.org/10.1016/S1470-2045(09)70035-X.

53. N. Brusselaers and J. Lagergren, "Maintenance Use of Non-Steroidal Anti-Inflammatory Drugs and Risk of Gastrointestinal Cancer in a Nationwide Population-Based Cohort Study in Sweden," *BMJ Open* 8, no. 7 (2018): 1–11, https://doi.org/10.1136/bmjopen-2018-021869.

54. F. V. N. Din, E. Theodoratou, S. M. Farrington, et al., "Effect of Aspirin and NSAIDs on Risk and Survival From Colorectal Cancer," *Gut* 59, no. 12 (2010): 1670–1679, https://doi.org/10.1136/gut.2009.203000.

Supporting Information

Additional supporting information can be found online in the Supporting Information section.

WILEY

International Journal of
Rheumatic Diseases

LETTER TO THE EDITOR

Case Report: Sarcoid Reaction Induced by Anti-TNF Therapy

Ana Catarina Moniz[1,2] 🔵 | Sónia Mota Faria[3] | Madalena Silveira Machado[4] | Manuela Zita Veiga[5] | Mariana Teixeira[6] | Tiago Saldanha[7] | Miguel Cordeiro[8] | Fernando Pimentel-Santos[1,2] | Carina Lopes[1,2]

[1]NOVA Medical School, Universidade Nova de Lisboa, Lisbon, Portugal | [2]Rheumatology Department, Hospital de Egas Moniz, Unidade Local de Saúde de Lisboa Ocidental, Lisbon, Portugal | [3]Clinical Pathology Department, Hospital Professor Doutor Fernando Fonseca, Unidade Local de Saúde de Amadora/Sintra, Amadora, Portugal | [4]Oncology Department, Instituto Português de Oncologia Dr. Francisco Gentil, Lisbon, Portugal | [5]Internal Medicine Department, Hospital de Egas Moniz, Unidade Local de Saúde de Lisboa Ocidental, Lisbon, Portugal | [6]Radiology Department, Hospital Universitario de Bellvitge, Barcelona, Spain | [7]Radiology Department, Hospital de Egas Moniz, Unidade Local de Saúde de Lisboa Ocidental, Lisbon, Portugal | [8]Ophtalmology Department, Hospital de Egas Moniz, Unidade Local de Saúde de Lisboa Ocidental, Lisbon, Portugal

Correspondence: Ana Catarina Moniz (acmoniz040@gmail.com)

Dear Editor,

Paradoxical reactions (PRs) are defined as exacerbations or new onset of noninfectious inflammatory skin or other organ changes upon the use of a substance that is theoretically therapeutic [1]. These reactions can occur with any drug group, but their association with biological agents is receiving more attention globally. Reports indicate that PRs are more common with antitumor necrosis factor (TNF) drugs compared to other biologics, with etanercept being the most frequently described anti-TNF in the literature. However, there are also reports on infliximab, adalimumab, golimumab and certolizumab [1–3]. PRs typically manifest 6–12 months after starting the offending drug but can also occur after discontinuation of the medication. These reactions can occur in various conditions such as Crohn's Disease, psoriasis, spondyloarthritis (SpA), rheumatoid arthritis, and juvenile idiopathic arthritis. The incidence of PRs associated with anti-TNF agents in axial spondylarthritis (axSpA) was estimated to be 2–23 cases per 1000 person-years [4–6]. Enterocolitis, psoriasis, and arthritis are the most described PRs associated with anti-TNF therapy, but less common reactions such as sarcoidosis-like lesions are increasingly being reported [7]. A drug-induced sarcoid reaction (DISR) is characterized by a systemic granulomatous tissue reaction that resembles sarcoidosis and occurs in temporal relation to the initiation of an offending drug [8].

1 | Case Report

We present a case of a 52-year-old man with an 8-year history of axSpA, who initially presented with inflammatory back pain (IBP), peripheral arthritis, and two episodes of acute anterior uveitis (AAU). He had a medical history of hypertension managed with amlodipine and valsartan. The axSpA was initially treated with nonsteroidal anti-inflammatory drugs (NSAIDs) for 1 year, followed by adalimumab for 2 years, which led to the development of paradoxical psoriasis. After consulting with a rheumatologist and dermatologist, the decision was made to discontinue adalimumab due to limited information on paradoxical psoriasis at the time. The patient then participated in a clinical trial evaluating golimumab for axSpA with ocular involvement.

One year after starting golimumab, the patient reported right flank pain radiating to the groin associated with dysuria. Laboratory tests revealed elevated creatinine (2.62 mg/dL, reference range [RR] 0.7–1.20 mg/dL), urea (93 mg/dL, RR 13–43 mg/dL) and total calcium (12.2 mg/dL, RR 8.6–10.0 mg/dL), along with increased C-reactive protein (1.02 mg/dL, RR <0.50 mg/dL). He was diagnosed with nephrolithiasis and underwent ureteral stent placement. Despite this, he continued to experience recurrent flank pain, and subsequent tests showed persistent kidney dysfunction, elevated total calcium (14.3 mg/dL, RR

8.6–10.0 mg/dL) and phosphorus (5.2 mg/dL, RR 2.5–4.5 mg/dL), and decreased parathyroid hormone (PTH) (8 pg/mL, RR 15–65 pg/mL) and 25-hydroxyvitamin D (58 nmol/L, RR 75–250 nmol/L). Urinalysis evidenced hemoglobinuria. Imaging revealed multiple supraclavicular, mediastinal, pelvic, and retroperitoneal enlarged lymph nodes (the largest infracarinal node measuring 27 × 26 mm)—Figure 1. A 24-h urine analysis revealed a urinary calcium of 416 mg (RR of 100–300 mg/24 h). Further investigations, including colonoscopy, endoscopy, and thyroid ultrasound were unremarkable.

The patient was admitted for observation and started therapy with intravenous (IV) fluids, furosemide, and pamidronate. Golimumab was suspended. During hospital admission, serum total calcium and kidney function progressively improved. A comprehensive laboratory workup revealed a PTH-related protein level (PTHrp) of 0.02 pmol/L (RR < 4.2 pmol/L), erythrocyte sedimentation rate (ESR) of 74 mm/h (RR < 20 mm/h), angiotensin-converting enzyme (ACE) of 109 U/L (RR 20–70 U/L), and 1,25-dihydroxyvitamin D of 68.20 pg/mL (RR 18–64 pg/mL). Interferon-Gamma Release Assay (IGRA) was not performed due to prior treatment for latent tuberculosis. Two weeks after golimumab suspension, a CT scan was repeated, showing lymph node size reduction, with the largest lymph node measuring 17 × 15 mm. The patient underwent an endobronchial ultrasound-guided transbronchial needle aspiration (EBUS-TBNA) for cytological and histological examinations (to rule out malignancy, particularly lymphoma). Microbiological studies were also conducted, including direct and cultural tests for *Mycobacterium tuberculosis*. Cytology smears revealed an heterogenous population of lymphocytes, and no malignant cells were found. Flow cytometric immunophenotyping of the lymphadenopathy aspirate was negative for lymphoproliferative disease and revealed a CD4+/CD8+ ratio of 4.3 (RR < 3.5). Histological examination was not possible due to insufficient sample material. The patient was discharged after 13 days with improved total serum calcium and creatinine levels. Golimumab remained suspended. One month later, the patient experienced a new episode of AAU and started prednisolone 40 mg/day, with a tapering regimen. Blood tests were repeated after 4 months, showing improvement in serum calcium and creatinine levels. A follow-up CT scan confirmed size regression of the lymphadenopathies, with the largest node slightly above 10 mm.

A diagnosis of sarcoid reaction associated with anti-TNF therapy was made. The patient continued treatment with prednisolone 5 mg/day as prescribed by the Ophthalmologist, with normal blood tests after 15 months of follow-up. Prednisolone was eventually stopped, but a rise in total serum calcium and ACE prompted a restart of low-dose prednisolone. A PET scan revealed mild metabolic activity in mediastinal and hilar lymphadenopathy. The patient maintained prednisolone 5 mg/day long-term, with stable calcium and ACE levels. Due to worsening IBP (Axial Spondyloarthritis Disease Activity Score—ASDAS 4.2) and contraindication for NSAIDs (due to deteriorated renal function), certolizumab was started while maintaining prednisolone to control the sarcoid reaction. Three months later, serum calcium, ACE, and renal function remained stable, with improvement in back pain and functionality (ASDAS 1.2). No new episodes of AAU were reported. Calcium or vitamin D supplementation was not given to prevent exacerbation of hypercalcemia associated with the sarcoid reaction.

2 | Discussion

Paradoxical reactions are abnormal immunological reactions that can affect various organs. While psoriasiform skin reactions are the most reported manifestations, there are increasing reports of less common reactions such as sarcoidosis and similar granulomatous skin and lung lesions [9–11]. Drug-induced sarcoid reactions (DISR) are a type of PR characterized by systemic granulomatous tissue reactions that resemble sarcoidosis and occur after starting a specific drug. Several biologics, including etanercept, infliximab, and adalimumab have been associated with DISR, with etanercept being the most reported (more than 100 cases described) [1]. Certolizumab, golimumab, rituximab, and tocilizumab are less associated with DISR. The exact relationship between these drugs and sarcoidosis is not fully understood, but DISR presents similarly to sarcoidosis as a multi-organ granulomatous disease that can affect any organ or system [12]. However, it is not clear if these drugs are truly causing sarcoidosis, rendering the immune system more susceptible to the development of sarcoidosis, exacerbating subclinical cases of sarcoidosis, or causing conditions that are distinct from sarcoidosis [8]. Clinical manifestations of DISR often involve the respiratory tract (90% of cases), with symptoms ranging from
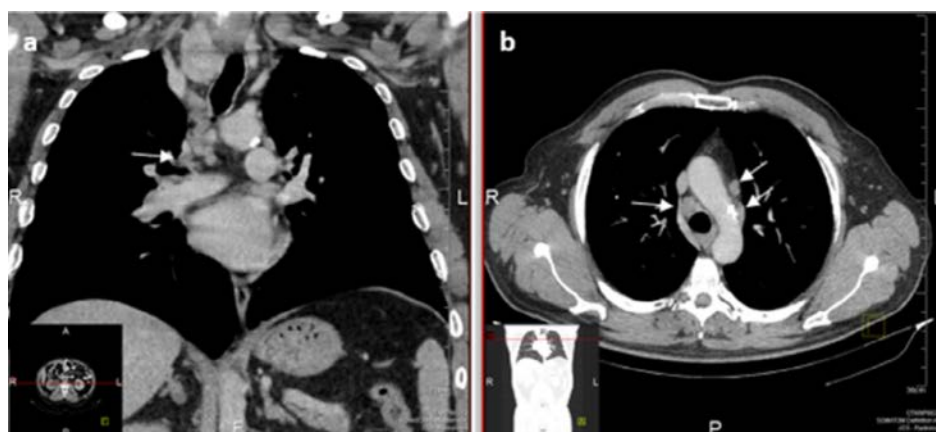
FIGURE 1 | Contrast-enhanced coronal (a) and axial (b) computed tomography at mediastinal windows show bilateral hilar and mediastinal lymphadenopathy (arrows).

hilar lymphadenopathy to fibrosis. Vitamin D dysregulation is common, caused by an increased conversion of vitamin D to its active form by activated macrophages in granulomas, leading to elevated levels of 1,25-dihydroxyvitamin D and potential complications such as hypercalciuria (50% of cases) and hypercalcemia (10% of cases). Renal involvement may result in renal calculi, while eye involvement, particularly uveitis, is reported in most cases (anterior uveitis accounting for 41%–81% of sarcoid uveitis) [13]. Uveitis in sarcoidosis tends to be bilateral and granulomatous, unlike the unilateral uveitis seen in SpA [14]. In this case, the uveitis was linked to SpA due to its clinical presentation and absence of specific granulomatous findings.

Diagnosing DISR and sarcoidosis involves excluding other potential causes through a comprehensive investigation, including primary hypoparathyroidism, cancer, and infection. Histological confirmation is crucial for a definitive diagnosis of sarcoidosis, particularly through the identification of noncaseating granulomatous inflammation. However, a presumptive diagnosis can be made based on clinical findings and laboratory tests. In this case, the sample size obtained was insufficient for histological analysis. It was not possible to repeat the procedure since the lymphadenopathies regressed following corticosteroid treatment, limiting further histological evaluation. Serum ACE is a commonly used biomarker and, although it has low sensitivity and specificity, genetic polymorphisms may affect its expression. When combined with other parameters such as blood and urine calcium levels, vitamin D, and immunoglobulin assays, it remains a valuable tool [12]. The presence of CD4+ lymphocytosis demonstrated by an elevated CD4+/CD8+ ratio, though typically determined in bronchoalveolar lavage fluid, can also be performed in lymphadenopathy aspirate. The normal ratio in lymphadenopathy samples is not universally established, but a ratio of > 3.5 is often indicative of sarcoidosis, especially when accompanied by elevated ACE levels and hypercalciuria [13, 14].

Treatment typically involves discontinuing the offending drug, with corticosteroids and anti-sarcoidosis therapies considered if necessary. Switching to a different drug within the same class may be an option in some cases, but severe reactions may warrant avoiding the same drug or class altogether [8, 15].

3 | Conclusion

We present a complex clinical case in which a patient experienced multiple PRs with various anti-TNF drugs. This required a multidisciplinary discussion among rheumatologists, pulmonologists, ophthalmologists, radiologists, and pharmacists to decide on the best therapeutic strategy. After thorough evaluation, certolizumab was chosen, as it is less commonly associated with PRs, especially DISR [1, 8]. Close monitoring will be crucial in the following months to ensure effective management of this challenging case.

Ana Catarina Moniz
Sónia Mota Faria
Madalena Silveira Machado
Manuela Zita Veiga
Mariana Teixeira
Tiago Saldanha
Miguel Cordeiro
Fernando Pimentel-Santos
Carina Lopes

References

1. I. Kremenevski, O. Sander, M. Sticherling, and M. Raithel, "Paradoxical Reactions to Biologicals in Chronic Inflammatory Systemic Diseases," *Deutsches Ärzteblatt International* 119 (2022): 88–95, https://doi.org/10.3238/arztebl.m2022.0067.

2. Z. Wang, M. D. Eugenio Capitle, M. D. Michael Jaker, M. D. Smita Mahendrakar, and R. Banerjee, "Golimumab Induced CNS, Pulmonary, and Cardiac Sarcoidosis-A Case Report and Literature Review," *American Journal of Medicine Case Reports* 4, no. 9 (2016): 298–300, https://doi.org/10.12691/ajmcr-4-9-1.

3. C. I. Daien, A. Monnier, P. Claudepierre, et al., "Sarcoid-Like Granulomatosis in Patients Treated With Tumor Necrosis Factor Blockers: 10 Cases," *Rheumatology* 48, no. 8 (2009): 883–886, https://doi.org/10.1093/rheumatology/kep046.

4. J. Braun, X. Baraliakos, J. Listing, et al., "Differences in the Incidence of Flares or New Onset of Inflammatory Bowel Diseases in Patients With Ankylosing Spondylitis Exposed to Therapy With Anti–Tumor Necrosis Factor α Agents," *Arthritis Care & Research (Hoboken)* 57, no. 4 (2007): 639–647, https://doi.org/10.1002/art.22669.

5. D. Fouache, V. Goeb, N. Massy-Guillemant, et al., "Paradoxical Adverse Events of Anti-Tumour Necrosis Factor Therapy for Spondyloarthropathies: A Retrospective Study," *Rheumatology* 48, no. 7 (2009): 761–764, https://doi.org/10.1093/rheumatology/kep083.

6. É. Toussirot and F. Aubin, "Paradoxical Reactions Under TNF-α Blocking Agents and Other Biological Agents Given for Chronic Immune-Mediated Diseases: An Analytical and Comprehensive Overview," *RMD Open* 2, no. 2 (2016): e000239, https://doi.org/10.1136/rmdopen-2015-000239.

7. A. Decock, G. Van Assche, S. Vermeire, W. Wuyts, and M. Ferrante, "Sarcoidosis-Like Lesions: Another Paradoxical Reaction to Anti-TNF Therapy?," *Journal of Crohn's and Colitis* 11 (2016): 378–383, https://doi.org/10.1093/ecco-jcc/jjw155.

8. A. Chopra, A. Nautiyal, A. Kalkanis, and M. A. Judson, "Drug-Induced Sarcoidosis-Like Reactions," *Chest* 154, no. 3 (2018): 664–677, https://doi.org/10.1016/j.chest.2018.03.056.

9. D. Koumaki, V. Koumaki, A. Katoulis, et al., "Adalimumab-Induced Scalp Psoriasis With Severe Alopecia as a Paradoxical Effect in a Patient With Crohn's Disease Successfully Treated With Ustekinumab," *Dermatologic Therapy* 33, no. 4 (2020): e13791, https://doi.org/10.1111/dth.13791.

10. N. Lian, L. Zhang, and M. Chen, "Tumor Necrosis Factors-α Inhibition-Induced Paradoxical Psoriasis: A Case Series and Literature Review," *Dermatologic Therapy* 33, no. 6 (2020): e14225, https://doi.org/10.1111/dth.14225.

11. A. Zangrilli, M. Bavetta, S. Mazzilli, V. Garofalo, and L. Bianchi, "Paradoxical Case Effects of Psoriasis Following Adalimumab Therapy: A Case Series," *Dermatologic Therapy* 31, no. 6 (2018): e12729, https://doi.org/10.1111/dth.12729.

12. E. Bargagli and A. Prasse, "Sarcoidosis: A Review for the Internist," *Internal and Emergency Medicine* 13, no. 3 (2018): 325–331, https://doi.org/10.1007/s11739-017-1778-6.

13. K. Oda, H. Ishimoto, K. Yatera, et al., "Relationship Between the Ratios of CD4/CD8 T-Lymphocytes in the Bronchoalveolar Lavage Fluid and Lymph Nodes in Patients With Sarcoidosis," *Respiratory Investigation* 52, no. 3 (2014): 179–183, https://doi.org/10.1016/j.resinv.2013.12.003.

14. T. Göktalay, P. Çelik, A. Ö. Alpaydın, et al., "The Role of Endobronchial Biopsy in the Diagnosis of Pulmonary Sarcoidosis," *Turkish Thoracic Journal* 17, no. 1 (2016): 22–27, https://doi.org/10.5578/ttj.17.1.004.

15. A. Baha, C. Hanazay, N. Kokturk, and H. Turktas, "A Case of Sarcoidosis Associated With Anti–Tumor Necrosis Factor Treatment," *Journal of Investigative Medicine High Impact Case Reports* 3, no. 1 (2015): 232470961557136, https://doi.org/10.1177/2324709615571366.

WILEY

International Journal of
Rheumatic Diseases

LETTER TO THE EDITOR

Comment on "Comparative Effectiveness of TNF-α and IL-6 Inhibitors on Bone Health Outcomes and Mortality in Rheumatoid Arthritis Patients"

Saraswati Sah[1] | Rachana Mehta[2] | Ranjana Sah[3,4] 🆔

[1]SR Sanjeevani Hospital, Kalyanpur, Siraha, Nepal | [2]Clinical Microbiology, RDC, Manav Rachna International Institute of Research and Studies, Faridabad, Haryana, India | [3]Department of Paediatrics, Dr. D. Y. Patil Medical College Hospital and Research Centre, Dr. D. Y. Patil Vidyapeeth (Deemed-to-be-University), Pune, Maharashtra, India | [4]Department of Public Health Dentistry, Dr. D. Y. Patil Dental College Hospital and Research Centre, Dr. D. Y. Patil Vidyapeeth (Deemed-to-be-University), Pune, Maharashtra, India

Correspondence: Ranjana Sah (ranjanasah384@gmail.com)

Dear Editor,

We read with great interest the study by Wang et al., which investigates the differential impact of TNF-α versus IL-6 inhibitors on osteoporosis, fracture risk, and mortality in rheumatoid arthritis (RA) patients using a large-scale, propensity-matched cohort derived from the TriNetX database [1]. While the authors conclude comparable effects on skeletal outcomes and a lower all-cause mortality associated with TNF-α inhibitors, several methodological and interpretive concerns warrant attention.

First, the study's central inference regarding all-cause mortality favoring TNF-α inhibitors raises concerns due to potential indication bias. IL-6 inhibitors are typically reserved for patients with more refractory disease or prior TNF-α treatment failure [2], yet the study excluded patients with prior treatment switches only post-index. Without adjusting for disease severity markers such as DAS28, CRP trends, or duration of untreated RA, which were not captured in the database, the observed mortality reduction may reflect channeling bias rather than a true pharmacologic advantage. Furthermore, while corticosteroid exposure was accounted for in subgroup analyses, the absence of cumulative dose quantification and treatment duration undercuts the validity of these stratifications, particularly given glucocorticoids' known effects on infection risk and mortality.

Second, although the authors state the fracture and osteoporosis outcomes were similar between groups, the endpoint definitions based solely on ICD-10 codes without confirmation through imaging (e.g., DXA scans) or biochemical parameters (e.g., serum osteocalcin, CTX) may have led to misclassification. This limitation is particularly relevant for subclinical osteoporosis, which may not be captured in claim-based data [3]. Moreover, the low absolute number of fracture events ($n = 10$ in each group) undermines the statistical power to detect meaningful differences and calls into question the reliability of the Cox model estimates for this outcome.

Third, while the adjusted hazard ratio for mortality (aHR 0.247, 95% CI 0.114–0.536) appears robust, the authors did not assess cause-specific mortality. This is critical given the differential immunomodulatory profiles of TNF-α and IL-6 inhibitors. IL-6 blockade has been associated with elevated lipid levels and potential cardiovascular risk [4], while TNF-α inhibitors are more closely linked to tuberculosis reactivation [5]. Without cause-specific data, attributing the mortality benefit to cardiovascular or infection-related protection remains speculative.

Finally, the study lacks granularity in medication adherence. While the inclusion criterion of "at least two prescriptions"

attempts to mitigate nonadherence, absence of data on dose intervals, drug discontinuation, or time to treatment failure limits clinical interpretability. The median follow-up of 365 days may also be insufficient to observe fracture development in RA patients, whose skeletal remodeling is slow and influenced by long-term inflammatory suppression [6].

In conclusion, while the study offers valuable real-world insights, the mortality benefit attributed to TNF-α inhibitors must be interpreted cautiously. Future prospective studies incorporating disease activity scores, adherence data, imaging-confirmed bone loss, and cause-specific mortality are needed to validate these findings.

Author Contributions

Saraswati Sah: conceptualization, methodology, validation, writing – original draft, writing – review and editing. **Rachana Mehta:** validation, investigation, writing – original draft, writing – review and editing. **Ranjana Sah:** supervision, project administration, validation, writing – original draft, writing – review and editing.

Disclosure

Generative AI tools, including Paperpal and ChatGPT-4o, were utilized solely for language, grammar, and stylistic refinement. These tools had no role in the conceptualization, data analysis, interpretation of results, or substantive content development of this manuscript. All intellectual contributions, data analysis, and scientific interpretations remain the sole work of the authors. The final content was critically reviewed and edited to ensure accuracy and originality. The authors take full responsibility for the accuracy, originality, and integrity of the work presented.

Ethics Statement

The authors have nothing to report.

Consent

The authors have nothing to report.

Data Availability Statement

The authors have nothing to report.

<div style="text-align: right">

Saraswati Sah
Rachana Mehta
Ranjana Sah

</div>

References

1. H. Wang, Y. Lee, I. Cheng, et al., "Comparative Effectiveness of TNF-α and IL-6 Inhibitors on Bone Health Outcomes and Mortality in Rheumatoid Arthritis Patients: A Retrospective Cohort Study," *International Journal of Rheumatic Diseases* 28 (2025), https://doi.org/10.1111/1756-185X.70204.

2. A. Alhendi and S. A. Naser, "The Dual Role of Interleukin-6 in Crohn's Disease Pathophysiology," *Frontiers in Immunology* (2023): 14, https://doi.org/10.3389/fimmu.2023.1295230.

3. A. O. Everhart, J. P. Brito, B. L. Clarke, et al., "Trends in Osteoporosis Drug Therapy Receipt Among Commercial and Medicare Advantage Enrollees in the United States, 2011–2022," *Journal of Clinical Endocrinology and Metabolism* (2025), https://doi.org/10.1210/clinem/dgae840.

4. F. Al-Rashed, H. AlSaeed, N. Almansour, F. Al-Mulla, Y. A. Hannun, and R. Ahmad, "IL-6R (Trans-Signaling) is a Key Regulator of Reverse Cholesterol Transport in Lipid-Laden Macrophages," *Clinical Immunology* 267 (2024): 110351.

5. M. V. de Oliveira, K. R. Bonfiglioli, C. M. F. Gomes, et al., "Tuberculin Skin Test Repetition After TNF-α Inhibitors in Patients With Chronic Inflammatory Arthritis: A Long-Term Retrospective Cohort in Endemic Area," *Advances in Rheumatology* 64 (2024): 70.

6. P. S. Kovalenko, I. S. Dydykina, P. O. Postnikova, S. I. Glukhova, and A. V. Smirnov, "Fractures of Vertebrae and Peripheral Bones in Patients With Rheumatoid Arthritis (Based on Long-Term Observation)," *Consilium Medicum* 26 (2024): 788–793.

EDITORIAL

Classification in Idiopathic Inflammatory Myopathies: Where Are We Now?

Keeran Shivakumar[1] | Ian Teh[2] | Latika Gupta[3,4,5] | Jessica Day[1,6,7]

[1]Department of Rheumatology, Royal Melbourne Hospital, Victoria, Australia | [2]Department of Rheumatology, Western Health, Victoria, Australia | [3]Department of Rheumatology, Royal Wolverhampton Hospitals NHS Trust, Wolverhampton, UK | [4]School of Infection, Inflammation and Immunology, College of Medicine and Health, University of Birmingham, Birmingham, UK | [5]Francis Crick Institute, London, UK | [6]Inflammation Division, Walter and Eliza Hall Institute of Medical Research, Victoria, Australia | [7]Department of Medical Biology, The University of Melbourne, Victoria, Australia

Correspondence: Jessica Day (jessica.day2@mh.org.au)

The classification of idiopathic inflammatory myopathies (IIMs) remains a significant challenge in the field of rheumatology and neuromuscular medicine. Despite advances in our understanding of these rare and heterogeneous diseases, the establishment of universally accepted classification criteria remains elusive. We recently highlighted substantial heterogeneity in the application of classification criteria, underscoring the need for unified frameworks [1].

This editorial examines the current landscape of IIM classification, highlighting the proliferation of competing frameworks, the evolving role of biomarkers, and the broader implications for clinical practice and research. We explore the key barriers to achieving consensus and highlight opportunities to balance scientific rigor with clinical utility, ultimately enhancing patient care and accelerating therapeutic innovation.

1 | Issue 1: Disease Heterogeneity, Rarity and the "Lump or Split" Dilemma

Idiopathic inflammatory myopathies (IIMs) represent a heterogeneous group of systemic autoimmune disorders and include polymyositis (PM), dermatomyositis (DM), clinically amyopathic dermatomyositis (CADM), immune-mediated necrotising myopathy (IMNM), anti-synthetase syndrome (ASyS), overlap myositis (OM), and inclusion body myositis (IBM). These conditions are characterized by a predilection for skeletal muscle

inflammation, although amyopathic forms exist. Additionally, these conditions often present with a spectrum of extra-muscular manifestations such as distinctive cutaneous lesions, interstitial lung disease, myocarditis, and arthritis. Variations in the clinical spectrum, prognosis, and therapeutic responses suggest distinct underlying pathophysiological mechanisms.

The rarity of IIM adds another layer of complexity to the classification dilemma. With limited patient populations available for study, generating robust data to support detailed subtyping is challenging, and the statistical power of many studies remains constrained. The scarcity of cases often necessitates lumping diverse clinical entities into broader categories to ensure sufficient cohort sizes for research, even if this oversimplifies the nuanced differences between subtypes. Historically, DM and PM have been studied together; however, contemporary literature indicates DM itself to be a highly heterogeneous condition characterized by distinct antibody-defined subtypes. Additionally, many conditions traditionally classified as PM have now been redefined into more precise subtypes such as IMNM and ASyS, rendering true PM extremely rare.

These issues of rarity and heterogeneity are reflected in the classification criteria landscape. A fundamental dilemma is whether classification criteria should adopt a broad framework which incorporates subtyping, as in the EULAR-ACR 2017 classification model [2] or whether IIM subtypes merit separate, detailed classification efforts, as exist for IMNM, IBM,

---

Keeran Shivakumar and Ian Teh contributed equally to this work.

CADM, and ASyS (Table 1). Over-arching IIM criteria promote standardization for research and reduce complexity. Distinct subtype classifications arguably enhance precision but risk fragmenting already limited research efforts.

2 | Issue 2: Disparate IIM Classification Efforts

The evolution of classification frameworks for IIM and the plethora of definitions employed in the contemporary literature highlights the complexities of classification. The pioneering framework established in 1975 by Bohan and Peter [3] focused on clinical features such as symmetrical proximal muscle weakness, elevated muscle enzyme levels, electromyographic abnormalities, and characteristic muscle biopsy findings. Despite its foundational importance, this early schema had notable limitations, including reliance on nonspecific electromyographic findings, imprecise definitions of DM skin lesions, and vague exclusion criteria. Over subsequent decades, the identification of new clinical subsets and an expanding spectrum of myositis-specific autoantibodies have rendered these early criteria increasingly inaccurate. As diagnostic techniques evolved, newer classification criteria were developed (Table 1). The EULAR/ACR classification criteria, introduced in 2017, represented a significant advancement by integrating clinical features, laboratory findings, muscle biopsy characteristics, and a defined autoantibody (anti-Jo1) [2]. Importantly, this represented the first data-driven classification system for IIMs which were validated with a robust methodology, a marked advance over previous criteria sets. However, the 2017 criteria have notable limitations: they do not include ASyS or OM as distinct subtypes and omit key clinical features such as mechanic's hands, shawl sign, and ILD, potentially leading to subtype misclassification and inflating the prevalence of polymyositis [4]. Additionally, IMNM was recognized as a distinct entity partway through the assembly of the derivation cohort, limiting its distinction from PM in the subclassification tree [2]. More broadly, another challenge across all IIM classification efforts is the substantial clinical heterogeneity within recognized subgroups, with important disease-specific features—such as anti-MDA-5 associated rapidly progressive ILD and the higher prevalence of malignancy linked to anti-TIF1-gamma and anti-NXP2 auto-antibodies [5]—often unaccounted for.

Efforts are currently underway to reassess and update the EULAR/ACR criteria [6]. Recent literature has highlighted the limitations of the ACR/EULAR classification criteria, noting that the inclusion of myositis-specific antibodies (MSAs), myositis-associated antibodies (MAAs), and neuromuscular imaging could enhance classification sensitivity [7, 8]. In parallel with the broader revision of EULAR/ACR criteria, several initiatives are focusing on refining the classification of specific IIM subtypes. For example, the absence of ASyS from the EULAR/ACR criteria is being addressed through a collaborative project aimed at developing dedicated criteria for ASyS as a distinct entity within the IIM framework: the CLASS project [9]. Beyond EULAR/ACR working group initiatives, other centres and collaborations have launched independent initiatives to refine IIM classification. These include efforts to classify amyopathic DM [10] and initiatives by the European Neuromuscular Centre (ENMC) targeting IBM [11], IMNM [12] and ASyS [13]. This growing landscape highlights the complexity of reaching a global consensus on the classification of IIM, with

TABLE 1 | A list of existing classification criteria of idiopathic inflammatory myopathies with their total citations and recent citation numbers as listed on Pubmed 17/02/25.

Classification criteria	Year	Total cites	Cites 2018–2024
IIM			
Bohan and Peter[3]	1975	715	371
Love[24]	1991	230	64
Dalakas[25]	1991	205	60
Tanimoto[26]	1995	71	25
Targoff[27]	1997	65	27
ENMC[28]	2004	304	186
Troyanov[29]	2005	139	63
Pestronk[30]	2011	39	20
EULAR/ACR[2]	2017	444	443
IBM			
Griggs[31]	1995	172	64
ENMC[32]	2013	134	102
ENMC – revision[11]	2014	14	14
Antisynthetase syndrome			
Connors[33]	2010	175	134
Solomon[34]	2011	118	97
Lega[35]	2015	103	80
Stenzel[13]	2024	2	2
IMNM			
ENMC[35]	2018	188	188
CADM			
Sontheimer[36]	2002	160	103
Concha[10]	2019	15	15

multiple consortia, not to mention numerous single-centre and discipline-specific initiatives, undertaking parallel efforts. It remains uncertain how these various efforts will be integrated with the proposed revision of EULAR/ACR IIM. We note that there have been at least 17 different classifications criteria proposed and used since the publication of the Bohan and Peter criteria (Table 1), suggesting that in real-world practice there is a lack of consensus on an accepted gold-standard criteria. This diversity underscores concerns highlighted in Section 1, that capturing the full heterogeneity of IIM within a single set of classification criteria may be inherently challenging.

Autoantibody testing presents its own constellation of challenges in IIM classification. Despite their central role in contemporary practice, significant issues persist with test standardization, interpretation, and accessibility. Commercial assays vary substantially in sensitivity and specificity, while immunoprecipitation—considered the gold standard—remains prohibitively

labor-intensive, expensive, and available only at specialized centers, creating substantial delays in diagnosis. Additionally, there is no unified model for interpreting these tests across laboratories and regions, with inconsistent reference ranges and reporting practices leading to potential misclassification. The validity of many newer antibody tests remains incompletely characterized, especially for antibodies like anti-HMGCR, anti-NXP2, and anti-MDA5, where clinical correlations continue to evolve. Further complicating matters, novel autoantibodies continue to emerge, suggesting our current panel captures only a fraction of the immunological diversity within IIMs. The ultimate solution may lie in precision phenotyping that integrates genetic profiling, comprehensive autoantibody screening, and molecular characterization to enable accurate classification and personalized therapeutic approaches that target specific pathophysiological pathways rather than broad clinical syndromes.

The evolution of classification criteria poses challenges in interpreting historical data. Researchers must navigate the divergence between past and current standards, integrating registry data and advancements in biomarkers and imaging technologies to refine classification systems [1]. For example, much of the existing evidence based on current myositis treatment strategies was derived from studies that collectively analyzed heterogeneous IIM populations without detailed consideration of distinct clinical subtypes. Similarly, our understanding of IIM malignancy risk predominantly stems from historical cohort per registry-based studies that may not have delineated subtypes as understood today.

3 | Issue 3: Rapid Advances in the Field Versus Prolonged, Labour-Intensive Data-Driven Classification Criteria Development

The field of IIM has experienced major advances that have transformed our understanding of these complex diseases. The discovery of novel autoantibodies has significantly refined our ability to delineate disease subtypes, while advances in imaging techniques, such as MRI and PET scans, have enhanced diagnostic precision by identifying subclinical muscle inflammation [14], patterns of muscle involvement, extra-muscular involvement [15] and targeting muscle biopsy [16]. Additionally, molecular studies have provided deeper insights into IIM pathophysiology, uncovering pathways and novel biomarkers [17]. Collectively, these advances have expanded the scope and complexity of classification, emphasizing the need for frameworks that accommodate rapidly evolving scientific knowledge.

However, the pace of discovery presents challenges for the field of classification. Developing robust, internationally accepted criteria requires extensive multidisciplinary collaboration, large-scale data collection, and careful validation, all of which take considerable time. Creation of the 2017 EULAR/ACR criteria, for example, began in 2004 [2], taking over a decade to publish, with clinical data collection taking place between 2008 and 2011. By the time of publication, commercially available autoantibody assays had evolved significantly and become more widely available, leaving a gap between the cohort data used to generate the criteria and the clinical phenotyping tools available to clinicians in practice. The prolonged timelines for classification

development can lead to frameworks that, while rigorous, may already be outdated by the time of their implementation. This creates a paradox where classification criteria, designed to standardize and advance the field, may lag behind current clinical and scientific knowledge. While data-driven classification criteria are regarded as the gold standard [18] because they provide evidence-based frameworks that promote reproducibility and standardization, they are inherently constrained by the quality and scope of the underlying dataset.

4 | Issue 4: Clinical Manifestations Versus Disease Pathophysiology

Traditionally, IIM classification systems have been led by clinicians with IIM-specific expertise and hence emphasize clinical features and organ-specific manifestations. This clinical approach has been instrumental in guiding diagnosis and treatment, but it risks oversimplifying the underlying biology and may fail to capture the shared molecular mechanisms that transcend organ-specific boundaries.

The advent of multi-omic profiling offers a transformative opportunity to rethink IIM classification from a molecularly driven, organ-agnostic perspective. Precision modeling may offer the most promising path forward for IIM classification. Liquid biopsies, which can capture circulating biomarkers including cell-free DNA, exosomes, and cytokines, represent a less invasive alternative to traditional muscle biopsies while potentially offering greater insights into disease activity and progression. Multi-omic studies integrating genomic, transcriptomic, proteomic, and metabolomic data are revealing molecular signatures that transcend traditional clinical boundaries, potentially redefining how we conceptualize these disorders [19]. Critically, emerging research on gene–environment interactions suggests that IIM development reflects complex interplays between genetic susceptibility and environmental triggers, including infections, medications, and ultraviolet exposure. Until we develop accurate classification systems incorporating these molecular insights, our field will likely remain decades behind other rheumatological conditions [20, 21] where newer pathophysiological drivers are established. The current literature continues to expand rapidly, often derived from cohorts using ambiguous or outdated classification criteria, creating a fragmented evidence base that impedes meaningful progress in understanding disease mechanisms and developing targeted therapies.

For example, DM is characterized by a prominent type 1 interferon signature [22]. As such, at a molecular level, DM shares greater similarity with other type 1 interferon-driven diseases, such as SLE, than with molecularly distinct myopathies like IMNM and IBM [23]. This observation raises critical questions about the appropriateness of classifying DM alongside other forms of myositis with fundamentally different underlying mechanisms.

5 | Issue 5: The Urgent Need for Unified and Updated Criteria

This is an exciting time in IIM research, with the field experiencing unprecedented expansion in clinical trials and therapeutic innovations. This rapidly evolving therapeutic landscape

highlights the pressing need for harmonized classification criteria to guide clinical research effectively. Beyond clinical trials, accurate disease definitions are also essential for developing clinical guidelines. Accurate and consistent classification also serves to attract research funding, direct research interest, and attract commercial investment by clearly delineating disease burden.

In spite of these challenges and limitations, there are clear paths forward. Future progress is contingent upon the synthesis of clinical data with contemporary molecular and imaging techniques, the establishment of dynamic, adaptable classification frameworks, and the strengthening of international collaborative networks. Open communication, transparency in data sharing, and sustained multidisciplinary engagement will be important to foster consensus and drive iterative refinement of classification systems. The ultimate solution may lie in precision phenotyping that integrates genetic profiling, comprehensive autoantibody screening, and molecular characterization to enable accurate classification and personalized therapeutic approaches that target specific pathophysiological pathways rather than broad clinical syndromes.

Author Contributions

Conceptualization: J.D. Data curation: J.D., K.S., I.T. Formal analysis: all authors Funding acquisition: J.D. Investigation: J.D., K.S., I.T. Methodology: all authors Project administration: J.D. Resources: J.D. Supervision: J.D., L.G. Validation: J.D., L.G. Visualization: all authors Writing – original draft preparation: K.S., I.T. Writing – review and editing: all authors.

Disclosure

L.G. and J.D.: The views and opinions expressed are solely those of the author and do not represent or reflect those of any affiliated institution.

Conflicts of Interest

The authors declare no conflicts of interest. J.D. has received consulting fees/research funding from NKARTA and CSL PTY LTD.

Data Availability Statement

The data that support the findings of this study are available from the corresponding author upon reasonable request.

References

Note: The references 24–36 are available in Supporting Information.

1. K. Shivakumar, E. Sun, O. Ma, L. Gupta, and J. Day, "Highlighting the Need for Consensus: Diverse Classification Strategies in Contemporary Research on Idiopathic Inflammatory Myopathies," *Arthritis & Rheumatology* 76, no. 10 (2024): 1573–1575, https://doi.org/10.1002/art.42932.

2. I. E. Lundberg, A. Tjarnlund, M. Bottai, et al., "2017 European League Against Rheumatism/American College of Rheumatology Classification Criteria for Adult and Juvenile Idiopathic Inflammatory Myopathies and Their Major Subgroups," *Annals of the Rheumatic Diseases* 76, no. 12 (2017): 1955–1964, https://doi.org/10.1136/annrheumdis-2017-211468.

3. A. Bohan and J. B. Peter, "Polymyositis and Dermatomyositis (First of Two Parts)," *New England Journal of Medicine* 292, no. 7 (1975): 344–347, https://doi.org/10.1056/NEJM197502132920706.

4. M. J. S. Parker, A. Oldroyd, M. E. Roberts, et al., "The Performance of the European League Against Rheumatism/American College of Rheumatology Idiopathic Inflammatory Myopathies Classification Criteria in an Expert-Defined 10 Year Incident Cohort," *Rheumatology (Oxford)* 58, no. 3 (2019): 468–475, https://doi.org/10.1093/rheumatology/key343.

5. A. G. S. Oldroyd, J. P. Callen, H. Chinoy, et al., "International Guideline for Idiopathic Inflammatory Myopathy-Associated Cancer Screening: an International Myositis Assessment and Clinical Studies Group (IMACS) Initiative," *Nature Reviews Rheumatology* 19, no. 12 (2023): 805–817, https://doi.org/10.1038/s41584-023-01045-w.

6. S. Glaubitz, D. Saygin, and I. E. Lundberg, "Current Efforts and Historical Perspectives on Classification of Idiopathic Inflammatory Myopathies," *Current Opinion in Rheumatology* 36, no. 6 (2024): 473–480, https://doi.org/10.1097/BOR.0000000000001042.

7. D. Saygin, S. Glaubitz, R. Zeng, et al., "Performance of the 2017 EULAR/ACR Classification Criteria for Adult and Juvenile Idiopathic Inflammatory Myopathies and Their Major Subgroups: A Scoping Review," *Clinical and Experimental Rheumatology* 42, no. 2 (2024): 403–412, https://doi.org/10.55563/clinexprheumatol/vuc5py.

8. Q. Luu, J. Day, A. Hall, V. Limaye, and G. Major, "External Validation and Evaluation of Adding MRI or Extended Myositis Antibody Panel to the 2017 EULAR/ACR Myositis Classification Criteria," *ACR Open Rheumatology* 1, no. 7 (2019): 462–468, https://doi.org/10.1002/acr2.11061.

9. S. Faghihi-Kashani, A. Yoshida, F. Bozan, et al., "Clinical Characteristics of Anti-Synthetase Syndrome: Analysis From the Classification Criteria for Anti-Synthetase Syndrome Project," *Arthritis & Rheumatology* 77, no. 4 (2025): 477–489, https://doi.org/10.1002/art.43038.

10. J. S. S. Concha, S. Pena, R. G. Gaffney, et al., "Developing Classification Criteria for Skin-Predominant Dermatomyositis: The Delphi Process," *British Journal of Dermatology* 182, no. 2 (2020): 410–417, https://doi.org/10.1111/bjd.18096.

11. J. B. Lilleker, E. Naddaf, C. G. J. Saris, et al., "272nd ENMC International Workshop: 10 Years of Progress – Revision of the ENMC 2013 Diagnostic Criteria for Inclusion Body Myositis and Clinical Trial Readiness. 16–18 June 2023, Hoofddorp, The Netherlands," *Neuromuscular Disorders* 37 (2024): 36–51. https://doi.org/10.1016/j.nmd.2024.03.001.

12. Y. Allenbach, A. L. Mammen, O. Benveniste, W. Stenzel, and Immune-Mediated Necrotizing Myopathies Working Group, "224th ENMC International Workshop:: Clinico-Sero-Pathological Classification of Immune-Mediated Necrotizing Myopathies Zandvoort, The Netherlands, 14–16 October 2016," *Neuromuscular Disorders* 28, no. 1 (2018): 87–99, https://doi.org/10.1016/j.nmd.2017.09.016.

13. W. Stenzel, A. L. Mammen, L. Gallay, et al., "273rd ENMC International Workshop: Clinico-Sero-Morphological Classification of the Antisynthetase Syndrome. Amsterdam, The Netherlands, 27–29 October 2023," *Neuromuscular Disorders* 45 (2024): 104453, https://doi.org/10.1016/j.nmd.2024.104453.

14. J. A. Day, N. Bajic, S. Gentili, S. Patel, and V. Limaye, "Radiographic Patterns of Muscle Involvement in the Idiopathic Inflammatory Myopathies," *Muscle & Nerve* 60, no. 5 (2019): 549–557, https://doi.org/10.1002/mus.26660.

15. G. Bentick, J. Fairley, S. Nadesapillai, I. Wicks, and J. Day, "Defining the Clinical Utility of PET or PET-CT in Idiopathic Inflammatory Myopathies: A Systematic Literature Review," *Seminars in Arthritis and*

Rheumatism 57 (2022): 152107, https://doi.org/10.1016/j.semarthrit.2022.152107.

16. S. Lassche, B. H. Janssen, T. Ijzermans, et al., "MRI-Guided Biopsy as a Tool for Diagnosis and Research of Muscle Disorders," *Journal of Neuromuscular Diseases* 5, no. 3 (2018): 315–319, https://doi.org/10.3233/JND-180318.

17. O. Benveniste, H. H. Goebel, and W. Stenzel, "Biomarkers in Inflammatory Myopathies – An Expanded Definition," *Frontiers in Neurology* 10 (2019): 554, https://doi.org/10.3389/fneur.2019.00554.

18. R. Aggarwal, S. Ringold, D. Khanna, et al., "Distinctions Between Diagnostic and Classification Criteria?," *Arthritis Care & Research (Hoboken)* 67, no. 7 (2015): 891–897, https://doi.org/10.1002/acr.22583.

19. S. Gao, H. Luo, H. Zhang, X. Zuo, L. Wang, and H. Zhu, "Using Multi-Omics Methods to Understand Dermatomyositis/Polymyositis," *Autoimmunity Reviews* 16, no. 10 (2017): 1044–1048, https://doi.org/10.1016/j.autrev.2017.07.021.

20. G. J. Brown, P. F. Cañete, H. Wang, et al., "TLR7 Gain-of-Function Genetic Variation Causes Human Lupus," *Nature* 605, no. 7909 (2022): 349–356, https://doi.org/10.1038/s41586-022-04642-z.

21. C. G. Vinuesa, N. Shen, and T. Ware, "Genetics of SLE: Mechanistic Insights From Monogenic Disease and Disease-Associated Variants," *Nature Reviews. Nephrology* 19, no. 9 (2023): 558–572, https://doi.org/10.1038/s41581-023-00732-x.

22. S. A. Greenberg, "Dermatomyositis and Type 1 Interferons," *Current Rheumatology Reports* 12, no. 3 (2010): 198–203, https://doi.org/10.1007/s11926-010-0101-6.

23. S. H. Jiang, M. Stanley, and C. G. Vinuesa, "Rare Genetic Variants in Systemic Autoimmunity," *Immunology and Cell Biology* 98, no. 6 (2020): 490–499, https://doi.org/10.1111/imcb.12339.

Supporting Information

Additional supporting information can be found online in the Supporting Information section.

EDITORIAL

Taiwan's National Health Insurance Research Database: A Silent Force Behind Global Changes in Clinical Practice and Guidelines

Ting-Chun Tseng[1,2] | Renin Chang[1,3] | Jin-Shuen Chen[4,5] | James Cheng-Chung Wei[6,7,8,9]

[1]Department of Medical Education and Research, Kaohsiung Veterans General Hospital, Kaohsiung, Taiwan | [2]Department of Internal Medicine, Kaohsiung Veterans General Hospital, Kaohsiung, Taiwan | [3]Institute of Medicine, Chung Shan Medical University, Taichung, Taiwan | [4]Department of Administration, Kaohsiung Veterans General Hospital, Kaohsiung, Taiwan | [5]Institute of Precision Medicine, National sun Yat-Sen University, Kaohsiung, Taiwan | [6]Shanxi Bethune Hospital, Shanxi Academy of Medical Sciences, Third Hospital of Shanxi Medical University, Tongji Shanxi Hospital, Taiyuan, China | [7]Department of Allergy, Immunology and Rheumatology, Chung Shan Medical University Hospital, Taichung, Taiwan | [8]Graduate Institute of Integrated Medicine, China Medical University, Taichung, Taiwan | [9]Institute of Medicine/Department of Nursing, Chung Shan Medical University, Taichung, Taiwan

Correspondence: Jin-Shuen Chen (dgschen@vghks.gov.tw) | James Cheng-Chung Wei (wei3228@gmail.com)

The Taiwan National Health Insurance Research Database (NHIRD) stands as one of the world's most comprehensive healthcare information systems. Emerging from Taiwan's universal National Health Insurance program in 1995, the NHIRD systematically captures claims data from beneficiaries who represent over 99.5% of the population. Since 2000, this repository has documented an extensive range of healthcare interactions, encompassing patient demographics, outpatient and inpatient claims, prescription records, and detailed medical facility information. Following its transition in 2016 to management by Taiwan's Ministry of Health and Welfare Data Science Centre, the NHIRD now supports advanced cross-database linkages, incorporating key clinical variables such as laboratory results, cancer staging, disability assessments, and socioeconomic indicators [1], representing a key strength when compared to other national health insurance databases (Table 1).

The NHIRD's strength lies in its well-validated data across a spectrum of health conditions, from common ailments to severe diseases including ischemic stroke, atrial fibrillation (AF), hypertension, diabetes, hyperlipidemia, and cancer. With

demonstrated modest to high sensitivity and positive predictive values, this database serves as an invaluable resource for understanding disease burden, optimizing treatment strategies, and evaluating outcomes [1, 2].

1 | From Evidence to Recommendations: Atrial Fibrillation as an Example

To demonstrate the NHIRD's influence on clinical practice, we looked into its contributions to the 2024 European Society of Cardiology (ESC) Guidelines for Atrial Fibrillation (AF) Management. Of the 1248 references screened from the guideline, approximately 1% (12 studies) originated from NHIRD analyses (Table 2), each providing significant insights into AF management strategies [15]. Several studies identified high-risk populations at elevated risk for thromboembolic events and stroke among Taiwanese patients [3, 4, 7, 8, 11]. A particularly influential study by Hsu et al. found that patients with concurrent hypertrophic cardiomyopathy (HCM) and AF experienced a high incidence of stroke, regardless of their CHA2DS2-VASc

---

Ting-Chun Tseng and Renin Chang contributed equally as the first authors.

TABLE 1 | Strengths and limitations of Taiwan's and Korea's national health insurance databases.

	Taiwan national health insurance research database	Korean national health insurance database
Strengths	• Covers over 99% of Taiwanese citizens (~23 million) under the National Health Insurance • Primarily claims data, including inpatient, outpatient, prescriptions, diagnoses, and interventions • Strong centralized linkage infrastructure since 2016 via Health and Welfare Data Science Center (birth, death, cancer registry, health surveys, socioeconomic data) • Unique encrypted identifiers; strong long-term follow-up • ICD-9-CM initially; transitioned to ICD-10 around 2016	• Covers approximately 97% of Koreans (~50 million) under the National Health Insurance Service • Primarily claims data plus national health screening data, including anthropometrics and lifestyle surveys (e.g., smoking, alcohol, exercise) • Linkage to external registries (e.g., death, cancer) possible but project-specific and approval-dependent • De-identified personal identifiers; strong long-term follow-up. • ICD-10 coding adopted from early 2000s • Availability of cohort sub-databases (e.g., National Sample Cohort) for targeted studies
Limitations	• Limited clinical detail; missing labs, imaging, disease severity or subtype, and lifestyle data unless linked • Potential coding errors and disease misclassification; ICD-9 to ICD-10 transition handling needed • Uninsured healthcare services not captured • Confounding by indication and unmeasured variables limits causal inference	• Limited clinical detail; risk of healthy screener bias due to health exam participation • Potential coding errors and disease misclassification • Uninsured healthcare services not captured • Confounding by indication and unmeasured variables limits causal inference

score. This finding directly influenced current practice, leading to a Class IB recommendation for non-vitamin K antagonist oral anticoagulants (NOACs) in HCM patients with AF [4, 15].

Further research enhanced our understanding of risk assessment strategies. Two studies demonstrated that dynamic monitoring of CHA2DS2-VASc and HAS-BLED scores provided superior risk prediction compared to static baseline measurements [5, 6]. This evidence supported the current Class IB recommendation for periodic reassessment of both thromboembolic and bleeding risks in AF management.

The database also yielded important insights into therapeutic approaches. Three studies investigating antidiabetic agents revealed potential protective effects against AF onset and related hospitalizations [12–14]. These findings influenced the guidelines' Class IIa recommendation to consider metformin or SGLT2 inhibitors for AF prevention in patients with type 2 diabetes mellitus [12, 13, 15]. Additional investigations expanded our knowledge of NOAC therapy, examining mortality outcomes in specific populations such as cancer patients [9], and evaluating their safety and efficacy in very elderly patients aged 90 years or older [10].

2 | Exploring Medication Risks and Benefits: An International Dialogue

The NHIRD has proven valuable for pharmacoepidemiologic research and pharmacovigilance efforts. A landmark investigation by Lee et al. in 2015 examined the association between fluoroquinolone therapy and the risk of aortic complications through a nested case–control analysis of 1477 cases and 147,700 matched controls [16]. The study revealed increased risks of

aortic aneurysm or dissection with both current use (rate ratio [RR], 2.43; 95% confidence interval [CI], 1.83–3.22) and past use (RR, 1.48; 95% CI, 1.18–1.86) of fluoroquinolones. These findings gained international validation when Pasternak et al. published corroborating evidence from Swedish national registers in 2018, demonstrating elevated risks of aortic complications with fluoroquinolone use compared to amoxicillin [17]. The cumulative evidence led the U.S. Food and Drug Administration to issue a safety warning that same year, advising against fluoroquinolone use in patients with or at risk for aortic aneurysm and recommending immediate discontinuation if suspicious symptoms develop [18].

Beyond drug safety, The NHIRD has also contributed significantly to our understanding of therapeutic benefits across various pharmacological interventions. Researchers have extensively studied medications including statins, metformin, and newer antidiabetic agents—such as thiazolidinediones, dipeptidyl peptidase-4 inhibitors, SGLT2 inhibitors, and GLP-1 receptor agonists—to evaluate their impact on diverse health outcomes [19]. A frequently cited investigation by Lee et al. examined metformin's potential protective effects against gastrointestinal cancers in a large Taiwanese cohort [20]. Their analysis revealed that diabetic patients not using anti-hyperglycemic medications showed at least double the cancer incidence compared to non-diabetic individuals, while metformin users demonstrated cancer rates similar to those without diabetes.

In addition, target trial emulation (TTE) has been increasingly embraced as a methodological framework for enhancing causal inference from observational data. A recent study by Yen et al. [21] applied sequential TTE in alignment with the two-step framework proposed by Hernán and colleagues [22]. Using NHIRD data, they compared the risks of major adverse

TABLE 2 | Synthesis summary of studies utilizing Taiwan's national health insurance research database in the 2024 European society of cardiology guidelines for the management of atrial fibrillation.

Title	Authors, publication year, and journal	Objective	Main study findings	Implications or influence on guideline
Different implications of heart failure, ischemic stroke, and mortality between nonvalvular atrial fibrillation and atrial flutter–a view from a national cohort study [3]	Lin et al. 2017. *J Am Heart Assoc*	To compare the incidence of ischemic stroke, heart failure hospitalization, and all-cause mortality between patients with nonvalvular atrial fibrillation (AF) and atrial flutter (AFL)	AF patients had significantly higher ischemic stroke, heart failure hospitalization, and mortality rates compared to AFL patients	Provides regional data on thromboembolic risk differences between AF and AFL
Stroke risk in hypertrophic cardiomyopathy patients with atrial fibrillation: a nationwide database study [4]	Hsu et al. 2020. *Aging (Albany NY)*	To determine the incidence of stroke and its risk factors in hypertrophic cardiomyopathy (HCM) patients with AF during long-term follow-up	HCM patients with AF had high stroke incidence regardless of CHA2DS2-VASc score	Oral anticoagulation (OAC) is recommended in all patients with AF and HCM, regardless of CHA2DS2-VASc score to prevent ischemic stroke and thromboembolism (Class I, Level B)
Relationship of aging and incident comorbidities to stroke risk in patients with atrial fibrillation [5]	Chao et al. 2018. *J Am Coll Cardiol*	To determine if the "Delta CHA2DS2-VASc score" is more predictive of ischemic stroke than the baseline CHA2DS2-VASc score in patients with AF	Delta CHA2DS2-VASc score better predicted ischemic stroke than baseline score	Individualized reassessment of thromboembolic risk is recommended at periodic intervals in patients with AF to ensure anticoagulation is started in appropriate patients (Class I, Level B)

TABLE 2 | (Continued)

Title	Authors, publication year, and journal	Objective	Main study findings	Implications or influence on guideline
Incident risk factors and major bleeding in patients with atrial fibrillation treated with oral anticoagulants: a comparison of baseline, follow-up and Delta HAS-BLED scores [6]	Chao et al. 2018. *Thromb Haemost*	To assess changes in bleeding risk factors and HAS-BLED scores in AF patients and determine whether the follow-up or Delta HAS-BLED score better predicts major bleeding than the baseline score	Follow-up and Delta HAS-BLED scores better predicted major bleeding than baseline score	Management of modifiable bleeding risk factors is crucial for safe anticoagulation use
Risk factors and incidence of ischemic stroke in Taiwanese with nonvalvular atrial fibrillation—a nationwide database analysis [7]	Lin et al. 2011. *Atherosclerosis*	To investigate the risk factors of ischemic stroke in Taiwanese patients with AF and compare them with western populations	AF, age, hypertension, diabetes mellitus, heart failure, previous ischemic stroke or transient ischemic attack, and peripheral arterial disease (PAD) identified as ischemic stroke risk factors	PAD predicts higher stroke and mortality risks in AF patients, emphasizing its role in risk stratification
Incident thromboembolism and heart failure associated with new-onset atrial fibrillation in cancer patients [8]	Hu et al. 2013. *Int J Cardiol*	To investigate the epidemiology of new-onset AF in cancer patients and its relation to thromboembolism, heart failure, and mortality	New-onset AF in cancer patients was associated with increased thromboembolism and heart failure but not mortality	New-onset AF in cancer patients warrants close monitoring for thromboembolic complications

(Continues)

TABLE 2 | (Continued)

Title	Authors, publication year, and journal	Objective	Main study findings	Implications or influence on guideline
Mortality associated with the use of non-vitamin K antagonist oral anticoagulants in cancer patients: dabigatran versus rivaroxaban [9]	Lin et al. 2021. *Cancer Med*	To assess the mortality outcomes of non-vitamin K antagonist oral anticoagulants (NOACs) in cancer patients with AF and venous thromboembolism (VTE)	Dabigatran was associated with lower cancer-related death, all-cause mortality, and major bleeding than rivaroxaban	DOACs show better safety and comparable efficacy to VKAs in cancer patients with AF and VTE
Oral anticoagulation in very elderly patients with atrial fibrillation: a nationwide cohort study [10]	Chao et al. 2018. *Circulation*	To investigate the risk of ischemic stroke, intracranial hemorrhage (ICH), and the net clinical benefit of OAC treatment in very elderly patients (≥90 years) with AF	Warfarin reduced ischemic stroke risk; NOACs had lower intracranial hemorrhage risk but similar stroke prevention efficacy	NOACs may be the preferred option for elderly AF patients, although their use is limited by prescription biases
Association of a family history of atrial fibrillation with incidence and outcomes of atrial fibrillation: a population-based family cohort study [11]	Chang et al. 2017. *JAMA Cardiol*	To measure the genetic and environmental contributions to AF and to estimate the association of a family history of AF with major adverse cardiovascular events (MACE)	Genetics accounted for 19.9% of AF variance; nonshared environmental factors accounted for 76.6%. A family history of AF did not predict worse MACE-free survival	Provides data on the association between family history and factors linked to incident AF

(Continues)

TABLE 2 | (Continued)

Title	Authors, publication year, and journal	Objective	Main study findings	Implications or influence on guideline
Association of metformin with lower atrial fibrillation risk among patients with type 2 diabetes mellitus: a population-based dynamic cohort and in vitro studies [12]	Chang et al. 2014. *Cardiovasc Diabetol*	To investigate whether metformin reduces the risk of AF in patients with type 2 diabetes mellitus (T2DM) and its effects on atrial cell myolysis and oxidative stress	Metformin was associated with lower AF risk, reduced myolysis, and oxidative stress in atrial cells, indicating a protective effect against AF	Metformin or SGLT2 inhibitors should be considered for individuals needing pharmacological management of diabetes mellitus to prevent AF (Class IIa, Level B)
Metformin use is associated with a lower incidence of hospitalization for atrial fibrillation in patients with type 2 diabetes mellitus [13]	Tseng et al. 2021. *Front Med (Lausanne)*	To compare the incidence of AF-related hospitalization between ever and never users of metformin in patients with newly diagnosed T2DM	Metformin users had lower AF-related hospitalization risk with a dose–response relationship observed	Metformin or SGLT2 inhibitors should be considered for individuals needing pharmacological management of diabetes mellitus to prevent AF (Class IIa, Level B)
Dipeptidyl peptidase-4 inhibitor decreases the risk of atrial fibrillation in patients with type 2 diabetes: a nationwide cohort study in Taiwan [14]	Chang et al. 2017. *Cardiovasc Diabetol*	To evaluate whether dipeptidyl peptidase-4 inhibitor (DPP4i) use is associated with a lower risk of new-onset AF in patients with diabetes treated with metformin	DPP4i users had lower AF risk compared to other second-line therapies; older age, hypertension, and IHD were independent AF risk factors	DPP-4i reduce the risk of new-onset AF and reaffirms that metformin is associated with lower rates of incident AF

kidney and cardiovascular events between patients with stage 5 chronic kidney disease, SGLT2 inhibitor users and nonusers. Importantly, the study followed two critical principles: synchronization of eligibility determination and treatment assignment at time zero, which avoided immortal time bias and maintained the comparability of treatment groups; and adequate confounding adjustment, which ensured that baseline differences between users and nonusers were addressed [21, 22]. By using these practices, the study shows how the target trial framework offers a methodical and disciplined procedure for operationalizing good practices in study design and data analysis, thereby enabling more credible and actionable causal inferences to be drawn from observational data [23].

3 | Early Diagnosis of Important Diseases

Population-based studies provide high-quality evidence with important clinical implications, particularly for rare autoimmune diseases. Wei et al. found that patients with immune thrombocytopenic purpura (ITP) had a 26.8-fold increased risk of developing systemic lupus erythematosus (SLE) over 16 years [24]. Their findings suggest that ITP may represent an early manifestation of SLE, underscoring the need for timely rheumatology referral to facilitate early diagnosis before organ involvement occurs. Early recognition of evolving SLE can also inform treatment decisions, such as delaying splenectomy or initiating disease-modifying therapy.

Population-based research plays a critical role in elucidating disease progression, guiding earlier interventions, and ultimately improving long-term patient outcomes. As analytical techniques evolve and cross-database linkages expand, the NHIRD is poised to make further impactful contributions to global healthcare.

Author Contributions

Writing – original draft preparation: Ting-Chun Tseng. Writing – review and editing: Ting-Chun Tseng and Renin Chang. Supervision: Jin-Shuen Chen and James Cheng-Chung Wei. All authors have read and agreed to the published version of the manuscript.

Conflicts of Interest

Renin Chang is currently the associate editor of International Journal of Rheumatic Diseases and had no role in the peer review process of or decision to publish this article. The other authors declared no conflicts of interest in writing this paper.

Data Availability Statement

The data that support the findings of this study are available on request from the corresponding author. The data are not publicly available due to privacy or ethical restrictions.

References

1. C. Y. Hsieh, C. C. Su, S. C. Shao, et al., "Taiwan's National Health Insurance Research Database: Past and Future," *Clinical Epidemiology* 11 (2019): 349–358.

2. C. H. Tang, F. Yu, C. Y. Huang, and D. Y. Chen, "Potential Benefits of Biologics on Stroke and Mortality in Patients With Rheumatoid Arthritis: A Nationwide Population-Based Cohort Study in Taiwan," *International Journal of Rheumatic Diseases* 22, no. 8 (2019): 1544–1552.

3. Y. S. Lin, T. H. Chen, C. C. Chi, et al., "Different Implications of Heart Failure, Ischemic Stroke, and Mortality Between Nonvalvular Atrial Fibrillation and Atrial Flutter—A View From a National Cohort Study," *Journal of the American Heart Association* 6, no. 7 (2017): e006406.

4. J. C. Hsu, Y. T. Huang, and L. Y. Lin, "Stroke Risk in Hypertrophic Cardiomyopathy Patients With Atrial Fibrillation: A Nationwide Database Study," *Aging (Albany NY)* 12, no. 23 (2020): 24219–24227.

5. T. F. Chao, G. Y. H. Lip, C. J. Liu, et al., "Relationship of Aging and Incident Comorbidities to Stroke Risk in Patients With Atrial Fibrillation," *Journal of the American College of Cardiology* 71, no. 2 (2018): 122–132.

6. T. F. Chao, G. Y. H. Lip, Y. J. Lin, et al., "Incident Risk Factors and Major Bleeding in Patients With Atrial Fibrillation Treated With Oral Anticoagulants: A Comparison of Baseline, Follow-Up and Delta HAS-BLED Scores With an Approach Focused on Modifiable Bleeding Risk Factors," *Thrombosis and Haemostasis* 118, no. 4 (2018): 768–777.

7. L. Y. Lin, C. H. Lee, C. C. Yu, et al., "Risk Factors and Incidence of Ischemic Stroke in Taiwanese With Nonvalvular Atrial Fibrillation—A Nation Wide Database Analysis," *Atherosclerosis* 217, no. 1 (2011): 292–295.

8. Y. F. Hu, C. J. Liu, P. M. Chang, et al., "Incident Thromboembolism and Heart Failure Associated With New-Onset Atrial Fibrillation in Cancer Patients," *International Journal of Cardiology* 165, no. 2 (2013): 355–357.

9. Y. S. Lin, F. C. Kuan, T. F. Chao, et al., "Mortality Associated With the Use of Non-Vitamin K Antagonist Oral Anticoagulants in Cancer Patients: Dabigatran Versus Rivaroxaban," *Cancer Medicine* 10, no. 20 (2021): 7079–7088.

10. T. F. Chao, C. J. Liu, Y. J. Lin, et al., "Oral Anticoagulation in Very Elderly Patients With Atrial Fibrillation: A Nationwide Cohort Study," *Circulation* 138, no. 1 (2018): 37–47.

11. S. H. Chang, C. F. Kuo, I. J. Chou, et al., "Association of a Family History of Atrial Fibrillation With Incidence and Outcomes of Atrial Fibrillation: A Population-Based Family Cohort Study," *JAMA Cardiology* 2, no. 8 (2017): 863–870.

12. S. H. Chang, L. S. Wu, M. J. Chiou, et al., "Association of Metformin With Lower Atrial Fibrillation Risk Among Patients With Type 2 Diabetes Mellitus: A Population-Based Dynamic Cohort and In Vitro Studies," *Cardiovascular Diabetology* 13 (2014): 123.

13. C. H. Tseng, "Metformin Use Is Associated With a Lower Incidence of Hospitalization for Atrial Fibrillation in Patients With Type 2 Diabetes Mellitus," *Frontiers in Medicine* 7 (2020): 592901.

14. C. Y. Chang, Y. H. Yeh, Y. H. Chan, et al., "Dipeptidyl Peptidase-4 Inhibitor Decreases the Risk of Atrial Fibrillation in Patients With Type 2 Diabetes: A Nationwide Cohort Study in Taiwan," *Cardiovascular Diabetology* 16, no. 1 (2017): 159.

15. I. C. Van Gelder, M. Rienstra, K. V. Bunting, et al., "ESC Guidelines for the Management of Atrial Fibrillation Developed in Collaboration With the European Association for Cardio-Thoracic Surgery (EACTS)," *European Heart Journal* 45, no. 36 (2024): 3314–3414.

16. C. C. Lee, M. T. Lee, Y. S. Chen, et al., "Risk of Aortic Dissection and Aortic Aneurysm in Patients Taking Oral Fluoroquinolone," *JAMA Internal Medicine* 175, no. 11 (2015): 1839–1847.

17. B. Pasternak, M. Inghammar, and H. Svanström, "Fluoroquinolone Use and Risk of Aortic Aneurysm and Dissection: Nationwide Cohort Study," *BMJ (Clinical Research Ed.)* 360 (2018): k678.

18. FDA Warns About Increased Risk of Ruptures or Tears in the Aorta Blood Vessel With Fluoroquinolone Antibiotics in Certain Patients (2018).

19. S. F. Sung, C. Y. Hsieh, and Y. H. Hu, "Two Decades of Research Using Taiwan's National Health Insurance Claims Data: Bibliometric and Text Mining Analysis on PubMed," *Journal of Medical Internet Research* 22, no. 6 (2020): e18457.

20. M. S. Lee, C. C. Hsu, M. L. Wahlqvist, H. N. Tsai, Y. H. Chang, and Y. C. Huang, "Type 2 Diabetes Increases and Metformin Reduces Total, Colorectal, Liver and Pancreatic Cancer Incidences in Taiwanese: A Representative Population Prospective Cohort Study of 800,000 Individuals," *BMC Cancer* 11 (2011): 20.

21. F. S. Yen, C. M. Hwu, J. S. Liu, Y. L. Wu, K. Chong, and C. C. Hsu, "Sodium-Glucose Cotransporter-2 Inhibitors and the Risk for Dialysis and Cardiovascular Disease in Patients With Stage 5 Chronic Kidney Disease," *Annals of Internal Medicine* 177, no. 6 (2024): 693–700.

22. M. A. Hernán, I. J. Dahabreh, B. A. Dickerman, and S. A. Swanson, "The Target Trial Framework for Causal Inference From Observational Data: Why and When Is It Helpful?," *Annals of Internal Medicine* 178, no. 3 (2025): 402–407.

23. E. L. Fu, "Target Trial Emulation to Improve Causal Inference From Observational Data: What, Why, and How?," *American Society of Nephrology: JASN* 34, no. 8 (2023): 1305–1314.

24. F. X. Zhu, J. Y. Huang, Z. Ye, Q. Q. Wen, and J. C. Wei, "Risk of Systemic Lupus Erythematosus in Patients With Idiopathic Thrombocytopenic Purpura: A Population-Based Cohort Study," *Annals of the Rheumatic Diseases* 79, no. 6 (2020): 793–799.

WILEY

LETTER TO THE EDITOR

Accuracy of Screening for Symptoms of Anxiety and Depression Among Patients With Rheumatoid Arthritis in Private Physiotherapy Practices

Davy Vancampfort[1,2,3] 🄳 | Isabel Zwahlen[1] | Veerle Gillis[4] | Emanuel Brunner[5,6] | Tine Van Damme[1,2]

[1]Department of Rehabilitation Sciences, KU Leuven, Leuven, Belgium | [2]University Psychiatric Centre KU Leuven, Kortenberg, Belgium | [3]Leuven Brain Institute, Leuven, Belgium | [4]University Hospital Gasthuisberg, Leuven, Belgium | [5]Department of Physiotherapy and Rehabilitation, Winterthur Cantonal Hospital, Winterthur, Switzerland | [6]Department of Health, OST – Eastern Swiss University of Applied Sciences, St. Gallen, Switzerland

Correspondence: Davy Vancampfort (davy.vancampfort@kuleuven.be)

Dear Editor,

Physiotherapists play a vital role in managing rheumatoid arthritis (RA) by improving physical function, reducing pain, and promoting joint mobility through tailored exercise, manual therapy, and patient education [1, 2]. Recent research [3, 4] highlights the importance of integrating psychological support into physiotherapy for RA patients. Given their frequent and extended interactions with patients, physiotherapists are well positioned to observe mental health issues such as anxiety and depression, which are often underdiagnosed in this population [5, 6]. Early identification of these conditions can improve treatment adherence and enhance overall outcomes [7]. However, physiotherapists often lack formal training in mental health screening, necessitating research on effective screening methods [6]. To address this gap in the literature, we assessed the ability of physiotherapists registered on the Axxon website, Belgium's physiotherapy professional organization, to identify anxiety and depression in RA patients using two brief observer-report mental health screening tools, that is, the Patient Health Questionnaire-2 (PHQ-2) [8] for depression and the Generalized Anxiety Disorder-2 (GAD-2) [9] for anxiety, compared to a numeric rating scale (NRS).

After providing informed consent, physiotherapists collected data over 6 months from newly referred RA patients who had been receiving treatment for 2 weeks. Patients had to meet the following criteria: (a) age 18 or older, (b) self-reported RA diagnosis, and (c) undergoing treatment with the participating

physiotherapist. Included patients completed the full versions of the PHQ-2 and GAD-2, that is, the PHQ-9 [10] and GAD-7 [11]. These are widely used self-report measures for assessing the severity of depressive and anxiety symptoms, respectively. These patient-completed assessments served as the reference standard for evaluating the accuracy of the physiotherapists' observer-report evaluations. Both scales evaluate symptom frequency over the past 2 weeks using a Likert scale: 0 (not at all), 1 (several days), 2 (more than half the days), and 3 (nearly every day). The PHQ-9 consists of nine items, with total scores ranging from 0 to 27. Depression severity was classified as mild (5–9), moderate (10–19), and severe (≥ 20). The GAD-7 includes seven items, with total scores ranging from 0 to 21, and anxiety severity classified as mild (5–9), moderate (10–14), and severe (≥ 15). Both instruments are reliable and valid for assessing mental health symptoms in patients with RA, with Cronbach's alpha values of 0.86 (PHQ-9) and 0.89 (GAD-7) in this study. Physiotherapists assessed their patients' depression and anxiety using a 0-to-10 NRS and then evaluated them using observed-report versions PHQ-2 and GAD-2. The PHQ-2 consists of the first two items of the PHQ-9, assessing "little interest or pleasure in doing things" and "feeling down, depressed, or hopeless." The GAD-2 consists of the first two items of the GAD-7, assessing "feeling nervous, anxious, or on edge" and "not being able to stop or control worrying." For both tools, the standard self-report stem question was modified to: "Over the last two weeks, how often has your patient been bothered by any of the following problems?" This adaptation enabled physiotherapists to assess depression and

---

anxiety levels based on clinical observations rather than patient self-report. No specific training was provided to physiotherapists to assess their ability to recognize these conditions independently. To minimize bias, physiotherapists were unaware of patients' questionnaire responses. Our study was approved by the Ethische Commissie Onderzoek UZ/KU Leuven (S67100) and registered on ClinicalTrials.gov (NCT 06785883). As no prior data were available for a sample size calculation, we analyzed the first 50 patients using MedCalc for Windows (Version 20.115, MedCalc Software, Ostend, Belgium). Key parameters from pilot data determined the required sample size of 97 patients (24 positive cases, 73 negative cases) to achieve a statistical power of 0.80 and significance level of 0.05. For the main analyses, missing data were handled using SPSS version 29.0 (IBM, Chicago) through multiple imputation, following established recommendations for ROC analyses. Based on PHQ-9 and GAD-7 scores, patients were categorized as having normal, mild (including moderate and severe cases above the cutoff), moderate (including severe cases above the cutoff), or severe anxiety or depressive symptoms. ROC curves were generated to assess the ability of physiotherapists' numeric rating scales (0–10) and the 2-item screening tests (PHQ-2, GAD-2) to detect these symptoms. The ROC curve plots sensitivity (hit rate) against 1 minus specificity (false alarm rate) for each possible cutoff, yielding 11 sensitivity-specificity pairs for the physiotherapists' ratings. This process was repeated for (a) mild, (b) moderate, and (c) severe symptom detection in both anxiety and depression. The proportion of the total area under the ROC curve (AUC) quantified classification accuracy, with AUC values interpreted as: $0.5 < \text{AUC} \leq 0.7$ (less accurate), $0.7 < \text{AUC} \leq 0.9$ (moderately accurate), and $0.9 < \text{AUC} < 1.0$ (highly accurate). An AUC of 1.0 indicates perfect discrimination, whereas 0.5 suggests classification no better than chance [12]. To compare the diagnostic accuracy of the physiotherapists' numeric rating scale and the 2-item screening tests, AUC values were analyzed using DeLong's method for correlated samples [13]. This analysis was conducted using MedCalc for Windows, Version 20.115 (MedCalc Software, Ostend, Belgium).

A total of 45 physiotherapists (36.9 ± 11.8 years; 20 male; experience $= 13.7 \pm 12.3$ years) participated, treating an average age of 17 patients with chronic pain per week. Fourteen had prior mental health-related training in managing chronic pain ($N = 10$), relaxation techniques ($N = 3$), and mindfulness-based stress reduction ($N = 1$). The study included 97 newly referred RA patients (age $= 57.5 \pm 14.8$ years; 22 male; illness duration $= 157.7 \pm 156.5$ months). The average anxiety and depression NRS scores were 3.2 ± 2.2 and 3.0 ± 2.2, respectively, whereas GAD-2 and PHQ-2 scores were 2.4 ± 1.5 and 2.2 ± 1.8. The prevalence of at least mild, moderate, and severe anxiety was 63.9%, 20.6%, and 2.1%, respectively; for depression, it was 64.9%, 28.9%, and 4.1%. The AUC values showed that GAD-2 performed significantly better than NRS for identifying mild and moderate anxiety (Table 1; Figures S1–S3). Similarly, PHQ-2 was significantly more accurate than NRS in detecting mild and moderate depression (Table 2; Figures S4–S6). No significant difference was found for severe anxiety and depression.

Our findings suggest that, compared to NRS, PHQ-2 and GAD-2 are more effelctive for screening mild to moderate anxiety and depression in RA patients. While NRS is commonly

TABLE 1 | Comparison of the accuracy of physiotherapists numeric anxiety ratings and the 2-Item Generalized Anxiety Disorder-2 (GAD-2) in screening for anxiety symptoms in patients with rheumatoid arthritis: Receiver operating characteristic curve analysis.

GAD-7	Numeric rating scale	GAD-2	p
$\geq$ mild	0.62	0.74	0.02*
$\geq$ moderate	0.55	0.87	< 0.001*
$\geq$ severe	0.63	0.99	0.16

Note: Values shown are the areas under the curve with analysis repeated for three cutoffs on the Generalized Anxiety Disorder-7 (GAD-7).
*Significant when $p < 0.05$.

TABLE 2 | Comparison of the accuracy of physiotherapists numeric depression ratings and the 2-Item Patient Health Questionnaire (PHQ-2) in screening for depressive symptoms in patients with rheumatoid arthritis: Receiver operating characteristic curve analysis.

PHQ-9	Numeric rating scale	PHQ-2	p
$\geq$ mild	0.72	0.83	0.02*
$\geq$ moderate	0.62	0.91	< 0.001*
$\geq$ severe	0.92	0.96	0.53

Note: Values shown are the areas under the curve with analysis repeated for three cutoffs on the Patient Health Questionnaire-9 (PHQ-9).
*Significant when $p < 0.05$.

used for pain assessment, it lacks sensitivity in detecting psychological distress. Integrating observer–report versions of the PHQ-2 and GAD-2 into physiotherapy practice offers a more comprehensive approach, enabling early interventions such as referrals to mental health professionals, stress management techniques, and psychologically informed physiotherapy. However, it is essential to exercise caution to avoid over-screening, which can lead to potential harms such as false positives, unnecessary labeling, and increased patient anxiety. Overdiagnosis may result in unwarranted interventions and strain healthcare resources, potentially detracting from care for those with more severe conditions. Therefore, mental health screening should be implemented judiciously, ensuring that it is targeted and accompanied by appropriate follow-up care. This balanced approach aligns with best-practice guidelines advocating for the concurrent treatment of physical and mental health in RA management, ensuring that interventions are both effective and appropriate. It is also important to note that while the PHQ-2 and GAD-2 are effective initial screening tools for identifying potential cases of depression and anxiety, their utility in monitoring symptom severity or detecting residual symptoms in patients already receiving treatment is limited. In such cases, more comprehensive assessments, such as the PHQ-9 and GAD-7, are recommended to evaluate treatment response and symptom progression. Therefore, while the PHQ-2 and GAD-2 are valuable for initial screening, their role in ongoing assessment of treated individuals should be complemented with more detailed instruments.

Despite promising results, our study has limitations. First, while well powered, the sample may not fully represent the diverse RA population due to the lack of data on disease severity

and comorbidities. Second, PHQ-2 and GAD-2 are screening tools, not diagnostic instruments, and further clinical evaluation is needed to confirm anxiety and depression diagnoses. Third, the psychometric properties of the observer-report versions of the PHQ-2 and GAD-2 have not been validated, as these instruments were originally developed and standardized for self-report use. While physiotherapists in our study administered the PHQ-2 and GAD-2 as observer-report measures and did not report any difficulties, we did not formally assess their experiences or the feasibility of this approach. Given the lack of validation for observer-rated use, employing the tools in this manner may affect the reliability and validity of the assessments. Fifth, the study was conducted in private physiotherapy settings, limiting its generalizability to other healthcare contexts, such as hospitals and community clinics, where implementation barriers may differ. Our findings have significant practical implications for physiotherapists treating RA patients, particularly in private practice. Incorporating PHQ-2 and GAD-2 into routine assessments can facilitate early identification of psychological distress, leading to timely interventions that improve treatment adherence and patient outcomes. Physiotherapists can collaborate with mental health professionals and those trained in psychologically informed approaches to enhance patient care. By integrating mental health screening into routine practice, physiotherapists can adopt a more biopsychosocial approach, improving patient engagement and satisfaction.

Future research should explore how clinical experience and training influence screening accuracy. Studies comparing outcomes between physiotherapists with and without formal mental health training could provide valuable insights. Additionally, research should assess the feasibility of implementing mental health screening tools across different physiotherapy settings and identify barriers to integration. Longitudinal studies examining the impact of early psychological interventions on RA symptoms, functional capacity, and quality of life are also needed. Finally, investigating how mental health screening influences adherence, pain management, and clinical outcomes would further support integrating mental health care into RA rehabilitation.

In conclusion, this study underscores the importance of screening for anxiety and depression in RA patients attending physiotherapy. The PHQ-2 and GAD-2 outperform NRS in identifying mild to moderate psychological distress, making them valuable additions to physiotherapy practice. Integrating these tools can enhance the biopsychosocial management of RA, addressing both physical and mental health needs. Further research should explore the long-term impact of early psychological interventions and strategies to optimize mental health screening in routine physiotherapy care.

Author Contributions

Davy Vancampfort: conceptualization, methodology, resources, formal analysis, writing – original draft; Isabel Zwahlen: validation, review and editing; Veerle Gillis: validation, review and editing; Emanuel Brunner: validation, review and editing; Tine Van Damme: conceptualization, methodology, project administration, supervision, data curation, review and editing.

Conflicts of Interest

The authors declare no conflicts of interest.

Data Availability Statement

The data that support the findings of this study are available on request from the corresponding author. The data are not publicly available due to privacy or ethical restrictions.

Davy Vancampfort
Isabel Zwahlen
Veerle Gillis
Emanuel Brunner
Tine Van Damme

References

1. B. Conley, S. Bunzli, J. Bullen, et al., "What Are the Core Recommendations for Rheumatoid Arthritis Care? Systematic Review of Clinical Practice Guidelines," *Clinical Rheumatology* 42, no. 9 (2023): 2267–2278, https://doi.org/10.1007/s10067-023-06654-0.

2. N. A. Allameen, Y. W. Lai, G. Lian, et al., "Physiotherapy and Occupational Therapy in Rheumatoid Arthritis: Bridging Functional and Comorbidity Gaps," *Best Practice & Research. Clinical Rheumatology* 39, no. 1 (2025): 102032, https://doi.org/10.1016/j.berh.2024.102032.

3. H. Chaplin, M. Sekhon, and E. Godfrey, "The Challenge of Exercise (Non-)adherence: A Scoping Review of Methods and Techniques Applied to Improve Adherence to Physical Activity and Exercise in People With Inflammatory Arthritis," *Rheumatology Advances in Practice* 7, no. 1 (2023): rkac096, https://doi.org/10.1093/rap/rkac096.

4. S. M. Abild, J. Midtgaard, A. Nordkamp, et al., "Maintaining Good Mental Health in People With Inflammatory Arthritis: A Qualitative Study of Patients' Perspectives," *International Journal of Qualitative Studies on Health and Well-Being* 19, no. 1 (2024): 2424015, https://doi.org/10.1080/17482631.2024.2424015.

5. C. M. Bastemeijer, J. P. van Ewijk, J. A. Hazelzet, and L. P. Voogt, "Patient Values in Physiotherapy Practice, a Qualitative Study," *Physiotherapy Research International* 26, no. 1 (2021): e1877, https://doi.org/10.1002/pri.1877.

6. R. L. McGrath, S. Shephard, T. Parnell, S. Verdon, and R. Pope, "Recommended Approaches to Assessing and Managing Physiotherapy Clients Experiencing Psychological Distress: A Systematic Mapping Review," *Physiotherapy Theory and Practice* 40, no. 11 (2024): 2670–2700, https://doi.org/10.1080/09593985.2023.2284823.

7. G. Gong, A. Dong, Z. Zhang, and J. Mao, "Medication Adherence and Predictive Factors Among Patients With Rheumatoid Arthritis: A COM-B Model Guided Structural Equation Modeling Analysis," *Patient Education and Counseling* 119 (2024): 108080, https://doi.org/10.1016/j.pec.2023.108080.

8. K. Kroenke, R. L. Spitzer, and J. B. Williams, "The Patient Health Questionnaire-2: Validity of a Two-Item Depression Screener," *Medical Care* 41 (2003): 1284–1292, https://doi.org/10.1097/01.MLR.0000093487.78664.3C.

9. K. Kroenke, R. L. Spitzer, J. B. Williams, P. O. Monahan, and B. Löwe, "Anxiety Disorders in Primary Care: Prevalence, Impairment, Comorbidity, and Detection," *Annals of Internal Medicine* 146 (2007): 317–325, https://doi.org/10.7326/0003-4819-146-5-200703060-00004.

10. R. L. Spitzer, K. Kroenke, and J. B. Williams, "Validation and Utility of a Self-Report Version of PRIME-MD: The PHQ Primary Care Study," *Journal of the American Medical Association* 282, no. 18 (1999): 1737–1744, https://doi.org/10.1001/jama.282.18.1737.

11. R. L. Spitzer, K. Kroenke, J. B. Williams, and B. Löwe, "A Brief Measure for Assessing Generalized Anxiety Disorder: The GAD-7," *Archives*

of Internal Medicine 166, no. 10 (2006): 1092–1097, https://doi.org/10.1001/archinte.166.10.1092.

12. M. Greiner, D. Pfeiffer, and R. Smith, "Principles and Practical Application of the Receiver-Operating Characteristic Analysis for Diagnostic Tests," *Preventive Veterinary Medicine* 45, no. 1–2 (2000): 23–41, https://doi.org/10.1016/s0167-5877(00)00115-x.

13. E. R. DeLong, D. M. DeLong, and D. L. Clarke-Pearson, "Comparing the Areas Under Two or More Correlated Receiver Operating Characteristic Curves: A Nonparametric Approach," *Biometrics* 44 (1988): 837–845.

Supporting Information

Additional supporting information can be found online in the Supporting Information section.

ORIGINAL ARTICLE

Patients With IgA Vasculitis and Kawasaki Disease Show Dysregulated Interferon Signature

Sevki Erdem Varol[1] | Cisem Cinar[2] | Nihan Burtecene[3] | Sezgin Sahin[4] | Mehmet Yildiz[4] | Kenan Barut[4] | Haluk Cokugras[3] | Sinem Firtina[2] | Ozgur Kasapcopur[4] 🔟 | Ayca Kiykim[3] 🔟

[1]Department of Pediatrics, Cerrahpasa School of Medicine, Istanbul University-Cerrahpasa, Istanbul, Türkiye | [2]Department of Medical Genetics, Cerrahpasa School of Medicine, Istanbul University-Cerrahpasa, Istanbul, Türkiye | [3]Department of Pediatric Immunology and Allergy, Cerrahpasa School of Medicine, Istanbul University-Cerrahpasa, Istanbul, Türkiye | [4]Department of Pediatric Rheumatology, Cerrahpasa School of Medicine, Istanbul University-Cerrahpasa, Istanbul, Türkiye

Correspondence: Ayca Kiykim (ayca.kiykim@iuc.edu.tr)

ABSTRACT

Objective: IgA vasculitis (IgAV) and Kawasaki disease (KD) are the most common forms of childhood vasculitis. Although various factors such as viral infections, genetic factors, and environmental factors are involved in the development of both diseases, their pathogenesis remains unclear. The interferon (IFN) signature, which reflects the activation of type I IFN signaling pathways, is a diagnostic and prognostic tool that contributes significantly to the pathogenesis and management of autoimmune diseases. In our study, we aimed to investigate the role of the IFN signature in patients with IgAV and KD.

Material and Methods: Thirty-two children with IgAV and four patients diagnosed with KD were included in the study. Serum levels of IL-1, IL-6, IL-8, IL-10, IL-17, IL-18, TNF-α, TNF-R1, TNF-R2, and IFN-gamma were analyzed in the serum samples of all participants, and the expression of IFN-related genes (*STAT1, IFI27, IFI44, IFI44L, IFIT1*, and *RSAD2*) was assessed in the patients and healthy controls ($n = 26$) to calculate the IFN score by RT-PCR method.

Results: A significant increase in the expression of three genes (*IFIT1, IFI44,* and *IFI27*) and decreased expression of the other three genes (*RSAD2, STAT1,* and *IFI44L*) was found in patients with IgAV and KD compared to the control group. Significantly higher IFN scores (IFN > 3) were found in patients with gastrointestinal involvement, in patients who required corticosteroid therapy, and in patients who had to be hospitalized. No significant difference in IFN levels was found between patients with and without renal involvement. Significantly higher serum IL-1 levels were found in patients with gastrointestinal symptoms with IgAV. High IFN scores were found in three out of four patients diagnosed with KD.

Conclusion: A dysregulated type 1 IFN signature was found in patients with IgAV and KD compared to the control group. A significantly increased risk of gastrointestinal involvement required corticosteroid therapy, and hospitalization was observed in patients diagnosed with IgAV who had high IFN levels. This underlines the idea that the IFN score could serve as a crucial prognostic indicator.

1 | Introduction

Immunoglobulin A vasculitis (IgAV) is the most common vasculitis in childhood and is a disease with multisystem involvement characterized by skin, kidney, gastrointestinal, and joint findings [1, 2]. It is also referred to as IgAV, as IgA deposits can be observed in small vessels [3]. Clinically, IgAV classically presents with palpable purpura without thrombocytopenia and coagulopathy, hematuria due to glomerulonephritis, arthritis, and arthralgia due to joint involvement, abdominal pain, gastrointestinal bleeding, and bowel obstruction due to gastrointestinal involvement [4]. Although most IgAV patients recover with conservative treatment, some patients require the use of corticosteroids [1, 5, 6]. Corticosteroids should be used in the presence of nephritis, orchitis, cerebral vasculitis, pulmonary hemorrhage, and significant gastrointestinal involvement [7–10].

Kawasaki disease (KD) is an acute febrile clinical illness with vasculitis in medium-diameter vessels that occurs more frequently in early childhood [1]. The main clinical findings include fever lasting at least 5 days, polymorphous rash, changes in the labial and oral mucosa, bilateral non-exudative conjunctivitis, unilateral cervical lymphadenopathy, and changes in the limbs [11]. In patients diagnosed with KD, the most important factor for prognosis is the presence of coronary artery involvement and early initiation of treatment during the acute phase of the disease [12, 13]. The main goal of treatment of KD is to suppress acute inflammation, reduce vascular damage, and prevent coronary artery involvement and thrombosis [11]. Initial treatment may include intravenous immunoglobulin, acetylsalicylic acid, corticosteroids in resistant cases, and drugs to suppress tumor necrosis factor (TNF) and interleukin 1 (IL-1) [11].

The interferon (IFN) signature refers to the dysregulated expression of a series of genes regulated by type I IFNs, a class of cytokines involved in the immune response to viral infections and other pathologic conditions, including autoimmune diseases [14, 15]. Type I IFNs, including IFN-α and IFN-β, bind to their receptors on the cell surface and trigger a signaling cascade that leads to the transcription of IFN-stimulated genes (interferon-stimulating genes; ISGs). The expression of these ISGs creates the IFN signature, which can be detected in various cell types and tissues [14].

The IFN signature has been observed in the blood and tissue cells of patients with systemic lupus erythematosus (SLE) and other autoimmune diseases, where it serves as a biomarker of active disease and influences treatment selection [14]. In dermatomyositis (DM), the IFN signature correlates with disease activity and has been shown to be more pronounced in patients with anti-melanoma differentiation gene 5 (MDA5) antibodies [16]. The IFN signature is also associated with the clinical severity of idiopathic inflammatory myopathies and has been proposed as a diagnostic tool [17].

The pathogenesis of IgAV and KD, the most common vasculitis in childhood, is not yet clearly understood. Although the importance of the type I IFN signaling pathway has been demonstrated in many autoinflammatory and autoimmune diseases, there is no study on this topic in IgAV and KD. In this context, we aimed to evaluate the role of the IFN signature measured in children with IgAV and KD in pathogenesis by comparison with healthy individuals.

2 | Materials and Methods

2.1 | Patients

Patients who met the diagnostic criteria for IgAV and KD between December 12, 2022 and March 1, 2024 in the Pediatric Rheumatology Department of Istanbul University-Cerrahpasa Pediatric Rheumatology, General Outpatient Clinic and Pediatric Emergency Outpatient Clinic were included in the study. Patients who did not meet the diagnostic criteria and who were receiving immunosuppressive treatment were excluded from the study.

The control group ($n = 26$) consisted of healthy individuals under the age of 18 who were admitted to the general pediatric outpatient clinic and had no chronic disease, acute infection, or drug use. The patients and healthy controls had a similar gender and age distribution. All patients and healthy controls were informed about the study, and informed consent was obtained from them and their families. The Ethics Committee of Istanbul University-Cerrahpasa (06.04.2023-660407) approved the human research, and written informed consent was obtained from all patients and/or their parents.

2.2 | Laboratory Examinations

2.2.1 | Acute Inflammatory Response

Acute inflammatory response including C-reactive protein (CRP), erythrocyte sedimentation rate [18], white blood cell (WBC) count, absolute neutrophil count [19], platelet count (PLT), hemoglobin concentration (g/dL) were recorded at the time of diagnosis. CRP ≥ 5 mg/L was considered as elevated CRP, WBC count $\geq 12\,000/mm^3$ as leukocytosis, ESR ≥ 20 mm/h as elevated ESR, and PLT $\geq 450\,000/mm^3$ as thrombocytosis.

2.2.2 | Serum Cytokine Analyses

Patient sera were collected at the time of diagnosis prior to treatment, frozen, and stored at 80°C until the measurement. IL-1, IL-6, TNF-α, IL-17, IL-8, IL-18, IFN-γ, IL-10, sTNFR1, and sTNFR2 were measured with Bioassay Technology Laboratory (BT-Lab, Shanghai, China) enzyme-linked immunoassay [20] kit. Dilution was performed according to the manufacturer's instructions.

2.2.3 | Interferon Signature

The peripheral blood samples were collected in ethylenediaminetetraacetic acid (EDTA)-coated tubes from the patients followed by total RNA isolation with an RNA isolation kit (Invitrogen, USA) prior to treatment. Complementary DNA (cDNA) was synthesized from 1000 ng of total RNA

using random primers and a cDNA synthesis kit (Applied Biosystems, USA). Real-time PCR analysis was performed using the BioRad CF96X system (Applied Biosystems, USA). Primers to all target genes (*STAT1, IFI27, IFI44, IFI44L, IFIT1,* and *RSAD2*) and the housekeeping gene (Beta-actin) were designed with the Primer3 program, and the primer sequences are available upon request. To calculate the IFN score, the relative expression of targeted genes was calculated by the $2^{-\Delta\Delta Ct}$ method, followed by *Z*-score-based standardized IFN score calculation [19] and IFN scores of 3 and more were considered significant.

2.3 | Statistics

The data were analyzed using the SPSS 29.0.2 program (New York, USA). The compatibility of the variables with the normal distribution was tested using the Kolmogorov–Smirnov test. For variables that did not conform to the normal distribution, the Mann–Whitney *U*-test was used for the comparison of means between two groups, and the Kruskal–Wallis test for the comparison of means between more than two groups. Spearman's rho correlation coefficient was used to analyze continuous variables, while the chi-squared test was used for categorical variables. Results are expressed as mean ± standard deviation. Correlations between parameters were reported using Pearson's or Spearman's correlation coefficient depending on the normality of the data. The results were considered statistically significant at $p < 0.05$.

3 | Results

3.1 | Clinical Presentation

A total of 32 patients with IgAV and 4 patients with KD were included in our study. Eight IgAV patients were excluded due to insufficient RNA amount, and the IFN signature was evaluated in 24 patients with IgAV and all patients with KD. Of these 28 patients, 16 (57.1%) were female and 12 (42.9%) were male. The mean age of the patients was 7.54 ± 3.79 years. Of the 24 patients diagnosed with IgAV, 14 (58.3%) were female and 10 (41.7%) were male. The mean age of these patients was 8.44 ± 3.23 years. Of the four patients diagnosed with KD, two were male and two were female. The mean age of the patients diagnosed with KD was 2.15 years.

Skin findings were present in all patients with IgAV at presentation. Joint involvement was found in 70.8% ($n = 17$), gastrointestinal involvement in 54.1% ($n = 13$), orchitis in 8% ($n = 2$), and kidney involvement in 16.6% ($n = 4$). When examining the distribution of rashes in the patients, all 24 patients had rashes on the lower extremities. Isolated rash on the lower extremities occurred in 15 patients (62.5%), rash on the upper extremities in addition to the rash on the lower extremities in 4 patients (16.6%), and rash on all extremities and the trunk in 5 patients (20.9%) (Table 1). Evaluation of the patients' classic laboratory findings revealed leukocytosis (WBC ≥ 12 000/mm³) in 12 (50%), elevated CRP ((≥ 5 mg/L) L) in 17 (70.8%), and elevated ESR (≥ 20 mm/h) in 12 (50%). Drug treatment (steroids and/or NSAIDs) was initiated in 19 (79.2%) patients

TABLE 1 | Symptoms seen in patients with IgAV.

	Number (=)	Percentage (%)
Skin		
Purpura	24	100
Subcutaneous edema	5	25
Joint		
Arthralgia only	17	70.8
Arthritis	7	29.2
Gastrointestinal		
Abdominal pain	13	54.1
Nausea and vomiting	11	45.8
Hematochezia	1	4.2
Hematemesis	1	4.2
Melena	3	12.5
Scrotal		
Scrotal edema	2	8
Scrotal pain	2	8.3
Renal		
Hematuria	4	16.7
Proteinuria	1	4.2

with IgAV, 14 (58.3%) of the patients received corticosteroids, 16 (66.6%) received non-steroidal anti-inflammatory drugs. Five (20.8%) of the patients were only recommended supportive therapies.

All patients with KD fulfilled the diagnostic criteria for classic Kawasaki disease. All patients had elevated CRP and ESR, three patients had thrombocytosis with leukocytosis and one patient lacked both parameters. Echocardiographic examination of the patients revealed dilated coronary arteries in one patient (*Z*-score between 2 and 2.5) and a giant aneurysm in one patient (*Z*-score ≥ 10) (Table 2). All patients were treated with IVIG and aspirin as first-line treatment. Two of the patients were found to be resistant to IVIG treatment. Patients with IVIG resistance also received a second dose of IVIG and high-dose steroids. As treatment with high-dose steroids did not respond, anakinra and infliximab were added.

3.2 | Interferon Signature

In our study, the gene expression of a total of 28 patients (24 with IgAV and 4 with KD) and 26 healthy children was evaluated for IFN signature analysis. Statistical analysis of gene expression data was performed using the Mann–Whitney *U* method. *IFIT1, IFI44*, and *IFI27* gene mRNA expressions were found to be higher in patients ($p = 0.0002$, $p < 0.0001$, and $p < 0.0001$, respectively), whereas *RSAD2, STAT1*, and *IFI44L*

TABLE 2 | Demographics, clinical, and laboratory data of patients with KD.

|	P1	P2	P3	P4
Gender	M	M	F	F
Age (months)	60	4.5	9.7	28.9
Duration of fever (days)	5	12	13	7
Response to IVIG	−	+	+	−
Coronary artery involvement	Dilatation	Giant aneurysm	−	−
Hospital stay length (days)	3	26	14	4
Hemoglobin (g/dL)	5	12	5	6
WBC (/mm^3)	5000	12860	34000	15600
ANC (/mm^3)	2600	9990	24700	9800
PLT (/mm^3)	248000	1115200	1482000	680000
CRP (mg/L)	20.8	57.2	206.3	32.3
ESR (mm/h)	81	52	35	37
IFN scores	3	4	2	3

Abbreviations: ANC, absolute neutrophil counts; CRP, C-reactive protein; ESR, Erythrocyte sedimentation rate; F, female; IFN, interferon; IVIG, intravenous immunoglobulin; M, male; P, patient; PLT, platelets; WBC, white blood cells.

gene mRNA expressions were lower in patients ($p < 0.0001$, $p < 0.0001$, and $p = 0.01$, respectively) compared to healthy controls (Figure 1).

When we evaluated the IFN scores, 18 IgAV patients (75%) had an IFN score of 3 or more. In IgAV patients, three (12.5%) patients had an IFN score of 6, one (4%) patient had an IFN score of 5, four (16.6%) patients had an IFN score of 4, 10 (41.6%) patients had an IFN score of 3, and six (25%) patients had an IFN score of 2. There were no IgAV patients with an IFN score of 1. The IFN scores of the Kawasaki patients were calculated as 3, 2, 3, and 4, respectively, for the patients listed in (Table 2).

Symptoms, clinical findings, need for hospitalization, need for corticosteroids, and IFN scores were statistically evaluated. There was no significant difference between the IFN scores of patients with and without joint involvement ($p = 0.89$). IFN scores were significantly higher in patients with gastrointestinal disease overall ($p = 0.009$), including abdominal pain ($p = 0.09$), nausea ($p = 0.008$), and invagination ($p = 0.021$). No significant difference was found with respect to hematemesis, melena, and hematochezia ($p = 0.789$, $p = 0.313$, and $p = 0.172$, respectively). IFN scores showed no significant difference in scrotal involvement, subcutaneous edema, and renal involvement ($p = 0.82$, $p = 0.46$, and $p = 0.59$, respectively). IFN scores were significantly higher in patients requiring corticosteroids ($p = 0.01$).

Patients with a high IFN score had a significantly higher risk of gastrointestinal tract involvement (OR: 4.5) (95% CI: 1.117–18.226) ($p = 0.034$).
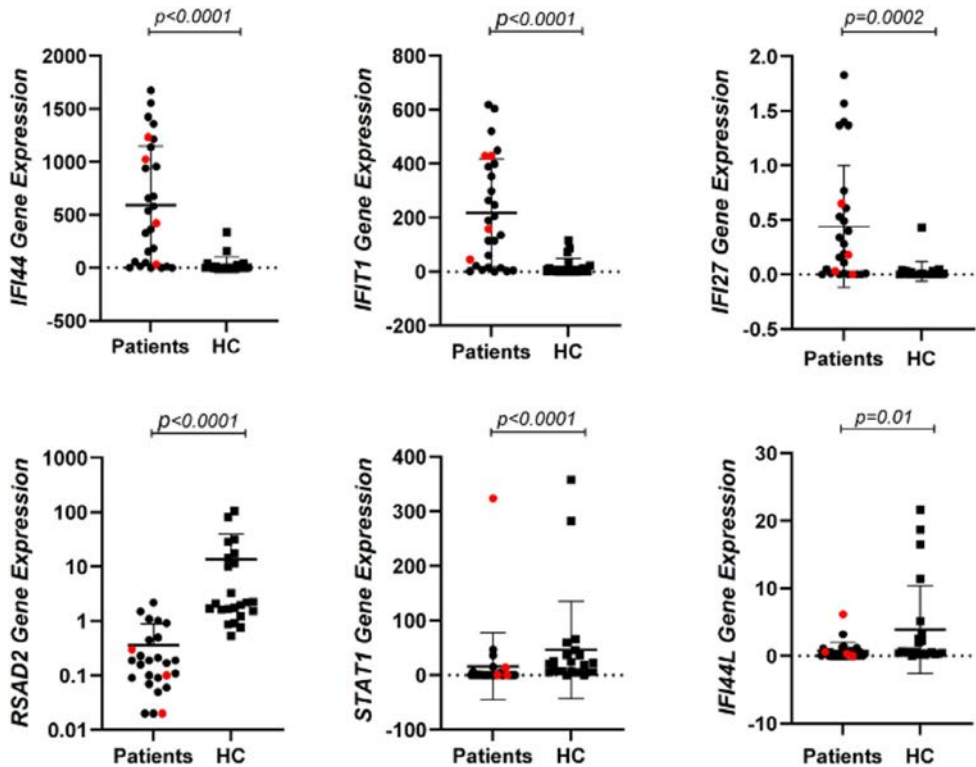
FIGURE 1 | Comparison of the IFN signature between patients and healthy controls. Red dots represent patients with Kawasaki Disease. Black dots represent patients with Immunoglobulin A vasculitis. HC, healthy controls.

Patients with a high IFN score had a significantly higher risk of corticosteroid use (OR: 4.6) (95% CI: 1.091–19.509) ($p = 0.038$).

3.3 | Comparison of IFN Score With Laboratory Data

Of the patients with IgAV who were included in the study for cytokine analysis, 14 (43%) were male and 18 (57%) were female. The mean age of the patients was 8.28 ± 3.06 years. Of the 45 children in the control group, 24 (53.3%) were male and 21 (47.7%) female. The mean age of the children in the control group was 8.14 ± 3.95 years. No statistically significant difference was found between the children in the patient group and the healthy control group in terms of gender distribution and age.

The laboratory data of patients with IgAV and the IFN score were analyzed using the Spearman correlation analysis method. When the hemoglobin level, WBC count, neutrophil count, lymphocyte count, and PLT were evaluated, no statistically significant correlation was found with the IFN score ($p = 0.503$, $p = 0.140$, $p = 0.366$, $p = 0.87$, and $p = 0.339$, respectively). No statistically significant correlation was found between erythrocyte sedimentation rate, CRP levels, leukocytosis, and IFN score ($p = 0.872$, $p = 0.530$, $p = 0.108$, respectively).

3.4 | Comparison of the Need for Hospitalization and the Duration of Hospitalization With the IFN Score

Need for hospitalization and length of hospital stay showed higher IFN scores ($p = 0.005$ and $p = 0.022$, respectively). The frequency of hospitalization was significantly higher in patients with a high IFN score (OR: 4.8) (95% CI: 1.190–19.36) ($p = 0.028$).

3.5 | Evaluation of the IFN Score in Patients With Kawasaki Disease

The IFN score was high in three patients with KD and low in one patient. The duration of fever, IVIG resistance, coronary artery involvement, duration of hospitalization, and IFN scores of the patients are shown in (Table 2).

Among the patients, patient number 2 developed IVIG resistance and had giant aneurysms in his coronary arteries. This patient had an IFN score of 4 (high). Patient number 3 developed IVIG resistance but had an IFN score of 2 (low). In patient number 1, dilation of the coronary arteries was observed and the IFN score was 3 (high). In patient number 4, the coronary artery was not affected and no IVIG resistance was detected. Patient number 4 also had an IFN score of 3 (high).

3.6 | Evaluation of Cytokine Levels in Patients With IgAV

The levels of IL-1, IL-6, IL-8, IL-10, IL-17, IL-18, TNF-α, TNF-R1, TNF-R2, and IFN-gamma were determined in serum samples from 31 patients with IgAV. Forty-five healthy children were included in the control group. In the patient group, 17 patients (54.8%) were female and 14 patients (45.2%) were male. The mean age of the patients was 8.28 ± 3.06 years.

In the control group, 24 (53.3%) children were male and 21 (46.7%) female. The average age of the control group was 8.14 ± 3.95 years. When comparing the patient and control groups in terms of gender and age, no significant difference was found between the two groups.

When comparing the groups, a significant difference was only found in the IL-6 values ($p = 0.045$). For the other cytokine levels, there was no statistically significant difference between the patient and control groups (Table 3).

3.7 | Comparison of Serum Cytokine Levels According to Clinical Findings in Patients With IgAV

The cytokine levels did not differ regarding arthritis in IgAV compared to healthy controls. However, in patients with arthralgia the serum levels of TNF-R2 and IL-8 were significantly higher ($p = 0.012$ and $p = 0.056$, respectively). Patients with abdominal pain had higher serum IL-1 and TNF-α levels ($p = 0.004$ and $p = 0.017$, respectively).

The presence of GI findings when evaluated together revealed higher serum IL-1 levels ($p = 0.004$), this was also true for vomiting ($p = 0.028$). In patients with melena, the serum IL-18 level was higher ($p = 0.025$), and in patients with intussusception serum levels of TNF-R1 and IFN-γ were significantly higher compared to patients without intussusception ($p = 0.033$ and $p = 0.033$, respectively).

Cytokine levels did not differ with regard to renal and/or scrotal involvement and diarrhea.

Serum levels of TNF-R1 and IFN were significantly lower in patients with isolated lower extremity rash ($p = 0.038$ and $p = 0.038$, respectively). A significant increase in the levels of IL-1, TNF-α, TNF-R1, and IFN-γ was found in patients receiving corticosteroids ($p = 0.013$, $p = 0.009$, $p = 0.045$, and $p = 0.045$, respectively).

There was no correlation between the IFN score and the serum cytokine levels (Spearman's rank correlation coefficient).

4 | Discussion

The etiopathogenesis of IgAV and KD, the most common childhood vasculitides, is not yet fully understood. This study aimed to investigate the type 1 IFN signature in IgAV and KD, as well as the relationship between cytokine levels, clinical findings, and IFN scores in patients with IgAV. To achieve this, we examined the expression of six genes (*IFI27*, *IFI44*, *IFI44L*, *IFIT1*, *RSAD2*, and *STAT1*) associated with the type 1 IFN signaling pathway. Our analysis revealed a significant increase in the expression of *IFIT1*, *IFI44*, and *IFI27* in patients with IgAV and KD compared to the control group. In contrast, the expression

	Patients ($n=32$)	Healthy controls ($n=45$)	p
Age (years)	8.29 ± 3.06	8.14 ± 3.95	0.86
Gender (female) (n, %)	18 (%56.3)	21 (%46.7)	0.55
IL-1 (ng/mL) median (min–max)	43.2 (3.81–226.2)	55.4 (3.8–222.9)	0.14
IL-6 (ng/mL) median (min–max)	68.8 (7.05–589.2)	83.1 (14.6–398.3)	**0.045**
IL-8 (ng/mL) median (min–max)	167.8 (54.5–994.2)	172.2 (50.8–1013.5)	0.98
IL-10 (pg/mL) median (min–max)	209.4 (10.3–1146.6)	238.1 (10.1–1019.7)	0.71
IL-17 (ng/mL) median (min–max)	82.9 (6.2–425.5)	87.1 (6.0–361.5)	0.37
IL-18 (ng/mL) median (min–max)	12.1 (1.5–95.7)	17.7 (1.4–68.5)	0.17
TNF-α (ng/mL) median (min–max)	164.5 (12.2–1183)	218.4 (11.4–886)	0.34
TNF-R1 (pg/mL) median (min–max)	7.09 (4,2-75,5)	9.4 (4.4–52.9)	0.07
TNF-R2 (ng/mL) median (min–max)	687.3 (338.7–2814.3)	659 (250.4–3401.8)	0.85
IFN-ɣ (ng/mL) median (min–max)	41.1 (24.3-41.1)	54.1 (25.2–270.4)	0.07

Note: Significant values are given in **bold**.

of *RSAD2, STAT1*, and *IFI44L* was decreased relative to controls (Figure 1).

Type 1 interferonopathies, which were first defined as an independent group of autoimmune diseases in 2011, now include dermatomyositis, systemic lupus erythematosus, and primary Sjogren's syndrome [15, 21, 22]. In addition, increased expression of type 1 IFN-related genes has been shown to be associated with disease activity in patients with rheumatoid arthritis [23]. A study by Batten et al. examined the type 1 IFN signature in ANCA-associated vasculitis and found that there was no increase in gene or protein expression of the type 1 IFN signaling pathway between ANCA-associated vasculitis and the healthy control group [24]. In our study, a significant increase in the expression of *IFIT1, IFI44*, and *IFI27* was found when the patient group with IgAV and KD was compared with healthy controls. This finding suggests that the type 1 IFN signaling pathway may play a role in disease pathogenesis. The fact that the expression of the *RSAD2, STAT1*, and *IFI44L* genes was reduced in the patient group compared to the control group indicates that there is a disturbance in the regulation of the IFN signaling pathway in the patient group.

Patients' IFN signature scores were calculated using the standardized IFN score calculation method based on the *Z*-score [25]. When comparing the IFN scores of patients diagnosed with IgAV with and without gastrointestinal tract involvement, the IFN score was significantly higher in patients with gastrointestinal tract involvement ($p=0.009$). The risk of gastrointestinal tract involvement was significantly higher (OR: 4.5) (95% CI: 1.117–18.226) in patients with high IFN scores ($p=0.034$). A high IFN score in patients with IgAV could be a biomarker for gastrointestinal involvement.

The IFN scores did not differ in IgAV patients with regard to renal involvement ($p=0.59$). This result suggests that the IFN score may not be an effective indicator of renal involvement in patients with IgAV. However, the limited sample size may have

affected the power of our results. Therefore, future studies with larger samples should be conducted to determine whether the IFN score can be a reliable biomarker for predicting renal involvement in IgAV patients. A longitudinal study to assess renal involvement should be warranted.

In IgAV patients, those requiring corticosteroid treatment had significantly higher IFN scores than those who did not ($p=0.01$). Additionally, patients with high IFN scores had a significantly increased risk of needing corticosteroid treatment (OR: 4.6, 95% CI: 1.091–19.509, $p=0.038$). High IFN scores may serve as an important prognostic factor for corticosteroid treatment necessity.

IgAV patients with gastrointestinal and renal involvement may require hospitalization. Those needing hospitalization had significantly higher IFN scores ($p=0.005$). A high IFN score was associated with a greater risk of hospitalization (OR: 4.8, 95% CI: 1.190–19.36, $p=0.028$) and longer hospital stays. These findings highlight the IFN score as a crucial prognostic marker.

This study aimed to investigate the IFN signature in KD patients. However, due to insufficient mRNA isolation, this was not possible in 6 of the 10 patients. The small sample size limits our assessment, but 3 of the 4 analyzed patients had high IFN scores. Future studies should reevaluate the IFN score in KD with a larger patient group.

There are few studies showing an increase in cytokines in patients with IgAV. In a study by Tae-Sun Ha, patients diagnosed with IgAV nephritis were compared with patients without nephritis, and it was found that serum and urinary TNF-α levels were significantly higher in patients with IgAV nephritis [26]. In a study of 20 IgAV patients conducted in Turkey, elevated levels of TNF-α, IL-1, and IL-6 were found in skin biopsies [27]. In addition, a gene polymorphism of IL-18, a proinflammatory cytokine, has been reported to play a role in the development of IgAV [28, 29]. In a study conducted by Novak et al. to evaluate anti-*Helicobacter pylori* antibodies in patients with IgAV, it was

shown that patients' TNF-α levels were elevated compared to the healthy control group [30]. We found IL-6 levels significantly lower in IgAV patients than in the control group ($p = 0.045$), suggesting a role for vascular inflammation in disease development. However, this contradicts the expected pro-inflammatory role of IL-6. No significant differences were observed in other cytokine levels between the patient and control groups.

There are studies that show an increased risk of IgAV in patients with familial Mediterranean fever (FMF) [31, 32]. In a study conducted on 80 IgAV patients in Turkey, a heterozygous mutation in the *MEFV* gene was found in 34% of patients [32]. In addition, patients carrying mutations in the *MEFV* gene were found to be younger and more likely to have arthritis and edema compared to those without mutations [32]. This study also showed that CRP and ESR values were higher in patients with *MEFV* mutations [32]. FMF is closely associated with dysregulation of interleukin-1 (IL-1), particularly IL-1β. Mutations in the *MEFV* gene, which encodes the pyrin protein, lead to uncontrolled IL-1β release, which is one of the main factors of inflammation in FMF [33]. IL-1 levels were significantly higher in IgAV patients with gastrointestinal involvement than in those without ($p = 0.0004$). This finding highlights a potential link between IgAV and FMF. While studies suggest that IgAV patients with MEFV mutations experience more arthritis and edema [32], no research has examined IL-1 levels in this group. Future studies should investigate both MEFV gene mutations and IL-1 levels in IgAV patients.

When comparing the cytokine levels of patients with and without joint symptoms (arthritis and/or arthralgia) in patients diagnosed with IgAV, it was found that TNF-R2 and IL-8 levels were statistically significantly higher in patients with joint symptoms ($p = 0.012$ and $p = 0.056$, respectively). There are studies in the literature showing that serum TNF receptors are elevated in patients with rheumatoid arthritis and juvenile rheumatoid arthritis [34, 35]. There is no autoimmune or autoinflammatory disease directly associated with IL-8. Elevated serum TNF-R2 and IL-8 levels as a result of immune dysregulation induced in patients with IgAV may be responsible for the joint symptoms experienced by patients.

When comparing patients with IgAV with and without melena, serum IL-18 levels were statistically significantly higher in patients with melena ($p = 0.025$). As mentioned above, studies have shown that a gene polymorphism of the proinflammatory cytokine IL-18 is associated with the development of IgAV. In our study, patients with melena had high serum IL-18 levels.

In the majority (68.8%) of IgAV patients in our study, the rash was limited to the lower extremities, while in some patients it spread to the upper extremities and trunk. No statistically significant results were found when comparing patients with and without isolated lower extremity rash in terms of hospitalization, corticosteroid requirements, renal involvement, and gastrointestinal involvement. In a large IgAV cohort conducted by Ekinci et al., subcutaneous edema on extremities was found to be significantly less frequent in patients with severe GI involvement than without [36]. When analyzing patients' cytokine levels with respect to rash distribution, TNF-R1 and IFN levels were significantly lower in patients with isolated lower extremity rash ($p = 0.038$ and $p = 0.038$, respectively). The significant increase in serum TNF-R1 and IFN-γ levels in patients whose rash spread to the trunk and upper extremities may be a sign of increased inflammation in the patients.

Our analysis found no significant difference in cytokine levels between IgAV patients with and without renal involvement. In contrast, Tae-Sun Ha's study reported significantly higher serum and urine TNF-α levels in IgAV nephritis patients [26]. We did not observe a similar increase in serum TNF-α levels in our nephritis group ($n = 5$), though our small sample size limits the generalizability of these findings.

In patients who required corticosteroids, IL-1, TNF-α, TNF-R1, and IFN-γ levels were significantly higher ($p = 0.013$, $p = 0.009$, $p = 0.045$, and $p = 0.045$, respectively), which may indicate increased inflammation in patients requiring corticosteroid treatment.

This work is important as it is the first study to examine the type 1 IFN signature in IgAV and KD, two childhood vasculitis. The results of this study will be important for future studies in expanded patient populations.

In our study, the IFN signature in patients with IgAV was evaluated, revealing dysregulation of the IFN signaling pathway. This finding suggests that the IFN pathway may play a crucial role in the pathogenesis of IgAV and raises the possibility that JAK inhibitors targeting this pathway could represent a novel therapeutic strategy. Notably, previous case reports have documented clinical improvement in patients with IgAV following JAK inhibitor treatment, further supporting this hypothesis [37, 38]. However, the precise mechanisms underlying IFN pathway dysregulation in IgAV remain unclear. Future studies, including larger-scale clinical trials, are warranted to confirm these findings and assess the therapeutic efficacy and safety of JAK inhibitors in this patient population.

The cross-sectional nature of our study, the lack of longitudinal data, and the limited number of KD patients are the limitations of this study. However, this is the first study to present the IFN signature in children with IgAV.

In conclusion, the IFN signature may provide an indication of gastrointestinal involvement and disease severity in the acute phase in patients with IgAV. Gastrointestinal involvement, corticosteroid requirement, hospitalization rate, and length of hospital stay are higher in IgAV patients with high IFN levels. As renal involvement may occur during the course of the disease, prospective studies are needed to demonstrate the efficacy of the IFN signature as a prognostic biomarker for renal involvement during follow-up.

manuscript. All authors provided critical feedback and helped shape the research, analysis, and manuscript.

Conflicts of Interest

Data Availability Statement

The data that support the findings of this study are available on request from the corresponding author. The data are not publicly available due to privacy or ethical restrictions.

References

1. K. Barut, S. Sahin, and O. Kasapcopur, "Pediatric vasculitis," *Current Opinion in Rheumatology* 28, no. 1 (2016): 29–38.

2. M. Piram and A. Mahr, "Epidemiology of Immunoglobulin A Vasculitis (Henoch–Schönlein): Current State of Knowledge," *Current Opinion in Rheumatology* 25, no. 2 (2013): 171–178.

3. Y. Song, X. Huang, G. Yu, et al., "Pathogenesis of IgA Vasculitis: An Up-to-Date Review," *Frontiers in Immunology* 12 (2021): 771619.

4. D. V. Parums, "A Review of IgA Vasculitis (Henoch-Schönlein Purpura) Past, Present, and Future," *Medical Science Monitor* 30 (2024): e943912-1.

5. E. Sag, E. D. Batu, and S. Ozen, "Childhood Systemic Vasculitis," *Best Practice & Research Clinical Rheumatology* 31, no. 4 (2017): 558–575.

6. Y. Bayındır, Ö. Başaran, Y. Bilginer, and S. Özen, "Vasculitis in Children," *Turkish Archives of Pediatrics* 59, no. 6 (2024): 517.

7. R. Bogdanović, "Henoch-Schönlein Purpura Nephritis in Children: Risk Factors, Prevention and Treatment," *Acta Paediatrica* 98, no. 12 (2009): 1882–1889.

8. P. F. Weiss, J. A. Feinstein, X. Luan, J. M. Burnham, and C. Feudtner, "Effects of Corticosteroid on Henoch-Schonlein Purpura: A Systematic Review," *Pediatrics* 120, no. 5 (2007): 1079–1087.

9. K. Barut, S. Şahin, A. Adroviç, and Ö. Kasapçopur, "Diagnostic Approach and Current Treatment Options in Childhood Vasculitis," *Turkish Archives of Pediatrics/Türk Pediatri Arşivi* 50, no. 4 (2015): 194.

10. Y. Ma, S. Zhang, J. Chen, H. Kong, and J. Diao, "Henoch-Schönlein Purpura With Scrotal Involvement: A Case Report and Literature Review," *Journal of Pediatric Hematology/Oncology* 43, no. 6 (2021): 211–215.

11. B. W. McCrindle, A. H. Rowley, J. W. Newburger, et al., "Diagnosis, Treatment, and Long-Term Management of Kawasaki Disease: A Scientific Statement for Health Professionals From the American Heart Association," *Circulation* 135, no. 17 (2017): e927–e999.

12. E. Rife and A. Gedalia, "Kawasaki Disease: An Update," *Current Rheumatology Reports* 22 (2020): 1–10.

13. H.-C. Kuo, "Diagnosis, Progress, and Treatment Update of Kawasaki Disease," *International Journal of Molecular Sciences* 24, no. 18 (2023): 13948.

14. L. Rönnblom and M.-L. Eloranta, "The Interferon Signature in Autoimmune Diseases," *Current Opinion in Rheumatology* 25, no. 2 (2013): 248–253.

15. E. C. Baechler, J. W. Bauer, C. A. Slattery, et al., "An Interferon Signature in the Peripheral Blood of Dermatomyositis Patients Is Associated With Disease Activity," *Molecular Medicine* 13 (2007): 59–68.

16. C. Cassius, R. Amode, M. Delord, et al., "MDA5+ Dermatomyositis Is Associated With Stronger Skin Type I Interferon Transcriptomic Signature With Upregulation of IFN-κ Transcript," *Journal of Investigative Dermatology* 140, no. 6 (2020): 1276–1279.e7.

17. L. Gallay, G. Mouchiroud, and B. Chazaud, "Interferon-Signature in Idiopathic Inflammatory Myopathies," *Current Opinion in Rheumatology* 31, no. 6 (2019): 634–642.

18. D. Özçeker, E. Ö. Yücel, S. S. Çimen, F. Dilek, N. Güler, and Z. Tamay, "Serum Autologous Skin Test in Children with Chronic Urticaria: Is it Related to The Severity of The Disease?," *Journal of Current Pediatrics* 18, no. 1 (2020): 85–94, https://doi.org/10.4274/jcp.2020.0008.

19. H. Kim, A. A. de Jesus, S. R. Brooks, et al., "Development of a Validated Interferon Score Using NanoString Technology," *Journal of Interferon & Cytokine Research* 38, no. 4 (2018): 171–185.

20. E. Mazzini, L. Massimiliano, G. Penna, and M. Rescigno, "Oral Tolerance Can Be Established via Gap Junction Transfer of Fed Antigens From CX3CR1+ Macrophages to CD103+ Dendritic Cells," *Immunity* 40, no. 2 (2014): 248–261.

21. K. Connelly, R. Kandane-Rathnayake, M. Huq, A. Hoi, M. Nikpour, and E. Morand, "Longitudinal Association of Type 1 Interferon-Induced Chemokines With Disease Activity in Systemic Lupus Erythematosus," *Scientific Reports* 8, no. 1 (2018): 3268.

22. O. Kimoto, J. Sawada, K. Shimoyama, et al., "Activation of the Interferon Pathway in Peripheral Blood of Patients With Sjögren's Syndrome," *Journal of Rheumatology* 38, no. 2 (2011): 310–316.

23. H. L. Wright, H. B. Thomas, R. J. Moots, and S. W. Edwards, "Interferon Gene Expression Signature in Rheumatoid Arthritis Neutrophils Correlates With a Good Response to TNFi Therapy," *Rheumatology* 54, no. 1 (2015): 188–193.

24. I. Batten, M. W. Robinson, A. White, et al., "Investigation of Type I Interferon Responses in ANCA-Associated Vasculitis," *Scientific Reports* 11, no. 1 (2021): 8272.

25. R. Pescarmona, A. Belot, M. Villard, et al., "Comparison of RT-qPCR and Nanostring in the Measurement of Blood Interferon Response for the Diagnosis of Type I Interferonopathies," *Cytokine* 113 (2019): 446–452.

26. T.-S. Ha, "The Role of Tumor Necrosis Factor-α in Henoch-Schönlein Purpura," *Pediatric Nephrology* 20 (2005): 149–153.

27. N. Besbas, U. Saatci, S. Ruacan, et al., "The Role of Cytokines in Henoch Schonlein Purpura," *Scandinavian Journal of Rheumatology* 26, no. 6 (1997): 456–460.

28. S. J. Park, J. S. Suh, J. H. Lee, et al., "Advances in Our Understanding of the Pathogenesis of Henoch-Schönlein Purpura and the Implications for Improving Its Diagnosis," *Expert Review of Clinical Immunology* 9, no. 12 (2013): 1223–1238.

29. O. Torres, R. Palomino-Morales, J. A. Miranda-Filloy, T. R. Vazquez-Rodriguez, J. Martin, and M. A. Gonzalez-Gay, "IL-18 Gene Polymorphisms in Henoch-Schönlein Purpura," *Clinical and Experimental Rheumatology* 28, no. 1 S57 (2010): 114.

30. J. Novák, Z. Szekanecz, J. Sebesi, et al., "Elevated Levels of Anti-*Helicobacter Pylori* Antibodies in Henoch–Schönlein Purpura," *Autoimmunity* 36, no. 5 (2003): 307–311.

31. R. Gershoni-Baruch, Y. Broza, and R. Brik, "Prevalence and Significance of Mutations in the Familial Mediterranean Fever Gene in Henoch-Schönlein Purpura," *Journal of Pediatrics* 143, no. 5 (2003): 658–661.

32. Z. B. Özçakar, F. Yalcinkaya, N. Çakar, et al., "MEFV Mutations Modify the Clinical Presentation of Henoch-Schönlein Purpura," *Journal of Rheumatology* 35, no. 12 (2008): 2427–2429.

33. P. R. Hesker, M. Nguyen, M. Kovarova, J. P.-Y. Ting, and B. H. Koller, "Genetic Loss of Murine Pyrin, the Familial Mediterranean Fever Protein, Increases Interleukin-1β Levels," *PLoS One* 7, no. 11 (2012): e51105.

34. B. Heilig, M. Wermann, H. Gallati, et al., "Elevated TNF Receptor Plasma Concentrations in Patients With Rheumatoid Arthritis," *Clinical Investigator* 70 (1992): 22–27.

35. B. Bjørnhart, P. Svenningsen, S. Gudbrandsdottir, et al., "Plasma TNF Binding Capacity in Patients With Juvenile Idiopathic Arthritis," *International Immunopharmacology* 5, no. 1 (2005): 73–77.

36. R. M. K. Ekinci, S. Balci, E. Melek, et al., "Clinical Manifestations and Outcomes of 420 Children With Henoch Schönlein Purpura From a Single Referral Center From Turkey: A Three-Year Experience," *Modern Rheumatology* 30, no. 6 (2020): 1039–1046.

37. Y.-F. Xu, Z.-Q. Li, W.-S. Yang, X.-W. Shi, and G.-M. Han, "Successful Treatment of Refractory IgA Vasculitis With Tofacitinib," *JAAD Case Reports* 30 (2022): 63–65.

38. Q. Sun, J. Bai, S. Wang, H. Fang, and J. Qiao, "JAK Inhibitors for Treating Steroid-Dependent IgA Vasculitis," *American Journal of Therapeutics* 31, no. 4 (2024): e476–e477.

WILEY

International Journal of
Rheumatic Diseases

ORIGINAL ARTICLE

Comparison of Outcomes Between Protocolized Tacrolimus-Based and Non-Protocolized Ciclosporin-Based Triple-Combination Therapy in Interstitial Lung Disease With Anti-MDA5-Positive Dermatomyositis: A Single-Center Retrospective Cohort Study

Risa Yamada | Masayoshi Harigai | Yasuhiro Katsumata [ID]

Department of Rheumatology, Tokyo Women's Medical University School of Medicine, Tokyo, Japan

Correspondence: Yasuhiro Katsumata (katsumata@twmu.ac.jp)

ABSTRACT

Aim: We retrospectively compared the outcomes of protocolized tacrolimus-based and non-protocolized ciclosporin-based triple-combination therapies in consecutive patients with newly diagnosed interstitial lung disease (ILD) and antimelanoma differentiation-associated gene 5 (MDA5)-positive dermatomyositis (DM).

Methods: Clinical data from consecutive adult patients with newly diagnosed anti-MDA5-positive DM-associated ILD in our hospital from 2013 to 2022 were analyzed. Recent cases received protocolized therapy with high-dose glucocorticoids (GCs), tacrolimus, and intravenous cyclophosphamide (IVCY). Earlier cases received non-protocolized ciclosporin-based triple-combination therapy. The observation period was 12 months. The outcomes included a composite of death or requirement for long-term domiciliary oxygen therapy (LTOT), mortality, GC and IVCY doses, and cytomegalovirus reactivation rates within 12 months.

Results: Protocolized therapy with tacrolimus ($n = 14$) and non-protocolized therapy with ciclosporin ($n = 10$) groups had similar baseline characteristics. No deaths or LTOT were observed in the protocolized therapy with the tacrolimus group, whereas four patients in the non-protocolized therapy with ciclosporin group experienced these outcomes (difference, 40 percentage points; 95% CI, 10 to 70; $p = 0.020$). The 12-month mortality rates were not significantly different between the two groups ($p = 0.16$). The protocolized therapy with the tacrolimus group had lower GC dosages at 6 months, more total cycles and cumulative doses of IVCY, and lower cytomegalovirus reactivation rates than the non-protocolized therapy with the ciclosporin group ($p < 0.05$).

Conclusions: Protocolized tacrolimus-based triple-combination therapy demonstrated better outcomes than non-protocolized ciclosporin-based triple-combination therapy in patients with anti-MDA5-positive DM-associated ILD. Reduced GC doses and more intensive IVCY use also presumably contributed to better outcomes in the protocolized therapy with the tacrolimus group.

1 | Introduction

Idiopathic inflammatory myopathies (IIMs) are a heterogeneous group of disorders in which a common feature is chronic inflammation of skeletal muscle, leading to muscle weakness [1]. Dermatomyositis (DM) is a subtype of IIM with characteristic cutaneous findings, such as heliotrope rash and Gottron's sign/papules [2, 3]. In addition, a subgroup of patients with DM classified as clinically amyopathic dermatomyositis (CADM) present with cutaneous lesions without muscle weakness. Interstitial lung disease (ILD) is a common pulmonary symptom and a major cause of morbidity and mortality in patients with IIMs, with a prevalence ranging from 19.9% to 86% [4]. ILD's initial presentation and clinical course in IIMs are heterogeneous, and its management is complex and requires close patient follow-up. Some patients are even asymptomatic; thus, ILD may be an incidental finding on radiological examination [4]. In contrast, rapidly progressive (RP)-ILD, mainly associated with anti-melanoma differentiation-associated gene 5 (MDA5) antibodies, is a life-threatening complication; up to 50% of ILD patients with anti-MDA5-positive DM die within 6 months after diagnosis despite treatment, including high-dose glucocorticoids (GCs) [5, 6]. Early diagnosis and therapeutic intervention are critical for preventing the progression from initial inflammatory activity to end-stage disease with irreversible fibrosis and diffuse alveolar damage [7].

A prospective, multicenter, single-arm study demonstrated that ILD patients with anti-MDA5-positive DM treated with triple-combination therapy (high-dose GCs, tacrolimus, and intravenous cyclophosphamide [IVCY]) had higher 6-month survival rates than historical controls who received only GCs or GC and sequential combination therapy [8]. The American College of Rheumatology (ACR)/American College of Chest Physicians (CHEST) Guideline conditionally recommends upfront combination therapy (triple therapy) for people with RP-LD and MDA-5 over monotherapy as first-line treatment [9]. However, a cluster analysis using a large-scale multicenter retrospective cohort of patients with myositis-associated ILD failed to show the survival benefits of triple-combination therapy (GCs, tacrolimus/ciclosporin, and IVCY) over dual-combination therapy or GC monotherapy in any of the clusters. Cumulative survival rates were even lower in the triple-combination therapy group than in the controls in clusters positive for anti-MDA5 antibodies but without supplemental oxygen requirement [10].

We aimed to retrospectively investigate the outcomes of protocolized tacrolimus-based triple-combination therapy in consecutive adult patients with newly diagnosed and previously untreated anti-MDA5-positive DM-associated ILD in our hospital and compare these outcomes with those of non-protocolized ciclosporin-based triple-combination therapy in historical controls.

2 | Materials and Methods

2.1 | Study Population and Data Collection

Clinical data from all consecutive adult (≥ 18 years old) patients with newly diagnosed and previously untreated anti-MDA5-positive DM-associated ILD in our hospital from 2013 to 2022 were enrolled. At our hospital, patients newly diagnosed with or suspected of having classic DM/CADM were admitted for systemic evaluation regardless of disease severity. Classic DM and CADM were diagnosed according to Bohan and Peter's criteria [11, 12], Sontheimer's criteria [2], or the 2017 European League Against Rheumatism (EULAR)/ACR classification criteria for adult and juvenile IIMs and their major subgroups [3]. In addition, when the word "DM" is used solely in this paper, it means both "classic DM" and "CADM". Anti-MDA5 antibodies were measured by enzyme-linked immunosorbent assay (ELISA) using commercial ELISA kits or those developed by Sato et al. as described previously [13, 14]. Clinical, radiological, and laboratory data and information on adverse events were collected retrospectively from the electronic medical records. Disease duration was defined as the duration from ILD onset until GC initiation. Serious adverse event (SAE) was defined as an adverse event that resulted in death, was life-threatening, required hospitalization or prolongation of existing hospitalization, resulted in persistent or significant disability or incapacity, or was a birth defect. Renal impairment was defined as an increase in the serum creatinine level to > 1.5-fold greater than the baseline level [8]. Chronic kidney disease (CKD) was defined as an estimated glomerular filtration rate (eGFR) [15] $= 194 \times$ (serum creatinine)$^{-1.094} \times$ (Age)$^{-0.287} \times$ [0.739 if female] $< 60 \, \text{mL/min}/1.73 \, \text{m}^2$. This study was approved by the ethics committee of Tokyo Women's Medical University (registration number 3534) and adhered to the principles of the Helsinki Declaration.

2.2 | Assessment of ILD

ILD was defined as the presence of diffuse parenchymal lung disease, such as reticular opacity, ground-glass opacity, and honeycombing on high-resolution computed tomography (HRCT) according to the American Thoracic Society/European Respiratory Society International Multidisciplinary Consensus Classification [16]. Patients with DM were routinely scanned using HRCT during the initial assessment and during the course of ILD at our hospital. Pulmonary function tests (PFTs) were performed on most patients as an initial assessment; however, the tests were not performed after treatment in some patients. Serum ferritin and Krebs von den Lungen-6 (KL-6) levels were measured in our hospital's central laboratory per our daily clinical practice. For KL-6, a clinical cut-off value of 500 U/mL has been established to distinguish patients with ILDs from healthy subjects and patients with lung diseases other than ILDs [17].

2.3 | Treatment

In our institution, our strategy for treating patients with anti-MDA5-positive DM-associated ILD was switched from non-protocolized ciclosporin-based triple-combination therapy to protocolized tacrolimus-based triple-combination therapy following the favorable results reported by Tsuji [8]. Recent cases (2017–2022; protocolized therapy with tacrolimus group [protocolized-TAC group]) were treated with protocolized triple-combination therapy with high-dose GCs, tacrolimus, and IVCY, according to the previous report by Tsuji [8]. Prednisolone or equivalent GC dose was initially administered at 1 mg/kg/day for 4 weeks; thereafter, the existing dose was reduced by 10% every 2 weeks when the dosage was > 30 mg/day and every 2–4 weeks when it was ≤ 30 mg/day. Tacrolimus was adjusted to retain 12-h

blood trough levels within the 10–12 ng/mL range. IVCY was initiated at 500 mg/m^2 of body surface area (BSA) biweekly, then gradually increased to a maximum of 1000 mg/m^2 of BSA; this was implemented with the goal of a nadir leukocyte count of 2000–3000/μl or a 50% reduction from baseline. After the sixth IVCY administration, the interval was extended to 4–8 weeks. The planned number of IVCY administrations was 10–15. Earlier patients (2013–2016; non-protocolized therapy with ciclosporin group [non-protocolized-CS group]) were treated with high-dose GCs, ciclosporin (target 2-h postdose blood level of 800–1000 ng/mL) [18], and IVCY, where the GC and IVCY regimens were individually tailored by the treating physicians. GC pulses were administered to patients in both groups at the discretion of the treating physicians. Plasmapheresis was not performed in any patient. Supplemental oxygen was administered according to the treating physicians' discretion. Long-term domiciliary oxygen therapy (LTOT) was administered when resting PaO$_2$ was ≤ 55 mmHg or SpO$_2$ was ≤ 88% at rest. Trimethoprim/sulfamethoxazole or atovaquone was routinely used for the prophylaxis of Pneumocystis pneumonia (PCP). Patients were regularly monitored for serum cytomegalovirus (CMV) antigenemia and, if they were positive for CMV antigenemia, were treated with ganciclovir or valganciclovir at an early stage. All patients received COVID-19 vaccination during the pandemic.

2.4 | Outcomes

The primary outcome was the composite of death from any cause or requirement for LTOT (used for at least 15 h per day) at home within 12 months after GC initiation. This composite outcome was newly adapted from a randomized controlled trial on nocturnal oxygen therapy for chronic obstructive pulmonary disease [19]. For composite outcomes, any patient who died was not counted as the one who required LTOT. The secondary outcomes included 12-month mortality, GC and IVCY doses, and CMV reactivation rates.

2.5 | Statistical Analyses

Continuous variables are presented as mean (standard deviation, SD). Categorical variables were described as counts and proportions (%). The observation period for the survival analyses began from the first visit when ILD was diagnosed in each patient and continued for 12 months or was censored when each event (death or requirement for LTOT) occurred for the first time within 12 months. Missing data were handled using available case analysis; each analysis was based on subjects with available data on the included variables. Two-group comparisons were performed using Fisher's exact test and Welch's t-test for categorical and continuous variables, respectively. The Jonckheere–Terpstra trend test was used to analyze the ordered differences among the groups. Relative risk was calculated as the ratio of the probability of an event occurring between the protocolized-TAC and non-protocolized-CS groups using the Haldane–Anscombe correction [20]. Time-to-event analyses were performed using Kaplan–Meier analysis with the log-rank test. Two-sided $p < 0.05$ were considered statistically significant. No correction for multiple comparisons was made, and p were interpreted as exploratory results, except for the primary

composite outcome of death or requirement for LTOT. Statistical analyses were performed using Microsoft Excel software (version 2021; Microsoft, Redmond, WA) and JMP Pro statistical software (version 17.0.0; SAS Institute, Cary, NC).

3 | Results

3.1 | Clinical Characteristics of Patients with Anti-MDA5-Positive DM-Associated ILD

Of the 31 hospitalized patients with anti-MDA5-positive DM-associated ILD during the study period, seven patients were excluded because they were initially treated at another hospital. Among the 24 remaining patients with anti-MDA5-positive DM-associated ILD, 14 and 10 received tacrolimus- and ciclosporin-based triple-combination therapies, respectively. The disease duration was not significantly different between the two groups. As detailed in Table 1, other characteristics such as age, sex, baseline PFT and arterial blood gas results, and baseline serum ferritin and KL-6 levels were not significantly different between the two groups.

3.2 | Primary Composite Outcome of Death or Requirement for LTOT and Secondary Outcome of Death

None of the protocolized-TAC group patients died or required LTOT. Treatment of five patients deviated from the protocol in the protocolized-TAC group: four patients received fewer IVCY cycles (6–9 cycles) according to the treating physicians' discretion, and GC tapering was suspended between 6 and 12 months in one patient while she was treated by a non-specialist doctor. In the non-protocolized-CS group, 4/10 (40%) patients died ($n = 2$) or required LTOT ($n = 2$) due to RP-ILDs. As shown in Table 2, a significant difference between the two groups in the composite outcome was observed (difference, 40 percentage points; 95% confidence interval [CI], 10 to 70; $p = 0.02$). Among patients with baseline serum ferritin levels > 500 ng/mL ($n = 15$), the difference between the two groups in the composite outcome was 38 percentage points (95% CI, 4 to 71; $p = 0.20$), and the relative risk was 0.16 (95% CI, 0.01 to 2.66). Among patients with baseline serum ferritin levels > 1000 ng/mL ($n = 5$), the difference between the two groups in the composite outcome was 33 percentage points (95% CI, −20 to 87; $p = 1.00$), and the relative risk was 0.44 (95% CI, 0.033 to 7.52). Among patients with baseline ABG PaO$_2$ levels < 80 mmHg ($n = 8$), the difference between the two groups in the composite outcome was 60 percentage points (95% CI, 17 to 103; $p = 0.20$), and the relative risk was 0.21 (95% CI, 0.02 to 3.12). As shown in Figure 1A, time-to-event analyses indicated that the protocolized-TAC group had better composite outcomes than the non-protocolized-CS group ($p < 0.01$). As shown in Table 2, the 12-month mortality rates were not significantly different between the protocolized-TAC and non-protocolized-CS groups (0/14 [0%] vs. 2/10 [20%]; difference, 20 percentage points; 95% CI, −5 to 45; $p = 0.16$). As shown in Figure 1B, the time-to-event analysis indicated no significant difference between the two groups in mortality ($p = 0.09$). The proportions of patients who required supplemental oxygen at hospitals (either temporarily or permanently) were not significantly different between the protocolized-TAC and non-protocolized-CS

TABLE 1 | Baseline characteristics of patients with anti-MDA5-positive DM-associated ILD.

	Protocolized therapy with tacrolimus group ($n=14$)	Non-protocolized therapy with ciclosporin group ($n=10$)	p[a]
Female, n (%)	10 (71%)	7 (70%)	1.00
Age, years, mean (SD)	51 (9.7)	54 (7.8)	0.42
Disease duration[b], days, mean (SD)	34 (48)	38 (74)	0.88
Current or ex- smoker, n (%)	10 (71%)	3 (30%)	0.095
Heliotrope rash, n (%)	3 (20%)	3 (30%)	0.67
Gottron's sign or papules, n (%)	14 (100%)	8 (80%)	0.16
Muscle weakness, n (%)	2 (10%)	1 (10%)	1.00
Skin ulcer, n (%)	3 (20%)	0 (0%)	0.24
Dysphagia, n (%)	1 (10%)	0 (0%)	1.00
Arthritis, n (%)	10 (71%)	6 (60%)	0.67
Fever, n (%)	3 (20%)	3 (30%)	0.67
ILD, n (%)	14 (100%)	10 (100%)	1.00
Anti-MDA5 antibodies, n (%)	14 (100%)	10 (100%)	1.00
Anti-Ro/SS-A antibodies, n (%)	2 (20%) ($n=11$)	0 (0%) ($n=8$)	0.49
WBC count, /μL, mean (SD)	5140 (1610)	5530 (1300)	0.52
Lymphocyte count, /μL, mean (SD)	920 (380)	830 (470)	0.61
Serum CK, U/L, mean (SD)	173 (130)	252 (229)	0.34
Serum LDH, U/L, mean (SD)	321 (146)	381 (103)	0.25
Serum albumin, mg/dL, mean (SD)	3.2 (0.6)	3.3 (0.3)	0.87
Serum creatinine, mg/dL, mean (SD)	0.56 (0.10)	0.64 (0.19)	0.21
Serum CRP, mg/dL, mean (SD)	1.00 (1.17)	1.20 (1.08)	0.67
Serum ferritin, ng/mL, mean (SD)	655 (465)	891 (834)	0.43
Serum KL-6, U/mL, mean (SD)	615 (187)	748 (411)	0.36
ABG PaO$_2$, mmHg, mean (SD)	88.3 (12.5) ($n=13$)	79.7 (12.9)	0.12
ABG SaO$_2$, %, mean (SD)	96.8 (0.9) ($n=13$)	96.3 (2.0)	0.56
PFT %VC, %, mean (SD)	79.7 (14.7) ($n=13$)	86.0 (17.9)	0.38
PFT %FVC, %, mean (SD)	83.2 (16.8) ($n=13$)	89.3 (19.3)	0.44
PFT %D$_{LCO}$, %, mean (SD)	54.8 (10.4) ($n=11$)	61.2 (14.2)	0.26

Abbreviations: ABG, arterial blood gas; CK, creatine kinase; D$_{LCO}$, diffusing capacity of the lung for carbon monoxide; DM, dermatomyositis; FVC, forced vital capacity; ILD, interstitial lung disease; KL-6, Krebs von den Lungen-6; LDH, lactate dehydrogenase; MDA5, melanoma differentiation-associated gene 5; PFT, pulmonary function test; SD, standard deviation; VC, vital capacity; WBC, white blood cell.
[a]p were determined using Fisher's exact test for categorical variables and Welch's t-test for continuous variables.
[b]Disease duration was defined as the duration from ILD onset until glucocorticoid initiation.

groups (3/14 [20%] vs. 5/10 [50%]; difference, 29 percentage points; 95% CI, −9 to 70; $p=0.20$).

3.3 | GC And IVCY Doses

Among the live patients, the mean prednisolone dosages at 6 months were 18 and 23 mg/day in the protocolized-TAC and non-protocolized-CS groups, respectively (mean difference, 5.4 mg/day; 95% CI, 0.1 to 10.7 mg/day; $p=0.046$) (Figure 2A), and 9 and 12 mg/day at 12 months in the protocolized-TAC and non-protocolized-CS groups, respectively (mean difference, 2.5 mg/day; 95% CI, −0.4 to 5.5 mg/day; $p=0.086$) (Figure 2B). According to the treating physicians' discretion, GC pulses were administered to 10/14 [71%] and 6/10 [60%] patients in the protocolized-TAC and non-protocolized-CS groups, respectively (difference, 11 percentage points; 95% CI, −27 to 50; $p=0.67$). More total cycles and cumulative doses of IVCY were administered to the protocolized-TAC group than to the non-protocolized-CS group ($p<0.001$ in both comparisons) (Figure 2C,D).

| Outcome	Protocolized therapy with the tacrolimus group	Non-protocolized therapy with the ciclosporin group	Difference (95% CI)[a]	Relative risk (95% CI)[a,b]	p[a,c]
			percentage points		
Composite outcome: death or requirement for LTOT[d]					
Event at 12 months of follow-up—number/total number (%)	0/14 (0%)	4/10 (40%)	40 (10 to 70)	0.08 (0.005 to 1.36)	0.020
Rate per 100 person-yr	0.0	58.1			
Death					
Event at 12 months of follow-up—number/total number (%)	0/14 (0%)	2/10 (20%)	20 (−5 to 45)	0.15 (0.008 to 2.77)	0.16
Rate per 100 person-yr	0.0	23.3			

Abbreviations: CI, confidence interval; LTOT, long-term oxygen therapy.

[a]*p *No correction for multiple comparisons was made.

[b]Relative risk was calculated as the ratio of the probability of an event occurring between the protocolized therapy with tacrolimus and non-protocolized therapy with ciclosporin groups using the Haldane–Anscombe correction.

[c]P-values were determined using Fisher's exact test.

[d]For the composite outcome, any patient who died was not counted as the one who required LTOT.
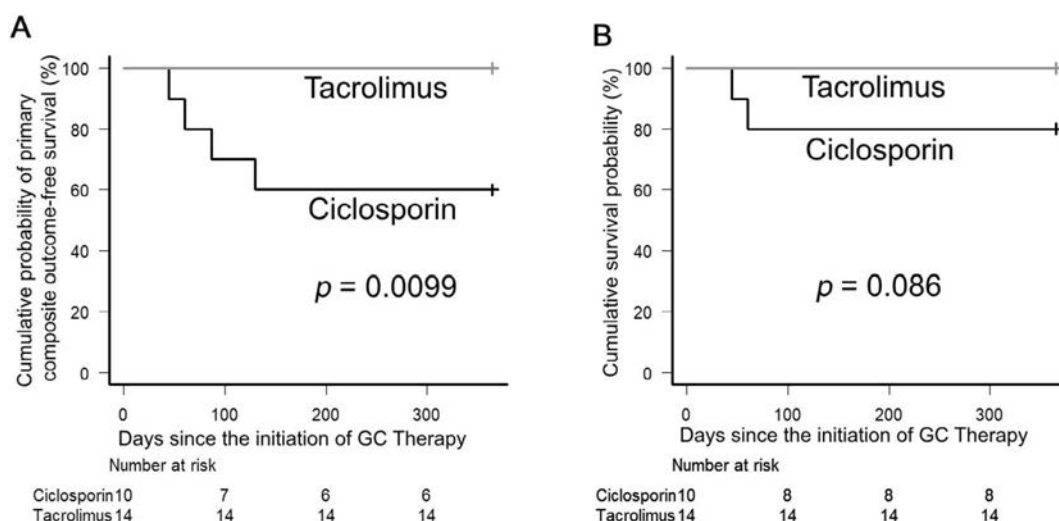
FIGURE 1 | Kaplan–Meier analyses of the primary and secondary outcomes. Kaplan–Meier plots of time to (A) death from any cause or requirement for LTOT (composite outcome) and (B) death within 12 months after initiation of GCs. p-values were determined using the log-rank test. GC, glucocorticoid; LTOT, long-term domiciliary oxygen therapy.

3.4 | Adverse Events

The adverse events are summarized in Table 3. CMV reactivation was more frequently observed in the non-protocolized-CS group than in the protocolized-TAC group (8/10 [80%] vs. 5/14 [40%]; difference, 40 percentage points; 95% CI, 9 to 80; p = 0.047).

PCP was observed in two patients in the non-protocolized-CS group. Patients complicated with these active infections were withdrawn from IVCY, tacrolimus, and ciclosporin and treated with drugs such as ganciclovir, valganciclovir, and trimethoprim/sulfamethoxazole. None of the patients had COVID-19. Renal impairment was observed in 9 and 3 patients in the
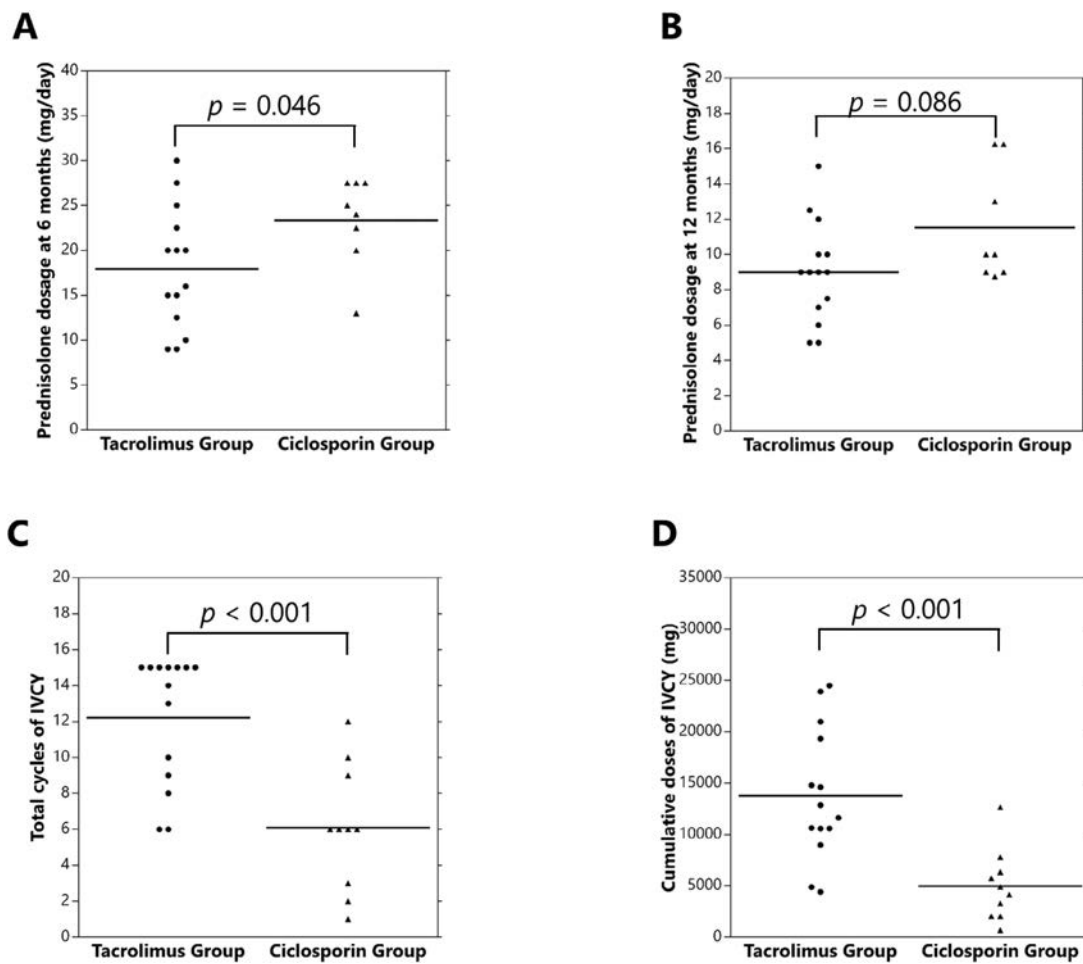
FIGURE 2 | Comparison of treatments other than tacrolimus and ciclosporin between the protocolized therapy with tacrolimus and non-protocolized therapy with ciclosporin groups. GC dosage at 6 (A) and 12 (B) months. Total cycles (C) and cumulative doses (D) of IVCY. p were determined using Welch's t-test. Horizontal lines represent the means of the groups. GC, glucocorticoid; IVCY, intravenous cyclophosphamide.

protocolized-TAC and non-protocolized-CS groups ($p=0.21$), respectively, and seven and two of these patients progressed to CKD ($p=0.21$). Thrombotic microangiopathy (TMA) did not occur. SAEs of infection were observed in one and three patients in the protocolized-TAC and non-protocolized-CS groups, respectively, and SAEs excluding infection were observed in two and one patients in the protocolized-TAC and non-protocolized-CS groups, respectively. No adverse events leading to death or discontinuation of IVCY or tacrolimus/ciclosporin were observed.

3.5 | Changes in Clinical Variables

Over 12 months, statistically significant decreasing trends in serum ferritin levels were observed in the protocolized-TAC and non-protocolized-CS groups (Figure 3A,B). Although not statistically significant, a decreasing trend in serum KL-6 levels over 12 months was observed in the protocolized-TAC and non-protocolized-CS groups (Figures 3C,D). In a deceased patient in the non-protocolized-CS group, the serum KL-6 levels were 1047 U/mL initially, elevated to 1663 U/mL, and decreased to 363 U/mL at the time of death because of sepsis. In another deceased patient in the non-protocolized-CS group, the serum KL-6 levels were 1005 U/mL initially, decreased to 977 U/mL

in 2 weeks, and then gradually increased up to 2798 U/mL at the time of death because of PCP and exacerbated ILD. Over 12 months, statistically significant decreasing trends in serum anti-MDA5 titers were observed in the protocolized-TAC group (Figures 3E). Although not statistically significant, an increasing trend in the percent predicted forced vital capacity (%FVC) over 6 months were observed in the protocolized-TAC group (Figure 3F). The analyses of anti-MDA5 titers and %FVC were not conducted due to the limited availability of these data in the non-protocolized-CS group.

4 | Discussion

This study demonstrated that the protocolized triple-combination therapy with high-dose GCs, tacrolimus, and IVCY demonstrated better outcomes than non-protocolized ciclosporin-based triple-combination therapy, individually tailored by the treating physicians in patients with anti-MDA5-positive DM-associated ILD. Although the ACR/CHEST guideline conditionally recommends triple therapy, including GCs with two additional agents (rituximab, cyclophosphamide, intravenous immune globulin, calcineurin inhibitor [tacrolimus/ciclosporin], mycophenolate, and JAK inhibitor) for people with anti-MDA5-positive DM-associated RP-ILD as first-line treatment, there is insufficient

TABLE 3 | Adverse events.

Adverse event	Protocolized therapy with the tacrolimus group (n = 14)[a]	Non-protocolized therapy with the ciclosporin group (n = 10)[a]
Any adverse event	14 (100%)	10 (100%)
Any SAE	3 (20%)	3 (30%)
SAE of infection	1 (7%)	3 (30%)
SAE, excluding infection	2 (10%)	1 (10%)
Infection		
Any infection, excluding CMV	3 (20%)	3 (30%)
Bacterial infection	3 (20%)	2 (20%)
PCP	0	2 (20%)
Invasive pulmonary aspergillosis	1 (7%)	1 (10%)
Herpes zoster	1 (7%)	0
CMV antigenemia/infection	5 (40%)[b]	8 (80%)
Impaired glucose tolerance	6 (40%)	5 (50%)
Hypertension	2 (10%)	5 (50%)
Dyslipidemia	6 (40%)	6 (60%)
Cardio vascular disease	1 (7%)	0
Fragility fracture	2 (10%)	0
Corticosteroid-induced psychiatric disorder	0	1 (10%)
Leukopenia	8 (60%)	4 (40%)
Thrombocytopenia	0	1 (10%)
Elevation of liver enzymes	0	2 (20%)
Renal impairment	9 (60%)	3 (30%)
Progression to CKD	7 (50%)	2 (20%)
Tremor	5 (40%)	0
Hemorrhagic cystitis	0	0

Abbreviations: CI, confidence interval; CKD, chronic kidney disease; CMV, cytomegalovirus; PCP, Pneumocystis pneumonia; SAE, serious adverse event.

[a]p Values are the number (%).

[b]$p = 0.047$ versus the non-protocolized therapy with ciclosporin group using Fisher's exact test. The difference (95% CI) was 40 percentage points (9 to 80), and the relative risk (95% CI) was 0.45 (0.21 to 0.96).

evidence to recommend one specific treatment regimen [9]. The guideline panel mentioned that they preferred tacrolimus to ciclosporin because of its perceived improved effectiveness [9]. The direct comparison of tacrolimus and ciclosporin was hardly reported for anti-MDA5-positive DM-associated ILD. Although a randomized, open-label trial was conducted on polymyositis/ DM-associated ILD, only 30% of the study subjects had anti-MDA5 antibodies; thus, subgroup analyses based on autoantibody status were not performed [21]. The results of our study might support the view of the ACR/CHEST guideline. However, it was unclear whether the superiority of the protocolized-TAC group stemmed from the tacrolimus itself or the difference in the GC and IVCY regimens between the two triple-combination therapies. In connection with this issue, a meta-analysis reported that tacrolimus was superior to ciclosporin in improving graft survival and preventing acute rejection after kidney

transplantation [22]. In addition, because there was more significant evidence of tacrolimus as a treatment option for lupus nephritis, tacrolimus, but not ciclosporin, was recommended in the EULAR recommendations for the management of systemic lupus erythematosus 2023 update [23].

More intensive use of IVCY and reduced doses of GCs also presumably contributed to the better outcomes in the protocolized-TAC group. Sasai et al. also suggested that the early administration of sufficient doses of IVCY might help maintain long-term remission [24]. In our study, CMV reactivation was more frequently observed in the non-protocolized-CS group than in the protocolized-TAC group, and PCP was observed only in the non-protocolized-CS group. These opportunistic infections, which require temporary withdrawal from tacrolimus/ciclosporin and IVCY, might be associated with higher GC doses. In this
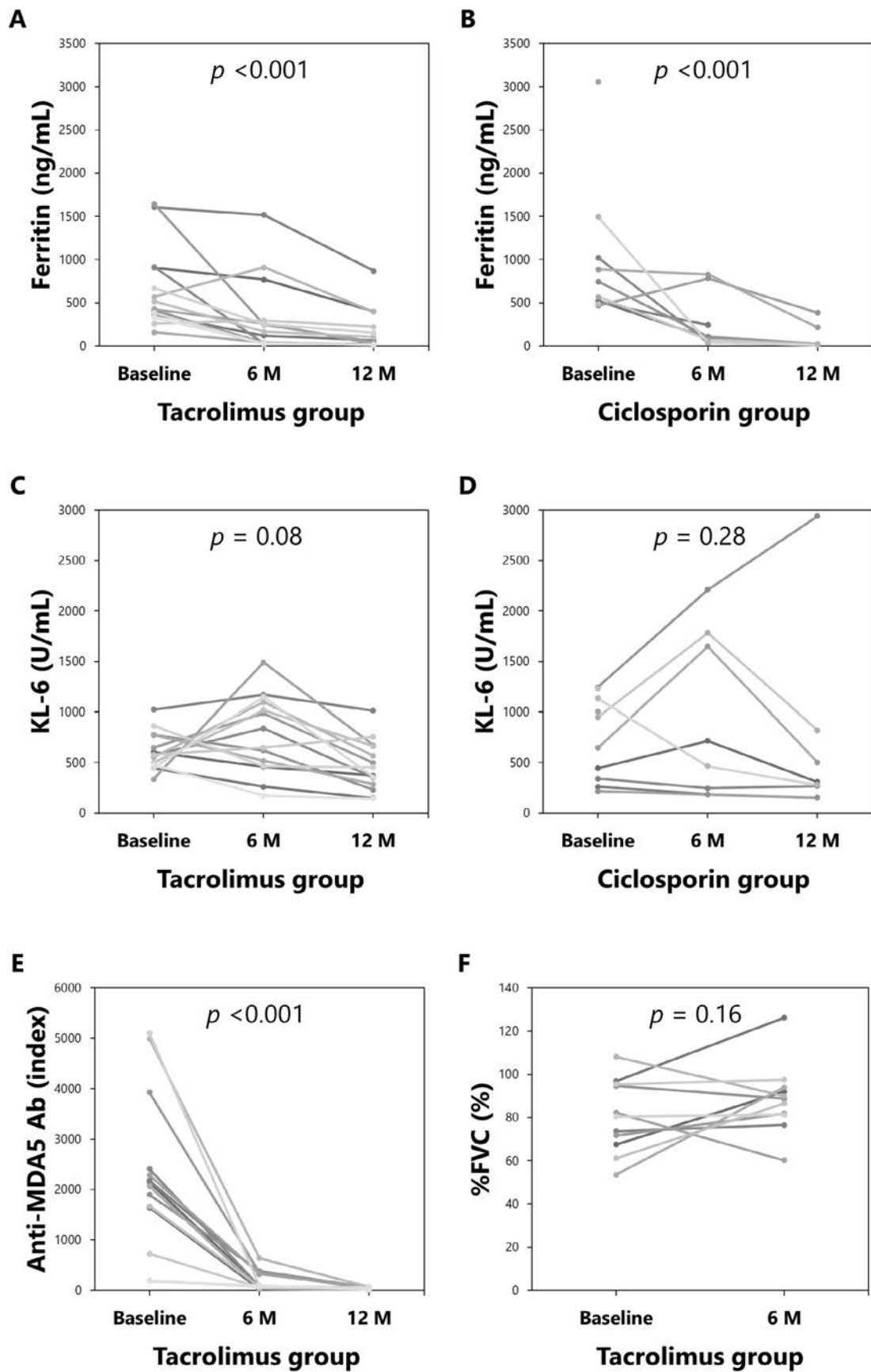
FIGURE 3 | Legend on next page.

FIGURE 3 | Changes in clinical variables among the protocolized therapy with tacrolimus group ($n=14$[a]) and the non-protocolized therapy with ciclosporin group ($n=10$[b]). Temporal changes in serum ferritin levels among the protocolized therapy with tacrolimus group (A) and the non-protocolized therapy with ciclosporin group (B), serum KL-6 levels among the protocolized therapy with tacrolimus group (C) and the non-protocolized therapy with ciclosporin group (D), anti-MDA5 antibody titers among the protocolized therapy with tacrolimus group (E), and %FVC among the protocolized therapy with tacrolimus group (F). [a]Data on %FVC at baseline and at 6 months were available for 11 patients. [b]Data from the non-protocolized therapy with ciclosporin group were demonstrated only for serum ferritin and KL-6 levels due to data availability, and two patients in the non-protocolized therapy with ciclosporin group died within 6 months. p were determined using the Jonckheere–Terpstra trend test. KL-6, Krebs von den Lungen-6; MDA5, melanoma differentiation-associated gene 5; %FVC, percent predicted forced vital capacity.

context, reduced GC doses may have been associated with the better overall survival rates even though CMV infection did not directly cause death in the patients included in this study.

The primary composite outcome of death or the requirement for LTOT in this study was not used in previous studies on anti-MDA5-positive DM-associated ILD; they mostly used 6-month or 1-year survival rates as primary outcomes [25]. However, considering that upfront combination therapy (triple therapy) has improved prognosis, short-term survival rates are no longer the best primary outcomes of studies on anti-MDA5-positive DM-associated ILD. The 5-year survival rate was 100% among participants in the previous trial [24]. Thus, adopting this primary composite outcome from a clinical trial on chronic obstructive pulmonary disease is reasonable [19]. The validity of this outcome should be verified in future studies. Furthermore, consistent with other studies [26], all deaths and the requirement for LTOT occurred within 6 months after GC initiation. Thus, this study's 6-month and 12-month rates for the primary composite outcome of death or the requirement for LTOT and secondary outcome of death were the same.

The inclusion criteria might have resulted in a better overall survival rate in our cohort than in previous reports. In the conventional definition of RP-ILD ("rapidly progressive within 3 months of the onset of symptoms" [5]), it takes up to 3 months without treatment to judge that the ILD is not RP-ILD. However, in our hospital, if the patient with DM-associated ILD had predictive features of RP-ILD, such as anti-MDA5 antibodies and hyperferritinemia, GC treatment was initiated even if rapidly progressive symptoms were not apparent. The mean disease duration in this study was approximately 1 month. Consequently, the ILD in some patients might have been chronic even without intensive immunosuppressive therapy, and the precise rate of RP-ILD according to the conventional definition was not determined. However, anti-MDA5-positive DM-associated ILDs in Japanese patients are mostly RP-ILD [5]. In addition, treatment delay, even for a few weeks, can greatly affect the outcomes of anti-MDA5-positive DM-associated RP-ILD [8]. Thus, it was clinically reasonable to include all patients with ILD without waiting up to 3 months to determine whether their ILD was RP-ILD.

Inconsistent with the results of the previous [8] and present studies, cluster analysis using a large-scale multicenter retrospective cohort did not support a better prognosis in patients with anti-MDA5-positive DM-associated ILD treated initially with triple-combination therapy compared with those treated initially with dual-combination therapy or GC monotherapy [10]. The authors of the cluster analysis study speculated that patients with more severe ILD were likely to be included in the triple-combination

therapy group in their cohort: they stated that clinical characteristics were somewhat different between the triple-combination therapy group and the dual-combination therapy or GC monotherapy group in individual clusters. In contrast, as discussed above, in this study, the ILD in some patients might have been mild even without triple-combination therapy.

Although not statistically significant, renal impairment and CKD tended to occur more frequently in the protocolized-TAC group than in the non-protocolized-CS group; end-stage kidney disease did not develop in any of the patients. Tsuji et al. also reported that the mean eGFR declined from 98.1 to 75.3 in patients who received basically the same tacrolimus-based triple-combination therapy and suggested that a high blood tacrolimus concentration might exert some influence on renal function and that when renal function seems to deteriorate seriously, it may be necessary to reduce or withdraw the potentially contributing medication, such as tacrolimus [8]. In a randomized, open-label trial on polymyositis/DM-associated ILD, the target blood trough level for tacrolimus was 5–10 ng/mL, and renal impairment was observed in 10% and 25% of the tacrolimus and ciclosporin groups, respectively [21]. The ACR/CHEST guideline alerted potential renal toxicity of calcineurin inhibitors (tacrolimus/ciclosporin) [9].

This study has several limitations. First, the study's reliance on an uncontrolled study design and retrospective data with a limited number of study subjects raises concerns about potential confounding factors and selection biases that may influence the reported outcomes, warranting cautious interpretation of the results and conclusions drawn. Nevertheless, all consecutive previously untreated patients hospitalized in our hospital during the study period were included in the analyses of this study, and all data were obtained on time as per routine clinical practice. Furthermore, randomized controlled trials are not feasible considering the severe and rapidly progressive nature of this rare disease [27]. Second, the treatment of five patients deviated from the protocol in the protocolized-TAC group: Four patients received fewer cycles of IVCY (6–9 cycles) according to the treating physicians' discretion, and GC tapering was suspended between 6 and 12 months in one patient while she was treated by a non-specialist doctor. Third, in the non-protocolized-CS group, treatment was decided and arranged by attending physicians, although a general treatment strategy had been developed and shared in our division. Fourth, assessment of ILD was not sufficient; scores were not calculated for lung HRCT images, and post-treatment PFTs were not performed in some patients. Fifth, because the two comparison groups spanned different periods (2013–2016 vs. 2017–2022), improvement in general supportive care and infection control practices may have affected the outcomes. Sixth, the primary outcome measure adapted from a randomized controlled

trial on nocturnal oxygen therapy for chronic obstructive pulmonary disease has not been validated in ILDs associated with myositis and has to be validated in future studies to confirm its clinical relevance. Finally, because the subjects of this study were of Japanese ethnicity only, generalizability must be confirmed in patients with different ethnic backgrounds.

5 | Conclusions

In conclusion, the protocolized triple-combination therapy with high-dose GCs, tacrolimus, and IVCY demonstrated better primary and secondary outcomes than non-protocolized ciclosporin-based triple-combination therapy and was well tolerated in patients with anti-MDA5-positive DM-associated ILD. The combination of tacrolimus, reduced GC doses, and more intensive use of IVCY also presumably contributed to better outcomes in the protocolized-TAC group. However, the potential renal toxicity of calcineurin inhibitors (tacrolimus/ciclosporin) is warranted, and further studies are needed to explore the best strategies for anti-MDA5-positive DM-associated ILD.

Author Contributions

R.Y. and Y.K. drafted the research proposal and protocol, and wrote the first draft of the manuscript. All authors were involved in acquisition and analyses of the data and drafting or revising this article critically for important intellectual content, and approved the final version to be published. Dr. Yasuhiro Katsumata had full access to all relevant data from the study and takes responsibility for their integrity and the accuracy of the analyses performed.

Ethics Statement

This study was approved by the ethics committee of Tokyo Women's Medical University (registration number 3534) and adhered to the principles of the Helsinki Declaration.

Conflicts of Interest

Y.K. received speaker's fee from AstraZeneca K.K. and GlaxoSmithKline K.K. M.H. received research grants from Boehringer-Ingelheim Japan Inc. and Asahi Kasei Corp., and speaker's fee from Boehringer-Ingelheim Japan Inc. M.H. was a consultant for Boehringer-Ingelheim. R.Y. declares no competing interests.

Data Availability Statement

The data that support the findings of this study are available from the corresponding author upon reasonable request.

References

1. I. E. Lundberg, M. de Visser, and V. P. Werth, "Classification of Myositis," *Nature Reviews Rheumatology* 14, no. 5 (2018): 269–278, https://doi.org/10.1038/nrrheum.2018.41.

2. R. D. Sontheimer, "Would a New Name Hasten the Acceptance of Amyopathic Dermatomyositis (Dermatomyositis siné Myositis) as a Distinctive Subset Within the Idiopathic Inflammatory Dermatomyopathies Spectrum of Clinical Illness?," *Journal of the American Academy of Dermatology* 46, no. 4 (2002): 626–636.

3. I. E. Lundberg, A. Tjarnlund, M. Bottai, et al., "2017 European League Against Rheumatism/American College of Rheumatology Classification Criteria for Adult and Juvenile Idiopathic Inflammatory Myopathies and Their Major Subgroups," *Annals of the Rheumatic Diseases* 76, no. 12 (2017): 1955–1964, https://doi.org/10.1136/annrheumdis-2017-211468.

4. J. Morisset, C. Johnson, E. Rich, H. R. Collard, and J. S. Lee, "Management of Myositis-Related Interstitial Lung Disease," *Chest* 150, no. 5 (2016): 1118–1128, https://doi.org/10.1016/j.chest.2016.04.007.

5. T. Gono, Y. Kawaguchi, T. Satoh, et al., "Clinical Manifestation and Prognostic Factor in Anti-Melanoma Differentiation-Associated Gene 5 Antibody-Associated Interstitial Lung Disease as a Complication of Dermatomyositis," *Rheumatology (Oxford)* 49, no. 9 (2010): 1713–1719, https://doi.org/10.1093/rheumatology/keq149.

6. X. Lu, Q. Peng, and G. Wang, "Anti-MDA5 Antibody-Positive Dermatomyositis: Pathogenesis and Clinical Progress," *Nature Reviews Rheumatology* 20, no. 1 (2024): 48–62, https://doi.org/10.1038/s41584-023-01054-9.

7. M. Fathi, S. Barbasso Helmers, and I. E. Lundberg, "KL-6: A Serological Biomarker for Interstitial Lung Disease in Patients With Polymyositis and Dermatomyositis," *Journal of Internal Medicine* 271, no. 6 (2012): 589–597, https://doi.org/10.1111/j.1365-2796.2011.02459.x.

8. H. Tsuji, R. Nakashima, Y. Hosono, et al., "Multicenter Prospective Study of the Efficacy and Safety of Combined Immunosuppressive Therapy With High-Dose Glucocorticoid, Tacrolimus, and Cyclophosphamide in Interstitial Lung Diseases Accompanied by Anti-Melanoma Differentiation-Associated Gene 5-Positive Dermatomyositis," *Arthritis & Rhematology* 72, no. 3 (2020): 488–498, https://doi.org/10.1002/art.41105.

9. S. R. Johnson, E. J. Bernstein, M. B. Bolster, et al., "2023 American College of Rheumatology (ACR)/American College of Chest Physicians (CHEST) Guideline for the Treatment of Interstitial Lung Disease in People With Systemic Autoimmune Rheumatic Diseases," *Arthritis & Rheumatology* 76, no. 8 (2024): 1182–1200, https://doi.org/10.1002/art.42861.

10. T. Gono, K. Masui, S. Sato, and M. Kuwana, "Mortality Risk Stratification Using Cluster Analysis in Patients With Myositis-Associated Interstitial Lung Disease Receiving Initial Triple-Combination Therapy," *Frontiers in Medicine* 9 (2022): 883699, https://doi.org/10.3389/fmed.2022.883699.

11. A. Bohan and J. B. Peter, "Polymyositis and Dermatomyositis (First of Two Parts)," *New England Journal of Medicine* 292, no. 7 (1975): 344–347, https://doi.org/10.1056/NEJM197502132920706.

12. A. Bohan and J. B. Peter, "Polymyositis and Dermatomyositis (Second of Two Parts)," *New England Journal of Medicine* 292, no. 8 (1975): 403–407, https://doi.org/10.1056/NEJM197502202920807.

13. M. Hanaoka, Y. Katsumata, H. Kawasumi, Y. Kawaguchi, and H. Yamanaka, "KL-6 Is a Long-Term Disease-Activity Biomarker for Interstitial Lung Disease Associated With Polymyositis/Dermatomyositis, but Is Not a Short-Term Disease-Activity Biomarker," *Modern Rheumatology* 29, no. 4 (2019): 625–632, https://doi.org/10.1080/14397595.2018.1553488.

14. T. Gono, Y. Okazaki, A. Murakami, and M. Kuwana, "Improved Quantification of a Commercial Enzyme-Linked Immunosorbent Assay Kit for Measuring Anti-MDA5 Antibody," *Modern Rheumatology* 29, no. 1 (2019): 140–145, https://doi.org/10.1080/14397595.2018.1452179.

15. S. Matsuo, E. Imai, M. Horio, et al., "Revised Equations for Estimated GFR From Serum Creatinine in Japan," *American Journal of*

Kidney Diseases 53, no. 6 (2009): 982–992, https://doi.org/10.1053/j.ajkd.2008.12.034.

16. S. American Thoracic and S. European Respiratory, "American Thoracic Society/European Respiratory Society International Multidisciplinary Consensus Classification of the Idiopathic Interstitial Pneumonias. This joint statement of the American Thoracic Society (ATS), and the European Respiratory Society (ERS) was adopted by the ATS board of directors, June 2001 And by the ERS Executive Committee, June 2001," *Am J Respir Crit Care Med* 165, no. 2 (2002): 277–304, https://doi.org/10.1164/ajrccm.165.2.ats01.

17. N. Ishikawa, N. Hattori, A. Yokoyama, and N. Kohno, "Utility of KL-6/MUC1 in the Clinical Management of Interstitial Lung Diseases," *Respiratory Investigation* 50, no. 1 (2012): 3–13, https://doi.org/10.1016/j.resinv.2012.02.001.

18. T. Kotani, S. Makino, T. Takeuchi, et al., "Early Intervention With Corticosteroids and Cyclosporin A and 2-Hour Postdose Blood Concentration Monitoring Improves the Prognosis of Acute/Subacute Interstitial Pneumonia in Dermatomyositis," *Journal of Rheumatology* 35, no. 2 (2008): 254–259.

19. Y. Lacasse, F. Series, F. Corbeil, et al., "Randomized Trial of Nocturnal Oxygen in Chronic Obstructive Pulmonary Disease," *New England Journal of Medicine* 383, no. 12 (2020): 1129–1138, https://doi.org/10.1056/NEJMoa2013219.

20. S. Tenny and M. R. Hoffman, *Relative Risk*, StatPearls, Treasure Island (FL) (StatPearls, 2024), https://www.ncbi.nlm.nih.gov/books/NBK430824/.

21. T. Fujisawa, H. Hozumi, Y. Kamiya, et al., "Prednisolone and Tacrolimus Versus Prednisolone and Cyclosporin A to Treat Polymyositis/Dermatomyositis-Associated ILD: A Randomized, Open-Label Trial," *Respirology* 26, no. 4 (2021): 370–377, https://doi.org/10.1111/resp.13978.

22. A. C. Webster, R. C. Woodroffe, R. S. Taylor, J. R. Chapman, and J. C. Craig, "Tacrolimus Versus Ciclosporin as Primary Immunosuppression for Kidney Transplant Recipients: Meta-Analysis and Meta-Regression of Randomised Trial Data," *BMJ* 331, no. 7520 (2005): 810, https://doi.org/10.1136/bmj.38569.471007.AE.

23. A. Fanouriakis, M. Kostopoulou, J. Andersen, et al., "EULAR Recommendations for the Management of Systemic Lupus Erythematosus: 2023 Update," *Annals of the Rheumatic Diseases* 83, no. 1 (2024): 15–29, https://doi.org/10.1136/ard-2023-224762.

24. T. Sasai, R. Nakashima, H. Tsuji, et al., "Long-Term Prognosis of Antimelanoma Differentiation-Associated Gene 5-Positive Dermatomyositis With Interstitial Lung Disease," *Journal of Rheumatology* 50, no. 11 (2023): 1454–1461, https://doi.org/10.3899/jrheum.2023-0371.

25. H. Wang, J. Lv, J. He, et al., "The Prevalence and Effects of Treatments of Rapidly Progressive Interstitial Lung Disease of Dermatomyositis/Polymyositis Adults: A Systematic Review and Meta-Analysis," *Autoimmunity Reviews* 22, no. 8 (2023): 103335, https://doi.org/10.1016/j.autrev.2023.103335.

26. H. You, L. Wang, J. Wang, et al., "Time-Dependent Changes in RPILD and Mortality Risk in Anti-MDA5+ DM Patients: A Cohort Study of 272 Cases in China," *Rheumatology (Oxford)* 62, no. 3 (2023): 1216–1226, https://doi.org/10.1093/rheumatology/keac450.

27. D. Saygin, V. Werth, J. J. Paik, et al., "Current Myositis Clinical Trials and Tribulations," *Annals of the Rheumatic Diseases* 83, no. 7 (2024): 826–829, https://doi.org/10.1136/ard-2023-224652.

WILEY

International Journal of
Rheumatic Diseases

ORIGINAL ARTICLE

Antimigratory, Anti-Invasive and Anti-Inflammatory Effects of Bergenin in Rheumatoid Arthritis by Downregulating the Wnt/β-Catenin Pathway

Haoyu Yang[1,2] | Xunhao Wang[1] | Jiayan Zhu[1] | Yuzhou Liu[2] | Gang Zhao[1,2] | Jingyi Mi[1,2]

[1]Suzhou Medical College of Soochow University, Suzhou, China | [2]Department of Orthopedics, Wuxi Ninth People's Hospital Affiliated to Soochow University, Wuxi, Jiangsu, China

Correspondence: Jingyi Mi (mijingyi@yeah.net) | Gang Zhao (zhaogangmd@suda.edu.cn)

ABSTRACT

Background: This study investigates antimigratory, anti-invasive, and anti-inflammatory mechanisms of Bergenin in patients with rheumatoid arthritis (RA) by focusing on the pathways involved.

Methods: In vitro, TNF-α-induced MH7A cells were used to assess Bergenin's effects on cell proliferation (CCK-8), migration (wound healing, Transwell assays), and apoptosis (flow cytometry). mRNA levels of IL-6 and MMPs were quantified by qRT-PCR, and protein expression was analyzed using ELISA and western blot. The Wnt/β-catenin pathway was examined through immunofluorescence and western blotting with or without LiCl. An adjuvant-induced arthritis (AIA) rat model was used to monitor clinical symptoms and analyze synovial tissue.

Results: Bergenin inhibited the proliferation, migration, and invasion of TNF-α-induced MH7A cells, while promoting apoptosis. It reduced IL-6 and MMPs expression, with these effects reversed by LiCl. In vivo, Bergenin alleviated paw swelling, arthritis score, and synovial pathology in AIA rats, reducing pro-inflammatory factors.

Conclusions: Bergenin exerts antimigratory, anti-invasive, and anti-inflammatory effects in rheumatoid arthritis by modulating the Wnt/β-catenin pathway, suggesting its potential as a therapeutic option for rheumatoid arthritis.

1 | Introduction

Rheumatoid arthritis (RA) is an inflammatory disorder characterized by synovial inflammation, vasculogenesis, abnormal synovial hyperplasia, and cartilage and bone destruction [1–3]. Although the exact cause of RA remains unclear, it is widely recognized that inflammatory mediators play a crucial role in the development of RA by disrupting the interaction between catabolic and anabolic factors in chondrocytes, ultimately resulting in cartilage damage [4]. Fibroblast-like synoviocytes (FLSs) [5], which constitute approximately 70% of the total synovial membrane cells [6], are the main effector cells in RA [7]. During disease progression, these cells exhibit tumor-like proliferation and secrete various matrix metalloproteinases (MMPs), which accelerate RA progression [6]. Several factors, particularly tumor necrosis factor-α (TNF-α)

Haoyu Yang and Xunhao Wang equally contributed to this work.

and interleukin (IL)-1β, are pivotal in the initiation and maintenance of inflammatory and destructive processes within the affected joint [8–11]. Therefore, it is hypothesized that inhibiting the proliferation and motility of synovial cells and suppressing the production of inflammatory factors might offer crucial therapeutic strategies for RA.

The Wnt/β-catenin pathway contributes to RA pathogenesis [12–14]. Inhibition of Wnt signaling has been associated with bone remodeling in catabolic models and may facilitate bone erosion, which is observed in patients with RA [15]. When Wnt/β-catenin signaling is aberrantly activated in chondrocytes, degradation of the cartilage matrix is promoted—a process implicated in both osteoarthritis and RA [16]. In patients with RA, Wnt1 overexpression has been associated with stimulation of fibronectin and pro-MMP3 production. Wnt1 also induces the production of Wnt signaling proteins that promote intercellular adhesion, cell proliferation, and survival [17]. Although a close association between the Wnt pathway and RA has been established, the specific interactions and mechanisms of prevention remain to be elucidated to enable effective treatment targeting this pathway.

There is an urgent need to develop novel therapeutic approaches that reduce toxicity and side effects for the treatment of RA [18–20]. Bergenin, a coumarin-class compound, is a white, loosely needled crystalline or powdery substance primarily found in plants belonging to families, including Saxifragaceae, Fabaceae, and Primulaceae [21, 22]. Bergenin is an active constituent extracted from herbs, including Bergenia, and exhibits a broad spectrum of pharmacological functions in traditional Chinese medicine [23], including antitumor, anti-inflammatory, analgesic, and immune-boosting effects [24–27]. It is known for its low toxicity and is considered promising for the development of new drugs. For instance, Jung et al. synthesized acylated derivatives of Bergenin and evaluated their anti-inflammatory effects in cell culture, as well as their anti-anesthetic effects in morphine-dependent mice, highlighting their potent anti-inflammatory activity and ability to reverse anesthesia in vitro [28]. Moreover, research by de Oliveira and colleagues found that Bergenin, through inhibition of TNF-α production, exhibits analgesic and anti-inflammatory properties with potential for controlling inflammatory pain [29]. Consequently, Bergenin demonstrates various medicinal properties, making it a noteworthy candidate for investigation in pharmaceutical research.

Currently, there is limited empirical research on the effects and mechanisms of action of Bergenin in RA. This study aimed to explore its therapeutic potential using cytological and animal models. Our results show that Bergenin promotes apoptosis, inhibits cytoskeletal reorganization and cell migration in MH7A cells (immortalized TNF-α-induced RA FLSs used as a cellular model of RA), and reduces the levels of proinflammatory cytokines and matrix MMPs. It also suppresses the Wnt/β-catenin signaling pathway, resulting in reduced inflammation and cellular invasion. In the adjuvant-induced arthritis (AIA) rat model, Bergenin demonstrated significant therapeutic efficacy. These findings suggest that Bergenin is a promising natural compound for the treatment of RA.

2 | Materials and Methods

2.1 | Reagents and Materials

Bergenin (Figure 1A, Catalogue Number: HY-N0017) with ≥ 98% purity was supplied by MedChemExpress (MCE). Recombinant human TNF-α (Catalogue Number: 300-01A-50ug) was obtained from Pepro-Tech (Rocky Hill, NJ, USA). Freund's Complete Adjuvant (CFA, Catalogue Number: F8170-10) was sourced from Jiangsu MagBioTech Co. Ltd. Primers for IL-6, MMPs, and GAPDH were manufactured by Shanghai Sangon Biotech Co. Ltd. Antibodies for GAPDH, Wnt1, β-catenin (Abcam, MA, USA) and MMPs, Caspases, GSK-3β, p-GSK-3β (ProteinTech, Wuhan, China; Cell Signaling Technology Inc., MA, USA) were used. Secondary antibodies and FITC-labeled antibodies were provided by ProteinTech Group. ELISA kits and Matrigel (Yubo Biotech, Shanghai, China) were used. Transwell chambers (Corning, Shanghai Aiyun Biotech Co. Ltd.) and the Annexin V-FITC Apoptosis Detection Kit (Senbeijia Biotechnology Co. Ltd., Nanjing, China) were used for apoptosis assays. The Caspase 3 Activity Assay Kit (Beyotime Biotech Inc., Shanghai, China) was also applied.

2.2 | Cell Culture and Animal

The human MH7A FLS cell line (Bena Culture Collection, catalogue number: BNCC371792, RRID: CVCL_0427) was cultured in DMEM (Gibco, USA) supplemented with 1% penicillin/streptomycin and 10% fetal bovine serum at 37°C and 5% CO_2. Male SD rats (200 ± 20 g) were provided by the Changzhou Cawens Experimental Animal Co. Ltd. (SCXK(Su)2022–0273). The animal procedures were approved by the Ethics Committee of Wuxi Ninth People's Hospital (Ethics Protocol No: KS2023077) and followed the National Animal Care Guidelines.

2.3 | CCK-8 Assay

The MH7A cells were seeded in 96-well plates (2×10^4/ well) and treated with varying concentrations of Bergenin for 24 and 48 h in the presence of TNF-α (10 ng/mL), or not. Subsequently, CCK-8 reagent (10 μL) was added for 1 h incubation. Thereafter, the absorbance values (OD, 450 nm) were recorded for analysis.

2.4 | Fluorescent Phalloidin Staining and Immunofluorescence Assay

Cells (2×10^5/well) were seeded in 24-well plates and cultured with or without TNF-α (10 ng/mL) or various concentrations of Bergenin. After treatment, the cells were fixed with 4% paraformaldehyde (15 min), permeabilized with 0.25% Triton X-100 in PBS (15 min) and incubated with 3% bovine serum albumin for 1 h. For β-catenin immunofluorescence, cells were incubated with rabbit anti-β-catenin antibody overnight at 4°C, followed by FITC-conjugated secondary antibody (1 h; 37°C). Fluorescence was observed under a microscope. F-actin and nuclei were stained with FITC-conjugated phalloidin (2 h) and
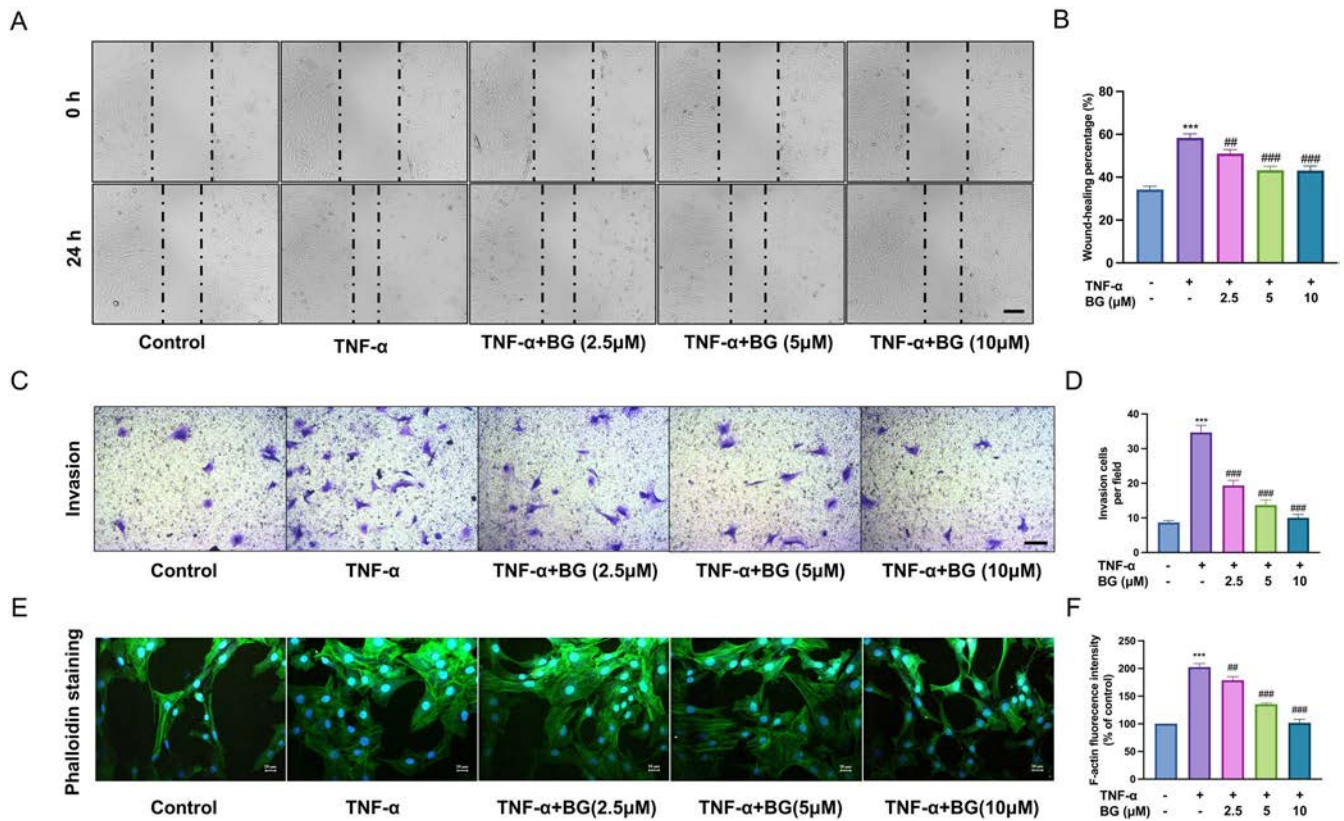
FIGURE 1 | Bergenin inhibited cell mobility and cytoskeletal reorganization. (A, B) The wound healing assay was utilized to evaluate the migratory capacity of the cells. MH7A cells were cultured with medium supplemented with TNF-α (10 ng/mL), in the presence of Bergenin (2.5, 5, and 10 μM) for 0 and 24 h, or not, it showed that Bergenin inhibited the migratory capacity of the cells. Scale bar = 200 μm. (C, D) Cell invasion was observed and determined through a transwell invasion assay. The MH7A cells were subjected to distinct treatment with TNF-α (10 ng/mL) for 24 h. The invading cells were visualized following staining and recorded under a microscope, it showed Bergenin inhibited the invasive capacity of the cells. Scale bar = 50 μm. (E, F) Displays representative images of cells stained with fluorescent phalloidin. F-Actin positive staining was indicated as a Green fluorescence signal and cell nuclei stained with DAPI showed a blue manifestation, it showed Bergenin inhibited cytoskeleton reorganization of the cells. Scale bar = 50 μm. ***$p < 0.001$ versus control group; ##$p < 0.01$ and ###$p < 0.001$ versus TNF-α group.

DAPI (15 min). The fibrous morphology was observed using confocal laser scanning microscopy.

2.5 | Wound Healing Assay

On the first day, MH7A cells were seeded and cultured in serum-free medium in six-well plates (5×10^5/well). On the second day, a scratch was made on the cell monolayer using a sterile pipette tip. The monolayers were rinsed with PBS to remove detached cellular fragments. Subsequently, 10 ng/mL TNF-α alongside a range of Bergenin concentrations was added to stimulate experimental cells. After a 24 h incubation period with Bergenin, a Nikon microscope (Tokyo, Japan) was used to capture images of the wounded areas. The dimensions of the initial wound and area that had healed were subsequently quantified using Adobe Photoshop software (USA), which calculates the percentage of wound closure.

2.6 | Transwell Assay

Initially, the Transwell inserts, featuring an 8 μm pore size, were precoated with or without Matrigel (300 μg/m, BD Biosciences,

Oxford, UK). Subsequently, cells were introduced into the upper compartment (2×10^5/mL) in a serum-free medium and subsequently exposed to Bergenin. Concurrently, the lower compartment was added with 0.6 mL DMEM with both 10 ng/mL TNF-α and 10% FBS to serve as a chemotactic agent. After 24 h incubation, a cotton-tipped swab was used to meticulously wipe away the cells remaining in the upper chamber. A 4% paraformaldehyde solution was added into the lower chamber to fix the invading cells (30 min, 4°C); then, the cells were stained with a crystal violet solution (10 min, room temperature). Images of stained cells within three randomly selected fields of view were obtained with an optical microscope (Nikon, Tokyo, Japan). The ImageJ software was utilized to conduct the enumeration of invasive cells.

2.7 | Functional Enrichment Analysis of Common Differentially Expressed Genes (DEGs)

DEGs were identified using the R package "limma" with criteria |log$_2$ FC| ≥ 0.5 and $p < 0.05$. DEGs were visualized using heat maps and volcano plots generated by "pheatmap" and "ggplot2" packages. To delve deeper into the potential roles of the DEGs mentioned above, the R package "clusterProfiler" was utilized to

conduct analyses pertaining to the Gene Ontology (GO) and the Kyoto Encyclopedia of Genes and Genomes (KEGG), with a significance threshold set at $p < 0.05$. This analysis was conducted to clarify the pathways related to the common DEGs [30].

2.8 | ELISA Assay

After treatment, cell culture supernatants were centrifuged, collected, and stored at −20°C for ELISA. For the in vivo studies, rats were euthanized with sodium pentobarbital (40 mg/kg) 24 h after the final oral dose. Blood was collected from the abdominal aorta and allowed to coagulate for 1 h at room temperature, then centrifuged at 5000 rpm for 15 min at 4°C to separate serum. Serum samples were stored at −80°C before cytokine quantification using commercial ELISA kits. Cytokine levels were determined from standard curves, and the mean of duplicate tests was used for statistical analysis.

2.9 | Western Blot Assay

Cellular lysis was performed using RIPA buffer supplemented with 1% PMSF (Beyotime, Shanghai, China). Equal amounts of denatured protein samples were resolved by 10% SDS-PAGE and transferred to nitrocellulose membranes (Millipore, MA). Membranes were blocked with 5% skimmed milk (1 h, room temperature) and incubated overnight at 4°C with primary antibodies against GAPDH, MMPs, Caspases, Wnt1, GSK-3β, p-GSK-3β, and β-catenin. After incubation with horseradish peroxidase-conjugated secondary antibodies (1:5000, 1 h, room temperature), the protein bands were visualized using an ECL substrate kit (Biosharp, Hefei, China). The experiment was repeated three times to ensure reliability.

2.10 | Quantitative Reverse Transcription (qRT)-PCR Assays

Cells were incubated overnight and treated with Bergenin (2.5, 5, and 10 μM) and TNF-α (10 ng/mL) for 24 h at 37°C. Total RNA was isolated using TRIzol reagent (Beyotime, Shanghai, China) and reverse transcribed into cDNA using the BeyoRT III First Strand cDNA Synthesis Kit (Beyotime). qRT-PCR was performed with SYBR Green qPCR Mix (Beyotime) on a Q1000 qRT-PCR machine (Longgene, Hangzhou, China) following the manufacturer's instructions. The cycling conditions included an initial denaturation (2 min, 95°C), followed by 40 cycles of denaturation (15 s, 95°C), annealing (20 s, 60°C), and extension (30 s, 72°C). Gene expression was quantified relative to GAPDH using the 2-Δ(ΔCt) method.

2.11 | Establishment of AIA Model

The AIA rat model is commonly used to study autoimmune joint diseases, including RA. The model was prepared as follows: there were four groups in total and five male SD rats in each group were randomly selected to conduct the following procedures after an adaptation period. The groups were the AIA model, Bergenin low-dose (5 mg/kg), Bergenin high-dose (10 mg/kg),

and a control. Each single rat was immobilized on the operating table and 0.1 mL of CFA was subcutaneously injected into the left hind paw metatarsal footpad, except for those in the control group who received a similar volume of normal saline. Two weeks later, Bergenin was intravenously administrated every other day in the low-dose group and high-dose group accordingly for a period of 3 weeks. Throughout the treating phase with varying drug concentrations, the record of the body weight of each rat was performed at a 4-day interval. The severity and changes in arthritis before and after treatment with different agents were reflected by measuring the arthritis index [31].

2.12 | Histopathological Examination

Right hind paw tissue samples were excised for histopathological analysis, fixed in 4% paraformaldehyde, and decalcified in 10% EDTA-PBS (pH 7.4). The specimens were then dehydrated through a series of ethanol solutions, embedded in paraffin, and sectioned into 5 μm slices. After hematoxylin and eosin (H&E) staining, the sections were examined under an optical microscope. Inflammatory cell infiltration, pannus formation, and synovial hyperplasia were scored blindly using the following scale: 0 = none; 1 = minimal; 2 = slight; 3 = moderate; 4 = severe.

2.13 | Statistical Analysis

Data were analyzed statistically using GraphPad Prism 9.0 software (GraphPad Software Inc., located in San Diego, California). Experimental data are presented as mean ± standard deviation (SD). Data analysis was performed using one-way analysis of variance (ANOVA) and the Student's t-test.

3 | Results

3.1 | Effects of Bergenin on the Proliferation of MH7A Cells

As shown in Figure S1A, Bergenin at lower concentrations had no significant impact on the MH7A cells proliferation within the first 24 h and 48 h. However, as the concentration increased, Bergenin at 20, 40, and 80 μM demonstrated cytotoxicity to MH7A cells (Figure S1B,C). Consequently, we opted for the safer range of higher concentrations, specifically 2.5, 5, and 10 μM of Bergenin, for further investigations into its anti-proliferative effects. The results showed that the inhibition by Bergenin (2.5, 5, and 10 μM) of TNF-α-mediated MH7A cell proliferation was enhanced with the increase of dose (Figure S1D). Hence, we selected the concentrations of 2.5, 5, and 10 μM of Bergenin as the experimental doses.

3.2 | Bergenin Inhibited the Mobility and Cytoskeletal Reorganization

Figure 1A shows increased migration of MH7A cells after TNF-α treatment. Bergenin dose-dependently reduced the migration of TNF-α-stimulated MH7A cells (Figure 1B). The Transwell assay (Figure 1C) revealed an increase in invasive cells in the TNF-α

group, whereas Bergenin treatment significantly reduced invasiveness in a dose-dependent manner (Figure 1D).

To assess the effect of Bergenin on cytoskeletal reorganization, phalloidin staining was performed. TNF-α stimulation increased F-actin fluorescence intensity and induced cell protrusions and pseudopodia formation (Figure 1E). Bergenin reduced F-actin intensity and the number of protrusions (Figure 1F), indicating that Bergenin inhibited F-actin expression in TNF-α-induced MH7A cells.

3.3 | Bergenin Increased the Apoptotic Rate of TNF-α-Stimulated MH7A Cells

Bergenin at concentrations of 2.5, 5, and 10 μM exhibited significant anti-proliferative activity (Figure S1B–D). Further investigations were conducted to assess the apoptotic rate in MH7A cells between groups. Flow cytometry analysis revealed that the apoptotic rate in MH7A cells was effectively and dose-dependently elevated with the administration of Bergenin (Figure S2A). Additionally, caspase-3, caspase-8, and caspase-9 were detected to further determine whether Bergenin induced caspase-dependent apoptosis (Figure S2B,C).

3.4 | Bergenin Suppress the Production of Pro-Inflammatory Factors in TNF-α-Stimulated MH7A Cells

Extensive research has demonstrated that specific proinflammatory factors and MMPs profoundly influence the pathological behavior of RA-FLSs, including articular cartilage erosion in RA progression, as documented in the literature. The outcomes indicated that treatment with Bergenin at various concentrations (2.5, 5, and 10 μM) resulted in a dose-dependent suppression of IL-6, MMPs (Figure 2A–C). Bergenin has the potential to reduce the synthesis and emission of several pro-inflammatory factors and a variety of pivotal MMPs.

3.5 | Screening of DEGs and GO and KEGG Enrichment Analysis

Differential analysis identified 16 282 DEGs in the RA group, of which 51 were upregulated and 142 were downregulated. Figure 3A shows a volcano plot of these DEGs, with red and blue nodes representing upregulated and downregulated genes, respectively. Gene expression heat maps highlight the most significantly altered genes in the TNF-α and TNF-α + BG groups.

Enrichment analysis revealed that the common DEGs were linked to cellular growth, development, and inflammatory responses. GO analysis (Figure 3B) focused on terms, including multicellular organism development and anatomical structure development. KEGG analysis identified enriched pathways, including the Wnt signaling pathway, AMPK pathway, osteoclast differentiation, and longevity regulation. Although the AMPK pathway has known roles in inflammation and metabolism, its involvement in RA remains insufficiently studied. Conversely, the Wnt/β-catenin pathway is well established in RA pathogenesis and represents a clearer therapeutic target.

3.6 | Bergenin Blocked TNF-α-Triggered Activation of Wnt/ß-Catenin Pathway

According to published literature, the aberrant Wnt/β-catenin pathway is closely associated with RA pathogenesis, including abnormal proliferation, inflammatory responses, and the migratory and invasive behavior of RA-FLSs [32]. As shown in Figure 4A, Bergenin treatment appears to suppress Wnt/β-catenin signaling activated by TNF-α. TNF-α has been identified as an agonist of the Wnt/β-catenin pathway, which was further validated by immunofluorescence experiments in this study (Figure 4B). Enhanced nuclear β-catenin intensity and translocation were observed following TNF-α (10 ng/mL) administration. However, Bergenin treatment inhibited β-catenin nuclear translocation in a concentration-dependent manner. These results confirm that Bergenin blocked TNF-α-mediated Wnt/β-catenin signaling in MH7A cells.

3.7 | LiCl Counteracted the Negative Effects of Bergenin on Mobility and Inflammation

To comprehensively validate Bergenin's inhibitory effect on the Wnt/β-catenin pathway, LiCl, a Wnt/β-catenin agonist, was introduced into the experiment to closely observe its potential reversal of Bergenin-induced changes in relevant protein expressions, as well as its impact on the inflammation and mobility of MH7A cells. The results from experiments after the administration of LiCl showed that the negative regulation of Bergenin could be reversed by LiCl, as shown in Figure 5A; the expressions of Wnt1(one of WNT ligand), p-GSK-3β, and β-catenin were elevated. Moreover, LiCl counteracted the effects of Bergenin on MH7A cells, resulting in an increased migration index (Figure 5B) and a higher number of invasive cells (Figure 5C). In addition, after LiCl treatment, the expression levels of several inflammatory factors, including MMPs and IL-6 (Figure 5D), were quantified. These results indicated that Bergenin suppresses the Wnt/β-catenin pathway and thereby reduces both mobility and inflammation in TNF-α-stimulated cells.

3.8 | Bergenin Exerted Therapeutic Effects in AIA Rats

To assess Bergenin's in vivo efficacy in RA, we used a CFA-induced AIA rat model (Figure 6A). The results (Figure 6B) showed significant weight loss in AIA rats starting on day 8, which was partially reversed by Bergenin in a dose-dependent manner. Paw swelling peaked on day 8 in AIA rats; however, Bergenin significantly reduced swelling in a dose-dependent fashion. Arthritis scores increased in AIA rats from day 12, whereas the Bergenin-treated groups showed significant reductions.

Histopathological analysis (Figure 6C,D) demonstrated reduced inflammation and joint pathology in Bergenin-treated rats. H&E staining of major organs showed no apparent toxicity (Figure S3). ELISA analysis (Figure 6E) indicated that Bergenin
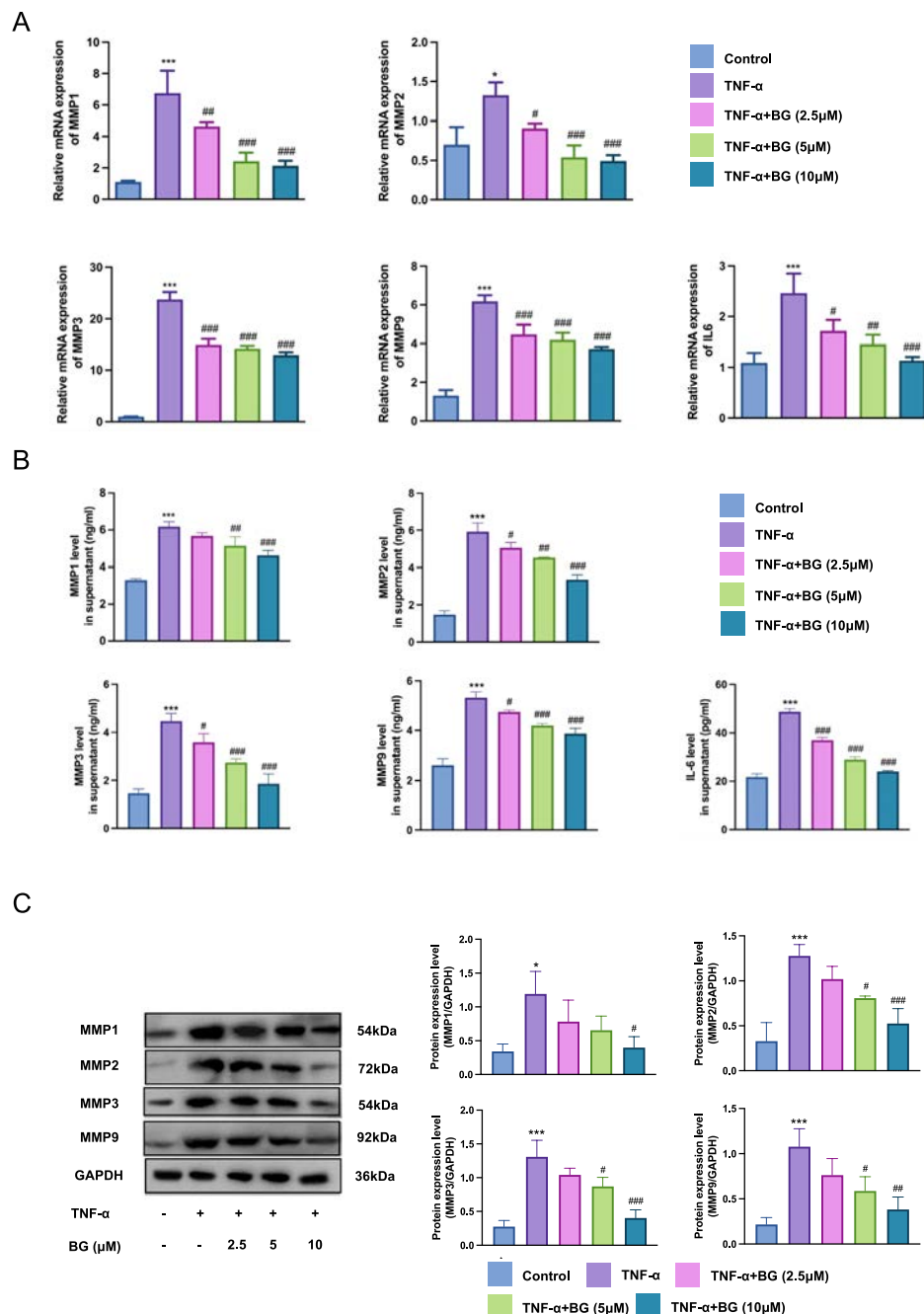
FIGURE 2 | Bergenin suppressed the production of proinflammatory factors in TNF-α-stimulated MH7A cells. MH7A cells were cultured with 10 ng/mL TNF-α for a duration of 24 h, administrating Bergenin (2.5, 5, and 10 μM), or not. Subsequently, (A) The mRNA level of MMP1, MMP2, MMP3, MMP9, and IL-6 were quantified using qRT-PCR. (B) Protein expression was quantified using ELISA and (C) western blot. *$p < 0.05$, ***$p < 0.001$ versus control group; and #$p < 0.05$, ##$p < 0.01$, ###$p < 0.001$ versus TNF-α group, respectively.

reduced serum levels of TNF-α, IL-1β, IL-6, and IL-17 in AIA rats. These findings suggest that Bergenin effectively alleviated RA symptoms and improved histopathological outcomes without observable toxicity.

4 | Discussion and Conclusions

The main clinical symptom of RA is inflammatory synovitis, and its clinical manifestations include chronic, symmetrical, and peripheral polyarthritis, resulting in joint pain, swelling,

and functional impairment [33]. This study validated Bergenin's therapeutic effects on cell mobility, inflammation, and apoptosis in TNF-α-treated MH7A cells, revealing its potential to disrupt Wnt/β-catenin signaling. Using an AIA rat model that mimics human RA symptoms—including joint swelling, synovial infiltration, and cartilage degradation—we assessed the anti-arthritic effects of Bergenin in vivo. The results showed that Bergenin reduced limb swelling and arthritis index scores, indicating its therapeutic potential. Pathological examination of AIA rat knee joints (H&E staining) revealed that Bergenin alleviated cartilage damage, inflammatory cell infiltration,
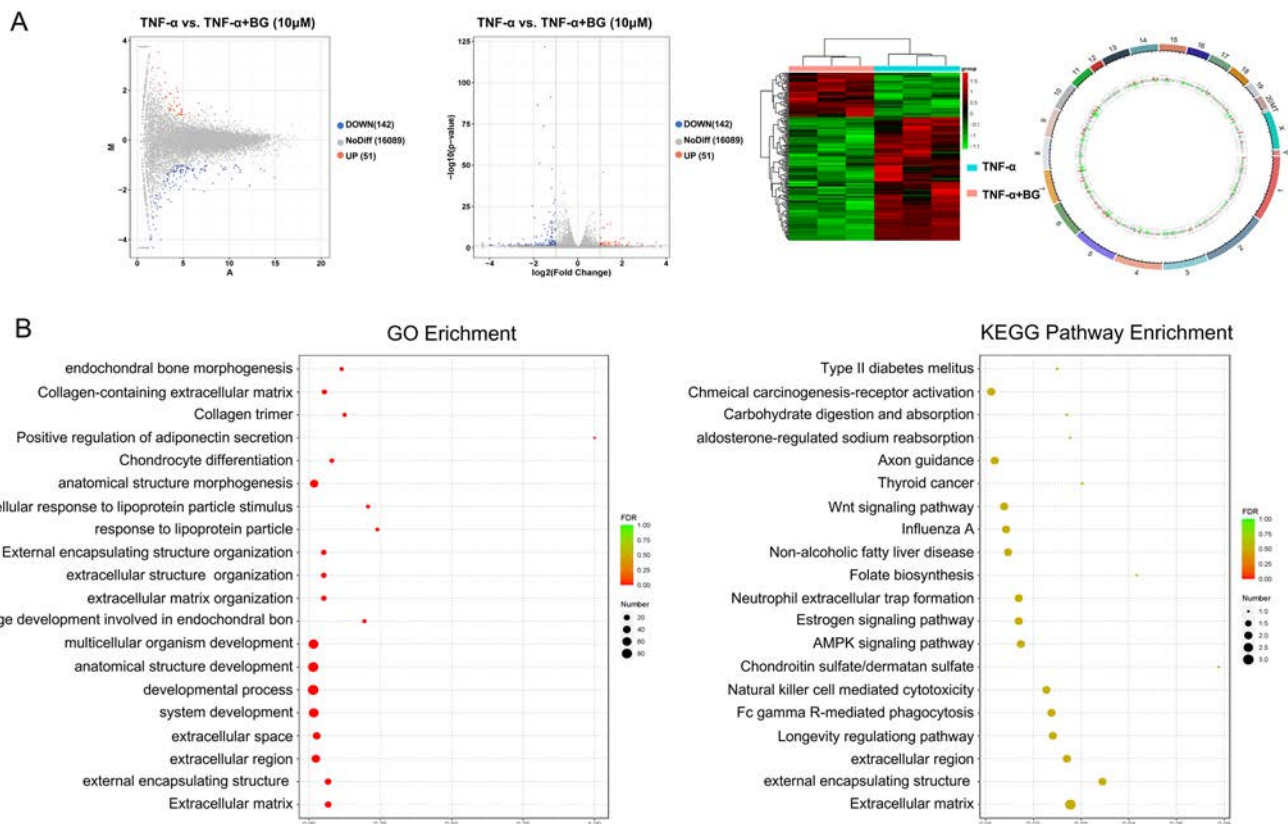
FIGURE 3 | Summary of the DEGs screening and the subsequent enrichment analysis. (A) Depict the volcano plot of identified DEGs. (B) GO and KEGG enrichment analysis. The circle size corresponds to the gene count. The rich factor on the X-axis indicated pathway enrichment level, and the analysis was facilitated by the Metascape online platform. Each circle dot represented a GO or KEGG term, with the network layout of selected terms and the thickness of the edge between them reflecting the degree of terms similarity.

synovial hyperplasia, and pannus formation. These findings demonstrate that Bergenin attenuates the progression and severity of articular damage in the AIA rat model, which were summarized in Figure S4.

Chronic inflammation of the synovium in affected joints is a hallmark of RA, and inhibiting this inflammation may effectively alleviate the disease. FLSs within inflamed RA joints, which act as key effector cells, are characterized by rapid proliferation and diminished apoptosis. These cells persistently synthesize IL-1β, IL-6, IL-17, and TNF-α, which are several vital proinflammatory factors. This ultimately results in joint damage and synovial or systemic inflammation [34]. The synthesis and accumulation of MMPs within the joints of patients with RA are driven by proinflammatory factors [35], particularly TNF-α. FLSs primarily produce MMPs (also known as collagenases), which degrade fibrillar collagen and the extracellular matrix [36]. Bergenin exerts anti-arthritic activity via its anti-inflammatory and antioxidant potential [37], which encouraged us to explore the in-depth effects and mechanisms of Bergenin in RA. In the present study, Bergenin exhibited several anti-inflammatory properties according to the results of qPCR, western blotting, and ELISA. In animal studies, Bergenin showed a dose-dependent inhibitory effect (5 mg/kg and 10 mg/kg) on the production of serum IL-1β, IL-6, IL-17, and TNF-α. Treatment with Bergenin at 2.5, 5, and 10 μM effectively curtailed the synthesis of IL-6 and MMPs in TNF-α-induced MH7A cells. Flow cytometry data indicated

that Bergenin increased the apoptotic rate of MH7A cells in a dose- and time-dependent manner. According to our findings, Bergenin possesses significant anti-inflammatory efficacy against TNF-α-induced FLSs and AIA in rats, suggesting that Bergenin may have antirheumatic effects.

RA FLSs augment the secretion of inflammatory factors and display malignant, tumor-like behavior, characterized by enhanced cell mobility. These properties significantly contribute to cartilage degradation and bone damage [38]. RA FLSs can migrate toward the cartilage and bone, subsequently invading the extracellular matrix—an essential step in joint damage in patients with RA [39]. Inhibition of the hyperactive migratory and invasive behavior of FLSs is considered a potential therapeutic strategy. We documented the impact of Bergenin on inhibiting the cellular motility of TNF-α-induced MH7A cells at 2.5, 5, and 10 μM. This effect was quantified using wound healing and Transwell invasion assays. The important process of cell motility involves reorganization of the actin cytoskeleton and the formation of lamellipodia and filopodia [35]. In studies of TNF-α-induced MH7A cells, phalloidin staining results demonstrated that Bergenin curtailed F-actin expression and hindered cytoskeletal reorganization. The inhibitory effect of Bergenin on MMP expression significantly contributed to its suppressive effects on FLS mobility.

Research on the Wnt pathway suggests that this signaling cascade is activated during RA progression, contributing to
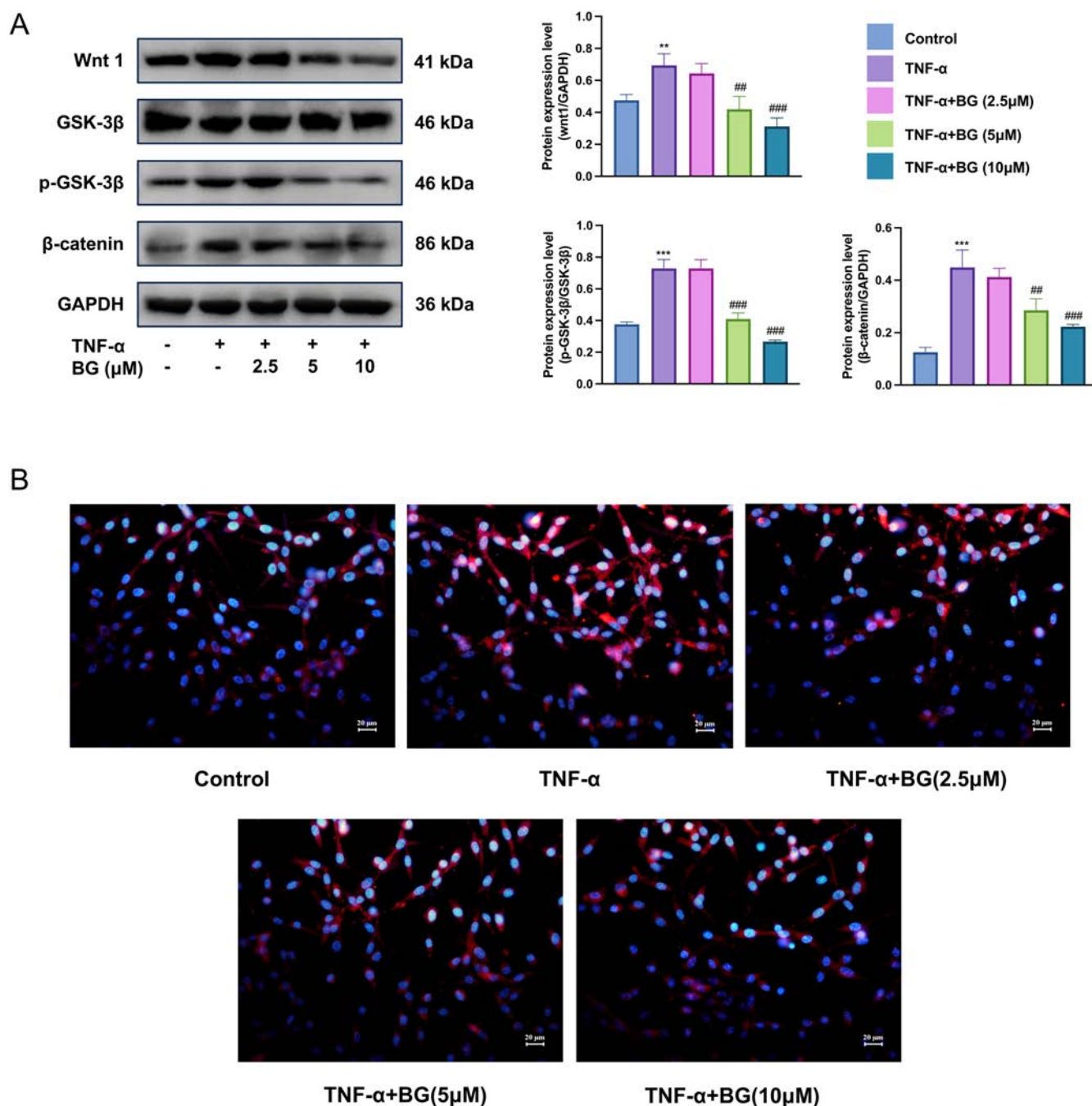
FIGURE 4 | Bergenin blocked TNF-α-triggered Wnt/ß-catenin. (A) MH7A cells were incubated with 10 ng/mL TNF-α, either with or without the addition of Bergenin for a period of 24 h. Following this incubation, Wnt1 (one of WNT Ligands), GSK-3β, p-GSK-3β, and β-catenin within the MH7A cells were evaluated. (B) The cellular localization of β-catenin was detected using immunofluorescent staining and photographically examined. The results showed that Bergenin inhibited the Wnt/ß-catenin signaling-related genes. Scale bar = 50 μm. **$p < 0.01$ and ***$p < 0.001$ versus control group; and ##$p < 0.01$, ###$p < 0.001$ versus TNF-α group.

increased synovial cell proliferation, synovitis, and pannus formation [36]. Under normal conditions, in the absence of a Wnt ligand, GSK-3β phosphorylates cytoplasmic β-catenin, targeting it for degradation. However, the Wnt ligand can bind to a receptor complex that leads to phosphorylation at the Ser9 residue, thereby inactivating GSK-3β. This inactivation prevents β-catenin phosphorylation and degradation. As β-catenin stabilizes and accumulates in the cytoplasm, it translocates to the nucleus to initiate Wnt-responsive gene expression [37]. In our present study, we observed that Bergenin reduced the expression

of Wnt1, p-GSK-3β, and both the expression and translocation of β-catenin under TNF-α-treated conditions, suggesting that Bergenin inhibits activation of the Wnt/β-catenin pathway. LiCl, an agonist of the Wnt/β-catenin pathway, is known to deactivate GSK-3β by phosphorylating it at Ser9 [40]. To delineate the role of Wnt/β-catenin signaling in the effects of Bergenin on TNF-α-induced FLSs, a combination treatment of LiCl and Bergenin was conducted in vitro. The findings indicated that LiCl counteracted the inhibitory effect of Bergenin on Wnt/β-catenin signaling in MH7A cells, effectively reversing Bergenin's suppression
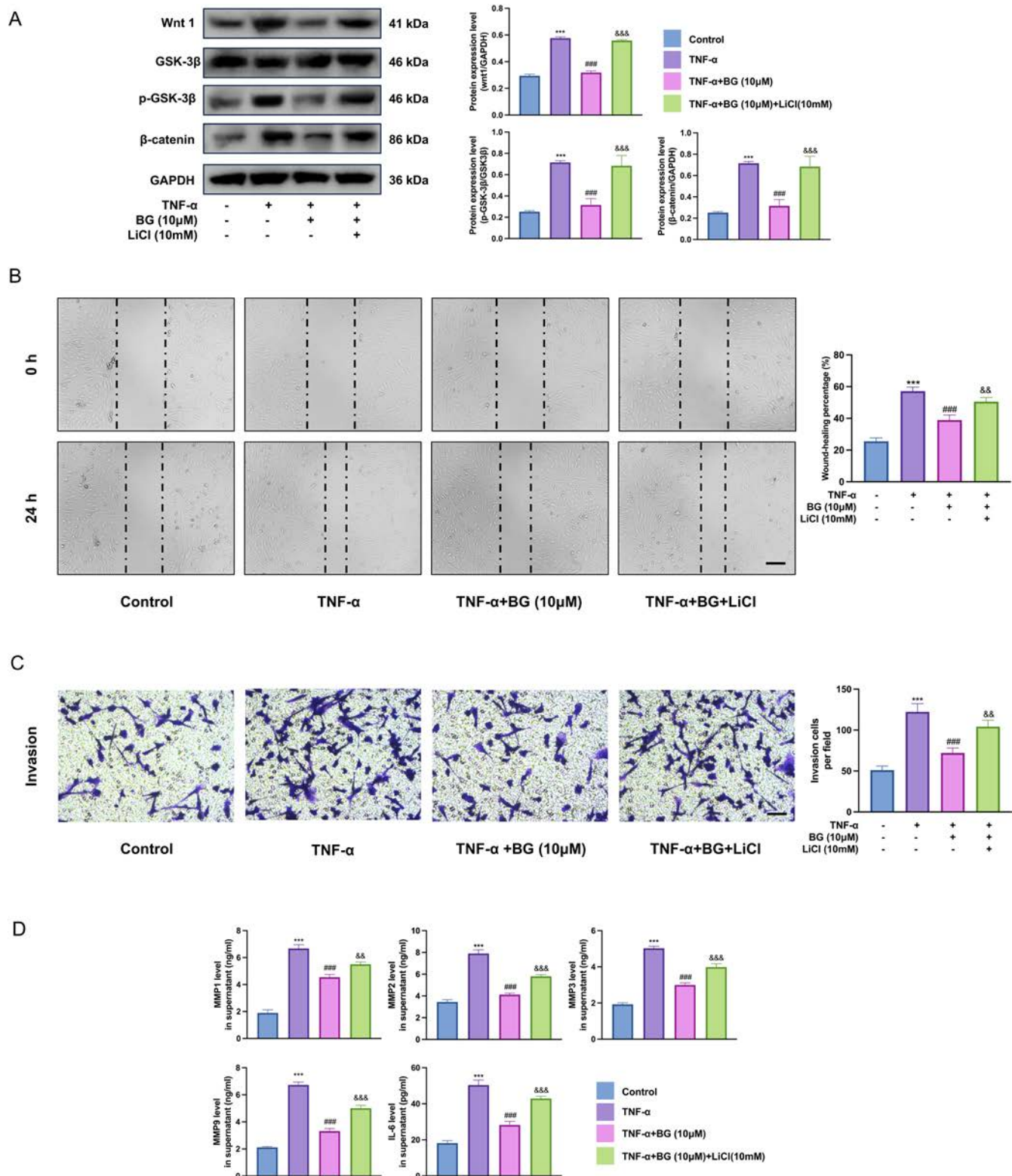
FIGURE 5 | LiCl reversed the negative influence of Bergenin on MH7A cells. (A) In the presence or absence of Bergenin ($10\,\mu$M) and LiCl ($10\,$mM), the MH7A cells were cultured with TNF-α for 1 day. Subsequently, the translational expression of Wnt1, GS3K-3β ' p-GS3K-3β, β-catenin was assessed using western blotting. (B) Migration ability was calculated as (a-b)/a*100%, "a" equals scratch width at 0 h, and "b" equals scratch width at 24 h. Scale bar $= 200\,\mu$m. (C) Cell invasion was observed and determined through a transwell invasion assay. The invading cells were visualized following staining and recorded under a microscope. Scale bar $= 50\,\mu$m. (D) IL-6, MMP1, MMP2, MMP3, and MMP9 were quantified using ELISA. ***$p < 0.001$ versus control group; ###$p < 0.001$ versus the TNF-α group; &&$p < 0.01$, &&&$p < 0.001$ vs. TNF-α + $10\,\mu$M BG group.
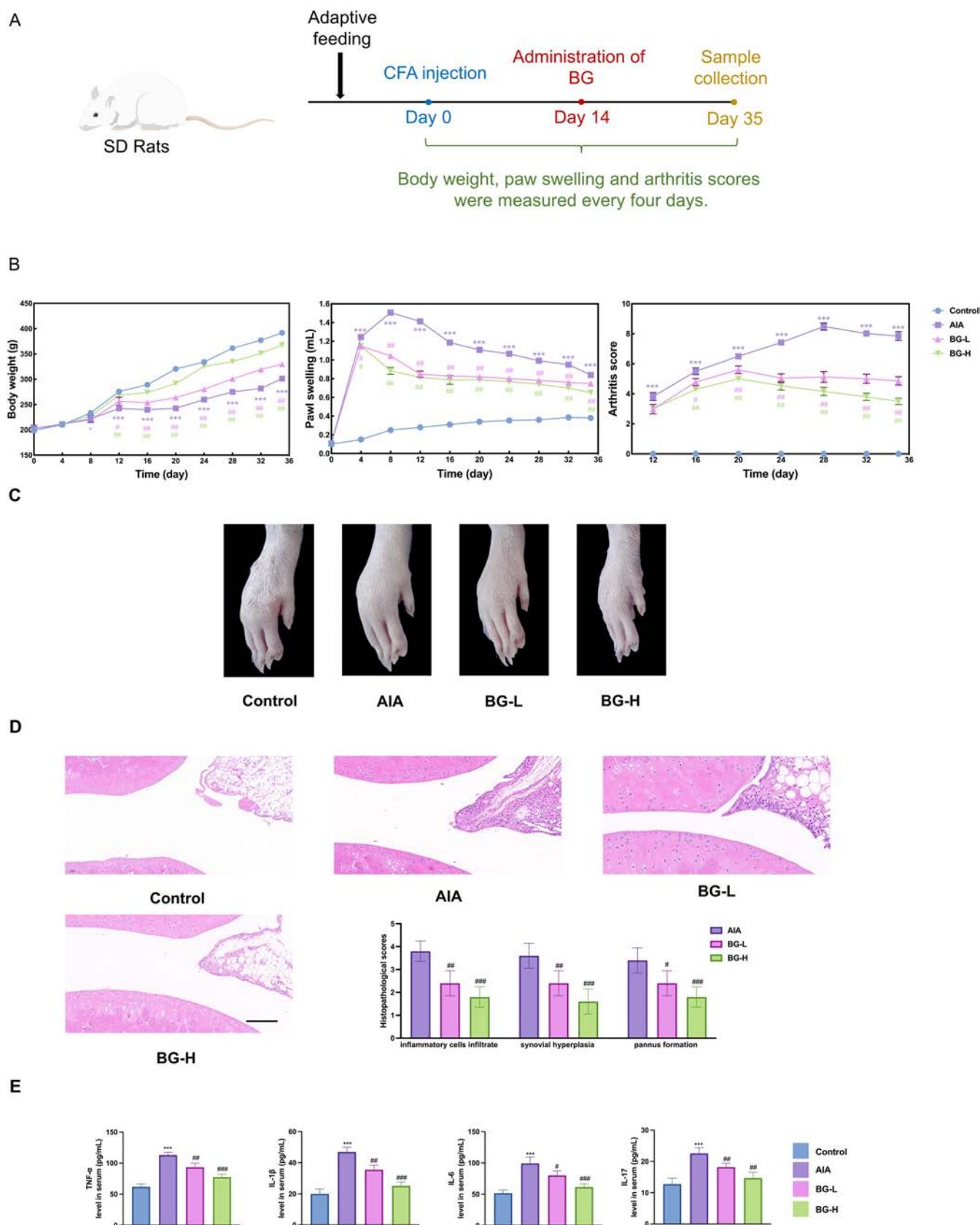
FIGURE 6 | Bergenin exerted therapeutic effects in vivo. (A) The procedure for evaluating the anti-arthritic effects of Bergenin in AIA rats was conducted. (B) The influence of Bergenin on body weight, paw edema, and the arthritis index was assessed in AIA rats. (C) Paws from different groups. (D) Tissue sections obtained as representative samples. Post-immunization with CFA, the right hind paws were harvested and sectioned on day 35 for histological assessment and quantification of tissue damage. Scale bar = 100 μm. (E) TNF-α, IL-1β, IL-6, and IL-17 were assessed with ELISA. Each group contain five rats ***$p < 0.001$ versus control group; and #$p < 0.05$, ##$p < 0.01$, ###$p < 0.001$ versus AIA group.

of cellular inflammation and mobility. Collectively, our findings demonstrate that modulation of Wnt/β-catenin signaling is likely integral to the therapeutic efficacy of Bergenin in correcting aberrant cellular activities associated with RA FLSs.

While this study provides valuable insights into the potential therapeutic effects of Bergenin for RA, it is essential to acknowledge several inherent limitations: (1) Preclinical model and translational gap: The efficacy and mechanistic investigations were conducted exclusively in a rat model of AIA. Although AIA is a widely used and valuable preclinical model for studying inflammatory arthritis and screening potential therapeutics, it does not fully recapitulate the complexity and heterogeneity of RA in humans. Key differences include the acute, induced nature of AIA versus the chronic, autoimmune-driven pathology of human RA; variations in disease progression; and potential species-specific differences in drug metabolism, pharmacokinetics, and immune responses. Consequently, the robust efficacy observed in AIA rats may not directly translate to equivalent clinical efficacy in human patients. (2) Mechanistic depth: Although we explored the impact on Wnt/β-catenin signaling and cytokine modulation, the precise molecular mechanisms underlying the observed therapeutic effects warrant further in-depth investigation. Additional studies using cell-specific knockouts, more extensive signaling pathway analysis, or exploration of interactions with other relevant pathways would provide a more nuanced understanding. (3) Dosing regimen and long-term effects: The study employed a specific dosing regimen. The optimal therapeutic window, potential dose dependency of effects beyond the tested range, and long-term consequences of sustained treatment remain to be fully elucidated. Furthermore, the relatively short treatment period in the model may not reflect chronic treatment requirements in human disease.

In conclusion, our study demonstrated that Bergenin exhibits significant anti-arthritic properties in both cellular and animal models. These effects are attributed to its ability to inhibit RA-FLS cell growth and mobility, induce apoptosis, and suppress MMP and cytokine production by modulating the Wnt/β-catenin pathway. Based on bioinformatics analysis and experimental validation, these findings suggest that Bergenin is a promising candidate for the treatment of RA.

Conflicts of Interest

The authors declare no conflicts of interest.

Data Availability Statement

The data that support the findings of this study are available from the corresponding author upon reasonable request.

References

1. D. L. Scott, F. Wolfe, and T. W. Huizinga, "Rheumatoid Arthritis," *Lancet* 376, no. 9746 (2010): 1094–1108.

2. I. B. McInnes and G. Schett, "The Pathogenesis of Rheumatoid Arthritis," *New England Journal of Medicine* 365, no. 23 (2011): 2205–2219.

3. Q. W. Lv, W. Zhang, Q. Shi, et al., "Comparison of Tripterygium Wilfordii Hook F With Methotrexate in the Treatment of Active Rheumatoid Arthritis (TRIFRA): A Randomised, Controlled Clinical Trial," *Annals of the Rheumatic Diseases* 74, no. 6 (2015): 1078–1086.

4. S. F. Ahmad, M. A. Ansari, A. Nadeem, et al., "The Tyrosine Kinase Inhibitor Tyrphostin AG126 Reduces Activation of Inflammatory Cells and Increases Foxp3(+) Regulatory T Cells During Pathogenesis of Rheumatoid Arthritis," *Molecular Immunology* 78 (2016): 65–78.

5. C. Carlens, M. P. Hergens, J. Grunewald, et al., "Smoking, Use of Moist Snuff, and Risk of Chronic Inflammatory Diseases," *American Journal of Respiratory and Critical Care Medicine* 181, no. 11 (2010): 1217–1222.

6. A. Barton and J. Worthington, "Genetic Susceptibility to Rheumatoid Arthritis: An Emerging Picture," *Arthritis and Rheumatism* 61, no. 10 (2009): 1441–1446.

7. J. Karami, S. Aslani, M. N. Tahmasebi, et al., "Epigenetics in Rheumatoid Arthritis; Fibroblast-Like Synoviocytes as an Emerging Paradigm in the Pathogenesis of the Disease," *Immunology and Cell Biology* 98, no. 3 (2020): 171–186.

8. F. M. Brennan and I. B. McInnes, "Evidence That Cytokines Play a Role in Rheumatoid Arthritis," *Journal of Clinical Investigation* 118, no. 11 (2008): 3537–3545.

9. A. Paradowska, W. Maśliński, A. Grzybowska-Kowalczyk, and J. Łącki, "The Function of Interleukin 17 in the Pathogenesis of Rheumatoid Arthritis," *Archivum Immunologiae et Therapiae Experimentalis (Warsz)* 55 (2007): 329–334.

10. M. Narazaki, T. Tanaka, and T. Kishimoto, "The Role and Therapeutic Targeting of IL-6 in Rheumatoid Arthritis," *Expert Review of Clinical Immunology* 13, no. 6 (2017): 535–551.

11. X.-m. Tong, J.-c. Wang, Y. Shen, J.-j. Xie, J.-y. Zhang, and J. Jin, "Inhibition of Inflammatory Mediators and Related Signaling Pathways by Macrophage-Stimulating Protein in Rheumatoid Arthritis Synovial Fibroblasts," *Inflammation Research* 60 (2011): 823–829.

12. R. Hayat, M. Manzoor, and A. Hussain, "Wnt Signaling Pathway: A Comprehensive Review," *Cell Biology International* 46, no. 6 (2022): 863–877.

13. Q. Ding, W. Hu, R. Wang, et al., "Signaling Pathways in Rheumatoid Arthritis: Implications for Targeted Therapy," *Signal Transduction and Targeted Therapy* 8, no. 1 (2023): 68.

14. P. Prajapati and G. Doshi, "An Update on the Emerging Role of Wnt/β-Catenin, SYK, PI3K/AKT, and GM-CSF Signaling Pathways in Rheumatoid Arthritis," *Current Drug Targets* 24, no. 17 (2023): 1298–1316.

15. G. Schett, J. Zwerina, and J.-P. David, "The Role of Wnt Proteins in Arthritis," *Nature Clinical Practice Rheumatology* 4, no. 9 (2008): 473–480.

16. F. Orsini, C. Crotti, G. Cincinelli, et al., "Bone Involvement in Rheumatoid Arthritis and Spondyloarthritis: An Updated Review," *Biology* 12, no. 10 (2023): 1320.

17. C.-g. Miao, Y.-y. Yang, X. He, et al., "Wnt Signaling Pathway in Rheumatoid Arthritis, With Special Emphasis on the Different Roles in

Synovial Inflammation and Bone Remodeling," *Cellular Signalling* 25, no. 10 (2013): 2069–2078.

18. H. Bastian, E. Feist, and G. R. Burmester, "Therapeutic Strategies in Rheumatoid Arthritis," *Internist* 52, no. 6 (2011): 645–656.

19. J. S. Smolen and G. Steiner, "Therapeutic Strategies for Rheumatoid Arthritis," *Nature Reviews. Drug Discovery* 2, no. 6 (2003): 473–488.

20. M. Zhu, Q. Ding, Z. Lin, et al., "New Targets and Strategies for Rheumatoid Arthritis: From Signal Transduction to Epigenetic Aspect," *Biomolecules* 13, no. 5 (2023): 766.

21. W. Frick, J. Hofmann, H. Fischer, and R. R. Schmidt, "The Structure of Bergenin," *Carbohydrate Research* 210 (1991): 71–77.

22. H. S. Kim, H. K. Lim, M. W. Chung, and Y. C. Kim, "Antihepatotoxic Activity of Bergenin, the Major Constituent of *Mallotus japonicus*, on Carbon Tetrachloride-Intoxicated Hepatocytes," *Journal of Ethnopharmacology* 69, no. 1 (2000): 79–83.

23. D. Zhou, X. Qin, Z. R. Zhang, and Y. Huang, "Physicochemical Properties of Bergenin," *Pharmazie* 63, no. 5 (2008): 366–371.

24. H. L. Pu, X. Huang, J. H. Zhao, and A. Hong, "Bergenin Is the Anti-arrhythmic Principle of *Fluggea virosa*," *Planta Medica* 68, no. 4 (2002): 372–374.

25. H. A. De Abreu, S. L. I. Aparecida Dos, G. P. Souza, D. Pilo-Veloso, H. A. Duarte, and A. F. D. C. Alcântara, "Antioxidant Activity of (+)-Bergenin: A Phytoconstituent Isolated From the Bark of Sacoglottis Uchi Huber (Humireaceae)," *Organic & Biomolecular Chemistry* 6, no. 15 (2008): 2713–2718.

26. K. Wang, Y. F. Li, Q. Lv, X. M. Li, Y. Dai, and Z. F. Wei, "Bergenin, Acting as an Agonist of PPARgamma, Ameliorates Experimental Colitis in Mice Through Improving Expression of SIRT1, and Therefore Inhibiting NF-kappaB-Mediated Macrophage Activation," *Frontiers in Pharmacology* 8 (2017): 981.

27. L. Yang, Y. Zheng, Y. M. Miao, et al., "Bergenin, a PPARgamma Agonist, Inhibits Th17 Differentiation and Subsequent Neutrophilic Asthma by Preventing GLS1-Dependent Glutaminolysis," *Acta Pharmacologica Sinica* 43, no. 4 (2022): 963–976.

28. J. C. Jung, E. Lim, S. H. Kim, N. S. Kim, M. Jung, and S. Oh, "Practical Synthesis and Biological Evaluation of Bergenin Analogs," *Chemical Biology & Drug Design* 78, no. 4 (2011): 725–729.

29. C. M. de Oliveira, F. R. Nonato, F. O. de Lima, et al., "Antinociceptive Properties of Bergenin," *Journal of Natural Products* 74, no. 10 (2011): 2062–2068.

30. L. Chen, C. Chu, J. Lu, X. Kong, T. Huang, and Y. D. Cai, "Gene Ontology and KEGG Pathway Enrichment Analysis of a Drug Target-Based Classification System," *PLoS One* 10, no. 5 (2015): e0126492.

31. A. Alsaber, J. Pan, A. Al-Herz, et al., "Influence of Ambient Air Pollution on Rheumatoid Arthritis Disease Activity Score Index," *International Journal of Environmental Research and Public Health* 17, no. 2 (2020): 416.

32. G. Yang, C. C. Chang, Y. Yang, et al., "Resveratrol Alleviates Rheumatoid Arthritis via Reducing ROS and Inflammation, Inhibiting MAPK Signaling Pathways, and Suppressing Angiogenesis," *Journal of Agricultural and Food Chemistry* 66, no. 49 (2018): 12953–12960.

33. M. M. Rahman, M. R. Khasru, M. A. Rahman, et al., "Quality of Life Assessment by SF-36 Among the Patients With Rheumatoid Arthritis," *Mymensingh Medical Journal* 31, no. 3 (2022): 586–591.

34. N. Li, Q. Xu, Q. Liu, et al., "Leonurine Attenuates Fibroblast-Like Synoviocyte-Mediated Synovial Inflammation and Joint Destruction in Rheumatoid Arthritis," *Rheumatology (Oxford)* 56, no. 8 (2017): 1417–1427.

35. G. Murphy and H. Nagase, "Reappraising Metalloproteinases in Rheumatoid Arthritis and Osteoarthritis: Destruction or Repair?," *Nature Clinical Practice. Rheumatology* 4, no. 3 (2008): 128–135.

36. C. J. Malemud, "Matrix Metalloproteinases and Synovial Joint Pathology," *Progress in Molecular Biology and Translational Science* 148 (2017): 305–325.

37. S. S. El-Hawary, R. Mohammed, S. Abouzid, Z. Y. Ali, and A. Elwekeel, "Anti-Arthritic Activity of 11-O-(4′-O-Methyl Galloyl)-Bergenin and Crassula Capitella Extract in Rats," *Journal of Pharmacy and Pharmacology* 68, no. 6 (2016): 834–844.

38. G. Nygaard and G. S. Firestein, "Restoring Synovial Homeostasis in Rheumatoid Arthritis by Targeting Fibroblast-Like Synoviocytes," *Nature Reviews Rheumatology* 16, no. 6 (2020): 316–333.

39. N. Bottini and G. S. Firestein, "Duality of Fibroblast-Like Synoviocytes in RA: Passive Responders and Imprinted Aggressors," *Nature Reviews Rheumatology* 9, no. 1 (2013): 24–33.

40. H. P. Hao, L. B. Wen, J. R. Li, et al., "LiCl Inhibits PRRSV Infection by Enhancing Wnt/Beta-Catenin Pathway and Suppressing Inflammatory Responses," *Antiviral Research* 117 (2015): 99–109.

Supporting Information

Additional supporting information can be found online in the Supporting Information section.

International Journal of
Rheumatic Diseases

| ORIGINAL ARTICLE

Endophilin A2, a Potential Therapeutic Target for Lupus, Promotes Lupus Progression

Lu-Qi Yang[1] | You-Yu Lan[2] | You-Qiang Wang[3] | Si-Yu Feng[1] | An-Fang Huang[2] 🔟 | Wang-Dong Xu[1] 🔟

[1]Department of Evidence-Based Medicine, School of Public Health, Southwest Medical University, Luzhou, Sichuan, China | [2]Department of Rheumatology and Immunology, The Affiliated Hospital, Southwest Medical University, Luzhou, Sichuan, China | [3]Department of Laboratory Medicine, Affiliated Traditional Chinese Medicine Hospital of Southwest Medical University, Luzhou, Sichuan, China

Correspondence: An-Fang Huang (loutch211@163.com) | Wang-Dong Xu (loutch123@163.com)

ABSTRACT

Objective: Endophilin A2 (EPA2) is a member of the Endophilin family. The relationship between EPA2 and SLE pathogenesis is unclear.

Methods: Plasma levels of EPA2 in SLE patients and healthy controls were detected by ELISA, and EPA2 mRNA levels of SLE patients were explored by qRT-PCR. EPA2 siRNA adenovirus was further injected into pristane-induced lupus mice, and the histological and serological changes were observed. In vitro, EPA2 siRNA adenovirus was transfected to human umbilical vein endothelial cells (HUVECs) in the presence of growth differentiation factor 15 (GDF15), and the proliferation, migration, and tube-forming ability of HUVECs were discussed.

Results: Plasma EPA2 levels were significantly higher in SLE patients than in healthy controls ($p < 0.001$), and EPA2 mRNA levels were significantly higher in SLE patients than in healthy controls as well ($p = 0.030$). Lupus mice exhibited splenomegaly, severe histologic damage, and high levels of autoantibodies (antinuclear antibody (ANA), anti-double-stranded DNA antibody (anti-dsDNA), and immunoglobulin G (IgG)) (vs. the control group, all $p < 0.05$). After injection of EPA2 siRNA adenoviruses, the lupus mice showed a lower proportion of CD11b$^+$LY-6C$^+$, F4/80$^+$, CD11c$^+$, CD19$^+$, CD8$^+$, Th1$^+$, Th2$^+$, Th17$^+$ cells and reduced expression of pro-inflammatory cytokines, and autoantibodies (vs. the adenoviral empty vector group, all $p < 0.05$). Addition of EPA2 siRNA adenovirus to HUVECs resulted in decreased GDF15 mRNA levels and reduced cell proliferation, migration and tube formation. However, in the presence of GDF15, EPA2-mediated effects were reversed, and the proliferation, migration, and tube formation ability of HUVECs were enhanced.

Conclusion: EPA2 may regulate angiogenesis through GDF15, and then involve in SLE pathogenesis.

1 | Introduction

Systemic lupus erythematosus (SLE) is a common rheumatic disease associated with a variety of autoantibodies as well as immune complex deposition, which ultimately leads to multi-organ damage and a lot of clinical manifestations [1, 2]. Many patients with SLE have cardiovascular comorbidities, and part of the mortality in SLE patients is induced by cardiovascular-related death [3, 4]. To date, the clear etiology of SLE has not been elucidated, and available studies suggest that genetic and environmental factors may correlate with SLE pathogenesis [5]. It is known that the risk of SLE may be attributed to genetics, and there is a higher prevalence of SLE in women than in men [6]. Homozygous twins with SLE have a higher concordance

rate than heterozygous twins [7]. This suggests that the risk of developing SLE may be highly heritable.

Endophilin A2 (EPA2) is a membrane-bound protein encoded by the SH3GL1 gene. EPA2 is closely related to cellular endocytosis [8] and is involved in the regulation of a variety of biological functions, such as autophagy [9–11]. Current studies have found that EPA2 is involved in tumor metastasis, neuromodulation, viral body production, and vascular function. EPA2 is highly expressed in neoplastic diseases such as colorectal cancer, breast cancer, and osteosarcoma, as well as rheumatoid arthritis (RA) [12–15]. EPA2 was found to be a disease-associated protein in adolescent idiopathic scoliosis [16, 17]. Therefore, EPA2 may be a biomarker for some diseases. The study by Norin et al. revealed that EPA2 may regulate T cells in RA patients, and there were higher serum EPA2 levels in RA patients than in healthy controls.

Angiogenesis, or the development of new capillaries from existing vessels, is associated with inflammation. Effector cells in the inflammatory phase release pro-angiogenic molecules that promote the formation and invasion of new blood vessels, allowing inflammatory cells to invade. Studies have shown that EPA2 is a regulator of endothelial cell migration during angiogenesis. EPA2 is expressed in endothelial cells, which are required for developmental and pathological angiogenesis. EPA2 promotes endothelial cell migration by regulating VEGFR2 internalization and downstream signaling [18]. Thus, EPA2 may be involved in regulating angiogenesis, and excessive angiogenesis may promote the development of SLE. A previous study by our group showed that SLE patients had elevated levels of growth differentiation factor 15 (GDF15) [19]. GDF15 was accepted to be involved in angiogenesis, and GDF15 stimulates the proliferation of human umbilical vein endothelial cells (HUVECs) and promotes vascular development. Since the proliferation of endothelial cells plays an important role in angiogenesis, GDF15 may be a potential angiogenic factor for tissue regeneration [20–23]. Indeed, SLE is a disease significantly associated with impairment of vascular function. Based on this, we speculate that EPA2 may affect endothelial cells migration and angiogenesis by regulating GDF15 signaling, which in turn promotes the development of SLE.

To date, there are no studies of EPA2 associated with SLE. Therefore, the aim of this study was to investigate the association of EPA2 with the pathogenesis of SLE. In this study, we first discussed plasma EPA2 levels in SLE patients and EPA2 mRNA levels in SLE patients. Second, we conducted a lupus mice model to confirm the role of EPA2 in lupus development. Finally, in vitro experiments, we discussed the role of EPA2 on HUVECs proliferation, migration, and tube formation through regulating GDF15. This study revealed the potential of EPA2 as a biomarker for SLE and demonstrated the role of EPA2 in promoting lupus development by regulating GDF15.

2 | Materials and Methods

2.1 | Study Population

For population study, we included 3 independent case–control studies. The first was to analyze plasma levels of EPA2 in SLE patients, and this part included 81 SLE patients and 81 healthy controls. The second part was to discuss EPA2 mRNA levels in 34 SLE patients and 34 healthy controls, which was used to demonstrate expression profile of EPA2 in SLE plasma. Moreover, we validated EPA2 plasma levels from an independent SLE cohort (81 SLE patients and 81 healthy controls). Diagnosis of SLE was made according to the classification criteria of the American College of Rheumatology (ACR) in 1997. Data about clinical and laboratory characteristics of SLE patients were collected. Systemic lupus erythematosus disease activity index (SLEDAI) was calculated according to the SLE Disease Activity Index 2000 version (SLEDAI-2K). All SLE patients were from the Department of Rheumatology and Immunology of the Affiliated Hospital of Southwest Medical University, and healthy controls were from the Center for Disease Control and Prevention of Jiangyang District and the Health Examining Center of Affiliated Traditional Chinese Medicine Hospital of Southwest Medical University.

2.2 | Animal Models

Thirty-two female C57BL/6J mice (6–8 weeks) were purchased from GemPharmatech (Chengdu, China). After 1 week of acclimatization feeding, the mice were randomly divided into 4 groups of 8 mice each using completely randomized grouping. Three groups of mice were injected intraperitoneally with 0.5 mL pristane (Sigma Aldrich, St Louis, USA) to induce lupus. The other group was injected with phosphate-buffered saline solution (PBS). After 3 months' observation, EPA2 siRNA adenovirus and empty vector adenovirus were diluted in sterilized saline and injected into part of the pristane-induced lupus mice. Different kinds of adenoviruses were injected into the tail vein for 5 and 7 days, and then EPA2 mRNA levels in the spleen were evaluated. Five days' injection of EPA2 siRNA adenovirus showed the best knockdown efficiency (Figure S1). In the following study, all mice were euthanized after injection of EPA2 siRNA adenovirus for 5 days. Cardiac blood was collected and centrifuged to obtain serum. The liver, spleen, and kidneys were weighed and photographed.

2.3 | Enzyme-Linked Immunosorbent Assay (ELISA)

Plasma from each patient and control subject was separated, and then the plasma was stored in a −80°C freezer until use. Plasma EPA2 was detected using an ELISA kit (Abebio, Wuhan, China). In addition, mouse serum was collected after centrifugation for detection of antinuclear antibody (ANA), anti-double-stranded DNA antibody (anti-dsDNA), and immunoglobulin G (IgG) (CUSABIO, Wuhan, China). The data were measured at 450 nm using an enzyme marker.

2.4 | Quantitative Real-Time PCR Analysis (qRT-PCR)

Total RNA from the whole blood of the patient and control subjects was extracted using the Whole Blood Total RNA Kit (Sangon Biotech, Shanghai, China), and total RNA from cells was extracted using the Ultra Pure Total RNA Extraction Kit (Sangon

Biotech, Shanghai, China). cDNA was synthesized using reverse transcriptase reagent (Vazyme, Nanjing, China). cDNA was amplified using SYBR dye (Vazyme, Nanjing, China). All qRT-PCR analysis was performed in triplicate and normalized to glyceraldehyde-3 phosphate dehydrogenase (GAPDH). Relative mRNA levels of EPA2 and GDF15 were calculated for each sample using the $2^{-\Delta\Delta Ct}$ method. Primer sequences were shown in Table S1.

2.5 | Flow Cytometry

Mouse spleens were ground using a $70\,\mu m$ cell filter to prepare single-cell suspensions. Leukocytes were obtained by removing erythrocytes on ice using erythrocyte lysis buffer (Beyotime, Shanghai, China). Monocytes, dendritic cells, B cells, macrophages, and T cells were detected using CD11b-FITC, LY-6C-PE-CY7, CD11c-APC, CD19-PE, F4/80-BV421, CD3-BV510, and CD8-percp-cy5.5. For Th1, Th2, Th17, and Treg cells, the proportion of the cells were detected by markers of CD4-BV421, interferon-γ (IFN-γ)-FITC, interleukin-4 (IL-4)-PE-CY7, IL-17A-PE, and Foxp3-AF647. All antibodies were purchased from BD Biosciences (California, USA). All data were analyzed by FlowJo software (v10.8.0, Treestar, USA).

2.6 | Cytometric Bead Array (CBA)

The BD Cytometric Bead Array Mouse Cytokine Kit was used to detect expression of inflammatory cytokines IL-2, IL-4, IL-6, IL-10, IFN-γ, and TNF-α in mouse serum. Experiments were performed according to the CBA kit instructions. Briefly, $50\,\mu L$ of serum samples, $20\,\mu L$ of mixed microspheres, and $20\,\mu L$ of PE detection antibody were gently mixed and incubated for 2 h at room temperature, protected from light. Data were collected using a BD FACSCantoII flow cytometer. A standard curve was obtained, and the sample content was calculated using FCAP Array software.

2.7 | Histopathology and Immunofluorescence Analysis

Mice kidneys were prepared by dehydration, trimming, embedding, sectioning, staining, sealing, and microscopic examination; hematoxylin–eosin (HE) staining and Masson staining were performed to observe the renal histopathology and renal fibrosis. HE and Masson scores were calculated according to the degree of renal tissue damage and the percentage of area of renal fibrous tissue expression, respectively [24, 25]. The site and intensity of immune complex expression in the mice's kidneys were observed by immunofluorescence staining under a laser confocal microscope.

2.8 | Cell Culture and Processing

Twenty-five milliliters of fetal bovine serum, 5 mL of endothelial cell growth supplement, and 5 mL of penicillin–streptomycin were added to 500 mL of ECM (Sciencell, USA) basal medium, which was configured as fresh medium. HUVECs were cultured in a 37°C incubator at 5% CO_2. HUVECs were transfected with the EPA2 siRNA adenoviral vector. For discussing the role of EPA2 in HUVECs proliferation, migration, and tube formation

by regulating GDF15, we first transfected HUVECs with EPA2 siRNA adenoviruses, and then we treated the cells with recombinant human GDF15. The concentration is 100 ng/mL with a 24h intervention.

2.9 | Proliferation

Cell proliferation capacity was evaluated using a cell counting kit (CCK-8; Sigma). HUVECs were spread in 96-well plates at a density of 2×10^3 cells for 24h. Ten microliters of CCK-8 solution was added to each well, and the absorbance at 450nm was measured by an enzyme marker.

2.10 | Migration

Migration was determined using transwell cell culture inserts (8um, Corning). HUVECs (3×10^4 cells) were placed in the upper layer of the transwell, and serum-containing ECM was placed below the cell-permeable membrane. After 24h of incubation, the cells were fixed with 4% paraformaldehyde for 15m, washed, and then stained with 0.1% crystal violet for 20m. Three fields of view were photographed in each well, counted using ImageJ, and the average value was taken for statistical analysis.

2.11 | Tube Formation

Each well in a 24-well plate was coated with $80\,\mu L$ matrigel (Lablead, Beijing, China), and then HUVECs were added to the matrigel-coated wells at a density of 5×10^4 cells per well. After 8h, photographs were taken with a light microscope, and the number of nodes and total tube length were calculated using the Angiogenesis Analyzer plug-in for ImageJ.

2.12 | Determination of Sample Size

The sample size was determined based on the research experience of the subject group and the ability of the group to actually collect samples. After completing the inclusion of samples, power was applied to conduct post hoc analysis as a means of calculating the actual test efficacy of the included sample size. The test efficacy for EPA2 plasma levels in the two case–control studies was both 1.000, and the test efficacy for EPA2 mRNA levels for qRT-PCR analysis was 0.970.

2.13 | Statistical Analysis

All data were analyzed using SPSS 26.0 statistical software. Quantitative data were expressed as mean $\pm$ standard deviation (SD) according to the Shapiro–Wilk test if the data were normally distributed. Median (interquartile spacing) was used for non-normal distribution data. Qualitative data were expressed as frequencies and (or) percentages. The rank correlation coefficient was used to evaluate the relationship between two variables. The specificity and sensitivity of plasma EPA2 as a diagnostic marker for SLE were measured by receiver operating characteristics (ROC) curves. $p < 0.05$ was statistically significant.
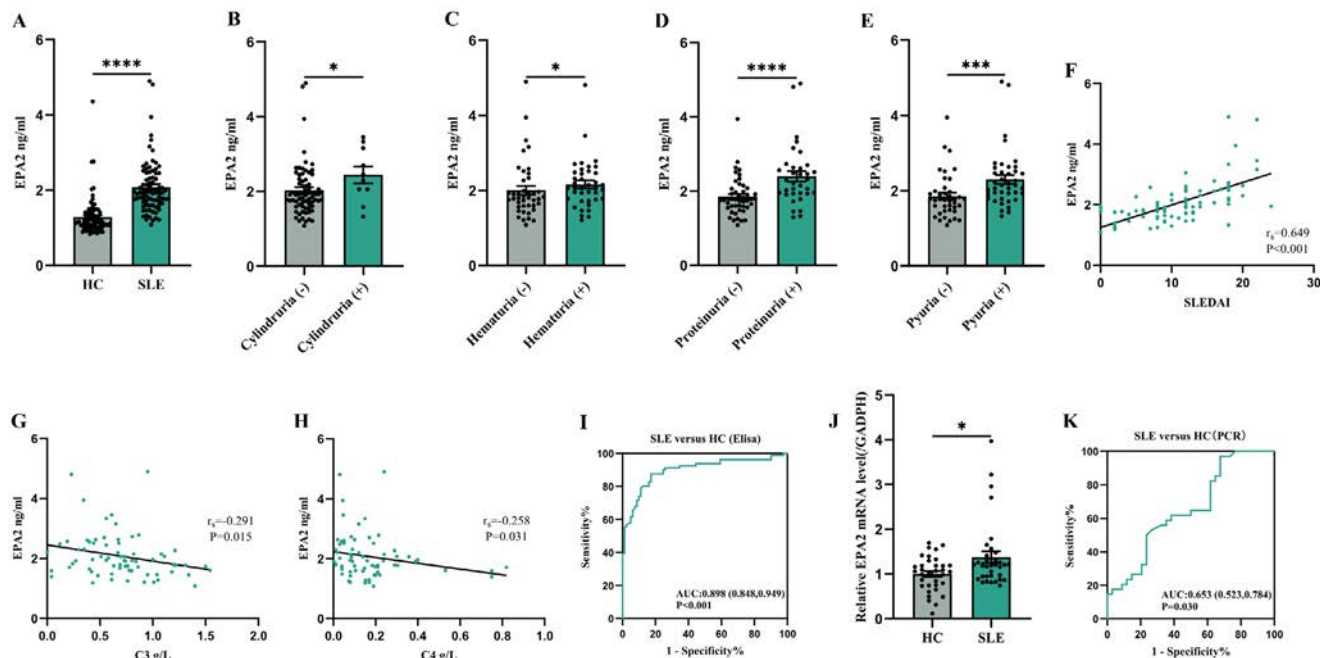
FIGURE 1 | Plasma and mRNA levels of EPA2 in SLE patients and healthy controls. (A) Plasma EPA2 levels in 81 SLE patients and 81 healthy controls were detected by ELISA. Comparison of EPA2 plasma levels between the two groups. (B–E) EPA2 plasma levels are associated with some clinical characteristics of SLE patients. (F–H) Correlation of plasma EPA2 levels with SLEDAI, C3, and C4. (I) Exploration of the potential of EPA2 plasma as a biomarker for SLE by receiver operating characteristics (ROC) curve analysis. (J) The mRNA levels of 34 SLE patients and 34 healthy controls were detected by qRT-PCR. (K) Exploration of the potential of EPA2 mRNA as a biomarker for SLE by receiver operating characteristics (ROC) curve analysis. $*p < 0.05$, $***p < 0.005$, $****p < 0.001$.

3 | Results

3.1 | Correlation Between Plasma Levels of EPA2 and SLE Patients

Clinical and laboratory characteristics of SLE patients and healthy controls for ELISA analysis are shown in Table S2. Plasma EPA2 levels were higher in SLE patients compared with healthy controls ($p < 0.001$, Figure 1A). Plasma EPA2 levels were significantly higher in SLE patients complicated with some clinical and laboratory features (including cylindruria, hematuria, proteinuria, and pyuria) compared to patients without these features (All $p < 0.05$, Figure 1B–E). Correlation analysis showed that plasma EPA2 levels were associated with a number of clinical and laboratory features, including SLEDAI ($r_s = 0.649$, $p < 0.001$, Figure 1F), C3 ($r_s = -0.291$, $p = 0.015$, Figure 1G), and C4 ($r_s = -0.258$, $p = 0.031$, Figure 1H). ROC curve analysis showed that plasma EPA2 distinguished SLE patients from healthy controls with an area under the curve of 0.898 (95% CI: 0.848–0.949, $p < 0.001$, Figure 1I). In addition, other clinical and laboratory characteristics were not significantly associated with plasma EPA2 levels ($p > 0.05$, Tables S3 and S4). We assessed the ability of plasma EPA2 to distinguish SLE from healthy controls. The diagnostic efficiency of plasma EPA2 was evaluated (Table S5). At the cut-off value of 1.533 ng/mL, the sensitivity, specificity, +LR, −LR, Youden's index, accuracy, PPV, and NPV were 0.827, 0.877, 6.724, 0.197, 0.704, 0.852, 0.870, and 0.835, respectively. To validate plasma levels of EPA2 in SLE patients, we used another independent SLE cohort, which included 81 SLE patients and 81 healthy controls (Table S6). We found that SLE patients also had significantly higher plasma EPA2 levels than healthy controls ($p < 0.001$, Figure S2A). Plasma

EPA2 levels were correlated with some clinical and laboratory characteristics of SLE patients (Figure S2B–I, Tables S7 and S8). ROC curve also found that plasma EPA2 may differentiate SLE from controls (Figure S2J).

3.2 | Peripheral Blood EPA2 mRNA Levels Were Higher in SLE Patients

Another cohort of SLE patients and healthy controls was conducted to discuss the expression profile of EPA2 mRNA. The characteristics of the patients and controls were shown in Table S9. There was no statistically significant difference in the age and gender of the study subjects in both groups. By exploring the differences between peripheral blood EPA2 mRNA levels in SLE patients and healthy populations, it was found that mRNA levels of EPA2 were higher in SLE patients than in healthy controls ($p = 0.030$, Figure 1J). ROC curve analysis showed that EPA2 mRNA levels distinguished SLE patients from healthy controls with an area under the curve of 0.653 (95% CI: 0.523–0.784, $p = 0.030$, Figure 1K). Correlation between EPA2 mRNA levels and SLE patients' clinical and laboratory features was listed in Tables S10 and S11.

3.3 | EPA2 siRNA Adenovirus Inhibited Kidneys Swelling in Lupus Mice

The weights of the liver, spleen, and kidneys were significantly increased in pristane-induced lupus mice compared to controls. Treatment with EPA2 siRNA adenovirus decreased the weights
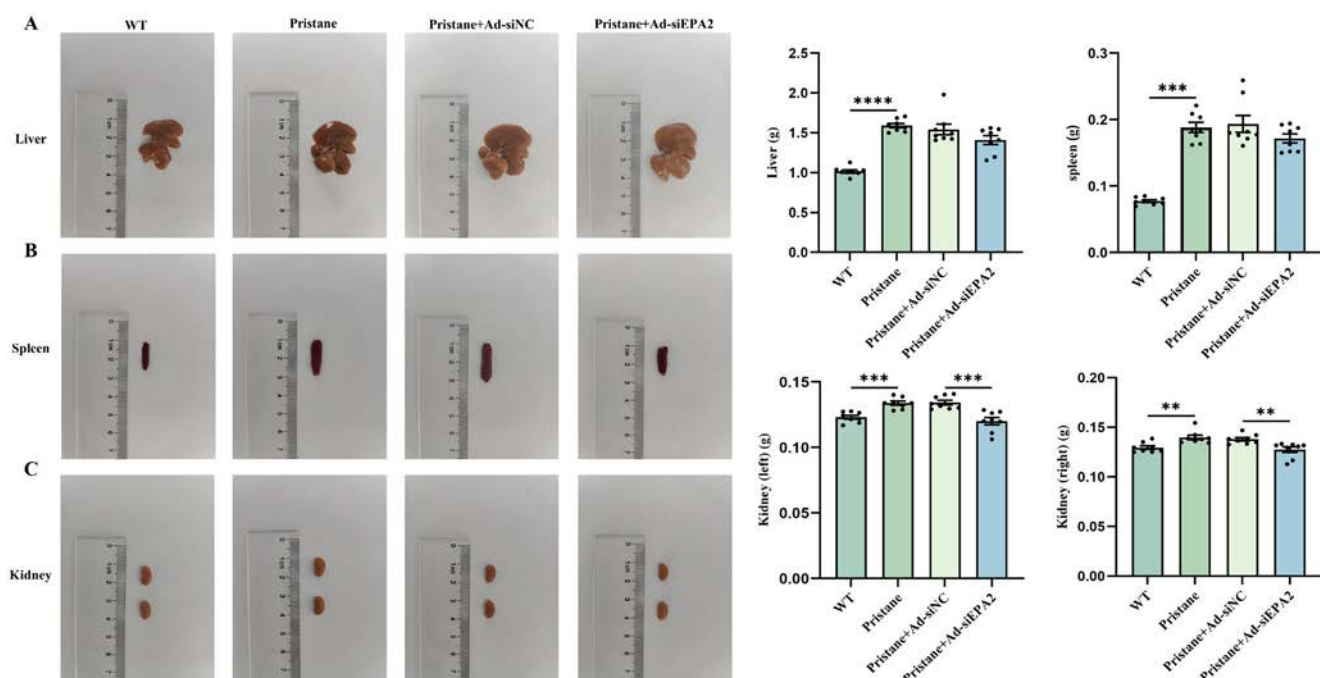
FIGURE 2 | Reduction of liver, spleen, and kidney enlargement in lupus mice after injection of EPA2 siRNA adenovirus. (A–C) Lupus mice (model group) were constructed by intraperitoneal injection of pristane into wild-type (WT) C57BL/6 J mice, and control mice were constructed by injection of PBS into WT mice. The lupus mice were injected with an adenoviral empty vector or EPA2 siRNA adenovirus. Representative pictures of liver, spleen, and kidney of four groups of mice (left) and statistical analysis of organ weights (right). Error bars are shown as mean ± standard deviation. 8 mice/group. $**p < 0.01$, $***p < 0.005$, $****p < 0.001$.

of kidneys but did not significantly decrease the weights of liver and spleen in lupus mice (Figure 2A–C).

3.4 | EPA2 siRNA Adenovirus Attenuates Renal Injury in Lupus Mice

Compared with controls, pristane-induced lupus mice exhibited glomerulosclerosis and necrosis, thickening of the basement membrane of the renal capsule, narrowing of the capillary lumen, localized crescent formation, nuclear deletion of renal tubular epithelial cells, dilatation of part of the renal tubule, thinning of the tubular wall, lymphocyte infiltration, and fibrous tissue hyperplasia. In addition, glomerular IgG deposition was significantly increased in lupus mice compared with control mice. However, HE, Masson, and immunofluorescence intensity scores indicated that the EPA2 siRNA adenovirus had a significant therapeutic effect in lupus mice (all $p < 0.05$, Figure 3A–C).

3.5 | Inhibition of EPA2 Reduces Inflammatory Cytokines and Autoantibodies Production

Pristane-induced lupus mice had significantly higher levels of ANA, anti-dsDNA, and IgG compared to control mice. Silencing of EPA2 in lupus mice significantly reduced ANA, anti-dsDNA, and IgG levels compared to adenoviral empty vector-treated lupus mice (Figure 4A–C). In pristane-induced lupus mice, serum IL-2, IL-4, IL-6, IL-10, IFN-γ, and TNF-α levels were higher than those in the control group (Figure 4D–I). The expression of all inflammatory cytokines was down-regulated after silencing EPA2 in the lupus mice.

3.6 | Silencing EPA2 Reversed Dysregulation of Immune Cells in Lupus Mice

The percentages of CD11b+LY-6C+, F4/80+, CD11c+, CD19+, CD8+, Th1+, Th2+, and Th17+ cells in the spleen of lupus mice were significantly higher than in control mice, and the proportion of Treg cells was lower in the lupus mice. After inhibition of EPA2, the lupus mice showed lower percentages of CD11b+LY-6C+, F4/80+, CD11c+, CD19+, CD8+, Th1+, Th2+, Th17+ cells, and a higher percentage of Treg cells (All $p < 0.05$, Figure 5A–I).

3.7 | EPA2 siRNA Adenovirus Down-Regulates the mRNA Levels of GDF15

It is known that EPA2 may regulate angiogenesis. Therefore, we conducted in vitro experiments to discuss whether silencing EPA2 may regulate the function of HUVECs. Moreover, in our previous study, we found that GDF15 may be involved in SLE pathogenesis by regulating angiogenesis. In this study, we also discuss the effects of EPA2 on HUVECs by regulating GDF15.

First, we discussed which titer (MOI = 50, MOI = 100, MOI = 200, MOI = 500) of adenoviral transfection of HUVECs may have the best effect, and immunofluorescence observation of the cells showed MOI = 100 to be the best (Figure 6A). Then, EPA2 siRNA adenoviral transfection of HUVECs was further conducted to discuss which time silencing EPA2 may inhibit EPA2 expression the best. Results showed that expression of EPA2 was mostly inhibited after 48 h (Figure 6B). In addition, qRT-PCR analysis showed that the GDF15 mRNA expression was significantly reduced in
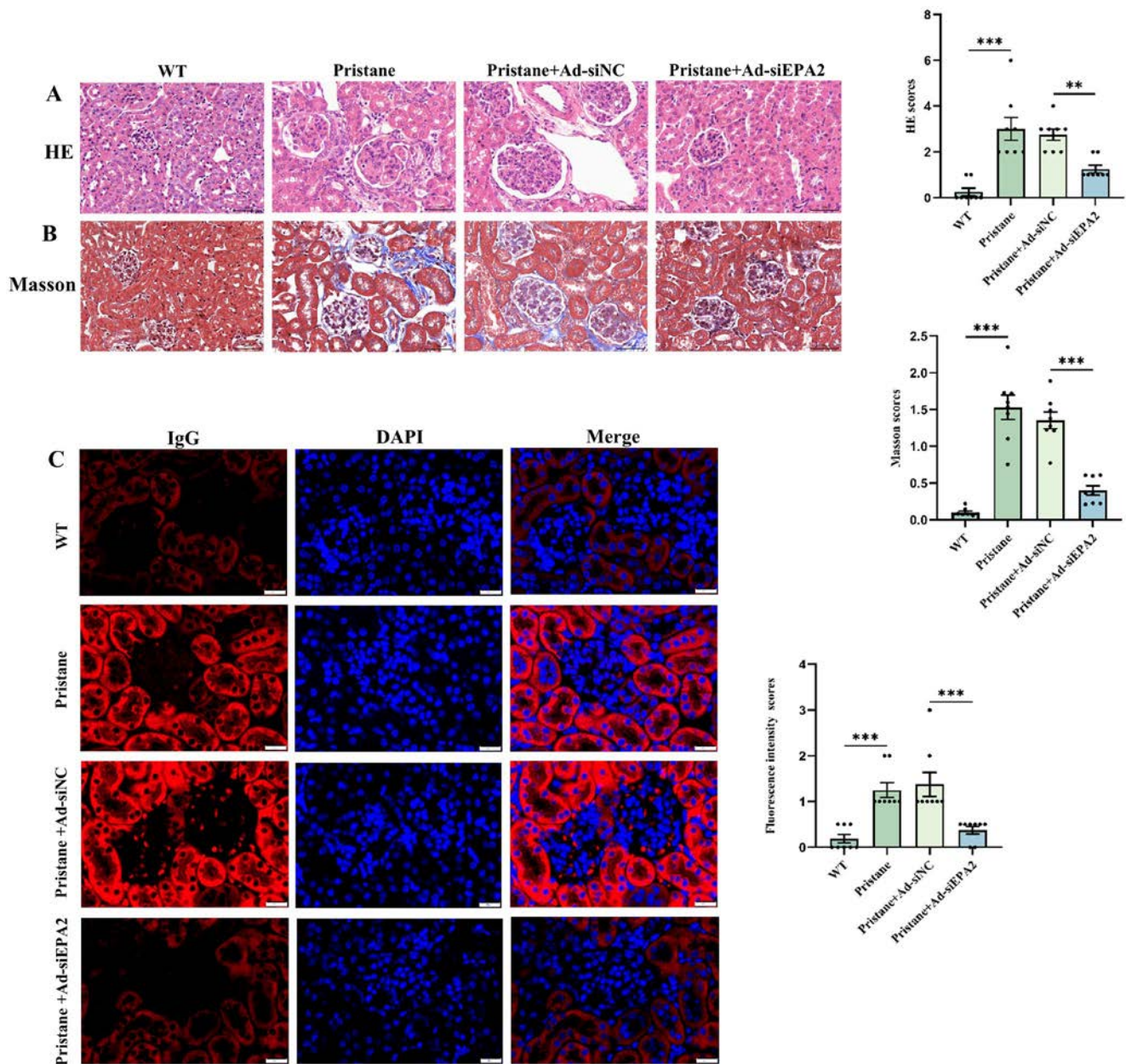
FIGURE 3 | EPA2 silencing attenuates kidney injury in lupus mice. (A–C) HE staining, Masson staining and immunofluorescence staining of the kidneys of mice in the control group, pristane-induced lupus group, adenovirus empty vector, and EPA2 siRNA adenovirus-injected groups. Acquisition of ×400 micrographs. Representative graphs of HE staining, Masson staining, and immunofluorescence of each group are shown on the left, and statistical scores of HE score, Masson score, and immunofluorescence score are shown on the right. Error bars are shown as mean ± standard deviation. 8 mice/group. **$p < 0.01$, ***$p < 0.005$.

the EPA2 siRNA adenovirus group compared with the control and empty vector adenovirus groups ($p < 0.05$, Figure 6C).

### 3.8 | Inhibition of HUVECs Proliferation by EPA2 Inhibition

HUVECs were transfected with empty vector adenovirus (MOI = 100) and EPA2 siRNA adenovirus (MOI = 100), and the proliferation of HUVECs was detected by CCK8. The results showed that the proliferation ability of HUVECs was significantly reduced in the EPA2 silencing group compared with the control and empty vector groups ($p < 0.05$, Figure 6D). Interestingly,

addition of GDF15 to the EPA2-silenced group significantly enhanced the proliferation ability of HUVECs ($p < 0.05$).

3.9 | Inhibition of HUVECs Migration by Suppression of EPA2

We discussed the effects of EPA2 on HUVECs migration. Transwell assay of HUVECs migration showed that the number of crystal violet staining was significantly reduced in the EPA2-silenced group compared with the control group and the empty vector group ($p < 0.05$, Figure 6E), suggesting that EPA2 silencing significantly reduced the migratory ability of HUVECs. After
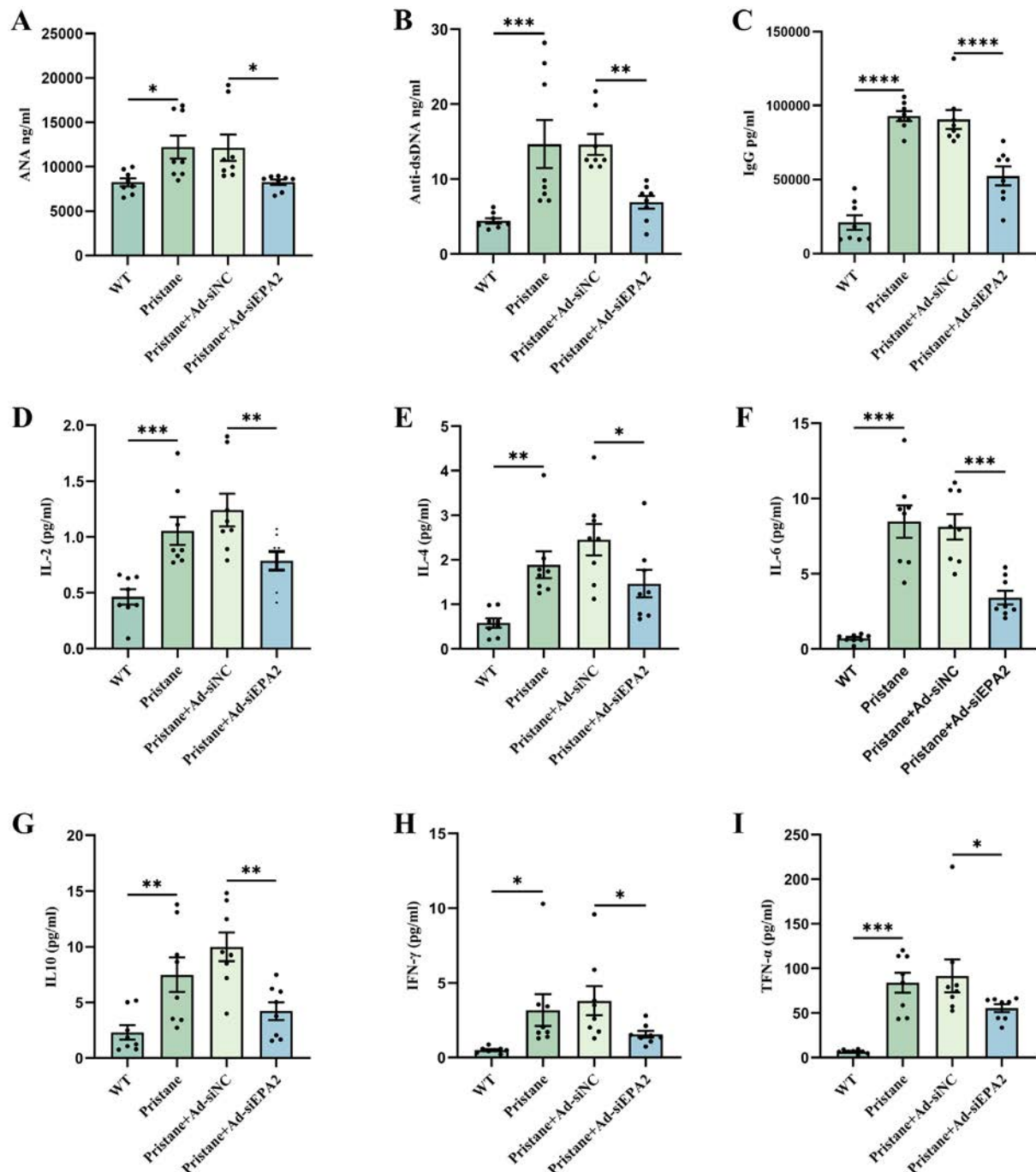
FIGURE 4 | Inhibition of EPA2 reduces autoantibodies and inflammatory cytokines production in lupus mice. (A–C) Concentrations of ANA, anti-dsDNA, and IgG in four groups of mice were measured by ELISA analysis. (D–I) Concentrations of inflammatory cytokines, including IL-2, IL-4, IL-6, IL-10, TNF-α, and IFN-γ, in four groups of mice were measured by CBA. Error bars are shown as mean ± standard deviation. 8 mice/group. $*p < 0.05$, $**p < 0.01$, $***p < 0.005$, $****p < 0.001$.

the addition of GDF15 to the EPA2-silenced group, the migratory ability of HUVECs was significantly enhanced ($p < 0.05$).

### 3.10 | Inhibiting EPA2 in HUVECs Reduces the Generation of Lumen-Like Structures

Based on the above-mentioned regulatory effects of EPA2 silencing on HUVECs' proliferation and migration, we discussed the effects of EPA2 on the angiogenesis of HUVECs. The results showed that compared with the empty vector adenovirus group, the number of

nodes in the EPA2-silenced group was significantly reduced, and the tube length was significantly shortened ($p < 0.05$, Figure 6F). On the contrary, the addition of GDF15 reversed EPA2 silencing-mediated effects. It is suggested that EPA2 silencing significantly inhibited the generation of lumen-like structures in HUVECs.

4 | Discussion

In the present study, 3 population-based case–control studies were conducted to discuss not only the correlation between
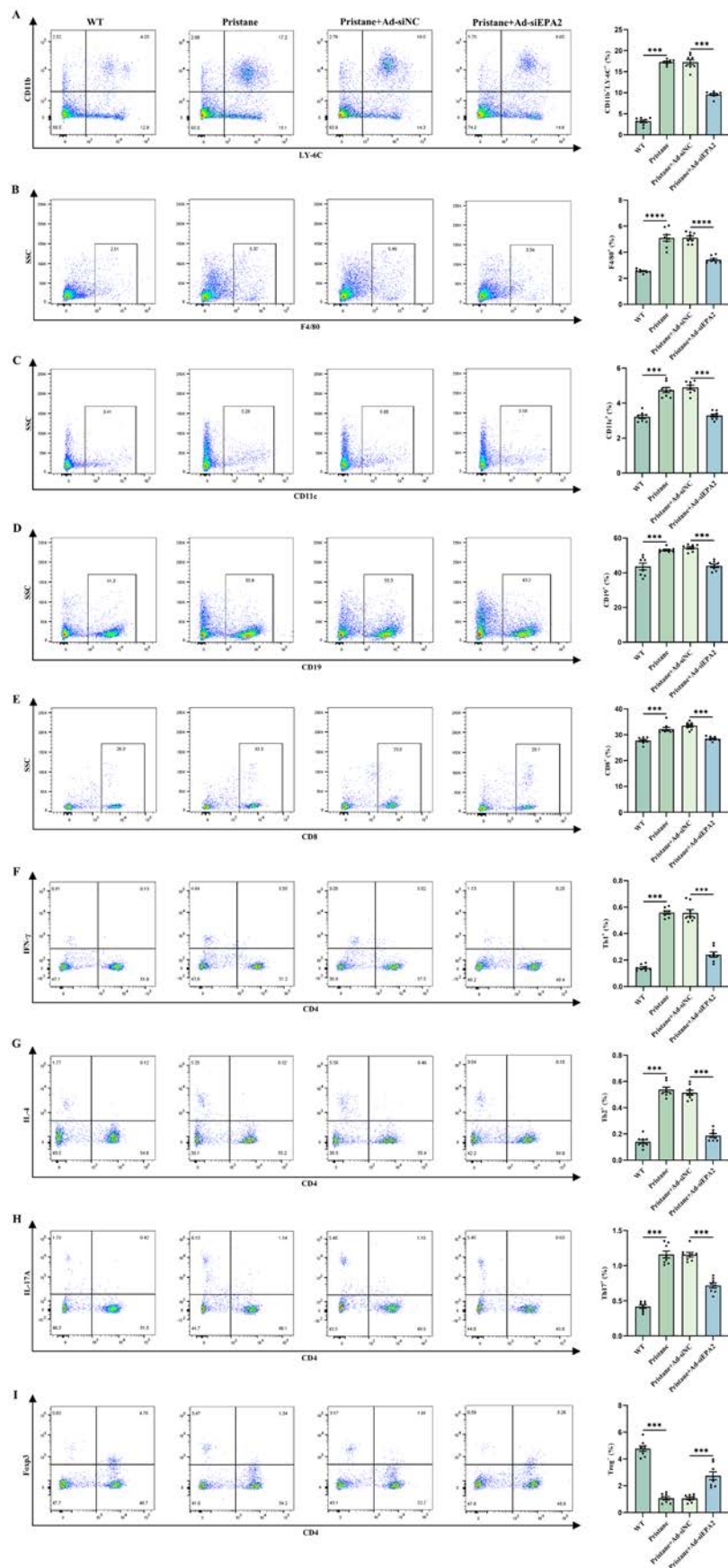
FIGURE 5 | Legend on next page.

FIGURE 5 | Distribution of immune cells in lupus mice after inhibiting EPA2 expression. Expression of different immune cells was analyzed using flow cytometry in four groups of mice, including wild-type mice injected with PBS, pristane-induced lupus mice, and pristane-induced lupus mice injected with adenoviral empty vectors or EPA2 siRNA adenovirus. (A) CD11b-FITC, LY-6C-PE-CY7; (B) F4/80-BV421; (C) CD11c-APC; (D) CD19-PE; (E–I) T cell subsets, and all cell proportions were first labeled with CD3^{+}. Representative flow plots are shown on the left, and statistical analysis of the corresponding immune cells is shown on the right. Error bars show mean ± standard deviation. 8 mice/group. ***$p < 0.005$, ****$p < 0.001$.
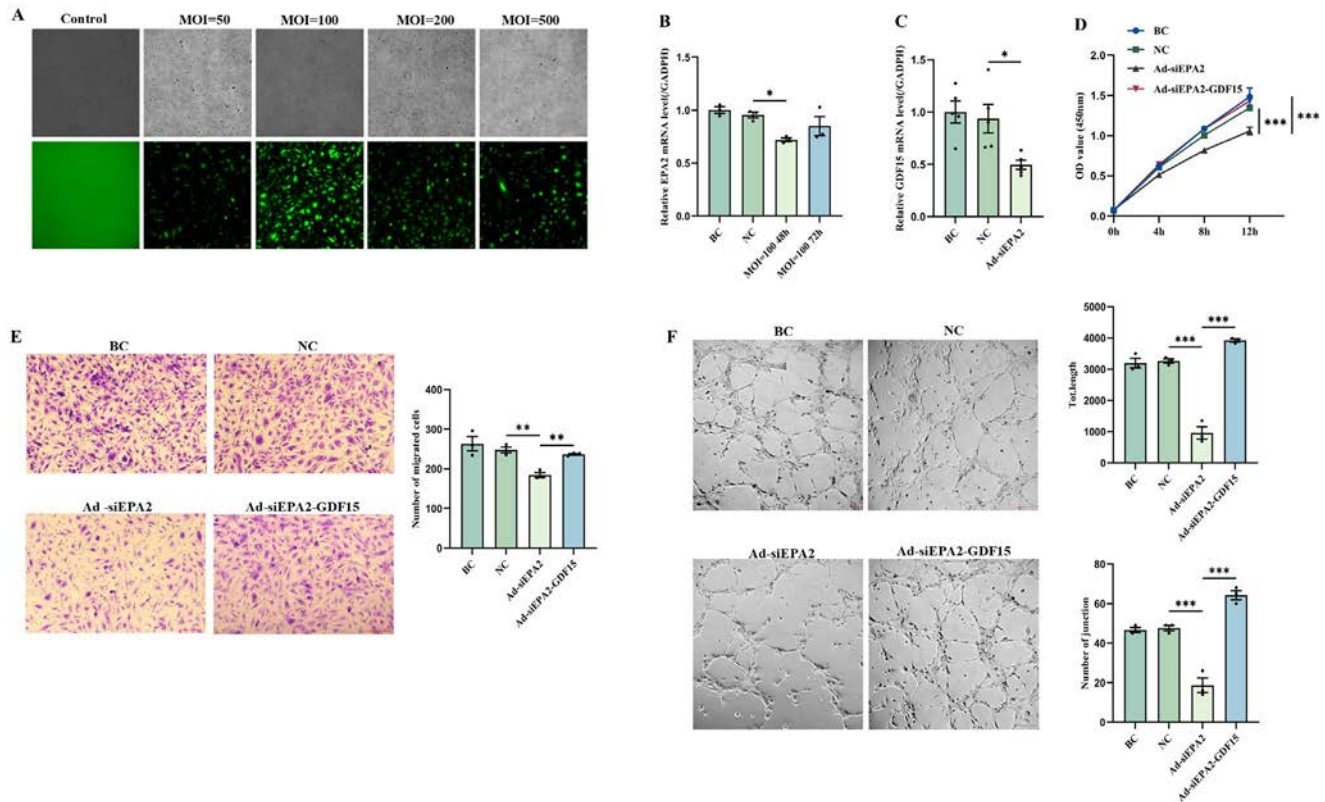
FIGURE 6 | Suppressing EPA2 inhibits proliferation, tube formation, and migration of HUVEC cells. (A) HUVECs were transfected with EPA2 siRNA adenovirus at different titers (MOI = 50, MOI = 100, MOI = 200, MOI = 500), and the transfection efficiency was observed under a fluorescence microscope at 48 h of transfection. (B) The optimal transfection time was detected by the qRT-PCR method ($N = 3$/group). (C) The relative mRNA levels of GDF15 in the control, adenovirus empty vector group, and EPA2 siRNA adenovirus group were detected by the qRT-PCR method ($N = 5$/group). (D) EPA2 siRNA transfection of HUVECs was carried out for 48 h for the proliferation assay. Cells were seeded in 96-well plates, and GDF15 recombinant protein was added; CCK-8 reagent was added after 24 h of incubation, and the absorbance at 450 nm was measured by an enzyme marker ($N = 5$/group). (E) HUVECs were transfected with EPA2 siRNA adenovirus, and a transwell assay was carried out and photographed after 48 h. Scale bar: 200 μm. For each experiment, 3 fields of view were randomly selected for cell counting, and the mean value was taken for statistical analysis. Each experiment was repeated 3 times. (F) HUVECs were transfected with EPA2 siRNA adenovirus to knock down EPA2 expression, and tube-forming experiments were performed at 48 h of transfection and photographed after 8 h. Scale bar: 200 μm. The total length of tube formation and the number of nodes were statistically analyzed. Each experiment was repeated 3 times. *$p < 0.05$, **$p < 0.01$, ***$p < 0.005$.

plasma EPA2 levels and SLE pathogenesis but also the association between peripheral blood EPA2 mRNA levels and SLE risk. The role of EPA2 in the development of lupus was further demonstrated by the establishment of a lupus mouse model, in which we explored the role of EPA2 in the development of lupus by treating lupus mice with EPA2 siRNA adenovirus. The results showed that both plasma and mRNA levels of EPA2 were higher in SLE patients, and silencing EPA2 significantly reduced kidney weight, slowed down kidney injury, and restored immune cell abnormalities. In in vitro experiments we demonstrated that EPA2 is associated with angiogenesis and may be involved in angiogenesis through regulating GDF15.

Dysregulation of T and B cell activation is a major feature of SLE. EPA2 is the only Endophilin family member expressed in hematopoietic cells, which is important for B cell-mediated humoral immunity and pathology [26, 27]. EPA2 can abnormally activate self-reactive T cells by regulating T cell receptor internalization, triggering, and driving RA. EPA2 deficiency was protective against autoimmune encephalomyelitis [15, 28]. Since SLE is also an autoimmune disease, we speculated that EPA2 might be involved in the pathogenesis of SLE. Our study confirmed that plasma EPA2 levels were much higher in SLE patients, and clinical subgroup analysis revealed that EPA2 expression was associated with a number

of indicators associated with acute kidney injury, such as tubular urine, hematuria, proteinuria, and pyuria. Our study also found a negative correlation between C3, C4, and EPA2 expression in SLE patients. Interestingly, EPA2 expression was significantly correlated with SLEDAI score. Plasma EPA2 levels could differentiate between SLE patients and healthy controls. In addition, we found that peripheral blood EPA2 mRNA levels were significantly higher in SLE patients than in healthy controls, and peripheral blood EPA2 mRNA showed the ability to differentiate SLE from healthy controls. All these suggest that EPA2 may be associated with SLE pathogenesis and may be a biomarker to distinguish SLE patients from healthy individuals. The diagnosis and treatment of SLE are highly dependent on biomarkers, but existing markers have significant shortcomings in terms of specificity and sensitivity. For example, the specificity of ANA is not high, the sensitivity and specificity of anti-dsDNA are not enough, and the levels of complement C3 and C4 are correlated with disease activity and may be affected by other factors such as infection. Therefore, there is a need to find new biomarkers to improve the efficiency and accuracy of early diagnosis of SLE. EPA2 has a good diagnostic ability with sensitivity and specificity of 0.827 and 0.877, respectively.

To further demonstrate the role of EPA2 in SLE pathogenesis, lupus mice were injected with EPA2 siRNA adenovirus. The results showed that EPA2 silencing could attenuate kidney injury and reverse the abnormality of immune cells, autoantibodies, and inflammatory cytokines in lupus mice. Interestingly, pristane-induced lupus mice exhibited enlarged livers, spleens, and kidneys, as well as renal injuries. The hepatomegaly, splenomegaly, and nephrometastasis were reduced in the lupus mice after silencing EPA2, and glomerulonephric necrosis was reduced. Renal lymphocyte infiltration was inhibited, and IgG deposition was reduced in lupus mice injected with EPA2 siRNA adenovirus. EPA2 silencing also significantly reduced ANA, IgG, and anti-dsDNA autoantibodies production in lupus mice. This confirms the role of EPA2 in promoting renal immune complex deposition. Some studies showed that EPA2 was positively correlated with the expression of IL-6 and TNF-α [29, 30]. It is well recognized that an imbalance of these pro-inflammatory factors is associated with SLE disease activity. In this study, lupus mice exhibited high levels of inflammatory cytokines, including IL-6 and TNF-α. After injecting with EPA2 siRNA adenovirus, the lupus mice showed down-regulated levels of IL-2, IL-4, IL-6, IL-10, TNF-α, and IFNγ. The findings suggest that silencing EPA2 inhibits the production of autoantibodies and inflammatory cytokines. In pristane-induced lupus mice, the frequencies of CD11b$^+$LY-6C$^+$, F4/80$^+$, CD11c$^+$, CD19$^+$, CD8$^+$, Th1$^+$, Th2$^+$, and Th17$^+$ cells were higher, and the frequency of Treg cells was lower. It is known that the imbalance of these cells promotes the pathogenesis of SLE. When injecting with EPA2 siRNA adenovirus in lupus mice, the imbalance of the immune cells was reversed. Interestingly, there are some potential off-target effects of EPA2 inhibition. First, EPA2 has homology with EPA1 and EPA3, and its function may be interfered with if the sequence is silenced. Second, EPA2 is involved in synaptic vesicle recycling and membrane remodeling, and its silencing may affect neuronal synaptic transmission, leading to behavioral abnormalities or cognitive

impairment. Third, EPA2 is associated with apoptosis regulation, and silencing EPA2 may lead to unintended cell death or abnormal proliferation by affecting mitochondrial membrane stability or caspase activation pathways. Fourth, EPA2 may indirectly regulate other pathways, leading to aberrant activation of signaling such as MAPKs and PI3K/AKT after EPA2 silencing.

To date, some studies have shown that the pathogenesis of cardiovascular diseases such as atherosclerosis, myocardial infarction, and heart failure may relate to insufficient angiogenesis. EPA2 may block subcutaneous deposition of oxLDL proteins when treating mice with atherosclerosis. EPA2 has a protective effect on cardiac function in ischemia-induced injury by attenuating cardiomyocyte apoptosis and decreasing the endoplasmic reticulum stress in response to myocardial infarction injury [31]. EPA2 may promote angiogenesis and may be protective against cardiovascular disease, suggesting a potential role in vascular function [32]. However, excessive angiogenesis may promote the development of autoimmune diseases and tumors. In glioblastoma, EPA2 may lead to activation of the MAPK cascade response and result in altered expression of genes associated with cell proliferation [33]. Reduced EPA2 expression was effective in inhibiting the phosphorylation activation of the AKT/GSK-3b/FAK signaling pathway and regulating cell proliferation [14]. A study found that silencing EPA2 reduced cancer cell migration [13]. In addition, a study showed that EPA2 promotes endothelial cell migration and angiogenesis. SLE pathogenesis was related to angiogenesis. Thus, we discussed whether EPA2 may regulate HUVECs function. Moreover, our previous study found that GDF15 correlated with SLE pathogenesis, and GDF15 may induce angiogenesis [29]. Therefore, in this study, we also explored whether EPA2 plays a role in angiogenesis through regulating GDF15. The results showed that HUVECs transfected with EPA2 siRNA had reduced proliferation, migration, and tube-forming ability, which was enhanced by the addition of GDF15 recombinant protein. It suggests that EPA2 may be involved in angiogenesis through regulating GDF15.

There are some innovations in the study. First, this study explored the plasma levels of EPA2 in SLE patients for the first time, revealing the ability of EPA2 as a diagnostic biomarker for SLE. Moreover, the potential of EPA2 as a biomarker for SLE was further verified by analyzing the expression of EPA2 in PBMCs of SLE patients and another independent cohort discussing EPA2 plasma levels, which will help the early detection and diagnosis of SLE in the future. Second, the functional study of the association between EPA2 and SLE pathogenesis was explored by carrying out animal experiments, which will provide a basis for targeting EPA2 for the treatment of SLE in the future. Third, this study revealed the role of EPA2 in angiogenesis by regulating GDF15, which provides a preliminary basis for future elucidation of whether EPA2 is involved in lupus progression by affecting GDF15.

There are several limitations in this study. First, plasma EPA2 levels correlated with some clinical and laboratory characteristics of SLE patients, and functional studies are needed to investigate how EPA2 modulates these characteristics. Second, in vitro studies have shown that EPA2 may be involved in angiogenesis through regulating GDF15, but whether EPA2 is involved in the

development of lupus through regulating GDF15 in vivo needs to be confirmed. Third, multicenter studies are needed to confirm the potential of EPA2 as a biomarker for SLE.

In summary, our study suggests that EPA2 was associated with the pathogenesis of SLE, EPA2 may be a biomarker for SLE, and EPA2 may be involved in SLE development by regulating GDF15.

Author Contributions

Study conception and design: L.-Q.Y., Y.-Y.L., Y.-Q.W., S.-Y.F., W.-D.X., A.-F.H. Acquisition of data, analysis, and interpretation of data: L.-Q.Y., Y.-Y.L., Y.-Q.W., S.-Y.F., W.-D.X., A.-F.H. Drafting the article: L.-Q.Y., W.-D.X., A.-F.H. Final approval of the version of the article to be published: all authors, and that all authors agree to be accountable for all aspects of the work.

Acknowledgments

The authors have nothing to report.

Ethics Statement

Animal studies were approved by the Animal Ethics Committee of Southwest Medical University (swmu20240050). All animal housing and experiments were conducted in strict accordance with laboratory animal care and use regulations. Population studies were approved by the Ethics Committee of Affiliated Hospital of Southwest Medical University (KY2020180). We certify that the study was performed in accordance with the World Medical Association's Declaration of Helsinki.

Consent

This study was conducted by obtaining written informed consent from all participants.

Conflicts of Interest

The authors declare no conflicts of interest.

Data Availability Statement

The data that support the findings of this study are available from the corresponding author upon reasonable request.

References

1. W. D. Xu, Y. Y. Chen, X. Wang, et al., "Development and External Validation of a Prediction Model for Interstitial Lung Disease in Systemic Lupus Erythematosus Patients: A Cross-Sectional Study," *Seminars in Arthritis and Rheumatism* 69, no. 11 (2024): 152556, https://doi.org/10.1016/j.semarthrit.2024.152556.

2. Y. Y. Tang, L. C. Su, Z. Qin, et al., "Serum Globulin Trajectory Discovery and Prediction in Systemic Lupus Erythematosus: Results From a Real-World Observational Cohort Study," *International Journal of Rheumatic Diseases* 27, no. 8 (2024): e15278, https://doi.org/10.1111/1756-185X.15278.

3. G. Guzmán-Martínez, C. Marañón, and C. Y. T. E. D. R. I. B. L. E. S. Network, "Immune Mechanisms Associated With Cardiovascular Disease in Systemic Lupus Erythematosus: A Path to Potential Biomarkers," *Frontiers in Immunology* 7, no. 13 (2022): 974826, https://doi.org/10.3389/fimmu.2022.974826.

4. J. Frostegård, "Systemic Lupus Erythematosus and Cardiovascular Disease," *Journal of Internal Medicine* 293, no. 1 (2023): 48–62, https://doi.org/10.1111/joim.13557.

5. A. F. Huang, L. Zhou, and W. D. Xu, "The Causal Associations of Inflammatory Cytokines With Obesity and Systemic Lupus Erythematosus: A Mendelian Randomization Study," *International Journal of Rheumatic Diseases* 27, no. 6 (2024): e15214, https://doi.org/10.1111/1756-185X.15214.

6. C. A. Odhams, A. L. Roberts, S. K. Vester, et al., "Interferon Inducible X-Linked Gene CXorf21 May Contribute to Sexual Dimorphism in Systemic Lupus Erythematosus," *Nature Communications* 10, no. 1 (2019): 2164, https://doi.org/10.1038/s41467-019-10106-2.

7. C. F. Kuo, M. J. Grainge, A. M. Valdes, et al., "Familial Aggregation of Systemic Lupus Erythematosus and Coaggregation of Autoimmune Diseases in Affected Families," *JAMA Internal Medicine* 175, no. 9 (2015): 1518–1526, https://doi.org/10.1001/jamainternmed.2015.3528.

8. J. A. Ross, Y. Chen, J. Müller, et al., "Dimeric Endophilin A2 Stimulates Assembly and GTPase Activity of Dynamin 2," *Biophysical Journal* 100, no. 3 (2011): 729–737, https://doi.org/10.1016/j.bpj.2010.12.3717.

9. J. Zhang, M. Tan, Y. Yin, et al., "Distinct Functions of Endophilin Isoforms in Synaptic Vesicle Endocytosis," *Neural Plasticity* 2015 (2015): 371496, https://doi.org/10.1155/2015/371496.

10. J. Li, B. Barylko, J. P. Eichorst, J. D. Mueller, J. P. Albanesi, and Y. Chen, "Association of Endophilin B1 With Cytoplasmic Vesicles," *Biophysical Journal* 111, no. 3 (2016): 565–576, https://doi.org/10.1016/j.bpj.2016.06.017.

11. Y. Liu, H. Q. Liu, J. Y. Xiao, et al., "Autophagy Is Involved in the Protective Effect of Endophilin A2 on H_2O_2-Induced Apoptosis in H9C2 Cardiomyocytes," *Biochemical and Biophysical Research Communications* 499, no. 2 (2018): 299–306, https://doi.org/10.1016/j.bbrc.2018.03.151.

12. H. Guan, P. Zhao, Z. Dai, X. Liu, and X. Wang, "SH3GL1 Inhibition Reverses Multidrug Resistance in Colorectal Cancer Cells by Downregulation of MDR1/P-Glycoprotein via EGFR/ERK/AP-1 Pathway," *Tumour Biology* 37, no. 9 (2016): 12153–12160, https://doi.org/10.1007/s13277-016-5092-0.

13. T. Baldassarre, P. Truesdell, and A. W. Craig, "Endophilin A2 Promotes HER2 Internalization and Sensitivity to Trastuzumab-Based Therapy in HER2-Positive Breast Cancers," *Breast Cancer Research* 19, no. 1 (2017): 110, https://doi.org/10.1186/s13058-017-0900-z.

14. E. Q. Li and J. L. Zhang, "Essential Role of SH3GL1 in Interleukin-6(IL-6)- and Vascular Endothelial Growth Factor (VEGF)-Triggered p130^{cas}-Mediated Proliferation and Migration of Osteosarcoma Cells," *Human Cell* 30, no. 4 (2017): 300–310, https://doi.org/10.1007/s13577-017-0178-6.

15. U. Norin, C. Rintisch, L. Meng, et al., "Endophilin A2 Deficiency Protects Rodents From Autoimmune Arthritis by Modulating T Cell Activation," *Nature Communications* 12, no. 1 (2021): 610, https://doi.org/10.1038/s41467-020-20586-2.

16. T. Yang, J. Z. Xu, Q. Z. Jia, et al., "Comparative Analysis of Sequence Alignment of SH3GL1 Gene as a Disease Candidate Gene of Adolescent Idiopathic Scoliosis," *Zhonghua Wai Ke Za Zhi* 48, no. 6 (2010): 435–438.

17. T. Yang, Q. Jia, H. Guo, et al., "Epidemiological Survey of Idiopathic Scoliosis and Sequence Alignment Analysis of Multiple Candidate Genes," *International Orthopaedics* 36, no. 6 (2012): 1307–1314, https://doi.org/10.1007/s00264-011-1419-z.

18. G. Genet, K. Boyé, T. Mathivet, et al., "Endophilin-A2 Dependent VEGFR2 Endocytosis Promotes Sprouting Angiogenesis," *Nature Communications* 10, no. 1 (2019): 2350, https://doi.org/10.1038/s41467-019-10359-x.

19. W. D. Xu, Q. Huang, C. Yang, R. Li, and A. F. Huang, "GDF-15: A Potential Biomarker and Therapeutic Target in Systemic Lupus Erythematosus," *Frontiers in Immunology* 13 (2022): 926373, https://doi.org/10.3389/fimmu.2022.926373.

20. S. Wang, M. Li, W. Zhang, et al., "Growth Differentiation Factor 15 Promotes Blood Vessel Growth by Stimulating Cell Cycle Progression

in Repair of Critical-Sized Calvarial Defect," *Scientific Reports* 7, no. 1 (2017): 9027, https://doi.org/10.1038/s41598-017-09210-4.

21. G. A. Bonaterra, N. Struck, S. Zuegel, et al., "Characterization of Atherosclerotic Plaques in Blood Vessels With Low Oxygenated Blood and Blood Pressure (Pulmonary Trunk): Role of Growth Differentiation Factor-15 (GDF-15)," *BMC Cardiovascular Disorders* 21, no. 1 (2021): 601, https://doi.org/10.1186/s12872-021-02420-9.

22. R. S. Lodi, B. Yu, L. Xia, and F. Liu, "Roles and Regulation of Growth Differentiation Factor-15 in the Immune and Tumor Microenvironment," *Human Immunology* 82, no. 12 (2021): 937–944, https://doi.org/10.1016/j.humimm.2021.06.007.

23. J. Wang, L. Wei, X. Yang, and J. Zhong, "Roles of Growth Differentiation Factor 15 in Atherosclerosis and Coronary Artery Disease," *Journal of the American Heart Association* 8, no. 17 (2019): e012826, https://doi.org/10.1161/JAHA.119.012826.

24. C. Yang, R. Li, L. C. Su, et al., "SHP2: Its Association and Roles in Systemic Lupus Erythematosus," *Inflammation Research* 72, no. 7 (2023): 1501–1512, https://doi.org/10.1007/s00011-023-01760-w.

25. P. Zhou, L. Yang, H. Li, et al., "IRG1/Itaconate Inhibits Hepatic Stellate Cells Ferroptosis and Attenuates TAA-Induced Liver Fibrosis by Regulating SLC39A14 Expression," *International Immunopharmacology* 146 (2025): 113945, https://doi.org/10.1016/j.intimp.2024.113945.

26. A. N. McShane and D. Malinova, "The Ins and Outs of Antigen Uptake in B Cells," *Frontiers in Immunology* 13 (2022): 892169, https://doi.org/10.3389/fimmu.2022.892169.

27. D. Malinova, L. Wasim, R. Newman, A. Martínez-Riaño, N. Engels, and P. Tolar, "Endophilin A2 Regulates B-Cell Endocytosis and Is Required for Germinal Center and Humoral Responses," *EMBO Reports* 22, no. 9 (2021): e51328, https://doi.org/10.15252/embr.202051328.

28. L. Q. Yang, A. F. Huang, and W. D. Xu, "Biology of Endophilin and It's Role in Disease," *Frontiers in Immunology* 14 (2023): 1297506, https://doi.org/10.3389/fimmu.2023.1297506.

29. A. A. Alfadda, R. M. Sallam, R. Gul, I. Hwang, and S. Ka, "Endophilin A2: A Potential Link to Adiposity and Beyond," *Molecules and Cells* 40, no. 11 (2017): 855–863, https://doi.org/10.14348/molcells.2017.0137.

30. M. Nakamura and N. Watanabe, "Ubiquitin-Like Protein MNSFβ/Endophilin II Complex Regulates Dectin-1-Mediated Phagocytosis and Inflammatory Responses in Macrophages," *Biochemical and Biophysical Research Communications* 401, no. 2 (2010): 257–261, https://doi.org/10.1016/j.bbrc.2010.09.045.

31. Y. Liu, R. Hu, H. Shen, et al., "Endophilin A2-Mediated Alleviation of Endoplasmic Reticulum Stress-Induced Cardiac Injury Involves the Suppression of ERO1α/IP$_3$R Signaling Pathway," *International Journal of Biological Sciences* 17, no. 13 (2021): 3672–3688, https://doi.org/10.7150/ijbs.60110.

32. X. Y. Liu, P. Li, X. S. Li, T. Simoncini, and Y. Cheng, "17β-Estradiol Nongenomically Induces Vasodilation Is Enhanced by Promoting Phosphorylation of Endophilin A2," *Gynecological Endocrinology* 38, no. 8 (2022): 644–650, https://doi.org/10.1080/09513590.2022.2088731.

33. T. Matsutani, T. Hiwasa, M. Takiguchi, et al., "Autologous Antibody to Src-Homology 3-Domain GRB2-Like 1 Specifically Increases in the Sera of Patients With Low-Grade Gliomas," *Journal of Experimental & Clinical Cancer Research* 31, no. 1 (2012): 85, https://doi.org/10.1186/1756-9966-31-85.

Supporting Information

Additional supporting information can be found online in the Supporting Information section.

| ORIGINAL ARTICLE

Modulation of Wnt/β-Catenin Signaling by STAT3 Inhibition Restores Myogenic Capacity in Sarcopenia

Suhong Zhang[1] | Xin Tao[1] | Minghui Fu[2] | Yue Li[1] | Gongbing Tu[1] | Dianfu Zhang[1] | Liping Yin[1] 🆔

[1]Department of Geriatrics, Nanjing Lishui People's Hospital, Zhongda Hospital Lishui Branch, Southeast University, Nanjing, Jiangsu, China | [2]Department of Orthopedics, Nanjing Lishui People's Hospital, Zhongda Hospital Lishui Branch, Southeast University, Nanjing, Jiangsu, China

Correspondence: Liping Yin (lipingyin168@163.com)

ABSTRACT

Background: Sarcopenia is a progressive disorder characterized by loss of skeletal muscle mass, strength, and function. Although STAT3 is known to regulate myogenic differentiation, its role in sarcopenia remains unclear.

Methods: STAT3 expression was assessed in skeletal muscle samples from sarcopenia patients and nonsarcopenic controls, as well as aged SAMP8 mice. C2C12 myoblasts were used to investigate the effects of STAT3 on proliferation and myogenic differentiation using gain- and loss-of-function approaches. The role of the Wnt/β-catenin pathway was examined using pathway-specific assays. In vivo, siRNA-mediated STAT3 knockdown was performed in aged SAMP8 mice to evaluate effects on muscle phenotype and endurance.

Results: STAT3 expression was significantly upregulated in muscle tissues from sarcopenia patients and aged mice, correlating with increased expression of the atrophy marker MuRF-1. STAT3 levels also rose during C2C12 cell differentiation. STAT3 overexpression suppressed C2C12 proliferation and myogenic differentiation, whereas knockdown enhanced both processes. Mechanistically, STAT3 inhibited Wnt/β-catenin signaling, reducing the expression of myogenic markers. In vivo, STAT3 silencing in aged mice increased muscle mass, improved treadmill performance, and decreased muscle atrophy markers.

Conclusion: STAT3 impairs myogenic proliferation and differentiation by negatively regulating the Wnt/β-catenin pathway, contributing to sarcopenia progression. Targeting STAT3 may serve as a promising therapeutic strategy for restoring muscle regeneration and function in sarcopenia.

1 | Introduction

Sarcopenia is a disorder caused by a persistent loss of weight, mass, and function of skeletal muscle. Clinical manifestations include decreased muscle strength, susceptibility to fatigue and falls, increased bone risk, and in severe cases, organ function can be involved, leading to cardiac and respiratory failure and even death [1, 2]. Aging, chronic diseases, and neurological damage are all contributing factors to sarcopenia [3, 4]. Approximately 50 million individuals globally are believed to suffer from sarcopenia, and this figure is expected to rise significantly as society ages, with projections suggesting that the number of people with sarcopenia could reach up to 500 million by 2050 [5]. Therefore, the pathogenesis and management of sarcopenia have attracted worldwide

---

Suhong Zhang and Xin Tao contributed equally to this study.

---

attention and research. Currently, there are various pathogenic mechanisms of sarcopenia, including reduced function of myosatellite cells, chronic inflammation, decreased function of nerves innervating skeletal muscle, oxidative stress, loss of mitochondrial function, and abnormal axis [6, 7]. Studies have provided evidence of progressive skeletal muscle loss because of aging. Aging causes a decline in the number of fast-twitch muscle fibers and satellite cells, which in turn leads to an imbalance in muscle homeostasis and impaired tissue regeneration [8]. Studies on the mechanisms of skeletal muscle cell proliferation and differentiation have revealed that once the skeletal muscle is stimulated by injury, myosatellite cells, which are in control of skeletal muscle maintenance, are activated to produce a large number of myogenic cells, which are called myoblasts [9]. These myogenic cells, which fuse to form new myotubes or merge with broken myotubes to reconstruct the myotube structure, participate in injury repair. The C2C12 mouse myoblast cell line was chosen as an in vitro model to examine the molecular pathways at play due to its established ability to develop into muscle cells. Consequently, examining the regulatory mechanisms that affect C2C12 cell growth and differentiation provides valuable understanding for enhancing muscle regeneration and addressing issues such as sarcopenia.

Signal Transducer and Activator of Transcription (STAT) is a fundamental pathway for growth factor and cytokine signaling, and STAT3 is an important component of the STAT family. STAT3 has been demonstrated to impede the myogenic differentiation of adult myoblasts [10]. Steyn et al. revealed that IL-6 induces myogenic differentiation of myoblasts through activation of JAK2-STAT3 signaling [11]. In contrast, Liu et al. indicated that glucosamine-induced endoplasmic reticulum stress negatively impacts myoblast differentiation by reducing STAT3 protein synthesis [12]. A recent study also identified STAT3 as notably elevated in sarcopenia and suggested it as a key regulatory gene [13]. STAT3′s role in muscle biology is complex; while it can stimulate muscle regeneration through satellite cell activation and improved mitochondrial activity, its excessive activation has been associated with muscle atrophy and fibrosis [13]. This duality underscores the necessity for precise mechanistic clarification of STAT3′s role specifically in sarcopenia, where regulation of muscle regeneration processes is crucial yet poorly understood. Thus, exploring STAT3's regulatory mechanisms in this context could reveal significant therapeutic opportunities. Additionally, the Wnt/β-catenin signaling pathway is considered pivotal in regulating muscle cell differentiation and regeneration [14, 15]. However, how STAT3 interacts with this pathway in the context of sarcopenia remains unclear. Therefore, this study aims to elucidate how STAT3 influences growth and differentiation of myoblasts specifically through its involvement with the Wnt/β-catenin signaling pathway. Utilizing both C2C12 cells and aged SAMP8 mice, we assess whether inhibiting STAT3 may enhance muscle regeneration, indicating its possible role as a therapeutic target for addressing sarcopenia.

2 | Methods

2.1 | Clinical Tissue

Muscle samples (quadriceps and skeletal muscle) were obtained via needle biopsy under local anesthesia from patients at Suzhou Municipal Hospital including six sarcopenia (aged ≥ 60 years)

(aged ≥ 60, mean age 68.6 ± 5.2 years, three males and three females) diagnosed according to the European Working Group on Sarcopenia in Older People 2019 (EWGSOP2) criteria [2] and six age-matched nonsarcopenia controls (mean age 67.8 ± 4.9 years, three males and three females). The exclusion criteria comprised neuromuscular illnesses, metabolic conditions, recent significant surgery or trauma, the use of corticosteroids, and inflammatory myopathies. The muscle tissue samples were biopsy-confirmed, and the study was granted approval by Joint Ethics Committee of the Ministry of Health and Suzhou Municipal Hospital (SMH-2024-021). The study was conducted following the Helsinki guidelines.

2.2 | Animal Study

Three- and 24-month-old male SAMP8 mice were obtained from GemPharmatech and allowed to acclimate for 1 week in standard conditions ($22°C \pm 2°C$, 12-h light/dark cycle). Five mice from each age category were euthanized, and the gastrocnemius (GA) muscle was removed for quantitative analysis. Twenty-four-month-old mice were divided into control (AAV9-NC) and experimental (AAV9-sh-STAT3) groups ($n = 5$ per group), receiving intraperitoneal injections of viral vectors (3×10^6 particles per mouse). The control vector (AAV9-NC) contained a scrambled shRNA sequence as a negative control. AAV9-shRNA and AAV9-sh-STAT3 were prepared as previously described [16]. Locomotor activity was tracked for 2 months postinjection. At endpoint, GA muscles were collected for qRT-PCR, Western blot, and histopathological analyses including H&E and Masson staining. Animal procedures were approved by Suzhou Municipal Hospital (SMH-2024-[A]154) and adhered to ARRIVE guidelines. Detailed reagents and kit information are available in Supplementary Table S1.

2.3 | Myoblast Culture and Differentiation

C2C12, a murine myoblast cell line acquired from ATCC, was cultured in a DMEM + FBS (10%) medium. Cells were evenly distributed 24 h before induction in a six-well plate. After they attained approximately 80% confluency, the cells were washed and transferred to another medium (DMEM + horse serum), which was changed every 48 h. In addition, cells in the STAT3 group or sh-STAT3 group were cultured in medium (DMEM + horse serum) containing the Wnt/β-catenin pathway activator LiCl (20 mmol/L) or the Wnt/β-catenin pathway inhibitor IWP2 (10 μM) for 48 h, respectively. Cells were harvested at days 0–5 to analyze STAT3 expression. Additionally, proliferation assays (CCK-8 and EdU) and myogenic differentiation markers (MyoG, MyoD1, MyHC) were assessed via Western blot. Detailed reagents and kit information are provided in Table S1.

2.4 | Lentiviral Preparation and Cellular Lipid Transfection

For STAT3 overexpression, the full-length STAT3 coding sequence was amplified and subsequently cloned into the pcDNA3.1 expression vector. For STAT3 knockdown, short

hairpin RNA (shRNA) sequences specifically targeting STAT3 were synthesized and cloned into the lentiviral vector pLentiGuide-Puro. Lentiviruses were packaged by cotransfecting HEK293T cells with the pLentiGuide-Puro vectors (containing either STAT3-specific or control shRNA sequences), along with the packaging plasmids PsPAX2 (2.2 µg) and the envelope plasmid pMD2.G (3 µg), using Lipofectamine 3000 transfection reagent (Invitrogen). The lentivirus was collected after 48 h for transducing C2C12 cells, filtered, and used to transduce C2C12 cells in the presence of 8 µg/mL polybrene. Cells were incubated with the lentiviral solution for 24 h before replacement with fresh growth medium. Successful overexpression or knockdown was confirmed using qRT-PCR and Western blot. Detailed primer and shRNA sequences are provided in Table S1.

2.5 | CCK-8 Assay

Cells transfected with different vectors were inoculated into 24-well plate medium (1×10^3 cells/well). After incubation for 4 days, 10% (v/v) CCK-8 reagent (Dojindo Laboratories, Kumamoto, Japan) was added to the culture medium, followed by incubation at 37°C for 4 h to infer cell viability. The OD value was determined at 450 nm using a microplate reader.

2.6 | EDU Assay

C2C12 cells transfected with different vectors were seeded onto sterile glass coverslips placed in 24-well plates and cultured to approximately 70%–80% confluency. Cells underwent treatment with EdU (10 µM) at 37°C for a duration of 2 h followed by fixation and permeabilization using paraformaldehyde and Triton-X (0.3%), respectively. Staining was done as mentioned in the kit. EdU-positive cells were quantified using a fluorescence microscope.

2.7 | Quantitative Real-Time PCR

Total RNA was isolated from quadriceps and skeletal muscles of patients and controls, GA muscles of SAMP8 mice, and C2C12 cells using TRIzol reagent. After cDNA synthesis, the target gene (STAT3) was amplified using a real-time quantitative PCR instrument. Gene expression was detected by $2^{\Delta\Delta C_t}$ and normalized to GAPDH. Table S1 mentions the used primer sequences.

2.8 | Western Blotting

Total protein was extracted from ground muscle tissues or C2C12 cell precipitates using PMSF prespiked with RIPA lysate. Proteins were denatured and separated using polyacrylamide microgels, shifted to nitrocellulose membranes, and then blocked with BSA (5%). Antibodies were added for incubation, color development reagents were added, and the membrane was then placed on an imaging system to properly display the bands. Table S2 mentions all the primary and secondary antibodies.

2.9 | Nucleocytoplasmic Separation

The nucleus and cytoplasm of C2C12 cells were separated using the Nucleoplasmic Separation and Extraction Kit. The distribution of β-catenin mRNA in the nuclear and cytoplasmic fractions was determined using qRT-PCR.

2.10 | Dual Luciferase Assay

C2C12 cells were cotransfected with either STAT3 overexpression or knockdown constructs (vector/STAT3 or sh-NC/sh-STAT3) along with TOPFlash or FOPFlash luciferase reporter plasmids using Lipofectamine 3000 (Invitrogen). After cell lysis, the GloMax 20/20 luminometer (Promega) was used to record the luciferase activity. The comparative luciferase activity was used to evaluate Wnt/β-catenin signaling activity. All transfections were performed in triplicate.

2.11 | Tests of Endurance Athletic Ability

The mice's locomoter capabilities were evaluated on a treadmill as previously described [17]. On the first day, mice began at 0 cm/s for 5 min, followed by running at 10 cm/s for another 5 min. On the second day, the treadmill's incline was adjusted to 5%, and the speed was increased by 13% every 2 min until the mice reached exhaustion. Exhaustion was characterized by a lack of movement in the hind limbs on the treadmill for more than 10 s. Data on running speed, distance, and time to exhaustion was recorded. Muscle strength was assessed with a grip strength meter. Mice were permitted to clutch the grid, and the maximum tension was documented during forelimb pulling. Every mouse was subjected to three trials, and the average value was determined. Body weight was recorded prior to testing for comparison.

2.12 | Histopathological Analysis

Immediately after anesthesia, mouse GA tissues were removed, fixed with paraformaldehyde, paraffin embedded, and prepared into sections (4 µm). Then, H&E staining and Masson staining were performed as per standard protocol. The GA tissue structure and fibrosis were observed. Three fields of view were randomly selected under the microscope for each sample, and at least three samples in each group were selected for quantitative analysis of cross-sectional area (CSA, µm²) of muscle fibers and fiber area with Image J software, respectively.

2.13 | Immunofluorescence Staining

Formalin-fixed, paraffin-embedded tissue sections underwent antigen unmasking using alkaline urea buffer. After blocking, sections were incubated with a primary anti-STAT3 antibody followed by washing, incubation with a fluorophore-tagged secondary antibody, and nuclear staining for visualization using fluorescence microscope. Signal intensity was analyzed on ImageJ. Table S2 enlists the antibodies details.

2.14 | Statistical Analysis

SPSS version 21.0 and GraphPad Prism version 8 were used for statistical interpretation. Group comparisons were evaluated using either the Student *t*-test or one-way ANOVA. Results are shown as the mean ± standard deviation. Pearson correlation analysis was applied to assess the association between gene expression levels, considering *p*-value < 0.05 as statistically significant.

3 | Results

3.1 | STAT3 Was Upregulated in Muscle During Sarcopenia

STAT3 is a key gene in sarcopenia and a promising therapeutic target [13]. To investigate STAT3 expression in sarcopenia, we examined the levels of STAT3 and its phosphorylated form (p-STAT3) in the quadriceps and skeletal muscle of sarcopenic and nonsarcopenic patients. We found that both STAT3 and p-STAT3 were upregulated in sarcopenic patients (Figure 1A,B). Similarly, their expression was also increased in the muscles of SAMP8 mice, with higher levels in 24-month-old mice compared to 3-month-old mice (Figure 1C,D). These findings were

consistent with the expression pattern of MuRF-1, a known muscle atrophy marker, suggesting that STAT3 could serve as a promising diagnostic marker in sarcopenia. Furthermore, both STAT3 and p-STAT3 levels were increased in C2C12 cells after the second day of differentiation, with a progressive rise during the differentiation process (Figure 1E,F). Overall, the expression levels of both STAT3 and phosphorylated STAT3 were heightened in the muscle tissue of sarcopenic individuals, SAMP8 mice, and C2C12 cells as they undergo differentiation, suggesting its potential role in the progression of sarcopenia.

3.2 | STAT3 Overexpression Impaired the Proliferation and Differentiation Potential of C2C12 Myoblasts

Next, STAT3 was overexpressed to observe the functional changes in C2C12 myoblasts. The STAT3 overexpression model was successfully constructed, and the biological changes of C2C12 cells were manifested in the reduction of cell viability and proliferation capacity (Figure 2A–D). The levels of Ki67 and PCNA proteins were notably reduced in the STAT3 model further demonstrating that STAT3 impeded the proliferation
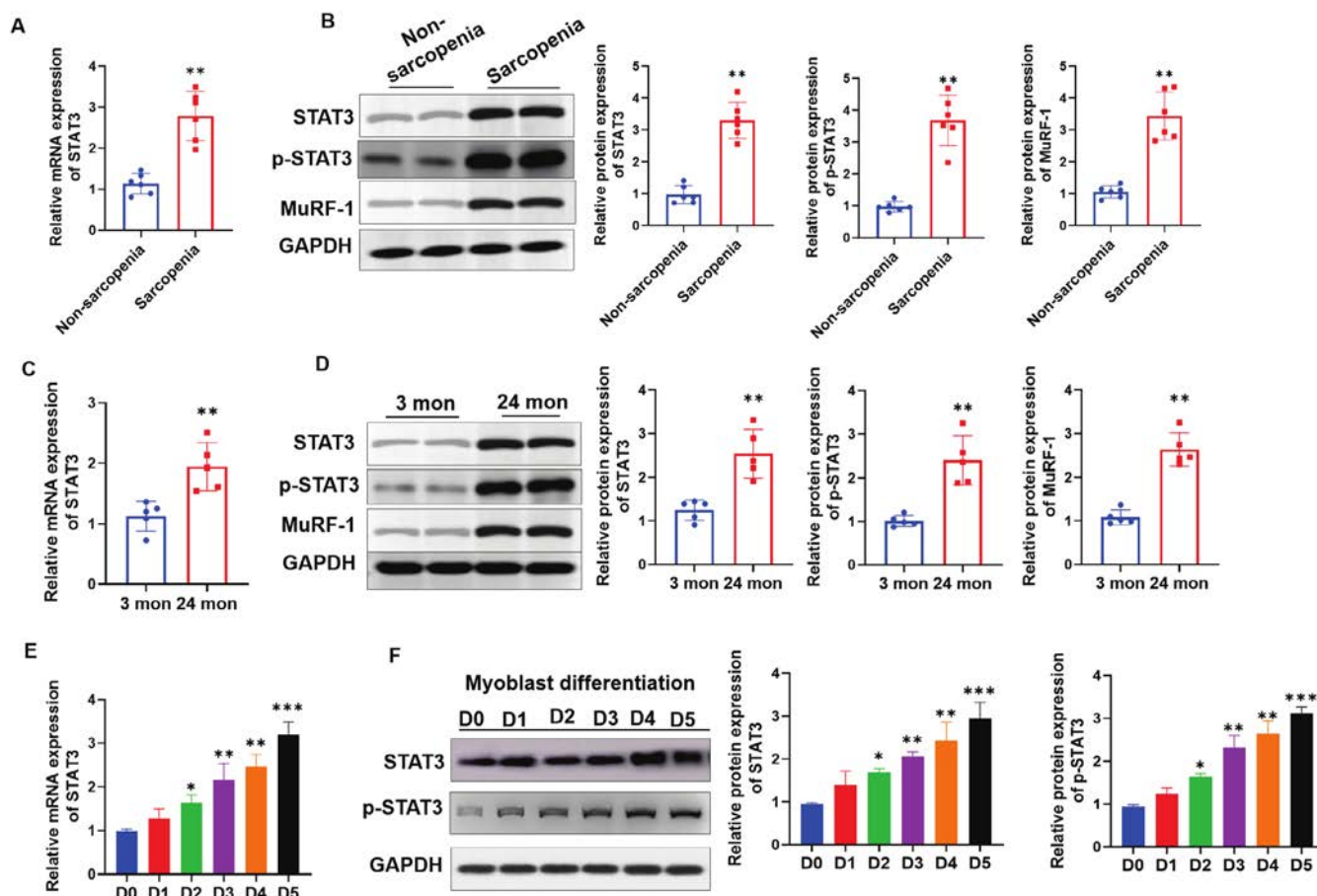
FIGURE 1 | STAT3 is upregulated in muscles during sarcopenia. (A) qPCR for mRNA levels of STAT3 in quadriceps muscle of sarcopenia and nonsarcopenia patients, *n* = 6. (B) Western blot for STAT3, p-STAT3 and MuRF-1 protein levels in sarcopenic and nonsarcopenic skeletal muscles, *n* = 6. (C) qPCR for mRNA levels of STAT3 in the muscle of 3 and 24 months old mice, *n* = 5. (D) Western blot for STAT3, p-STAT3 and MuRF-1 protein levels in the muscle of 3 and 24 months old mice, *n* = 5. (E, F) qPCR and Western blot examination of STAT3 and p-STAT3 levels during the cell differentiation of C2C12 cells from mouse adult myoblasts. *p < 0.05, **p < 0.01, ***p < 0.001.
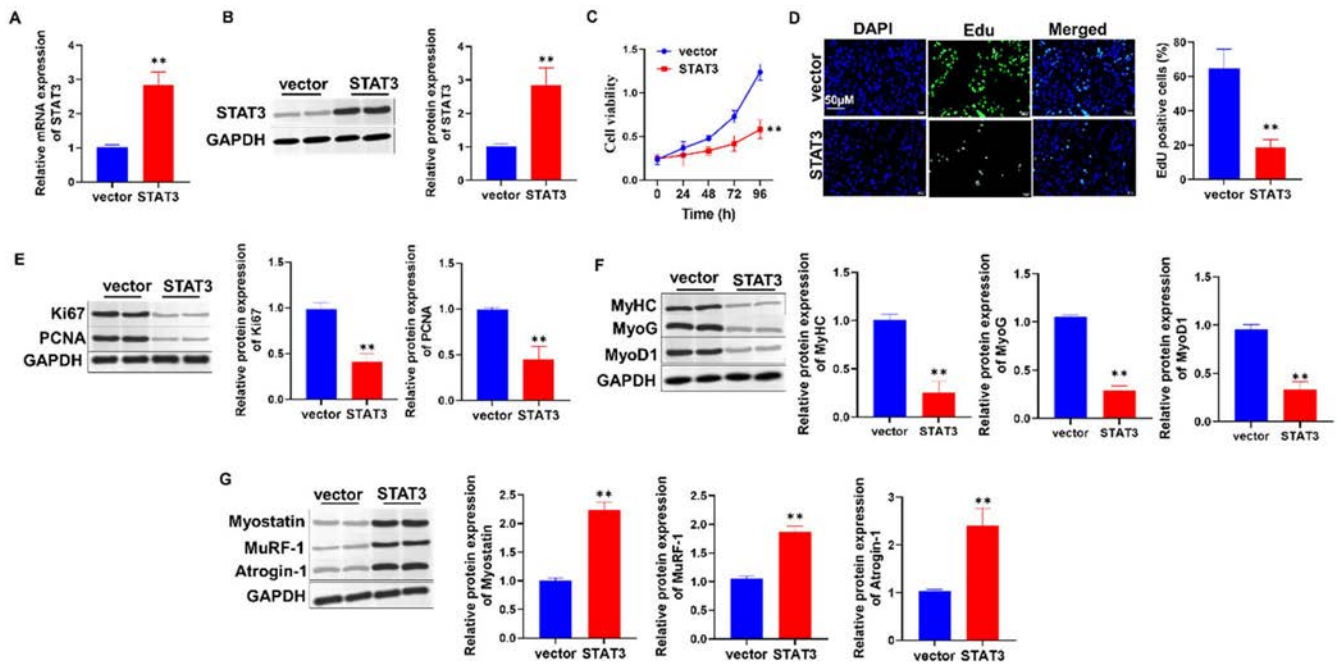
FIGURE 2 | STAT3 overexpression impaired the proliferation and differentiation potential of C2C12 myoblasts. (A, B) qPCR and Western blot to detect STAT3 overexpression effects. (C) CCK-8 determination of the effect of STAT3 overexpression on the cell proliferation of mouse adult myoblast C2C12 cells. (D) EdU determination of the influence of STAT3 overexpression on the proliferation of mouse adult myoblast C2C12 cells. (E) Western blot showing protein levels of proliferation-related proteins Ki67 and PCNA. (F) Western blot showing the protein expression levels of MyoG, MyoD1, and MyHC myogenic differentiation proteins. (G) The protein expression levels of muscle atrophy factors Atrogin-1, MuRF-1, and Myostatin were determined by Western blot. ** $p < 0.01$.

of C2C12 myoblasts (Figure 2E). In addition, myogenic differentiation has a vital part in muscle regeneration, and STAT3 inhibited the levels of myogenic differentiation proteins MyoG, MyoD1, and MyHC, suggesting that STAT3 hinders myogenic differentiation (Figure 2F). The levels of muscle atrophy factors Atrogin-1, MuRF-1, and Myostatin were notably upregulated by STAT3 further demonstrating that STAT3 worsens the progression of sarcopenia (Figure 2G). In short, elevated STAT3 levels exacerbated the progression of sarcopenia by inhibiting C2C12 myoblast proliferation, reducing their capacity to grow into muscle cells, and increasing muscle degeneration.
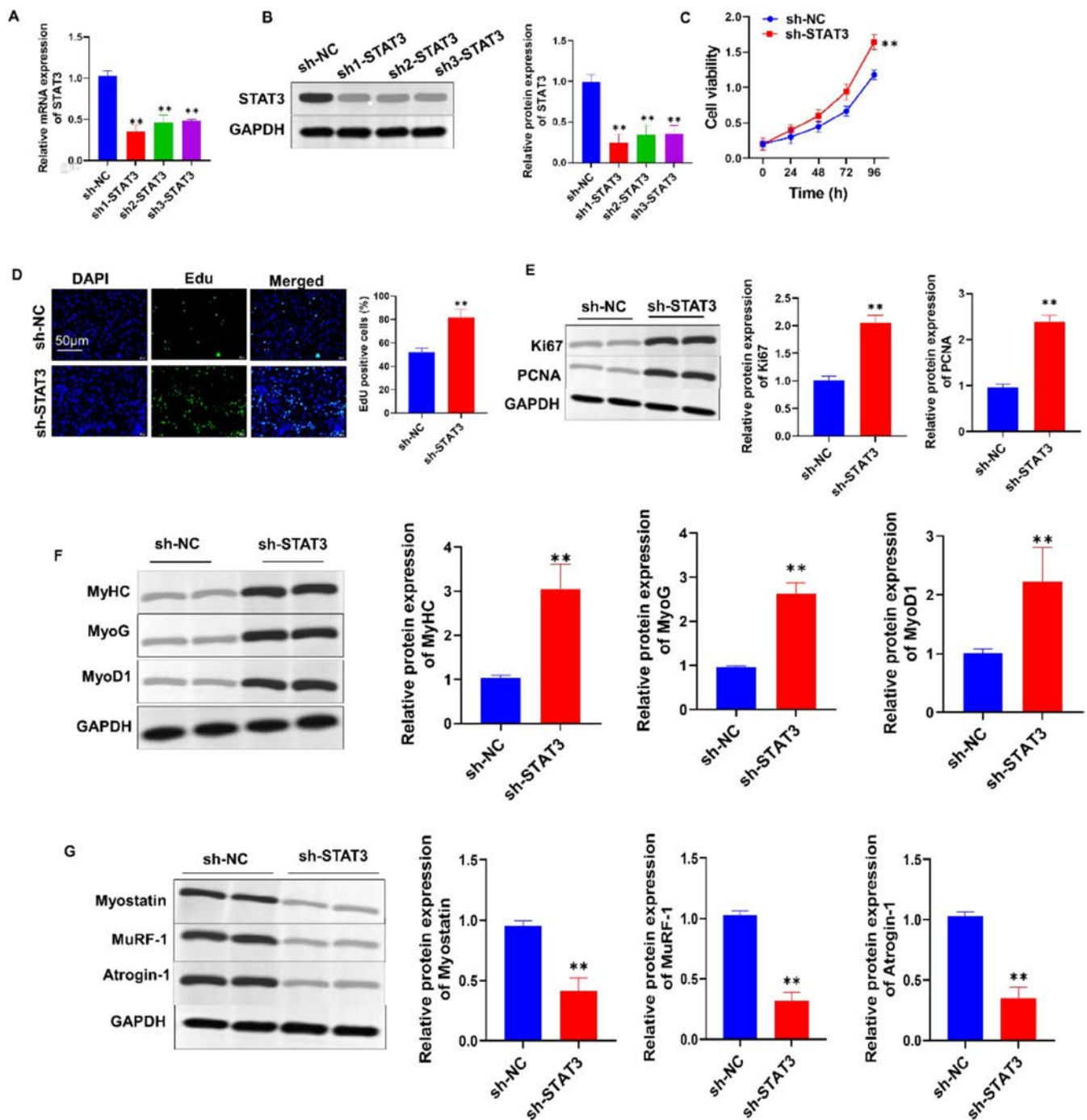
3.3 | STAT3 Deficiency Promoted Proliferation and Myogenic Differentiation of C2C12 Myoblasts

We next knocked out STAT3 to investigate the effect on proliferation and myogenic differentiation of C2C12 myoblasts. Three pairs of hairpin primers were designed for STAT3, and quantitative results revealed that all of them had a knockdown effect (Figure 3A). Among the three constructs, shRNA-1 showed the strongest knockdown and was used for most of the experiments. The cell viability and proliferation ability of C2C12 cells were notably enhanced after STAT3 knockdown (Figure 3B–D). The levels of Ki67 and PCNA proteins were also notably increased, further demonstrating that STAT3 deficiency promoted the proliferation of C2C12 cells (Figure 3E). The expression of muscle differentiation proteins MyoG, MyoD1, and MyHC was also notably elevated, indicating that STAT3 knockdown promoted

adult muscle differentiation (Figure 3F). In addition, the levels of muscle atrophy factors Atrogin-1, MuRF-1, and Myostatin were notably downregulated further demonstrating the potential therapeutic effect of STAT3 knockdown on sarcopenia (Figure 3G). In conclusion, reducing STAT3 levels promoted C2C12 myoblast proliferation, enhanced myogenic differentiation, and reduced muscle atrophy, implying that it has therapeutic capacity for sarcopenia.

3.4 | STAT3 Promoted the Progression of Sarcopenia by Modulating the Wnt/β-Catenin Pathway

Sufficient evidence suggested that the Wnt pathway activation leads to the production of satellite cells. However, the specific regulatory functions of Wnts in musculoskeletal diseases like sarcopenia are still being studied [14, 18]. Therefore, we initially hypothesized that STAT3 plays a regulatory role in sarcopenia through signaling of the Wnt/β-catenin pathway. The Wnt/β-Catenin pathway activity was measured using the TCF/LEF dual luciferase reporter gene, and knockdown of STAT3 enhanced luminescence signaling, whereas overexpression had the opposite effect (Figure 4A,B). Moreover, STAT3 knockdown upregulated the β-catenin phosphorylation. It upregulated the total β-catenin protein level, indicating that STAT3 knockdown suppressed the degradation of β-catenin, thereby increasing its protein levels and enhancing pathway activation (Figure 4C,D). Further detection of β-catenin protein in the cytoplasm and nucleus showed that the expression of this protein was notably elevated after STAT3 knockdown, confirming that STAT3 knockdown inhibited the β-catenin

FIGURE 3 | STAT3 deficiency promoted growth and differentiation of C2C12 myoblasts. (A, B) qPCR and Western blot to detect the knockdown effect of STAT3. (C) CCK-8 assay showing the effect of STAT3 knockdown on the proliferation of C2C12 cells in mouse myoblasts. (D) EdU determination of the effect of STAT3 knockdown on the growth of mouse adult myoblast C2C12 cells. (E) Western blot showing the protein levels of proliferation-related proteins Ki67 and PCNA. (F) Western blot was used to determine the protein expression levels of MyoG, MyoD1 and MyHC. (G) The protein expression levels of muscle atrophy markers Atrogin-1, MuRF-1, and Myostatin were determined by Western blot. **$p < 0.01$.

protein degradation, thereby enhancing the activity of the Wnt/β-catenin pathway (Figure 4E,F). In addition, we measured the protein levels of downstream target genes of the Wnt/β-catenin pathway, including Axin2, Cyclin D1, and LEF1, after STAT3 knockdown. The results showed that STAT3 knockdown significantly increased the protein levels of these targets (Figure 4G). To conclude, STAT3 inhibited the Wnt/β-catenin pathway, and reducing its expression increases β-catenin signaling activity.

3.5 | Activation of Wnt/β-Catenin Signaling-Mediated STAT3-Stimulated Myoblast Differentiation

To further confirm the role of Wnt/β-catenin signaling in STAT3-regulated myogenesis, we treated STAT3-overexpressing C2C12 cells with the Wnt activator LiCl and STAT3 knockdown cells with the Wnt inhibitor IWP2. LiCl restored the reduced
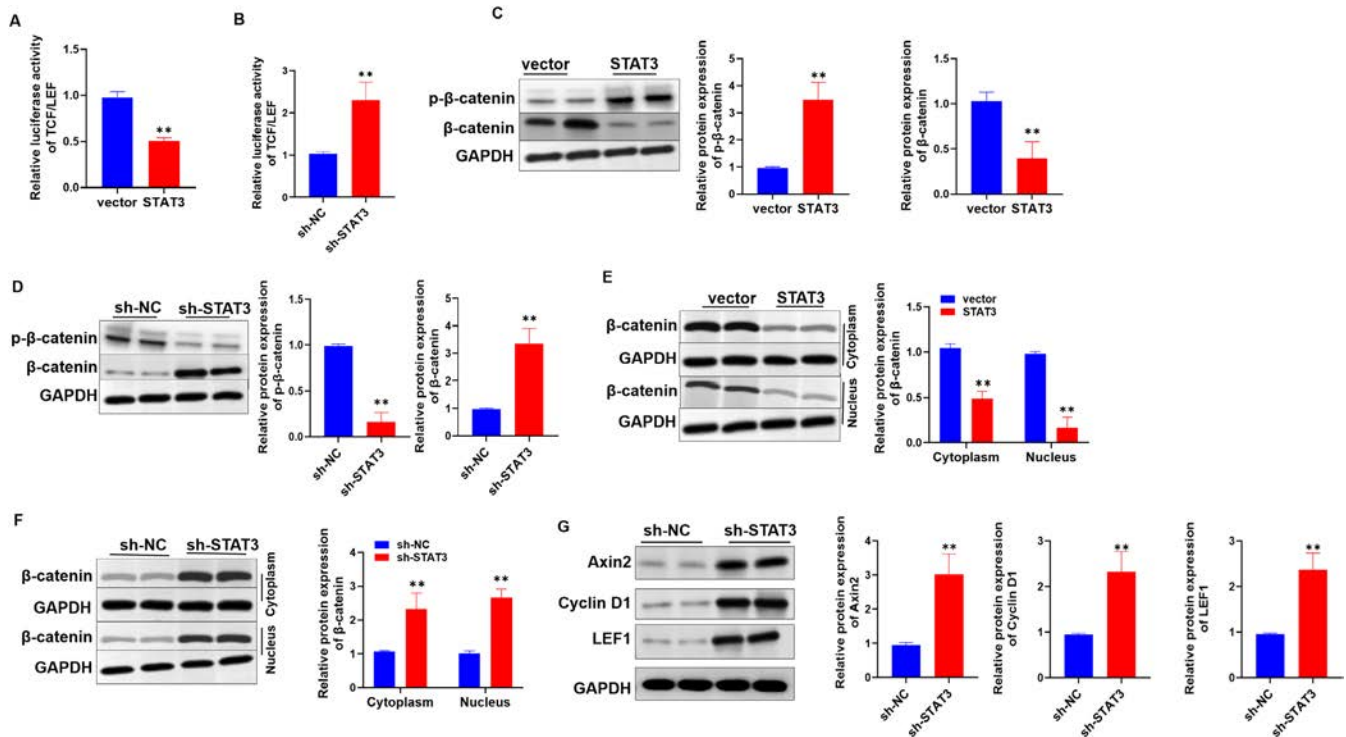
FIGURE 4 | STAT3 promoted the progression of sarcopenia by regulating the Wnt/β-catenin pathway. (A, B) TCF/LEF dual luciferase reporter gene assay system to assess Wnt pathway activity. (C, D) Western blot measurements of p-β-catenin and total β-catenin protein expression. (E, F) Western blot measurements of protein levels of β-catenin in the cytoplasm and nucleus. (G) Western blot measurements of protein levels of Axin2, Cyclin D1, and LEF1 after STAT3 silencing. **$p < 0.01$.

cell viability caused by STAT3 overexpression, while IWP2 suppressed the enhanced viability seen with STAT3 knockdown (Figure 5A,B). In addition, the levels of proliferation markers (Ki67 and PCNA) and β-catenin were decreased after STAT3 overexpression, but LiCl treatment reversed this decline (Figure 5C). Conversely, IWP2 blocked the increase in these markers caused by STAT3 knockdown (Figure 5D). Regarding myogenic differentiation, LiCl reversed the STAT3-induced downregulation of MyoG, MyoD1, and MyHC, while IWP2 blocked the upregulation of these markers following STAT3 knockdown (Figure 5E,F). These results showed that STAT3 suppressed Wnt/β-catenin activity, thereby impairing both proliferation and differentiation of myoblasts. Modulating Wnt signaling effectively reversed these effects, confirming that STAT3 exerted its function in sarcopenia at least in part through the Wnt pathway.

3.6 | STAT3 Silencing Enhanced Endurance Exercise Capacity and Muscle Mass in SAMP8 Aged Mice

To validate our findings in vivo, we used 24-month-old SAMP8 mice to assess whether STAT3 silencing could improve muscle performance and morphology. Following STAT3 knockdown, mice exhibited significant improvements in maximal running speed, total distance, time to fatigue, and grip strength, while body weight remained unchanged (Figure 6A–E). These results suggest that STAT3 silencing enhanced endurance capacity independent of body mass changes. Immunofluorescence analysis confirmed that

STAT3 expression was significantly reduced in GA muscles of the treated mice (Figure 6F). Consistent with in vitro findings, β-catenin protein levels were regulated, while muscle atrophy markers (Atrogin-1, MuRF-1, and Myostatin) were downregulated, supporting activation of the Wnt/β-catenin pathway in STAT3-silenced muscle (Figure 6G). Gross morphological observation revealed visibly larger GA muscles in STAT3 knockdown mice (Figure 6H). Histological analysis further showed an increase in muscle fiber CSA, indicating enhanced myofiber size and potential restoration of muscle function (Figure 6I,J). Additionally, the fibrotic area was reduced, suggesting improved muscle elasticity and reduced pathological remodeling (Figure 6K). Together, STAT3 silencing enhanced muscle quality and performance in aged mice, at least in part through Wnt/β-catenin signaling.

4 | Discussion

Sarcopenia is an increasingly recognized public health issue, with its prevention and management posing urgent clinical challenges. Past studies have demonstrated that promoting C2C12 myoblast differentiation supports muscle regeneration and offers therapeutic potential against sarcopenia [11]. In this study, we identified STAT3 as a critical modulator of myogenic proliferation and differentiation and explored its mechanistic role in the context of sarcopenia. While STAT3 is known to be activated in muscle-wasting conditions, its specific downstream effects remained unclear. Our findings provided evidence that STAT3 suppressed the Wnt/β-catenin pathway, thereby impairing muscle cell differentiation, and that STAT3 knockdown led
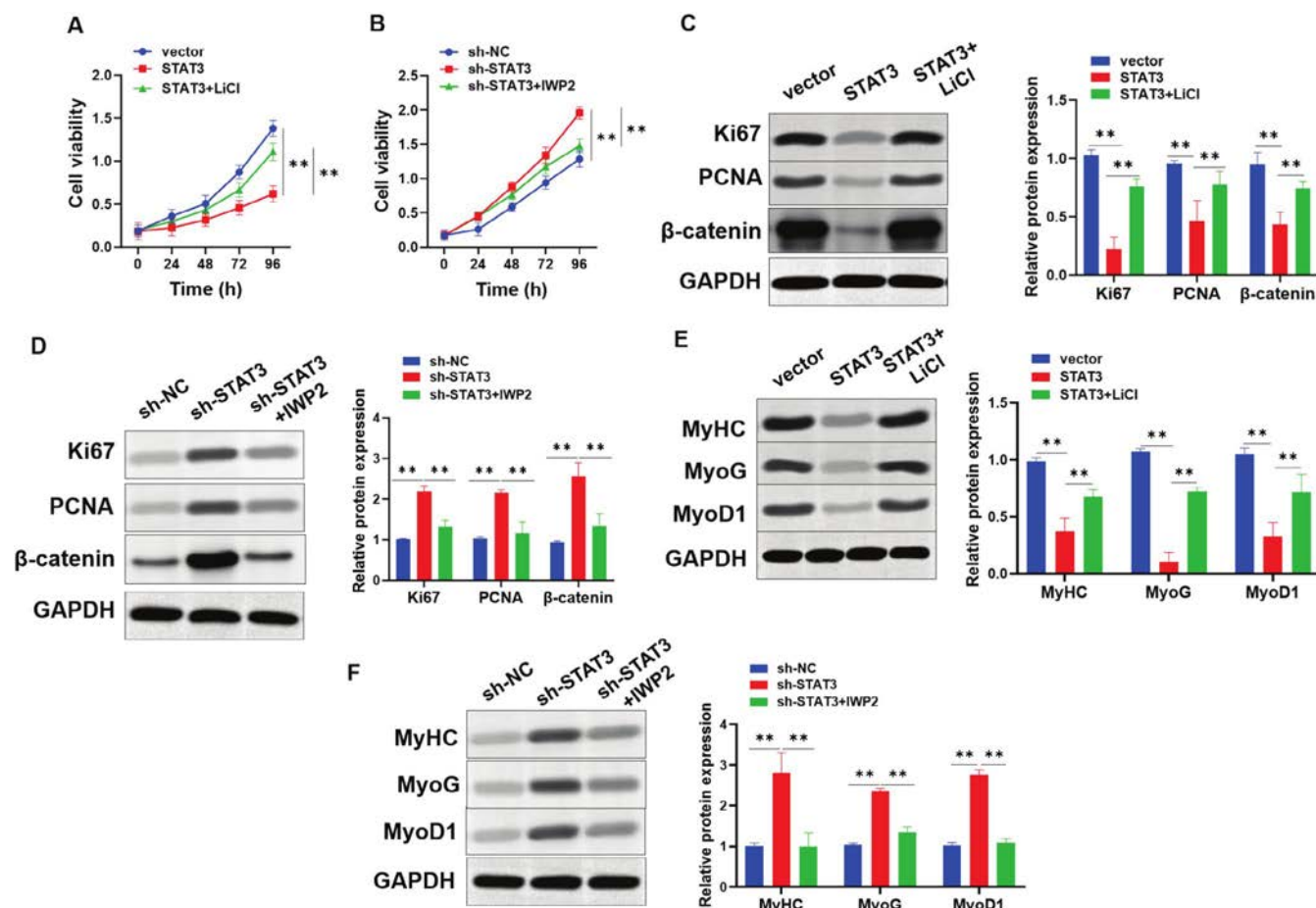
FIGURE 5 | Activation of Wnt/β-catenin signaling mediated STAT3-stimulated myoblast differentiation. (A, B) CCK-8 was used to determine the effects of STAT3, LiCl, and IWP2 on the proliferation of mouse adult myoblast C2C12 cells. (C, D) Western blot showing the effects of STAT3 and IWP2 on the protein levels of proliferation-related proteins Ki67, PCNA, and β-catenin. (E, F) Western blot to determine the effect of STAT3 knockdown and IWP2 on the protein expression levels of muscle differentiation proteins MyoG, MyoD1, and MyHC. **$p < 0.01$.

to functional improvements in muscle mass and endurance in aged SAMP8 mice.

Inflammatory cytokines, such as TNF-α, IL-6, and interferons, are increased in degenerative musculoskeletal disorders and are recognized for activating the JAK/STAT signaling pathway, which contributes to muscle wasting [19]. Notably, IL-6-mediated STAT3 phosphorylation has been proven to upregulate muscle wasting pathways [20]. STAT3 activation promotes MuRF1 and Atrogin-1 expression, thus causing protein breakdown and inhibiting myogenic signaling [21–23]. In our study, STAT3 knockdown resulted in downregulation of these atrophy markers and upregulation of MyoD, MyoG, and MyHC, indicating enhanced differentiation and reduced catabolism.

C2C12 cells are a standard in vitro model for skeletal muscle development. MyoD and MyoG are early differentiation markers, while MyHC expression peaks at later stages [24]. The observed increase in these factors upon STAT3 knockdown supports a role for STAT3 in negatively regulating myogenic progression. Maintaining the balance between differentiation and degradation is critical for preventing muscle loss, and targeting STAT3 offers a promising strategy to restore this balance.

The Wnt/β-catenin signaling pathway is a central regulator of muscle development and regeneration. β-catenin enhances MyoD transcriptional activity by promoting its interaction with E-box elements [25, 26]. The activation of this pathway drives myoblast fusion and myotube formation [27]. Our results confirmed that STAT3 suppressed Wnt/β-catenin signaling by limiting β-catenin accumulation and nuclear localization. Conversely, STAT3 knockdown led to β-catenin stabilization and nuclear translocation, thereby activating transcription of downstream myogenic targets. These findings were consistent with previous reports linking STAT3 to Wnt regulation in other disease contexts [28, 29].

Mechanistically, Wnt signaling is activated when β-catenin escapes proteasomal degradation by the Axin-APC-GSK3β destruction complex and accumulates in the nucleus to activate LEF/TCF-mediated transcription [30, 31]. Our in vitro and in vivo data supported this model, showing that STAT3 knockdown activated the Wnt pathway, improving muscle structure and function. These findings suggested that STAT3 was a critical upstream inhibitor of Wnt/β-catenin–mediated muscle regeneration.

Our study has some limitations. First, the sample size for human biopsies ($n = 6$ per group) is small, which may affect the strength of the results. Second, we did not explain in detail the specific regulatory mechanism by which STAT3 inhibits β-catenin. We suggest
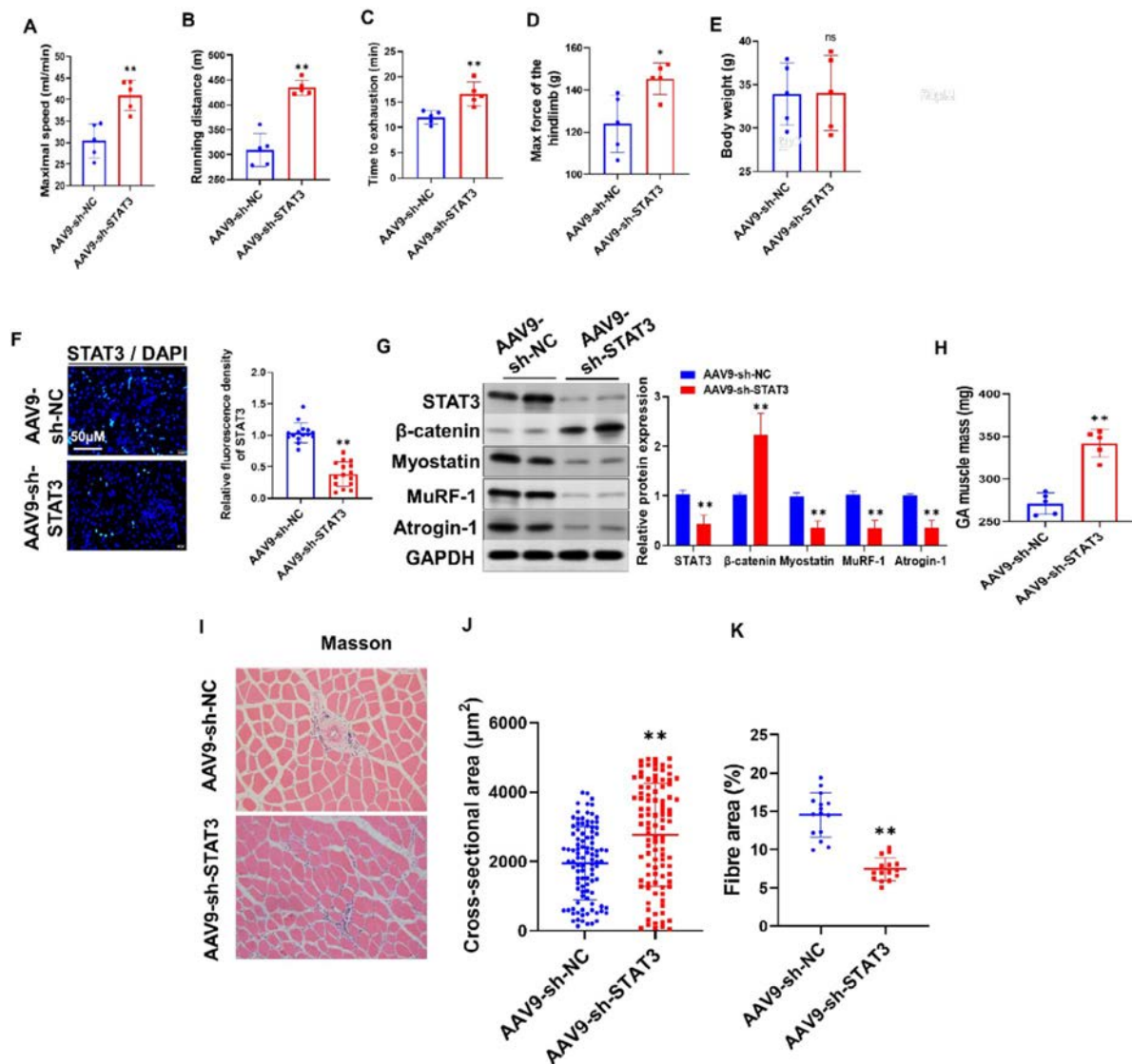
FIGURE 6 | STAT3 silencing enhanced endurance exercise capacity and muscle mass in SAMP8 aged mice. (A–E) Measurement of maximal running speed, distance, running-to-fatigue time, grip strength, and body weight in SAMP8 mice 2 months after STAT3 knockdown, $n = 5$. (F) IF staining to examine the fluorescence intensity of STAT3 in GA muscle tissue; three frames were selected for each sample. (G) Expression levels of STAT3, β-catenin, and muscle atrophy factors Atrogin-1, MuRF-1, and Myostatin in GA muscle of SAMP8 mice. (H) Representative images of GA muscle from AMP8 mice and quantitative results of muscle mass. (I) Schematic of H&E staining and Masson staining of GA muscle of AMP8 mice. (J) Quantitative results of muscle fiber CSA; 20 fibers were selected for each sample. (K) Quantitative results of fiber area; three frames were selected for each sample. ns $p > 0.05$, $*p < 0.05$, $**p < 0.01$.

this inhibition might involve interfering with β-catenin's binding to TCF/LEF transcription factors or affecting the transcription of downstream target genes [32]. Therefore, future research should include larger sample sizes and explore in more depth how STAT3 regulates the Wnt/β-catenin signaling pathway in sarcopenia.

In summary, our study identifies STAT3 as a key inhibitor of myogenic differentiation via Wnt/β-catenin signaling suppression. STAT3 knockdown elevates myogenic markers' expression, reduces atrophy-related proteins, and enhances muscle performance and mass in aged mice. These results show that STAT3 is a likely therapeutic target for sarcopenia. Future studies are needed to explore whether STAT3 may also influence myogenesis through additional signaling pathways beyond Wnt/β-catenin.

Author Contributions

S.Z. and X.T., study design, data acquisition, analysis, and manuscript drafting; M.F., patient recruitment, data interpretation; Y.L., G.T., and D.Z., in vivo, in vitro, and molecular assays; histological analysis and manuscript preparation; L.Y., supervision, critical revisions, and final manuscript draft. All authors read and approved the final version of the manuscript.

Conflicts of Interest

The authors declare no conflicts of interest.

Data Availability Statement

Data is available from the corresponding author upon request.

References

1. A. A. Damluji, M. Alfaraidhy, N. AlHajri, et al., "Sarcopenia and Cardiovascular Diseases," *Circulation* 147, no. 20 (2023): 1534–1553.

2. A. J. Cruz-Jentoft, G. Bahat, J. Bauer, et al., "Sarcopenia: Revised European Consensus on Definition and Diagnosis," *Age and Ageing* 48, no. 1 (2019): 16–31.

3. C. Coletti, G. F. Acosta, S. Keslacy, and D. Coletti, "Exercise-Mediated Reinnervation of Skeletal Muscle in Elderly People: An Update," *European Journal of Translational Myology* 32, no. 1 (2022): 10416.

4. K. A. Rygiel, M. Picard, and D. M. Turnbull, "The Ageing Neuromuscular System and Sarcopenia: A Mitochondrial Perspective," *Journal of Physiology* 594, no. 16 (2016): 4499–4512.

5. L. K. Chen, L. K. Liu, J. Woo, et al., "Sarcopenia in Asia: Consensus Report of the Asian Working Group for Sarcopenia," *Journal of the American Medical Directors Association* 15, no. 2 (2014): 95–101.

6. H. Nishikawa, S. Fukunishi, A. Asai, K. Yokohama, S. Nishiguchi, and K. Higuchi, "Pathophysiology and Mechanisms of Primary Sarcopenia (Review)," *International Journal of Molecular Medicine* 48, no. 2 (2021): 156.

7. Z. Zeng, J. Liang, L. Wu, H. Zhang, J. Lv, and N. Chen, "Exercise-Induced Autophagy Suppresses Sarcopenia Through Akt/mTOR and Akt/FoxO3a Signal Pathways and AMPK-Mediated Mitochondrial Quality Control," *Frontiers in Physiology* 11 (2020): 583478.

8. L. Larsson, H. Degens, M. Li, et al., "Sarcopenia: Aging-Related Loss of Muscle Mass and Function," *Physiological Reviews* 99, no. 1 (2019): 427–511.

9. A. S. Thooyamani and A. Mukhopadhyay, "PDGFRα Mediated Survival of Myofibroblasts Inhibit Satellite Cell Proliferation During Aberrant Regeneration of Lacerated Skeletal Muscle," *Scientific Reports* 11, no. 1 (2021): 63.

10. Y. Kataoka, I. Matsumura, S. Ezoe, et al., "Reciprocal Inhibition Between MyoD and STAT3 in the Regulation of Growth and Differentiation of Myoblasts," *Journal of Biological Chemistry* 278, no. 45 (2003): 44178–44187.

11. P. J. Steyn, K. Dzobo, R. I. Smith, and K. H. Myburgh, "Interleukin-6 Induces Myogenic Differentiation via JAK2-STAT3 Signaling in Mouse C2C12 Myoblast Cell Line and Primary Human Myoblasts," *International Journal of Molecular Sciences* 20, no. 21 (2019): 5273.

12. S. Y. Liu, L. K. Chen, Y. T. Chung, et al., "Glucosamine Inhibits Myoblast Proliferation and Differentiation, and Stimulates Myotube Atrophy Through Distinct Signal Pathways," *Journal of Nutritional Biochemistry* 135 (2025): 109762.

13. D. Liu, K. Wang, J. Wang, F. Cao, and L. Tao, "Identification of the Molecular Link: STAT3 Is a Shared Key Gene Linking Postmenopausal Osteoporosis and Sarcopenia," *Bone & Joint Research* 13, no. 8 (2024): 411–426.

14. W. Lin, S. K. H. Chow, C. Cui, et al., "Wnt/β-Catenin Signaling Pathway as an Important Mediator in Muscle and Bone Crosstalk: A Systematic Review," *Journal of Orthopaedic Translation* 47 (2024): 63–73.

15. L. Hu, W. Chen, A. Qian, and Y. P. Li, "Wnt/β-Catenin Signaling Components and Mechanisms in Bone Formation, Homeostasis, and Disease," *Bone Research* 12, no. 1 (2024): 39.

16. S. Zolotukhin, M. Potter, I. Zolotukhin, et al., "Production and Purification of Serotype 1, 2, and 5 Recombinant Adeno-Associated Viral Vectors," *Methods* 28, no. 2 (2002): 158–167.

17. X. Chen, Y. Zhang, Z. Deng, et al., "Keratocan Improves Muscle Wasting in Sarcopenia by Promoting Skeletal Muscle Development and Fast-Twitch Fibre Synthesis," *Journal of Cachexia, Sarcopenia and Muscle* 16, no. 1 (2025): e13724.

18. J. Wu, P. Ding, H. Wu, et al., "Sarcopenia: Molecular Regulatory Network for Loss of Muscle Mass and Function," *Frontiers in Nutrition* 10 (2023): 1037200.

19. X. Hu, J. li, M. Fu, X. Zhao, and W. Wang, "The JAK/STAT Signaling Pathway: From Bench to Clinic," *Signal Transduction and Targeted Therapy* 6, no. 1 (2021): 402.

20. F. Haddad, F. Zaldivar, D. M. Cooper, and G. R. Adams, "IL-6-Induced Skeletal Muscle Atrophy," *Journal of Applied Physiology (1985)* 98, no. 3 (2005): 911–917.

21. L. Zanders, M. Kny, A. Hahn, et al., "Sepsis Induces Interleukin 6, gp130/JAK2/STAT3, and Muscle Wasting," *Journal of Cachexia, Sarcopenia and Muscle* 13, no. 1 (2022): 713–727.

22. J. Aravena, J. Abrigo, F. Gonzalez, et al., "Angiotensin (1–7) Decreases Myostatin-Induced NF-κB Signaling and Skeletal Muscle Atrophy," *International Journal of Molecular Sciences* 21, no. 3 (2020): 1167.

23. M. Nowak, B. Suenkel, P. Porras, et al., "DCAF8, a Novel MuRF1 Interaction Partner, Promotes Muscle Atrophy," *Journal of Cell Science* 132, no. 17 (2019): jcs233395.

24. Y. L. Ye, Z. Kuai, D. D. Qian, et al., "GLP-2 Ameliorates D-Galactose Induced Muscle Aging by IGF-1/Pi3k/Akt/FoxO3a Signaling Pathway in C2C12 Cells and Mice," *Archives of Gerontology and Geriatrics* 124 (2024): 105462.

25. C. H. Kim, H. Neiswender, E. J. Baik, W. C. Xiong, and L. Mei, "Beta-Catenin Interacts With MyoD and Regulates Its Transcription Activity," *Molecular and Cellular Biology* 28, no. 9 (2008): 2941–2951.

26. S. Cui, L. Li, R. T. Yu, et al., "β-Catenin Is Essential for Differentiation of Primary Myoblasts via Cooperation With MyoD and α-Catenin," *Development* 146, no. 6 (2019): dev167080.

27. Y. Son, W. W. Lorenz, and C. M. Paton, "Linoleic Acid-Induced ANGPTL4 Inhibits C2C12 Skeletal Muscle Differentiation by Suppressing Wnt/β-Catenin," *Journal of Nutritional Biochemistry* 116 (2023): 109324.

28. J. Shi, Q. Su, F. Han, W. Chen, D. Zhang, and B. Xu, "MiR-337 Suppresses Pancreatic Cancer Development via STAT3/Wnt/β-Catenin Axis," *Anti-Cancer Drugs* 32, no. 7 (2021): 681–692.

29. M. T. Cantwell, J. S. Farrar, J. C. Lownik, et al., "STAT3 Suppresses Wnt/β-Catenin Signaling During the Induction Phase of Primary Myf5+ Brown Adipogenesis," *Cytokine* 111 (2018): 434–444.

30. D. B. Lybrand, M. Naiman, J. M. Laumann, et al., "Destruction Complex Dynamics: Wnt/β-Catenin Signaling Alters Axin-GSK3β Interactions In Vivo," *Development* 146, no. 13 (2019): dev164145.

31. A. Berthon, A. Martinez, J. Bertherat, and P. Val, "Wnt/β-Catenin Signalling in Adrenal Physiology and Tumour Development," *Molecular and Cellular Endocrinology* 351, no. 1 (2012): 87–95.

32. M. Shin, E. H. Yi, B. H. Kim, et al., "STAT3 Potentiates SIAH-1 Mediated Proteasomal Degradation of β-Catenin in Human Embryonic Kidney Cells," *Molecules and Cells* 39, no. 11 (2016): 821–826.

Supporting Information

Additional supporting information can be found online in the Supporting Information section.

WILEY

LETTER TO THE EDITOR

Calibrating Anti-Double-Stranded DNA Antibodies Detections Using Likelihood Ratios

Jiangfeng Zhao[1] | Kaiwen Wang[2] | Canchen Ma[2] | Zhenghan Zhao[3] | Li Guo[2] | Haiting Yang[1] | Shuang Ye[2]

[1]Rheumatology and Immunology Laboratory, Jiading Branch, Renji Hospital, Shanghai JiaoTong University School of Medicine, Shanghai, People's Republic of China | [2]Department of Rheumatology, Renji Hospital, School of Medicine, Shanghai JiaoTong University, Shanghai, People's Republic of China | [3]Chengdu Medical College, Chengdu, People's Republic of China

Correspondence: Shuang Ye (ye_shuang2000@163.com)

Dear Editor,

Anti-dsDNA antibodies are of diagnostic value for systemic lupus erythematosus (SLE) with up to 90% specificity. With a high relevance to the disease activity, monitoring changes in the titer of anti-dsDNA antibodies every 1–3 months is a standard practice that has been recommended by international guidelines for active SLE [1].

However, the variety of different quantitative assays for anti-dsDNA antibodies has posed a big challenge to align, compare, and interpret the laboratory results. In 1985, the World Health Organization (WHO) established the first International Standard (IS) material, IS-Wo/80, with International Units (IU/ml) for anti-dsDNA antibodies calibration [2]. With the exhaustion of the Wo/80 material, in 2019, the European Directorate for the Quality of Medicines & HealthCare (EDQM), part of the Biological Standards and Control Institute, prepared 15/174, an ampoule with a nominal value of 100 units [3]. Although 15/174 is not fully equivalent to Wo/80, it can serve as a reference reagent for anti-dsDNA antibodies testing. These standard materials are more efficient in terms of intra-assay quality control. The aim of the current study is to establish an inter-assay calibration using the likelihood ratios (LRs) approach.

The LR has been previously applied with regard to interpreting test results and assisting diagnosis [4]. The idea of LR refers to the ratio of the proportion of patients with a specific test result to the proportion of controls with the same test result. For example,

a test result with an LR of 1 indicates that the likelihood of this result occurring in a patient is the same as in the control. A test result with an LR of 10 means that the likelihood of this result occurring in the patient is 10 times higher than in the control population.

Thus, we enrolled 502 SLE patients, 498 disease controls, and 100 healthy donors (Table S1) to detect anti-dsDNA antibodies via seven different assays available in mainland China. SLE patients fulfilled the American College of Rheumatology/European League Against Rheumatism (ACR/EULAR) 2019 classification criteria [5]. Those with severe infections, malignancies, infectious diseases, and other such conditions were excluded. Additionally, SLE patients with concurrent conditions such as Rhupus were also excluded. The control group was matched with the SLE patient group in terms of age, gender, ethnicity, and other aspects before being included in the study. The study was approved by the Ethics Committee of Ren Ji Hospital Jiading Branch, Shanghai Jiao Tong University School of Medicine (Ethics number:2024–007). The distribution of test results was presented with test-specific LRs calculated (Figure 1A and Figure S1). The proportion of SLE patients who tested positive for anti-dsDNA, along with the sensitivity and specificity values for each test type, has been presented in Table S2. The corresponding test results for LR of test specificity at 0.1, 1, 10, and 30, along with the readout of the 15/174 reference materials and the cut-off values provided by assay manufacturers, were listed in Figure 1B. All seven assays had their cut-off values

---
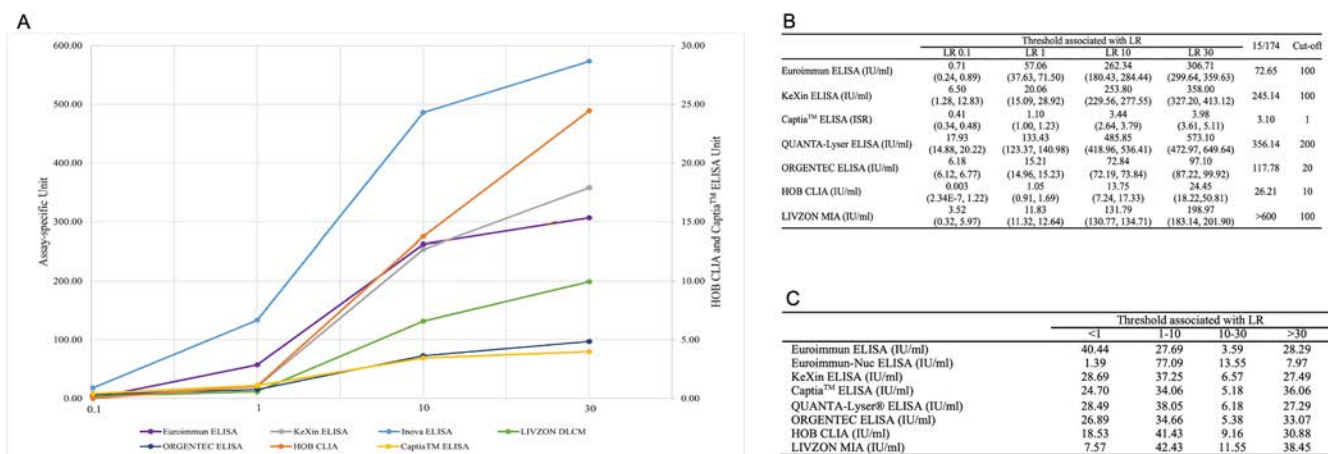
FIGURE 1 | Assay-specific thresholds associated with a LR of 0.1, 1, 10, 30 (A). LRs associated with the 15/174 reference materials (B). Fraction of SLE patients with results associated with selected LR ranges (C). ELISA: Enzyme-Linked Immunosorbent Assay. CLIA: Chemiluminescence immunoassay. MIA: Magnetic Barcode Immunofluorescence Luminescence Assay. A total of 502 SLE, 251 CTD other than SLE, 247 patients with non-CTD and 100 healthy donors were enrolled. SLE: Systemic Lupus Erythematosus; CTD: Connective Tissue Diseases; HD: Healthy Donors.

distributed between LR 1 to 10, and six out of seven assays had a 15/174 reference readout higher than the corresponding cut-off values. One assay (ELISA, Euroimmun, Germany) yielded a lower than cut-off 15/174 readout which suggested its suboptimal performance (low detection sensitivity [6]). The second, third, and fourth assays displayed a similar 15/174 reference LR at around 10, while the remaining three assays had a higher 15/174 reference LR beyond 30. Overall, the specificity likelihood ratios of the seven anti-dsDNA assays beyond 10 were 31%~50% after LR calibration among SLE patients (Figure 1C). Particularly, around 30% of the patient population demonstrated highly specific test results with an LR greater than 30 across the board. It is noteworthy that the proportion of anti-dsDNA antibodies detected by the MIA (LIVZON, China) within the LR intervals of 10–30 and > 30 is the highest among all methodologies. This is because MIA is a method that combines magnetic separation technology with immunofluorescence luminescence analysis. With a 15/174 reference readout beyond its upper detection limits, it should be cautious to deploy this very sensitive assay and be aware of the risk of generating false positive results. LR of 10 will serve as a critical threshold value; at this threshold, the sensitivity of detecting anti-dsDNA antibodies in patients with SLE will be highly beneficial.

There is no gold standard methodology for anti-dsDNA antibody detection. Even with the calibration of WHO international units (IU), inter-assay inconsistency is still problematic. Due to the different antigen sources and numerous detection platforms, the cut-off values, sensitivity, specificity, and linear range for assays are diverse. To address this issue, we introduced LRs to provide a quantitative reference interval among products from different brands or methodologies to improve consistency. In summary, a multi-assay cross-referenced approach is still the *status quo* regarding anti-dsDNA testing to establish a diagnosis. LR analysis may provide a useful tool to align different quantitative assays. Additionally, sticking with a validated assay with proper intra-assay quality control will be more viable for established SLE patients in terms of longitudinal assessment of anti-dsDNA antibodies.

Jiangfeng Zhao
Kaiwen Wang
Canchen Ma
Zhenghan Zhao
Li Guo
Haiting Yang
Shuang Ye

References

1. A. J. G. Swaak, J. Groenwold, and W. Bronsveld, "Predictive Value of Complement Profiles and Anti-dsDNA in Systemic Lupus Erythematosus," *Annals of the Rheumatic Diseases* 45 (1986): 359–366.

2. T. Feltkamp, T. B. Kirkwood, R. Maini, T. E. Feltkamp, R. N. Maini, and L. A. Aarden, "The First International Standard for Antibodies to Double Stranded Dna," *Annals of the Rheumatic Diseases* 47 (1988): 740–746.

3. B. J. Fox, J. Hockley, P. Rigsby, C. Dolman, P. L. Meroni, and J. Rönnelid, "A WHO Reference Reagent for Lupus (Anti-dsDNA) Antibodies: International Collaborative Study to Evaluate a Candidate Preparation," *Annals of the Rheumatic Diseases* 78, no. 12 (2019): 1677–1680.

4. W. Fierz, "Likelihood Ratios of Quantitative Laboratory Results in Medical Diagnosis: The Application of Bézier Curves in ROC Analysis," *PLoS One* 13, no. 2 (2018): e0192420.

5. M. Aringer, K. Costenbader, D. Daikh, et al., "European League Against Rheumatism/American College of Rheumatology Classification Criteria for Systemic Lupus Erythematosus," *Arthritis and Rheumatology* 71, no. 9 (2019): 1400–1412.

6. C.-J. Bauer, P. Karakostas, N. Weber, et al., "Comparative Analysis of Contemporary Anti-Double Stranded DNA Antibody Assays for Systemic Lupus Erythematosus," *Frontiers in Immunology* 7, no. 14 (2023): 1305865.

Supporting Information

Additional supporting information can be found online in the Supporting Information section.

LETTER TO THE EDITOR

Producing an Anti-dsDNA Antibody Reference Reagents to Calibrate Different Quantitative Assays in China

Jiangfeng Zhao[1] | Yuqing Zhu[2] | Canchen Ma[3] | Li Guo[3] | Haiting Yang[1] | Xueyu Zhang[2] | Zhenghan Zhao[4] | Shuang Ye[3] | Kaiwen Wang[3] 🄳

[1]Rheumatology and Immunology Laboratory, Jiading Branch, Renji Hospital, Shanghai Reference Lab for Autoantibodies Testing, Shanghai JiaoTong University School of Medicine, Shanghai, People's Republic of China | [2]Shanghai Center for Clinical Laboratory, Shanghai, People's Republic of China | [3]Department of Rheumatology, Renji Hospital, School of Medicine, Shanghai JiaoTong University, Shanghai, People's Republic of China | [4]Chengdu Medical College, Chengdu, People's Republic of China

Correspondence: Kaiwen Wang (wangkaiwen_1983@163.com)

Dear Editor,

Systemic lupus erythematosus (SLE) is a prototypic autoimmune disease characterized by the presence of an array of anti-nuclear autoantibodies [1]. Anti-dsDNA antibody serves as one of the immunological benchmarks of SLE and contributes to diagnosis [2]. Quantitative measurements of anti-dsDNA over time are also pivotal, as they may reflect SLE disease activity and the response to treatment. Abiding by international recommendations, SLE patients should be tested for anti-dsDNA quantitative values every 3–6 months during the follow-up [3]. The importance of anti-dsDNA IgG antibody detection in SLE, in terms of diagnosis and disease activity monitoring, is indisputable. However, the diversity of quantitative methodologies and the variety of a given assay produced by different manufacturers in the market pose critical unmet needs to standardize anti-dsDNA antibody test results. For example, the radio-immunoassay Farr (RIA) has gradually faded away from the market due to its bio-hazard issue; on the other hand, ELISAs are getting more popular [4] yet six different brands are available in the China market; in the meantime, more sensitive hi-tech armed chemiluminescence immunoassays (CLIA), magnetic barcode immunofluorescence assays (MIA) and magnetic bead flow Fluoroimmunoassay (MBFFI) are becoming part of the racing.

In 1985, the World Health Organization (WHO) established the first international standard substance (IS) of anti-dsDNA IgG antibody, Wo/80, and calibrated its concentration using international units (IU/ml) [5]. With the gradual depletion of Wo/80, in 2019, the European Biological Standards and Control prepared the 15/174 with a standard value of 100 units per ampoule. Although 15/174 is not exactly equivalent to Wo/80, it can be used as a reference reagent for anti-dsDNA IgG antibody to unify and quantify different detection methods of anti-dsDNA IgG antibody [6]. However, its accessibility is problematic. In light of the *status quo* of anti-dsDNA assays in China, that is, differences in methodology and manufacturers, hence the inconsistency of the test results, we need a Reference Reagent equivalent to Wo/80 as the constant in the equation more than ever.

With the depletion and availability issues of international standard materials, such as Wo/86 or 15/174, we have produced an anti-dsDNA local Reference Reagent in China. The reference reagent displayed a good stability and consistency in multiple quality control assays and was further tested for robustness by 38 independent laboratories. The launch of this local Reference Reagent for anti-dsDNA antibodies may facilitate data sharing and normalization, enhance test accuracy, and better interpretation.

The patient is an 18-year-old female SLE who was admitted to our hospital in 2023 due to a major flare of lupus characterized by thrombotic microangiopathy (TMA: microangiopathic hemolytic anemia, thrombocytopenia, and acute kidney injury). Her autoantibody laboratory tests revealed strong positive anti-dsDNA antibodies (both for ELISA method and Crithidia luciliae method, Figure 1A) with an ANA positive at 1:640

Jiangfeng Zhao and Yuqing Zhu contributed equally to this study.
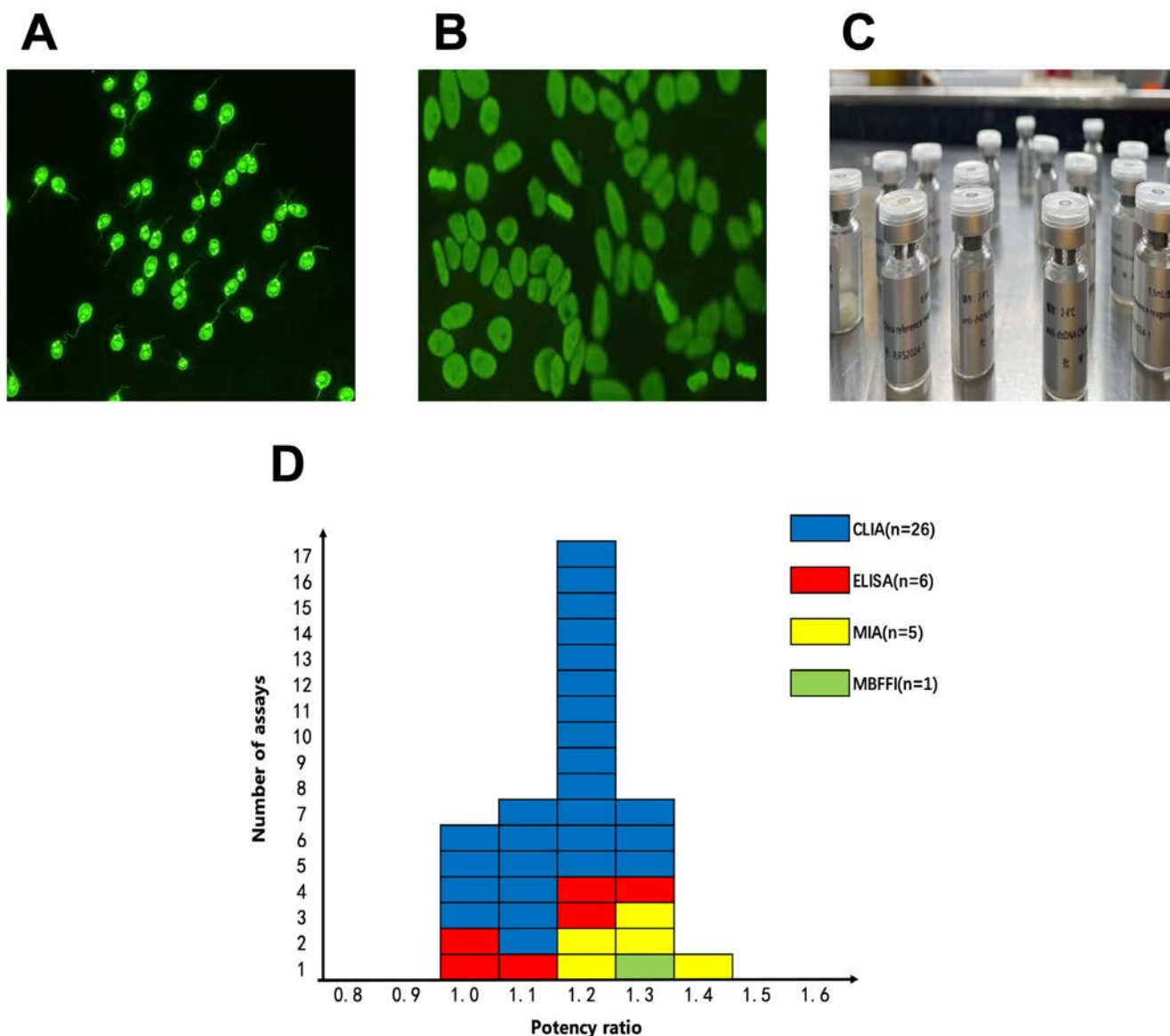
FIGURE 1 | Perform indirect immunofluorescence staining on Crithidia luciliae (A) and HEp-2 cells (B) using Anti-dsDNA Antibody Reference Reagents in China (C). The potency estimates for the anti-double-stranded DNA antibody reference reagent from 38 laboratories (D). CLIA, Chemiluminescence immunoassay; ELISA, Enzyme-linked immunosorbent assays; MBFFI, Magnetic Bead Flow Fluoroimmunoassay; MIA, Magnetic Barcode Immunofluorescence Luminescence Assay.

(homogenous pattern, Figure 1B). She underwent plasma exchange, and a total of 8 plasma exchange solutions (amounting to 13.5 L) were collected. Informed consent was obtained from the patient, and the study protocol was approved by IRB prior to carrying out the subsequent experiments (ethical approval number: 2024-005).

The lyophilized thrombin powder (5000 IU, Zhejiang Hengkang Pharmaceutical Co. Ltd., China) is mixed with the patient's plasma replacement solution in a ratio of 50 IU:1 mL, stirred gently until evenly mixed, left to stand at 37°C for 1 h, and then further placed at 4°C for 72 h. After centrifugation at 5000 rpm for 15 min, the supernatant is collected, filtered through a sterilized filter, and transferred into glass reagent bottles at 500 ul per vial (Figure 1C). Freeze-dry strictly in accordance with the Standard Operating Procedures for Vacuum Freeze Dryer (Ningbo Xinzhi Freeze-Drying Equipment Co. Ltd., Ningbo, China).

The commercial Anti-dsDNA Antibody ELISA Kit (Kexin Biotechnology Co. Ltd., Shanghai, China) was picked to evaluate the performance of the Anti-dsDNA Antibody local Reference Reagents (LRR). The LRR, which were stored at 4°C, showed that the coefficient of variation (CV) of the detection values was less than 5% for both inter-group and intra-group data in three consecutive days of testing, indicating good homogeneity of the reagent (Table S1). Next, we extended the detection time to 3 months to conduct a stability study of the LRR. The results showed again that the continuous detection values at 4°C for 3 months have a CV of less than 5% (Table S2). The results of accelerated destruction stability experiments showed that the CV% of the detected values of the LRR was still within 5% after being placed at 37°C for 24 h or 72 h (Table S3). Next, we conducted an inter-batch stability analysis of 10 batches of LRR, and the results yielded a similar CV% of less than 5% (Table S4). The titre of the anti-dsDNA antibody reference reagent remained above

90% after being stored at different temperatures for 12 months (Table S5).

Thirty-eight laboratories participated in the performance evaluation of the Anti-dsDNA Antibody LRR, with specific methodological details and a breakdown of reagents used provided in Table S6. The potency ratio was calculated based on the parallel test results of the LRR and a specific serum sample. Most of the ratio fell within the range of 1.0–1.4 (Figure 1D). The results indicate that the data follow a normal distribution, suggesting that the LRR can aid in accurately estimating the reference value for different methodologies. Our preliminary data in 38 independent labs suggested that the overall performance of the current ELISA and CLIA assays for anti-dsDNA in the market is generally good with the reference reagents. However, there are fewer data from MIA or MBFFI, making it impossible to fully evaluate those new methodologies [7].

As an academic rheumatology referral center in southeast China and the Shanghai reference lab for autoantibodies testing, we attempted to fulfill the commitment of providing a local standardization of anti-dsDNA measurements. By producing the anti-dsDNA local reference reagents, it helps to calibrate and unify different brands and methodologies. By no means is our LRR meant to substitute Wo/80 or 15/174; it is not intended to gauge an absolute value for a certain serum sample, but rather, it may reduce inter-batch variation to a given commercial kit, correct intra-assay (such as ELISAs) variations, and align inter-assay (such as ELISA and CLIA) results. Due to the exhaustion of the first international standard for anti-dsDNA-Wo/80, while some conventional methods can establish historical links to Wo/80 through early calibration exercises, many new assays cannot be traced back. The claim of anti-dsDNA antibodies with international standards and assigned definite International Units (IU) at the moment is largely unsubstantiated.

Author Contributions

Jiangfeng Zhao and Yuqing Zhu conducted experiments, making figures and tables, and drafting the manuscript. Canchen Ma and Li Guo performed clinical data. Haiting Yang performed bioinformatics analysis. Xueyu Zhang and Zhenghan Zhao collected clinical samples. Shuang Ye and Kaiwen Wang participated in revising the article and supplementing the data. All authors contributed to the article and approved the submitted version.

Conflicts of Interest

The authors declare no conflicts of interest.

Data Availability Statement

The authors confirm that the data supporting the findings of this study are available within the Supporting Information.

Jiangfeng Zhao
Yuqing Zhu
Canchen Ma

Li Guo
Haiting Yang
Xueyu Zhang
Zhenghan Zhao
Shuang Ye
Kaiwen Wang

References

1. E. M. Tan, A. S. Cohen, J. F. Fries, et al., "The 1982 Revised Criteria for the Classification of Systemic Lupus Erythematosus," *Arthritis and Rheumatism* 25 (1982): 1271–1277, https://doi.org/10.1002/art.1780251101.

2. Y. Sherer, A. Gorstein, M. J. Fritzler, and Y. Shoenfeld, "Autoantibody Explosion in Systemic Lupus Erythematosus: More Than 100 Different Antibodies Found in SLE Patients," *Seminars in Arthritis and Rheumatism* 34, no. 2 (2004): 501–537, https://doi.org/10.1016/j.semarthrit.2004.07.002.

3. G. Yaniv, G. Twig, D. B. Shor, et al., "A Volcanic Explosion of Autoantibodies in Systemic Lupus Erythematosus: A Diversity of 180 Different Antibodies Found in SLE Patients," *Autoimmunity Reviews* 14, no. 1 (2015): 75–79, https://doi.org/10.1016/j.autrev.2014.10.003.

4. M. Infantino, B. Palterer, G. Previtali, et al., "Comparison of Current Methods for Anti-dsDNA Antibody Detection and Reshaping Diagnostic Strategies," *Scandinavian Journal of Immunology* 96, no. 6 (2022): e13220, https://doi.org/10.1111/sji.13220.

5. T. Feltkamp, T. B. Kirkwood, R. Maini, T. E. Feltkamp, R. N. Maini, and L. A. Aarden, "The First International Standard for Antibodies to Double Stranded Dna," *Annals of the Rheumatic Diseases* 47, no. 9 (1988): 740–746, https://doi.org/10.1136/ard.47.9.740.

6. B. J. Fox, J. Hockley, P. Rigsby, C. Dolman, P. L. Meroni, and J. Rönnelid, "A WHO Reference Reagent for Lupus (Anti-dsDNA) Antibodies: International Collaborative Study to Evaluate a Candidate Preparation," *Annals of the Rheumatic Diseases* 78, no. 12 (2019): 1677–1680, https://doi.org/10.1136/annrheumdis-2019-215845.

7. M. Satoh, S. Tanaka, and E. K. Chan, "The Uses and Misuses of Multiplex Autoantibody Assays in Systemic Autoimmune Rheumatic Diseases," *Frontiers in Immunology* 21, no. 6 (2015): 181, https://doi.org/10.3389/fimmu.2015.00181.

Supporting Information

Additional supporting information can be found online in the Supporting Information section.

LETTER TO THE EDITOR

Alterations of Gut Microbiome and Serum Short-Chain Fatty Acids in Children With Enthesitis-Related Arthritis

Qi Zheng[1] | Yiping Xu[1] | Xubo Qian[2] | Bin Hu[1] | Qian Ma[1] | Li Guo[1] | Robert M. Dorazio[3] | Meiping Lu[1]

[1]Department of Rheumatology Immunology and Allergy, Children's Hospital, Zhejiang University School of Medicine, National Clinical Research Center for Child Health, Hangzhou, China | [2]Department of Pediatrics, Jinhua Hospital of TCM Affiliated to Zhejiang University of Traditional Chinese Medicine, Jinhua, China | [3]Children's Hospital, Zhejiang University School of Medicine, National Clinical Research Center for Child Health, Hangzhou, China

Correspondence: Robert M. Dorazio (rmdorazio@zju.edu.cn) | Meiping Lu (meipinglu@zju.edu.cn)

Dear Editor,

Enthesitis-related arthritis (ERA) is a subtype of juvenile idiopathic arthritis, in which altered microbiota associated with abnormal immune responses have been found [1]. However, the molecules and mechanisms underlying these associations are far from being identified. There are still many questions to be answered: (1) among the tens of thousands of gut microbiota, which bacteria are truly active or playing a pathogenic role in the development of ERA? (2) what is the relationship between the genotype and enterotype? (3) how does gut microbiota affect the immune system or mediate the onset of chronic arthritis? (4) how does gut microbiota metabolites affect disease progression? To answer some of these questions, we conducted a metagenomic study to identify gut microbiota composition in ERA patients at the species level and to thoroughly investigate the microbial components. We also measured short-chain-fatty acids (SCFAs) in the sera of ERA and healthy controls, and correlation analysis between clinical and laboratory indicators was performed to elucidate the possible pathways taken by intestinal microorganisms to influence human immunity.

Fourteen children with ERA (treatment naïve) and 20 healthy children were enrolled in the study (Figure S1). The median ages in the ERA group and control group were 11.79 (8.25–14.5) and 10.17 (7.75–14.5) years, respectively. There were no statistical differences in age ($p=0.086$), BMI ($p=0.077$), or sex ($p=0.089$) between the two groups (Table 1). A total of 14 ERA fecal

samples and 20 control fecal samples were collected. Microbial genomic DNA was isolated, and the quality of DNA was measured using the NanoDrop instrument (Thermo Scientific). A DNA library was constructed using the TruSeq DNA HT Sample Prep Kit. Qubit 2.0 was used for preliminary quantification; then inserted fragments of the library were detected by Agilent 2100. Metagenomic sequencing was completed, and paired-end Illumina NovaSeq data underwent quality control (FastQC) and host removal via KneadData (Trimmomatic, Bowtie2). Taxonomic profiling employed Kraken2 (confidence 0.2) with a custom microbial database (bacterial, fungal, archaeal, viral, and novel genomes) and Bracken for Bayesian abundance estimation. Functional annotation used HUMAnN2 (DIAMOND-aligned to UniRef90). Antibiotic resistance genes were identified via FMAP (CARD database) [2]. The R package ALDEx2 was used for the compositional analysis, and there were 8 genera that differed considerably in relative abundances between the ERA group and controls (effect size > 0.5 or ≤ 0.5). Of these 8 genera, the abundances of *Akkermansia*, *Campylobacter*, and *Gordonia* were lower in the ERA group, whereas the abundances of *Fusobacterium*, *Gemella*, *Lachnoclostridium*, *Propionispora*, and *Rhodococcus* were higher in the ERA group. The highest relative abundances among these 8 genera were those of *Lachnoclostridium* 0.7687% (0.3753%, 1.3265%) in the ERA group and 0.3196% (0.2216%, 0.4285%) in the control group. However, the abundances of the other 7 genera were much lower than those of *Lachnoclostridium* (Figure 1A,B). At the

Abbreviations: AS, ankylosing spondylitis; BMI, body mass index; ERA, enthesitis-related arthritis; HLA-B27, human leukocyte antigen-B27; IBD, inflammatory bowel disease; JIA, juvenile idiopathic arthritis; PCoA, principal coordinate analysis; SCFAs, short-chain fatty acids.

TABLE 1 | Clinical characteristics of ERA patients.

Characteristics	ERA ($n = 14$)	Control ($n = 20$)	p
Age, median (IQR)	11.79 (8.25–14.50)	10.50 (7.75–14.00)	$p = 0.086$
Male	12	12	$p = 0.089$
BMI median (IQR)	16.00 (14.70–19.95)	16.86 (14.43–20.68)	$p = 0.077$
Disease activity parameters			
JADAS, median (IQR)	15.40 (6.00–26.9)	—	
ESR, median (IQR)	55.50 (8.00–115.00)	—	
HLA-B27, positive, n (%)	13 (92.86)	—	
Cytokines			
IL-2, median (IQR), pg/mL	2.20 (1.00–3.50)	—	
IL-4, median (IQR), pg/mL	1.90 (1.00–6.10)	—	
IL-6, median (IQR), pg/mL	14.00 (1.30–439.40)	—	
IL-10, median (IQR), pg/mL	1.90 (1.00–4.40)	—	
TNF-α, median (IQR), pg/mL	1.30 (1.00–34.50)	—	
IFN-γ, median (IQR), pg/mL	2.80 (1.00–5.60)	—	
Cluster of differentiation			
CD3, median (IQR), %	66.90 (46.50–85.20)	—	
CD4, mean, (SD), %	33.87 (8.26)	—	
CD8, mean, (SD), %	29.49 (5.96)	—	
CD19, median (IQR), %	12.50 (4.80–30.70)	—	
CD3-CD16 + CD56+, median (IQR), %	11.40 (2.90–22.50)	—	
CD4/CD8, median (IQR)	1.13 (0.60–1.89)	—	
Immunoglobulin			
IgG, mean (IQR), IU/mL	13.20 (9.10–20.10)	—	
IgA, mean (IQR), IU/mL	2.64 (1.20–4.74)	—	
IgM, mean (IQR), IU/mL	1.36 (0.58–1.97)	—	
IgE, mean (IQR), IU/mL	18.50 (17.80–230.00)	—	

species level, we identified 25 species that differed considerably between the ERA group and controls (effect size > 0.5 or ≤ 0.5). The species *Anaerostipes_hadrus* had the highest relative abundance, followed by *Ruminococcus_gnavus* and *Clostridium_bolteae* (Figure 1A–F).

SCFAs were isolated from the blood samples of ERA and controls. Gas chromatography–mass spectrometry (GC–MS, Thermo TRACE 1310-ISQ) was used for quantitative analysis of SCFAs, including acetic acid, propionic acid, butyric acid, isobutyric acid, valeric acid, isovaleric acid, and hexanoic acid. The linear regression equation, precision, reproducibility, and limit of quantification of SCFAs standards were tested before being used to quantify SCFAs in samples. We identified 25 associations among the gut microbiome species, SCFAs, and the clinical phenotypes after p values were adjusted for multiple testing corrections using the "Holm" method (the Spearman's correlation, adjusted $p < 0.05$). In this study, most of the bacterial

species whose abundance was higher in ERA were anaerobic and gram-positive, including *Ruminococcus_gnavus*, which has been observed as one of the major contributions to altered intestinal microecology. This finding was consistent with that of Breban et al., who showed that SpA patients had the most notable change being a 2- to 3-fold increase in *Ruminococcus gnavus*, that correlated with disease activity [3]. *Ruminococcus_gnavus* belongs to the Lachnospiraceae family, which is considered to be an important member of human gut microbiota [4]. Significantly higher abundance of *Ruminococcus_gnavus* also was observed in the gut of IBD patients [5]. It was reported that glucorhamnan synthesized by *Ruminococcus_gnavus* can induce TNF-α secretion by dendritic cells, which is one of the core inflammatory cytokines in the pathogenesis of arthritis [6]. We did not find a direct correlation between *Ruminococcus gnavus* and clinical indicators; however, we noticed that IL-6 was positively related to *Actinomyces_graevenitzii*, which was also enriched in ERA patients compared to controls. We can infer that a group of gut
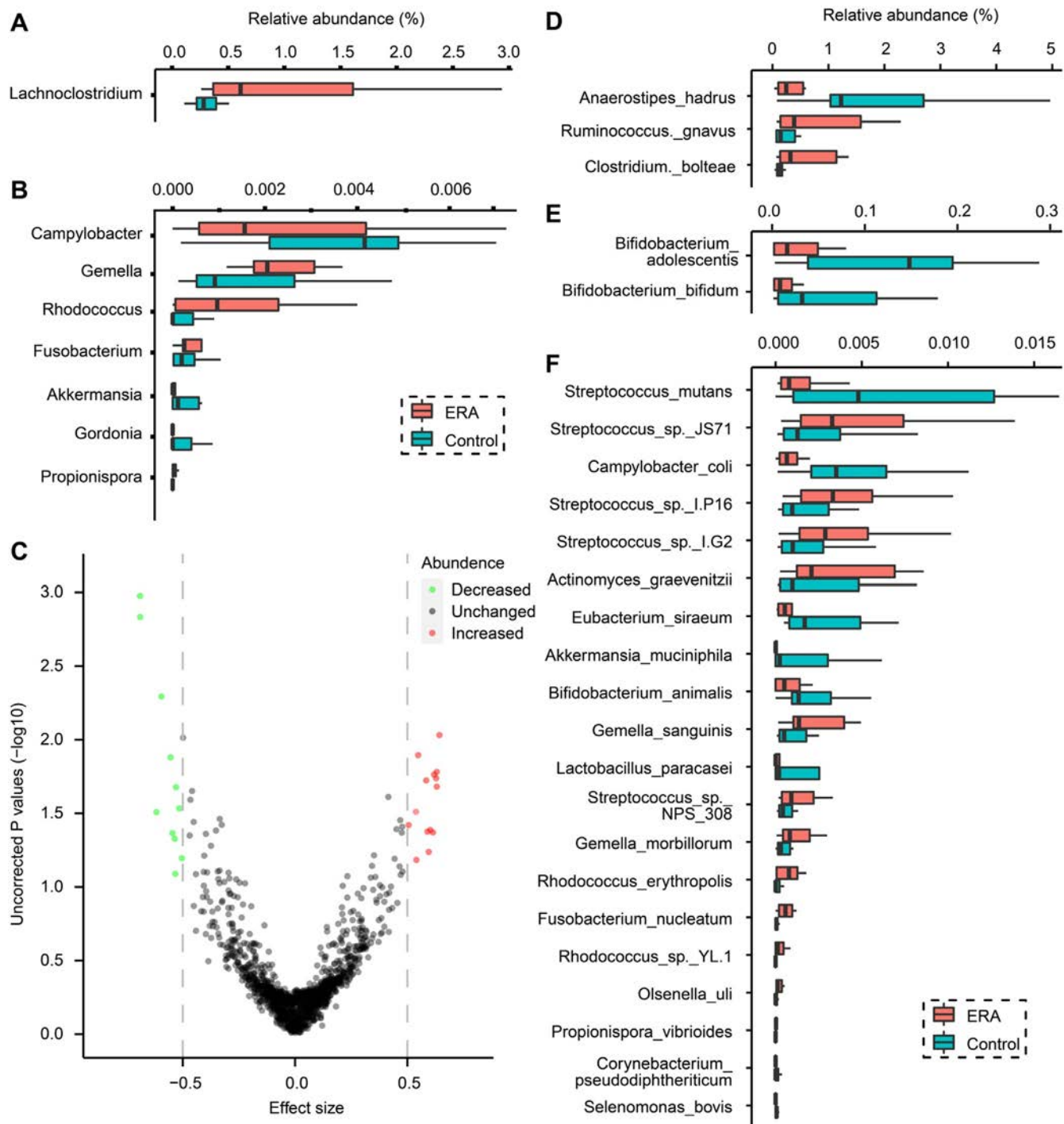
FIGURE 1 | Genera and species changed substantially between the ERA group and controls. (A, B) Box plots of the genera changed substantially between the two groups. The three vertical lines of each box represent the first, second (median), and third quartile, respectively, with the whisker extending to 1.5 inter-quartile range. (C) A volcano plot of the species. Green and red points represent the samples with the "effect size" lower than −0.5 or greater than 0.5. The effect size is the ratio of "the difference between groups" and "the maximum difference within groups." In general, the effect size cut-off is more robust than a *p* value. The difference is considered to be statistically significant if an effect size is lower than −0.5 or greater than 0.5. (D–F) Box plots of the species changed substantially between the two groups.

bacteria rather than one specific gut bacterium can produce an imbalance of the gut microbiome's ecology and can affect the disease progression in ERA patients.

Butyric acid was significantly decreased in ERA patients than normal (Figure S2). Interestingly, we noticed that butyrate-producing strains such as Clostridium bolteae and Fusobacterium nucleatum were significantly higher in ERA patients than in normal controls. Conversely, the concentration of serum butyrate was decreased in the ERA group. It was noted that an enhanced butyrate-consuming microbiome was observed in the gut of rheumatoid arthritis patients [7]. The gut

microbiota generate SCFA through carbohydrate fermentation of dietary fibers and improve glucose homeostasis with upregulation of butyrate production [8]. Butyrate is the major energy source for colonocytes and accounts for about 15% of SCFA in humans [9]. Butyrate can inhibit the growth of Salmonella, playing a role in innate immunity to maintain the homeostasis of the gut bacteria ecology [10]. Deficiency in SCFA production has been associated with autoimmune diseases, such as type 2 diabetes mellitus [11, 12]. Although butyrate plays an important role in the maintenance of intestinal homeostasis, detrimental effects were observed in the study of a mouse model in which butyrate-producing bacteria aggravated colitis symptoms and increased the mortality [13, 14]. Morris et al. showed that spent media from Fusobacterium nucleatum with a high level of SCFAs (such as butyrate) can induce the switch between

latency and lytic replication of Kaposi's sarcoma-associated herpesvirus via the activation of a stress-activated MAPK pathway [15]. In this study, butyric acid was positively correlated with *Actinomyces graevenitzii*, while the abundances of *Actinomyces graevenitzii were* correlated with IL-6. As a consequence, we hypothesize that the alteration of the gut microbiome was associated with cytokines (such as IL-6) that may be involved in the inflammatory microenvironment of the intestine of ERA patients (Figure 2).

Another finding of our study was that oropharyngeal flora, such as Streptococcus sp. I-P16, Streptococcus sp. I-G2, Actinomyces graevenitzil, and Olsenella uli were enriched in the intestine of patients with ERA (Figure 1F). Most of these bacteria were pathogenic or opportunistically pathogenic, leading to
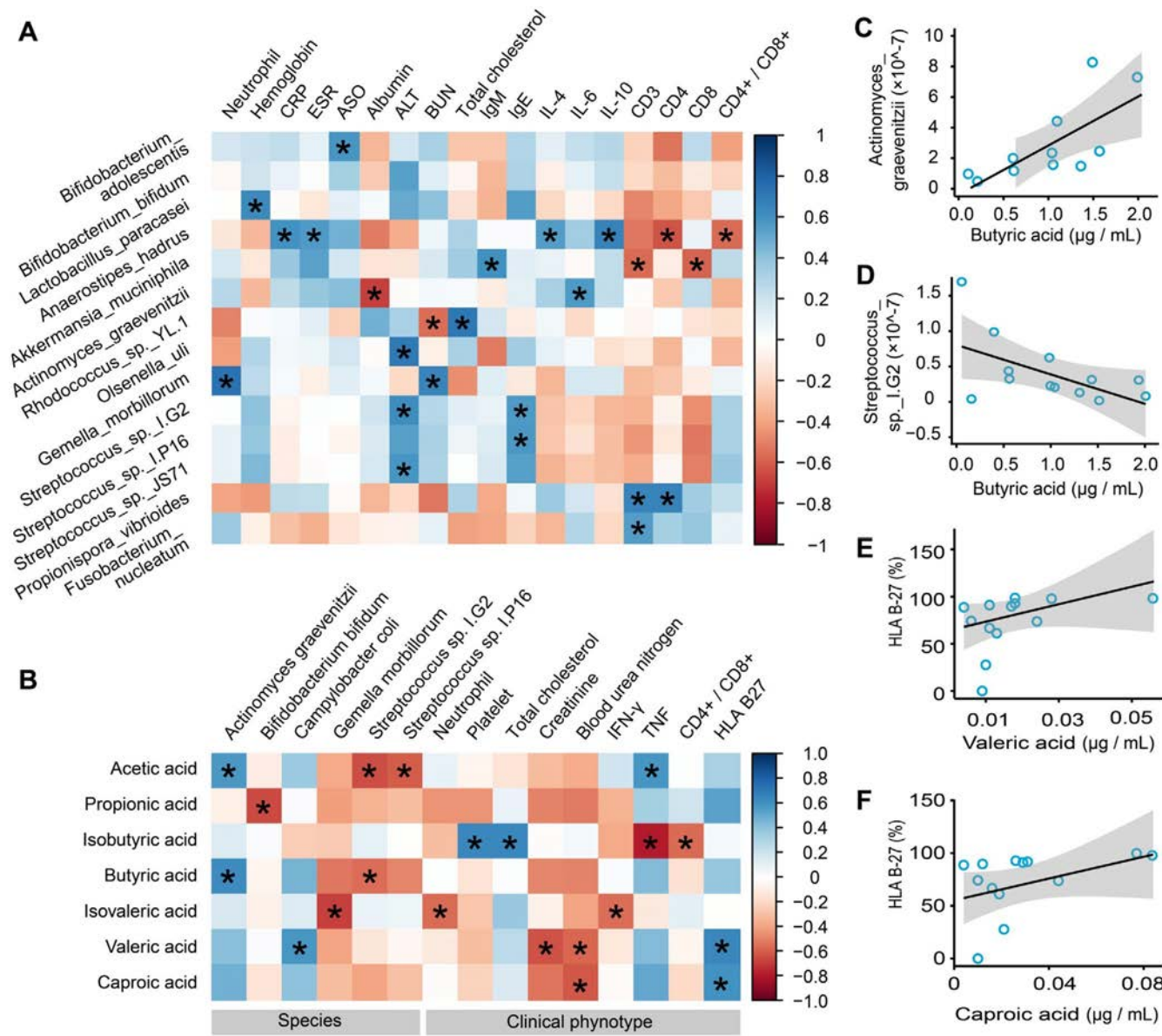
FIGURE 2 | (A) Correlations between the species, short-chain fatty acids (SCFAs), and phenotypes. Correlations between the species and phenotypes. The shade of a square represents the size of a correlation coefficient. A square with an asterisk indicates that the correlation coefficient reached statistical significance after the *p* values were adjusted for multiple testing corrections using the "holm" method. (B) Correlations between the SCFAs, species, and phenotypes. (C–F) Scatter plots of the relationships between the SCFAs and "species or phenotype." The angled line in a panel is the line of simple linear regression, and the shaded area shows the 95% confidence intervals for the fit.

bloodstream infection, septic arthritis, or osteomyelitis [16–19]; therefore, we can infer that enrichment and migration of oral-intestinal bacteria to the gut may be involved in the development of ERA. Correlation analysis found that the level of butyric acid was negatively correlated with Streptococcus sp. I-G2 abundance. Coincidentally, SCFA was found to have antimicrobial activity against *Streptococcus mutans*, *S. gordonii*, S. sanguis, *Candida albicans,* and other species by influencing the growth of competitor microorganisms [20]. Although the detailed mechanism of gut bacterial metabolic end products in the pathogenesis of ERA remains to be elucidated, the accumulating data indicate that immunomodulatory properties of SCFAs represent a new frontier for manipulation and prevention of arthritis.

Author Contributions

Qi Zheng: manuscript writing and research design. **Yiping Xu:** sample collection and manuscript writing. **Bin Hu, Qian Ma, and Li Guo:** clinical data collection. **Xubo Qian:** basic statistical analysis. **Meiping Lu:** review and modification of the article. **Robert M. Dorazio:** statistical analysis and review of the paper.

Ethics Statement

Informed consents were obtained from guardians as well as subjects age over 14 years. The study was approved by the institutional research ethics committee of Zhejiang University School of Medicine (2021-IRBAL-258).

Conflicts of Interest

The authors declare no conflicts of interest.

Data Availability Statement

The data that support the findings of this study are available on request from the corresponding author. The data are not publicly available due to privacy or ethical restrictions.

Qi Zheng
Yiping Xu
Xubo Qian
Bin Hu
Qian Ma
Li Guo
Robert M. Dorazio
Meiping Lu

References

1. H. Jethwa and S. Abraham, "The Evidence for Microbiome Manipulation in Inflammatory Arthritis," *Rheumatology* 56 (2017): 1452–1460.

2. E. A. Franzosa, L. J. McIver, G. Rahnavard, et al., "Species-Level Functional Profiling of Metagenomes and Metatranscriptomes," *Nature Methods* 15, no. 11 (2018): 962–968, https://doi.org/10.1038/s41592-018-0176-y.

3. M. Breban, J. Tap, A. Leboime, et al., "Faecal Microbiota Study Reveals Specific Dysbiosis in Spondyloarthritis," *Annals of the Rheumatic Diseases* 76, no. 9 (2017): 1614–1622.

4. A. Bell, J. Brunt, E. Crost, et al., "Elucidation of a Sialic Acid Metabolism Pathway in Mucus-Foraging *Ruminococcus Gnavus* Unravels Mechanisms of Bacterial Adaptation to the Gut," *Nature Microbiology* 4, no. 12 (2019): 2393–2404.

5. A. B. Hall, M. Yassour, J. Sauk, et al., "A Novel *Ruminococcus gnavus* Clade Enriched in Inflammatory Bowel Disease Patients," *Genome Medicine* 9, no. 1 (2017): 103.

6. M. T. Henke, D. J. Kenny, C. D. Cassilly, H. Vlamakis, R. J. Xavier, and J. Clardy, "*Ruminococcus gnavus*, A Member of the Human Gut Microbiome Associated With Crohn's Disease, Produces an Inflammatory Polysaccharide," *Proceedings of the National Academy of Sciences of the United States of America* 116, no. 26 (2019): 12672–12677.

7. J. Wang, B. Huang, L. Shi, et al., "Intestinal Butyrate-Metabolizing Species Contribute to Autoantibody Production and Bone Erosion in Rheumatoid Arthritis," *Science Advances* 8, no. 6 (2022): eabm1511.

8. D. J. Morrison and T. Preston, "Formation of Short Chain Fatty Acids by the Gut Microbiota and Their Impact on Human Metabolism," *Gut Microbes* 7, no. 3 (2016): 189–200.

9. L. K. Brahe, A. Astrup, and L. H. Larsen, "Is Butyrate the Link Between Diet, Intestinal Microbiota and Obesity-Related Metabolic Diseases?," *Obesity Reviews* 14 (2013): 950–959.

10. I. Gantois, R. Ducatelle, F. Pasmans, et al., "Butyrate Specifically Down-Regulates Salmonella Pathogenicity Island 1 Gene Expression," *Applied and Environmental Microbiology* 72, no. 1 (2006): 946–949.

11. J. Qin, Y. Li, Z. Cai, et al., "A Metagenome-Wide Association Study of Gut Microbiota in Type 2 Diabetes," *Nature* 490 (2012): 55–60.

12. Liping Zhao, Feng Zhang, Xiaoying Ding, et al., "Gut Bacteria Selectively Promoted by Dietary Fibers Alleviate Type 2 Diabetes," *Science* 359, no. 6380 (2018): 1151–1156.

13. H. Liu, J. Wang, T. He, et al., "Butyrate: A Double-Edged Sword for Health?," *Advances in Nutrition* 9 (2018): 21–29.

14. Q. Zhang, Y. Wu, J. Wang, et al., "Accelerated Dysbiosis of Gut Microbiota During Aggravation of DSS-Induced Colitis by a Butyrate-Producing Bacterium," *Scientific Reports* 6, no. 6 (2016): 27572.

15. T. L. Morris, R. R. Arnold, and J. Webster-Cyriaque, "Signaling Cascades Triggered by Bacterial Metabolic End Products During Reactivation of Kaposi's Sarcoma-Associated Herpesvirus," *Journal of Virology* 81, no. 11 (2007): 6032–6042.

16. D.-W. Hyun, J.-Y. Lee, M.-S. Kim, et al., "Pathogenomics of Streptococcus Ilei sp. Nov., a Newly Identified Pathogen Ubiquitous in Human Microbiome," *Journal of Microbiology* 59, no. 8 (2021): 792–806.

17. F. Somma, R. Castagnola, D. Bollino, and L. Marigo, "Oral Inflammatory Process and General Health. Part 2: How Does the Periapical Inflammatory Process Compromise General Health?," *European Review for Medical and Pharmacological Sciences* 15 (2011): 35–51.

18. S. Jiang, X. Gao, L. Jin, and E. C. Lo, "Salivary Microbiome Diversity in Caries-Free and Caries-Affected Children," *International Journal of Molecular Sciences* 17, no. 12 (2016): 1978.

19. C. Willmann, X. Mata, K. Hanghoej, et al., "Oral Health Status in Historic Population: Macroscopic and Metagenomic Evidence," *PLoS One* 13, no. 5 (2018): e0196482.

20. C. B. Huang, Y. Alimova, T. M. Myers, and J. L. Ebersole, "Short- and Medium-Chain Fatty Acids Exhibit Antimicrobial Activity for Oral Microorganisms," *Archives of Oral Biology* 56, no. 7 (2011): 650–654.

Supporting Information

Additional supporting information can be found online in the Supporting Information section.